Development of High Durability Concrete for the Arabian Gulf Environment

by

Nasser Rashid Shattaf

Thesis submitted in accordance with the requirements for the degree of

DOCTOR OF PHILOSOPHY

University of Sheffield
Department of Mechanical Engineering
Faculty of Engineering

March 1998

Dedicated to my wife,
son and daughter

Summary

Concrete is probably the most widely used construction material in the world. In the Arabian Gulf region, deterioration of concrete due to the aggressive environment is recognized to be the main factor affecting their structural integrity. The durability of concrete structures can be preserved by various protection methods; however, using cement replacement materials is one of the most effective and economic methods of maintaining their stability as well as extending their service life.

The aim of this project is to study four interrelated aspects, namely, (1) the effect of hot environment on the properties of fresh concrete incorporating mineral admixtures, (2), the influence of exposure environment on the engineering properties of hardened concrete, under various curing conditions, without and with mineral admixture, (3), the differences in porosity and pore structure of the same set of mixes, and, (4) the effect of outdoor exposure on the durability-related properties of concrete. To achieve the above aims, the experimental programme involved the study of five different mixes of combinations of silica fume/slag and silica fume. The effects of real exposure to the Arabian Gulf environment of these mixes subjected to four curing regimes, namely, continuous water curing, no water curing after demolding, and air drying after 3 and 7 days of initial water curing were investigated.

The properties investigated include (1) consistency and setting times of cement pastes, workability and workability loss with time, (2) engineering properties such as compressive strength, dynamic modulus of elasticity, pulse velocity, shrinkage, expansion and thermal expansion, (3) microstructural properties such as porosity and pore size distribution, (4) durability-related properties such as permeability, water absorption and carbonation depth.

The results show that exposure to hot environment results in rapid setting times, faster loss of slump, higher porosity, coarser pore structure and more permeable concretes. It was found that part cement replacement by silica fume and slag improves

the quality of concrete mixtures, refined the pore structure and produced concretes with very low porosity and continuous pore diameter in both indoor and outdoor environment. The properties of concrete containing mineral admixture appear to be more sensitive to poor curing than the plain concrete, with the sensitivity increasing with increasing amount of slag in the mixture.

Acknowledgements

The author wishes to express his very deep gratitude to ***Professor R N Swamy****, for his invaluable help and supervision throughout the period of the work.*

The author is greatly indebted to ***Dr. A. M. Alshamsi,*** *Associate professor at Department of Civil Engineering-UAE University, for his invaluable suggestions and local supervision during the study.*

The author would like to express his thanks to UAE University, Ministry of Public Works and Housing, for providing generous supply of the materials and equipment.

Special thanks are due to my friend and the technical staff for their help and co-operation in the laboratory work.

Finally, this work would not have been possible without the endless support of my wife.

TABLE OF CONTENTS

Title	i
Dedication	ii
Summary	iii
Acknowledgements	v
Table of Contents	vi
List of Figures	xii
List of Tables	xix
Notation	xxi
Chapter One INTRODUCTION	1
1.1 Introduction	1
1.2 Aims and Objectives	3
1.3 Thesis layout	4
Chapter Two **LITERATURE REVIEW**	6
2.1 Introduction	6
2.2 Problems of deterioration of concrete in the Arabian Gulf	7
2.3 Protection of concrete from deterioration	8
2.3.1 Protection by cover	9
2.3.2 Mineral admixtures	9
2.3.3 Curing	11
2.4 Properties of blended cement concrete	13
2.4.1 Setting time	13
2.4.2 Workability as a function of time	15
2.4.3 Compressive strength	18
2.4.4 Pulse velocity and modulus of elasticity	25
2.4.5 Thermal expansion	26

2.4.6 Permeability 26
2.4.7 Porosity and pore structure 29
2.4.8 Carbonation depth 30
2.5 Summary 31
Chapter Three **EXPERIMENTAL PROGRAMME** 33
3.1 Introduction 33
3.2 Over all test programme 33
3.3 Materials 35
3.2.1 Ordinary portland cement 35
3.2.2 Silica fume 36
3.2.3 Ground granulated blast-furnace slag 36
3.2.4 Aggregates 36
3.3.5 Water 38
3.3.6 Chemical admixture 38
3.4 Mixing 38
3.5 Exposure environments 39
3.5.1 Laboratory environment 39
3.5.2 Outdoor environment in Dubai 39
3.6 Curing 39
3.6.1 Air curing regime 39
3.6.2 3-day curing regime 40
3.6.3 7-day curing regime 40
3.6.4 Continuous water curing regime 40
3.7 Test programme 40
3.7.1 Consistency and Setting time 40
3.7.1.1 Apparatus 40
3.7.1.2 Consistency test procedure 41
3.7.1.3 Setting time test procedure 41
3.7.2 Workability as a function of time 42
3.7.3 Compressive strength 42
3.7.4 Ultrasonic pulse velocity 42
3.7.5 Dynamic modulus of elasticity 43
3.7.6 Shrinkage and expansion 43

lib

3.7.7 Water absorption 44

3.7.7.1 Test procedure 44

3.7.8 Oxygen permeability 44

3.7.8.1 Sample preparation 44

3.7.8.2 Test procedure 46

3.7.9 Carbonation depth 47

3.7.10 Porosity and pore structure 47

3.7.10.1 Apparatus 48

3.7.10.2 Presentation of results 48

3.7.10.3 Sample preparation 55

3.7.10.4 Test procedure 55

Chapter Four **FRESH CONCRETE PROPERTIES** **57**

4.1 Introduction 58

4.2 Aims and objectives

4.3 Consistency of cement paste 58

4.4 Setting times 58

4.4.1 Effect of mix type 59

4.4.2 Effect of environment 60

4.5 Workability 64

4.5.1 Workability loss with time: effect of binder 64

4.5.2 Workability loss with time: effect of environment 67

4.6 Conclusions 70

Chapter Five **ENGINEERING PROPERTIES** **71**

5.1 Introduction 71

5.2 Compressive strength 72

5.2.1 Early age compressive strength (less than 28 days) 72

5.2.2 Effect of curing , Indoor 80

5.2.3 Effect of mix type , Indoor 87

5.2.4 Effect of exposure environment 94

5.3 Ultrasonic pulse velocity 95

5.2.1 Early age pulse velocity 95

5.3.2 Effect of curing , Indoor 102

5.3.3 Effect of mix type , Indoor 109

5.3.4 Effect of exposure environment 114
5.4 Dynamic modulus of elasticity 115
5.4.1 Early age dynamic modulus 115
5.4.2 Effect of curing, Indoor 121
5.4.3 Effect of mix type , Indoor 128
5.4.4 Effect of exposure environment 133
5.4.5 Relationship between dynamic modulus and compressive strength 134
5.5 Shrinkage and expansion 139
5.5.1 Effect of curing , Indoor 139
5.5.2 Effect of mix type , Indoor 153
5.5.3 Effect of exposure environment 157
5.5.4 Effect of thermal expansion 157
5.6 Conclusions 170
Chapter Six **POROSITY AND PORE STRUCTURE** **172**
6.1 Introduction 172
6.2 Porosity 175
6.2.1 Effect of curing-6 months, indoor 175
6.2.2 Effect of mix type-6 months, indoor 179
6.2.3 Effect of exposure time 180
6.2.4 Effect of exposure environment 180
6.3 Pore structure 182
6.3.1 Effect of curing-6 months, indoor 182
6.3.2 Effect of mix type-6 months, indoor 201
6.3.3 Effect of exposure time 208
6.3.4 Effect of exposure environment 228
6.4 Conclusions 249
Chapter Seven **DURABILITY-RELATED PROPERTIES** **252**
7.1 Introduction 252
7.2 Aims and objectives 252
7.3 Oxygen permeability 253
7.3.1 Effect of curing, indoor 253
7.3.2 Effect of mix type, indoor 258
7.3.3 Effect of exposure environment 262

7.3.4 Effect of exposure time 270
7.3.5 Relationship between permeability and pore structure 272
7.3.6 Relationship between permeability and compressive strength 277
7.4 Carbonation depth 277
5.4.1 Effect of curing 279
5.4.2 Effect of mix type 280
5.4.3 Effect of exposure environment 283
7.5 Water absorption 286
5.5.1 Effect of curing 286
5.5.2 Effect of mix type 289
5.5.3 Effect of exposure environment 293
5.5.4 Relationship between water absorption and oxygen permeability 293
7.6 Conclusions 295
Chapter Eight **CONCLUSIONS AND RECOMMENDATIONS FOR FUTURE RESEARCH** 297
8.1 Overall conclusions 297
8.2 Limitations of present works 299
8.3 Recommendations for future works 299
REFERENCES 301

List of Figures

Figure	Title	Page
2.1	Influence of temperature on setting times of cement pastes	14
2.2	Influence of temperature on setting times of OPC and OPC/SF pastes	14
2.3	Influence of weather factors on evaporation rate	16
2.4	Workability as a function of time for OPC and OPC/SF concretes	17
2.5	Effect of temperature on slump and the water required to compensate for slump loss	19
2.6	Effect of temperature on the water required to change the slump	19
2.7	Effect of temperature on the increases of water required for concrete mix	20
2.8	Workability as a function of time for OPC and OPC/slag concretes	20
2.9	Influence of curing temperature on the strength of OPC and OPC/slag mortar	21
2.10	Influence of curing temperature on the strength of plain concrete at various ages	23
2.11	Influence of temperature during the first two hours after casting on the development of strength of concrete	23
2.12	Influence of exposure environment on the strength of mortar and concrete	24
2.13	Influence of curing temperature on the strength of concrete at 1 and 28 days	24
2.14	Influence of temperature on the permeability of cement paste	28
2.15	Effect of silica fume on the carbonation rate of concrete	32
3.1	Vicat apparatus	41
3.2	General view of the permeability cells	45
3.3	The components of oxygen permeameter	45

3.4	Schematic diagram of the permeability cell	46
3.5	Mercury porosimeter model Micromeritics pore sizer 9320	49
3.6	An example of porosimetry report	50
3.7	Parameters defining MIP pore size distribution threshold diameter and continuous pore diameter	54
4.1	Influence of cement replacement materials on consistency	59
4.2	Influence of mix type on setting times	61
4.3	Influence of environment on setting times	61
4.4	Influence of slag content on setting times	63
4.5	Relationship between the amount of superplasticizer and slag content	65
4.6	Effect of environment on workability loss with time	66
4.7	Influence of mix type on workability loss	69
5.1	Influence of mix type on compressive strength under air curing	73
5.2	Influence of mix type on compressive strength under 3d wet/air curing	74
5.3	Influence of mix type on compressive strength under 7d wet/air curing	75
5.4	Influence of mix type on compressive strength under continuous water curing	76
5.5	Influence of curing regime on compressive strength for mix A	81
5.6	Influence of curing regime on compressive strength for mix B	82
5.7	Influence of curing regime on compressive strength for mix C	83
5.8	Influence of curing regime on compressive strength for mix D	84
5.9	Influence of curing regime on compressive strength for mix E	85
5.10	Influence of mix type on compressive strength under continuous water curing	88
5.11	Influence of mix type on compressive strength under 3d wet/air curing	89
5.12	Influence of mix type on compressive strength under 7d wet/air curing	90
5.13	Influence of mix type on compressive strength under air curing	91
5.14	Influence of mix type on pulse velocity under continuous water curing	96
5.15	Influence of mix type on pulse velocity under 7d wet/air curing	98
5.16	Influence of mix type on pulse velocity under 3d wet/air curing	99
5.17	Influence of mix type on pulse velocity under air curing	100
5.18	Influence of curing regime on pulse velocity for mix A	103
5.19	Influence of curing regime on pulse velocity for mix B	104

5.20	Influence of curing regime on pulse velocity for mix C	105
5.21	Influence of curing regime on pulse velocity for mix D	106
5.22	Influence of curing regime on pulse velocity for mix E	107
5.23	Influence of mix type on pulse velocity under continuous water curing	110
5.24	Influence of mix type on pulse velocity under 3d wet/air curing	111
5.25	Influence of mix type on pulse velocity under 7d wet/air curing	112
5.26	Influence of mix type on pulse velocity under air curing	113
5.27	Influence of mix type on dynamic modulus of elasticity under continuous water curing	116
5.28	Influence of mix type on dynamic modulus of elasticity under 3d wet/air curing	117
5.29	Influence of mix type on dynamic modulus of elasticity under 7d wet/air curing	118
5.30	Influence of mix type on dynamic modulus of elasticity under air curing	119
5.31	Influence of curing regime on dynamic modulus of elasticity for mix A	122
5.32	Influence of curing regime on dynamic modulus of elasticity for mix B	123
5.33	Influence of curing regime on dynamic modulus of elasticity for mix C	124
5.34	Influence of curing regime on dynamic modulus of elasticity for mix D	125
5.35	Influence of curing regime on dynamic modulus of elasticity for mix E	126
5.36	Influence of mix type on dynamic modulus of elasticity under continuous water curing	129
5.37	Influence of mix type on dynamic modulus of elasticity under 3d wet/air curing	130
5.38	Influence of mix type on dynamic modulus of elasticity under 7d wet/air curing	131
5.39	Influence of mix type on dynamic modulus of elasticity under air curing	132
5.40	Relationship between dynamic modulus and compressive strength for all mixes under continuous water curing	135
5.41	Relationship between dynamic modulus and compressive strength for all mixes under 7d wet/air curing	136
5.42	Relationship between dynamic modulus and compressive strength for	137

	all mixes under 3d wet/air curing	
5.43	Relationship between dynamic modulus and compressive strength for all mixes under air curing	138
5.44	Influence of mix type on shrinkage and expansion under continuous water curing	140
5.45	Influence of mix type on shrinkage and expansion under 7d wet/air curing	141
5.46	Influence of mix type on shrinkage and expansion under 3d wet/air curing	142
5.47	Influence of mix type on shrinkage and expansion under air curing	143
5.48	Influence of curing regime on shrinkage and expansion for mix A	144
5.49	Influence of curing regime on shrinkage and expansion for mix B	145
5.50	Influence of curing regime on shrinkage and expansion for mix C	146
5.51	Influence of curing regime on shrinkage and expansion for mix D	147
5.52	Influence of curing regime on shrinkage and expansion for mix E	148
5.53	Influence of mix type on shrinkage and expansion under continuous water curing	149
5.54	Influence of mix type on shrinkage and expansion under 7d wet/air curing	150
5.55	Influence of mix type on shrinkage and expansion under 3d wet/air curing	151
5.56	Influence of mix type on shrinkage and expansion under air curing	152
5.57	Influence of curing regime on thermal expansion for mix A	160
5.58	Influence of curing regime on thermal expansion for mix B	161
5.59	Influence of curing regime on thermal expansion for mix C	162
5.60	Influence of curing regime on thermal expansion for mix D	163
5.61	Influence of curing regime on thermal expansion for mix E	164
5.62	Influence of mix type on thermal expansion under continuous water curing	165
5.63	Influence of mix type on thermal expansion under 7d wet/air curing	166
5.64	Influence of mix type on thermal expansion under 3d wet/air curing	167
5.65	Influence of mix type on thermal expansion under air curing	168
6.1	Influence of age and exposure environment on porosity	177

6.2	Influence of curing regime on pore size distribution for mix A	186
6.3	Differential pore size distribution for mix A	187
6.4	Influence of curing regime on pore size distribution for mix B	188
6.5	Differential pore size distribution for mix B	189
6.6	Influence of curing regime on pore size distribution for mix C	190
6.7	Differential pore size distribution for mix C	191
6.8	Influence of curing regime on pore size distribution for mix D	192
6.9	Differential pore size distribution for mix D	193
6.10	Influence of curing regime on pore size distribution for mix E	194
6.11	Differential pore size distribution for mix E	195
6.12	Influence of curing regime and mix type on total intrusion volume	196
6.13	Influence of curing regime and mix type on coarse pore volume	196
6.14	Influence of curing regime and mix type on threshold diameter	197
6.15	Influence of curing regime and mix type on continuous pore diameter	197
6.16	Influence of mix type on pore size distribution under air curing	202
6.17	Influence of mix type on pore size distribution under 3d wet/air curing	203
6.18	Influence of mix type on pore size distribution under 7d wet/air curing	204
6.19	Influence of mix type on pore size distribution under continuous water curing	205
6.20	Influence of curing regime on pore size distribution for mix A	210
6.21	Differential pore size distribution for mix A	211
6.22	Influence of curing regime on pore size distribution for mix B	212
6.23	Differential pore size distribution for mix B	213
6.24	Influence of curing regime on pore size distribution for mix C	214
6.25	Differential pore size distribution for mix C	215
6.26	Influence of curing regime on pore size distribution for mix D	216
6.27	Differential pore size distribution for mix D	217
6.28	Influence of curing regime on pore size distribution for mix E	218
6.29	Differential pore size distribution for mix E	219
6.30	Influence of mix type on pore size distribution under air curing	220
6.31	Influence of mix type on pore size distribution under 3d wet/air curing	221
6.32	Influence of mix type on pore size distribution under 7d wet/air curing	222
6.33	Influence of mix type on pore size distribution under continuous water	223

curing
6.34 Influence of specimens age and exposure environment on total intrusion volume 224
6.35 Influence of specimens age and exposure environment on coarse pores 226
6.36 Influence of specimens age and exposure environment on threshold diameter 229
6.37 Influence of specimens age and exposure environment on continuous pore diameter 231
6.38 Influence of curing regime on pore size distribution for mix A 233
6.39 Differential pore size distribution for mix A 234
6.40 Influence of curing regime on pore size distribution for mix B 235
6.41 Differential pore size distribution for mix B 236
6.42 Influence of curing regime on pore size distribution for mix C 237
6.43 Differential pore size distribution for mix C 238
6.44 Influence of curing regime on pore size distribution for mix D 239
6.45 Differential pore size distribution for mix D 240
6.46 Influence of curing regime on pore size distribution for mix E 241
6.47 Differential pore size distribution for mix E 242
6.48 Influence of mix type on pore size distribution under air curing 243
6.49 Influence of mix type on pore size distribution under 3d wet/air curing 244
6.50 Influence of mix type on pore size distribution under 7d wet/air curing 245
6.51 Influence of mix type on pore size distribution under continuous water curing 246
6.52 Influence of exposure environment and curing condition on volume of coarse pores 250
7.1 Influence of curing regime on oxygen permeability for mix A 255
7.2 Influence of curing regime on oxygen permeability for mix B 255
7.3 Influence of curing regime on oxygen permeability for mix C 256
7.4 Influence of curing regime on oxygen permeability for mix D 256
7.5 Influence of curing regime on oxygen permeability for mix E 257
7.6 Influence of mix type on oxygen permeability under air curing 259
7.7 Influence of mix type on oxygen permeability under 3d wet/air curing 259
7.8 Influence of mix type on oxygen permeability under 7d wet/air curing 260

7.9	Influence of mix type on oxygen permeability under continuous water curing	260
7.10	Influence of curing regime on oxygen permeability for mix A	263
7.11	Influence of curing regime on oxygen permeability for mix B	263
7.12	Influence of curing regime on oxygen permeability for mix C	264
7.13	Influence of curing regime on oxygen permeability for mix D	264
7.14	Influence of curing regime on oxygen permeability for mix E	265
7.15	Influence of mix type on oxygen permeability under air curing	268
7.16	Influence of mix type on oxygen permeability under 3d wet/air curing	268
7.17	Influence of mix type on oxygen permeability under 7d wet/air curing	269
7.18	Influence of mix type on oxygen permeability under continuous water curing	269
7.19	Relationship between oxygen permeability and coarse pore volume	274
7.20	Relationship between oxygen permeability and threshold diameter volume	275
7.21	Relationship between oxygen permeability and continuous pore diameter	276
7.22	Relationship between oxygen permeability and compressive strength	278
7.23	Effect of curing regime on carbonation depth of mix A	281
7.24	Effect of curing regime on carbonation depth of mix B	281
7.25	Effect of curing regime on carbonation depth of mix C	282
7.26	Effect of curing regime on carbonation depth of mix D	282
7.27	Effect of curing regime on carbonation depth of mix E	283
7.28	Effect of mix type on carbonation depth under air curing	284
7.29	Effect of mix type on carbonation depth under 3d wet/air curing	284
7.30	Effect of mix type on carbonation depth under 7d wet/air curing	285
7.31	Effect of mix type on carbonation depth under continuous wet curing	285
7.32	Effect of curing regime on water absorption for mix A	287
7.33	Effect of curing regime on water absorption for mix B	287
7.34	Effect of curing regime on water absorption for mix C	288
7.35	Effect of curing regime on water absorption for mix D	288
7.36	Effect of curing regime on water absorption for mix E	289
7.37	Effect of mix type on water absorption under air curing	291

7.38 Effect of mix type on water absorption under 3d wet/air curing 191

7.39 Effect of mix type on water absorption under 7d wet/air curing 192

7.40 Effect of mix type on water absorption under continuous water curing 292

7.41 Relationship between water absorption and oxygen permeability 294

List of Tables

Table	Title	Page
2.1	Influence of slag content on setting times	15
2.2	Influence of temperature on the modulus of elasticity	25
2.3	Development of porosity and water permeability with slag	29
3.1	Mix proportions used in the research	35
3.2	Mix proportions of cement paste	35
3.3	Chemical composition of OPC, SF, and GGBFS, percent by weight	36
3.4	Physical properties of aggregate used in the project	37
3.5	Chlorides and sulphates content in aggregate	37
3.6	Chemical tests on water	38
4.1	Initial and final setting times	60
4.2	Workability properties	64
4.3	Slump loss parameters for both laboratory and real outdoor environments	69
5.1	Compressive strength in the indoor environment	77
5.2	Compressive strength in the outdoor environment	78
5.3	Ultrasonic pulse velocity in the indoor environment	100
5.4	Ultrasonic pulse velocity in the outdoor environment	101
5.5	Dynamic modulus of elasticity in the indoor environment	120
5.6	Dynamic modulus of elasticity in the outdoor environment	121
5.7	Relationship between dynamic modulus and compressive strength	134
5.8	Shrinkage and expansion in microstrain in the indoor environment	155
5.9	Shrinkage and expansion in microstrain in the outdoor environment at 8 AM	156
5.10	Shrinkage and expansion in microstrain in the outdoor environment at 1 PM	169
6.1	Influence of curing regime on total porosity	176

6.2	Influence of curing regime on pore size distribution	183
6.3	Percentage of coarse and fine pores	184
6.4	Influence of curing regime on threshold diameter and continuous pore diameter	185
7.1	Influence of mix type on oxygen permeability	254
7.2	Relationship between oxygen permeability and pore structure	273
7.3	Relationship between oxygen permeability and compressive strength	277
7.4	Influence of curing and exposure condition on the depth of carbonation	280
7.5	Water absorption results for indoor and outdoor specimens	290
7.6	Relationship between water absorption and oxygen permeability	295

Notation

ACI	American Concrete Institute
Air curing	No water curing after demolding
Al_2O_3	Aluminum Oxide
BS	British Standard Institution
C	Carbon
CaO	Calcium Oxide
Cl	Chloride
CO_2	Carbon dioxide
d_{con}	Continuous pore diameter, μm
d_{th}	Threshold diameter, μm
E_d	Dynamic modulus of elasticity, GPa
Fe_2O_3	Ferric Oxide
f_{cu}	Compressive strength, MPa
Indoor	Laboratory environment
GGBFS	Ground granulated blast furnace slag
HRWRA	High range water reducer admixture
k	Intrinsic permeability, m^2
K_2O	Potassium Oxide
LOI	Loss on ignition
Mix A	400 OPC, kg/m^3 or Control mix
Mix B	378 OPC + 22 SF, kg/m^3
Mix C	323 OPC + 22 SF + 55 slag, kg/m^3
Mix D	323 OPC + 22 SF + 110 slag, kg/m^3
Mix E	323 OPC + 22 SF + 165 slag, kg/m^3
MgO	Magnesium Oxide
MIP	Mercury Intrusion Porosimetry

Na_2O	Sodium Oxide
OPC	Ordinary portland cement
Outdoor	Outdoor environment of Dubai
P_{cr}	Coarse pore volume, ml/g
RH	Relative humidity
SF	Silica fume
SF/slag	Mix comprise combination of OPC + SF + slag
SiO_2	Silica Oxide
SO_3	Sulphur Trioxide
SP	Superplasticizer
UAE	United Arab Emirates
UPV	Ultrasonic pulse velocity
WA	Water absorption
w/b	Water binder ratio
wet curing	Continuous water curing
wt	Weight
3d wet/air curing	3 day continuous water curing and then exposed to lab or outdoor environment
7d wet/air curing	7 day continuous water curing and then exposed to lab or outdoor environment

Chapter one

INTRODUCTION

1.1 Introduction

The hot environment of the United Arab Emirates (UAE) creates particular problems in the production of concrete for the construction industry. The high temperature of the fresh concrete results in a more rapid hydration of cement and accelerated setting time and slump loss. Further, if a high temperature is accompanied by a low relative humidity of the air, a rapid evaporation of some of the mix water takes place, causing loss of workability and plastic shrinkage cracks.

In severe environmental conditions like those prevalent in the coastal area of the Arabian Gulf countries, the predominant concrete deterioration factors such as corrosion of reinforcement, sulfate attack and thermal shrinkage cracking are accentuated by the geomorphic and climatic environmental conditions. It is the concrete-environment interaction that controls the performance of concrete in such conditions. The environment-durability-materials selection interaction, should therefore, receive considerable attention to ensure durable concrete in such environments. The selection of appropriate concrete materials that compensate for the aggressiveness of the exposure condition is, therefore, a critical factor in ensuring durability of concrete construction in severe exposure conditions.

The intense growth in construction activity during the last two decades in the Arabian Gulf region has made reinforced concrete and concrete blocks the most popular forms of construction. There has been an unprecedented demand for concrete buildings of all kinds, and the local construction industry, beset by an inadequate infrastructure and shortages of suitable materials, skilled manpower, equipment and inadequate specification and construction practices, has succeeded only in producing structures that are showing an alarming degree of deterioration within short time. The deterioration is linked to climatic/geomorphic environmental effects.

The early drying of concrete accompanied with high temperature, which usually takes place in hot environments may stop the cement hydration before the pores are blocked by hydration products, and thus a more continuous pore structures may be formed. The cover concrete is more sensitive to drying since it is more prone to lose water. The formation of continuous pore structure in cover concrete may provide and easy passage for the intrusion of aggressive agents, and therefore, the deterioration of concrete structures. Early drying can also lead to more shrinkage and cracking, and would aggravate the deterioration process of concrete.

It is well known that an elevated curing temperature will cause a high degree of hydration of cement at an early age, and therefore lead to continuous pore size distribution [1-3] of cement paste, higher permeability [1, 4-6] and lower strength [7-9] of concrete at later ages. However, not enough information is available for curing conditions occurring in large scale concrete production in the Arabian Gulf region, in which an elevated temperature could develop due to the release of the heat of cement hydration.

The use of blended cements or supplementary cementing materials such as fly ash (FA), ground granulated blast furnace slag (GGBFS) and silica fume (SF) has been reported to refine the pore structure [10-13] and increase the resistance of concrete to deterioration by aggressive chemicals such as chlorides [14]. These new composite cement materials are widely used and have improved the quality of concrete structures. Apart from improved durability properties, cement replacement materials also reduce the heat of hydration and thereby limit early age temperature rise [12]. The most widely quoted incentive for using blast-furnace slag, for example, in part substitution for portland cement, is concerned with economy of the final concrete mix, in terms of cost of constituents and/or energy [12] . In recent years blended cement concrete, because of its long term performance, has received considerable acceptance in the marine environment of the Arabian Gulf where a growing volume of investment in concrete construction is located. In addition to offshore oil industry structures, a causeway between Saudi Arabia and Bahrain has recently been constructed at a cost of $ 640 million, in which potland blast furnace cement is made up of 70-73% finely ground slag with 30-27% type I ordinary portland cement [15].

Concern related to concrete-durability problems should culminate in efforts to develop blended concrete mixes that are highly resistant to problems of deterioration in the local conditions of environment and resources. Therefore, an argument need to evaluate and develop concrete composite both in the laboratory and the field. In this research work, a new idea has been introduced using combination of OPC/SF/slag to control the durability problems in the Arabian Gulf environment.

1.2 Aims and Objectives

This study is aimed to develop and establish the properties of a high performance/high durability concrete using a combination of ordinary portland cement (OPC), silica fume (SF), ground granulated blast furnace slag (GGBFS) and exposed to an aggressive environment such as that found in the Arabian Gulf region. The properties studied include fresh concrete properties, engineering properties and durability-related properties. The concrete mixes are targeted to meet three criteria, namely, high strength, high workability and prolonged durability.

The main objectives of this project are outlined below and are discussed in greater detail in the relevant chapters. The main objectives are:

- To investigate the properties of fresh concrete to include the length of period within which the concrete can be transported, placed and finished in hot environment and to minimise the generation of heat when cast during hot summer season.
- To assess the effect of exposure environments on the engineering properties of concrete containing a combination of different mineral admixtures in terms of changes in strength and elasticity properties with time. The properties investigated include compressive strength, pulse velocity, dynamic modulus of elasticity, shrinkage and swelling. Thermal expansion was also determined.
- To evaluate the effectiveness of mineral admixture on the development of porosity and pore structure under various curing conditions in aggressive environments.
- To study the effect of exposure environments on the durability-related properties of these mixes. Water absorption and carbonation depth of the surface layer of concrete are of considerable importance, especially in relation to the thickness of the concrete cover. Also, gas permeation into concrete is not a simple function of porosity, but depends on the pore size distribution and continuous pore diameter.

While permeability of concrete is one of the most critical parameters in determining concrete durability, the effect of aggressive environmental conditions on the oxygen permeability of concrete with different mineral admixtures subjected to four curing regimes also have been evaluated.

The specific objective was to develop high durability concretes to be used in aggressive environments similar to that in the Arabian Gulf region.

1.3 Thesis layout

The thesis develops an understanding of the influence of Arabian Gulf environment, indoor and outdoor on the performance of high durability concrete. The thesis consists of eight chapters. A brief layout of the thesis is given below:

In chapter 1, the background to the project, related to deterioration of concrete construction is briefly discussed. The aims and objectives are then defined.

In chapter 2, a background of the research related to the durability and deterioration of concrete in the Arabian Gulf environment is briefly discussed. The literature related to the hot environment and mineral admixtures in concrete mixes and their effects on fresh concrete properties, engineering, durability and microstructural properties are reviewed.

Chapter 3 covers the materials used in this research; it covers the properties of ordinary portland cement, silica fume, slag, superplasticizer and fine and coarse aggregates. It also includes mixing, exposure environments, curing and details of the experimental programme carried out.

Chapter 4 reports on the fresh concrete properties such as consistency, setting times and workability as a function of time.

Chapter 5 presents the engineering properties such as compressive strength, pulse velocity, dynamic modulus of elasticity, relationship between compressive strength and dynamic modulus of elasticity, swelling, drying shrinkage, and thermal expansion.

Chapter 6 reports on porosity and pore size distribution of all concrete mixes used in this study under four curing regimes at different ages and under different exposure environments.

Chapter 7 discusses the durability related properties such as oxygen permeability, water absorption and carbonation depth.

Conclusions are shown at the end of each chapter. A summary of the limitation of the present work, overall conclusions and recommendations for future work is presented in chapter 8.

Chapter two

LITERATURE REVIEW

2.1 Introduction

The construction industry is considered to be one of the biggest industries in most developing countries. In general, a great proportion of the national income is spent on building the essential infrastructure required for social and economic development. Among the different materials available for construction, concrete materials have the best ecological profile and are widely used in every part of the word. The material is adaptable, economical, workable, durable and versatile. In the United Arab Emirates (UAE) and the Arabian Gulf region, large numbers of infrastructure projects were constructed in a short period of time. However, most of the reinforced concrete structures built in 70`s were also demolished soon after wards.

Concrete structures in the UAE deteriorate more rapidly than in most other areas of the world. The factors that have contributed to such a high rate of concrete deterioration include the aggressive environment, unsuitable specifications, unskilled labor, cement of dubious quality and poor aggregates. Another factor may be the rapid rate of construction, which is often demanded in the UAE.

As far as concrete materials and construction are concerned, UAE is characterized by an aggressive environment. The temperature often rises to above 45°C in May, June, July and August. The mean maximum temperature in summer can be as high as 45°C while the mean minimum ranges from 25°C to 30°C. The relative humidity ranges from 40 to 100% within a 24-hour period. These continuous and large daily fluctuations in both temperature and humidity initiate cycles of wetting and drying, causing subsequent adverse effects on hydration and the physical properties of concrete. Such effect often appear in the form of micro-cracking enhancing the permeability of concrete. Because of these climatic conditions the general awareness of the importance of curing in the production of durable concrete is nowadays taken into account. Concrete should be cured in hot climate in accordance to ACI Committee 305 report, and water curing, if used, should be continuous to avoid volume changes due to alternate wetting and drying

[16]. The committee states that the need for adequate continuous curing is greatest during the first few days after placement of concrete in hot climate.

Many researchers [17-19] have tried to solve the problem of concrete deterioration through many means and techniques such as using epoxy coated steel bars, galvanized reinforcement, polymer impregnated concrete, latex modified concrete, cathodic protection and the use of corrosion inhibitors. The use of mineral admixtures in concrete is now considered by major researches in many parts of the world as a simple and effective means of improving concrete durability. Using dense, high performance concrete with low permeability is one of the best means to ensure the long-term durability of concrete.

The traditional approach to overcoming the problem is to use large concrete cover with a relatively high cement content and, furthermore, to limit the crack widths thus reducing permeability; another approach is to use coated rebars. Remedial action may be needed to prolong the life of concrete before its deterioration has reached a stage where the concrete no longer serves its function. The results of many surveys into the causes of failure of concrete structures show that they are chloride contamination, sulfate attack, cover to reinforcement, water proofing, and carbonation.

In this research project, high performance, high durability concrete was studied in an attempt to see whether such material can prolong the durability of concrete structures exposed to aggressive environments. Such concretes have low water-binder ratio and incorporate chemical and mineral admixtures.

2.2 Problems of deterioration of concrete in the Arabian Gulf

The low durability of concrete structures in the Arabian Gulf is caused by corrosion of reinforcement, sulfate attack, environmental cracking, and carbonation. Condition surveys carried out on structures located along the Gulf sea-board in the Arabian Gulf, show an alarming degree of deterioration within a short span of 10 to 15 years [20-21].

The exposure conditions for concrete in the coastal areas of the Arabian Gulf constitute one of the most aggressive climatic environments in the world. In this region, interaction between concrete and environment controls material performance [20-23] and has resulted in premature deterioration and low durability of concrete structures to a level of major concern.

One aspect of the hot weather condition which has not been adequately researched, and yet may cause considerable physical disintegration and microcracking is the large fluctuation in the daily and seasonal temperature and humidity regimes. The temperature can vary by as much as 20°C during a typical summer day, and the relative humidity ranges from 40 to 100% over a period of 24 hours. Fluctuations of temperature cause cycles of expansion/contraction and hydration/dehydration resulting in microcracking and damage due to thermal incompatibility of concrete components [24, 25]. Corrosion and solubility of salts are accelerated with elevated of temperature which are a common feature in this region [26].

The failure of a structure may be caused by the environment to which the structure is exposed or by internal causes which may by physical and/or chemical attack from aggressive agents. The most important factor which leads to the deterioration of concrete is permeability, where gases and/or chlorides easily penetrate into the concrete. The performance of concrete depends not only on the exposure conditions but also on the quality of the concrete, which can vary widely; low quality concrete can be quite permeable, but good quality concrete is relatively impermeable.

All these effects interact concomitantly and cumulatively, and significantly increase concrete permeability and reduce its durability.

2.3 Protection of concrete from deterioration

Blended cements are increasingly used throughout the world due to the technical and economic benefits accrued due to their use [27]. However, in the Arabian Gulf, use of blended cements is dictated more by durability necessity, rather than by economic benefit, as these materials have to be imported and work out to be costlier than the cement. From this point of view, selection of appropriate blending is of importance. Several research studies carried out in the Arabian Gulf on the use of mineral admixtures have indicated the superior performance of these materials, particularly the two high profile supplementary cementing materials namely silica fume and GGBFS [25].

From a study of the performance of concrete and a review of the principal causes of concrete deterioration, it is clear that the permeability of concrete is the most important aspect determining its long term durability.

Al-Rabiah [28] carried out a study on the King Fahd Cause way (The cause way links the Kingdom of Saudi Arabia and Bahrain). In this project, 70-73% replacement

level of slag was used to replace OPC. After 10 years of service, he found from his investigation that the data indicated that the long term performance of GGBFS concrete had improved the properties of the concrete, and confirmed the benefits of the supplementary cementing materials in resisting the severe marine environment of the Gulf. The concrete was found to be sound, dense and showed no sign of deterioration or cracks in the super or substructure. Also, there was no indication of any attack by rock-barriers, oysters or sponges. Almost negligible carbonation of 8 mm has been observe at the cores taken from the concrete piles.

Studies carried out by Rasheeduzzafar [20] show that the main causal factors, in decreasing order of importance are corrosion of reinforcement, sulfate attack, salt weathering, and cracking caused by shrinkage, thermal, and humidity gradients. Spalling of concrete caused by rebar corrosion and cracking/degradation of concrete caused by salt attack, however, outweigh all other forms of deterioration. Both of these factors are the visible manifestations of excessive salt inclusion in concrete through the aggregates, mix water, and subsequent ingress through cracks and pores. Sulfate and chloride extensively contaminate the ground, ground water, and the moisture laden environment of the Gulf.

2.3.1 Protection by cover

The depth of cover plays an important role in the protection of reinforcement. It must provide protection against the ingress of moisture and air, and other deleterious chemicals from outside to reach the rebars as these would eventually cause corrosion of the embedded steel. The lower the cover, the more likelihood for an aggressive agent to penetrate into the concrete and thus cause initiation of corrosion .

When rust occurs, the resulting volume is larger than the iron from which it is formed, resulting in expansive forces that cause cracking and spalling of the concrete cover and, ultimately, the failure of the structure. Concrete deterioration is time-dependent, and is a result of many interactive and interdependent factors.

2.3.2 Mineral admixtures

In 1985, the publication of BS 8110 [29] confirmed the important role that had developed for the use of Ground Granulated Blast-furnace Slag (GGBFS) and Pulverized-Fuel Ash (PFA) in concrete. With the updating of existing standards and the development of new ones relating to GGBFS and PFA, composite cements and cement blends became available for wider use.

Blast-Furnace slag is produced as a by-product during the manufacture of iron in a blast-furnace. It results from the fusion of a limestone flux with ash from coke and the siliceous and aluminous residue remaining after the reduction and separation of the iron from the ore. To make GGBFS from blast furnace slag the processor has to water quench or otherwise rapidly cool the molten slag. The principle oxides in blast-furnace slag are the same as those in portland cement [30].

The slag is often produced as glassy pellets which are ground into a powder to form the basis of a cement. Ground granulated blast furnace slag is cementitious, and reacts with water, but the rate of reaction is slow and it is necessary to blend the powdered slag with portland cement to produce a cement that is of greater practical use. Numerous studies have been reported in which slag is used as partial replacement for portland cement; these studies have been summarized in several review [30-34].

A higher replacement level of slag tends to reduce strength development at early ages, but this loss can be recovered within six to twelve months depending on the GGBFS content [35]. However, using silica fume will enhance the early strength of slag concrete even with high levels of slag [36].

Silica fume (SF) which is also known as microsilica, is a by-product resulting from the reduction of quartz with coal in electric arc furnace in the manufacture of silicon metal and silicon alloys. It contains more than 75% silicon, with a mean particle size in the range of 0.1 to 0.2 μm. First experiments on the use of silica fume in concrete were carried out by the Norwegian Institute of Technology in Trondheim in 1950. The first field application of silica fume was made in the construction of Blinddtarmen Tunnel in Oslo [37].

Electric furnace of submerged-arc type in which quartz is reduced by carbon at very high temperature is used to produce silicon, ferrosilicon and other silicon alloys. The chemical reactions taking place within the furnace are known to be complex. However, one of the reactions involves the formation of SiO_2 vapor which oxidizes and condenses in the form of very tiny spheres. This material is a non-crystalline silica. The type of silica fume formed may change in its chemical properties as the raw materials change according to the desired product. For example, high-purity quartz, coal, and wood chips are charged in the oven when silicon metal is produced [37]. However, the charge also contains an iron-bearing material, when ferrosilicon alloy is manufactured. The plants containing submerged-arc furnaces vary considerably in design. However, as

far as silica fume is concerned, it is useful to distinguish between two type of furnace, those with and without heat recovery system. The exhaust gases exit at about 800°C. Most of carbon is burnt at this temperature, resulting in a light color silica fume [37]. Meanwhile, when the furnace is not equipped with heat recovery system, the gases leave the furnace at about 200°C and contain some unburned carbon. This results in a gray color silica fume. The preferred material is that produced during the production of ferrosilicon because the silica fume produced contains 90-95% SiO_2.

The use of blended cement has become an essential component of a global strategy required in the development of high durability concrete; their economic and engineering benefits have already been well established. To provide the desired corrosion protection to steel reinforcement, the concrete develops its characteristics, on the basis of its cement components. Portland cement is now more likely to be blended with mineral admixtures such as ground granulated blast-furnace slag, silica fume and fly ash, in order to enhance the basic characteristics of the resulting concrete, both in its fresh and hardened states.

2.3.3 Curing

Durability and engineering properties give an indication of the quality of concrete, and their performance is intimately associated with the curing regime. In fact curing regimes play an important role in determining the pore structure and permeability of blended cement concrete and hence affects its durability. Curing is more important in the Gulf environment with high temperatures during summer. The intense direct solar radiation on concrete surface may raise the concrete surface temperature. Low daytime humidity and frequent drying winds during summer results in extremely rapid and excessive evaporation of moisture from concrete surface. During summer, curing should commence immediately after finishing concrete to minimize drying shrinkage cracking. The method of application and duration of curing varies depending on the type of concrete and on the environmental condition. From site practice the wet hessian curing method for a minimum period of 7 days is the most popular. The CIRIA Report [38] stated that 22 % of the publications dealing with concrete curing recommended this period, and that the wet hessian curing method was the most frequently used one. The ACI committee 308 [39] recommended 7 days for type I cement.

Continual water loss from young hardened concrete could result in complete stoppage of hydration processes. According to Payne and Dransfield [40], if the relative

humidity within the pores of the concrete drops to less than 80%, then no further significant hydration will take place. Tests have shown that the relative humidity drops to less than 80% in one day in the top 6 mm under severe environmental conditions and in the top 20 mm within 7 days [40]. Powers and Neville [35,41] indicated that the hydration of cement can take place only when the vapor pressure in the capillaries is sufficiently high, about 80% of saturation pressure. Khan and Ayers [42] from their study on silica fume concrete recommend a continuous water curing of 3 days for silica fume concrete. On the other hand, Hussain et al [43] recommends a wet curing of 7 days as an absolute minimum.

The variations in the curing practice of silica fume concrete may be largely attributed to the lack of standard specifications, which are tied to insufficient background data on silica fume concrete, in general, and its curing in particular. The ACI committee 308 report [39] provides guidelines for the curing of normal portland cement concrete, but does not include concretes made with mineral admixtures such as silica fume.

With the cement replacement materials such as slag curing takes on much more important role than with portland cement due to the low hydration processes [44]. BS 8110 [29] requires longer curing periods for slag concrete than for normal concretes. Swamy [12,13] showed that slag concrete with 50% or more cement replacement need longer water curing than plain concrete. Similarly it is suggested by Hussain et al [43] that for blended cement concrete with slag, the curing period should be extended to at least 14 days.

However, it should be noted that most of the technical benefits associated with the use of mineral admixtures in concrete cannot be achieved until the pozzolanic reaction has progressed; according to this, a minimum water curing is essential. Therefore, after casting the concrete, concrete mixes containing slag or silica fume must be protected from drying especially in the hot environment. In Arabian Gulf weather, in addition to customary precautions against water evaporation, effective steps should be taken for maintaining the concrete temperature until sufficient cement hydration has occurred to ensure continual hydration and pozzolanic reaction.

2.4 Properties of blended cement concrete

2.4.1 Setting time

The term setting is used to describe the stiffening of the cement paste; i.e. The change from fluid to rigid state. In measuring setting time two terms are used:-

I- Initial setting time.

II- Final setting time.

These two terms are used to describe arbitrary chosen stages of setting. The method used to find these setting times is described in chapter 4 of this report. There are many factors affecting setting time such as cement composition, cement fineness, water-cement ratio, chemical and mineral admixture and ambient temperature.

The standard initial set of commercial portland cement is known to range from approximately 2 to 4 hours, and the final set from 5 to 8 hours [35]. In site concrete mixtures the set usually occurs later than this because of the usually higher w/c ratio. Furthermore, concrete may set earlier in hot environments due to the presence of high temperatures. This observation is illustrated by the tests of Popovics and Malhotra [45] which show that an increase in temperature from 15 to 30°C reduced the time of initial set by approximately half. Other results confirm the above finding, see Figs. 2.1 and 2.2 [46, 47].

Many published reports show that the addition of silica fume up to 10% by weight of cement in concrete mixtures (250 to 300 kg/m^3 cement content) either has no effect or alters the time of set of reference concrete only slightly [37]. For example, Malhotra et al [36,48] reported that the addition of 5 or 10% silica fume to either superplasticized or non- superplasticized concrete with w/b ratio of 0.4 did not result in any significant increase of setting time. However, when 15% SF was added with a high dosage of a superplasticizer, both the initial and final setting times were delayed by approximately 1 and 2 hours respectively. This delay was due to the relatively high dosage rates of superplasticizer needed when the amount of SF used was high.

Usually, an increase in time of setting can be expected when GGBFS is used as a replacement for part of the portland cement in concrete mixtures [49]. The initial rate of reaction between GGBFS and water, being slower than that of portland cement and water, causes an increase in setting times. Typical results on a British slag cement are shown in Table 2.1 [44]. The Table shows that both initial and final setting times were increased by more than 2 hours when slag content was increased from 0 to 70%. Also,

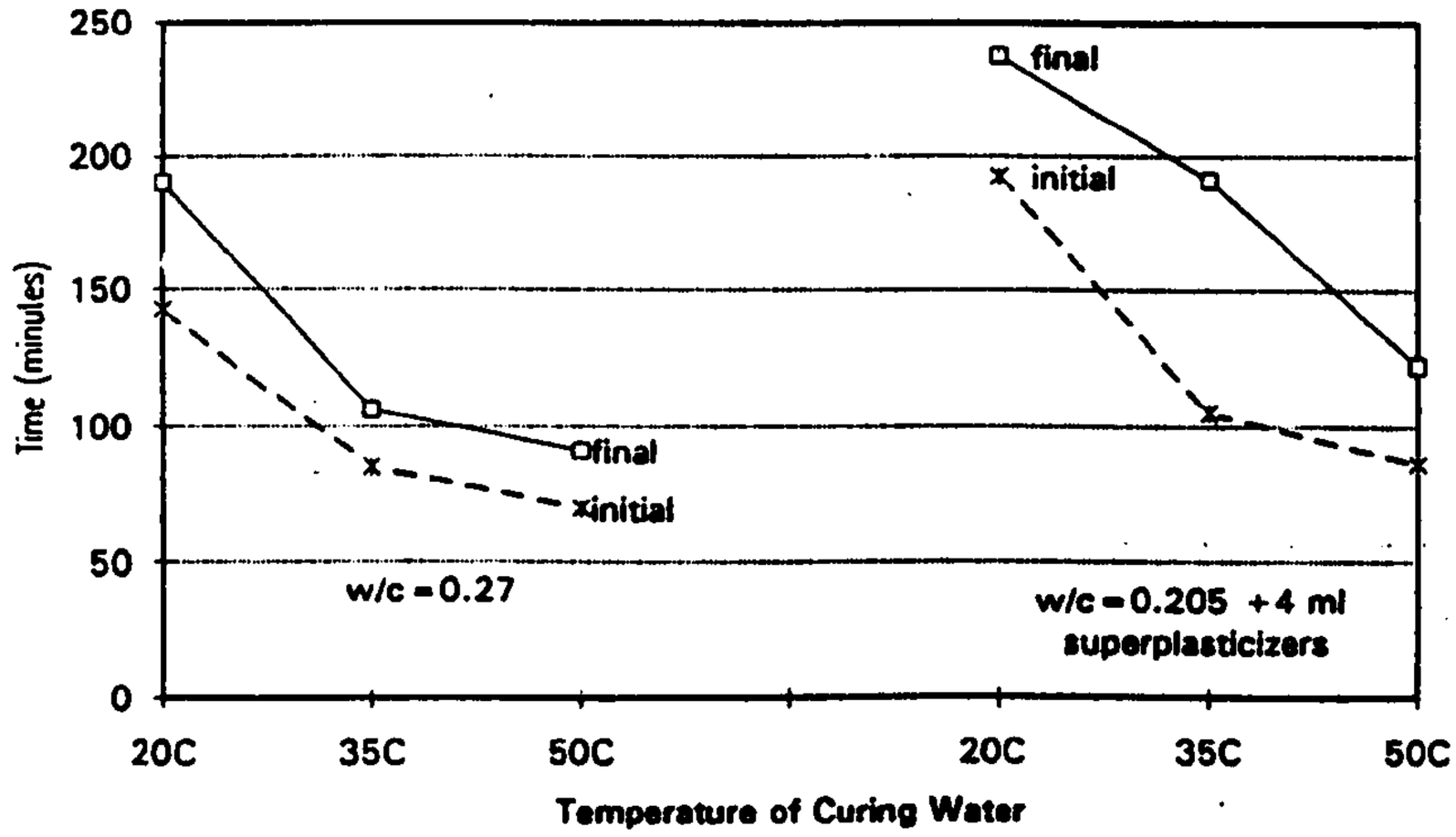

Fig. 2.1: Influence of temperature on setting time of cement pastes [46].

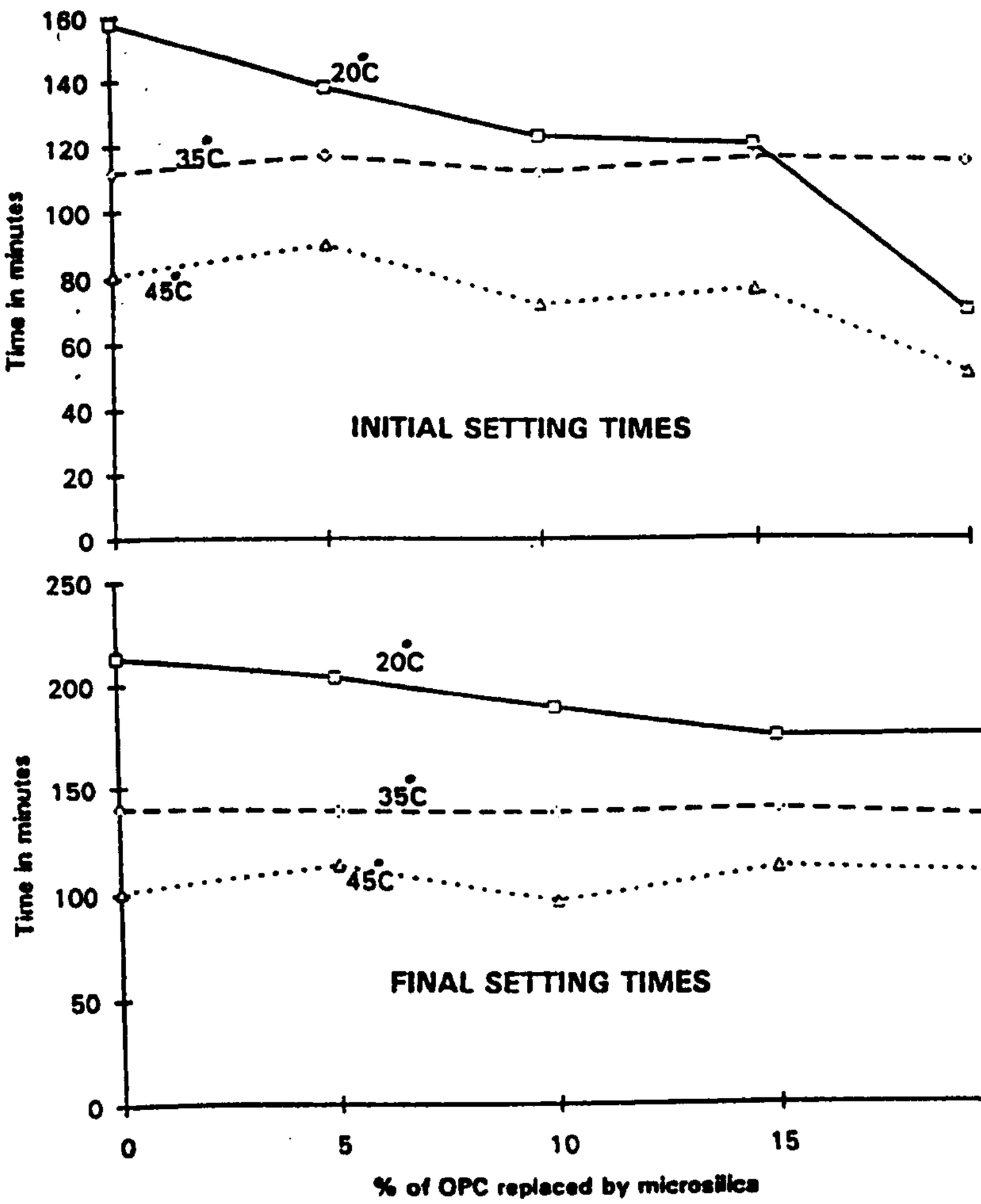

Fig. 2.2: Influence of temperature on setting time of OPC and OPC/SF pastes [47].

Dubbovoy et al [50] determined setting time for various levels of GGBFS. From their results, they concluded that the replacement level of 50% slag for cement significantly retards setting times compared to 25% or even 40% slag replacement. Initial set retardations for the 25 and 50% slag content mixtures were 32 and 86 minutes respectively. Final set retardations were 45 and 75 minutes for the 25 and 50% slag content mixtures.

Table 2.1 Influence of slag content on setting times [44].

Slag content, % of weight	Initial setting time, minutes	Final setting time, minutes
0	126	173
30	163	208
50	187	241
70	262	309

2.4.2 Workability as a function of time

Workability is affected by the properties of the mix constituents such as grading of the aggregate, cement content, maximum size of aggregates and the physical properties of the aggregates. Nonetheless the most important factor is water content.

When SF is used in concrete, water demand is expected to increase due to the very fine vitreous particles of SF which have a very high surface area compared to OPC and GGBFS. The major effect of SF on the workability of concrete is to increase the cohesiveness and reduce the bleeding. The increased cohesiveness means slump loss. The slump loss due to incorporation of SF could be compensated by the use of water reducing agents. Decreasing the friction between aggregate particles enhances the workability of concrete and this is obtained by paste content of the mixture [51].

Hot weather factors affect the workability of concrete in two ways as follows:

Temperatures accelerate setting time

High temperatures are known to accelerate the setting of cement, see Fig. 2.1 [46]. As a results of this, workability will be lost faster in hotter environment.

High evaporation rate

High temperatures, low humiditys and solar radiation accelerate the evaporation rate of water from concrete. Fig. 2.3 [52] shows the effect of weather factors on evaporation. As a results of this, workability of concrete will be lost faster in hot dry environments

than in cool moist ones, this may have serious consequences on compaction and therefore strength and durability.

In addition to the effect of hot weather factors on workability, initial concrete temperature and type of cement are two more important factors that control workability. Fig. 2.4 [47] show relationships between slump loss and time in different environments. The results shown in Fig. 2.5 [53] indicate that an increase of 11°C (20°F) in temperature reduces the slump by about 25 mm. It also illustrates that additional water

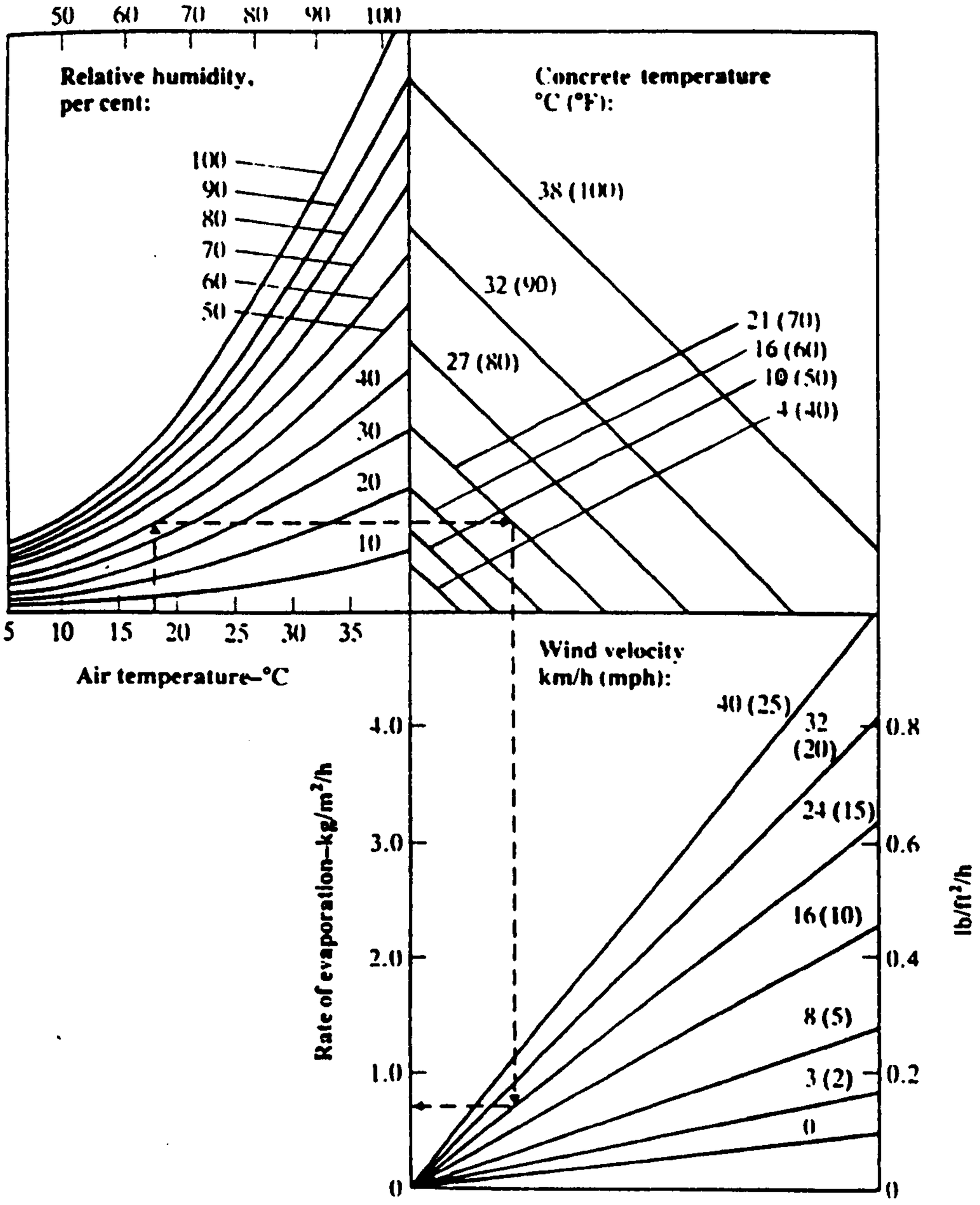

Fig. 2.3: Influence of weather factors on evaporation rate [52].

is required to compensate for slump loss at high temperatures. Furthermore, the percentage of additional water required to increase the slump by 25 mm changes with temperature. For example, 4.5 % is required at 49°C but only 2.25% and 2 .5% are required at 4°C and 27°C respectively [16,54].

Fig. 2.6 [9] confirms the above results by showing that the percentage of water required to change the slump by 25 mm increases as concrete temperature increases. Thus, more water is required in hot environments in order to maintain a constant slump. For example Fig. 2.7 [53] shows that an additional 18.2 kg of water per cubic yard is needed to maintain a slump of 3- inches (76 mm) as temperature is increased from 4°C to 38°C. This additional water content could reduce the compressive strength and durability significantly [16,54,55].

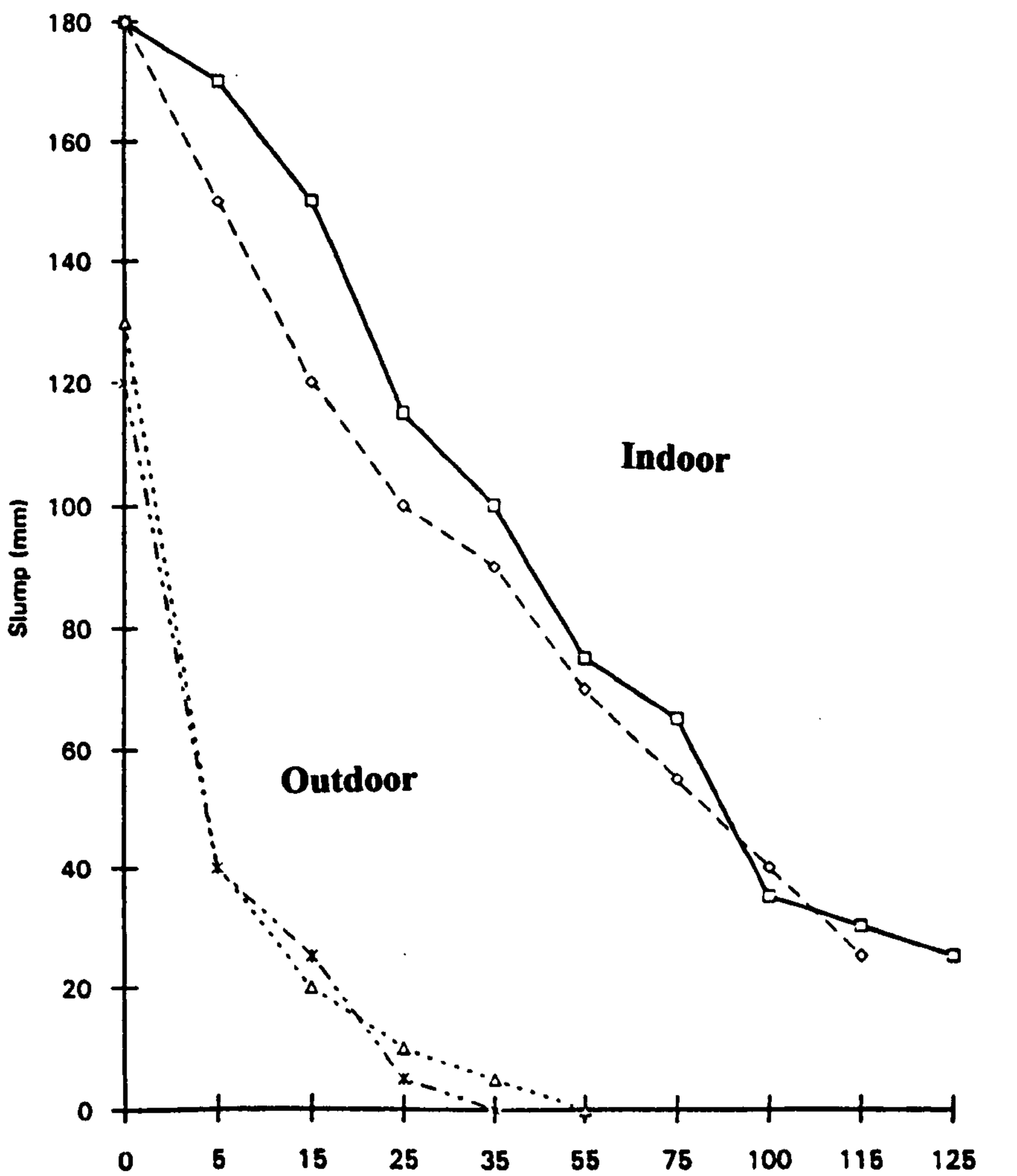

Fig. 2.4: Workability as a function of time for OPC and OPC/SF concretes [47].

It is interesting, however to see that the results produced by Shalon [56] do not confirm the above findings. He reported that no effect of temperature on slump was observed for temperatures up to 40°C and for relative humiditys between 20-70%. The slump fell rapidly only when temperature was above 50°C or relative humiditys lower than 20%. However, test data by others [53,54] show otherwise.

The addition of silica fume to concretes having cement content more than 250 kg/m^3 reduces workability [57].

The above results are confirmed by Malhotra and Carrette[48] who show that the water content to maintain a given slump of concrete varied almost linearly with the amount of silica fume added. Nonetheless, the increased water demand can be reduced or even eliminated to a level lower than the water content of the control concrete by using a superplasticizing admixture.

Little information is available regarding workability loss with time when GGBFS is used. Lea and Frigione reported that slag reduced rate of slump loss [49]. Four mixes were evaluated by Meusel and Rose [58] to study slump loss, two with a 50% blend of slag and two using plain concrete. The binder content was constant for the four mixes, and the initial slump was 150 mm. Slump tests were taken every 15 minutes until such a point that the slump fell below 50 mm, or when the lapse of time of 2 hours was reached as seen in Fig. 2.8 [58]. The slag mix and the portland cement mix were compared at two temperatures of 24°C and 27°C. From the results of the tests they concluded that no significant differences were found between the slag and plain concrete. Also they concluded that no significant effects were observed between the two temperatures, but these two temperatures are too close to give effective information on the role of temperature on workability.

2.4.3 Compressive strength

The rate development of strength and the ultimate strength are controlled by the hydration and pozzolanic reactions of cement and mineral admixtures, because strength development is related to the pore-filling process which takes place with the formation of hydration products. It is well known that early age strength of slag/OPC concrete is generally lower than the strength of OPC concrete, even though at later ages, the strength development of such concrete is equal to or higher than the plain concrete [59].

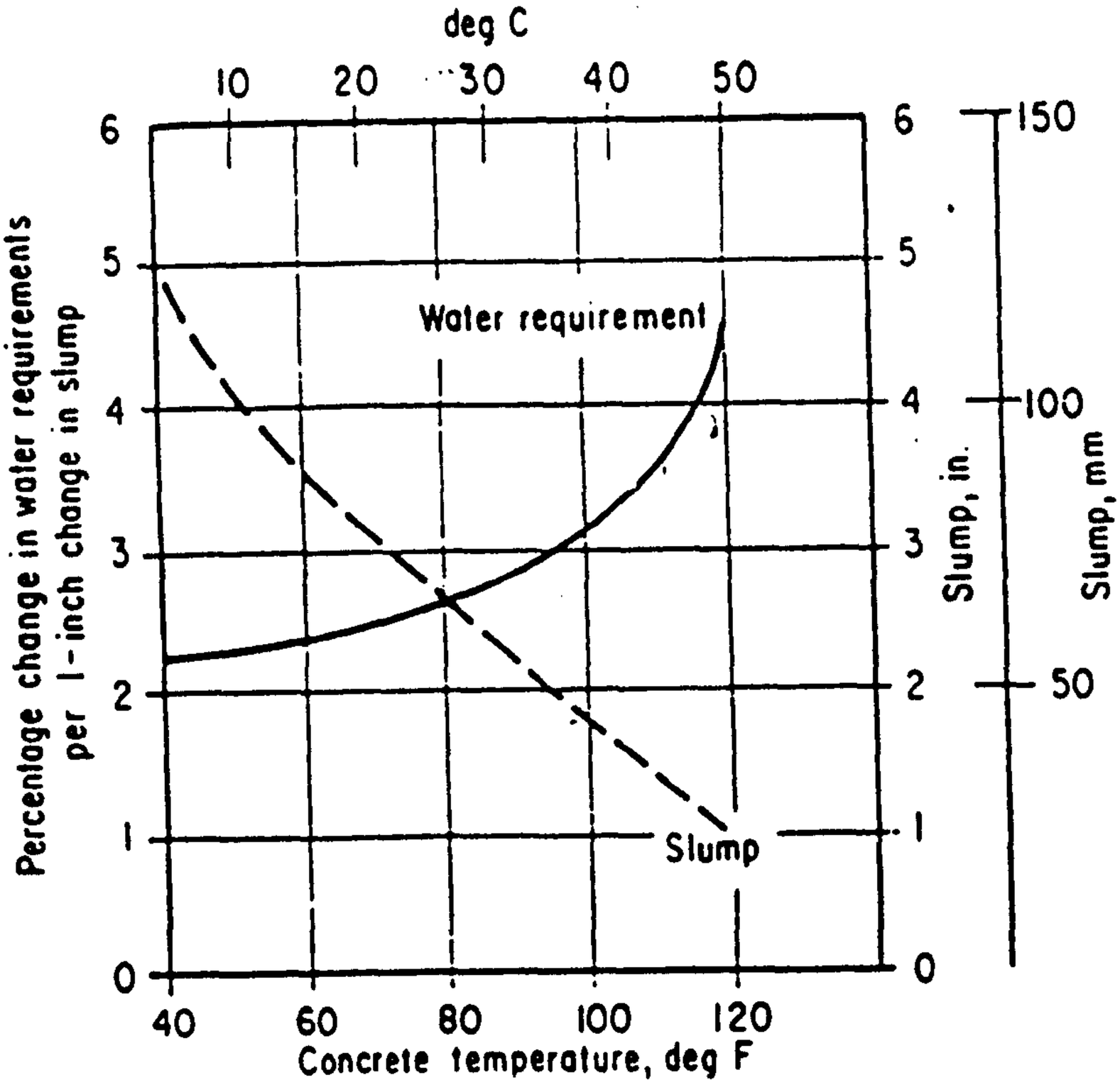

Fig. 2.5: **Effect of temperature on slump and water required to compensate for slump loss [53].**

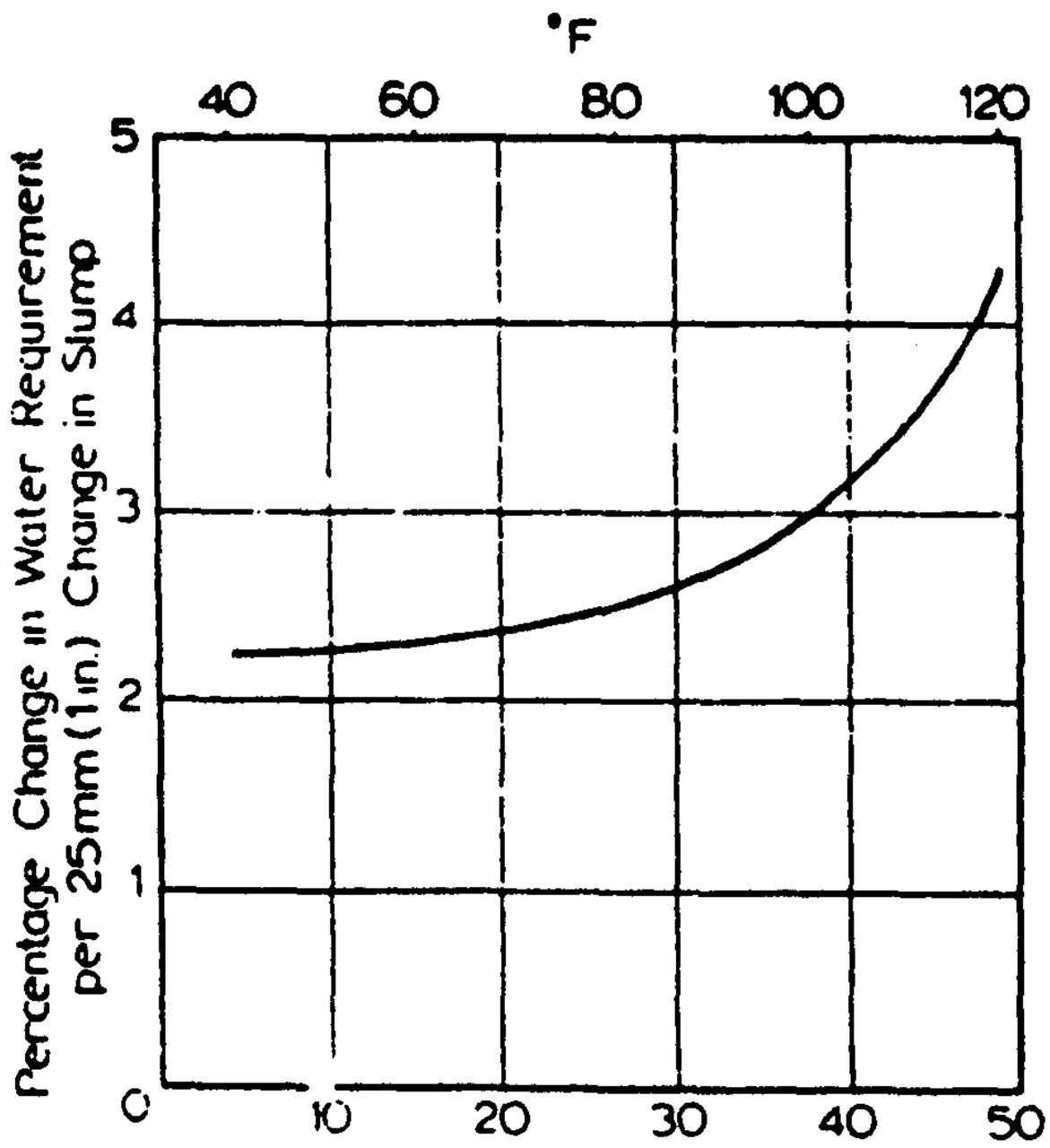

Fig. 2.6: **Effect of temperature on the water required to change the slump [9].**

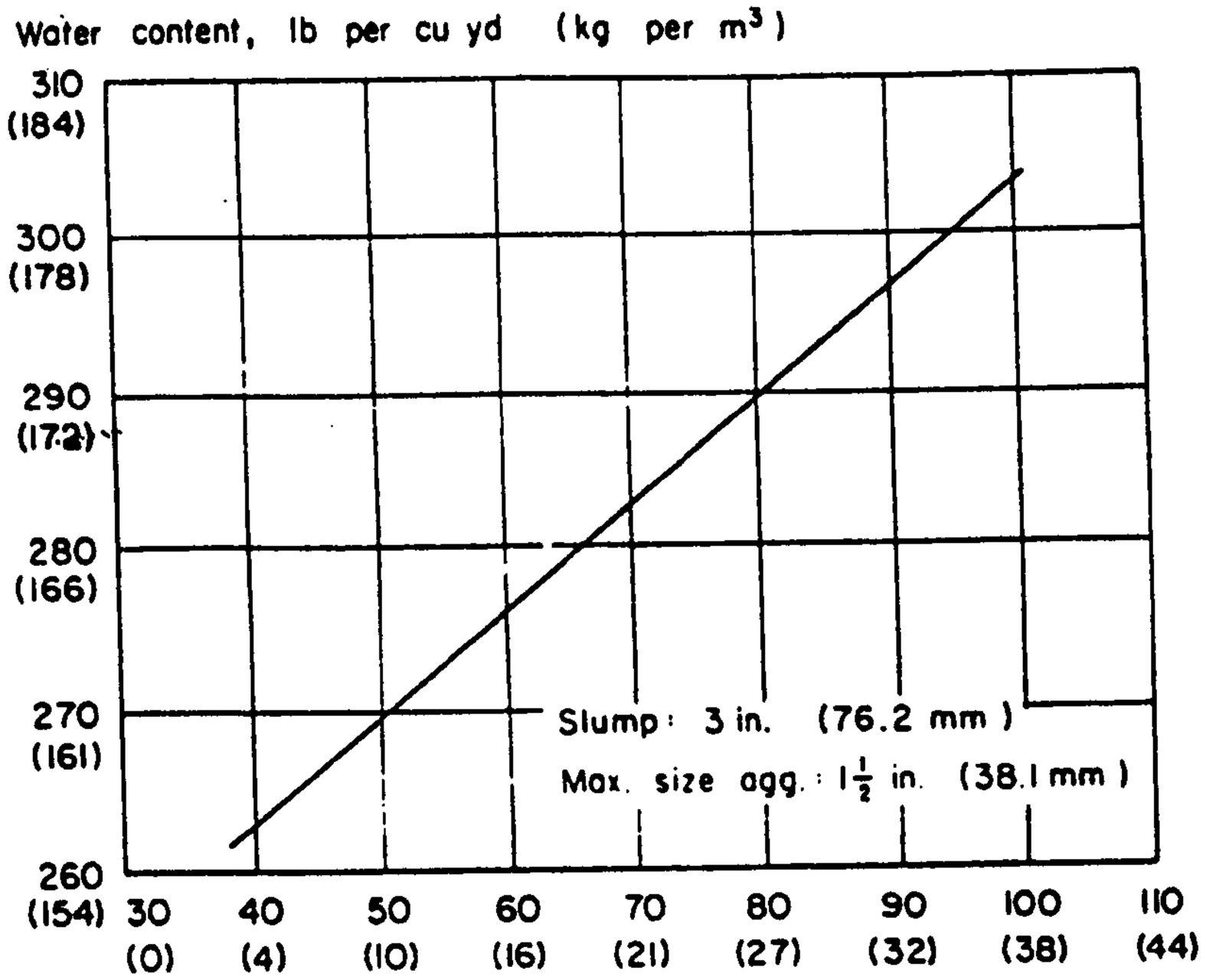

Fig. 2.7: **Effect of temperature on the increases of water required for concrete mix [53].**

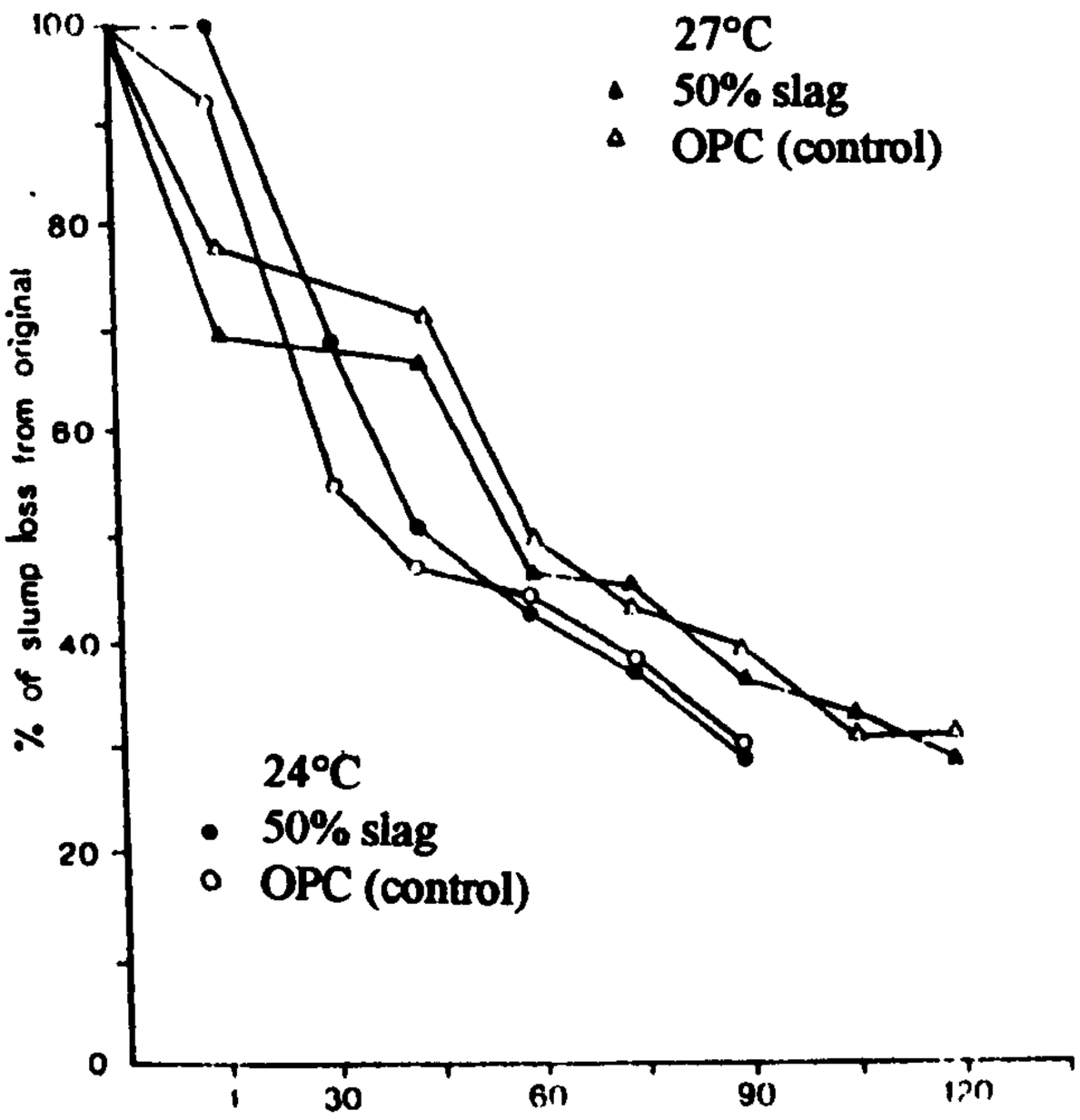

Fig. 2.8: **Workability as a function of time for OPC and OPC/slag concretes [58].**

Increased curing temperature is commonly used in concrete construction to activate the chemical reaction of cement to obtain the strength at earlier ages. Hwang and Lin [60] carried out investigations using three curing temperature (20, 50 and 80°C) to study the effect of curing temperature on the reaction of slag at ages of 1, 7 and 28 days. They found from the results shown in Fig. 2.9 [60] that specimens cured under 50°C tended to have the best results when tested at 28 days; the slag concrete exhibited better development of strength than plain concrete. The results also indicate that the strength of the specimens cured at 80°C was lower than that cured at 50°C. Similar results have also been reported by Hogan and Meusel [61] who showed that increased strengths developed by steam curing of mortar containing slag.

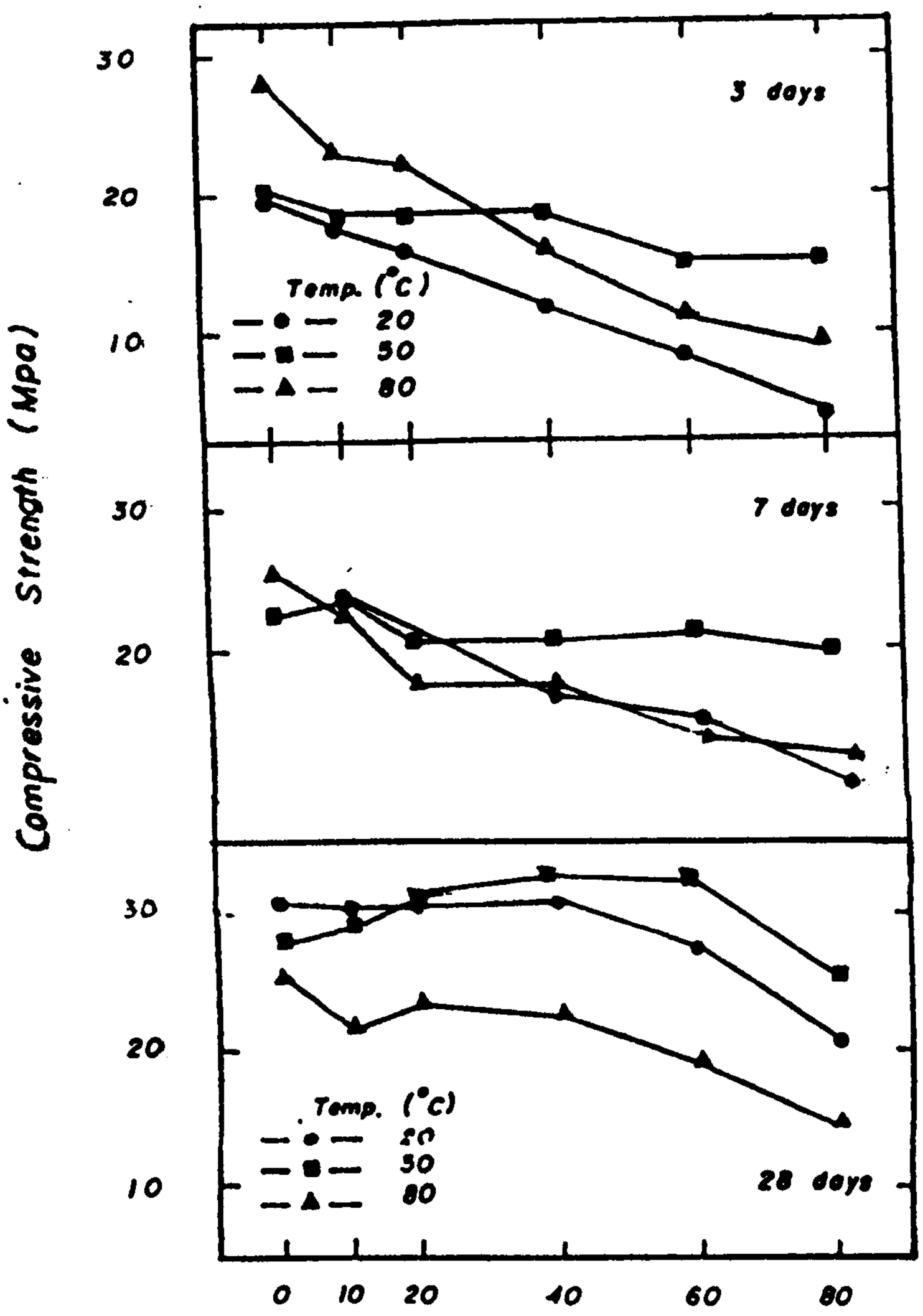

Fig. 2.9: Influence of curing temperature on the strength of OPC and OPC/slag mortar [60].

The influence of temperature during the early stages of hardening is clearly seen on the later strength. Although higher temperatures during mixing and placing increase the very early strength, it may adversely affect the strength from about 3-days onwards, as shown in Fig. 2.10 [53].

Fig. 2.11 shows strength development of concrete with effect of temperature during the first two hours after mixing with w/c ratio of 0.53 [62]. The temperature range was 4 to 46°C (0 to 115°F), and all specimens were cured at 21°C (70°F) beyond the age of two hours. It can be seen from the figure that higher the initial curing temperature, the lower the strength at later ages.

Qamaruddin et al [63] carried out investigation using two type of exposure environment, laboratory environment and outside Arabian Gulf environment. They found that, in general, the compressive strength of specimens cured inside the laboratory was higher than their respective values when the corresponding specimens were cured outside, when tested at 28 day, as shown in Fig. 2.12. Similar results have been reported by Al-Mashary [64] who also investigated the effect of hot weather on compressive strength. The study concluded that hot weather curing tends to increase the early concrete strength but decreases the 28 day strength. The reduction in the 28 day strength due to 50°C curing temperature, with other factors fixed, were found to be between 3% and 9% compared to the 21°C curing temperature.

Fig. 2.13 [35] shows that the effect of curing temperature on strength of concrete tested at 1 and 28 days. This figure illustrate that, when concrete is mixed, placed, and cured at elevated temperatures, it normally develops higher early strength than concretes cured at normal temperatures but at 28 days or later strengths are generally lower.

The results of the effect of high temperature on compressive strength of concrete are highlighted in Fig. 2.10 [53]. The temperatures of the concrete at the time of mixing, casting, and curing were 23°C, 32°C, 40°C and 45°C (73°F, 90°F, 105°F and 120°F), respectively. The specimens were moist- cured at 23°C after 28 days until the time of test. The test using identical concretes of the same w/c ratio, shows that while higher concrete temperature give higher early strength than concrete at 23°C, at later ages lower ultimate strength is recorded. If the water content had been increased to maintain the same slump (without increasing cement content), the reduction in strength would have been even greater than shown.

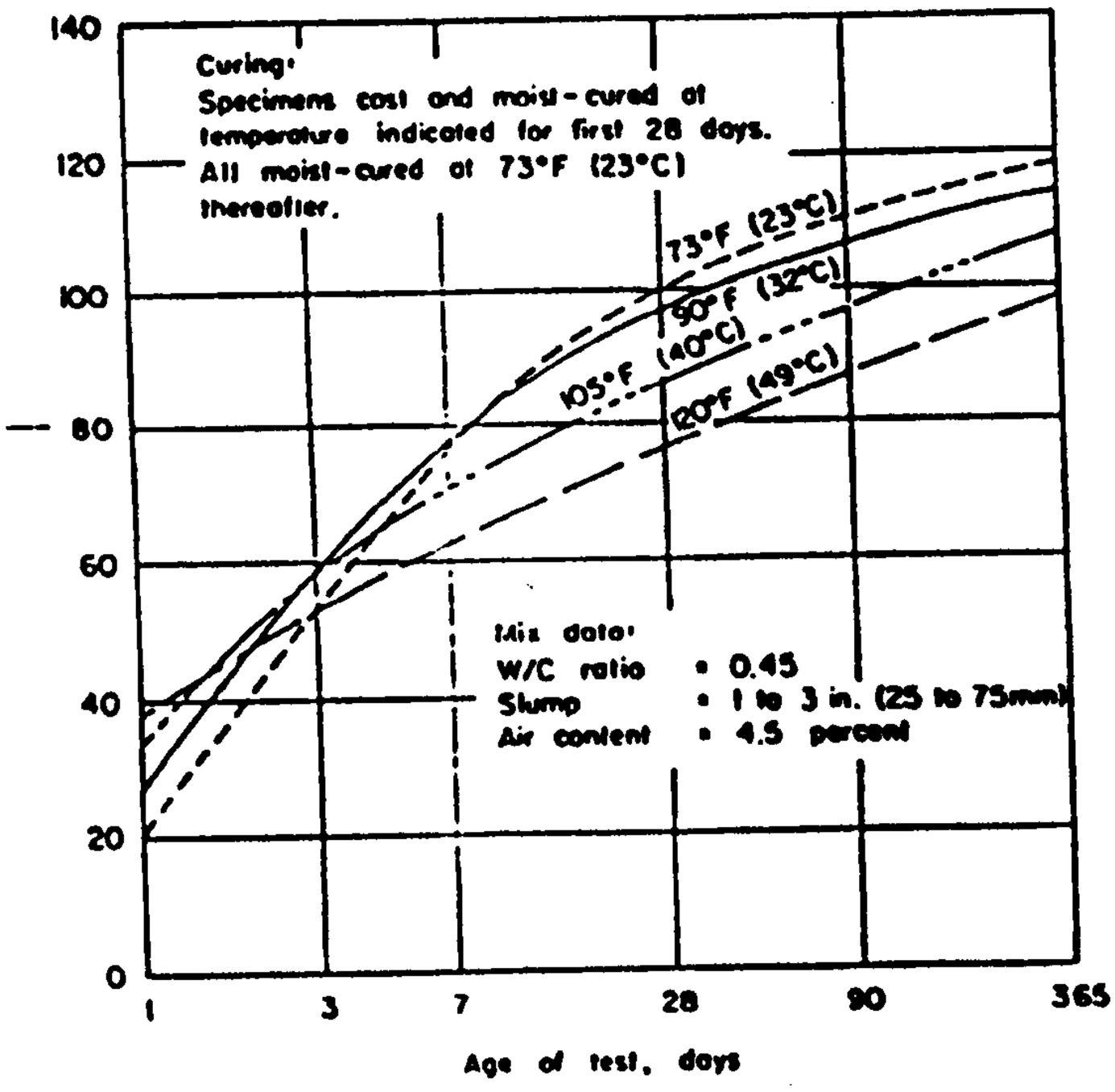

Fig. 2.10: **Influence of curing temperature on the strength of plain concrete at various ages [53].**

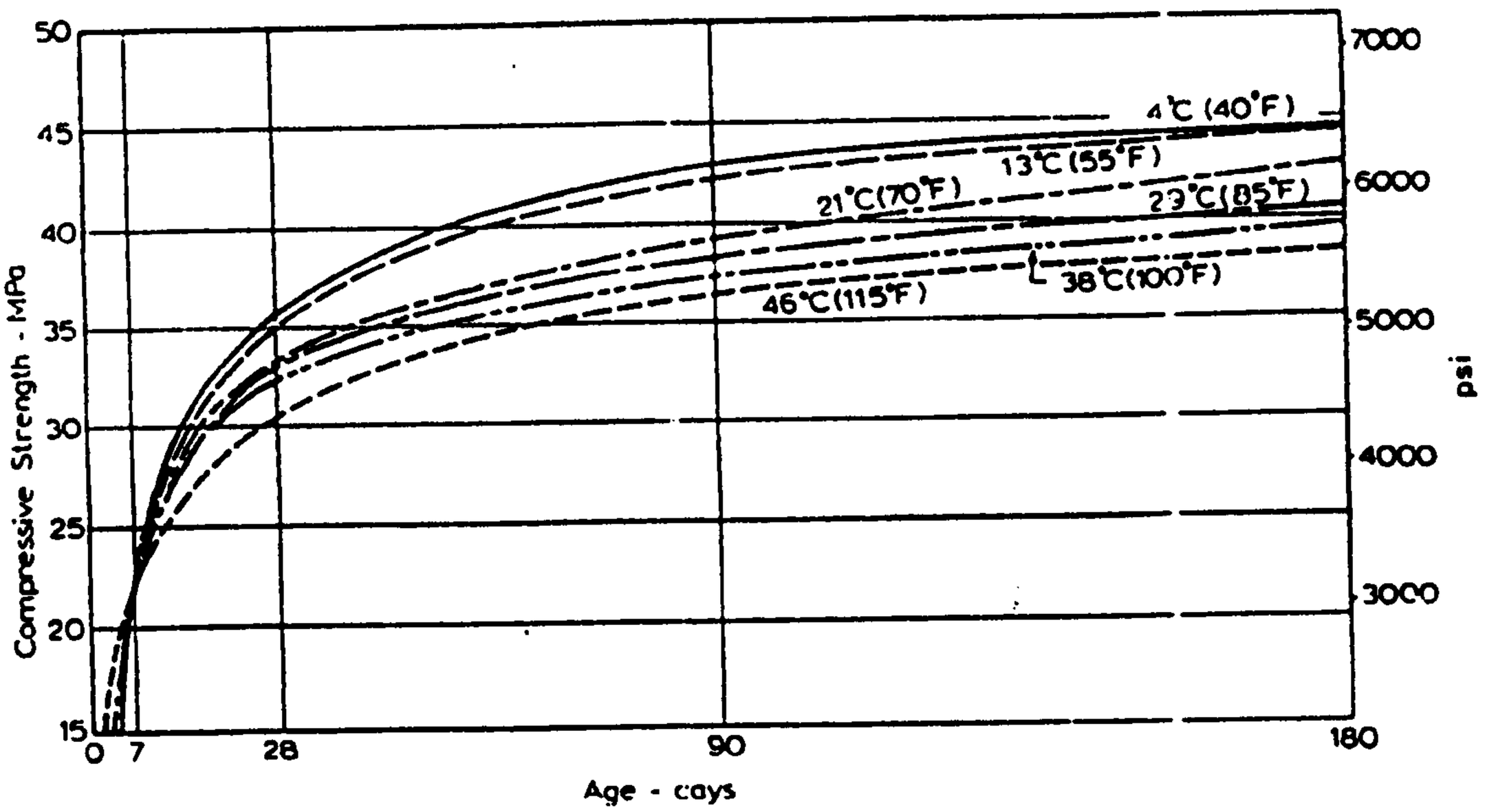

Fig. 2.11: **Influence of temperature during the first two hours after casting on the development of strength of concrete [62].**

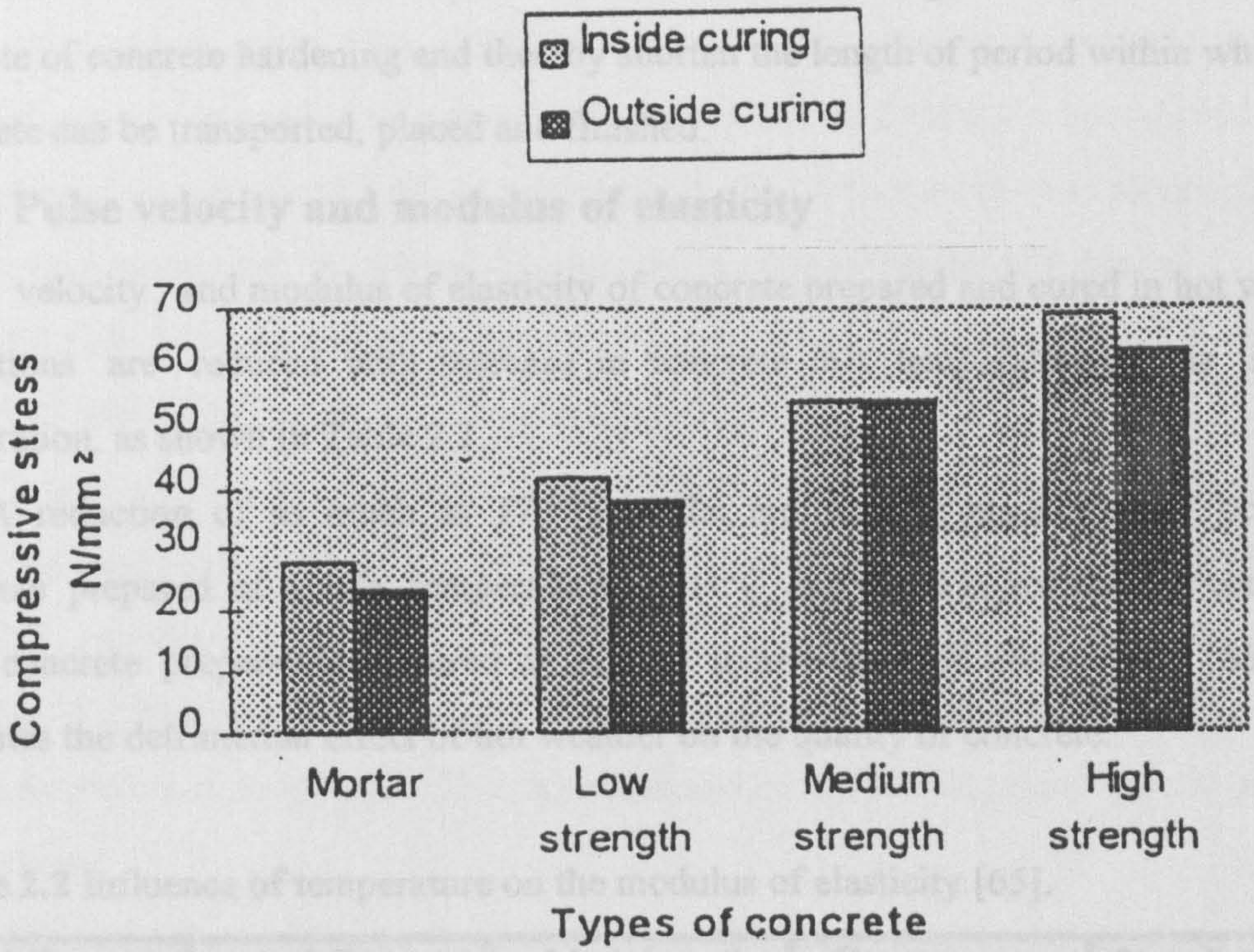

Fig. 2.12: Influence of exposure environment on the strength of mortar and concrete [63].

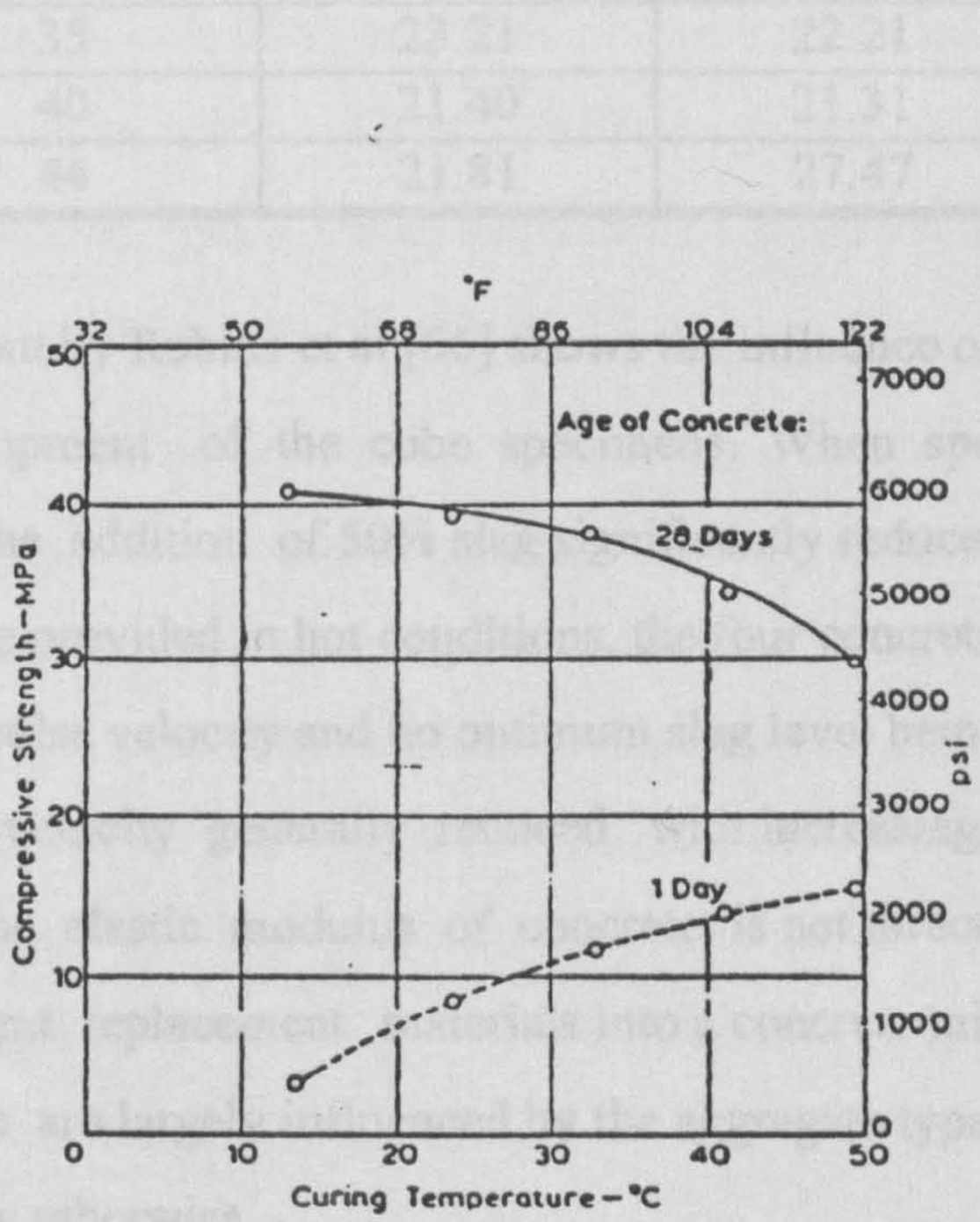

Fig. 2.13: Influence of curing temperature on the strength of concrete at 1 and 28 days [35].

Besides increasing the mixing water requirement and reducing strength, high temperatures of fresh concrete have other harmful effects. Higher temperatures increase the rate of concrete hardening and thereby shorten the length of period within which the concrete can be transported, placed and finished.

2.4.4 Pulse velocity and modulus of elasticity

Pulse velocity and modulus of elasticity of concrete prepared and cured in hot weather conditions are reduced with increase in concrete mix temperature at the time of preparation, as shown in Table 2.2.

A reduction of as much as 17.6% in the modulus of elasticity can occur for concrete prepared at a mix temperature of 44°C, and cured in hot weather compared with concrete prepared and cured at normal temperature of about 27°C [65]. This indicates the detrimental effect of hot weather on the quality of concrete.

Table 2.2 Influence of temperature on the modulus of elasticity [65].

Mix	Mix temperature °C	Modulus of elasticity, GPa	Compressive strength, MPa	% reduction in modulus of elasticity
ME-4	27	25.65	25.82	0.0
ME-2	35	23.21	22.21	3.4
ME-3	40	21.40	21.31	8.1
ME-1	44	21.81	27.47	17.6

A study carried out by Robins et al [66] shows the influence of slag content on the pulse velocity development of the cube specimens. When specimens were dried continuously in air, the addition of 50% slag significantly reduced the pulse velocity. When water curing was provided in hot conditions, the four concretes behaved similarly with little change in pulse velocity and no optimum slag level being evident. In normal conditions, the pulse velocity generally reduced with increasing slag content. Mehta [51] suggested that the elastic modulus of concrete is not directly influenced by the incorporation of cement replacement materials into a concrete mixture, and that these properties of concrete are largely influenced by the aggregate type. However, test data by others [13, 66] show otherwise.

Wainwright and Tolloczko [67] carried out a laboratory investigation into the effects of subjecting concretes to normal (20°C) and heat cyclic curing. Concretes with two cement contents of 300 and 450 kg/m^3 (Grade 25 and 45) were made with slag

replacement levels of 0, 50 and 70% by mass of total binder. For the Grade 45 concrete at the age of 1 day the modulus of elasticity of the three mixes increased due to the heat-cycled curing from 35.0, 25.5 and 18.5 GPa, for replacement levels of 0, 50 and 70% of slag, at normal temperature to 39.5, 35.5 and 26.0 GPa, for heat-cycled curing respectively. At the age of 7 days a reduction for the OPC concrete was observed due to heat curing compared to normal curing, and concretes registered values of 41.5, 45.0 and 45.5 GPa for replacement levels of 0, 50 and 70% of slag at heat cycled curing, and 43.0, 39.0 and 36.5 GPa at normal temperature respectively.

Klieger and Isberner reported [49] similar values of modulus of elasticity for concretes containing portland blast furnace slag cement compared with OPC concrete.

The modulus of elasticity of SF concrete has also been found to be similar to that of plain OPC concrete [68]. Khayat and Aitcin [69] reported that the increase in compressive strength of concrete is accompanied by a lower degree of gain in modulus of elasticity.

2.4.5 Thermal expansion

Like most engineering materials, concrete has a coefficient of thermal expansion. In addition to the composition of the mix and the type of aggregate, its value depends on the temperature change. It is to be expected, therefore, that the mineral admixture will have little influence on this property. Wainwright [44] reported investigation carried out by Bamforth who indicated that a small reduction of about 3% in thermal expansion was observed for concrete containing 75% slag.

The influence of the mix proportions on thermal expansion arises from the fact that the two main constituents of concrete, hydrated cement paste and aggregate, have different thermal coefficients of expansion, and the coefficient of concrete is a resultant of these two values. The coefficient of thermal expansion of hydrated cement paste is higher than the coefficient of the aggregate [35]. It can be added that this difference may have a deleterious effect when combined with other actions. Thermal shock which produces a temperature differences of 50°C between the surface of concrete and its core has been reported to cause cracking [70].

2.4.6 Permeability

For all concretes, it is generally recognized that the durability of concrete is related to its permeability to liquids and gases which has an important bearing upon the possible degree and rate of deterioration of the concrete and corrosion of the embedded

reinforcing steel when exposed to water carrying ions such as chlorides and sulfates. Permeability to either liquid or gases can be measured in variety of ways. These include not only the monitoring of steady flow through the specimens [71], but also by many other methods such as air permeability by the Figg method [72] and the Initial Surface Absorption Test [73] which is designed to evaluate the relative permeability of the surface only.

The use of blended cements as a portion of the cementitious material in concrete decreases permeability under adequate curing. Graf and Grube [74], have reported that with adequate curing, slag can reduce permeability compared with equivalent plain concrete. As the slag content increases, the permeability of concrete decreases [44,75]. Others [76] have found that the use of slag as a part replacement of cement results in a lower chloride permeability than the equivalent OPC concrete. The addition of silica fume to such slag concrete further reduces the chloride permeability. Dhir [30] related such observations to the continued hydration which occurs beyond 28 days which causes slag concretes to develop higher strength in the long term when water cured.

Swamy [77] carried out investigation on oxygen permeability using three types of mixes, plain OPC, OPC/slag and OPC/slag/SF. Concrete samples of 50-mm dia. x 35-mm high were used. The samples were then dried in an oven at 105°C for about 24 hours. The concretes with combination of OPC/slag /SF or OPC/slag were seen to possess reduced permeability even at 7 days, and at 28 days, the values of permeability for concretes with slag or slag/SF under continuous water curing are only about one-half of that of the control PC concretes, irrespective of the nature of curing. Obviously with continued drying, the permeability values will change, but it is unlikely that the trend will be totally reversed to make slag and slag/SF concretes worse than OPC concrete.

The permeability of slag cement has been shown to depend on curing conditions. Kasai et al [78] have studied the effects of curing periods on permeability. They found that, for curing periods of up to 7 days slag specimens were more permeable than the plain OPC specimens. The difference between the two mixes was seen to decrease with increasing curing periods. Bakker [79] on the other hand, showed that, contrary to Kasai [78], he found that for 7 days cured specimens and tested at the end of curing period, slag specimens were less permeable than the plain OPC specimens. He [79] has reasoned that, in addition to the hydrate formation around the slag and clinker particles, there are further hydrate precipitations in the 'gaps' between adjacent particles.

Heat curing of both types of concrete (plain and blended cement concrete) lead to increase permeability. Skurdal [57] measured the permeability coefficient of a plain concrete and 10% silica fume concrete (replaced by weight of cement) under three curing temperatures, 20, 30 and 50°C. Both mixes had 28 day cube strengths of about 32 MPa at 20°C curing. The permeability coefficients under normal curing were consistently lower than for the 30 and 50°C, and these values were 7.2 $x10^{-13}$, 27 $x10^{-13}$ and 90 $x10^{-13}$ m/s respectively for OPC concrete, and the corresponding values for SF concrete were 0.5 $x10^{-13}$, 0.8 $x10^{-13}$ and 74 $x10^{-13}$ m/s respectively.

Goto and Roy [1] investigated the effect of temperature on the porosity and permeability of pure cement pastes, as shown in Fig. 2.14, they found that the permeability of the samples at 60°C was greater than that at 27°C. This indicates the adverse effect of temperature on the permeability of pure cement. Bakker [79] explained such observations that the permeability is influenced by the amount of gel formed, and the locality where the gel is precipitated within the capillaries. Temperature affects both the amount of gel formed and its locality and therefore, it influences permeability. At normal temperature (20°C), the hydration of cement paste will be normal resulting in a uniform distribution of the cement gel with a more closure of capillaries and lower permeability [52]. It is therefore important to reduce the temperature of fresh concrete when concreting in hot climates.

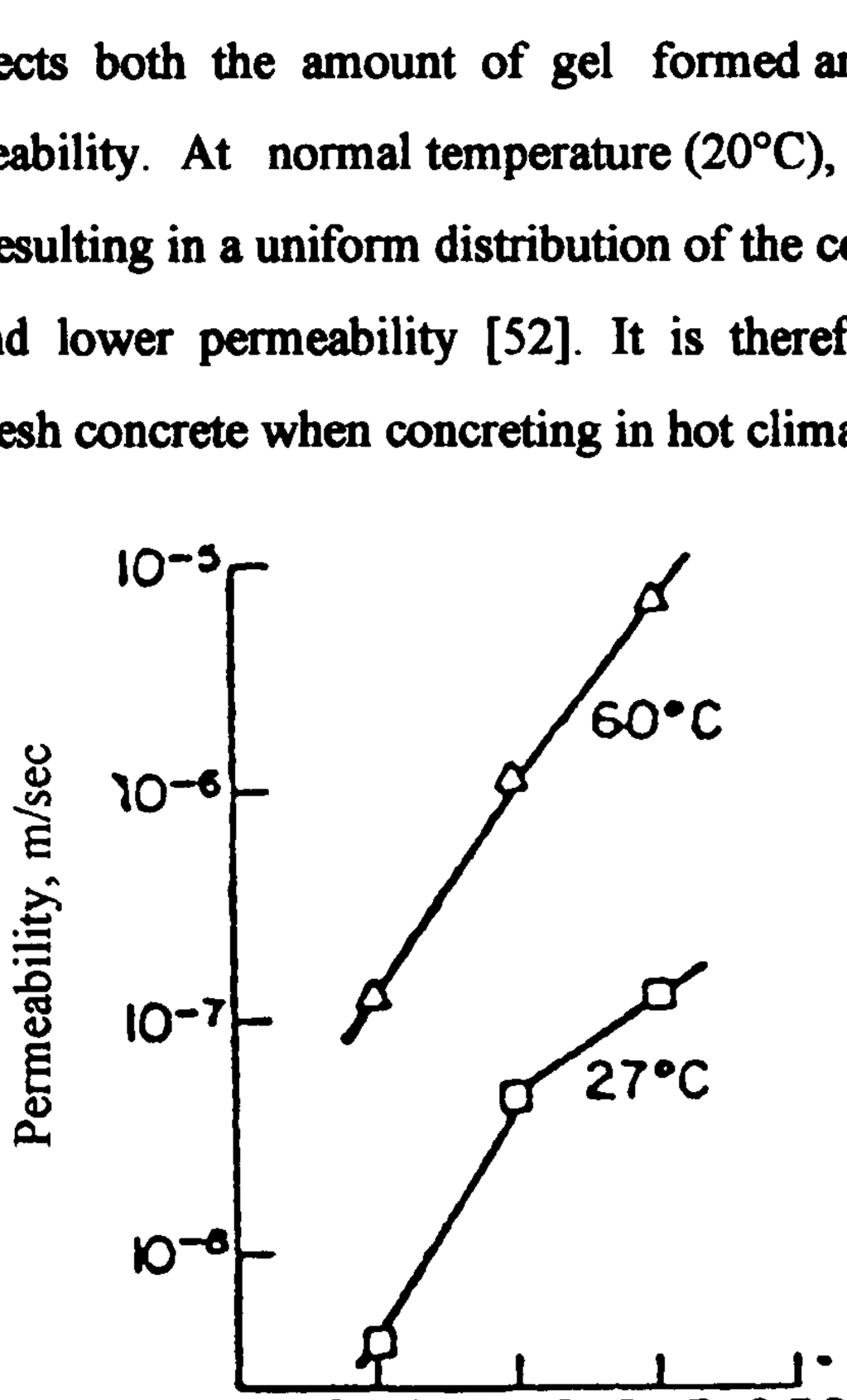

Fig. 2.14: Influence of temperature on the permeability of cement paste [1].

2.4.7 Porosity and pore structure

Porosity is a property of the volume of a given sample, and represents the content of pores which are not necessarily inter-connected and may not, therefore, allow the passage of a gas or fluid, but is significant for determining the strength and controlling the durability of concrete. It follows, also, that concrete with a high porosity need not necessarily be highly permeable, but higher porosity may entail greater permeability [1].

One of the most important properties of mineral admixtures when used as replacement for portland cement, is their ability to greatly reduce the porosity, and refine the pores. A measure of pore size distribution of these materials is more definitive and can lead to a basic understanding of many phenomena occurring within the material.

Swamy [77] has reported on the role of slag in developing a very fine pore structure, and high water tightness, and this is shown in Table 2.3. These data show dramatic improvements that slag can impart to control the total pore volume and water permeability of concrete.

Table 2.3 Development of porosity and water permeability with slag [77].

Mix	slag specific	Cylinder comp.st., MPa		Total pore volume, mm^3/g				Water permeability	
type	area m^2/kg	7 day	28 day	3 day	7 day	28 day	91 day	Depth of penetration mm	Diffusion coefficient $x10^{-2}$ mm
OPC	None	48.9	59.5	64.9	57.4	46.7	33.5	12.3	2.27
slag 1	453	27.7	58.7	60.4	55.9	30.7	13.0	8.1	0.99
slag 2	786	36.4	67.8	68.5	47.6	22.8	12.0	7.1	0.76
slag 3	1160	64.8	101.8	41.5	31.6	16.8	11.9	2.9	0.13

Mehta [80], and Manmohan and Mehta [10] have demonstrated a relationship between pore structure-permeability-durability for blended cement. The pore structure of silica fume cement pastes has been studied by Sellevold [68] using water adsorption, and mercury penetration. They concluded that increasing silica fume dosage at constant w/b ratio did not change the total porosity as measured by water adsorption, but led to a refinement of the pore structure. Sellevold has also reported a study carried out by Traetteberg who measured mercury penetration in mortars with varying silica fume

contents, and concluded that silica fume was very efficient in subdividing the pore space.

Roy and Parker [2] investigated the effect of 60% of slag on the pore size distribution. The use of plain OPC resulted in a higher threshold diameter of about 0.0125 μm whereas slag cement was significantly lower at about 0.0035 μm. Roy and Idorn [81] suggested that the pore structure of concrete containing slag is changed through the reaction of slag with calcium hydroxide, and alkalis released during portland cement hydration. Pores in concrete, normally containing calcium hydroxide, are then in part filled with calcium silicate hydrates resulting in reduction in the total pore volume and pore size [81,82].

Another explanation as to the superiority of the pore size distribution of blended cements is given by Feldman [83]. He concluded from his investigation that the nature of the pore structure appears to be related to the calcium hydroxide content. Calcium hydroxide produces an inhomogenous body with poor bonding between the major components. Therefore, slag is superior in terms of durability to the lower permeability and calcium hydroxide content.

Silica fume is not quite similar to slag. It is highly pozzolanic compared to slag. When used in cement paste, it leads to a reduction in calcium hydroxide content which is consumed by the reaction with silica fume. The decrease in calcium hydroxide content is almost linear with increasing silica fume content in mature pastes [84]. As is the case with all pozzolanic reactions, prolonged moist curing of concrete containing silica fume is necessary, specially because of its permeability contribution.

Roy and Parker [2] and Goto and Roy [1] have studied the effect of curing temperature on the pore size distribution of cement pastes. They [2] found that higher temperatures increase the number of large pores, and this effect was maximized when the curing temperature was increased from 60 to 90°C. Neville has reported that the main effect of silica fume is to reduce the permeability of the hydrated cement paste, but not necessarily its total porosity [35].

2.4.8 Carbonation depth

Carbonation occurs progressively from the outside surface of concrete exposed to CO_2, The use of ground granulated blast furnace slag in the concrete mix entails an even greater necessity for good curing. Wainwright [44] has suggested that GGBFS concrete is more affected by carbonation due to poor curing than OPC concrete but that they

perform similarly with adequate curing. In order to achieve this similarity, slag concretes will normally require a longer curing period than the portland cement concretes.

High slag contents (more than 50%) lead to a greater depth of carbonation [85,86]. Osborne [85] has reported that the use of GGBFS with poorly cured concrete exhibited very high carbonation depths of 10 to 20 mm after one years exposure. However, when the slag content in the mix is below 50%, and the concrete is exposed to CO_2 at a concentration of 0.03%, there was only a marginal increase in carbonation.

Small variations in temperature have little effect on carbonation but a high temperature increases the rate of carbonation unless drying overshadows the temperature effect. Jones [87] reported that the reason why carbonation increases as temperature decreases is not clear, since it would be normally be expected that a diffusion-based phenomenon should obey thermo-dynamic laws and gaseous flux reduces with temperature. It would, therefore, appear that carbonation in GGBFS concrete is strongly affected by other reactions, and is not a simple diffusion process [87].

Jones [87] carried out accelerated carbonation test over 20 weeks using different levels of silica fume. As shown in Fig. 2.15 the rates of carbonation of the 20 and 30% silica fume concrete are indeed very much higher than that of the control mix or even the mix with 10% silica fume.

Yamato et al also carried out an investigation; they found that the 10% silica fume concrete carbonates only marginally faster than plain concrete [87].

2.5 Summary

The use of mineral admixture such as silica fume and slag in the Arabian Gulf region needs intensive investigation. GGBFS and SF can impart significant benefits to the quality and durability of concrete. Enhancement of the quality of the internal microstructure and pore refinement are the most direct results of incorporation these materials.

It is true that the permeability and porosity of these cement replacement materials is lower than that of plain concrete, but this is only true when samples are adequately cured. The rate of water loss is greatly accelerated by the environment of the Arabian Gulf States; i.e. low humidity, high temperature and persistent winds. Preventing or reducing water loss from concrete can be achieved in many ways. Application of

additional water by ponding or wet hessian is widely used or, alternatively, the use of coatings and membranes can help in reducing water loss.

The most important parameters controlling permeability of concrete are the relative humidity and degree of curing of the concrete. Permeability increases with drying and with age for plain and blended cement concretes. Longer moist curing of concrete is thus essential to achieve the lowest permeability and to realize the full benefits of blended cement concrete.

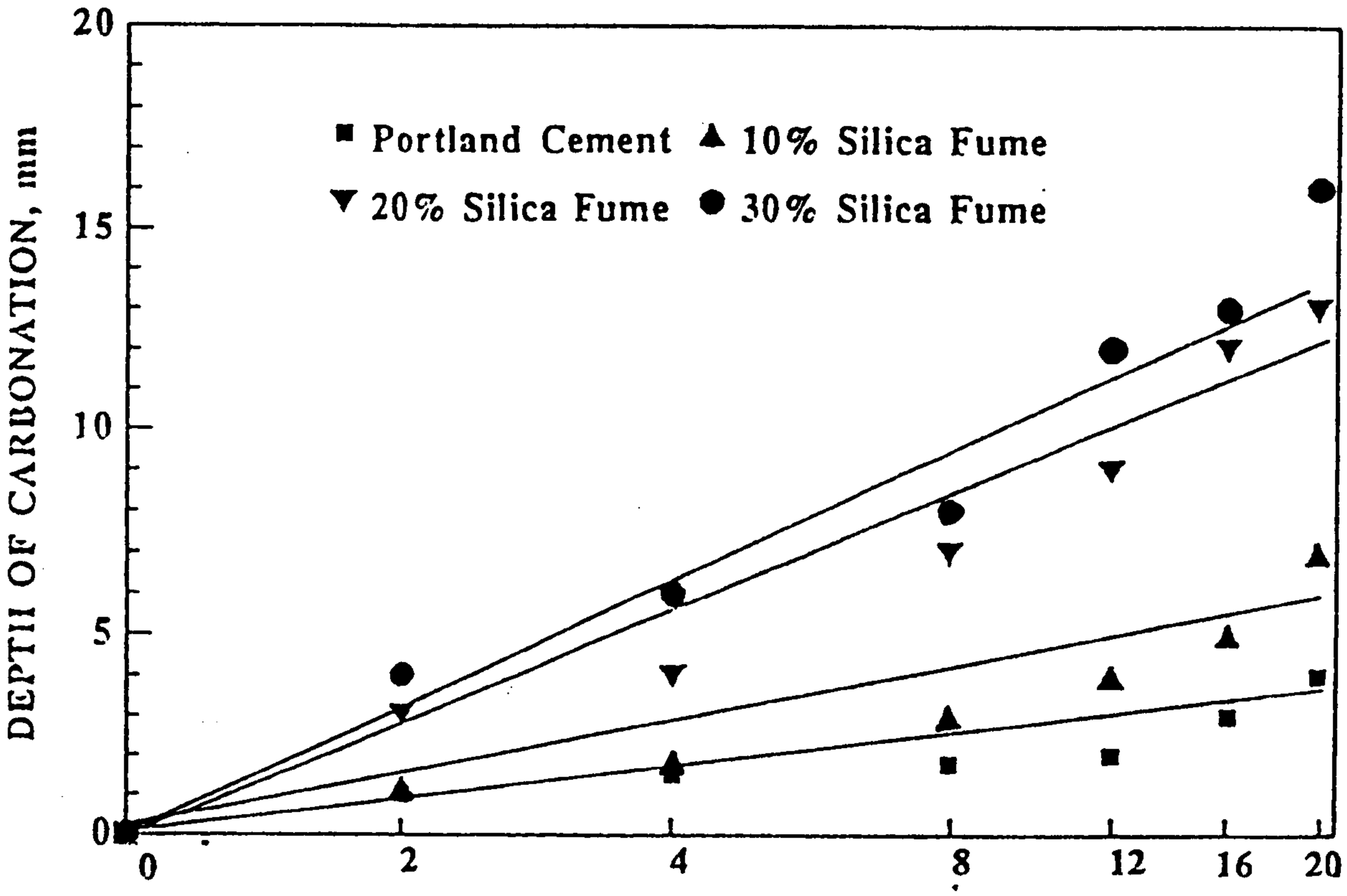

Fig. 2.15: Effect of silica fume on the carbonation depth of concrete [87].

Chapter three

EXPERIMENTAL PROGRAMME

3.1 Introduction

Blended cements incorporating mineral admixtures such as fly ash (FA), ground granulated blast-furnace slag (GGBFS) and silica fume(SF) are being increasingly used throughout the world for their technological and economic benefits. They are known to improve the durability performance of concrete in severe environmental conditions, by refining the pore structure which results in low-permeability concrete [10-13]. In the Arabian Gulf region, which is one of the world's most aggressive environments for concrete durability, the predominant concrete deterioration results from chloride ingress, sulphate attack and shrinkage cracking [88,89], all of which are closely linked to climatic environmental effects. The proper selection of concrete materials then becomes a major consideration in design and construction, in order to ensure durable concrete in aggressive exposure conditions. Therefore, the use of mineral admixtures, minimum cement contents, low water-binder ratios and good quality materials should receive special attention to ensure better durability, and long serviceability life of concrete structures. In this study, the properties of a high performance concrete, using a combination of ordinary portland cement, silica fume, and ground granulated blast-furnace slag, exposed to the real aggressive environment of the Arabian Gulf region, have been investigated.

3.2 Over all test programme

To produce a high performance concrete, a low water-binder (w/b) ratio incorporating mineral admixtures and a high range water reducer (SP) were considered essential. The criteria considered for the proportions of concrete mixes were:

1- High durability.

2- High workability.

3- High early strength and continued long-term strength development.

Five concrete mixes were designed having similar slumps in the range of 175-200 mm, using a minimum cement content, together with mineral and chemical admixtures to produce dense and low-permeability concrete. The mix proportions adopted are shown in Table 3.1.

Mix A with ordinary portland cement (OPC) alone was adopted as the control mix. The total cementitious material content was kept constant at 400 kg/m^3 for mixes A, B and C. In mixes D and E, the total cementitious content was increased to 455 and 510 kg/m^3. These mixes were adopted after a large number of trial mixtures were carried out with an initial total cementitious material content of 370 kg/m^3, and a target slump of 175-200 mm. The results showed that to obtain the required slump with a w/b = 0.35, it was necessary to increase the superplasticizer content to 20 l/m^3 (23.7 kg/m^3) for the plain cement concrete or to increase the total cementitious materials. Therefore, to minimise the amount of superplasticizer, and to get good workability, the total cementitious materials was increased by 30 kg/m^3 for all mixes with similar amount of binders, i.e. mixes A, B and C. For the last 15 years, reinforced concrete structures had been build in the United Arab Emirates (UAE) with a total cement content in the range of 300-350 kg/m^3 in order to resist the severe environment in the country. The minimum OPC content was therefore kept at 323 kg/m^3 to maintain the same percentage of the initial trials as well as to cover the minimum cement content requirement in the UAE. The amount of slag was also increased to produce high performance concrete with very low permeability. The use of slag enhances workability, and decreases the amount of superplasticizer. In mixes B to E shown in Table 3.1 the amount of SF was kept constant at 22 kg/m^3 to evaluate the effect of different levels of slag.

In addition to the concrete mixes, five cement and blended cement pastes (400 gm each) were used for tests for consistency and setting times, the details of which are shown in Table 3.2. To comply with the standards, the paste content of these mixes was fixed at 400 gm, and the mass of OPC, SF and GGBFS was reduced to represent the percentage of the total binder content in mixes D and E, to get mixes with proportions similar to that of the concrete mixes.

Table 3.1: Mix proportions used in the research.

Mix type	OPC kg/m^3	SF kg/m^3	GGBFS kg/m^3	Free w/b ratio	SP L/m^3	Coarse aggregate kg/m^3	Fine aggregate kg/m^3	Slump mm	Total binder content kg/m^3
A	400	-	-	0.35	12.5	881	1077	175-200	400
B	378	22	-	0.35	12.0	881	1077	175-200	400
C	323	22	55	0.35	9.5	881	1077	175-200	400
D	323	22	110	0.35	7.0	838	1023	175-200	455
E	323	22	165	0.35	5.0	798	976	175-200	510

Table 3.2: Mix proportions of cement paste.

Mix type	Total binder content, gm	OPC/SF/GGBFS %	OPC/SF/GGBFS gm	w/b
A	400	100/0/0	400/0/0	0.295
B	400	94.5/5.5/0	378/22/0	0.300
C	400	81/5.5/13.5	323/22/55	0.300
D	400	71/5/24	284/19/97	0.300
E	400	63/4/33	253/17/130	0.300

3.3 Materials

3.3.1 Ordinary portland cement

The cement used in this investigation was ordinary portland cement (OPC), manufactured and supplied by Ajman cement factory in the UAE. The cement complied with the requirements of BS 12 :1991 [90]. It had a fineness of about 310 m^2/kg and a specific gravity of about 3.12. Table 3.3 shows the chemical composition of the cement.

3.3.2 Silica fume (SF)

The silica fume used was in slurry form, with 50% solids and 50% water by mass; it was an Elkem product imported from Norway. It contained over 90% of SiO_2, as shown in Table 3.3.

3.3.3 Ground Granulated Blast-Furnace Slag (GGBFS)

The GGBFS was supplied by Slagment (Pty) Ltd in Johannesburg, South Africa. It had a fineness of about 380 m^2/kg, and a specific gravity of about 2.89. Table 3.3 shows its chemical composition.

3.3.4 Aggregates

Coarse aggregates

The coarse aggregates used were a fully crushed Gabbro stone with a maximum size of 10 mm. Their source location is Aldaid in the western region of the UAE. It is widely used in the UAE. It had no chlorides and sulphates, and has generally, been found to be unreactive to alkali-aggregate reactivity. The general properties of the coarse aggregate were found to conform with BS 882:1992 [91], as shown in Table 3.4.

Table 3.3: Chemical composition of OPC, SF, and GGBFS, percent by weight.

Constituent, percent	OPC	SF	GGBFS
SiO_2	21.60	90.0-96.0	32.4
Al_2O_3	5.45	0.5-3.0	16.8
Fe_2O_3	3.70	0.2-0.8	0.74
MgO	0.70	0.5-1.5	10.5
CaO	64.90	0.1-0.5	32.0
Na_2O	0.20	0.2-0.7	0.20
K_2O	0.30	0.4-1.0	1.03
SO_3	1.85	-	1.56
C	-	0.5-1.4	-
*LOI=(C+S)	1.00	0.7-2.5	-
fineness m^2/kg	310	18,000	380

* LOI - loss on ignition.

Table 3.4: Physical properties of aggregate used in the project.

Sieve size mm	Fine aggregate		Coarse aggregate		All-in aggregate	
	Cumulative % Passing	BS 882:1992	Cumulative % Passing	BS 882:1992	Cumulative % Passing	BS 882:1992
14	100	-	100	100	100	100
10	100	-	89	85-100	95	95-100
5	100	-	11	0-25	60	30-65
2.36	72	65-100	1	0-5	40	20-50
1.18	47	45-100	-	-	26	15-40
0.600	29	25-80	-	-	16	10-30
0.300	15	5-48	-	-	8	5-15
0.150	5	-	-	-	3	0-8
fineness modulus	3.32		6.01		-	
Water absorption % by dry mass	1.65		0.83		-	
Specific gravity	2.81		2.87		-	

Fine aggregates

Fine aggregates from two sources were used. The first was a dark brown sand from Aldaid, and the other was a desert dune sand; the proportions were 90% of dark sand to 10% of dune sand. The sands also contained no chlorides and sulphates, and they were unreactive so far as alkali-aggregate reactivity was concerned. The sands complied with zone M for sand grading (Table 3.4). The general properties of blended sand were found to conform with BS 882:1992 [91]. Table 3.5 shows the chloride and sulphate content in the aggregates.

Table 3.5: Chlorides and sulphates content in aggregate.

Aggregate type	Fine aggregate		Coarse aggregate	
Test	Results (PPM)	MPWH *	Results (PPM)	MPWH *
Chlorides	0.009	0.06	0.005	0.02
Sulphates	0.067	0.30	0.084	0.30

*MPWH= Ministry of public works and housing specification.

3.3.5 Water

Drinkable water of the City of Dubai was used for mixing and curing the specimens. It had no chlorides and sulphates and conformed to BS 3148:1980 [92], as shown in Table 3.6.

3.3.6 Chemical admixture

A high range water reducing admixture was used in this investigation, namely, Conplast SP 430 (SP). It is a high performance superplasticizer admixture, which complies with BS 5075: 1982 [93] . Conplast SP 430 is generally used to significantly improve the workability of concrete, without increasing water demand. This admixture provides excellent acceleration of strength gain at early ages, by permitting a reduction in w/c in a concrete mix, and it also improves the long-term durability by reducing concrete permeability. It is chloride-free, and is based on selected sulphonated naphthalene polymers, suitable for use with all types of portland cement and cement replacement materials such as FA, GGBFS and SF [94].

Table 3.6: Chemical tests on water.

Test	Results (PPM)	Max. allowed [92] (PPM)
Chlorides	160	500
Sulphates	36	1000
Total dissolved solids	220	2000
PH-Value	7.73	-

3.4 Mixing

The concrete materials were mixed in a pan mixer with 56 litre capacity. The coarse aggregates were loaded first, followed by the fine aggregates. Then the mixer was started, and run for 30 seconds. Half the amount of water was then added and mixed for approximately 30 seconds. Cement, slag and silica fume were then added slowly during further mixing to ensure uniform mixing. Finally, the remaining mixing water including the superplasticizer was added, and the mixing continued until full dispersion of the superplasticizer and SF was achieved. Adjustment was made for the water in the SF

slurry as well as in the aggregates. The concrete mixtures were cast in steel moulds in three layers and compacted using a vibrating table.

3.5 Exposure environments

Two environments were used to simulate indoor and outdoor environments in the UAE They were as follows:-

3.5.1 Laboratory environment

The concrete laboratory of the Building materials laboratory of the Ministry of Public Works and Housing was used for the laboratory environment studies. The temperature and the relative humidity in this laboratory was usually about 23±2°C and 70±10%RH respectively.

3.5.2 Outdoor environment in Dubai

In addition to the laboratory environment, samples were also kept in the real outdoor environment of Dubai. The daily mean maximum temperature in this condition in the summer is usually about 45°C, with accompanying relative humidity of about 30%RH. The daily mean minimum night temperature is in the range of 30°C, with a relative humidity of about 95%RH. In winter, the daily mean maximum temperature and relative humidity are usually about 24°C and 95%RH respectively, with the daily mean minimum temperature and relative humidity of about 18°C and 30%RH [95]. These were recorded regularly in both environments; for the shrinkage and expansion tests in this environment, the temperature and RH were recorded at early morning and mid day during the testing.

3.6 Curing

Four curing regimes were used for both normal laboratory environment and outdoor environment. After casting, all the samples were immediately covered by a polythene sheet, with the exception of air-cured samples which were left uncovered. After 24-hours, the samples were demoulded and placed in their respective environment until the day of the test. The curing regimes used are as follows:

3.6.1 Air curing regime

The samples, after demoulding, were cured in air until the day of testing.

3.6.2 3-day curing regime

Samples, after demoulding, were cured in a water tank in the exposure environment for a period of 2-days, after which they were removed from the water tank and placed in air in the same environment until the day of testing.

3.6.3 7-day curing regime

Samples, after demoulding, were cured in a water tank in the exposure environment for a period of 6-days, after which they were removed from the water tank and placed in air at the same environment until the day of testing.

3.6.4 Continuous water curing regime

Samples, after demoulding, were immersed in a water tank in the exposure environment until the day of testing.

3.7 Test Programme

The following tests were carried out to assess the different properties of the concrete and paste mixes under consideration:

3.7.1 Consistency and setting time

For the determination of the initial and final setting times, a neat cement paste of a standard consistency had to be used. It was, therefore, necessary to determine for any given mix the water content of the paste which will produce the desired consistency.

The aim of the consistency test was to determine the water-binder (w/b) ratio for cement paste with a given consistency. The purpose of the setting time test was to find the initial and final setting times. The Vicat apparatus was used to measure consistency and setting time, in accordance with the British standard test BS 4550:1978 [96].

3.7.1.1 Apparatus

The Vicat apparatus is shown in Fig. 3.1. It is consists of a plunger which measures the depth of penetration (consistency) of a 10 mm diameter plunger under its own weight. Initial and final set needles were used to determine the initial and final setting times.

3.7.1.2 Consistency test procedure

The cement sample of 400 gm in weight, and the measured quantity of water were prepared. A trial paste of cement and water was mixed, and placed in the mould within a time limit of 4 minutes ±15 seconds. Using the 10 mm diameter plunger shown in Fig. 3.1 fitted into the needle holder, the mould was placed on the base of the Vicat apparatus. The plunger was then brought into contact with the top surface of the paste, and released under the action of its weight. The plunger penetrated the paste to a point 5 ±1 mm from the bottom of the mould. The water content of the standard paste was then expressed as a percentage by weight of dry cement, the usual range of values being between 26 and 33 percent.

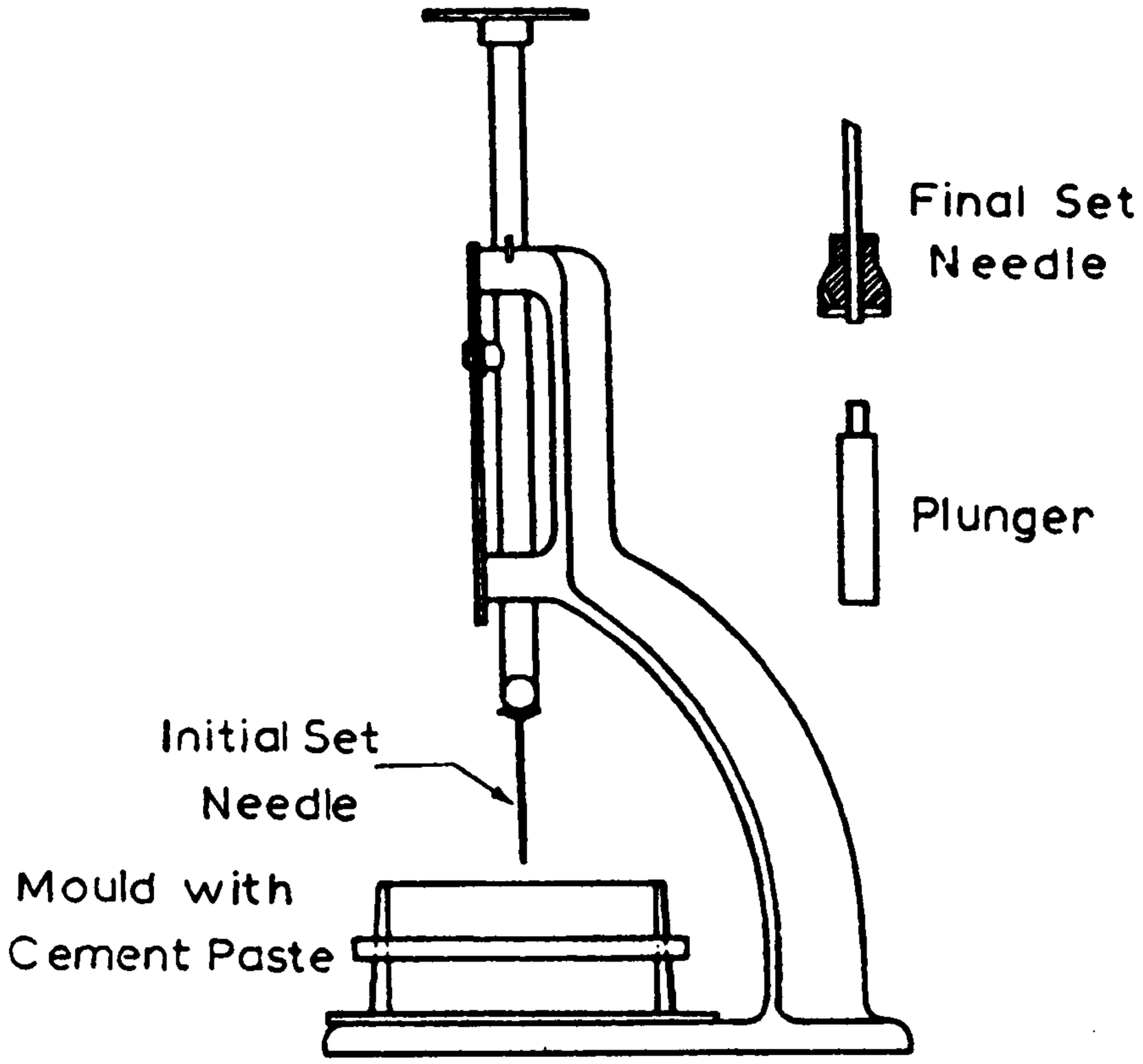

Fig. 3.1: Vicat apparatus [35].

3.7.1.3 Setting time test procedure

After finding the water content required for the standard consistency, rod B (1.13 mm diameter needle) was used to determine the initial setting time. This needle, acting under a prescribed weight, is used to penetrate a paste of the standard consistency placed in the special conical mould. Initial set is said to have taken place when the paste

stiffens, and the needle penetrates only to a point 5 ±1 mm from the bottom. A minimum time of 45 minutes is given by BS 4027:1980 [97] for OPC.

Final set time is then measured by the final set needle. This needle includes a hollow metal attachment so as to leave a circular cutting edge 5 mm in diameter. Final set is said to have taken place when the needle, gently lowered to the surface of the paste, makes an impression on it but the circular cutting edge fails to do so. British standard BS 4027:1980 [97] prescribes the final setting time as a maximum of 10 hours for OPC.

3.7.2 Workability as a function of time

The workability as a function of time of concrete was measured using the standard slump test BS 1881:1983 [98]. Slump measurement is not considered to be the ideal test for measuring the workability of concrete. It was, however, adopted for use in this study, since this test is widely used and easy to perform. The tests were performed on the five mixes shown in Table 3.1. All mixes were made to nominally the same slump of about 175-200 mm when tested in the laboratory environment.

3.7.3 Compressive strength

The test for compressive strength was carried out in accordance with BS1881:1983 [99], using 100 mm concrete cubes. The results recorded are the average of two samples.

3.7.4 Ultrasonic pulse velocity

The ultrasonic pulse velocity (UPV) test was carried out in accordance with BS 1881:1986 [100] on 100x100x500 mm concrete prisms. The measurement of UPV is usually used to determine:

1- The homogeneity of the concrete.

2- Changes of concrete state due to hydration of cement and aggressive environment.

3- The presence of cracks, voids and imperfections.

The results recorded are the average of two samples.

The following equation was used to calculate USPV [100]:

$$V = L/N \tag{3.2}$$

where:

V = Ultrasonic pulse velocity, km/s.

L= Length of the specimen, km.

N = Transit time, second.

3.7.5 Dynamic modulus of elasticity

The dynamic modulus of elasticity (E_d) test was carried out in accordance with BS 1881:1990 [101], using 100x100x500 mm concrete prisms. The test measures the fundamental resonant frequency of the test specimen. The E_d value is calculated from the fundamental resonant frequency. The following equation was used to calculate E_d [101].

$$E_d = 4\,F^2 L^2 \rho \times 10^{-15} \tag{3.1}$$

where:

E_d = The Dynamic modulus of elasticity, GPa.

F = Frequency of fundamental mode of longitudinal vibration, Hz.

L = Length of the specimen, mm.

ρ = The density of concrete, kg/m^3.

3.7.6 Shrinkage and expansion (strain)

The tests for shrinkage and expansion were carried out using a 200 mm mechanical Demec strain gauge in accordance with BS 1881:1986 [102], using 100x100x500 mm concrete prisms. The results recorded are the average of two samples.

The result for each sample was recorded as the average of 4 readings taken on the four sides of the prism.

3.7.7 Water absorption

The test for water absorption was carried out in accordance with BS 1881:1983 [103], using 100 mm concrete cubes. The results recorded are the average of two samples.

3.7.7.1 Test procedure

The specimens were placed in a drying oven in which the temperature was controlled at 105°C for 72 ± 2 hours. The specimens were then removed from the oven and placed in dry air-tight vessels for 24 hours ± 30 minutes. After that the specimens were weighed and immediately completely immersed in water at a temperature of approximately 20°C and left immersed at a depth of about 25 ±5 mm of water over the top surface of the specimens for 30 minutes ±30 seconds. The water absorption was then calculated as the mass of water absorbed expressed as a percentage of the dry mass of the specimen.

3.7.8 Oxygen permeability

Permeability is a property which determines the ease with which gases, liquids and dissolved ions such as chloride or sulphate ions or carbon dioxide, can permeate through concrete. The oxygen permeability was determined by a gas permeameter which was developed by Cabrera and Lynsdale [71]. It is an easy, simple and relatively accurate test. Fig. 3.2 shows a general view of four of the cells, Fig. 3.3 shows in detail the component of the cell and Fig. 3.4 shows schematic diagram of the permeability cell [71]. The permeability cell consists of oxygen supply cylinder, accurate pressure gauge, bubble flowmeter and specimen holder.

3.7.8.1 Sample preparation

The test for oxygen permeability was carried out using concrete cores, 50.8 mm (2 inch) in diameter and about 35 mm thickness, cored from 100x100x100 mm concrete cubes. The cores were taken from side face at right angles to the trawled face (the top face in the exposure environment was the trawled face); each core was then sliced using a diamond saw into two specimens after rejecting the top and bottom 10-15 mm from the end faces to avoid variations in the results. The results recorded are the average of two specimens. The samples were removed from their respective curing environment at the age of the test, cored and placed in an Ethanol solution to stop the hydration until the test was carried out at Sheffield university. Before testing, the samples were placed

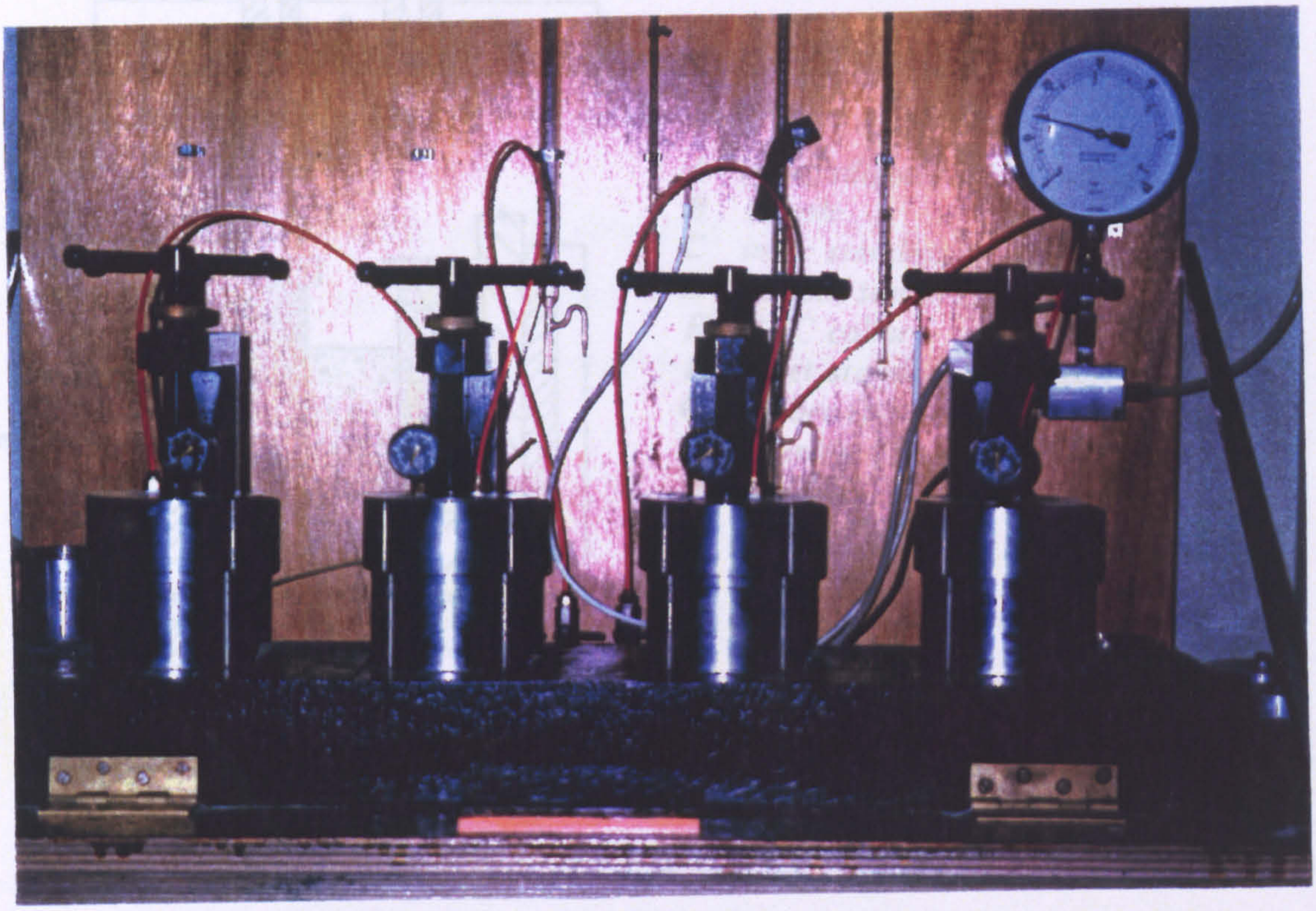

Fig. 3.2: General view of the permeability cells.

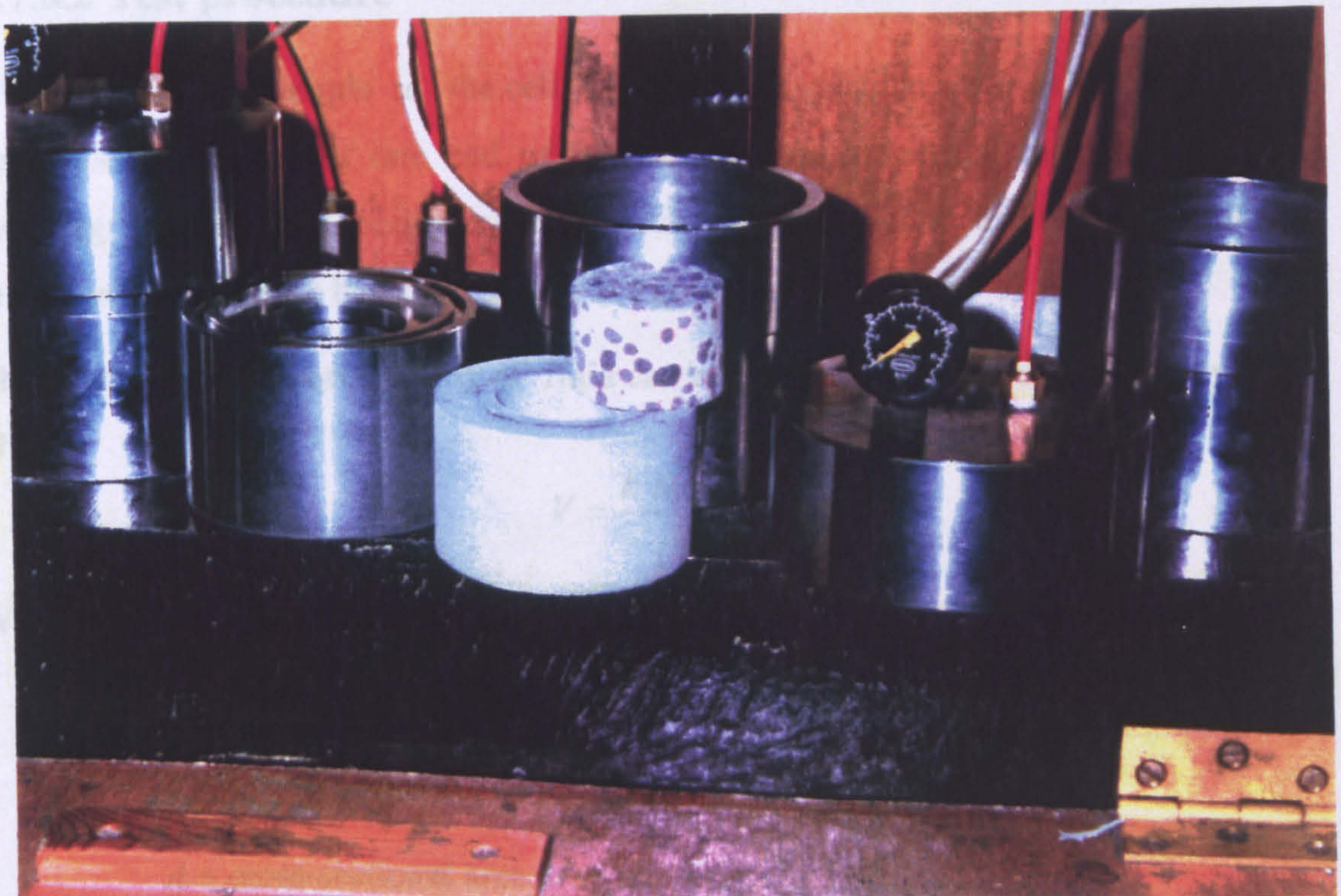

Fig. 3.3: The components of gas permeameter.

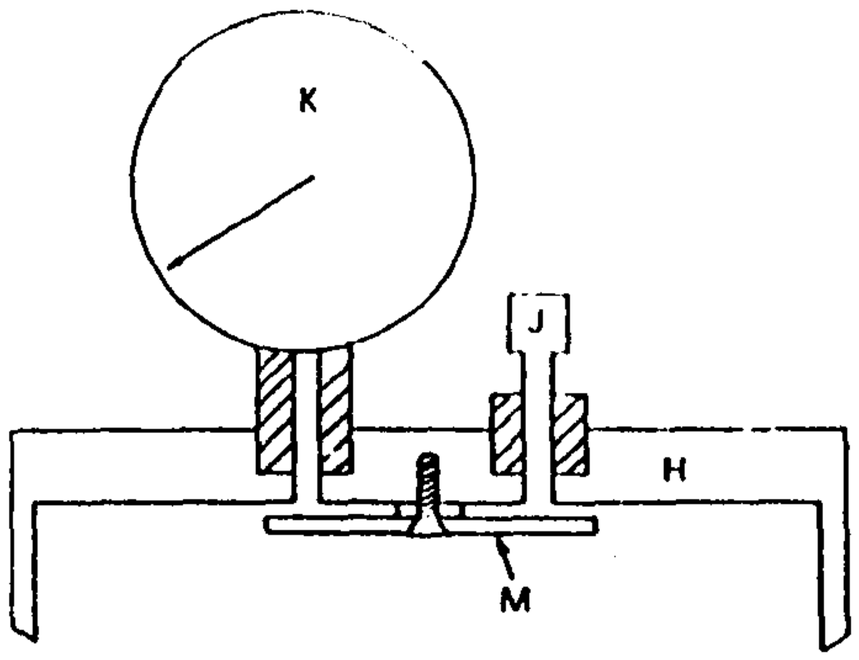

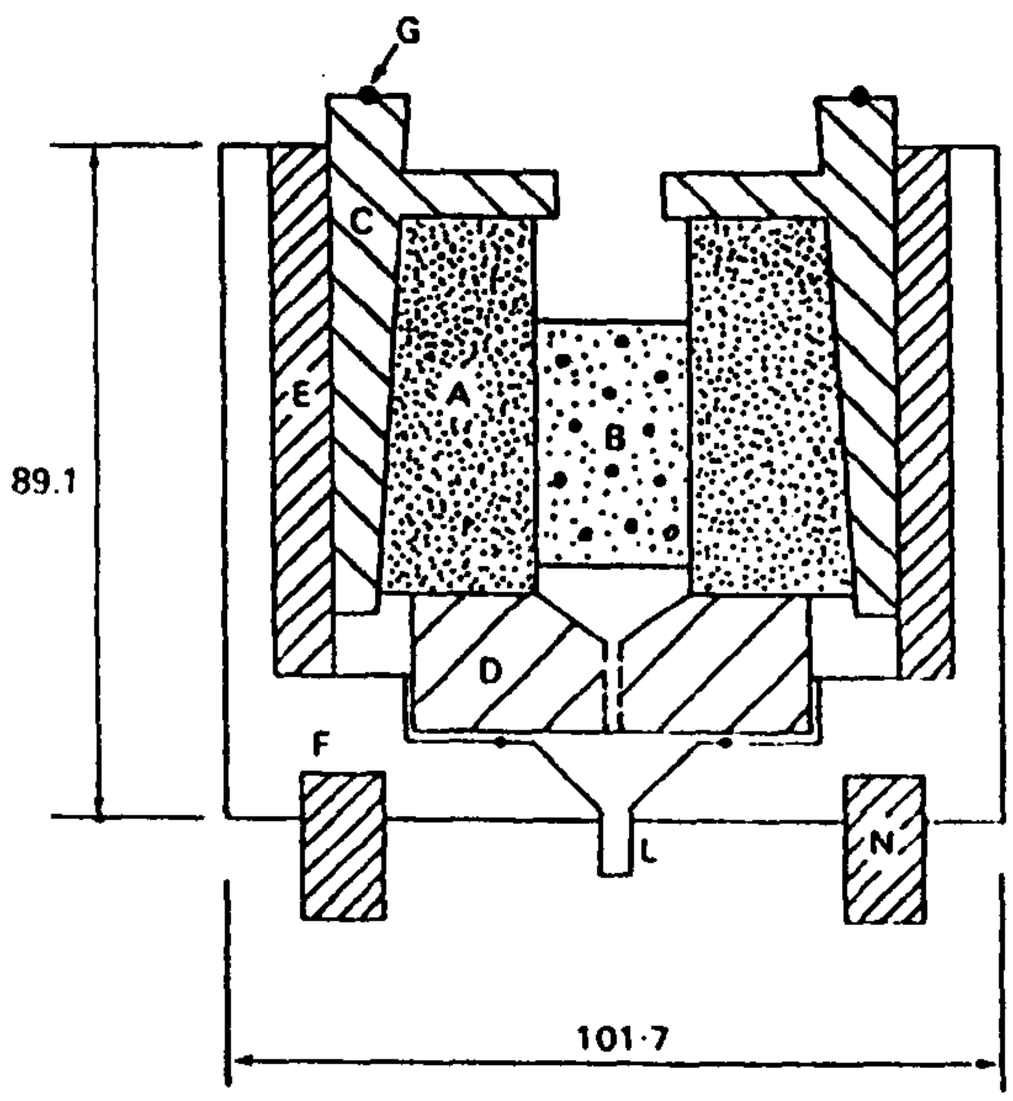

A inner silicon rubber cylinder
B sample
C inner stainless steel cylinder
D bottom stainless steel hollow seating
E PVC collar
F outer stainless steel body of cell
G rubber O-ring
H stainless steel cap of cell
J gas inlet
K pressure gauge
L gas outlet
M plastic circular baffle
N sitting guides

Fig 3.4: Schematic diagram of the permeability cell [71]

in an oven at 105°C for 24 hours. They were then put in an air-tight vessel until they reached room temperature before the start of the test.

3.7.8.2 Test procedure

After putting the sample in the cell, Oxygen was applied at a pressure of 1 bar above atmospheric pressure at one end of the sample and collected at the other end. After reaching a steady state condition, the flow rate was measured by one of the bubble flow meters mounted on the board, as shown in Fig. 3.2.

The coefficient of permeability of fluid can be determined according to D'Arcy's law [71]:

$$V = \frac{k A \Delta P}{\mu l} \tag{3.3}$$

Where:

V = flow rate, cm^3/s

k = coefficient of permeability, m^2

A = cross-sectional area of specimen, m^2

ΔP = (P1-P2)

μ = viscosity of gas, Ns/m^2

P_1 = absolute applied pressure, bar

P_2 = pressure at which the flow rate is measured, usually 1 bar

l = length of specimen, m

When a compressible fluid, such as oxygen is used, D'Arcy's equation should be modified using the expression proposed by Grube and Lawrence [104], which calculates the volume of fluid at the average pressure within the specimen:

$$k = \frac{2 P_2 V l \mu}{A(P_1^2 - P_2^2)} \tag{3.4}$$

For oxygen at 20°C with value of $\mu = 2.02 \times 10^5$ Ns/m^2 and P_2 at atmospheric pressure (1 bar), equation 3.4 can be written as,

$$k = \frac{2 P_2 V l \times 2.02 \times 10^{16}}{A(P_1^2 - P_2^2)} \tag{3.5}$$

3.7.9 Carbonation depth

The test for carbonation depth was performed in accordance with RILEM Draft recommendation CPC - 18 . The concrete samples used were 100 mm cubes. Each cube was split into two pieces. Carbonation was measured on the freshly broken surface . A solution of 1% phenolphthalein remains uncoloured at carbonated materials at low PH values and turns pink with PH values over 9.2 [105]. The results recorded are the average of two samples. On average, about 36 carbonation depth readings were taken for each sample, 18 readings for each specimens, 9 readings on each face.

3.7.10 Porosity and pore structure

Mercury intrusion porosimetry (MIP) has become widely used for evaluating the pore structure of hardened cements pastes, mortars and concrete. Mercury, which is a non-wetting liquid, will intrude open pores of the sample at high pressure [106]. The relationship between the applied pressure (P) and the pore diameter (d) is given by the Washburn equation [106], which is given as follows:

$$P = -\frac{\phi \gamma \cos\theta}{d} \tag{3.6}$$

where:

P = pressure required to intrude a pore.

d = diameter of intruded pore.

γ = surface energy of the liquid.

θ = contact angle between the liquid and the pore wall.

If γ and θ are constant for an intrusion liquid, d is inversely proportional to P. Note that in equation (3.6) the factor $\phi = 4$ is due to the assumption that all the pores are cylindrical in shape.

3.7.10.1 Apparatus

The instrument used in this research was a micromeritics Pore Sizer (model 9320). The instrument is designed for a maximum operation pressure of 30,000 psi (207 MPa) (Fig. 3.5). The instrument mainly consists of the following parts:

- Two low and one high pressure ports.
- Penetrometer, i.e. a high quality glass container for the sample

Pump and oxygen cylinder for generating the pressure for the low and high pressure.

Control keys for evacuation of the sample, applying the low and high pressure and monitoring the progress of the test.

3.7.10.2 Presentation of results

Data analysis was carried out using the MIP equipment with relevant software. The porosimetry report consists of a display of results covering several pages with data displayed on spread sheets, and several pages of graphs including pore size distribution plots. All the data are summarised in one page; and this page shows the experimental parameters and intrusion data summary, the most relevant of which are total pore volume, total pore surface area, median pore diameter, sample density and other measurements.

Fig. 3.6 gives a typical example of the porosimetry report. The first page shows the experimental parameters and intrusion data summary. The next page is the spreadsheet data.

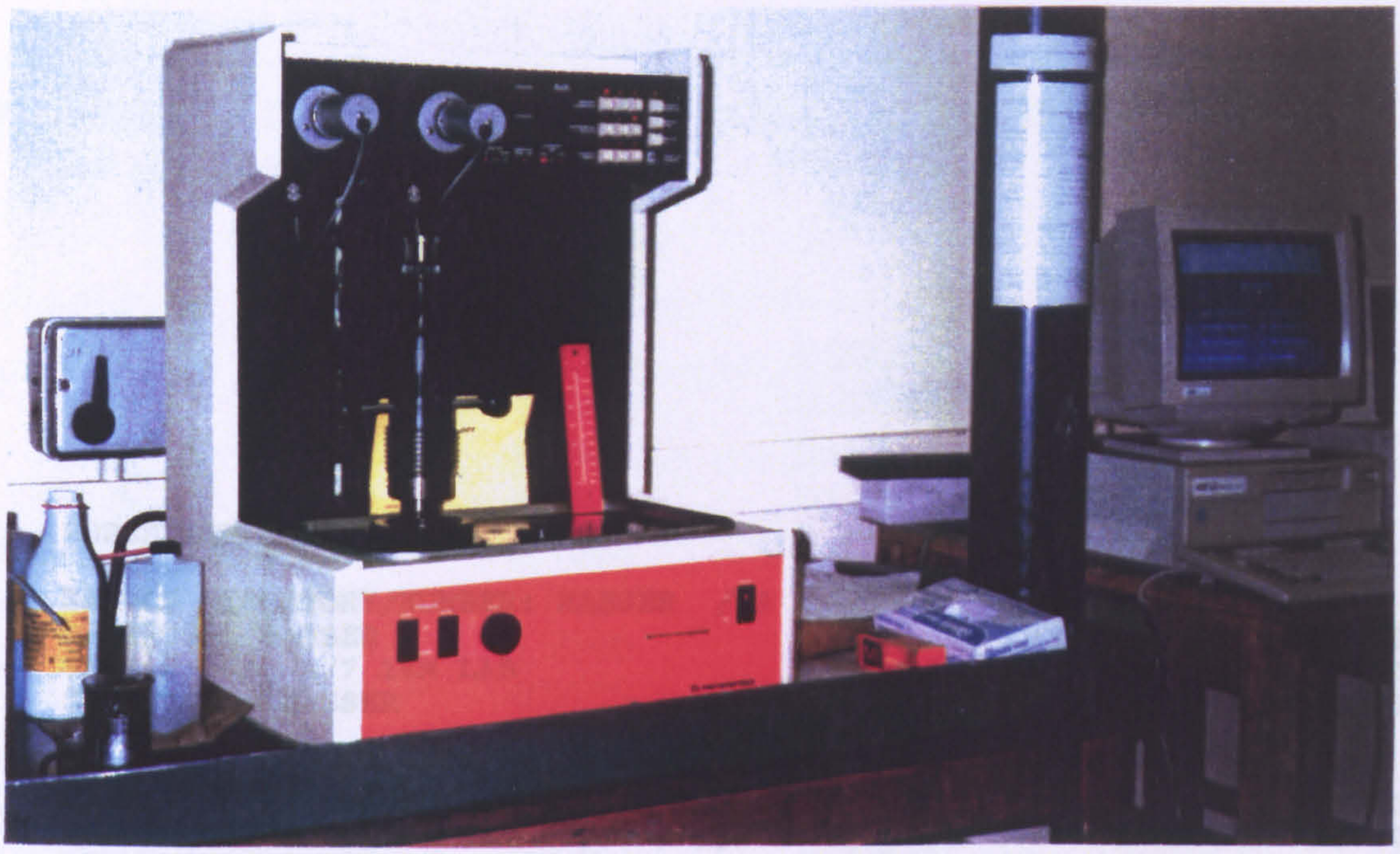

Fig. 3.5: Mercury porosimeter model Micromeritics pore sizer 9320

In a standard MIP report the following information is obtained:

Total Intrusion Volume: This is the maximum volume of mercury intruded into the sample at the highest pressure during the test.

Total Pore (surface) Area: This is the surface area within the pores determined as a function of pressure range, based on the assumption of cylindrical geometry.

Median Pore Diameter (volume): This is the pore diameter which corresponds to 50% value of total intrusion volume obtained from the cumulative intrusion volume curve.

Median Pore Diameter (area): This is the pore diameter which corresponds to 50% the value of total pore surface area in the cumulative pore area.

Average Pore Diameter: This is determined from the pore volume divided by the pore area assuming that all pores are right cylinders.

Bulk Density: This is a measurement that occurs at the initial mercury filling pressure. It takes the same value, which includes all open and closed pores as well as interstitial particle spacing, divided by the sample mass.

Apparent (skeletal) Density: This is a measurement of the samples solid phase, i.e., the sample volume minus all open pores as measured from total intrusion at the highest pressure, which is then divided by the sample mass. If there are no hidden, closed pores, then apparent density equals the true density of the material.

SAMPLE DIRECTORY/NUMBER: NASSER /18
OPERATOR: NASSER
SAMPLE ID: A/7 18M LAB
SUBMITTER: NASSER

LP 09:34:11 09/22/96
HP 09:58:31 09/22/96
REP 16:22:41 09/28/96

PENETROMETER NUMBER:	10-0380	ADVANCING CONTACT ANGLE:	117.0 deg
PENETROMETER CONSTANT:	21.63 µL/pF	RECEDING CONTACT ANGLE:	117.0 deg
PENETROMETER WEIGHT:	68.9488 g	MERCURY SURFACE TENSION:	485.0 dyn/cm
STEM VOLUME:	1.1310 mL	MERCURY DENSITY:	13.5537 g/mL
MAXIMUM HEAD PRESSURE:	4.4500 psi	SAMPLE WEIGHT:	2.0509 g
PENETROMETER VOLUME:	5.9200 mL	SAMPLE+PEN+Hg WEIGHT:	138.7900 g

LOW PRESSURE:
MERCURY FILLING PRESSURE: 0.9975 psia
LAST LOW PRESSURE POINT: 25.8581 psia

HIGH PRESSURE:

RUN TYPE:	AUTOMATIC
RUN METHOD:	EQUILIBRATED
EQUILIBRATION TIME:	5 seconds
MAXIMUM INTRUSION VOLUME:	0.0010 mL/g

INTRUSION DATA SUMMARY

TOTAL INTRUSION VOLUME =	0.0364 mL/g
TOTAL PORE AREA =	5.733 sq-m/g
MEDIAN PORE DIAMETER (VOLUME) =	0:0659 µm
MEDIAN PORE DIAMETER (AREA) =	0.0052 µm
AVERAGE PORE DIAMETER (4V/A) =	0.0254 µm
BULK DENSITY =	2.2331 g/mL
APPARENT (SKELETAL) DENSITY =	2.4308 g/mL
POROSITY =	8.13 %
STEM VOLUME USED =	37 %

(a) Summary sheet

Fig. 3.6: An example of porosimetry report

PRESSURE psia	PORE DIAMETER μm	MEAN DIAMETER μm	CUMULATIVE VOLUME ml/g	INCREMENTAL VOLUME ml/g
1.00	128.0609	128.0609	0.0000	0.0000
49.72	4.9401	5.2970	0.0003	0.0003
121.04	4.2506	4.5953	0.0003	0.0000
149.87	2.5694	3.4100	0.0008	0.0005
248.69	1.8237	2.1966	0.0013	0.0005
403.02	1.4239	1.6238	0.0016	0.0003
500.52	1.0554	1.2396	0.0019	0.0003
703.85	0.8523	0.9539	0.0023	0.0004
1002.84	0.7063	0.8521	0.0029	0.0006
1511.00	0.5136	0.6112	0.0034	0.0005
1768.82	0.4251	0.5231	0.0038	0.0004
1941.64	0.3170	0.0016	0.0042	0.0004
1999.97	0.2552	0.0019	0.0046	0.0004
2388.94	0.1815	0.0023	0.0054	0.0008
2668.92	0.1274	0.0029	0.0063	0.0009
3038.24	0.0845	0.0034	0.0076	0.0013
3461.90	0.0722	0.0038	0.0092	0.0016
4000.72	0.0658	0.0042	0.0106	0.0014
5251.55	0.0639	0.0648	0.0112	0.0006
5997.22	0.0590	0.0589	0.0131	0.0019
7990.05	0.0535	0.0562	0.0152	0.0021
10000.39	0.0479	0.0507	0.0170	0.0018
12502.78	0.0420	0.0450	0.0187	0.0017
15000.11	0.0369	0.0395	0.0202	0.0015
16852.43	0.0319	0.0344	0.0213	0.0011
17491.09	0.0243	0.0281	0.0225	0.0012
19987.45	0.0213	0.0228	0.0229	0.0004
21684.93	0.0160	0.0186	0.0237	0.0008
22484.25	0.0128	0.0144	0.0289	0.0052
23253.41	0.0102	0.0115	0.0300	0.0011
24980.59	0.0085	0.0094	0.0313	0.0013
25065.06	0.0082	0.0091	0.0330	0.0017
27465.72	0.0076	0.0076	0.0362	0.0032
28281.38	0.0076	0.0076	0.0363	0.0001
29966.72	0.0073	0.0076	0.0364	0.0001

(b) Spread sheet

Fig. 3.6: An example of porosity report

From the spreadsheet data, the precise intrusion volumes for each equilibrium pressure identify any anomalies that could significantly affect sample characteristics. A total of five columns of data provide full details of pore characteristics.

In the first column, equilibrium pressure attained during the analysis is listed in psia. These pressures are automatically corrected for mercury head pressure when the penetrometer is in the vertical position during high pressure analysis.

The second column, pore diameter in micrometers for each pressure point, as calculated by the Washburn equation [3.6] is given. The remaining three columns provide the following data for each pressure point: Mean pore diameter (in μm), cumulative intrusion volume (in ml/g) and incremental intrusion volume (in ml/g).

The following curves are usually used to analyse the pore size distribution:

Cumulative intrusion pore volume curve:

In this work, the pore size distribution data are presented in the form of the cumulative intrusion pore size distribution curves, the pore volume parameter being expressed in millilitres per gram. while the pore diameters are expressed in micrometers. The volumes intruded are accumulated from the largest pore diameter measured to the smallest one. Logarithmic scale of the abscissa was chosen for the pore diameter. This type of curves has the advantage of giving readily the following information, namely, the general pore size distribution of the specimen, total intrusion volume, coarse pore volume, threshold diameter and maximum continuous pore diameter.

Log differential intrusion volume:

Another way used for presenting the data of this work is d(volume)/d log(diameter) against pore diameter; this curve is frequently used to indicate the amount of intrusion between two diameters, the maximum continuous pore diameter (i.e., the pore at which the maximum intrusion is filled) and its location.

Additional common curves can be used for presenting the data in other ways. the differential intrusion volume (dV/dD-D) curve also shows the intrusion values between diameters. The increment intrusion volume (dV-D) curves show the increment of intrusion volume.

The discussion of the characteristics of the pore structure shall be dealt with using the following parameters:

Total porosity

This is the total pore volume divided by bulk sample volume, or total intrusion volume multiplied by bulk density.

Total intrusion volume

This is the maximum volume of mercury intruded into the sample at the highest pressure during the test.

Coarse pore volume

Because of the existence of pores of different kinds, some of which contribute to permeability and some of which do not, it is important to distinguish between coarse and fine pores. If the pores are coarse and interconnected, they contribute to transport of fluid and gases through concrete so the concrete then has a high permeability. On the other hand, if the pores are fine or discontinuous it will be ineffective with respect to transport, then the permeability of the concrete is low.

It has been suggested by Goto and Roy [1] and Hooton [11] that the pore relevant to permeability are those with diameter of at least 50 or 150 nm. These pores have to be continuous. Pores which are ineffective with respect to flow, that is to permeability, include, in addition to discontinuous pores, those which contain adsorbed water and those which have a narrow entrance, even if the pores themselves are large.

Nyame and Illston [107], Mehta [108] and Hooton [109] have suggested other values for this coarse pore diameter which ranges from 0.090-0.150 μm. In this study, it is suggested that coarse pores which is greater than 0.1 μm contribute to poor durability.

Threshold diameter

Feldman and Beaudoin [110] defined that the threshold diameter corresponds to the diameter where the initial rapid increase in dV/dD curves occurs. Mehta and Manmohan [111] defined 'the threshold diameter' as the diameter of the largest pores present at which mercury begins to penetrate into the pores of the specimens. Winslow and Diamond [106] defined that the 'threshold diameter represents the minimum diameter of pores which is geometrically continuous throughout all regions of the hydrated cement paste'.

In this work, the threshold diameter is taken as defined by other researchers [112-114] and as shown in Fig. 3.7 via the turning point of the intrusion curve; above this point there is comparatively little intrusion into the specimens, and immediately below, the greatest portion of the intrusion.

Continuous pore diameter

Nyame and Illston [107] defined the continuous pore radius as the pore radius at which dV/dP has a maximum value. Roy and Parker [2] also used dV/dP - R plot to determine the maximum continuous pore radius. However, in this study the continuous pore diameter is as shown in Fig. 3.7 is interpreted as the pore at which the maximum intrusion is filled.

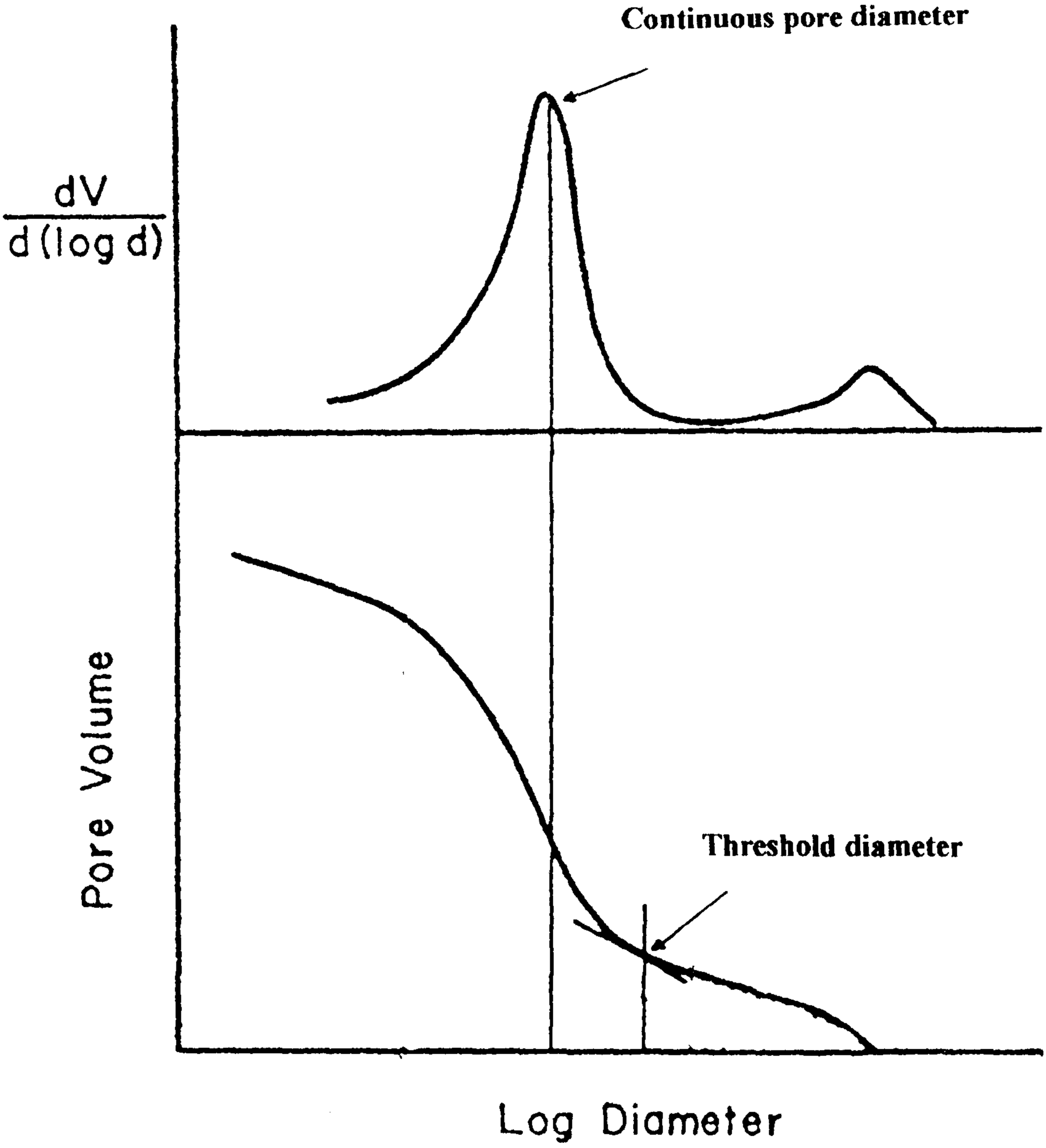

Fig. 3.7: Parameters defining MIP pore size distribution threshold diameter and continuous pore diameter [112]

3.7.10.3 Sample preparation

The sample preparation is a very important factor which affects the pore structure in many ways. For example; the location of the sample must be chosen carefully and taken the same way for all the samples. Near surface samples may be affected by carbonation. External forces may damage or deform the pore structure such as the samples obtained from cubes used after the compressive strength test.

Forty concrete prisms, 100x100x500 mm, were cast for porosity and pore structure tests. The samples were removed from their respective curing environment at the age of the test; cores were then taken, and submerged in an ethanol solution and kept tightly in a plastic jar to stop the hydration until the test at Sheffield University. The 50.8 mm (2 inch) diameter cores were taken from the side face at right angles with the trowelled face (the top face in the exposure environment was the trowelled face) and, at the middle of the prism. Each core was then sliced using a diamond saw into two specimens (30 mm thickness) after rejecting the top and bottom 15-20 mm from the end faces to avoid any variation on the results. The mortar from each sample was carefully taken by breaking the core by chisel; then small pieces of mortar, 3-6 mm in size, were taken from the middle part with a hand clipper, i.e. no coarse aggregate particle was present, not even the smallest one, because such particles can be seen to have a great effect on pore size distribution when MIP results are interpreted. Oven drying, however, is still considered by many researchers [115] as the standard procedure of drying. In this work, ovendrying at 105°C was used for all the samples, on the assumption of the necessity of complete removal of water from the sample prior to the intrusion of mercury. All samples were weighed before oven drying and after; oven drying time had been gauged by repeated drying, as necessary, of a few preliminary samples. Once all the test samples had achieved constant weight losses (approximately 3.5 hours), they were kept in a desiccator during cooling. The sample weights ranged approximately from 2.00-2.20 grams. The results recorded represent the test of one specimen.

3.7.10.4 Test procedure

A dry sample of about 2 g was weighed and put into the penetrometer; the sample was then subjected to evacuation to evacuate the sample pores from gases. This was to allow the mercury to inject into the small pores. Then the sample pores were filled by

mercury by systematically increasing the pressure on mercury. Both the pressure and mercury intruded are recorded automatically by the machine. Systematically using Washburn equation the pore size distribution was calculated.

The porosity and pore size distribution were obtained using pressure up to 30,000 psi (207 MPa). A contact angle of 117°C was used in equation [3.5]. This value was used by Winslow and Diamond [106] for oven dried samples.

Chapter four

FRESH CONCRETE PROPERTIES

4.1 Introduction

The need for excellent workability characteristics of concrete is extremely important, in order to avoid mixing, placing and compacting problems, and to obtain satisfactory long-term performance of the concrete. Workability is affected by the properties of the mix constituents as well as the environmental conditions. Climatic conditions in the Arabian Gulf region increase the evaporation rate of water from the concrete causing immediate workability loss. High temperatures also accelerate the setting time of concrete, insufficient compaction and enhanced tendency for pre-setting cracking and plastic shrinkage cracks [26,35]. The addition of more water to the fresh concrete to compensate for this workability loss during casting will adversely affect the engineering and durability properties of hardened concrete.

4.2 Aims and objectives

The main objectives of this part of the project are as follows:

- To investigate the properties of fresh concrete to include the length of period within which the concrete can be transported, placed and finished in hot environment in the Arabian Gulf area.
- To investigate the role of slag if the concrete with and without slag is mixed and cast after period of time in the outdoor environment during summer season of the Arabian Gulf.

The fresh properties investigated include consistency and setting times, workability and workability loss with time. The full details of the experimental programme are presented in chapter three and the test results are presented below:

4.3 Consistency of cement paste

The consistency of cement paste was measured following the procedure outlined in Chapter 3. The influence of cement replacement materials on consistency is shown in Fig. 4.1 and Table 4.1. The results indicate no significant effects of the presence of silica fume or slag. The SF was presented only in small quantities whereas slag helps to enhance the workability properties. The net results was no major change in the consistency properties of the resulting cement paste. The water demand increased from 29% to 30% only for standard consistency when 5.5% of silica fume was used to replace OPC. Alshamsi et al [116] have shown that the replacement level of 5% silica fume increased the water demand from 27.5% to 30%, while 15% replacement can increase the water demand significantly up to 37.5% at the same consistency. He attributed these observation to the small particle size of SF leading to higher water demand.

The inclusion of GGBFS as part replacement of OPC had also no major effect on consistency results. Mix C (81% OPC + 5.5% SF + 13.5% slag) exhibited similar consistency to mix B and any further increase in slag content (mixes D and E) exhibited similar values (30%). This may be attributed to the fact that the fineness of the slag used in this study (380 m^2 /kg) was of the same order as the finesses of cement (310 m^2 /kg). The effect of GGBFS is similar to the results reported by others. Reeves [117] carried out a series of laboratory tests using slag replacement levels of 0, 30, 50, and 70% on pastes made to a standard consistency. He found that there was no differences in the water demand between plain OPC and blended cement pastes, which ranged from 26.5% to 25.8%.

4.4 Setting times:

Table 4.1 shows initial and final setting times for the five pastes in both indoor (20±2°C) and outdoor environments (39±3°C). In this investigation, silica fume and a range of slag contents up to 33% of the total cemetitious material were used in making the cement paste. In addition to the laboratory environment, the effect of hot environment on the five different mixes was studied. All the specimens were covered by polythene sheet after placing in the mould until the end of the test to avoid surface cracks and to minimise water loss from the sample.

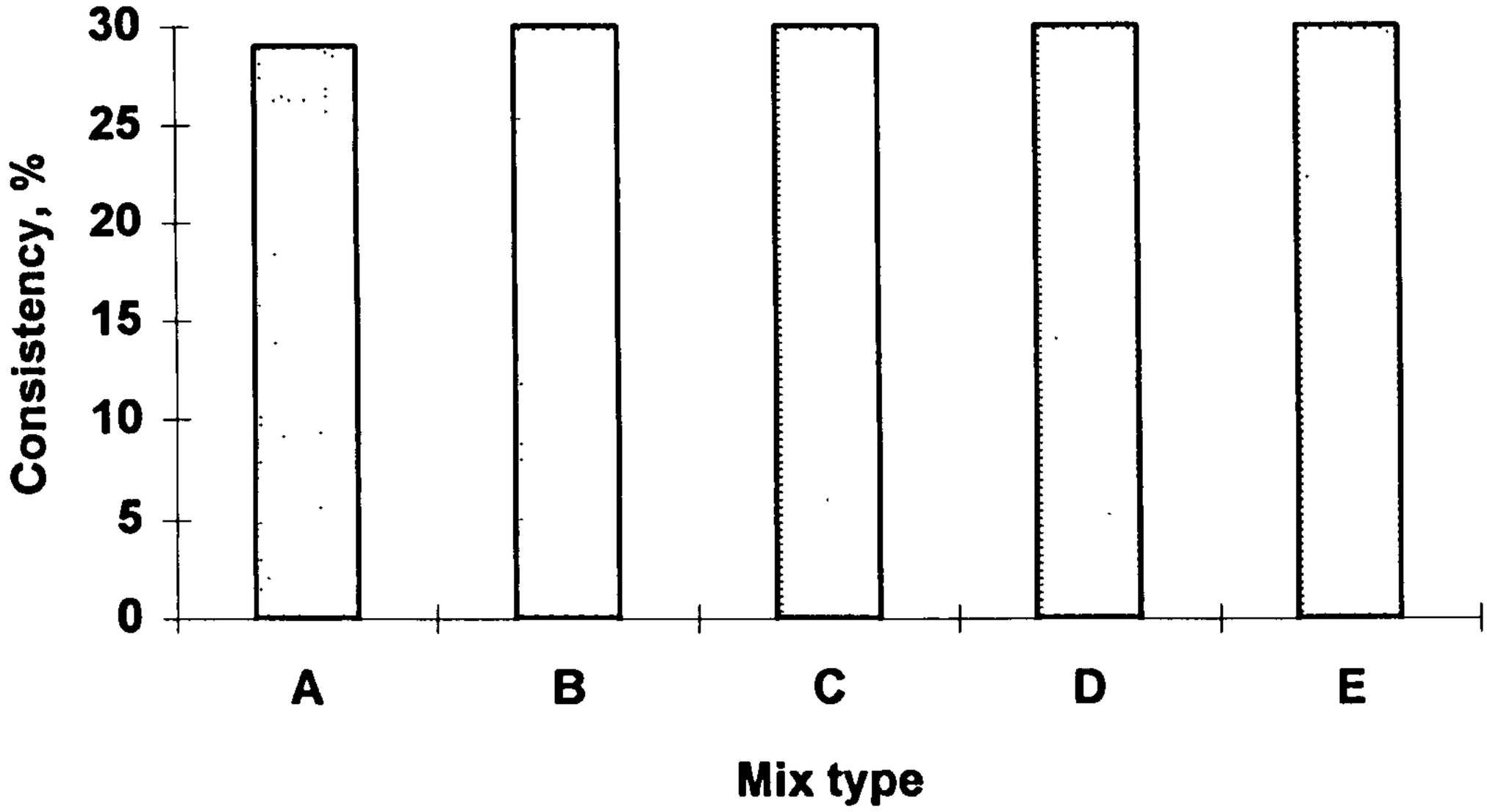

Fig. 4.1: Influence of mix type on consistency.

4.4.1 Effect of mix type

Table 4.1 and Fig. 4.2 show the influence of silica fume and slag content on the initial and final setting times. It can be seen that, in the indoor environment, the inclusion of 5.5% of SF shows no significant effect on the setting times, and that both setting times are similar to that of plain OPC. Alshamsi et al [116] also found that the addition of microsilica with a superplasticizer with mild retardation effects delayed the setting times of pastes. They suggested that this retardation is due to the fact that microsilica replaces part of the OPC thus reducing the early stiffening potential. While the addition of microsilica, without chemical admixture, in percentages less than or equal to 10% had little effect on setting times, higher percentages produced significant influence. Increases in both setting times of between 6 to 20% of that of the control were observed when 20% of the OPC was replaced by microsilica. On the other hand, investigations by Pistilli et al [118] show that, ordinary concrete mixtures (with 250 to 300 kg/m^3 cement) incorporating small amounts of silica fume, up to 10% by mass of cement, exhibit no significant difference in setting times compared to conventional concrete.

Table 4.1: Initial and final setting times.

Mix type	OPC/SF/Slag	Standard	Indoor		Outdoor	
	%	Consistency %	Initial hr:min	Final hr:min	Initial hr:min.	Final hr:min.
A	100/0/0	29	2:04	3:27	0:55	1:53
B	94.5/5.5/0	30	2:03	3:40	1:10	2:10
C	81/5.5/13.5	30	2:45	4:15	1:28	2:32
D	71/5/24	30	3:28	4:33	1:52	2:42
E	63/4/33	30	3:47	4:49	2:04	2:47

On the other hand, the inclusion of slag shows a retardation in both setting times. Mix C which contains the smallest amount of slag presented the smallest values of initial and final setting times among the mixes containing slag, these values are higher than those of the control mix by 33 and 23% for initial and final setting times respectively. The other mixes D and E containing slag also showed delay in setting times. Initial and final setting times of mixes D and E were extended by more than one hour in the laboratory environment compared to that of the control mix (mix A). The retardation of the initial and final setting times as exhibited by mix E was higher by 83 and 40% respectively, compared with those of the control mix. Many published reports confirm the above findings when using OPC/GGBFS paste; The presence of slag in the mix leads to retardation at normal temperature, typically 30 to 60 minutes [49]; Hwang and Shen [119], for example, explain this retardation due to the presence of slag, and the phenomenon may lie in the fact that increments in the slag content will reduce the amount of C_3S and C_3A formed. Reeves and Wainwright [44,117] have reported that this retardation is due to the initial rate of reaction between GGBFS and water being slower than that of portland cement and water, causing an increase in setting time.

The principal factor influencing times of setting is the level of cement replacement. The water/binder ratio has a much less significant influence on the time of setting. High range water reducing admixtures also generally exercised retardation effect [77,120].

4.4.2 Effect of environment

The results presented in Table 4.1 and Fig. 4.3 show that as temperature increases, setting times are reduced for all mixes, for both plain OPC as well as for the blended

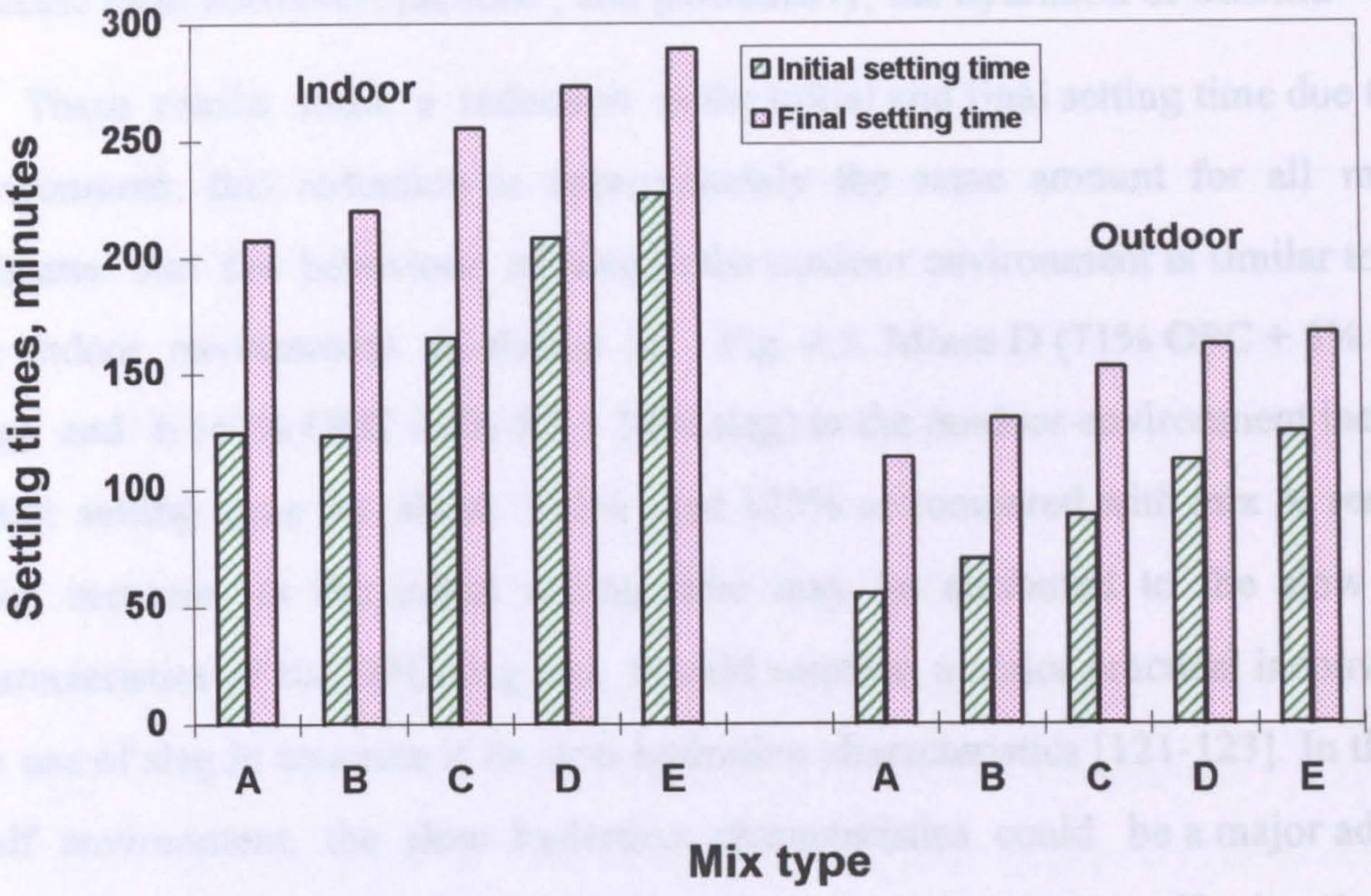

Fig. 4.2: Influence of mix type on setting times.

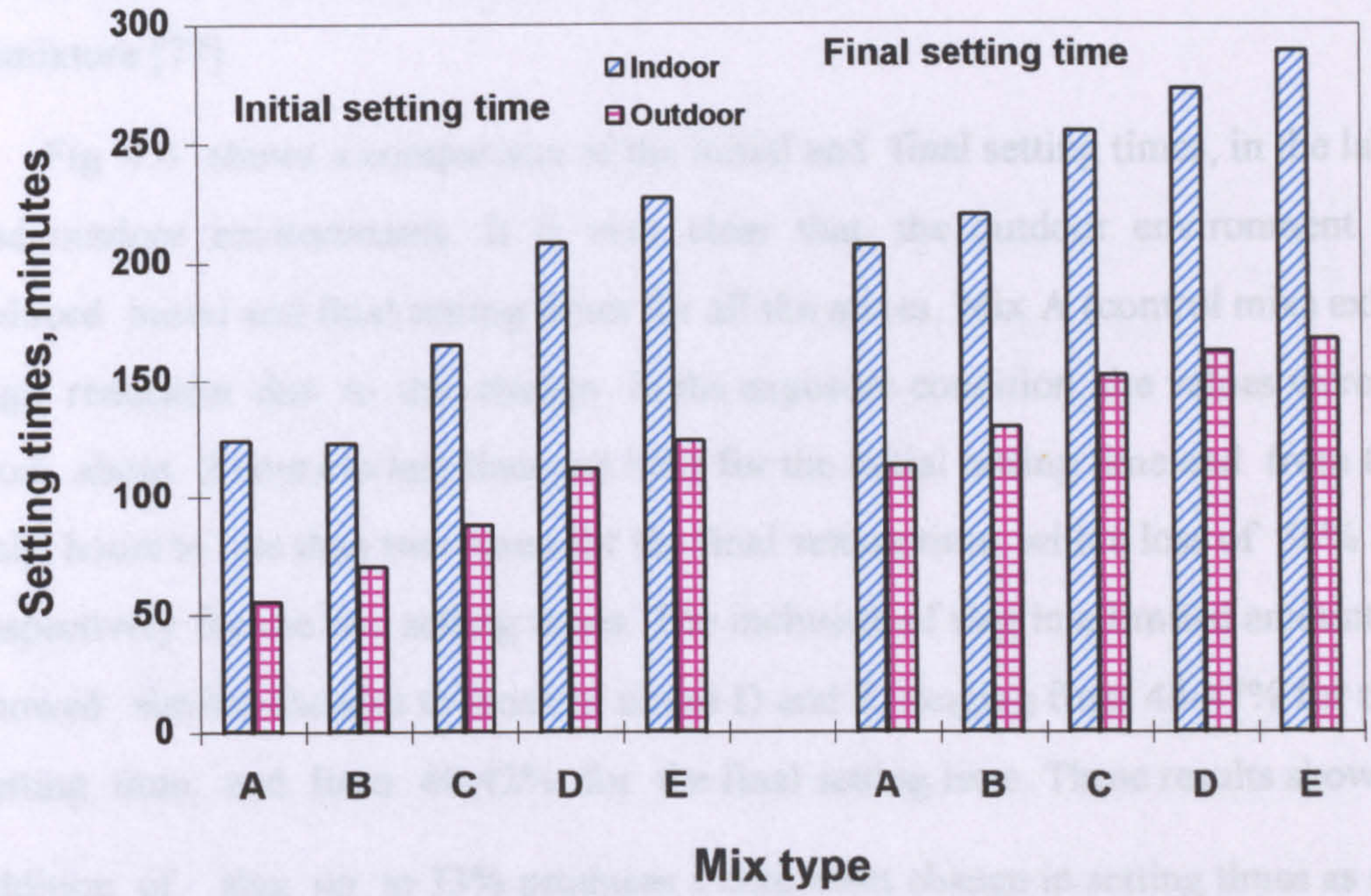

Fig 4.3: Influence of environment on setting times.

cement pastes. This trend is expected because the higher temperatures are known to increase most chemical reactions , and particularly, the hydration of cement.

These results show a reduction in the initial and final setting time due to outdoor environment; this reduction is approximately the same amount for all mixes. This indicates that the behaviour of slag in the outdoor environment is similar to that of in the indoor environment as shown in Fig. 4.3. Mixes D (71% OPC + 5% SF + 24% slag) and E (63% OPC + 4% SF + 33% slag) in the outdoor environment increased the initial setting time by about 104% and 125% as compared with mix A, respectively. This increase in the initial setting time may be attributed to the slow hydration characteristics of the OPC-slag mix. In cold weather, a major practical inconvenience in the use of slag in concrete is its slow hydration characteristics [121-123]. In the Arabian Gulf environment, the slow hydration characteristics could be a major advantage in using slag, because the heat of hydration is a major factor affecting the long term durability of concrete. When present in an adequate amount, slag can also eliminate internal microcracking by reducing the thermal strains due to temperature rises in large members, specially in hot environment. Thus increased slag setting times can ensure not only the low heat of hydration but also extended concrete casting times in hot environment, which leads to a better retardation effect than that of the chemical admixture [77].

Fig 4.4 shows a comparison of the initial and final setting times, in the laboratory and outdoor environments. It is very clear that, the outdoor environment leads to reduced initial and final setting times for all the mixes. Mix A (control mix) exhibited a high reduction due to the change in the exposure condition: the values were reduced from about 2 hours to less than one hour for the initial setting time and from three and half hours to less than two hours for the final setting time, with a loss of 56% and 45% respectively for the two setting times. The inclusion of slag in a limited amount (mix C) showed similar changes to those of mixes D and E, ranging from 45-47% for the initial setting time, and from 40-42% for the final setting time. These results show that the addition of slag up to 33% produces a consistent change in setting times as shown in Fig. 4.4.

The results of Hogan and Meusel [49] indicate that the initial setting time is extended one-half to one hour at temperatures of 23°C; little, if any change is found in setting time due to using of slag at temperatures above 29°C.

Wainwright [44] has reported a study carried out by Taylor and Woodrow who conducted an investigation into the setting times of concretes with slag replacement levels of 25% and 50%. They measured setting times using a penetration resistance test on specimens kept at 5, 15 and 25°C. Their conclusions were that at low temperatures the setting time is marginally increased by the use of slag, but that at higher temperatures (i.e. 15 and 25°C) there was little difference.

All the results reported above are on tests carried out on small specimens. The conditions under which the specimens have been kept in the laboratory may not reflect conditions on site, particularly with respect to the heat generated in deep members cast in hot climates. Slag reduces stresses arising from temperature rise due to heat of hydration by delaying the setting times which then delays the occurrence of the maximum thermal stresses, which, in turn, reduce the possibility of early age thermal microcracking. Heat generation will be reduced as the percentage of slag is increased, and this could have a significant effect in reducing thermal gradients and thermal cracks caused by the heat of hydration.

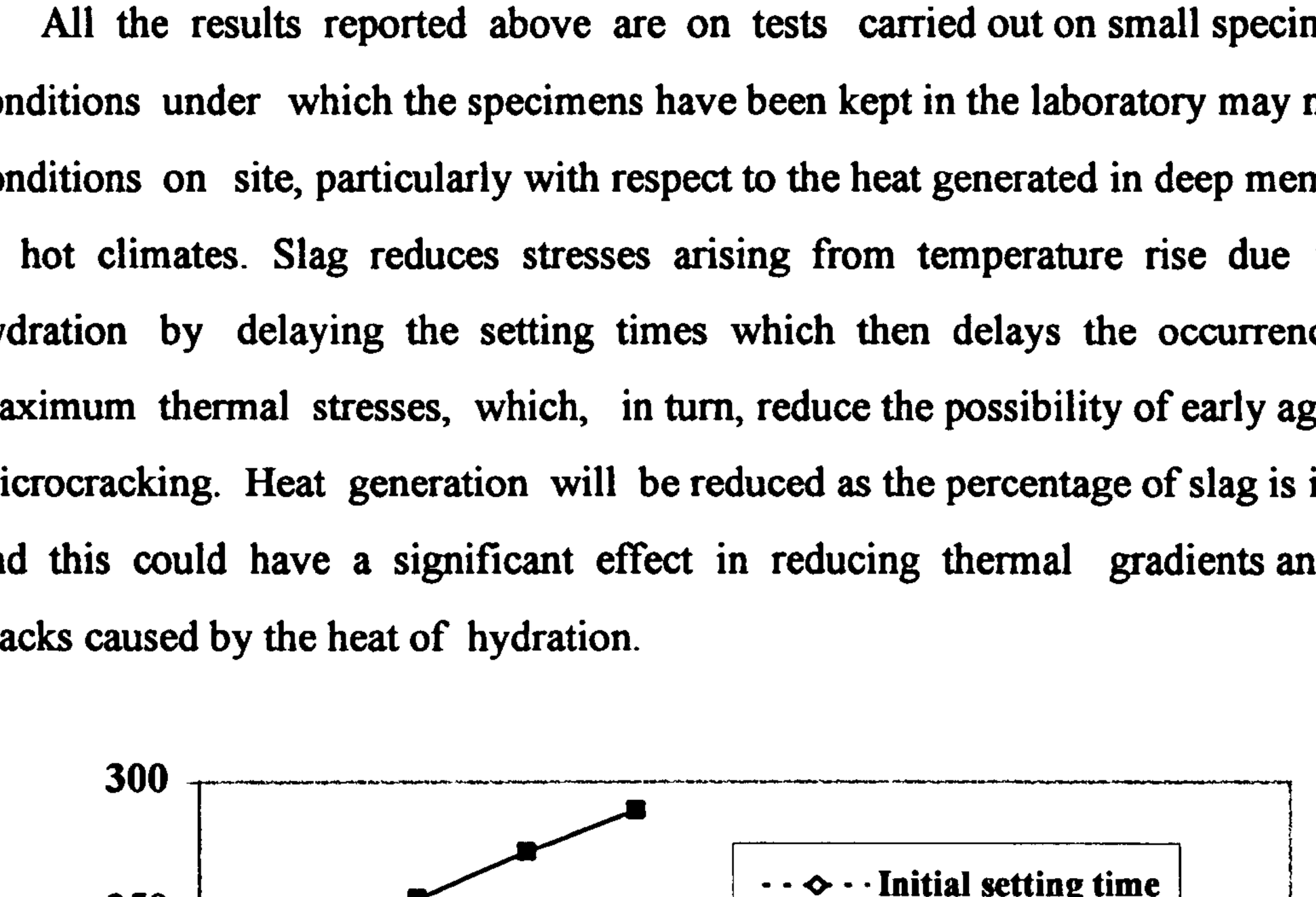

Fig. 4.4: Influence of slag content on setting times.

4.5 Workability

All the concrete mixes were proportioned to give a nominal slump of about 175-200 mm when tested in the laboratory environment soon after mixing. There was a need for high workability to start with in order to illustrate clearly the effect of environment on workability. The superplasticizer dosages needed for mixes A and B to reach a slump of about 190 mm were 12.5 and 12 l/m^3 respectively. On the other hand, the amount of HRWRA required for the mixes with slag was less, and decreased progressively with increase in the slag content as shown in Fig. 4.5. For mix E, the HRWRA required was 5 l/m^3 at the same slump and w/b ratio, as shown in Table 4.2.

Fig. 4.5 shows the relationship between the amount of superplasticizer and percentage of GGBFS content, It is clear from the figure that as the slag content increased from 0 to 33%, the amount of superplasticizer decreased to about 40% of that needed for plain OPC.

Table 4.2: Workability properties.

Mix type	OPC kg/m^3	SF kg/m^3	GGBFS kg/m^3	Free w/b	SP430 L/m^3	Slump Indoor mm	Slump Outdoor mm*	Total binder kg/m^3
A	400	-	-	0.35	12.5	190	100	400
B	378	22	-	0.35	12.0	190	100	400
C	323	22	55	0.35	9.5	195	140	400
D	323	22	110	0.35	7.0	195	170	455
E	323	22	165	0.35	5.0	190	170	510

* Initial slump values with similar proportions materials which were kept in the outdoor environment under solar radiation and ambient temperature before mixing.

4.5.1 Workability loss with time: effect of binder

The workability loss with time was measured using the standard slump test BS 1881:1983 [98]. The concrete mix was remixed for 1 minute every 7 minutes, and the slump taken every 15 minutes. The tests were performed on the five mixes as shown in Table 4.2. All mixes were made to nominally the same slump of about 175-200 mm when tested in the laboratory environment.

From visual examination, it was found that the inclusion of slag lead to better cohesiveness and workability. This is the consequence of a better dispersion of the

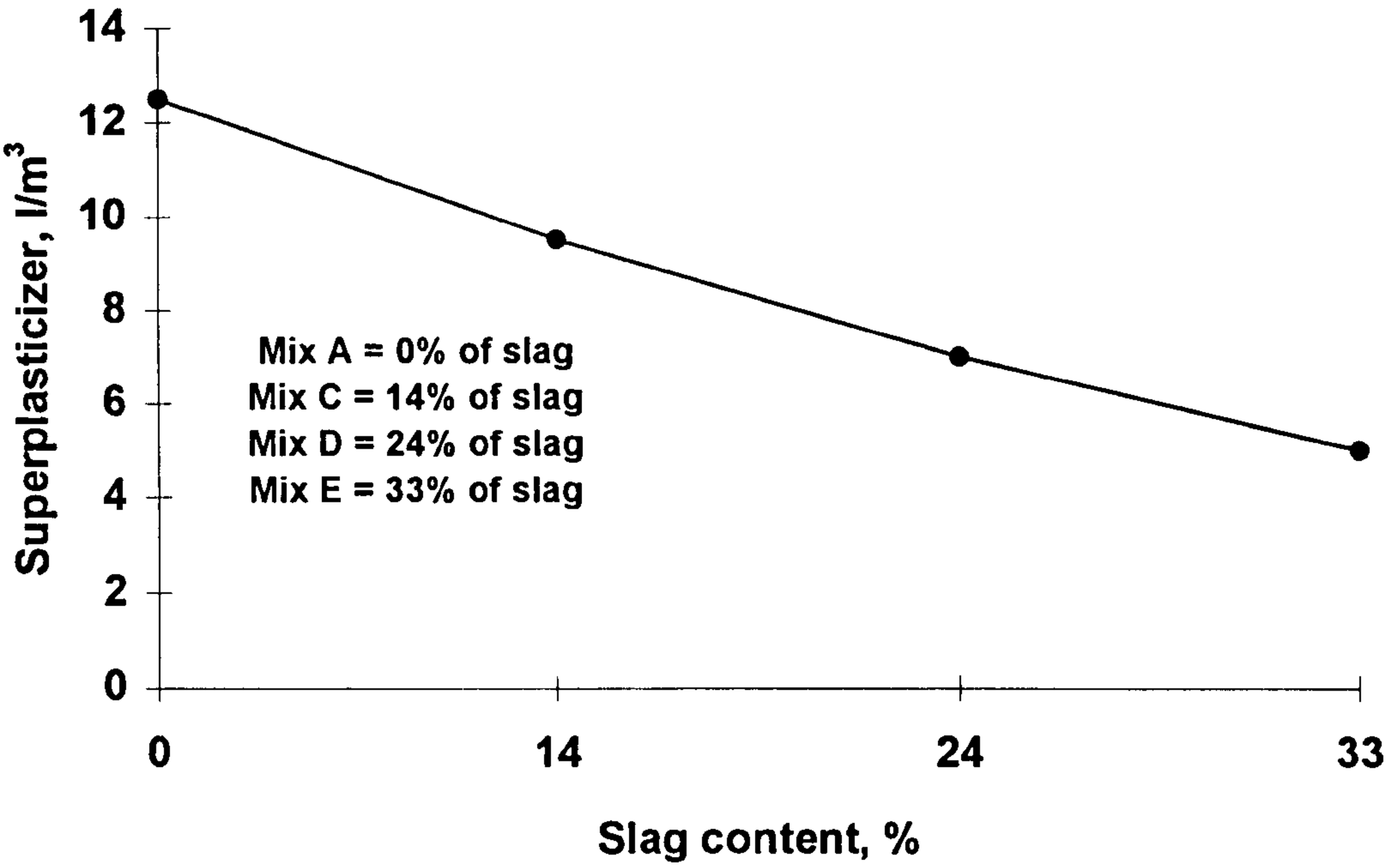

Fig. 4.5: Relationship between the amount of superplasticizer and slag content.

cementitious particles and of the surface characteristics of the GGBFS particles, which absorbs little water during mixing [49].

Fig. 4.6 shows that in indoor environment mix A (400 OPC) exhibited the smallest loss of slump. The presence of silica fume (378 OPC + 22 SF) slightly reduced the slump as compared to the control mix A; the slump loss was about 6% during the first 30 minutes. The presence of a limited amount of slag in mix C (323 OPC + 22 SF + 55 slag), on the other hand, did not increase the slump loss as compared with mix B. On the other hand, the additional slag in mixes D and E showed 11.4% and 22.9% increase in loss of slump during the first 30 minutes compared to mix C. Subsequent to start of mixing, as the amount of GGBFS increased the loss of slump increased, due to the fact that, mixes containing slag had less amount of superplasticizer to extend the workability. Other published results confirm this finding. Cesareni and Frigione reported that, GGBFS increase the rate of slump loss [124], whereas Meusel and Rose [58] indicate that concrete containing slag at 50% substitution rate yielded slump loss equal to that of concrete without slag. Others [125] indicate that the use of slag reduces slump loss, particularly when the portland cement used in the blend exhibits rapid slump loss. It has also been found that mixes containing slag have been sometimes found to exhibit an early loss of slump, but there are also reports of a low rate of slump loss.

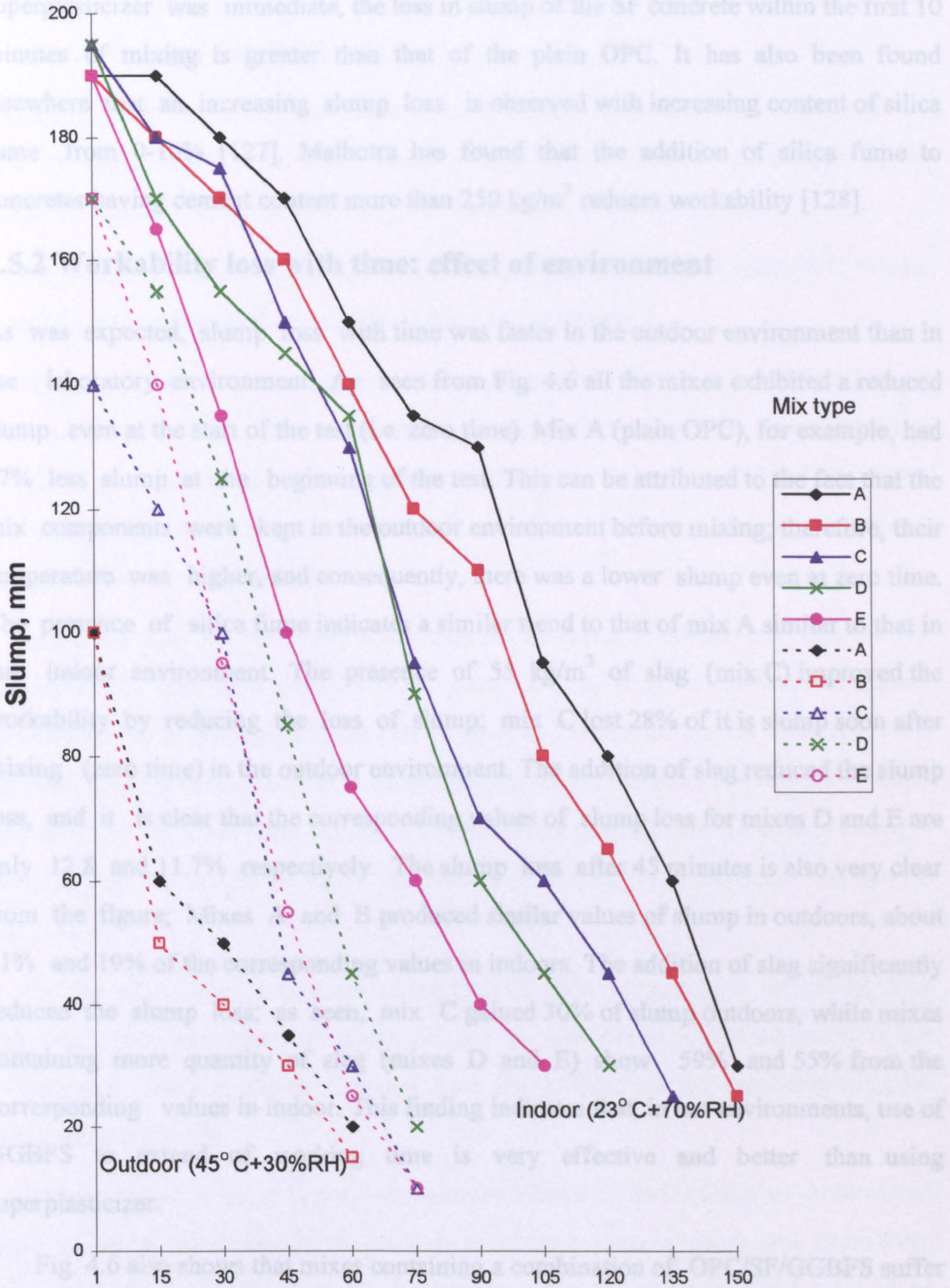

Fig. 4.6: Effect of environment on workability loss with time.

Mangilardi [126] arrived at a similar finding; he found that when the addition of superplasticizer was immediate, the loss in slump of the SF concrete within the first 10 minutes of mixing is greater than that of the plain OPC. It has also been found elsewhere that an increasing slump loss is observed with increasing content of silica fume from 0-10% [127]. Malhotra has found that the addition of silica fume to concretes having cement content more than 250 kg/m^3 reduces workability [128].

4.5.2 Workability loss with time: effect of environment

As was expected, slump loss with time was faster in the outdoor environment than in the laboratory environment. As seen from Fig. 4.6 all the mixes exhibited a reduced slump even at the start of the test (i.e. zero time). Mix A (plain OPC), for example, had 47% less slump at the beginning of the test. This can be attributed to the fact that the mix components were kept in the outdoor environment before mixing; therefore, their temperature was higher, and consequently, there was a lower slump even at zero time. The presence of silica fume indicates a similar trend to that of mix A similar to that in the indoor environment. The presence of 55 kg/m^3 of slag (mix C) improved the workability by reducing the loss of slump; mix C lost 28% of it is slump soon after mixing (zero time) in the outdoor environment. The addition of slag reduced the slump loss, and it is clear that the corresponding values of slump loss for mixes D and E are only 12.8 and 11.7% respectively. The slump loss after 45 minutes is also very clear from the figure; Mixes A and B produced similar values of slump in outdoors, about 21% and 19% of the corresponding values in indoors. The addition of slag significantly reduced the slump loss; as seen, mix C gained 30% of slump outdoors, while mixes containing more quantity of slag (mixes D and E) show 59% and 55% from the corresponding values in indoor. This finding indicates that, in hot environments, use of GGBFS to extend of working time is very effective and better than using superplasticizer.

Fig. 4.6 also shows that mixes containing a combination of OPC/SF/GGBFS suffer slump loss at a slower rate than the mix A (plain OPC) in outdoor environment, which is due to the evaporation of the superplasticizer from mix A. This may be explained as follows:

1- Mixes containing slag/SF lose water and superplasticizer at a slower rate than the plain OPC mix, due to less bleeding.

2- The absorption of water in the mixes containing GGBFS is slower than that in OPC because of the lower rate of hydration. Therefore, more water will remain unhydrated during first 30 minutes.

3- Because slag has a slightly lower relative density than OPC (2.89 compared to 3.12), replacement at an equal mass-to-mass basis will result in an increase in the powder volume, which should lead to an increase in workability [44].

4. The colour of the mixes containing GGBFS is lighter than that of plain OPC, which should lead to less absorption of heat due to solar radiation.

Whiting [129, 130] has suggested two quantitative parameters to define loss of slump with time. These include the "slump half-time', defined as the time needed for the slump to decrease to 50% of its initial value, and "slump pot-life', defined as the time needed for slump to decrease to a value of 25 mm (1 inch). These parameters are shown in Table 4.3 and Fig. 4.7.

Table 4.3 and Fig. 4.7 serve to illustrate the influence of the two environments on the workability loss with time for both plain OPC as well as the blended cement combination. It is interesting to see that mixes A and B showed shorter half- lives only after two minutes in real outdoor environment. However, this half- life was not reached even after 100 minutes when testing in the laboratory environment. This observation is confirmed by the results of other researchers [47,53,55,57] as discussed in chapter 2 (Fig. 2.4).

On the other hand, mixes containing GGBFS show betterment in workability loss with time. This retardation of hydration due to presence of slag is a blessing in hot environments, since it allows enough time for mixing, placing and compacting the concrete at the job site.

There is high variation in pot-lives between laboratory and outdoor environment of mixes A and B. For example; the pot-lives in laboratory environment were about three times the pot-lives in the outdoor environment. On the other hand, the pot-lives of mixes containing slag (i.e. mixes C, D and E) in the laboratory environment were about twice that in the to outdoor environment.

Table 4.3: Slump loss parameters (minutes) for both laboratory and real outdoor environments.

Environment	Laboratory environment		Outdoor environment	
Mix type	half- life[a]	Pot- life[b]	half- life[a]	Pot- life[b]
A	112	155	2	55
B	100	150	2	50
C	76	135	30	60
D	75	125	40	70
E	50	110	30	63

[a] Half- life: The time (minutes) required for concrete to lose 50% of initial slump.

[b] Pot- life: The time (minutes) required for concrete slump to fall below 25 mm.

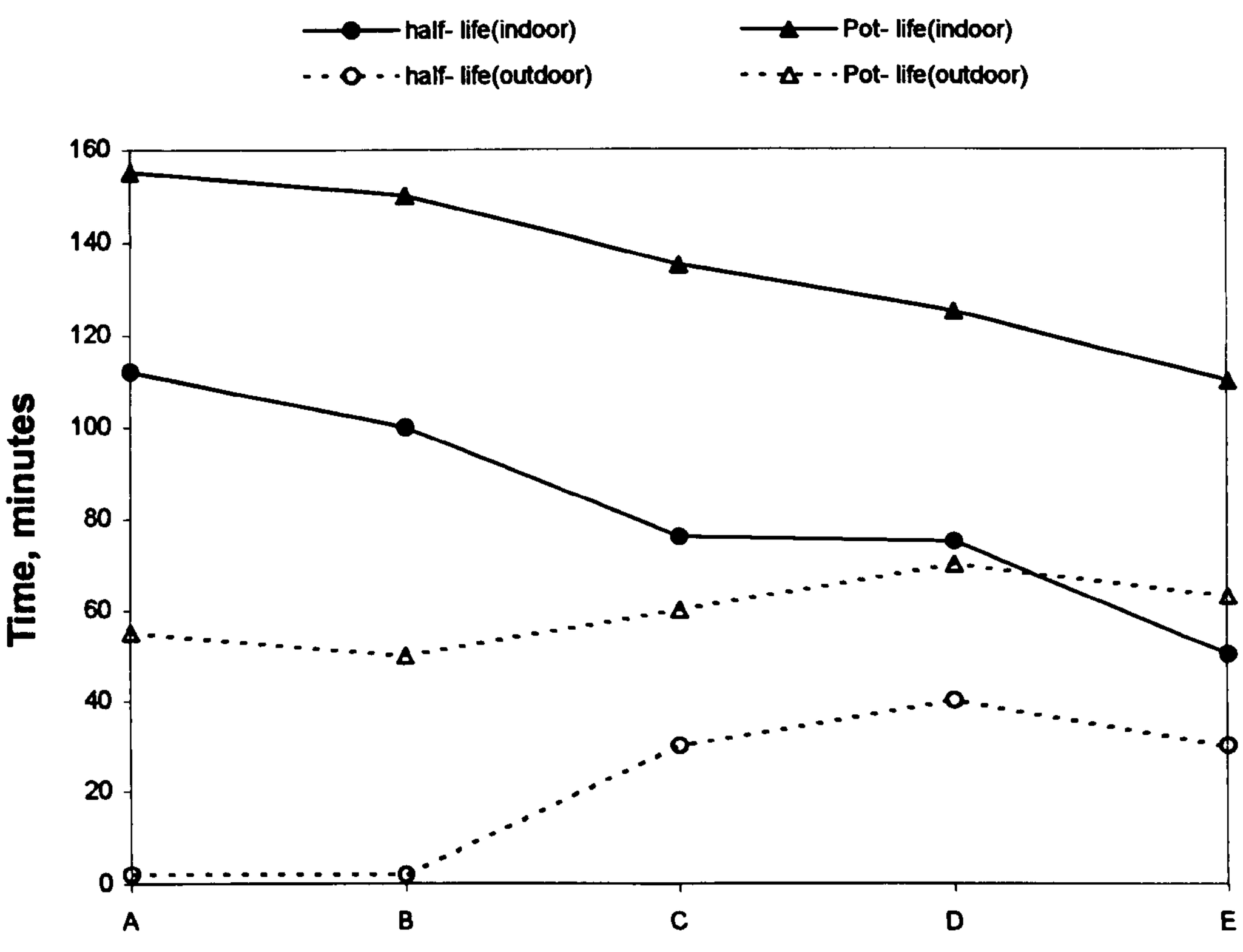

Fig. 4.7: Influence of mix type on workability loss.

4.6 Conclusions

The results obtained from this part of the research lead to the following conclusions:

1. The inclusion of GGBFS as replacement of OPC has no major effect on consistency results.
2. In the indoor environment, the inclusion of 5.5% of SF shows no si¸nificant effect on the setting times, and both setting times are similar to that of plain OPC.
3. The inclusion of GGBFS showed an increase in both setting times for both environments.
4. In the outdoor environment a reduction in the initial and final setting time was observed, this reduction was approximately by the same amount for all mixes.
5. The inclusion of GGBFS and chemical admixture showed a faster loss of slump than plain OPC concrete when tested in the laboratory environment, while plain OPC concrete in real outdoor environment showed a faster loss of slump than the GGBFS concrete.
6. The effect of chemical admixture in hot environment was limited. Using GGBFS to extend working time is better than using a superplasticizer, although the later is required from other consideration.
7. The inclusion of GGBFS reduced the amount of superplasticizer.

Chapter Five

ENGINEERING PROPERTIES

5.1 Introduction

The new composite cement materials are widely used and have improved the quality of portland cements. Apart from improved durability properties, the most widely quoted incentive for the utilisation of ground granulated blast furnace slag (GGBFS) is the part substitution portland cement with an industrial by product. To compensate the low early strength of concrete mixes resulting from the use of GGBFS, silica fume (SF) was used in this study. One of the advantages of part replacement of ordinary portland cement (OPC) with slag is the economy of the final concrete mix. Besides having the ability to reduce temperature rise during hydration, the use of GGBFS in concrete is beneficial to many engineering properties of concrete in the fresh and hardened states. Compared to portland cement, slag cements have a reduced water demand, and improve the short and long term engineering properties. Moreover, the use of blended cement materials has been reported to increase the resistance of the resulting concrete to deterioration by aggressive chemicals such as chlorides [12,131]. The increased durability of concrete with mineral admixtures is attributable to its ability to reduce permeability, and it also results from the finer pore structure [12,29,69,131]. In this chapter, the long term properties of slag concrete incorporating a constant amount of SF, both as part replacement of cement are presented. Compressive strength, ultrasonic pulse velocity, dynamic modulus of elasticity, shrinkage and expansion are discussed. In addition, since strength in compression is commonly accepted as a general index of concrete quality, the relationship between compressive strength and dynamic modulus of elasticity is also discussed. All properties were determined for different curing regimes in two environments (indoor and outdoor), and at different ages.

5.2 Compressive strength

On of the inherent disadvantages of portland cement concrete is the time required to develop its full strength under normal conditions. The time taken to achieve a specific strength is a practical and economic factor important in construction technology. The most satisfactory source to achieve high strength and high early strength therefore appears to be the cement binder itself [132].

5.2.1 Early age compressive strength (less than 28 days)

Figs. 5.1-5.4 present the early age compressive strength for all mixes in both environments, indoor as well as outdoor, and these are also quantified in Tables 5.1 and 5.2. In the indoor environment the 1-day compressive strength of all the mixes varied from 20 to 30 MPa; mixes B and C exhibited the highest values followed by the control mix (mix A), as an increase in the amount of slag caused the compressive strength to decrease. On the other hand, there was no significant effect of moist curing on the first day in this environment. A similar trend was found for the 3 day compressive strength but with an increase in strength of about 33% to 40% for all the mixes.

These values increased by more than double after 7 days, with strength values in the range from 43-70 MPa, and further ageing up to 14 days increased the strength of 7 wet/air cured specimens significantly. Mix B (378 OPC + 22 SF) under all curing conditions exhibited values of compressive strength higher than those of mix A (400 OPC); this increase in strength was observed from the first day of casting, and it also produced the highest values of compressive strength among the five mixes at early ages. This is due to the high reactivity and fineness of silica fume. This finding is in agreement with those of Alkhaja[133]who studied the effect of 10% silica fume on the early age compressive strength at controlled temperature and humidity (23°C + 65%RH). In his tests, he found that, the increase in compressive strength was about 15.3, 7.7, 10.4, 18.5 and 18.3% at 1, 3, 7, 28, and 33 days respectively. Other research studies [134,135] have indicated that the 1 day compressive strength of silica fume concrete is generally equal to or slightly higher than the strength of plain concrete regardless of whether the silica fume is used as direct replacement or as an admixture, Carette [135] related such observation to the early start of the pozzolanic reaction due to the use of silica fume, although this may also be partially accounted for by the filler effect of silica fume resulting in a denser matrix structure. Contrary to this finding, it

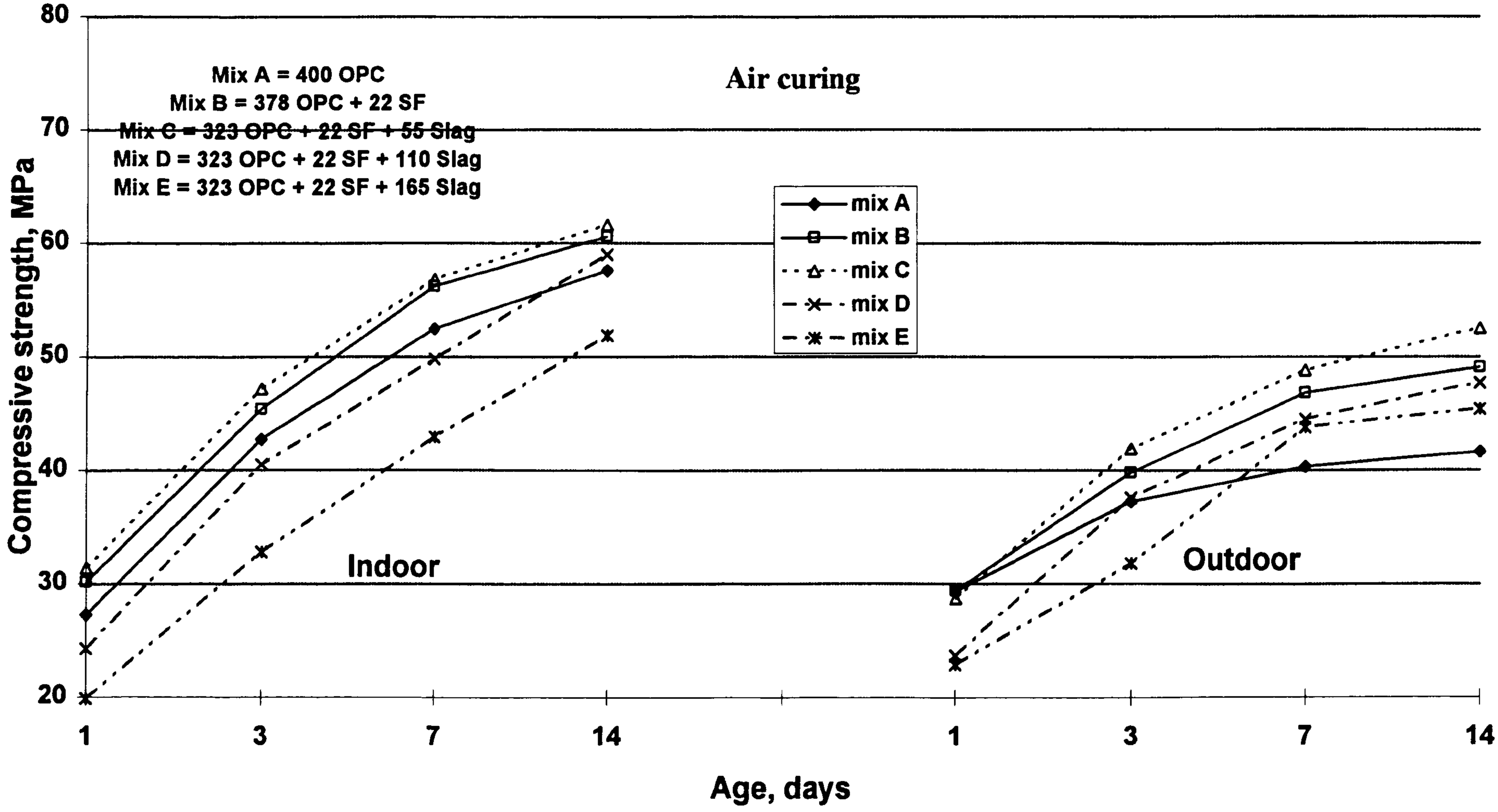

Fig. 5.1 : Influence of mix type on compressive strength under air curing.

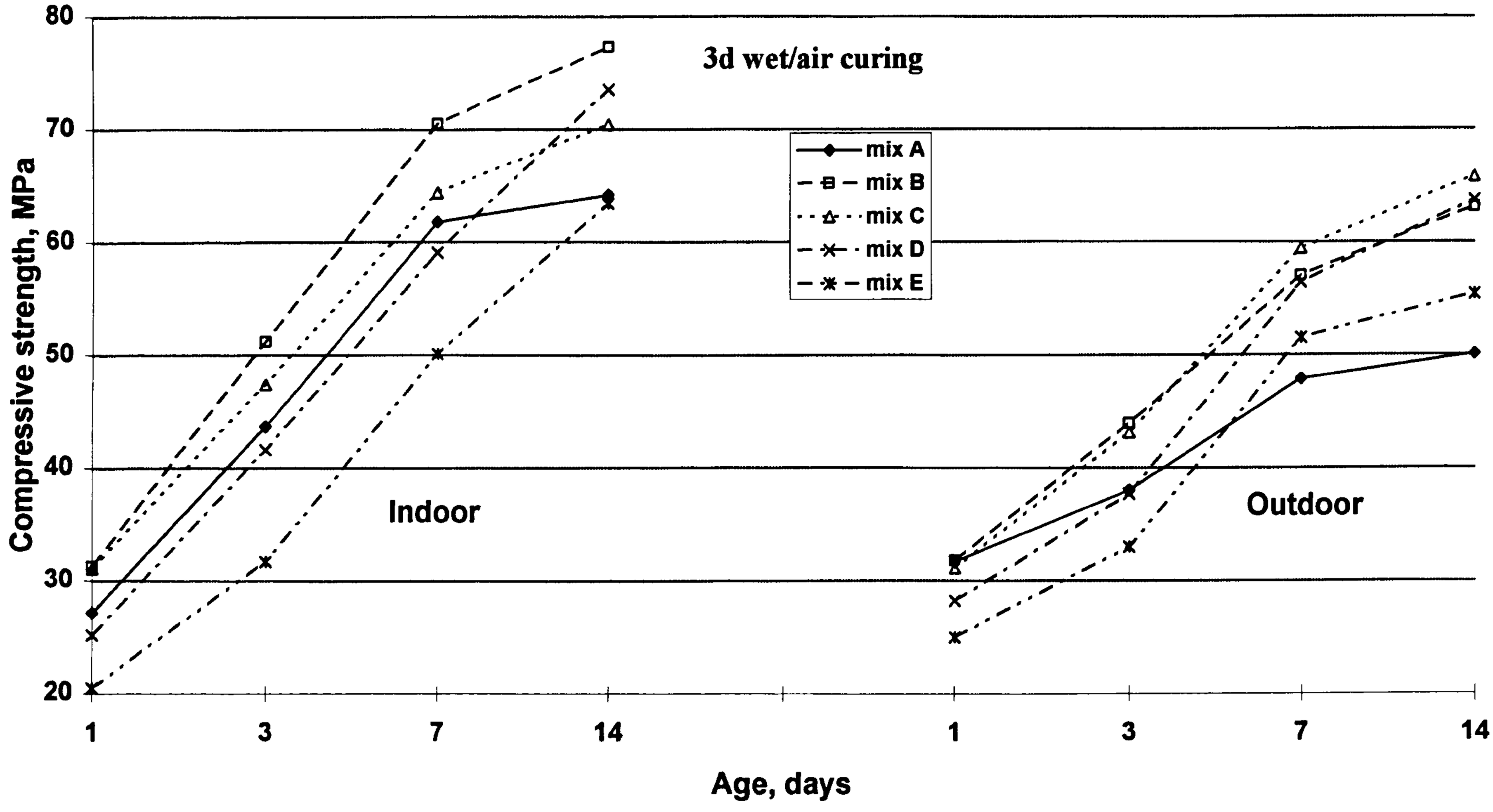

Fig. 5.2 : Influence of mix type on compressive strength under 3d wet/air curing.

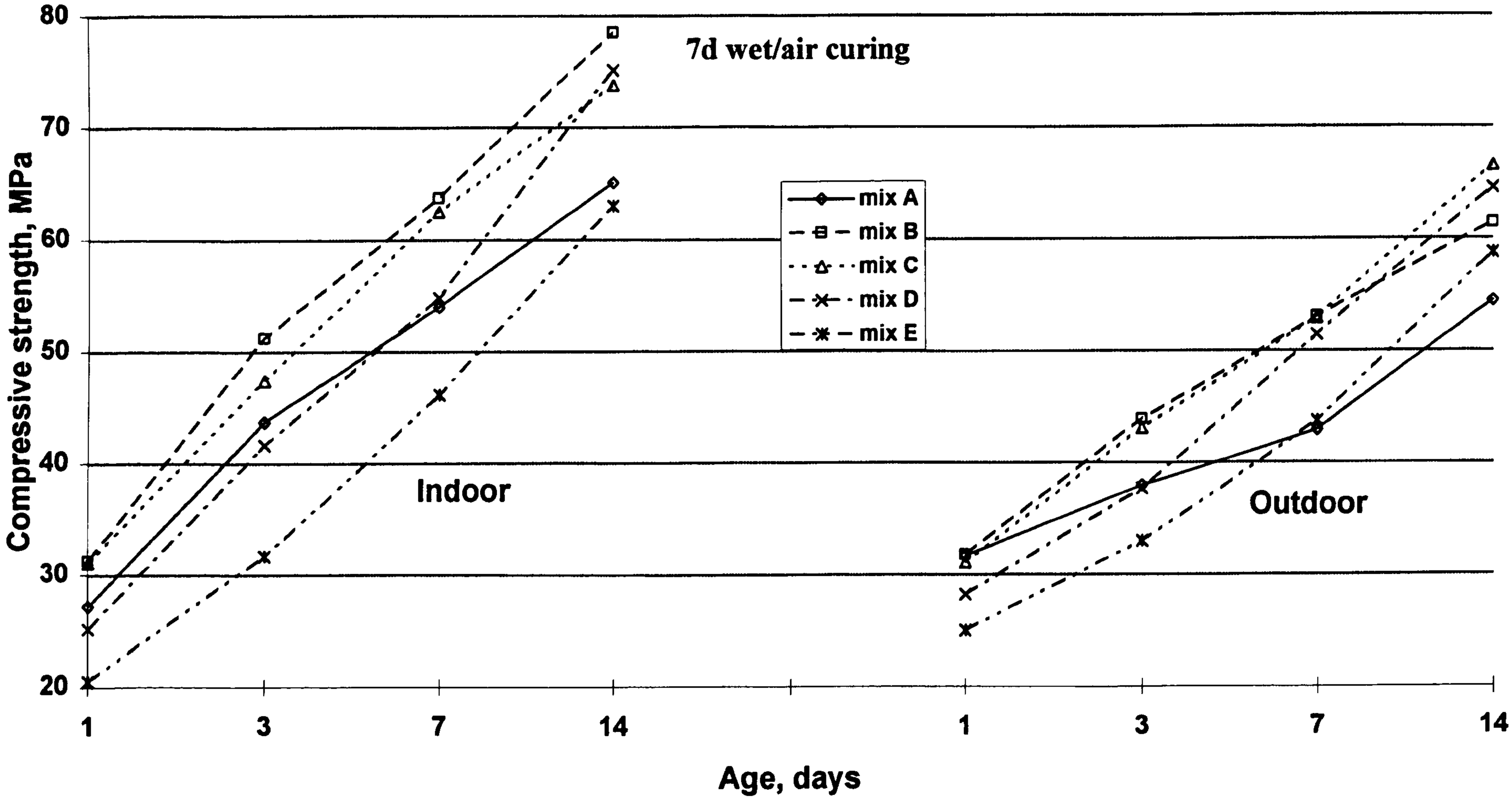

Fig. 5.3 : Influence of mix type on compressive strength under 7d wet/air curing.

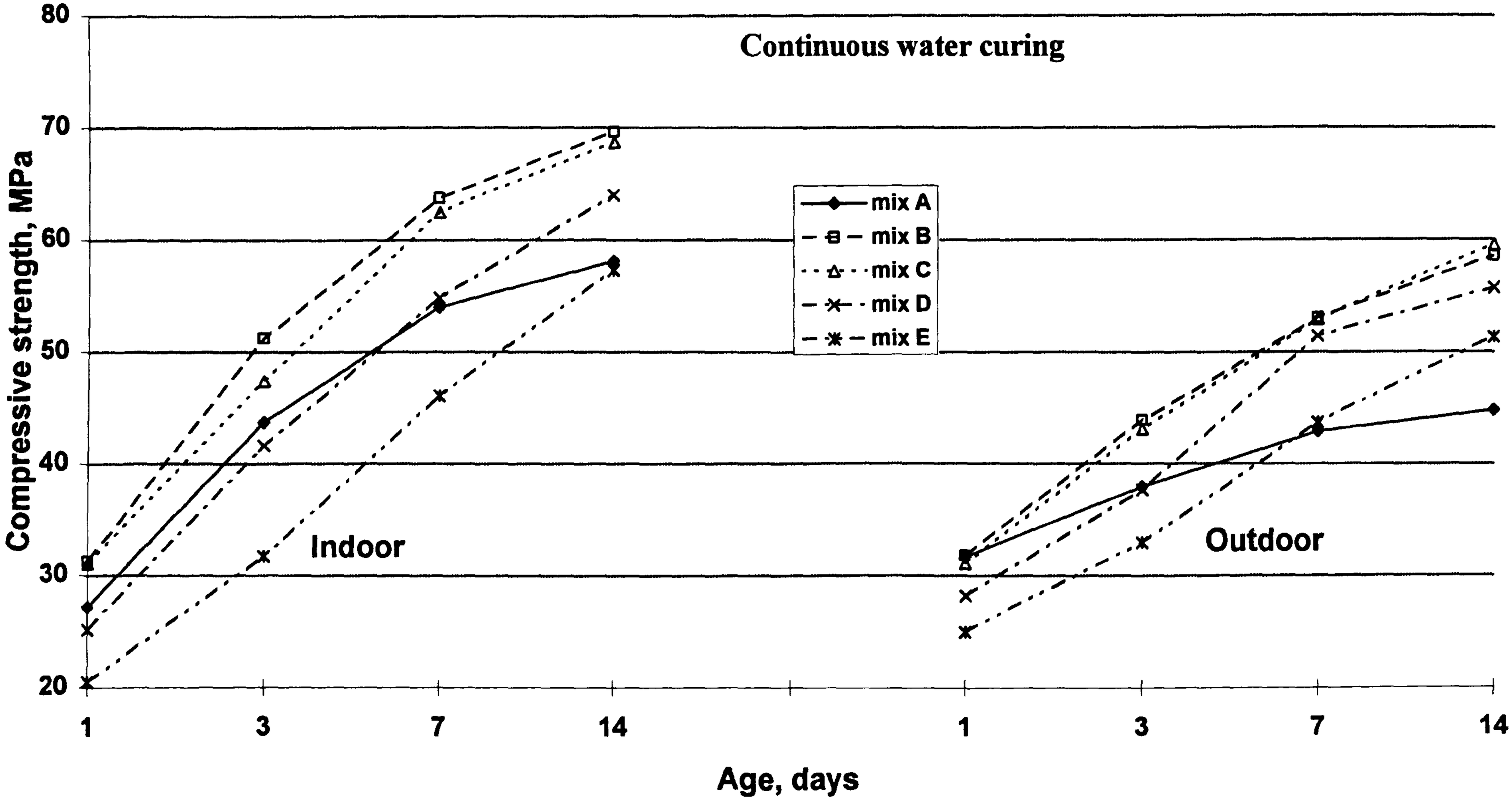

Fig. 5.4 : Influence of mix type on compressive strength under continuous water curing.

has been reported [136] that, for moist curing near to 20°C, it has been established that the strength development of silica fume concrete is slower than that of a control concrete of equal 28 day compressive strength. This difference increases with increasing silica fume dosage and decreasing temperature.

Mix C which had a limited amount of slag (323 OPC + 22 SF + 55 slag) produced values of compressive strength lower than that of mix B at early ages, which indicates that this small reduction in compressive strength of mix C is due to the low amount of slag added, and therefore, its small effect; the inclusion of silica fume in mix C, on the

Table 5.1 Compressive strength (MPa) in the indoor environment.

Age	(days)	1	3	7	14	28	91	182	365	540
Mix	Curing	MPa	MPa	MPa	MPa	MPa	MPa	MPa	MPa	MPa
A	air	27.3	42.7	52.5	57.6	58.2	59.9	55.6	56.0	57.4
	3d w/a	27.2	43.7	61.8	64.2	69.0	69.1	68.3	65.1	67.4
	7d w/a	27.2	43.7	54.0	65.1	69.4	71.2	71.1	69.6	73.6
	wet	27.2	43.7	54.0	58.1	63.6	65.0	73.1	73.2	71.7
B	air	30.2	45.4	56.2	60.6	67.9	69.4	68.4	66.9	67.8
	3d w/a	31.3	51.2	70.5	77.3	83.8	84.5	85.4	84.0	81.4
	7d w/a	31.3	51.2	63.7	78.5	88.9	89.2	87.5	87.5	88.1
	wet	31.3	51.2	63.7	69.6	77.7	79.7	86.5	91.8	90.5
C	air	31.4	47.2	56.8	61.6	68.7	69.7	66.9	63.3	65.1
	3d w/a	31.1	47.4	64.4	70.4	82.0	82.8	85.1	79.7	82.9
	7d w/a	31.1	47.4	62.5	73.7	82.8	86.2	92.3	88.0	85.7
	wet	31.1	47.4	62.5	68.7	75.6	79.0	90.2	91.0	94.1
D	air	24.3	40.5	49.8	59.0	60.2	63.9	63.6	62.0	62.8
	3d w/a	25.2	41.6	59.1	73.5	76.4	82.2	84.5	76.3	80.1
	7d w/a	25.2	41.6	54.8	75.1	79.0	88.2	91.1	84.6	86.5
	wet	25.2	41.6	54.8	64.0	74.6	85.5	95.5	94.8	92.9
E	air	20.0	32.8	42.9	51.9	54.8	58.4	61.2	57.0	57.7
	3d w/a	20.5	31.7	50.1	63.4	69.4	73.3	77.0	72.0	74.6
	7d w/a	20.5	31.7	46.1	63.0	75.6	81.7	86.2	80.0	82.1
	wet	20.5	31.7	46.1	57.3	69.1	80.6	83.1	87.2	90.0

Table 5.2 Compressive strength (MPa) in the outdoor environment.

Age	(days)	1	3	7	14	28	91	182	365	540
Mix	Curing	MPa	MPa	MPa	MPa	MPa	MPa	MPa	MPa	MPa
A	air	29.3	37.3	40.3	41.6	44.2	47.0	51.0	58.1	56.6
	3d w/a	31.7	38.0	47.9	50.1	57.1	60.4	63.0	69.7	66.9
	7d w/a	31.7	38.0	42.9	54.4	59.2	61.4	66.7	70.5	65.5
	wet	31.7	38.0	42.9	44.8	49.5	57.0	67.0	66.9	66.9
B	air	29.4	39.8	46.8	49.1	52.0	53.9	57.4	58.9	55.0
	3d w/a	31.8	43.9	57.0	63.1	66.1	70.0	79.4	77.3	72.0
	7d w/a	31.8	43.9	53.0	61.4	71.1	73.2	81.9	83.0	75.5
	wet	31.8	43.9	53.0	58.5	60.5	64.8	73.7	79.8	80.0
C	air	28.7	41.9	48.8	52.5	54.7	55.5	55.0	57.0	51.9
	3d w/a	31.1	43.1	59.4	65.8	64.6	70.0	74.5	76.5	72.0
	7d w/a	31.1	43.1	52.9	66.5	65.8	74.2	78.5	79.7	73.7
	wet	31.1	43.1	52.9	59.5	59.8	62.4	68.0	72.6	73.3
D	air	23.7	37.6	44.5	47.7	48.9	51.9	56.9	59.6	52.1
	3d w/a	28.2	37.7	56.4	63.7	67.0	69.4	76.0	74.2	70.1
	7d w/a	28.2	37.7	51.4	64.5	68.7	75.3	77.9	79.9	71.3
	wet	28.2	37.7	51.4	55.7	56.7	63.0	68.1	78.3	81.0
E	air	22.9	31.8	43.8	45.4	48.3	50.7	55.9	54.7	48.2
	3d w/a	25.0	33.0	51.5	55.4	59.9	63.2	71.0	71.8	65.1
	7d w/a	25.0	33.0	43.7	58.7	60.1	68.1	74.8	72.4	67.4
	wet	25.0	33.0	43.7	51.3	54.0	58.2	67.9	72.9	72.0

other hand, produced values of compressive strength higher than that of mix A (400 OPC). It is clear from these figures and Table 5.1 that the early gain in compressive strength of concrete incorporating SF and GGBFS results from a combination of factors, such as high reactivity and fineness of SF, and hence an early start of pozzolanic reaction, and the increased rate of hydration of the OPC due to the presence of SF and GGBFS. The contribution from the physical and chemical effects of SF in hydrating portland cement concrete, however, starts immediately after mixing, and follows a course of action similar to that of the OPC itself. Mix D (323 OPC + 22 SF +

110 slag) caused a reduction in the strength at early ages (1 and 3 days) compared to that of concrete made with only OPC. This loss in strength could be compensated by the addition of as little as 10% SF. A similar approach was taken by Malhotra [36] and a noticeable strength increase was recorded during the early ages in moist curing [51] when most of the pozzolanic reaction takes place. As the amount of slag increased the compressive strength decreased. Because the reactivity of GGBFS is lower than 'hat of portland cement, the initial compressive strength (0-7 days) of slag concrete (mix E) is low compared to that of plain concrete, silica fume concrete or even mixes containing limited amount of slag (mix C). This is due to the fact that the slag proportion is higher, and it could not contribute as a binder until at a later age. Others researchers [50,67,137,138] have come to similar findings.

The effect of water curing on the development of compressive strength at early age is very clear; at 7 days after casting, under continuous drying in air all mixes exhibited values in the range of 43-57 MPa, whereas the corresponding values under 3d wet/air curing were in the range of 50-70 MPa; this was the case with all cementitious materials studied, which indicates the importance of early age water curing. Similar findings have also been reported by others [139,140].

These data also show the effect of exposure environment on compressive strength. It is clear that the increased ambient temperature in the outdoor environment accelerates the hydration reaction in the control and blended cement concrete. This is reflected in higher strength at first day for all mixes under investigation compared with corresponding strength achieved under the indoor environment condition. Cebeci [7] has studied the effect of simultaneous changes in the curing temperature (17°C and 37°C) on the strength development of plain concrete at various ages. The results indicate that, under water curing, the high temperature leads to an increase in the compressive strength at early ages (i.e. 3, 7 and 28 days) while decreasing the compressive strength beyond 90 days.

Studies were also made by Rose [8] to determine the effect of three curing environments, 10, 23 and 32°C on concrete containing 0, 30 and 50% slag; he found that, for pure cement the curing temperature increased compressive strength at early ages (3 and 7 days) to obtain values higher than those at low temperature, and this trend was reflected at 28 days. On the other hand, slag concrete produced values of compressive strength at temperatures 23 and 32°C higher than the value at 10°C.

In this study, compressive strength was found to be affected more by outdoor condition than the indoor condition. All mixes exhibited development in compressive strength on the first day, but after that all the mixes exhibited a slower rate of strength gain, under the four curing conditions. For example, at 14 days, mix A under continuous air curing exhibited the highest loss in compressive strength of about 16 MPa; the inclusion of silica fume (mix B) reduced this loss, the corresponding loss with mix B was 11 MPa. On the other hand, the inclusion of slag (mix C) also reduced this loss and the loss in strength value for this mix was 9 MPa; and further increase in the slag content produced less loss in compressive strength than the control mix, the corresponding losses for mixes D and E being 11 and 6 MPa, respectively.

In the outdoor environment, significant increase was observed due to exposure environment on the one day compressive strength. For example, mix E specimens showed an increase of about 14.5 and 18% for air cured and wet cured specimens respectively, while mixes A and D showed little increase due to outdoor environment on the first day. At 3 days after casting, mix E (which contained the highest amount of slag) specimens cured in water showed an increase of about 4% in compressive strength values due to outdoor exposure. Others [8] have shown that the strength of slag concrete at high temperature was improved. Mixes A to D showed a reduction in compressive strength of about 3 to 7 MPa, this reduction in compressive strength due to exposure environment may be attributed to the fact that the large and continuous daily fluctuation in both temperature and relative humidity initiates cycles of wetting and drying, which causing subsequent adverse effects on hydration and the physical properties of concrete. In addition to this, a direct influence of solar radiation and low relative humidity at mid day in hot climates is the excessive loss of water especially after casting when for specimens placed in outdoor environment during the first 24 hours, this loss of water may lead to reduction or complete stoppage of hydration.

5.2.2 Effect of curing, Indoor

The effect of curing regime on compressive strength is shown in Figs. 5.5-5.9 and Tables 5.1 and 5.2. These data show that specimens initially cured in water for period of 7 days or even 3 days resulted in higher strength for all mixes and in both environments. Longer curing periods obviously allow more time for hydration to take place and hence contribute to stronger material [141].

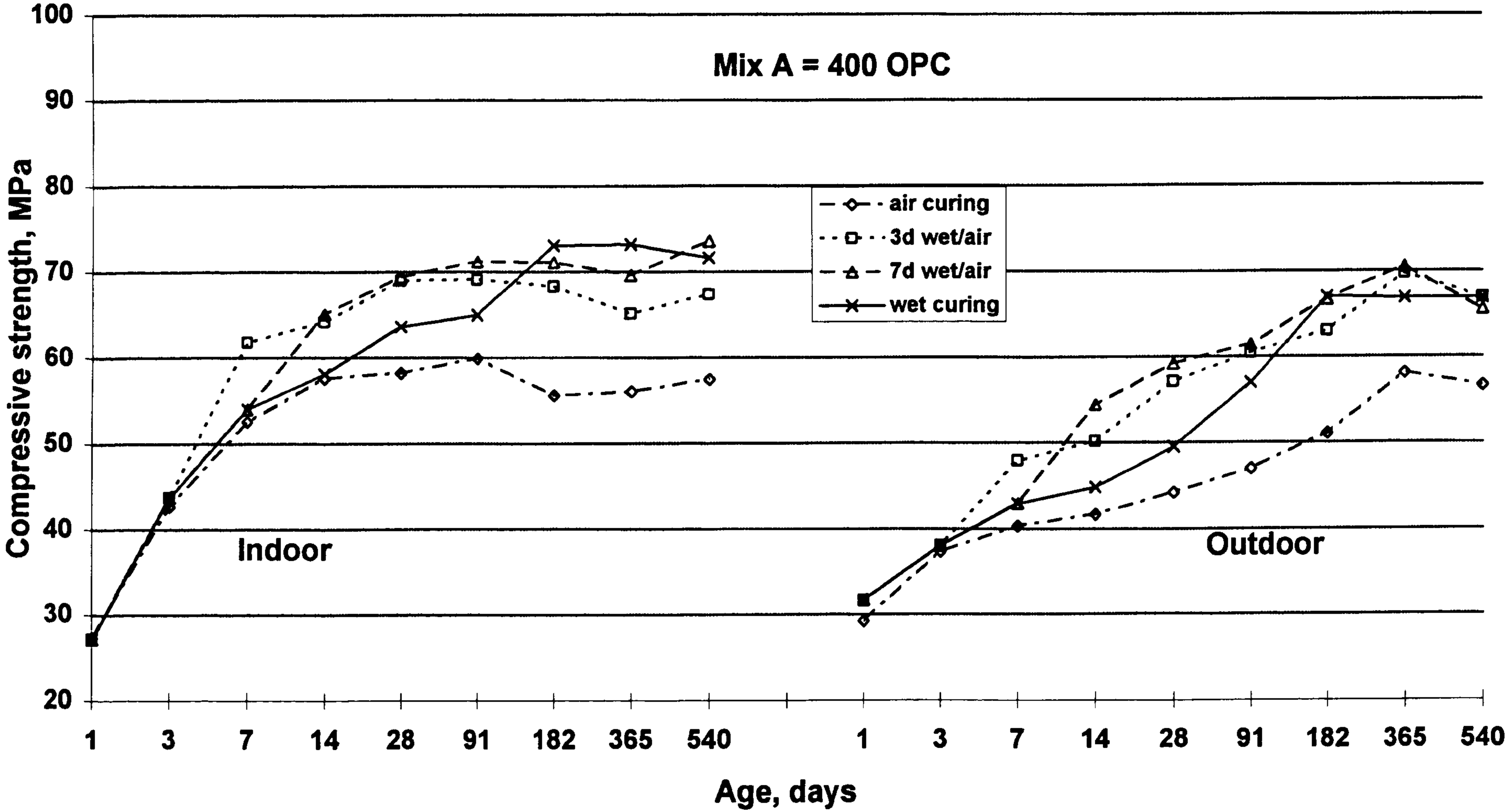

Fig. 5.5 : Influence of curing regime on compressive strength for mix A.

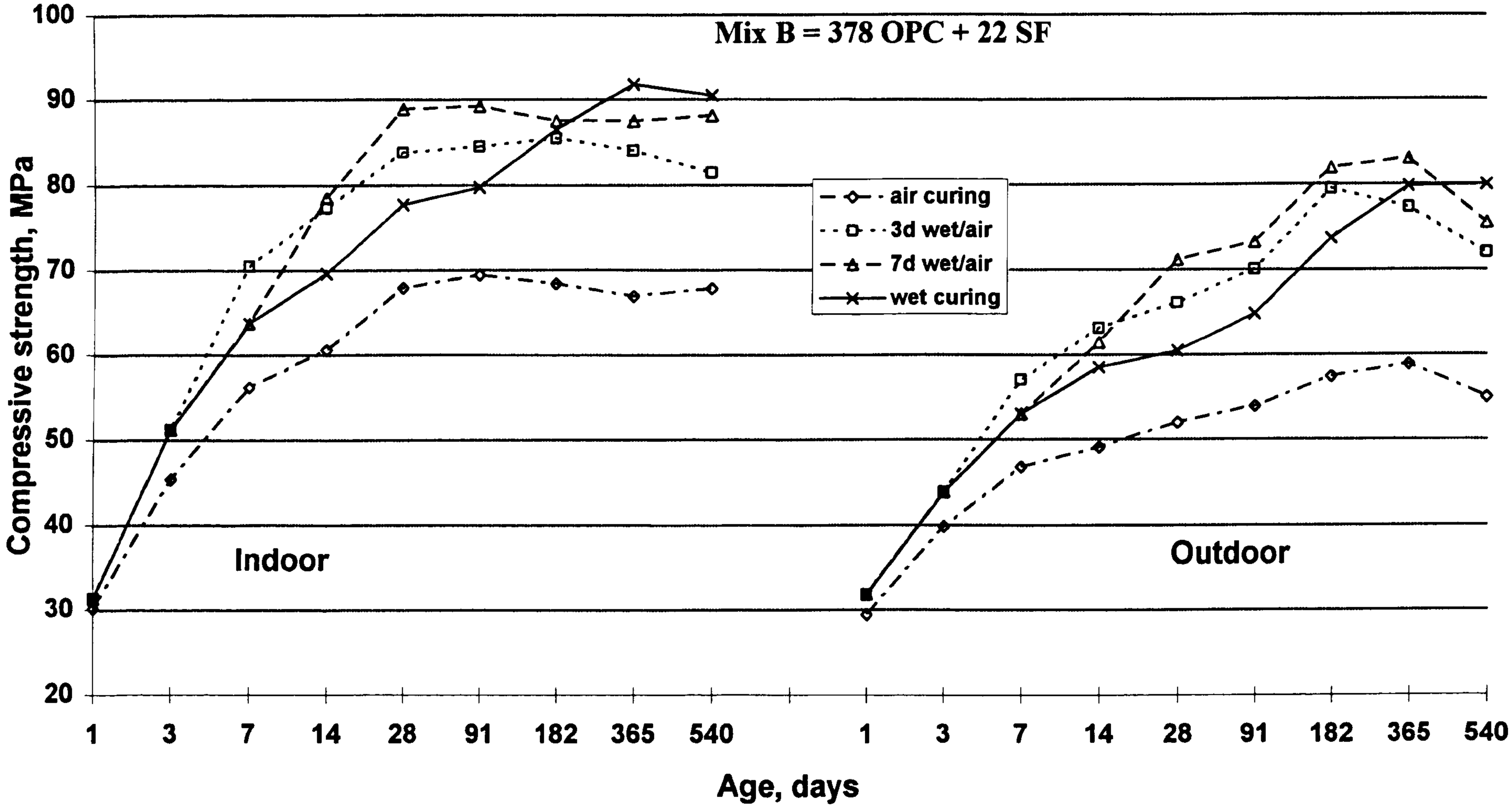

Fig. 5.6 : Influence of curing regime on compressive strength for mix B.

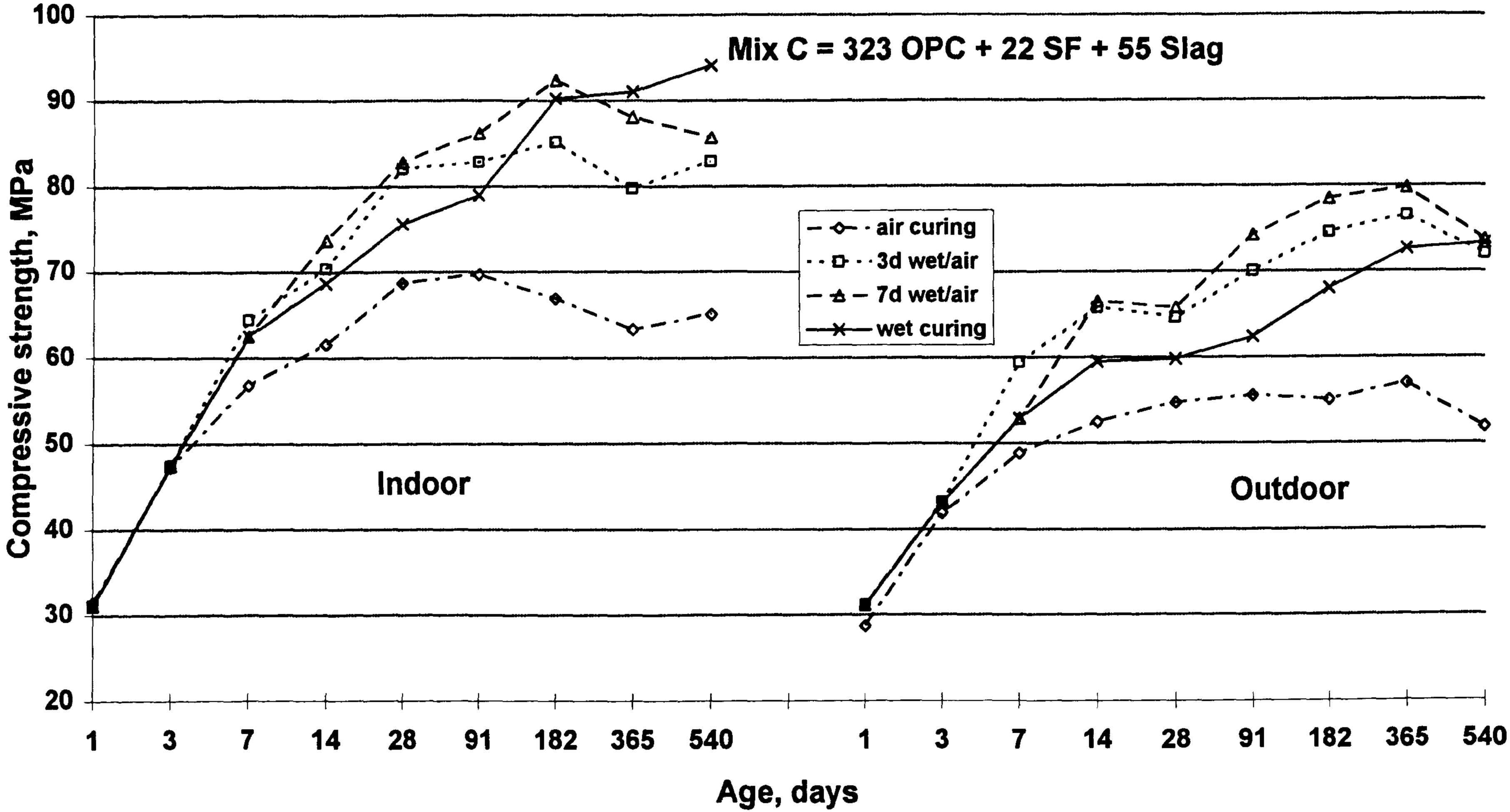

Fig. 5.7 : Influence of curing regime on compressive strength for mix C.

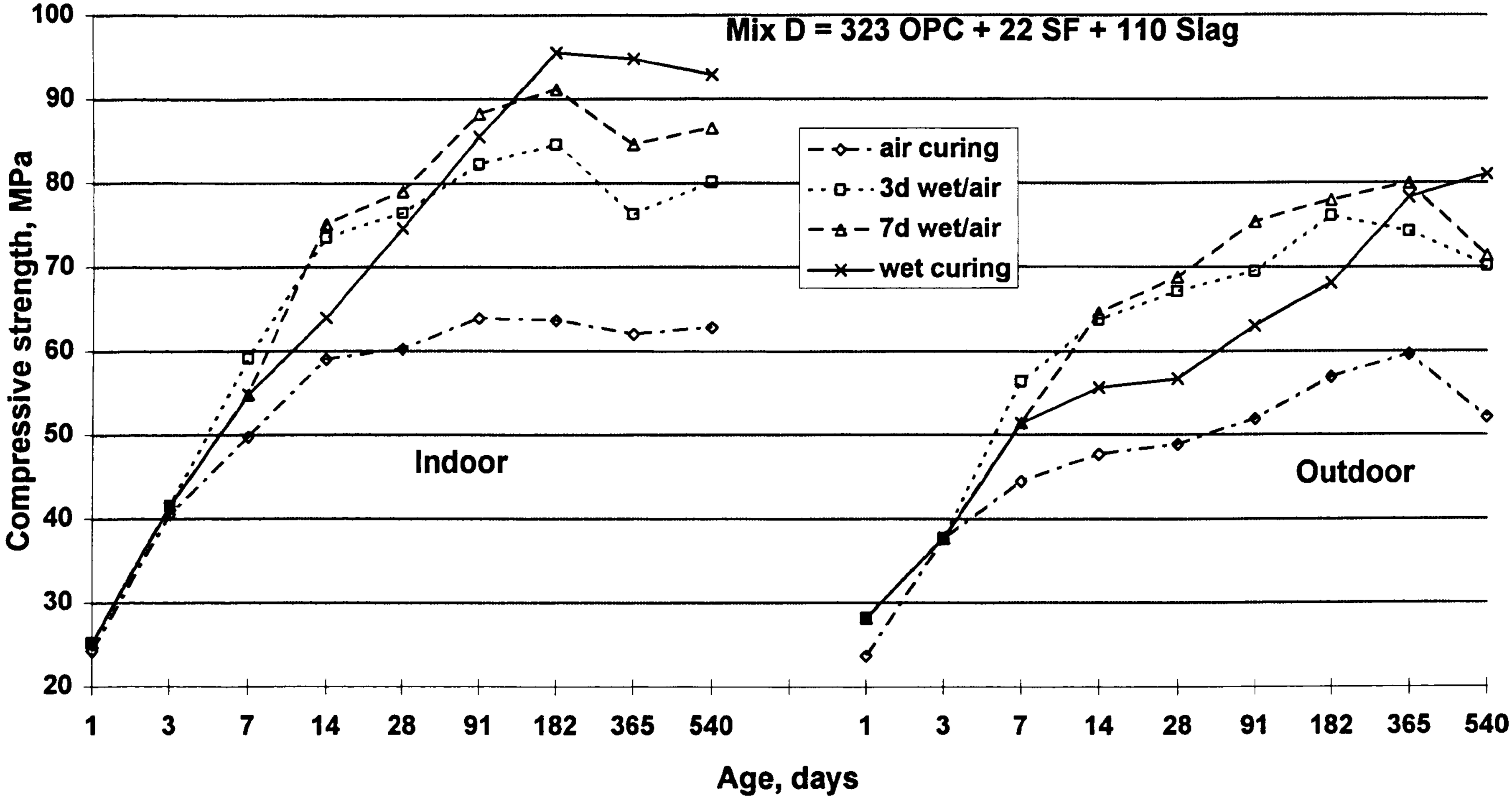

Fig. 5.8 : Influence of curing regime on compressive strength for mix D.

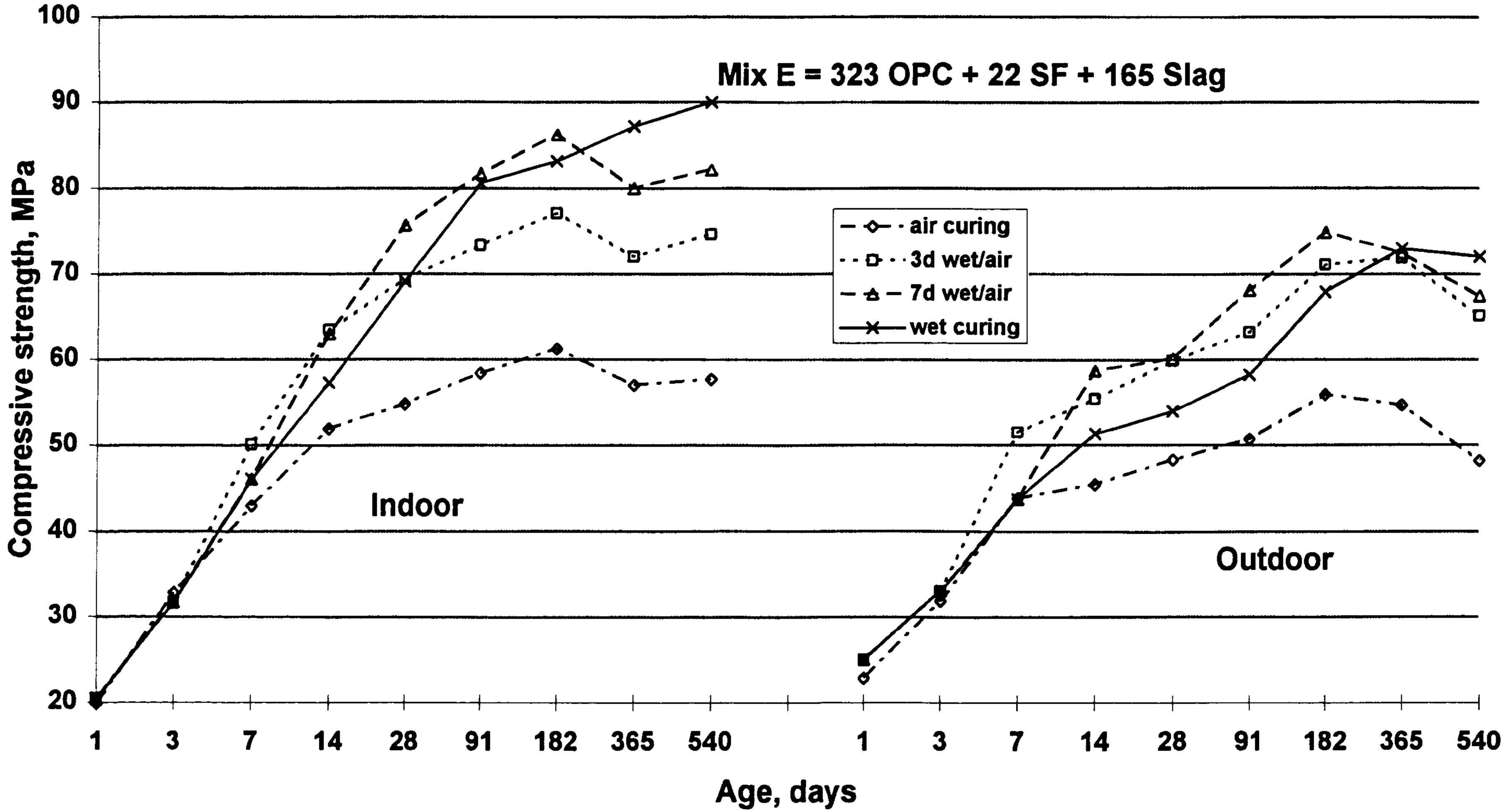

Fig. 5.9 : Influence of curing regime on compressive strength for mix E.

Fig. 5.5 shows the influence of curing on the compressive strength of mix A (400 OPC). Specimens under continuous water curing in the indoor environment showed values of compressive strength at 28 days lower than those of concrete initially cured in water for 3 or 7 days. Such phenomenon has been observed by many researchers [47,142,143]. The explanation suggested by Popovics [143] is based on the observation that drying decreases the volume of the hardened cement paste. These volume reductions are caused by the increased surface tension in water-filled small pores during drying, which reduces the distance between the surfaces of the hydrated cement gel. The strength is then increased due to the increased bond between these surfaces. In addition to this, Popovics reported that fully saturated concretes are expected to be lower in strength than dry samples due to the internal water pressure exerted on the surface of the cement gel when external pressure is applied [142].

A similar trend was found at 91 days. It is clear from the figure that, the compressive strength beyond six months is more affected by the extent of early age water curing. Specimens cured continuously in water exhibited slightly higher compressive strength values. On the other hand, prolonged air curing showed significant reduction in compressive strength starting at 14 days, to exhibit a maximum reduction of 17 MPa at 6 months when compared with the corresponding value under continuous water curing.

Mixes B and C exhibited similar trend to mix A but with different values; at 12 months indoor under air curing, both mixes showed a reduction in compressive strength of about 25 to 28 MPa respectively, when compared with the corresponding value under continuous water curing. This increase in the reduction of compressive strength may be attributed to the fact that mixes containing silica fume or SF/slag are more sensitive to water curing than the control mix.

In Fig. 5.9 the variation in the compressive strength development of mix E with age under various curing regimes are shown. The figure shows that at 28 days, the continuous water curing in indoor environment exhibited similar compressive strength, 69.1 MPa, compared with the 3d wet/air curing values of 69.4 MPa. On the other hand, the difference between both continuous water and 7d wet/air cured concretes and air cured concrete strengths is much greater with SF/slag than plain concrete which means that exposure to a drying was detrimental to strength development. As a consequence, more attention should be paid on job sites, and a minimum 7 day curing period has to

be recommended to achieve the strength potential of SF/slag concrete. At 18 months, the maximum value of compressive strength was registered for specimens under continuous water curing of 90 MPa, followed by 7d wet/air, 3d wet/air and air cured specimens with values of 82.1, 74.6 and 57.7 MPa, respectively.

Although the gap appears to grow bigger slowly with time between various curing regimes, in mix A this gap appears smaller than that in mixes containing slag and it is appears to be constant beyond 6 months. Mixes D and E shows similar trends. This means that the strength development of all the mixes have responded to the curing conditions at different levels depending on the type of cementitious material. Clearly curing times have to be increased to allow adequate strength development of mixes with slag [34].

Mix A specimens continuously cured in water show values approximately similar to the specimens cured 7d wet/air or even 3d wet/air, while significant development in strength was observed for specimens continuously cured in water, of about 25%, compared to specimens continuously dried in air. A similar trend was found for the other mixes, the corresponding values for mixes B, C, D and E being 33, 44, 48 and 56%, more than the strength values under air curing. This observation shows the importance of early age curing to develop the strength of concrete specially when mineral admixtures are used.

5.2.3 Effect of mix type, Indoor

Figs. 5.10 and 5.13 show the effect of mix types on compressive strength properties. These data show that the presence of silica fume helps to enhance early and long term strength (mix B), but the additional presence of slag in mix C produced similar strengths to mix B with reduced portland cement content. The optimum slag content appears to be given by mix D, and any further increase in slag (mix E) lowered the strength slightly. Overall, the mixes B and C have similar values of strength under all the curing conditions, particularly at later ages. In water curing conditions all the mixes in the indoor environment exceeded their 28 day target strength of 60 MPa.

Under continuous water curing, mix A presented the lowest compressive strength at 28 days and beyond to reach steady values beyond 6 months; the value at 18 months indoor was 71.7 MPa. The presence of silica fume showed superior development at early ages and in the long term; the compressive strength in the period from 28-90 days

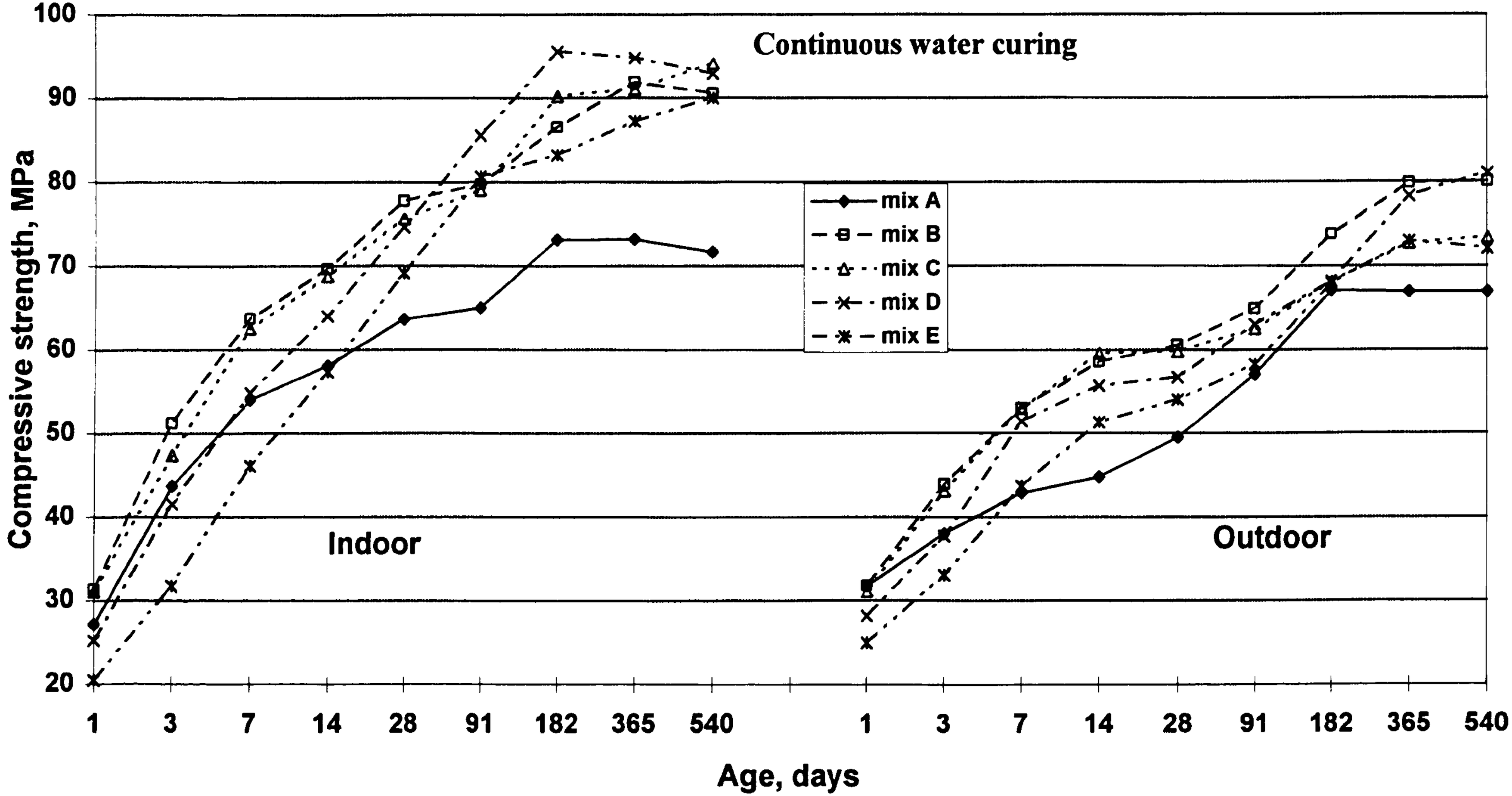

Fig. 5.10 : Influence of mix type on compressive strength under continuous water curing.

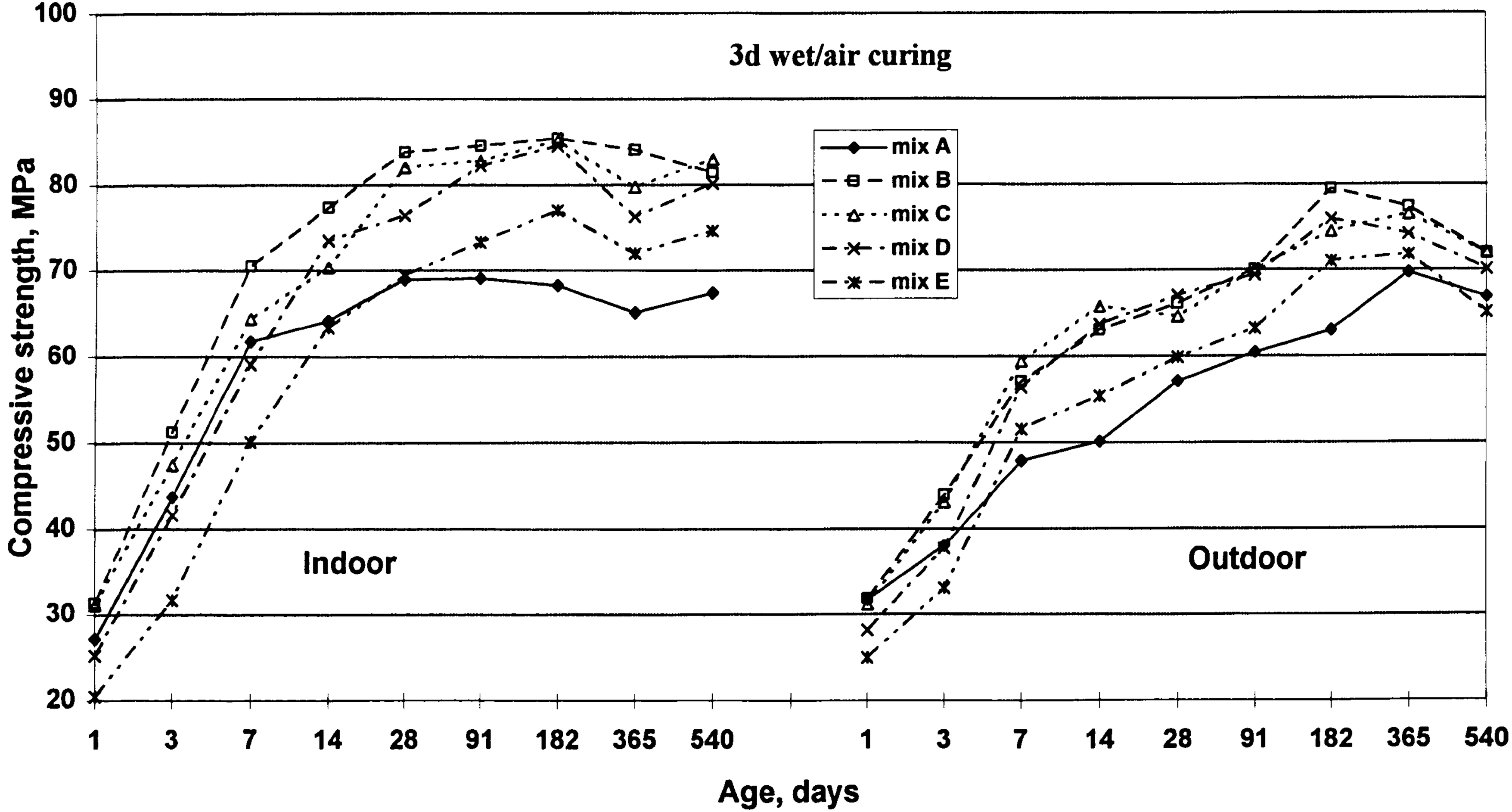

Fig. 5.11 : Influence of mix type on compressive strength under 3d wet/air curing.

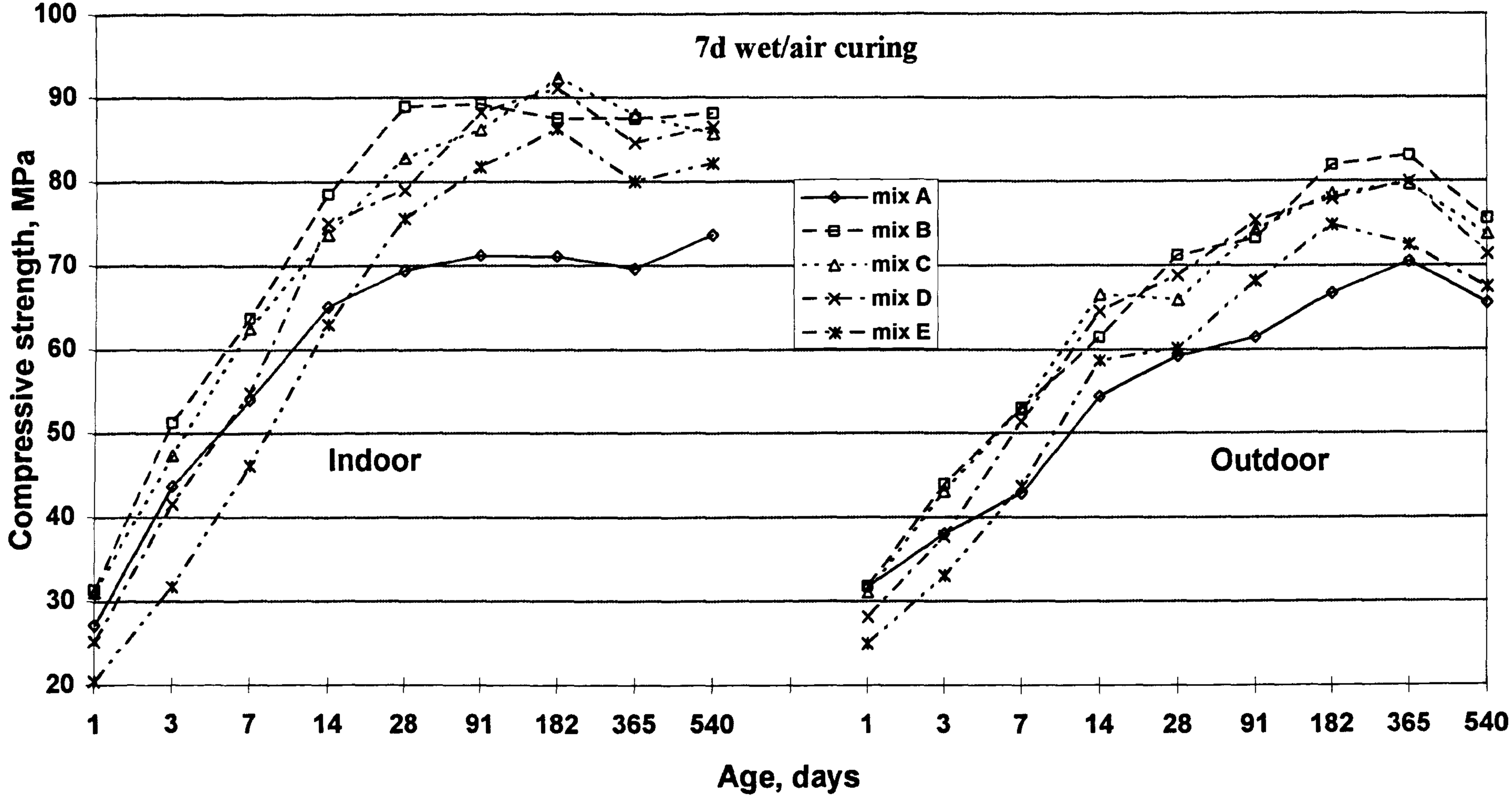

Fig. 5.12 : Influence of mix type on compressive strength under 7d wet/air curing.

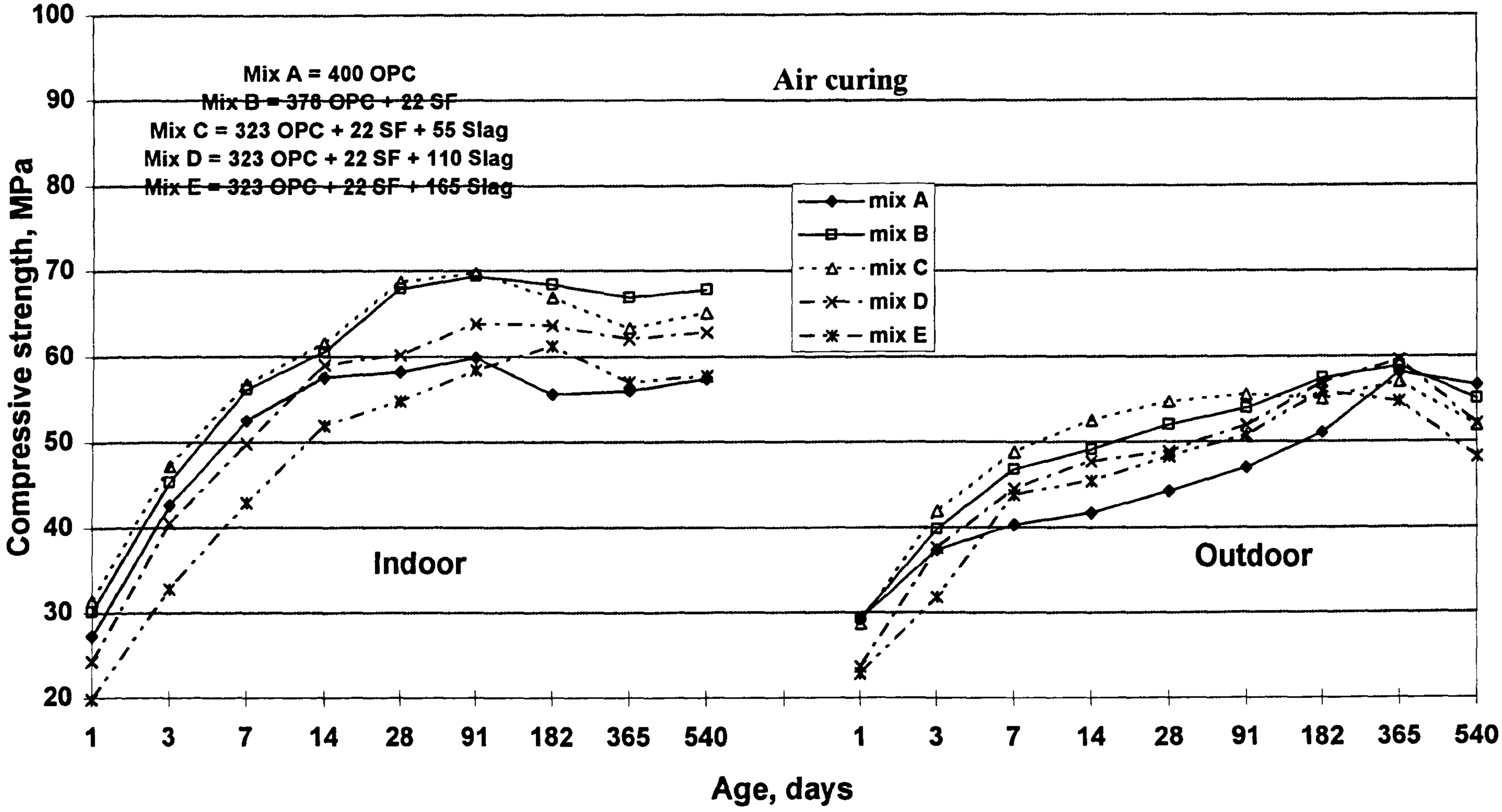

Fig. 5.13 : Influence of mix type on compressive strength under air curing.

was higher than the corresponding value of mix A by 18%. The corresponding value at 18 months was of 21% more than mix A, which indicates the continuity of strength development due to the influence of silica fume in the long term. Many investigations have measured strength development with respect to time for silica fume concretes, Johansen reported [136] little effect of silica fume on the strength gain between 28 days and 1 year and between 1 and 3 years for moist cured specimens. Mix C (323 OPC + 22 SF + 55 slag) showed a similar trend to mix B. The addition of slag (mixes D and E) followed the expected pattern, the early age strength of blends in the indoor environment was lower than for pure cement, whereas very high strength was obtained in the long term (18 months) compared with mix A. These increase were as much as 30 and 25% for mixes D and E respectively. Similar results have been reported by others [61,81,139,144].

At 28 days, mix B yielded the highest value of compressive strength and registered an increase of about 14.1 MPa over the control mix value, similar values of compressive strength were obtained for both mix C and mix D, 74.6 and 75.6 MPa with an increase of about 18% over the control mix. Mix E with the highest amount of slag showed slightly higher strength than mix A due to slag hydration. At 91 days, mixes B, C and E showed similar values of about 80 MPa. Mix D exhibited slightly higher strength than these mixes, of about 85.5 MPa. On the other hand, mix A showed a reduction of compressive strength of about 20 MPa compared with the corresponding value of mix D, this is logical because mix D contained 5.5 % SF and 24.2% slag and both binders are effectively under adequate water curing to produce high strength concrete.

The compressive strength development for all mixes in the indoor environment under 3d wet/air curing is shown in Fig. 5.11. A reduction in compressive strength has been found for all mixes when compared with continuous water curing; this reduction is high for mixes A and E at 18 months, which showed values of compressive strength of about 67.4 and 74.6 MPa respectively. Mixes B, C and D exhibited strength of 81.4, 82.9 and 80.1 MPa, respectively.

Fig. 5.12 shows a comparison of compressive strength development under 7d wet/air curing. The development of compressive strength is similar to that of 3d wet/air cured concretes but with higher strength values due to the influence of good curing at early age. Mixes B, C and D exhibited similar compressive strength values in the long

term (12-18 months), higher than that of the control mix, which indicates the pozzolanic activity of these mixes at this stage and confirms the possibility of continuing the strength development at later ages. Mix E (with the largest amount of slag) exhibited values of strength lower than mixes B to D but with increasing water curing, (as shown in Fig. 5.10) it can develop similar values to these mixes at 18 months. Mix A exhibited the lowest strength at 28 days and beyond, and exhibited a reduction in the strength of about 8 to 15 MPa than the corresponding values of the other mixes at 18 months. The values registered at 18 months were 67.8, 65.1, 62.8, 57.7 and 57.4 MPa for mixes B, C, D, E and A respectively.

Development of compressive strength of all mixes under air curing is shown in Fig. 5.13. Mix A gave the lowest value at 6 months and beyond, followed by mix E which gave the lowest values up to age of 91 days, then gave similar values to mix A at 12 and 18 months. The inclusion of silica fume in mix B (378 OPC + 22 SF) exhibited the highest values of compressive strength at early age and in the long term, 18% higher than that of mix A (400 OPC) specimens when tested at 18 months. This is in agreement with Khan et al [139] who investigated plain OPC mortar specimens and compared them with silica fume concrete subjected to water curing for 0, 3, 7, 14 days and continuously water cured and tested at 28 days. The results showed that silica fume specimens obtained higher strength than plain OPC under all the curing regime. Roy [144] explain such observation due to the high rate of hydration of cement containing silica fume compared to OPC concrete; this high hydration due to silica fume is attributed to the fact that silica fume particles accelerate the hydration of tricalcium silicate (C_3S), the cement compound primarily responsible for strength development at early ages. Mix C with limited amount of slag exhibited compressive strength values higher than that of the control mix due to pore refinement of both SF and slag. Mix D showed a reduction in compressive strength compared with mix C at early ages, but similar values at long term due to the increase in slag content (110 kg/m^3). The adverse effect of no water curing on compressive strength of blended cement concrete can be readily seen in the figure 5.10-5.13, the gap appears to be bigger slowly with increasing water curing between mix A and the blended cement concretes. Under air curing this gap appears smaller between mix A and the other mixes which is in the range of 0.3 - 7.7 MPa at 18 months, while under 3d wet/air curing the corresponding values is in the range of 7.2-15.5 MPa. Any further increase in water curing increases this value, the

corresponding values under 7d wet/air curing is in the range of 8.5-14.5 MPa, whereas the corresponding values under continuous water curing is in the range of 18.9 - 22.4 MPa.

5.2.4 Effect of exposure environment

In order to provide a realistic simulation of daily temperature fluctuations, the actual ambient temperature variation in Dubai for the six summer months of April to September were analysed for an 18 month period to investigate its effect on compressive strength. Significant effects were found for all the mix specimens exposed to outdoor environment. All the data are given in Figs. 5.1 to 5.13 and Table 5.1 and 5.2. All the mixes at later ages under the four curing regimes show lower compressive strength in the outdoor environment compared with those in the laboratory environment. Also, with the exception of continuous water curing, all mixes in the outdoor environment produced losses in compressive strength beyond 1 year.

In the outdoor environment, mix A specimens, under continuous water curing showed the lowest value of compressive at 28 days of 49.5 MPa, followed by mix E and D of 54 and 56.7 MPa respectively; the highest value was shown by mixes B and C with 60.5 and 59.8 MPa respectively. On the other hand, as seen from Fig. 5.10 under both exposure environment, the outdoor environment exhibited losses on compressive strength for all concretes compared with indoor environment.

The adverse effect of absence of water curing and hot environment on compressive strength can readily seen in Fig. 5.13 which shows losses in compressive strength for all mixes. Mix A exhibited the lowest values from 7 day to 6 months of 40 to 50 MPa; respectively, the corresponding values in the indoor environment were 52.5 and 55.6 MPa. The compressive strength of both the SF/slag concrete (mixes D and E) in the outdoor environment at 6 months were 56.9 and 55.9, with an increase of about 6 MPa than the control mix, the corresponding values in the indoor environment were 63.6 and 61.2 MPa, respectively. Mixes B and C showed the highest values of compressive strength at 6 months, which gave values of 57.4 and 55.0 MPa, respectively, the corresponding values in the indoor environment were 68.4 and 66.9 MPa, respectively. Beyond 12 months all the mixes exhibited compressive strength loss due to the hot environment. These losses may contributed due to air drying, particularly when silica fume is present in the mixes. Carette [145] found a non-negligible drop in the

compressive strengths measured on 150 mm x 300 mm cylinders between 3 months and 2 years in the case of specimens of silica fume concrete cured in air, while a control concrete cured in the same conditions exhibited no significant variations of strength. De Larrard et al [145] explain this phenomenon quantitatively by self-stresses caused by the drying of the specimen.

The compressive strength developments of all the mixes under 3d wet/air and 7d wet/air curing subjected to both environmental conditions are shown in Figs. 5.11 and 5.12. Similar trend has been found for both curing regimes, with a reduction of compressive strength values in the outdoor environment. For example, the control mix (mix A) specimens under 7d wet/air curing at 28 days in the outdoor exhibited the lowest compressive strength, 59.2 MPa, followed by mix E, 66.1 MPa. The SF concrete (mix B) exhibited the largest compressive strength values in the outdoor environment compared with the other mixes, with a value of 71.1 MPa at 28 days. The inclusion of slag in mixes C and D exhibited compressive strength values at corresponding age of 65.8 and 68.7 MPa.

5.3 Ultrasonic pulse velocity

The ultrasonic pulse velocity test data were used to examine the effect of mix composition, curing regime and exposure environment on the internal structure of all the concrete mixes. The ultrasonic pulse technique is increasingly used for non-destructive evaluation of concrete, and it is hoped that the data presented here will be helpful in such monitoring of concrete in the Gulf environment.

5.3.1 Early age pulse velocity

Figs. 5.14 to 5.17 and Tables 5.3 and 5.4 show the effect of mix type on pulse velocity for the period of 1 to 28 days for both environments. In general, between 1 and 3 days rapid increase in pulse velocity was observed under the four curing regimes, the differences being slightly less for air-cured specimens. Beyond 3 days, this difference was higher for mixes B to E under wet curing. These trends could be explained by the different rates of hydration and the availability of water for hydration. In the indoor environment, all mixes under continuous water curing (Fig. 5.14) showed that the increase in pulse velocity values between 1 and 7 days occurred at a rapid rate, this increases being in the range of 8-15%. For the period of 1 to 14 days there were no significant differences between the control mix (mix A) and mix B or mix C. On the

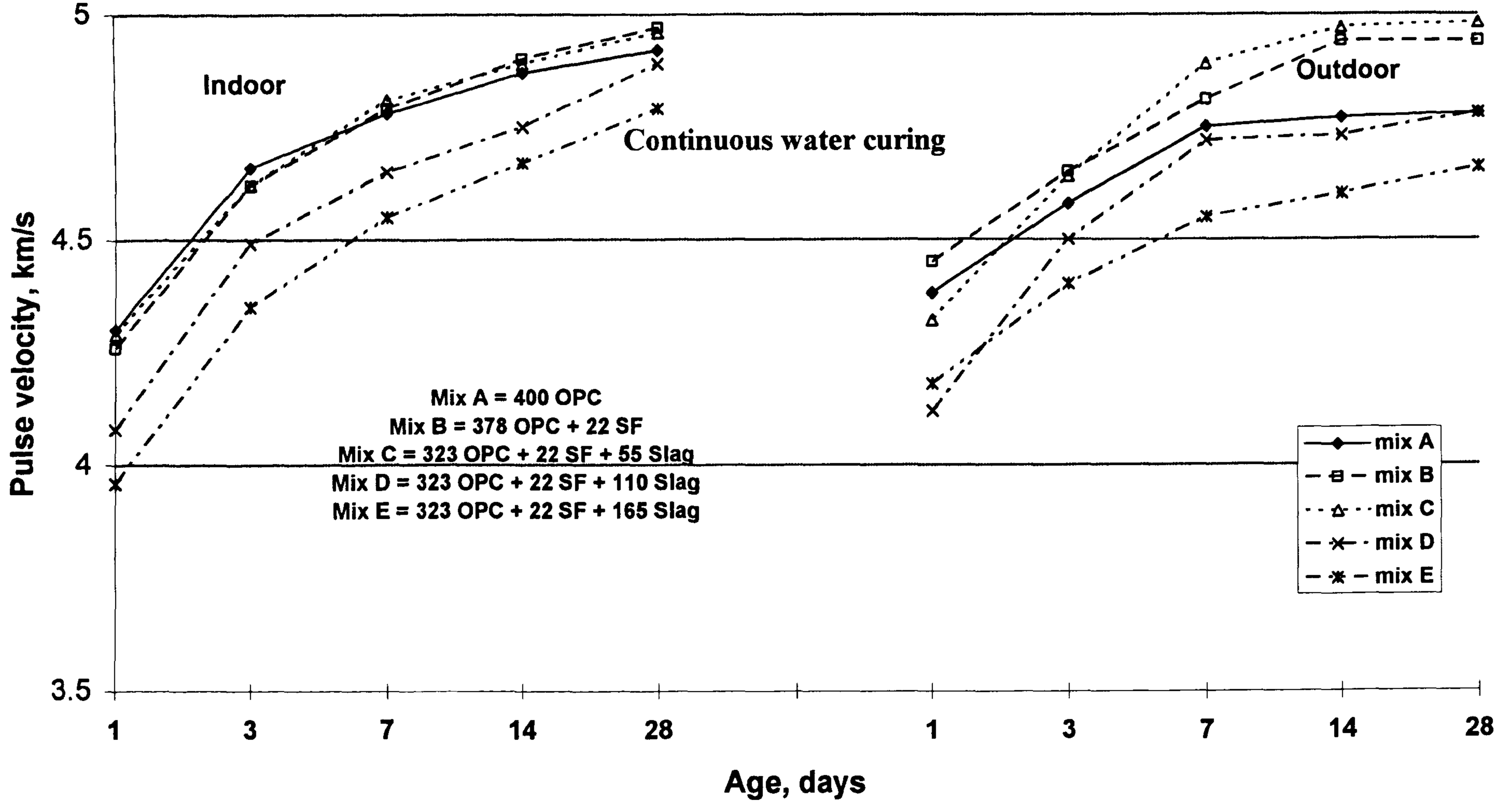

Fig. 5.14 : Influence of mix type on pulse velocity under continuous water curing.

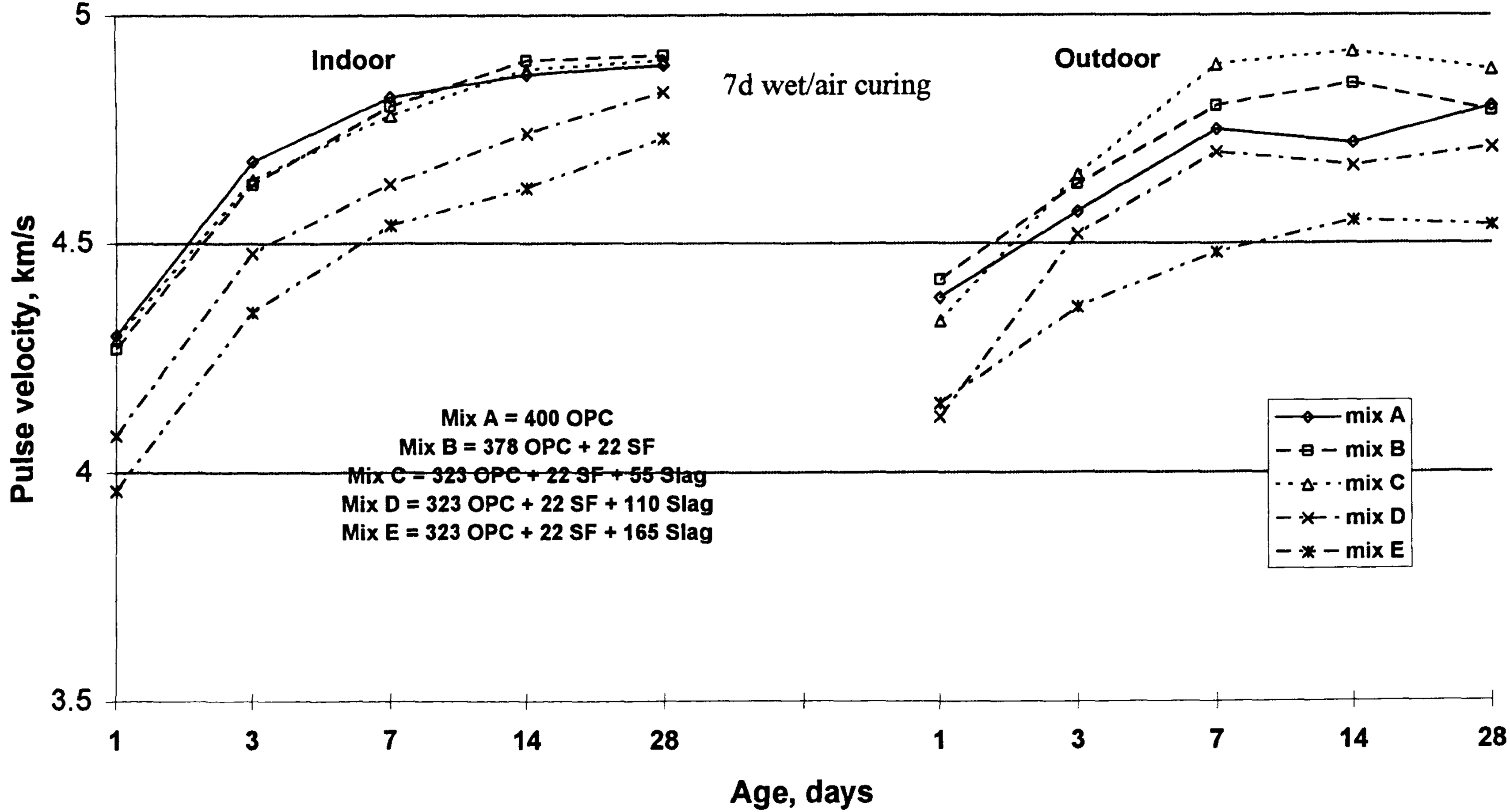

Fig. 5.15 : Influence of mix type on pulse velocity under 7d wet/air curing.

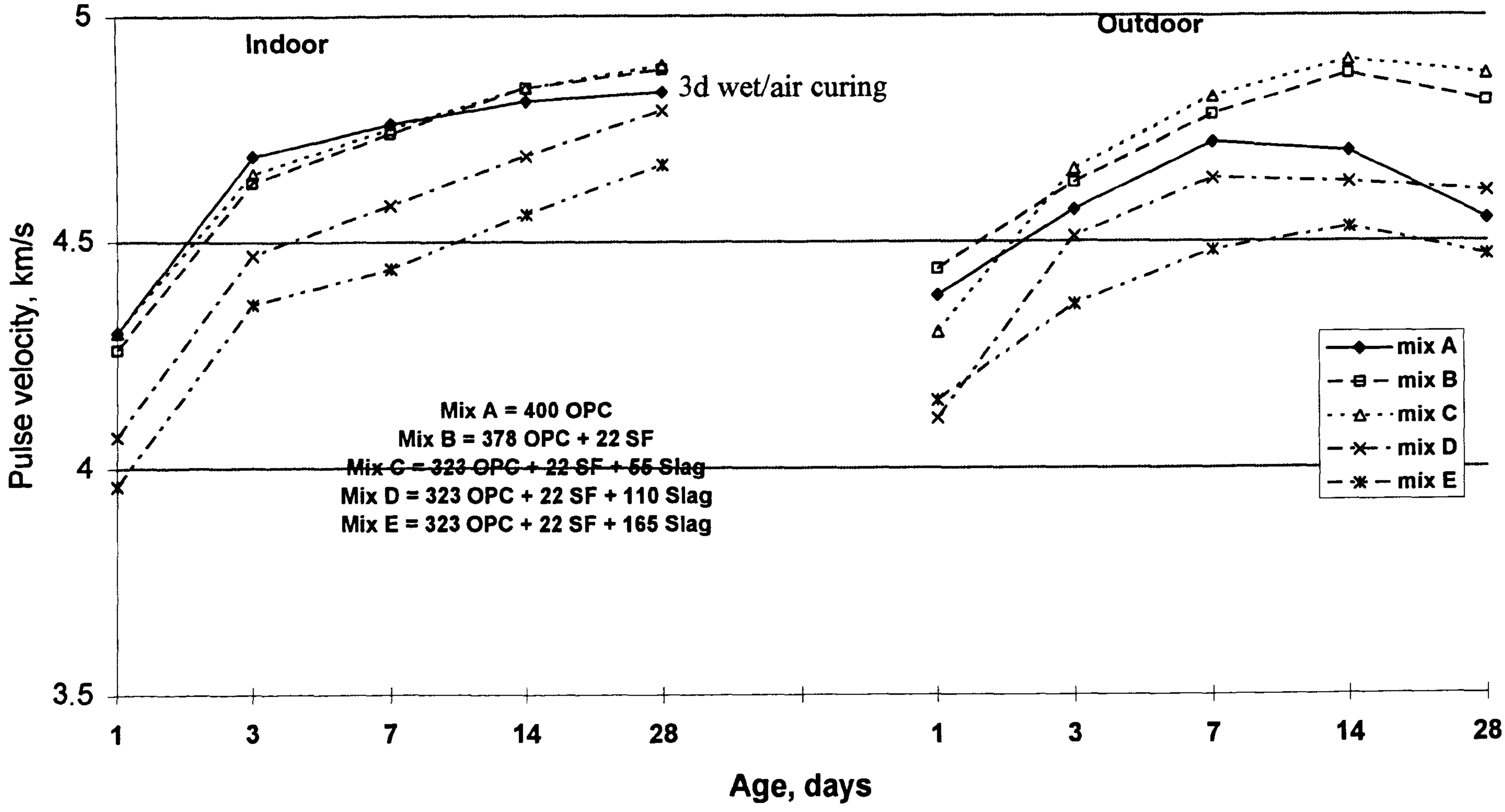

Fig. 5.16 : Influence of mix type on pulse velocity under 3d wet/air curing.

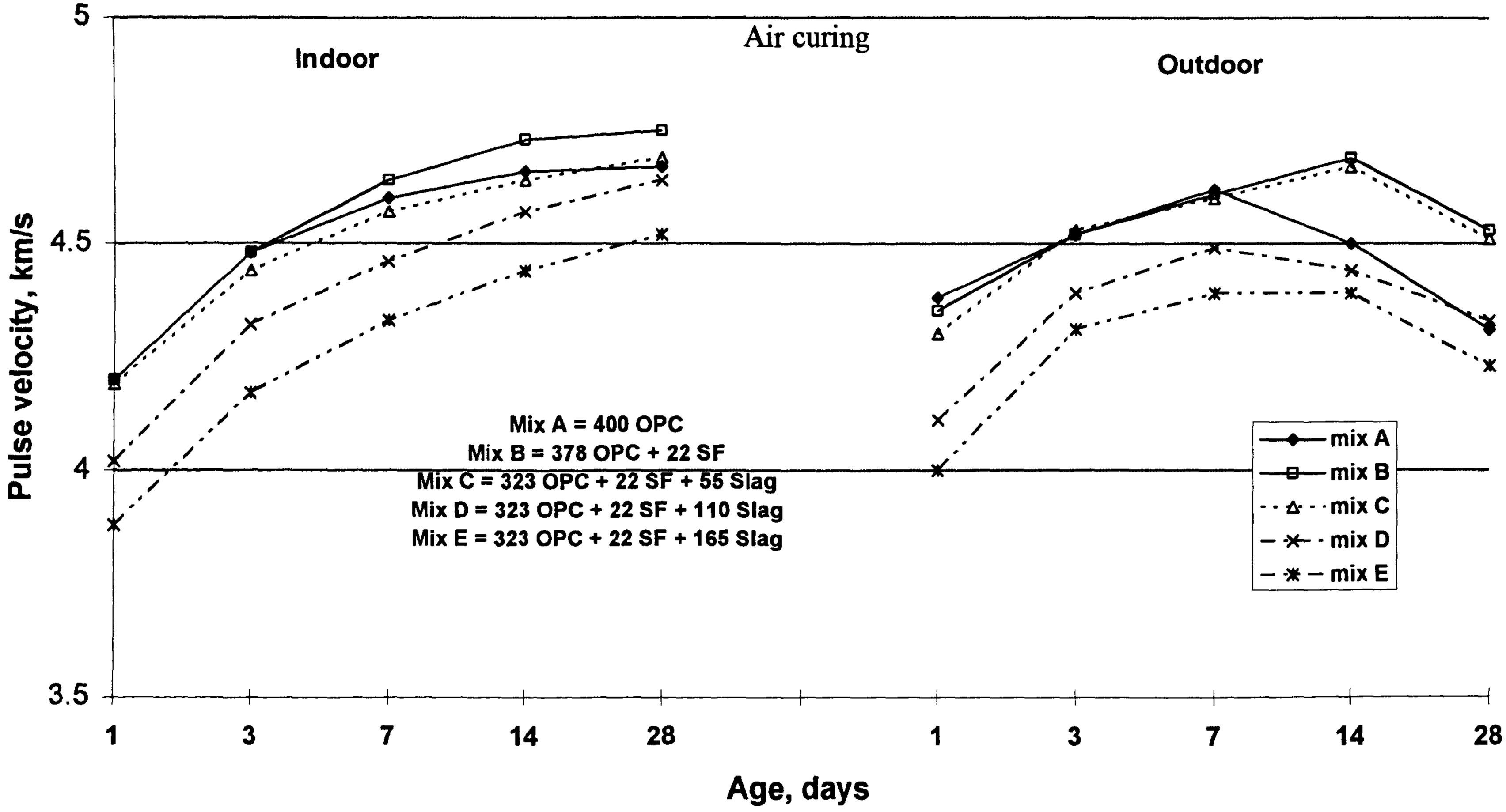

Fig. 5.17 : Influence of mix type on pulse velocity under air curing.

other hand, mixes containing slag in large amounts exhibited lower values of pulse velocity; as the amount of slag increased the pulse velocity decreased for the same period, although by closer inspection of the graphs it appears that mix A specimens performed better for the period of 1 to 3 days. At 7 days and beyond mixes B and C began to perform better than mix A to present values of 4.97 and 4.96 km/s for mixes B and C at 28 days respectively. The continuous hydration of slag (mix D) reduced the gap between the control mix and mixes D or E from 0.22 km/s at 1 day to only

Table 5.3 Ultrasonic pulse velocity (km/s) in the indoor environment.

Age	(days)	1	3	7	14	28	91	182	365	540
Mix	Curing	km/s	km/s	km/s	km/s	km/s	km/s	km/s	km/s	km/s
A	air	4.20	4.48	4.60	4.66	4.67	4.53	4.35	4.30	4.24
	3d w/a	4.30	4.69	4.76	4.81	4.83	4.66	4.46	4.38	4.37
	7d w/a	4.3.0	4.68	4.82	4.87	4.89	4.73	4.52	4.47	4.41
	wet	4.30	4.66	4.78	4.87	4.92	5.00	4.98	5.11	5.07
B	air	4.20	4.48	4.64	4.73	4.75	4.70	4.56	4.42	4.40
	3d w/a	4.26	4.63	4.74	4.84	4.88	4.80	4.64	4.46	4.45
	7d w/a	4.27	4.63	4.80	4.90	4.91	4.85	4.71	4.50	4.49
	wet	4.26	4.62	4.79	4.90	4.97	5.05	5.11	5.14	5.09
C	air	4.19	4.44	4.57	4.64	4.69	4.74	4.61	4.45	4.42
	3d w/a	4.30	4.65	4.75	4.84	4.89	4.91	4.78	4.60	4.56
	7d w/a	4.29	4.64	4.78	4.88	4.90	4.94	4.81	4.61	4.57
	wet	4.29	4.62	4.81	4.89	4.96	5.07	5.10	5.15	5.14
D	air	4.02	4.32	4.46	4.57	4.64	4.66	4.54	4.42	4.37
	3d w/a	4.07	4.47	4.58	4.69	4.79	4.79	4.72	4.52	4.46
	7d w/a	4.08	4.48	4.63	4.74	4.83	4.88	4.78	4.57	4.53
	wet	4.08	4.49	4.65	4.75	4.89	5.01	4.98	5.07	5.03
E	air	3.88	4.17	4.33	4.44	4.52	4.56	4.43	4.30	4.26
	3d w/a	3.96	4.36	4.44	4.56	4.67	4.72	4.65	4.40	4.36
	7d w/a	3.96	4.35	4.54	4.62	4.73	4.80	4.73	4.48	4.43
	wet	3.96	4.35	4.55	4.67	4.79	4.95	4.95	5.04	5.00

Table 5.4 Ultrasonic pulse velocity (km/s) in the outdoor environment.

Age (days)		1	3	7	14	28	91	182	365	540
Mix	Curing	km/s	km/s	km/s	km/s	km/s	km/s	km/s	km/s	km/s
A	air	4.38	4.52	4.62	4.50	4.31	4.30	4.28	4.27	4.25
	3d w/a	4.38	4.57	4.72	4.70	4.55	4.45	4.41	4.40	4.37
	7d w/a	4.38	4.57	4.75	4.72	4.80	4.55	4.48	4.43	4.40
	wet	4.38	4.58	4.75	4.77	4.78	4.99	5.00	5.05	5.05
B	air	4.35	4.52	4.61	4.69	4.53	4.25	4.19	4.20	4.20
	3d w/a	4.44	4.63	4.78	4.87	4.81	4.64	4.50	4.44	4.41
	7d w/a	4.42	4.63	4.80	4.85	4.79	4.67	4.51	4.43	4.46
	wet	4.45	4.65	4.81	4.94	4.94	5.02	5.05	5.05	5.06
C	air	4.30	4.53	4.60	4.67	4.51	4.31	4.30	4.30	4.30
	3d w/a	4.30	4.66	4.82	4.90	4.87	4.79	4.78	4.60	4.56
	7d w/a	4.33	4.65	4.89	4.92	4.88	4.87	4.81	4.65	4.66
	wet	4.32	4.64	4.89	4.97	4.98	5.04	5.10	5.08	5.08
D	air	4.11	4.39	4.49	4.44	4.33	4.24	4.23	4.24	4.17
	3d w/a	4.11	4.51	4.64	4.63	4.61	4.65	4.47	4.44	4.46
	7d w/a	4.12	4.52	4.70	4.67	4.71	4.71	4.55	4.52	4.50
	wet	4.12	4.50	4.72	4.73	4.78	4.86	4.88	4.89	4.91
E	air	4.00	4.31	4.39	4.39	4.23	4.14	4.10	4.10	4.10
	3d w/a	4.15	4.36	4.48	4.53	4.47	4.46	4.30	4.31	4.27
	7d w/a	4.15	4.36	4.48	4.55	4.54	4.55	4.41	4.33	4.34
	wet	4.18	4.40	4.55	4.60	4.66	4.73	4.77	4.78	4.86

0.03 km/s at 28 days for mix D and from 0.34 km/s at 1 day to 0.13 km/s at 28 days for mix E. In outdoor environment, with the exception of mix A, all mixes exhibited higher values up to 3 days when exposed to outdoor environment. The pulse velocity values at 3 days in the outdoor were 4.58, 4.65, 4.64, 4.50 and 4.40 km/s for mixes A, B, C, D and E respectively, the corresponding values in indoor environment were 4.66, 4.46, 4.62, 4.49 and 4.35 km/s for mixes A, B, C, D and E respectively. Mix C exhibited the highest pulse velocity at 7 days and beyond followed by mixes B, A, D and E, respectively. Mix D exhibited a very rapid increase in pulse velocity compared to the

control mix, to produce an increase of 14% at 7 days when compared to the value at 1 day, the corresponding increase for mix A being 8%.

The influence of 7d wet/air and 3d wet/air curing on the five mixes are presented in Figs. 5.15 and 5.16, the trend in pulse velocity for the five mixes is similar to the trend obtained for specimens under continuous water curing.

Under air curing, mixes A, B and C exhibited similar values of pulse velocity at 1 day which is about 4.20 km/s. Mixes D and E exhibited lower values than the other mixes, i.e., 4.02 and 3.88 km/s, respectively. This is due to the fact that the presence of slag slows down early hydration of concrete. The adverse effect of air curing, continued drying, on the early pulse velocity values was pronounced at 1 day and beyond, when compared with wet specimens, a significant drop in pulse velocity of air-cured specimens was found.

In outdoor environment, at the age of 7 days, mixes A and D specimens exhibited their largest pulse velocity value and did not show any further improvement in pulse velocity development beyond this age, but the mixes B, C and E showed increases in pulse velocity up to 14 days. Beyond that age all the mixes exhibited losses in the pulse velocity due to exposure environment and drying condition; this loss of pulse velocity at early ages may give an indication of damage occurring in the microstructure of these specimens.

5.3.2 Effect of curing, Indoor

Figs. 5.18 to 5.22 and Tables 5.3 and 5.4 show the effects of curing conditions on pulse velocity for all the mixes; the data show that under continuous water curing, all the mixes showed increasing pulse velocity, reflecting the increases in compressive strength and the development of the pore structure, as well as the development of a dense internal structure. Beyond 28 days, the wet-cured specimens continued to show higher pulse velocity values whereas loss in pulse velocity of 7d wet/air, 3d wet/air and air-cured specimens was observed beyond 28 days for mixes A and B and beyond 91 days for mixes C to E. At 28 days, the pulse velocity of all mixes of wet-cured specimens was higher by about 0.22 to 0.27 km/s than those of the air-cured specimens.

When drying, concretes cured in the laboratory and concretes given 3 days or 7 days wet curing followed by drying showed losses in pulse velocity after 28 days for the three curing conditions (Fig 5.18), while compressive strength showed continued

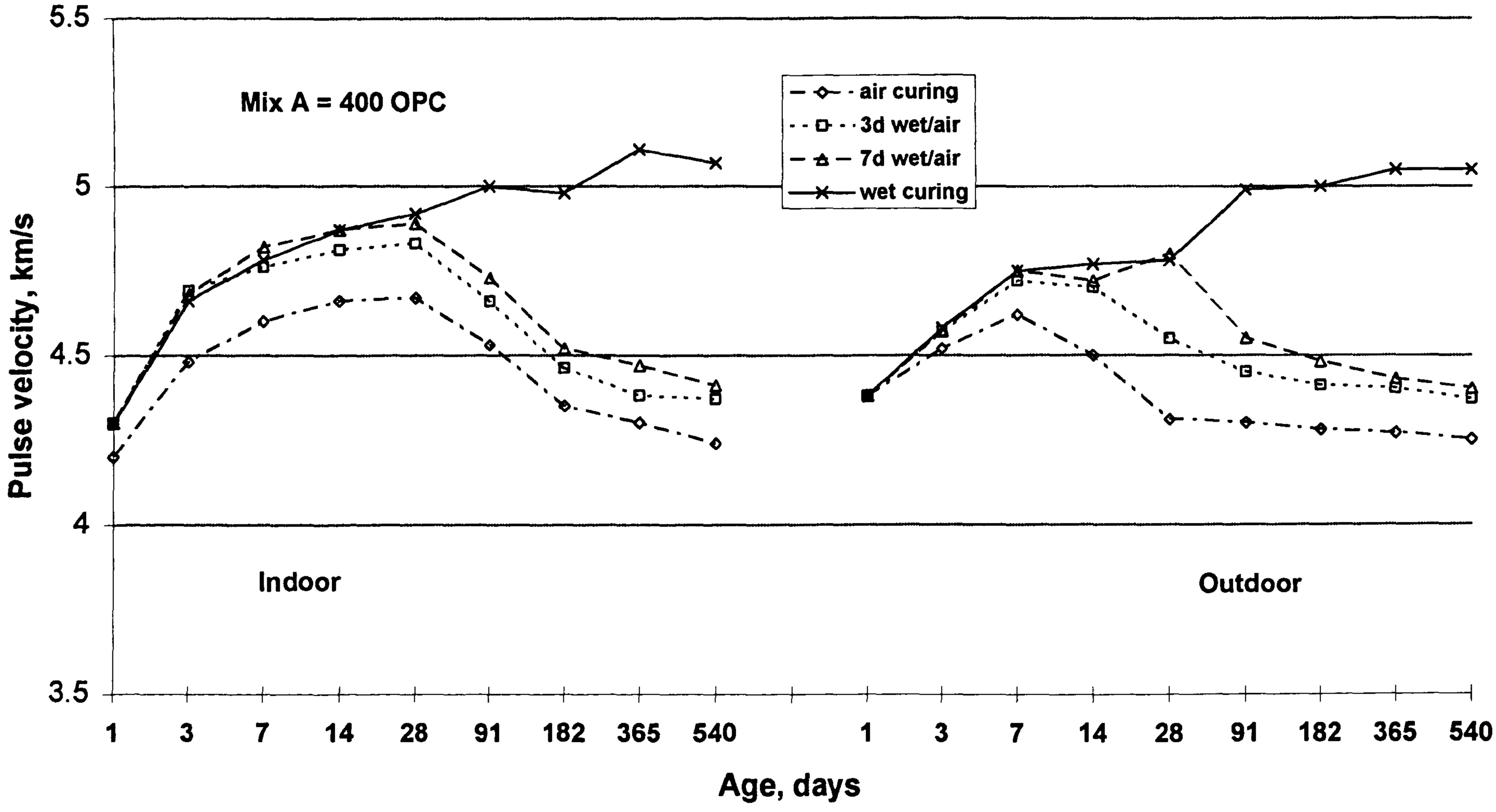

Fig. 5.18 : Influence of curing regime on pulse velocity for mix A.

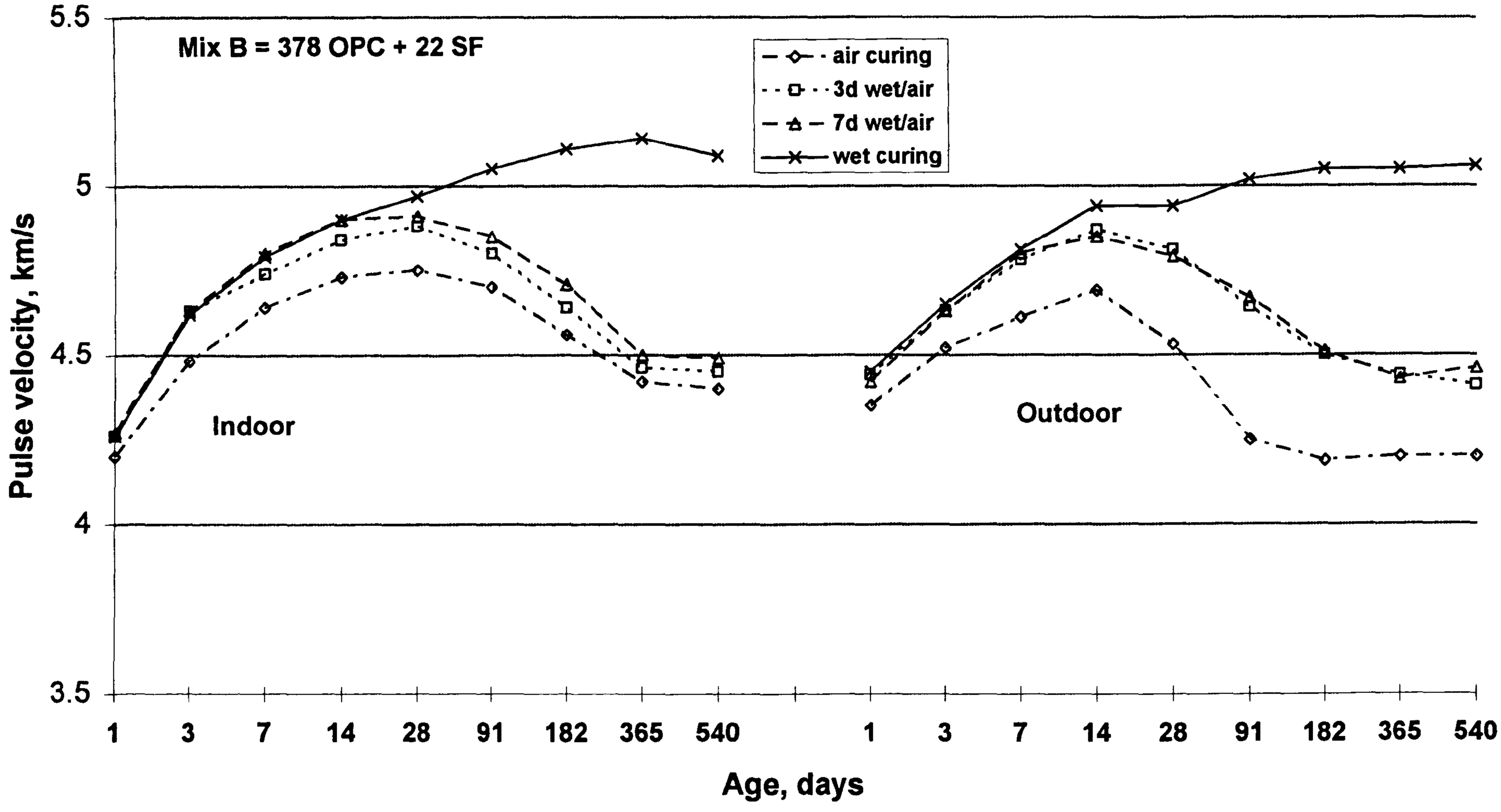

Fig. 5.19 : Influence of curing regime on pulse velocity for mix B.

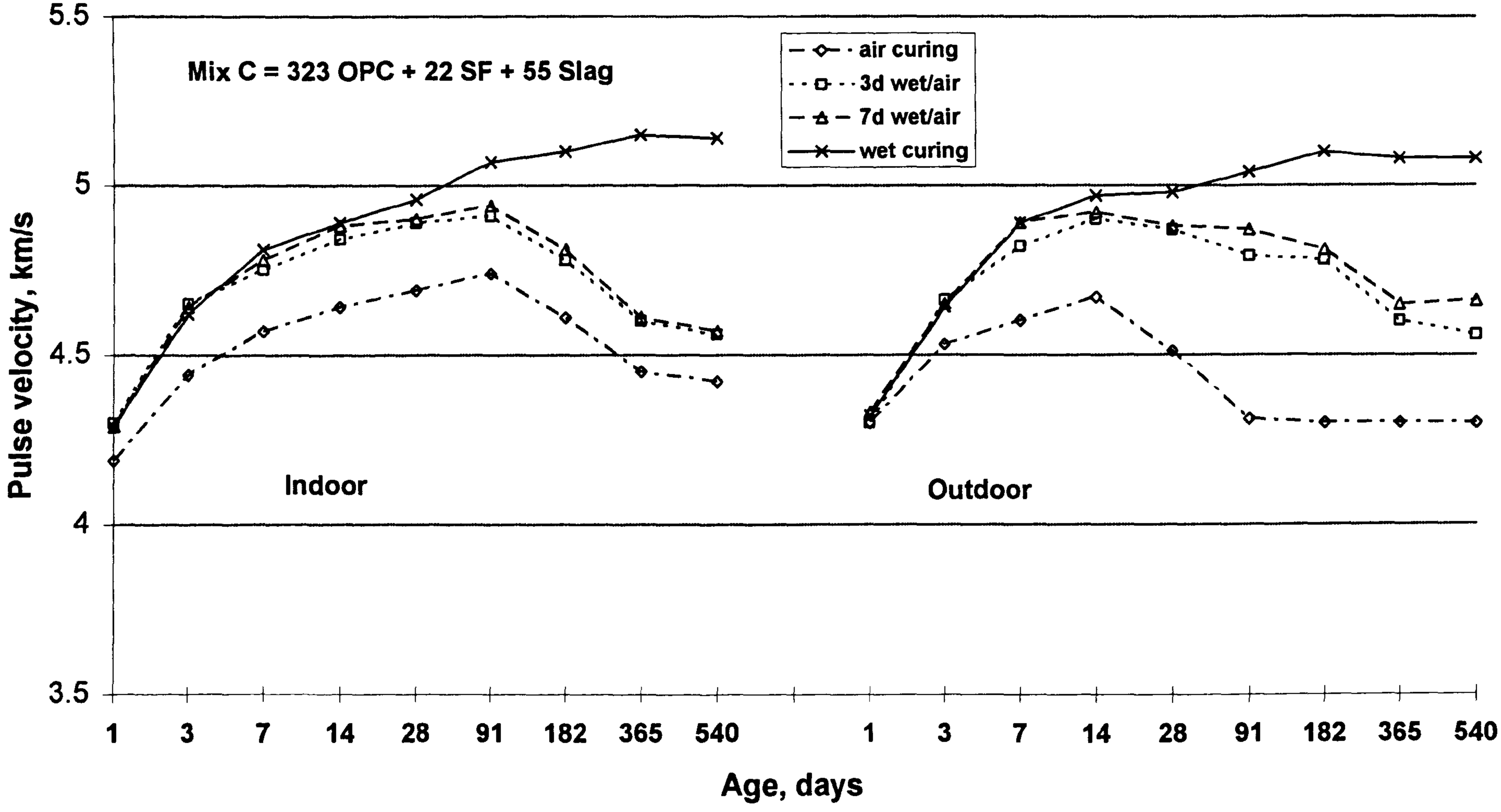

Fig. 5.20 : Influence of curing regime on pulse velocity for mix C.

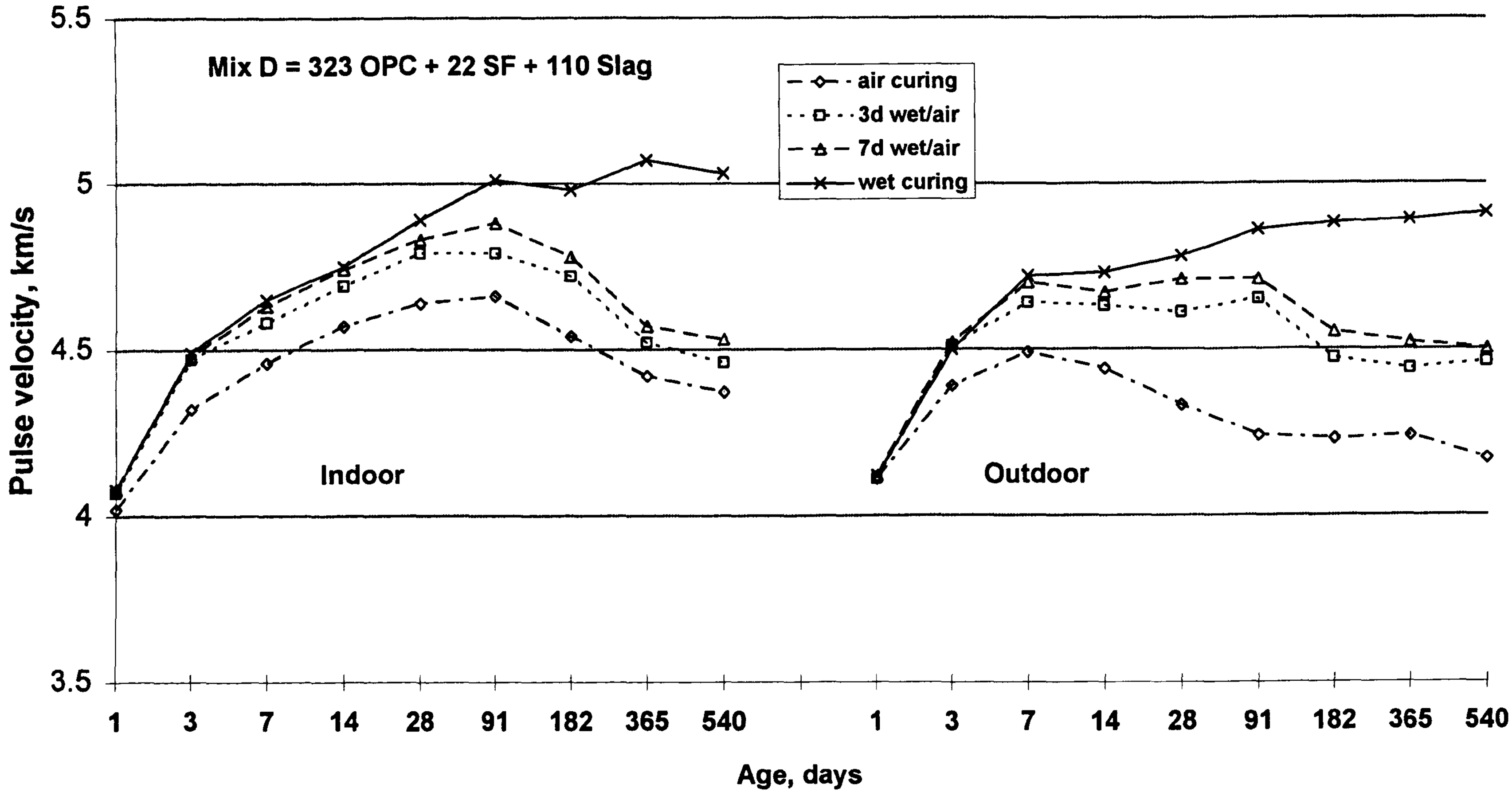

Fig. 5.21: Influence of curing regime on pulse velocity for mix D.

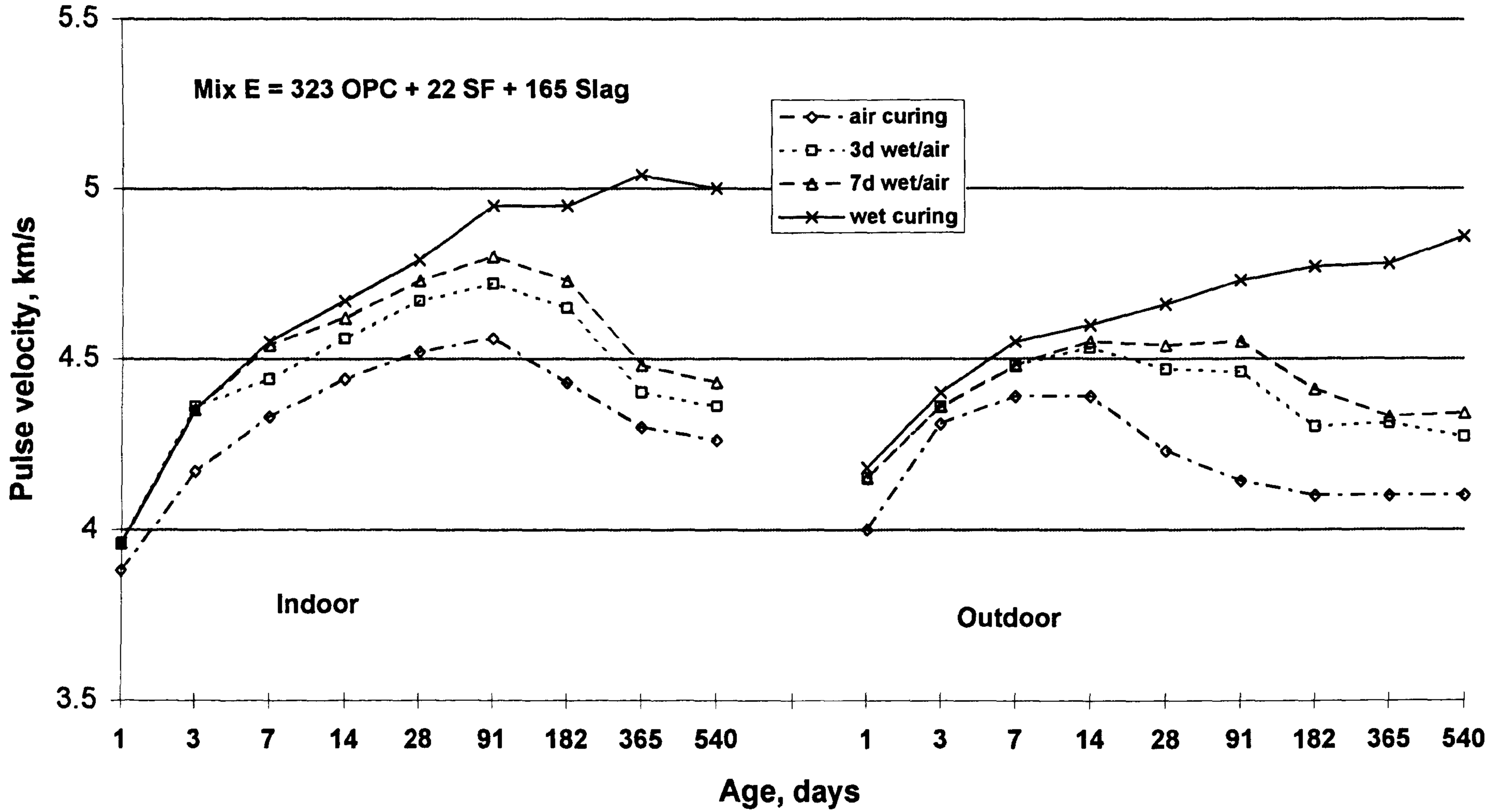

Fig. 5.22 : Influence of curing regime on pulse velocity for mix E.

increase up to 91 days. loss of pulse velocity is an indication of loss of moisture from the specimens and possible of internal microcracking. On the other hand, compressive strength again showed development up to one year for the same curing regimes, which gives no indication of internal microcracking, while the pulse velocity showed continuous losses until reaching a steady state beyond one year.

Prolonged drying can thus create adverse internal microcracking not readily indicated by compressive strength values. These results thus show that, except for the case of moist curing, compressive strength should not be used as a criterion of concrete quality beyond 28 days in the environment similar to the indoor environment used in this study, and beyond 7 days in outdoor environment, since pulse velocity varies quite widely with compressive strength when insufficiently cured concrete begins to dry with time. Popovics [143] reported that the primary reason for keeping the concrete wet at early ages is the prevention of cracking.

Fig. 5.18 shows the development of pulse velocity with age for the control mix under the four curing conditions. The figure shows that the greatest loss in pulse velocity occurs when the specimens are dried continuously in air to give maximum loss at 18 months with a value of pulse velocity similar to that at 1 day, 4.20 km/s. The maximum value was registered at 28 days, about 4.67 km/s, whereas limited water curing of even 3 days improves performance of concrete. There was not much difference between 3d wet/air and 7d wet/air curing, but the values jumped to 4.83 and 4.89 km/s for 3d wet/air and 7d wet/air curing specimens respectively showing marginal increases, over air-cured specimens at 28 days. A steady difference of losses between air-cured and 3d wet/air cured specimens and between 3d wet/air and 7d wet/air cured specimens in pulse velocity was observed beyond 28 days of age.

At the age of 28 days, wet-cured and 7d wet/air-cured specimens exhibited similar pulse velocity values of 4.92 and 4.89 km/s compared with 4.67 and 4.83 for air cured and 3d wet/air-cured ones. Beyond this age, only wet-cured specimens exhibited improved performance obtain a maximum value at 12 months of 5.11 km/s. However, the effect of curing was pronounced after 28 days on air-cured, 3d wet/air-cured and 7d wet/air-cured specimens compared with continuous water-cured specimens. The pulse velocity of air-cured, 3d wet/air and 7d wet/air-cured at 28 days of age for mix A were about 5, 2 and 1% less than that for wet cured specimens, while at the age of 18 months the corresponding values were about 20, 16 and 15% less than those of wet-cured

specimens respectively, which indicates that the most important finding is that specimens exposed to air drying show much greater loss in pulse velocity than the wet-cured specimens at later ages.

A similar comparison for development of pulse velocity is presented in Fig. 5.19 for mix B (378 OPC + 22 SF) subjected to the four curing regimes. The pulse velocity development behaviour under the four curing conditions followed the trend of mix A with small differences between their values. The increases in pulse velocity for air-cured, 3d wet/air and 7d wet/air cured specimens occurred up to 28 days and beyond that, there was a reduction in pulse velocity up to 18 months, whereas the continuous water cured specimens still showed pulse velocity development. At the age of 18 months, the pulse velocity of wet-cured specimens was higher by 13, 14 and 16% than 7d wet/air, 3d wet/air and air-cured specimens respectively, and this shows the effect of air drying, which usually happens in the Arabian Gulf region; this effect of drying is more pronounced at later ages which indicates that there are changes taking place which appear as losses in pulse velocity.

Figs. 5.20 to 5.22 and Table 6.3 show the effect of the four curing conditions on pulse velocity of SF/slag concrete (mixes C, D and E). The figures and data show that pulse velocity behaviour of 3d wet/air and 7d wet/air-cured specimens of these mixes follows generally the behaviour of air-cured specimens. The pulse velocity values increased with age, the increase was sharp in the first 7 days and afterwards a gradual increase up to 91 days was observed, and reduction in pulse velocity was observed beyond 91 days. Wet-cured specimens exhibited development in the pulse velocity with age up to 12 months for all the mixes (mixes C, D and E), although the gap appeared to grow wider slowly with time between specimens dried in air and moist cured specimens.

5.3.3 Effect of mix type, Indoor

Figs. 5.23 to 5.26 show the effect of mix type on the development of pulse velocity up to 18 months under the four curing conditions studied in this project. Generally, all the mixes exhibit similar trends. In the laboratory environment, under wet curing mixes B and C presented better development of pulse velocity than mix A at 28 days and beyond. Mixes with high amount of slag (mix E) exhibited the lowest values up to 28

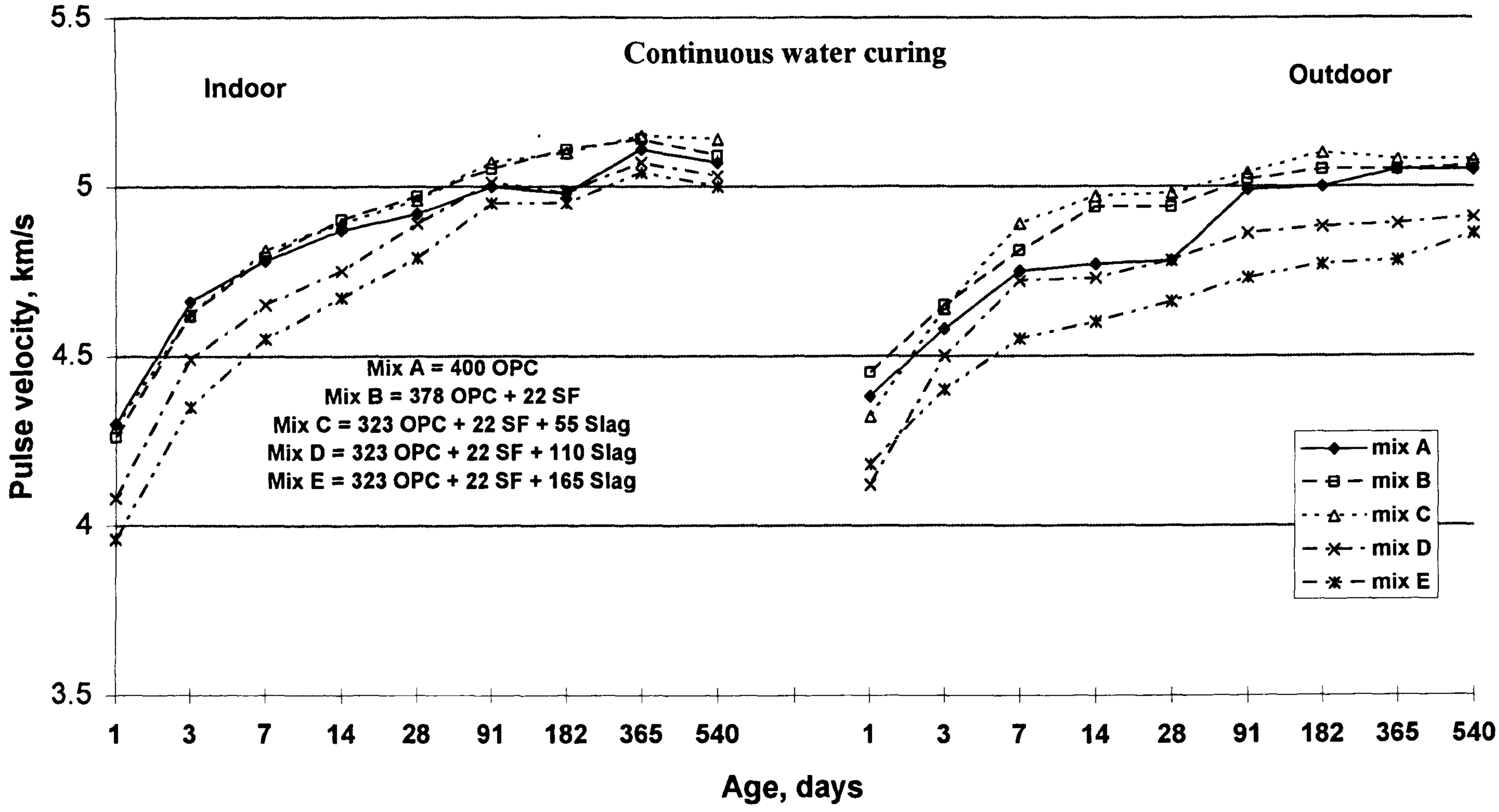

Fig. 5.23 : Influence of mix type on pulse velocity under continuous water curing.

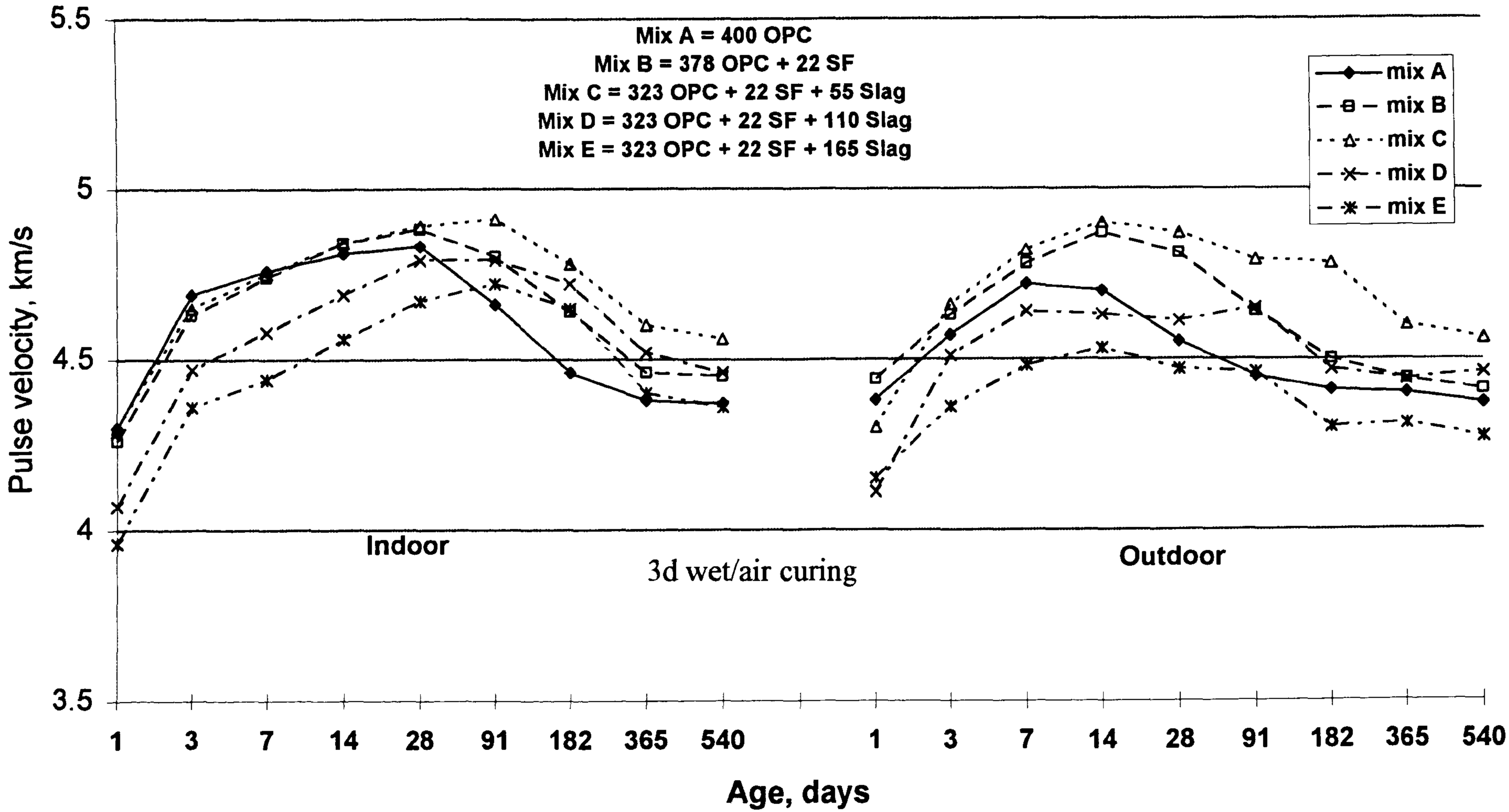

Fig. 5.24 : Influence of mix type on pulse velocity under 3d wet/air curing.

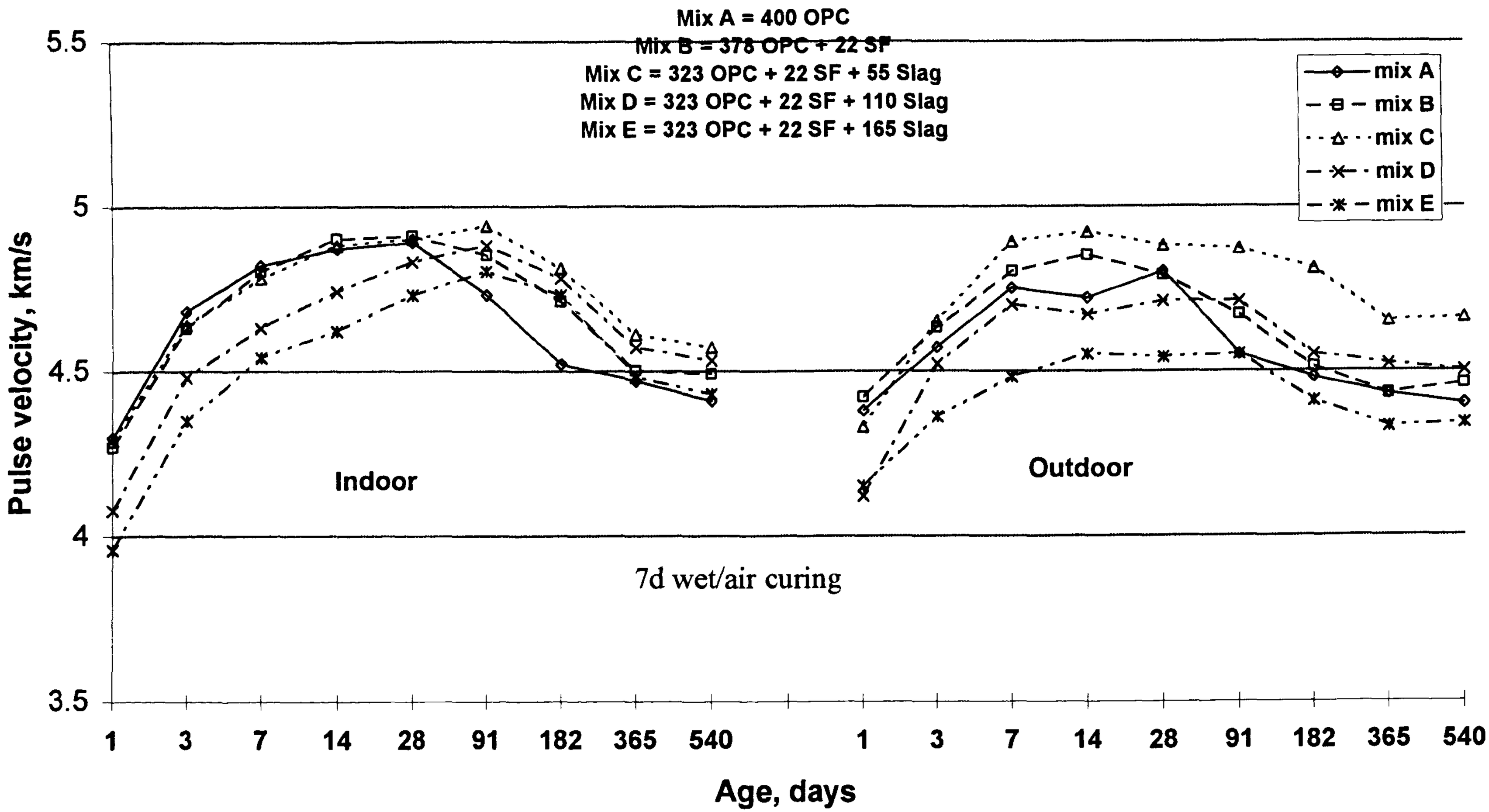

Fig. 5.25 : Influence of mix type on pulse velocity under 7d wet/air curing.

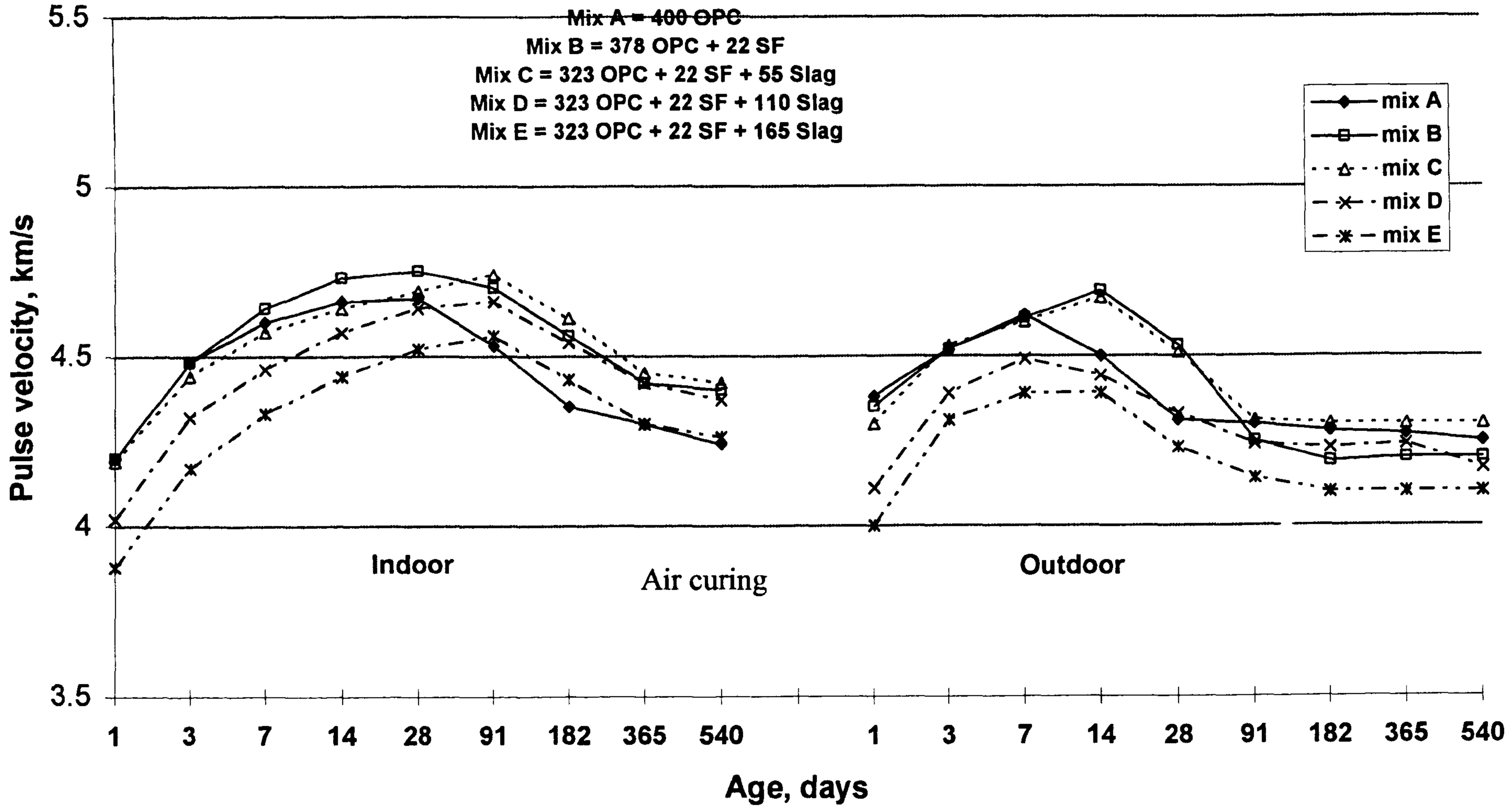

Fig. 5.26 : Influence of mix type on pulse velocity under air curing.

days, beyond that, the improvement at later ages was very clear, the gap between mix E and mix A reduced from 9% at 1 day to only 1% at 18 months.

Drying in air, without or with initial water curing, has much worse effect on OPC concrete (mix A) than on concrete with mineral admixture (mixes B to E). Mix A showed increasing pulse velocity up to 28 days, and then produced sharp losses to give the lowest values of pulse velocity in the long-term. Using either silica fume (mix B) or silica fume with slag in the other mixes exhibited good development of pulse velocity at early age and in the long-term, compared with mix A. As a result it can be said that the rate of gain of pulse velocity at early ages for silica fume or SF/slag concretes increases far more with the addition of silica fume. Mix C showed a slight improvement in pulse velocity at early ages compared to mixes with a higher amount of slag; this is due to using a smaller amount of slag which contributes to improve the long term pulse velocity without any reduction at early ages.

5.3.4 Effect of exposure environment

These figures and the data in Tables 5.3 and 5.4 present the effect of exposure environment on pulse velocity. In general, with the exception of continuous wet curing, all mixes in the outdoor environment exhibited loss in pulse velocity beyond 7-14 days after casting, while this trend was observed between 28-91 days in the indoor environment. The above trend is more clear for specimens under continued air drying.

The pulse velocity for specimens of mixes A, D and E subjected to air curing decreased beyond 7-days when cured in the outdoor environment. This characteristic did not appear before 14-days in mixes B and C. Moreover, this trend occurred beyond 91-days for mixes C, D and E in the laboratory environment, while mixes A and B exhibited similar loss after only 28-days in the laboratory environment, which indicates that the inclusion of silica fume or silica fume with a small amount of slag improves the pulse velocity in the outdoor environment, and delays the formation of micro-cracking. On the other hand, all mixes exposed to the outdoor environment exhibited pulse velocity values less than the corresponding values in the laboratory environment at later ages, which also indicates that water curing is more critical in the outdoor environment than in the laboratory environment; similar findings have also been observed for the pore size distribution as discussed later.

Mix E which contains the highest amount of slag presented the lowest values of pulse velocity in the outdoor environment both at early ages and in the long term. On the other hand, Mix C with limited amount of slag exhibited the highest values of pulse velocity under similar conditions.

5.4 Dynamic modulus of elasticity

The dynamic modulus of elasticity is a key factor in estimating the deformation of structural members, as well as being a fundamental factor in determining the modular ratio, which is used in the design of sections of members subjected to flexure. It has been successfully correlated with compressive strength and the static modulus of elasticity [146]. The dynamic modulus is also a factor indicating the dynamic response of concrete members, and is thus an important factor in the design of tall buildings and other structures [147].

Figs. 5.27 to 5.39 and Tables 5.5 and 5.6 show the results of the dynamic modulus of elasticity tests for all the mixes in both indoor and outdoor environmental conditions. Similar to the pulse velocity, the dynamic modulus of elasticity increases with time particularly in the wet curing condition, and continued to rise gradually particularly at later ages.

5.4.1 Early age dynamic modulus

Tables 5.5 and 5.6 and Figs. 5.27 to 5.30 show the effects of mix type on early dynamic modulus. The figures show very rapid development of dynamic modulus of elasticity on the first day and up to 7 days under all curing conditions, and for all the mixes. The figures show that the effect of wet and continuous drying curing conditions on dynamic modulus of elasticity is similar to that on pulse velocity. However, all the mixes are highly affected by early wet curing condition. On the other hand, all the mixes cured in a drying environment exhibit the lowest values of dynamic modulus of elasticity similar to pulse velocity and compressive strength at early and later ages.

Between the period of 1 to 3 days, under continuous water curing, all the mixes containing slag showed a lower dynamic modulus than the control concrete; at 7 days, mix C with limited amount of slag exhibited similar modulus of elasticity as the control concrete. This means that slag with silica fume has the effect of significantly increasing the dynamic modulus at early and later ages in both environmental conditions. This occurs as a result of the increasing degree of hydration through the higher surface area

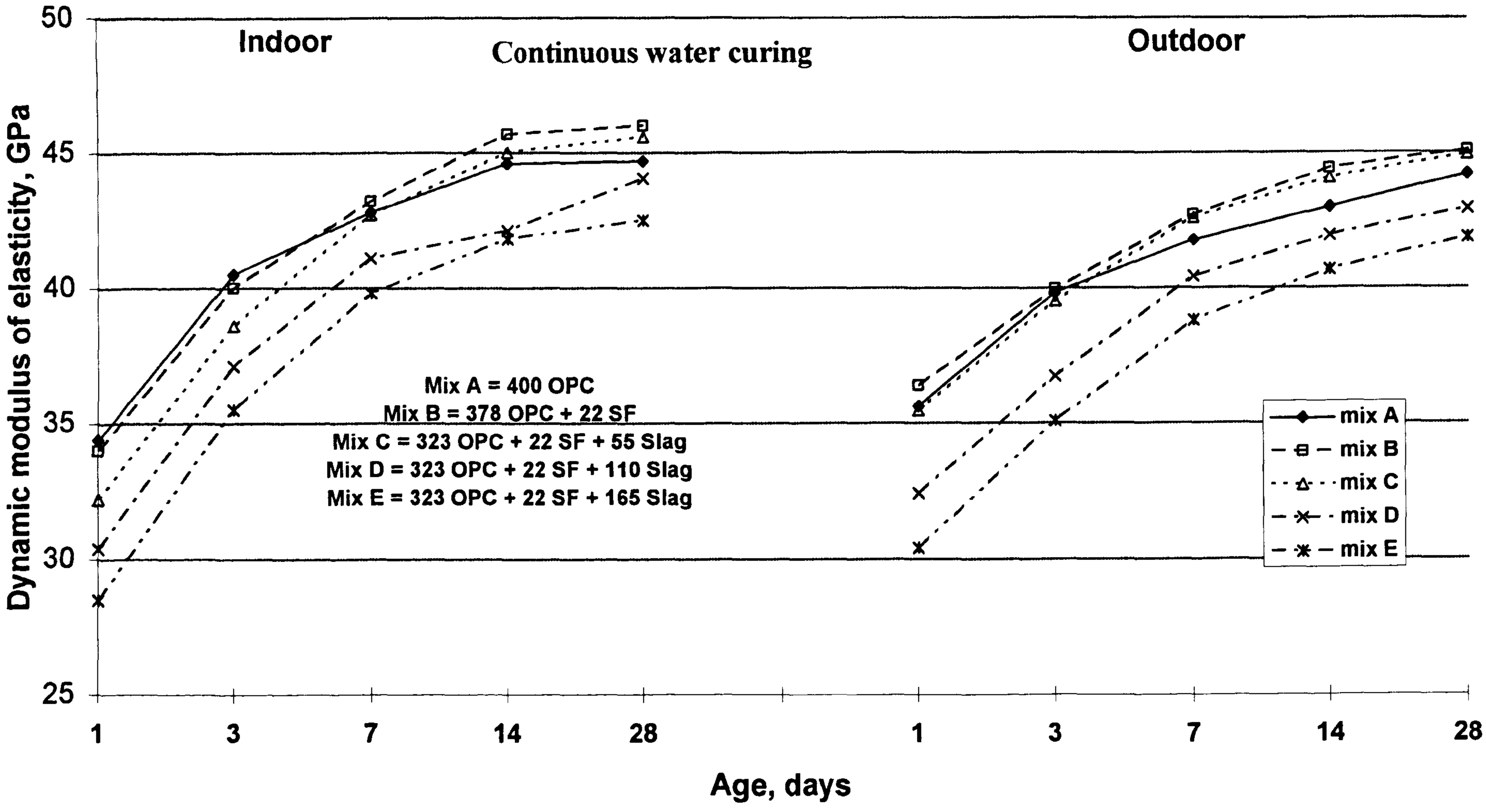

Fig. 5.27: Influence of mix type on dynamic modulus of elasticity under continuous water curing.

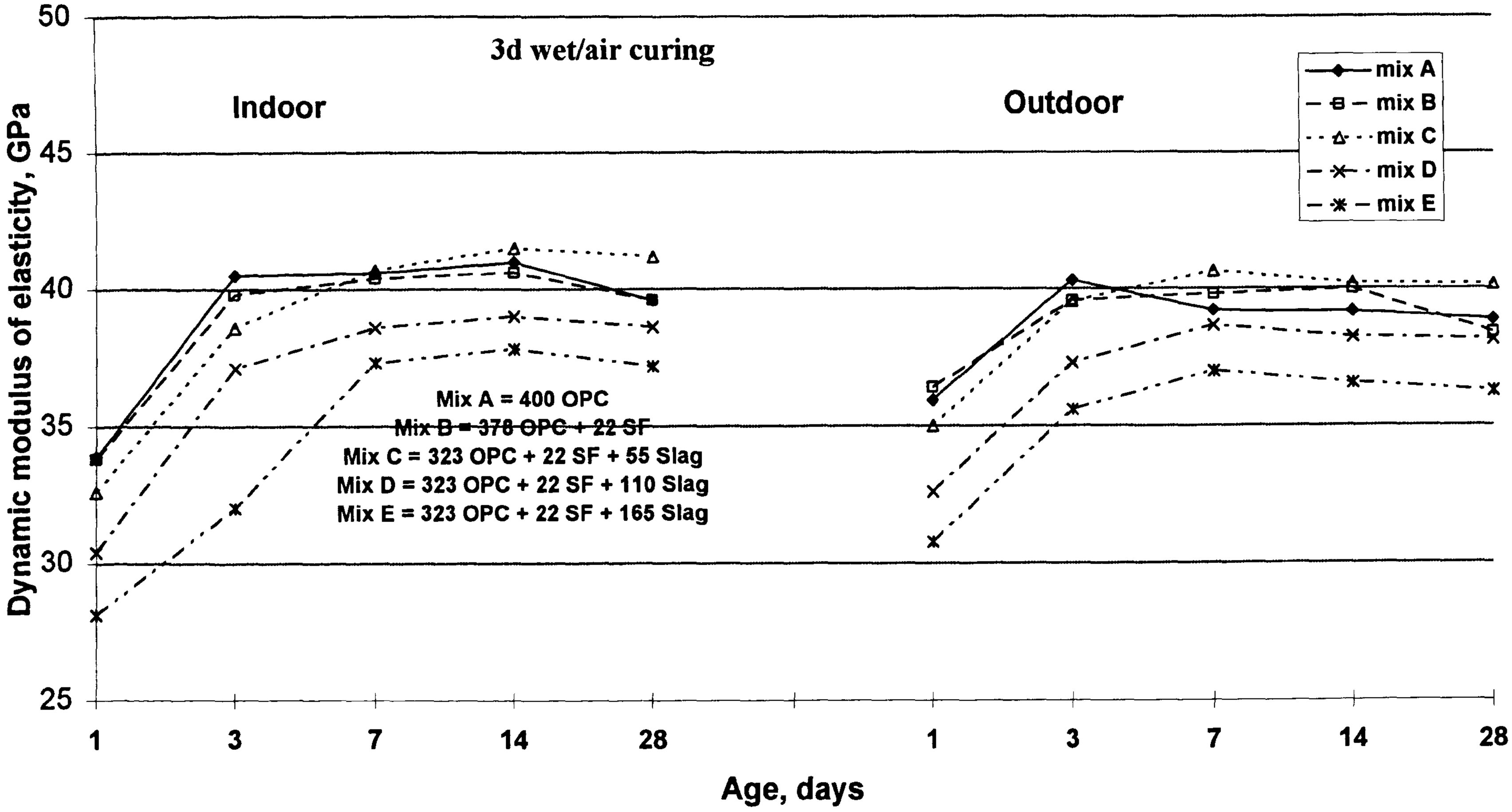

Fig. 5.28: Influence of mix type on dynamic modulus of elasticity under 3d wet/air curing.

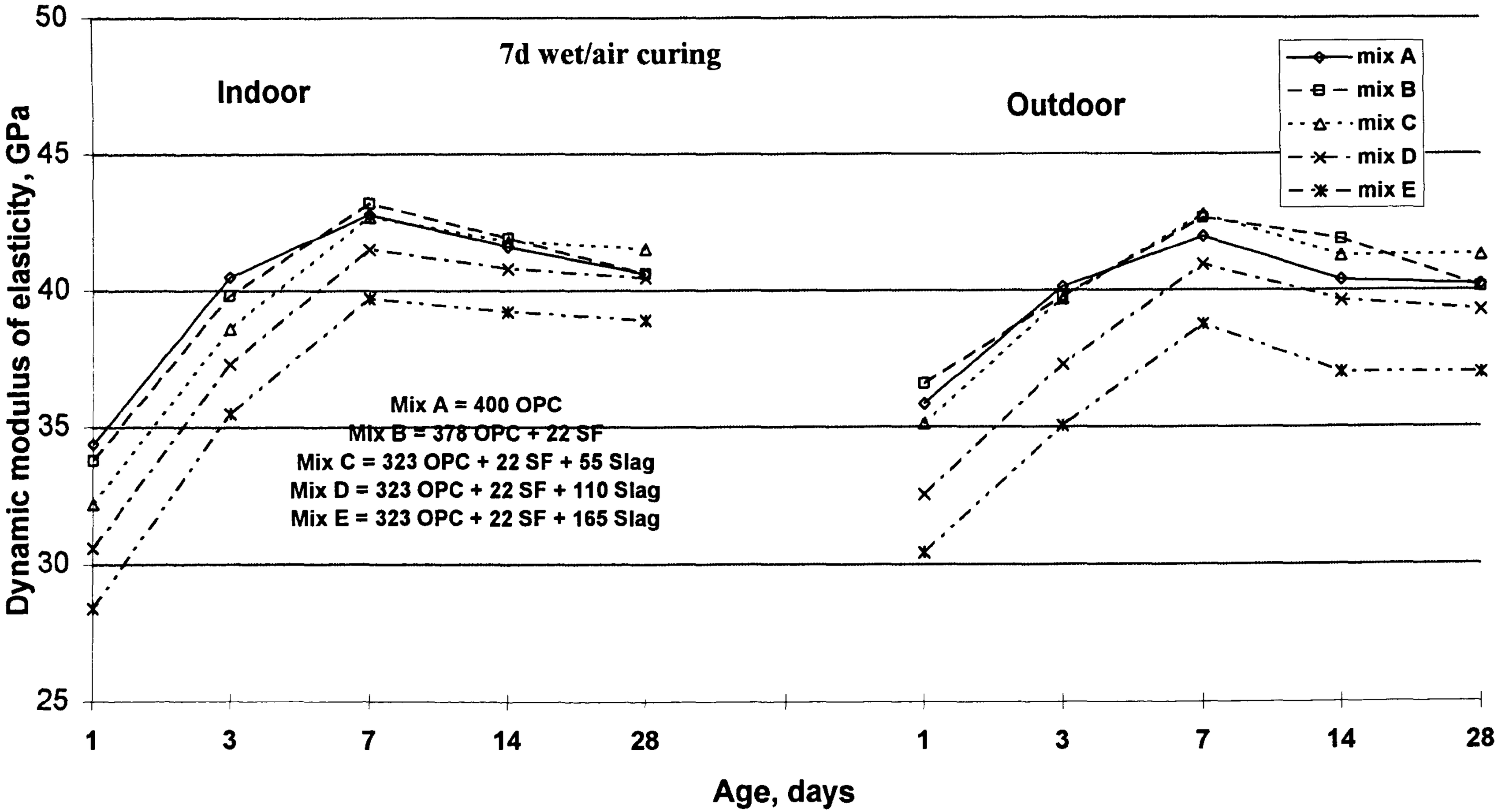

Fig. 5.29: Influence of mix type on dynamic modulus of elasticity under 7d wet/air curing.

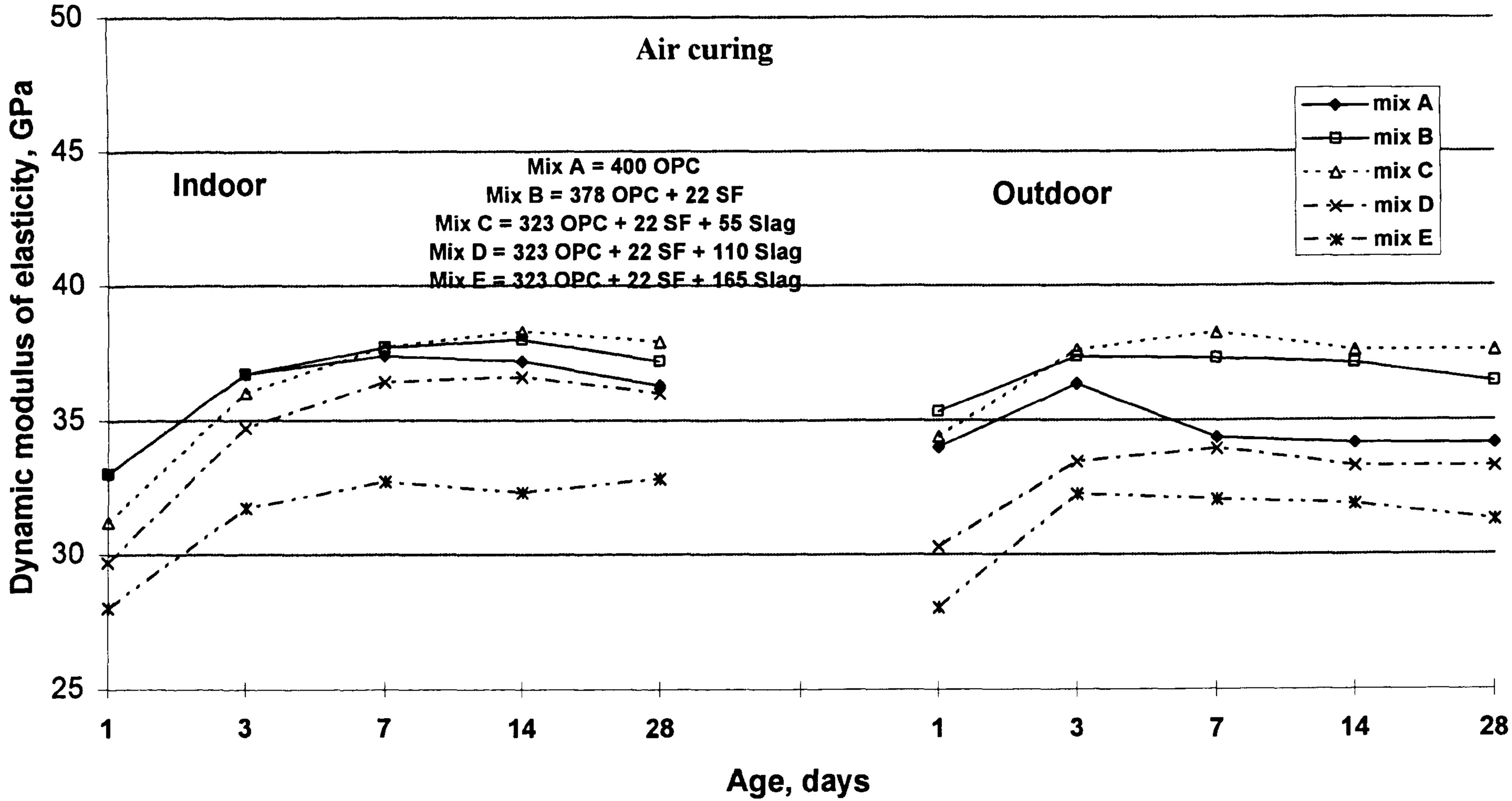

Fig. 5.30: Influence of mix type on dynamic modulus of elasticity under air curing.

of silica fume which is highly reactive, thus compensating the lower degree of hydration resulting from the high level of slag as in mixes D and E. Mix E (with large amount of slag) showed a marginally lower elastic modulus value than the other mixes, whereas mix B (silica fume concrete) developed similar modulus to that of the control mix at the age of 1 to 7 days and higher than the control mix beyond this age, in the same way as pulse velocity. With the exception of wet-cured specimens, all the mixes exhibited slight reduction in modulus of elasticity beyond 14 days.

Table 5.5 Dynamic modulus of elasticity (GPa) in the indoor environment.

Age (days)		1	3	7	14	28	91	182	365	540
Mix	Curing	GPa	GPa	GPa	GPa	GPa	GPa	GPa	GPa	GPa
A	air	33.0	36.7	37.4	37.2	36.3	35.0	34.6	34.0	33.9
	3d w/a	33.9	40.5	40.6	41.,0	39.6	38.5	37.6	37.6	37.5
	7d w/a	34.4	40.5	42.8	41.6	40.6	39.5	38.3	38.3	38.3
	wet	34.4	40.5	42.8	44.6	44.7	46.8	47.2	47.7	47.9
B	air	33.0	36.7	37.7	38 0	37.2	35.7	35.1	35.7	35.6
	3d w/a	33.8	39.8	40.4	40.6	39.6	38.0	37.0	37.2	37.3
	7d w/a	33.8	39.8	43.2	41.9	40.6	39.2	38.2	38.1	37.9
	wet	34.0	40.0	43.2	45.7	46.0	47.0	47.6	48.3	48.8
C	air	31.2	36.0	37.7	38.3	37.9	36.2	35.9	35.8	36.2
	3d w/a	32.6	38.6	40.7	41.5	41.2	39.3	38.9	38.9	38.9
	7d w/a	32.2	38.6	42.7	41.8	41.5	39.8	39.4	39.4	39.4
	wet	32.2	38.6	42.7	45.0	45.6	47.0	47.6	48.0	49.3
D	air	29.7	34.7	36.4	36.6	36.0	34.6	34.2	34.5	34.6
	3d w/a	30.4	37.1	38.6	39.0	38.6	37.2	36.5	36.4	36.8
	7d w/a	30.6	37.3	41.5	40.8	40.4	39.0	38.1	37.9	37.6
	wet	30.4	37.1	41.1	42.1	44.0	45.5	45.7	47.0	47.5
E	air	28.0	31.7	32.7	32.3	32.8	31.3	32.3	32.3	32.2
	3d w/a	28.1	32.0	37.3	37.8	37.2	36.0	34.7	34.7	34.9
	7d w/a	28.4	35.5	39.7	39.2	38.9	37.6	36.4	36.5	36.4
	wet	28.5	35.5	39.8	41.8	42.5	43.9	44.3	45.7	46.6

Table 5.6 Dynamic modulus of elasticity (GPa) in the outdoor environment.

Age	(days)	1	3	7	14	28	91	182	365	540
Mix	Curing	GPa	GPa	GPa	GPa	GPa	GPa	GPa	GPa	GPa
A	air	34.0	36.3	34.4	34.2	34.2	34.2	34.3	34.2	34.6
	3d w/a	35.9	40.3	39.2	39.2	38.9	38.9	38.8	38.5	37.6
	7d w/a	35.9	40.1	42.0	40.4	40.2	40.5	40.1	38.8	38.3
	wet	35.6	39.8	41.8	43.0	44.2	45.9	46.5	47.1	47.2
B	air	35.3	37.4	37.3	37.1	36.4	36.0	35.9	35.7	35.1
	3d w/a	36.4	39.6	39.8	40.0	38.4	38.0	37.8	37.1	37.0
	7d w/a	36.6	39.8	42.5	41.9	40.1	39.4	38.5	38.0	38.2
	wet	36.4	40.0	42.7	44.4	45.1	46.4	46.7	47.6	47.6
C	air	34.4	37.6	38.3	37.6	37.6	37.7	37.6	37.6	35.9
	3d w/a	35.0	39.5	40.6	40.2	40.2	40.1	39.3	38.8	38.9
	7d w/a	35.1	39.7	42.8	41.3	41.3	40.6	40.1	39.3	39.4
	wet	35.5	39.5	42.6	44.1	45.0	46.0	46.4	47.0	47.6
D	air	30.3	33.4	33.9	33.3	33.3	34.0	34.2	34.0	34.2
	3d w/a	32.6	37.3	38.6	38.3	38.2	38.0	37.9	37.0	36.5
	7d w/a	32.6	37.3	41.0	39.6	39.3	39.2	39.0	37.9	38.1
	wet	32.4	36.7	40.4	41.9	42.9	43.9	44.5	45.1	45.7
E	air	28.0	32.2	32.1	31.9	31.3	31.5	31.3	31.5	31.4
	3d w/a	30.8	35.6	37.0	36.6	36.3	36.1	35.7	35.4	34.7
	7d w/a	30.4	35.0	38.8	37.0	37.0	37.1	36.7	35.2	36.4
	wet	30.4	35.1	38.8	40.7	41.9	42.7	43.0	44.1	44.3

In the outdoor environment, under the four curing regimes, all the mixes exhibited higher modulus of elasticity at 1 day compared to those in indoor environment. At 7 days and beyond, all the mixes exhibited losses in modulus values due to exposure to hot environment, and this loss ranged from 0.3 to 2.7 GPa at 28 days for all the mixes.

5.4.2 Effect of curing, Indoor

Figs 5.31 to 5.35 show the development of dynamic modulus of elasticity with age for all the mixes in different curing conditions and in both environments. Generally, all the mixes show similar higher degree of elastic modulus when cured continuously in water,

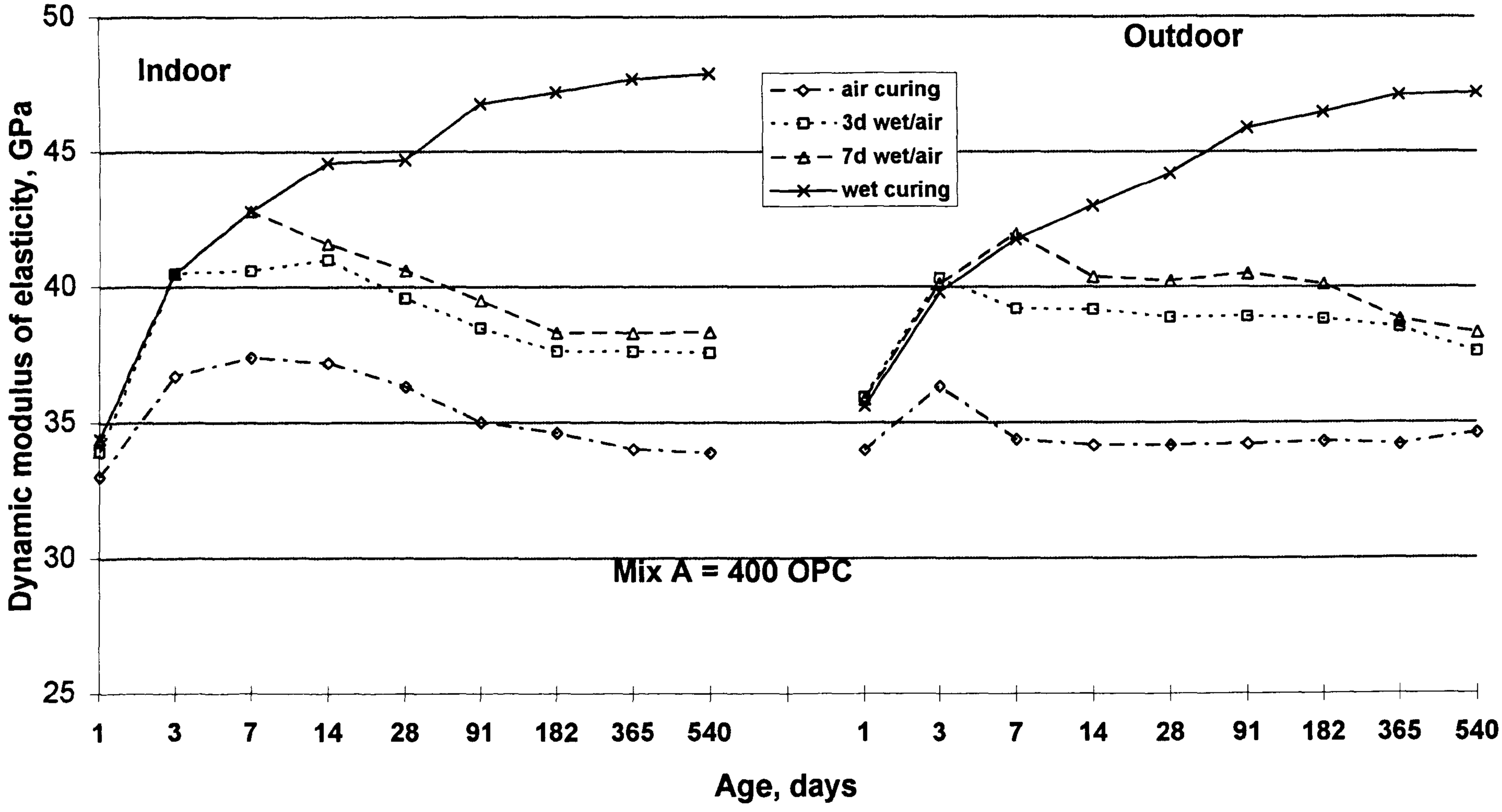

Fig. 5.31: Influence of curing regime on dynamic modulus of elasticity for mix A.

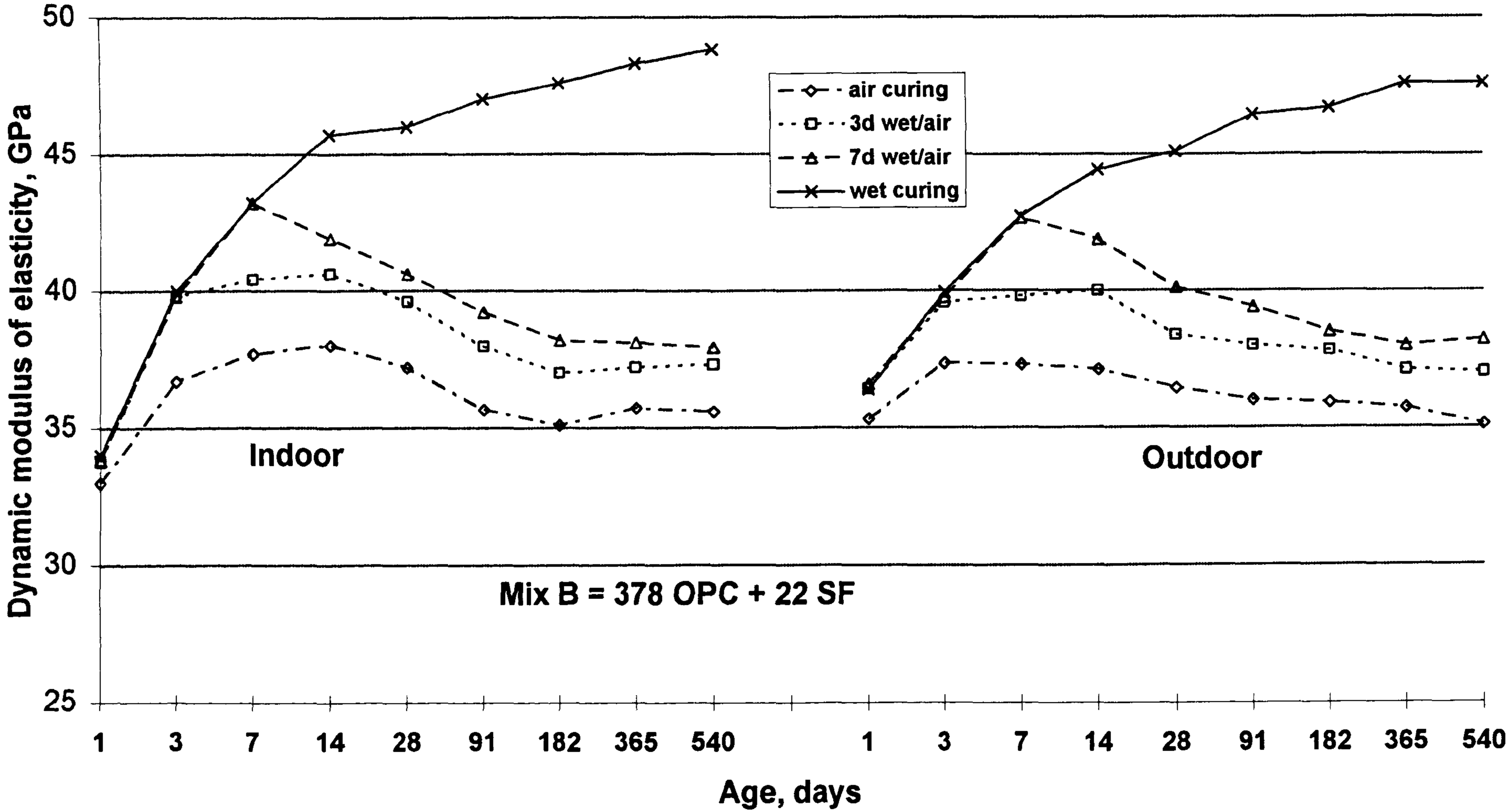

Fig. 5.32: Influence of curing regime on dynamic modulus of elasticity for mix B.

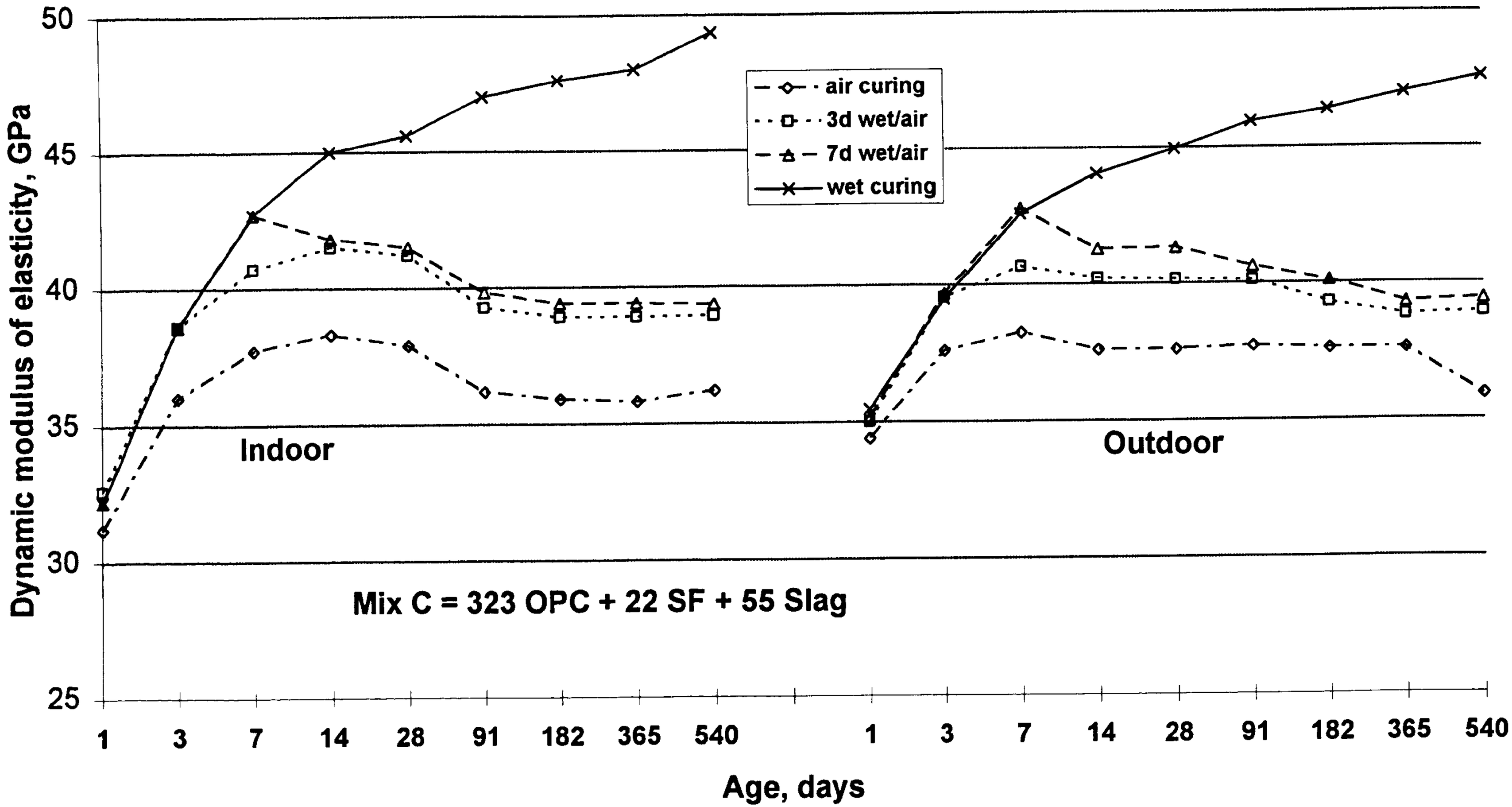

Fig. 5.33: Influence of curing regime on dynamic modulus of elasticity for mix C.

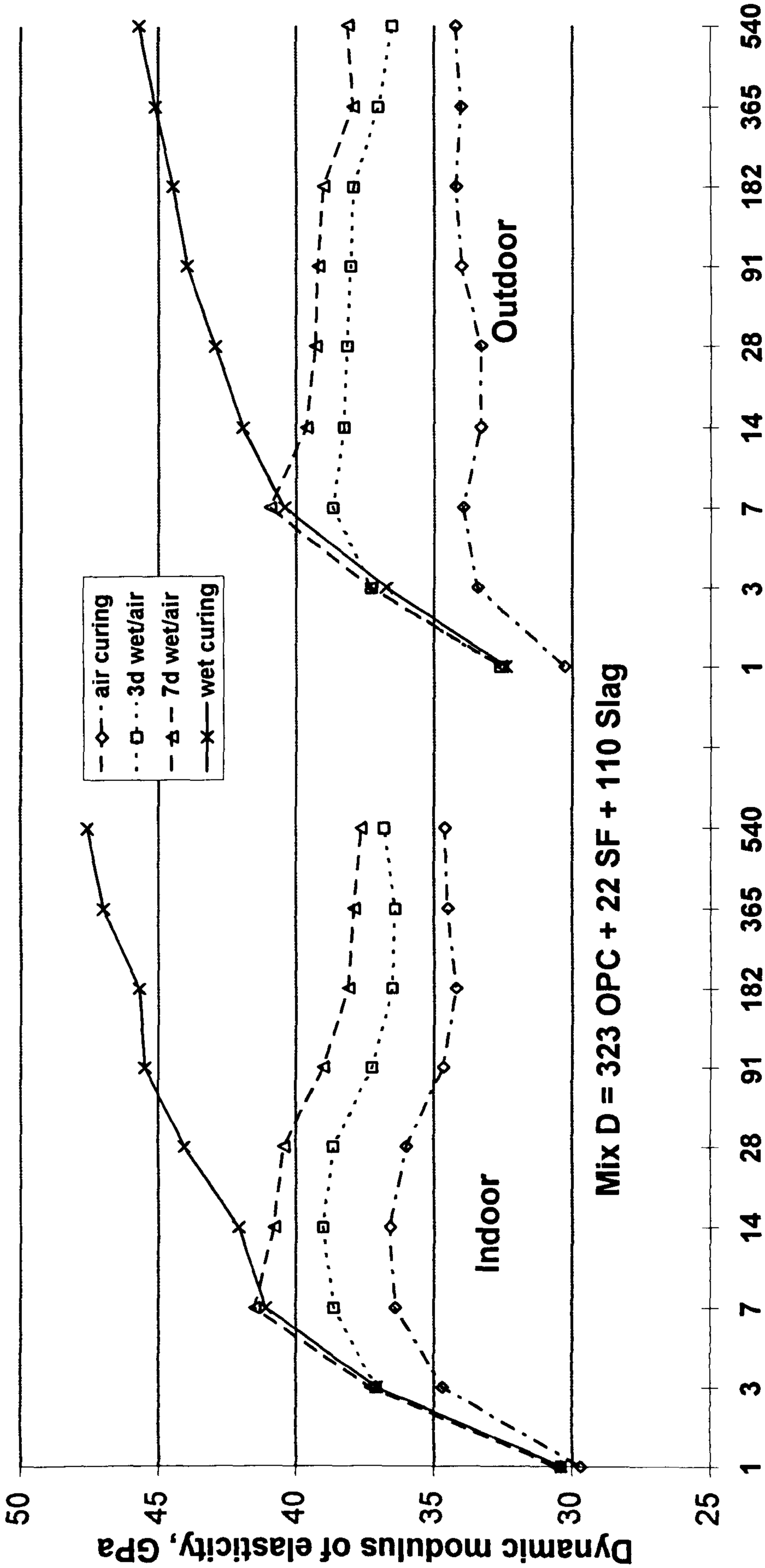

Fig. 5.34: Influence of curing regime on dynamic modulus of elasticity for mix D.

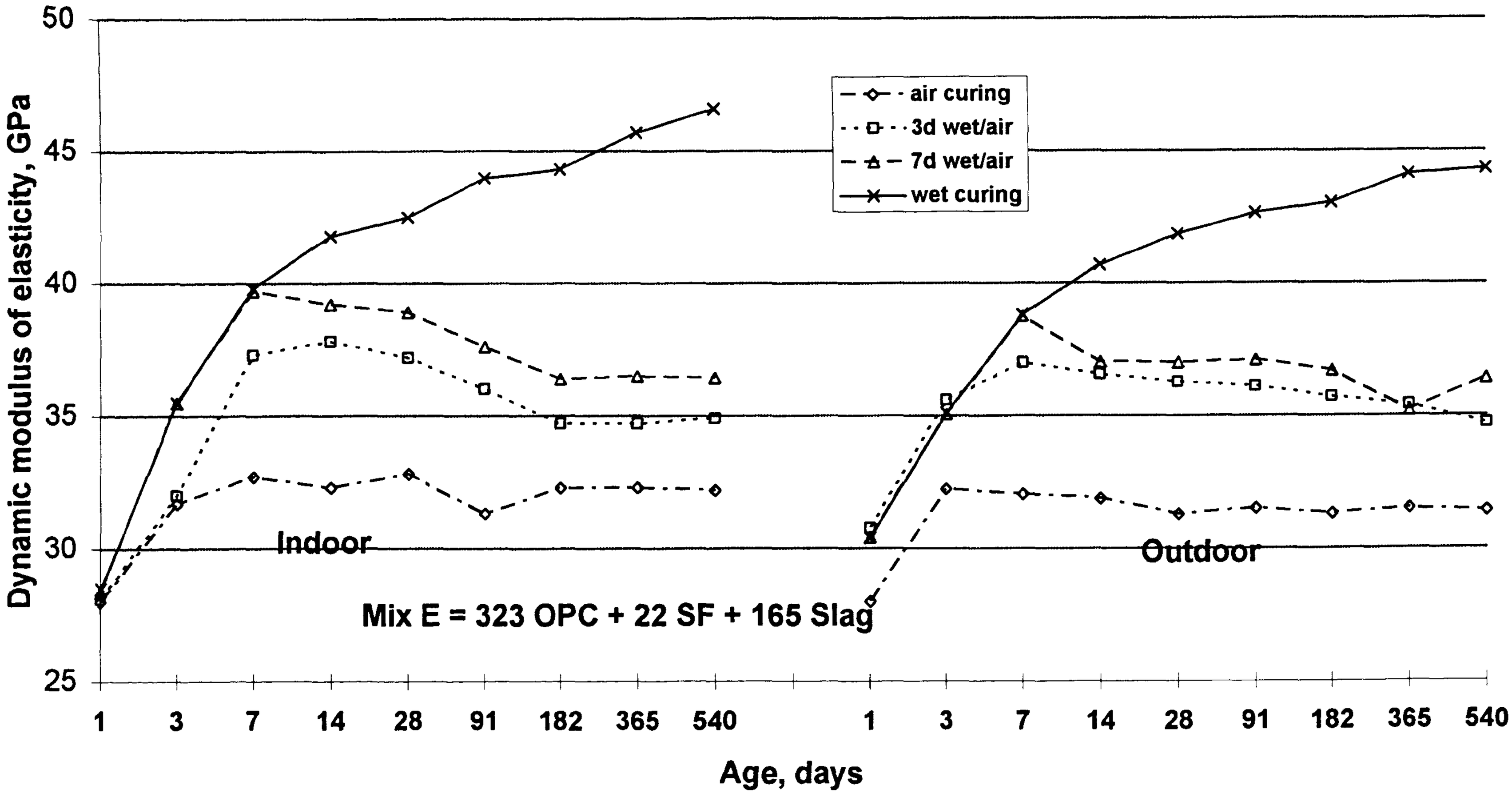

Fig. 5.35: Influence of curing regime on dynamic modulus of elasticity for mix E.

and similar loss of elastic modulus of some 25% at later ages when exposed to prolonged drying. This loss in elastic modulus can be attributed to internal microcracking as shown earlier by the pulse velocity data. This phenomenon was also observed at early ages from 7-14 days for all specimens initially cured in water and then dried in air. Lydon [148] however, attributed the reduction of dynamic modulus to water loss on drying, which is likely to occur at a greater rate with the latter. On the other hand, others [13] have reported that, this reduction of modulus of elasticity due to formation of microcracking. In fact, this loss is due to internal microcracking arising from moisture loss.

Fig. 5.31 shows the dynamic modulus of elasticity development for the control mix under the four curing conditions. The wet-cured specimens yielded the highest elastic modulus values at early ages and in the long term compared to 7d wet/air, 3d wet/air and air-cured specimens, and reached a maximum value at 18 months of 47.9 GPa. Drying in air continuously showed a reduction of 23% at 28 days and 41 % at 18 months. Curing initially in water for 3 days helped to develop the performance of concrete and produce values better than air curing; future increase in water curing to 7 days increased the elastic modulus, the values at 18 months being 33.9, 37.5 and 38.3 GPa for air-cured, 3d wet/air and 7d wt/air-cured specimens respectively. From the figure it appears that drying in air affected the internal microstructure, and reflected the effect of drying as losses in elastic modulus increasing with time.

Fig. 5.32 shows the development of dynamic modulus of elasticity with age for silica fume concrete under the four curing regimes. The trend in dynamic modulus of elasticity for the different curing regimes is similar to those obtained for the control mix. The wet-cured specimens yielded the highest dynamic modulus values compared with the other curing regimes. For example, at the age of 18 months, the dynamic modulus of wet cured specimens were 48.8 GPa. Significant reduction was observed due to drying in air, the corresponding values of air-cured, 3d wet/air-cured and 7d wet/air-cured specimens were 35.6, 37.3 and 37.9 GPa, respectively.

The influence of various curing regimes on dynamic modulus of elasticity development for mixes C, D and E are shown in Figs. 5.33 to 5.35. From the trend shown in these figures it is clear that there were significant differences in the long term between the wet cured specimens and the other three curing regimes. The maximum reduction was observed for air cured specimens followed by 3d wet/air and 7d wet/air

curing. Similar to the trend in the other mixes, the wet cured specimens of SF/slag yielded the highest dynamic modulus of elasticity. On the other hand, the effect of drying in air was more pronounced in the long term, and it decreased with increasing water curing.

5.4.3 Effect of mix type , Indoor

Figs. 5.36 to 5.39 show the effect of mix type on the dynamic modulus of elasticity. The values of the modulus of elasticity can be seen in Table 5.5 where the mix type can be seen to affect the dynamic modulus of elasticity. Under wet curing the dynamic modulus of all concretes continued to increase up to 18 months except mix A which reached a steady state after 6 months. At 6 months, similar values were obtained for mixes A, B and C. Mixes D and E yielded lower values than the other mixes of about 4 and 6% respectively. At 18 months, mixes C and B exhibited the highest values, while mix A showed lower values than these mixes due to the low hydration of OPC at this age. On the other hand, mix containing slag (mix D) showed significant development due to the continued slag hydration and presented similar value to mix A. Also, mix E decreased the gap with mix A from 2.9 GPa at 6 months to 1.3 GPa at 18 months.

Under 3d wet/air and 7d wet/air curing, a comparison of the five mixes shows that mix C (323 OPC + 22 SF + 55 slag) produced the highest values of modulus of elasticity at 28 days and beyond. On the contrary, mix E showed the lowest modulus of elasticity at any given specimen age, as seen in Figs. 5.37 and 5.38. In addition to this, the general trend of mix D results at long term was approximately similar to those of the SF/OPC or plain OPC mixes. Under 7d wet/air curing mix A and B showed the highest reduction compared with the results at both 7-days and 18 months; these reductions were about 11 and 12% respectively. On the other hand, mixes containing slag exhibited lower reduction in the range of 8 to 9%.

In general the adverse effect of air curing on dynamic modulus development in all mixes is readily seen, all the concretes reached a maximum dynamic modulus at 14 days and indeed the control mix (mix A) showed a considerable reduction in dynamic modulus beyond this age and reached it is minimum value of 33.9 GPa at 18 months; this is reduction of about 9% compared with its maximum value. Mix B exhibited 6% reduction. On the other hand, mixes C, D and E containing slag exhibited less reduction, of about 2 to 5% compared with its maximum value. At 14 days and beyond, the B and C mixtures were close to each other, showed almost equal dynamic modulus values and had higher dynamic modulus than the other mixes, while mix E

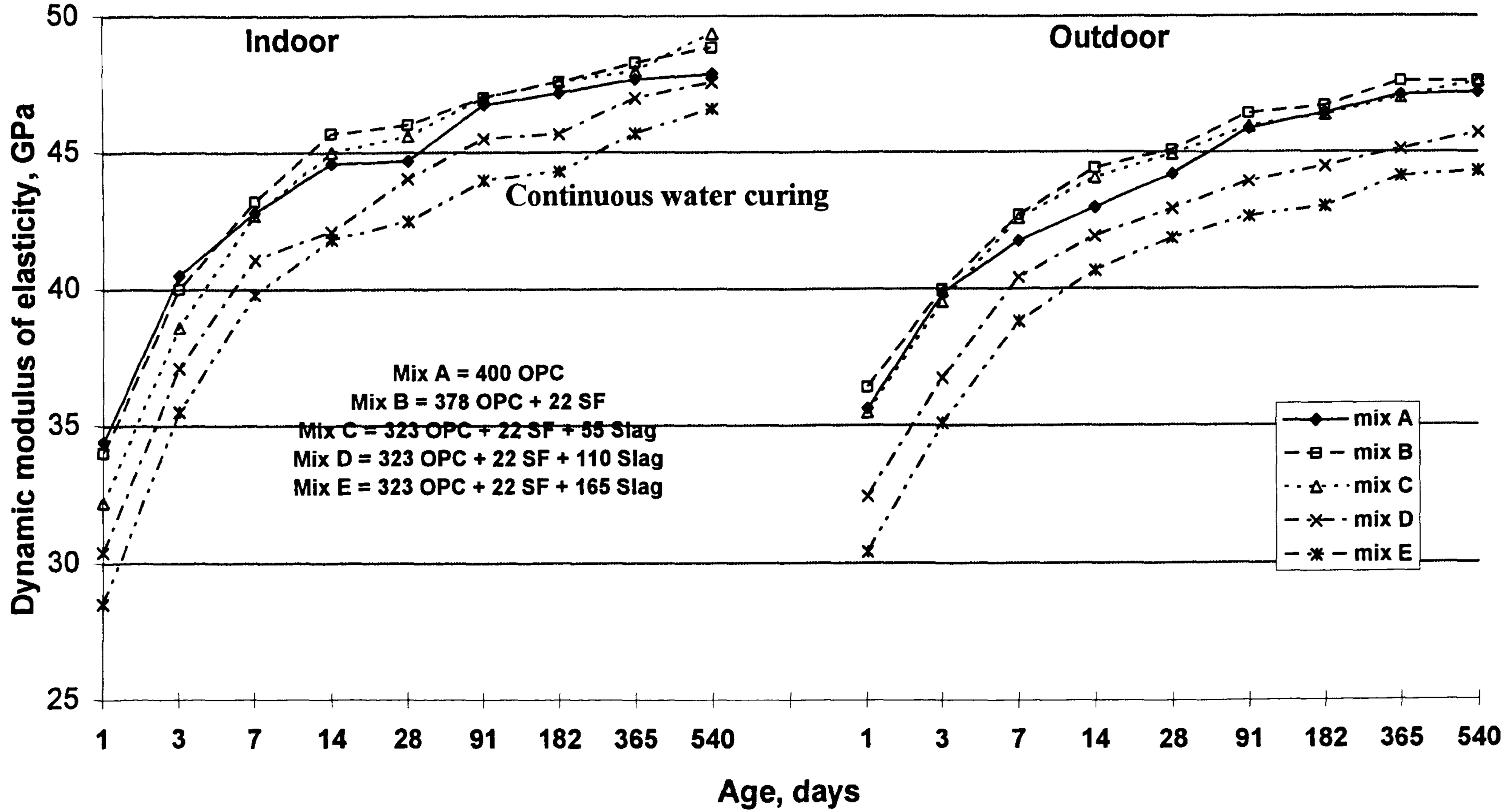

Fig. 5.36: Influence of mix type on dynamic modulus of elasticity under continuous water curing.

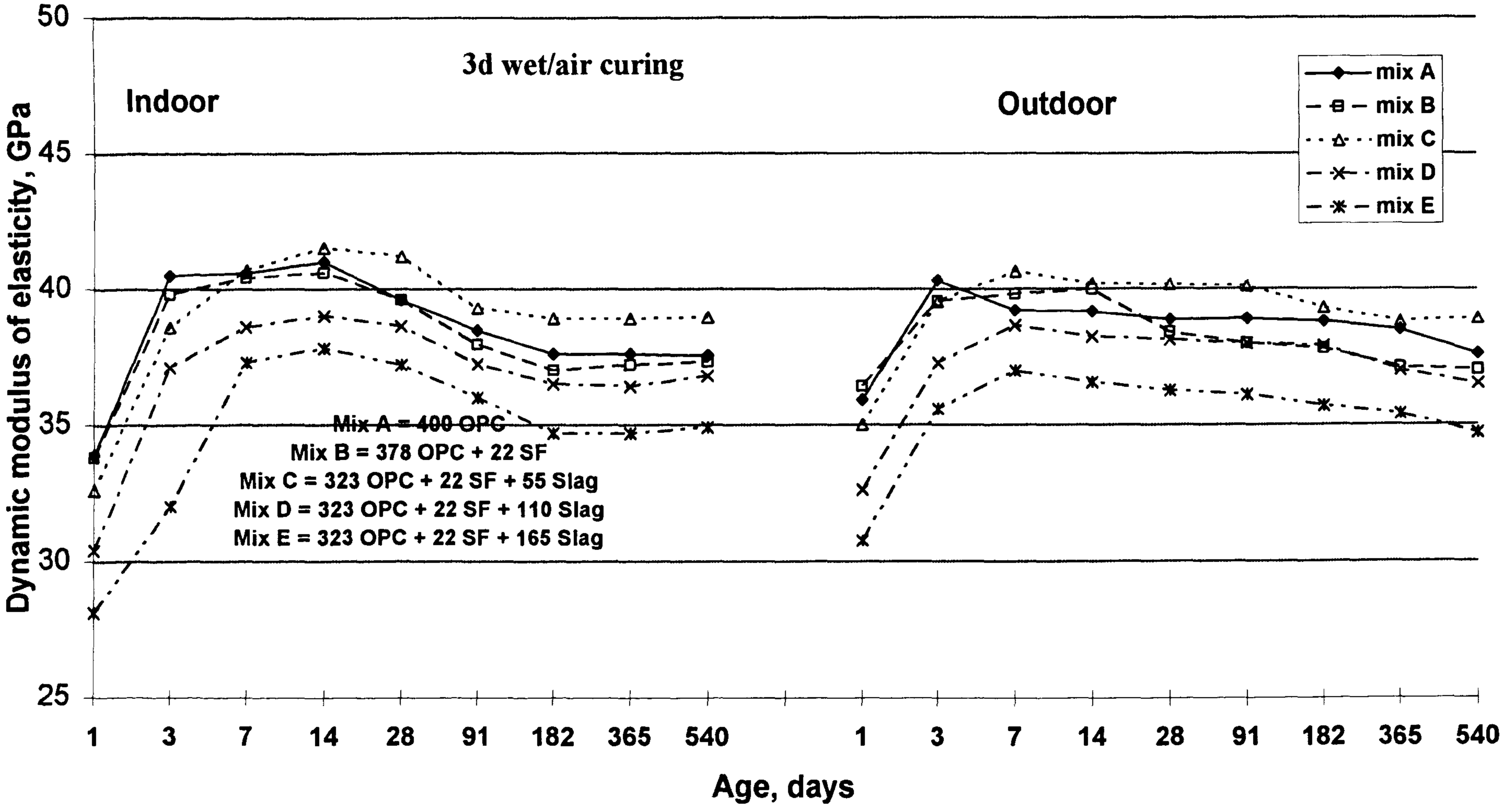

Fig. 5.37: Influence of mix type on dynamic modulus of elasticity under 3d wet/air curing.

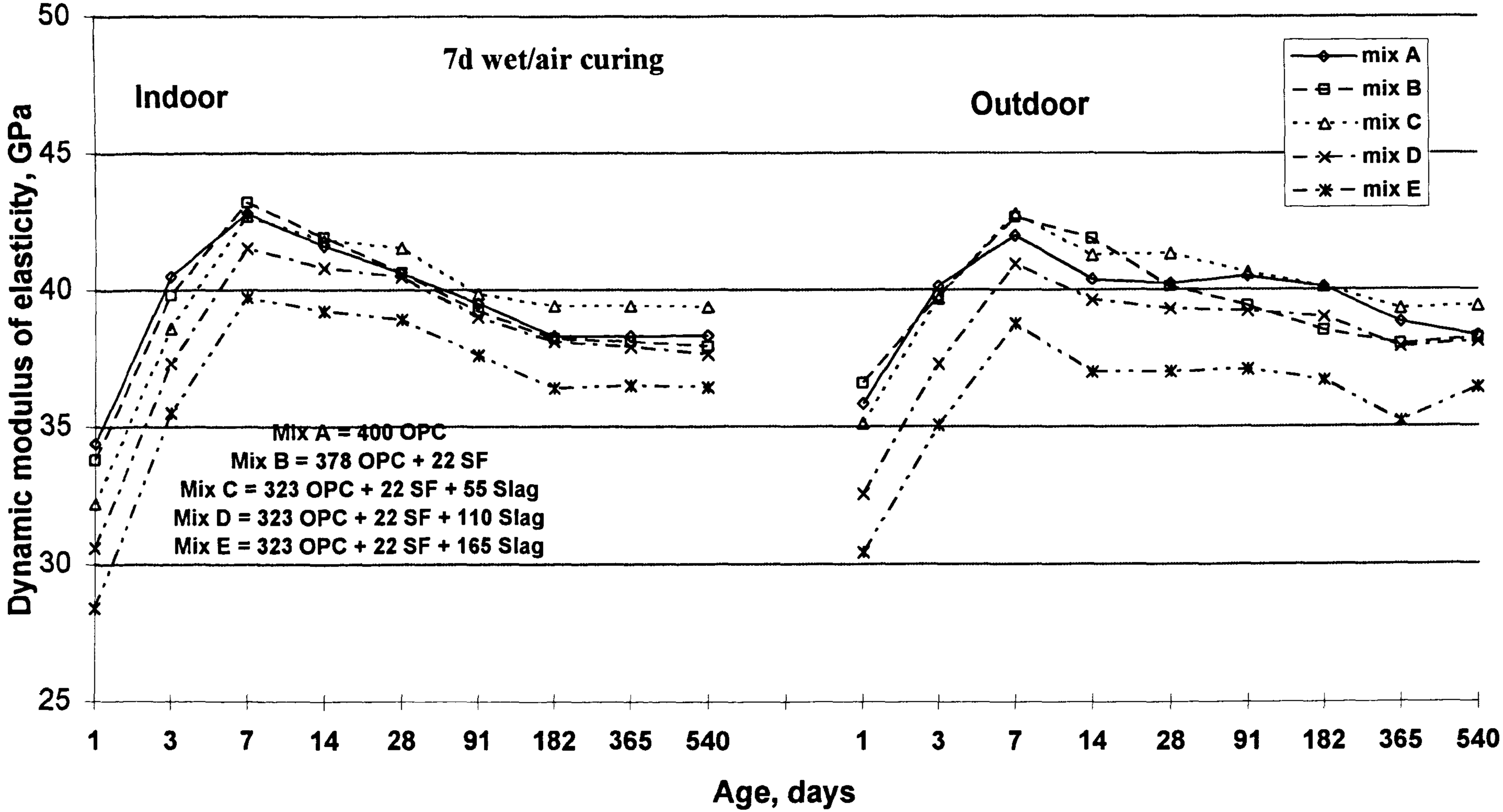

Fig. 5.38: Influence of mix type on dynamic modulus of elasticity under 7d wet/air curing.

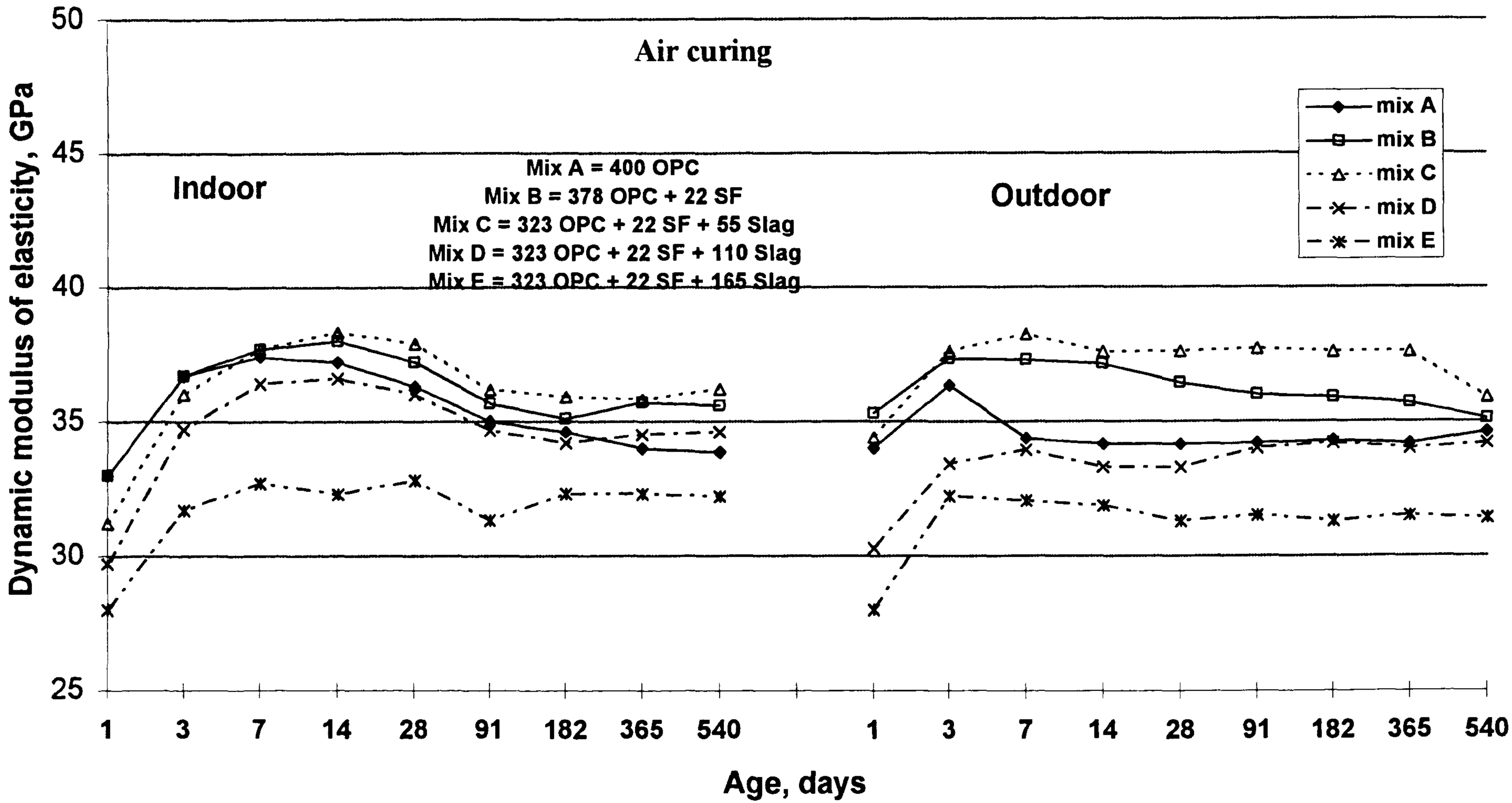

Fig. 5.39: Influence of mix type on dynamic modulus of elasticity under air curing.

exhibited the lowest values of dynamic modulus of elasticity which remained constant at early age and later at about 32 GPa, indicating more than the other concretes the adverse effect of the absence of water curing on the development of dynamic modulus for a relative high slag content. This is confirmed by pulse velocity results which show a pattern similar to that observed in dynamic modulus.

5.4.4 Effect of exposure environment

The effect of exposure environment on the dynamic modulus of elasticity is also shown in Figs. 5.27 to 5.39 and Tables 5.5 and 5.6 presented earlier. These data emphasise that the development of dynamic modulus of elasticity is affected by curing regime as well as cement type and exposure environment. For all the five mixes, the initial rate of development of the dynamic modulus was rapid on the first day in the outdoor environment, while at 3 days and beyond, the outdoor environment slowed down this rate similar to or less than that in the indoor environment. Specimens subjected to continuous wet curing in the outdoor exhibited values lower than the corresponding values in the indoor specially during the period from 91 to 540 days. This reduction in the dynamic modulus may be attributed to the fact that, after casting, the specimens were immediately exposed to the hot environment for about 24 hours; during this period, the adverse effect of the hot environment could have increased the surface temperature of specimens up to 60°C, and together with direct solar radiation, caused high evaporation and accelerated the hydration process. The temperature then dropped to about 30°C at night of the same day which caused thermal shrinkage. This high temperature and also the high variation in temperature may cause adverse effects on concrete, and this appears as loss of elasticity at later ages. Abbasi and Al-Tayyib [65] reported that the pulse velocity and modulus of elasticity of concrete prepared and cured in hot weather conditions are reduced with increase in the concrete mix temperature at the preparation time. Mixes D and E exhibited a greater loss in the elastic modulus in the outdoor environment, indicating that mixes containing a relatively high amount of slag is affected more in the outdoor environment, so far as the modulus of elasticity criterion is concerned. On the other hand, mix C with a limited amount of slag produced the highest values of elastic modulus in the outdoor environment.

Mixes subjected to 7 days water curing and then exposed to air drying in the outdoor environment showed sudden loss of dynamic modulus of elasticity for all the mixes after 7 days, whereas this loss was gradual in the indoor environment. This is considered to be due to the rapid loss of water from specimens in the outdoor environment; leading to restricted

hydration in the concrete and initiating microcracking, and thus stopping the development of the dynamic modulus. Therefore, keeping concrete wet during most of its hydration period in hot environment, leads to producing a high quality concrete with a high modulus of elasticity arising from the development of its pore structure.

5.4.5 Relationship between dynamic modulus and compressive strength

The general relationship between the modulus of elasticity and compressive strength is well established, and is well known for OPC concrete, and models to predict these properties have also been developed. In this study, a number of empirical functions were tried in an attempt to relate strength to the dynamic modulus. The relations between compressive strength, f_{cu} and dynamic modulus of elasticity was found for all the mixes and in both environments under various curing conditions and these are as shown in Figs. 5.40-5.43 using the following equation:

$$E_d = a(f_{cu})^b \qquad (5.1)$$

where E_d = dynamic modulus of elasticity, GPa.

f_{cu} = compressive strength, MPa.

a and b are constants related to the properties of the concrete and the materials in each mix.

The correlation results presented in Table 5.7 indicate that there is poor correlation between compressive strength and dynamic modulus of elasticity for specimens exposed to a drying environment, or initially cured in water and then exposed to drying in air. These correlation factors ranged from 0.29-0.34, while specimens continuously

Table 5.7 Relationship between dynamic modulus and compressive strength.

Curing regime	Equation	R^2
Air curing	$E_d = 20.5(f_{cu})^{0.134}$	0.29
3d wet/air	$E_d = 23.0(f_{cu})^{0.12}$	0.34
7d wet/air	$E_d = 23.8(f_{cu})^{0.117}$	0.32
Wet curing	$E_d = 12.1(f_{cu})^{0.31}$	0.88

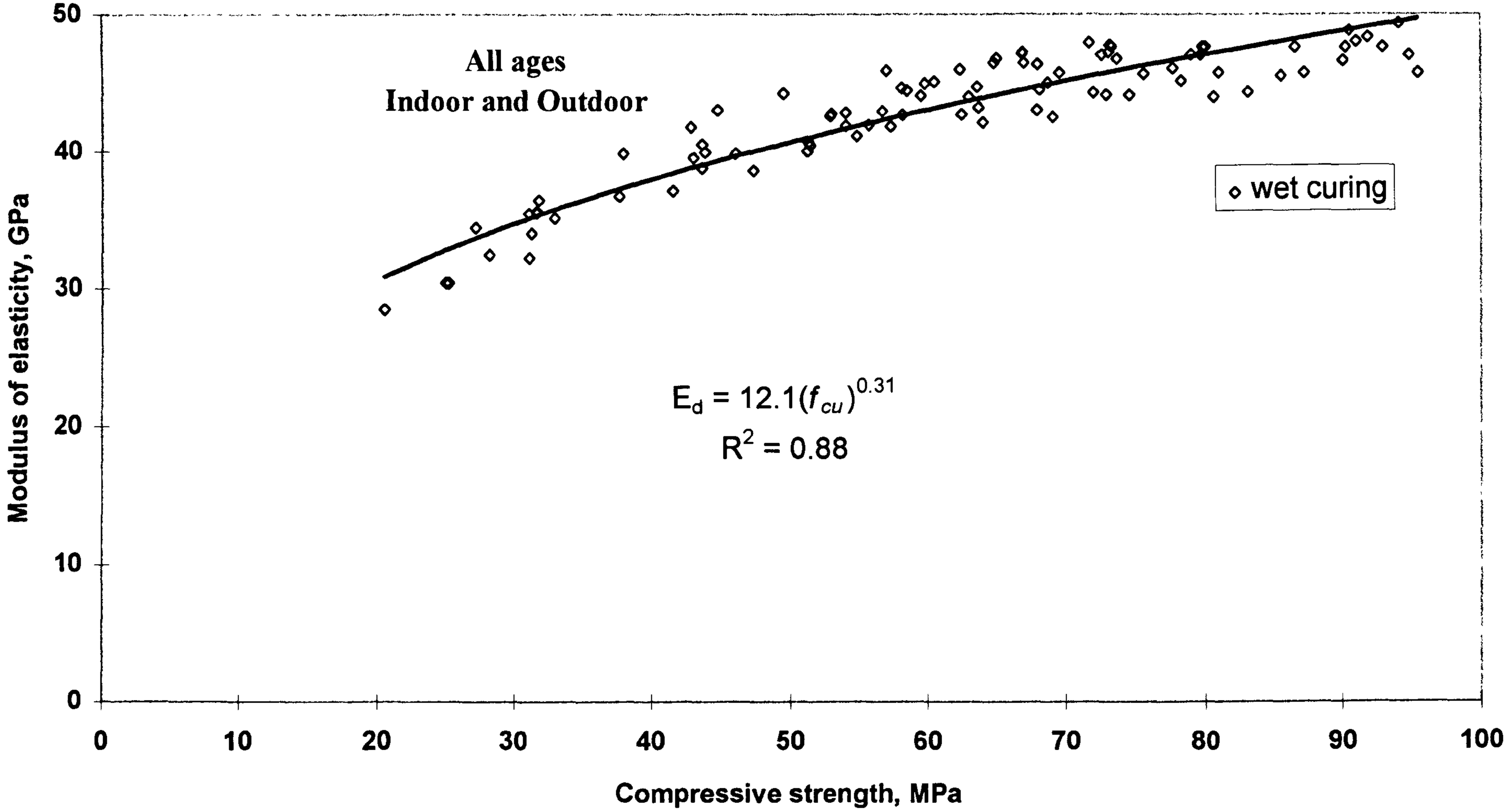

Fig. 5.40 : Relationship between dynamic modulus and compressive strength for all mixes under continuous water curing.

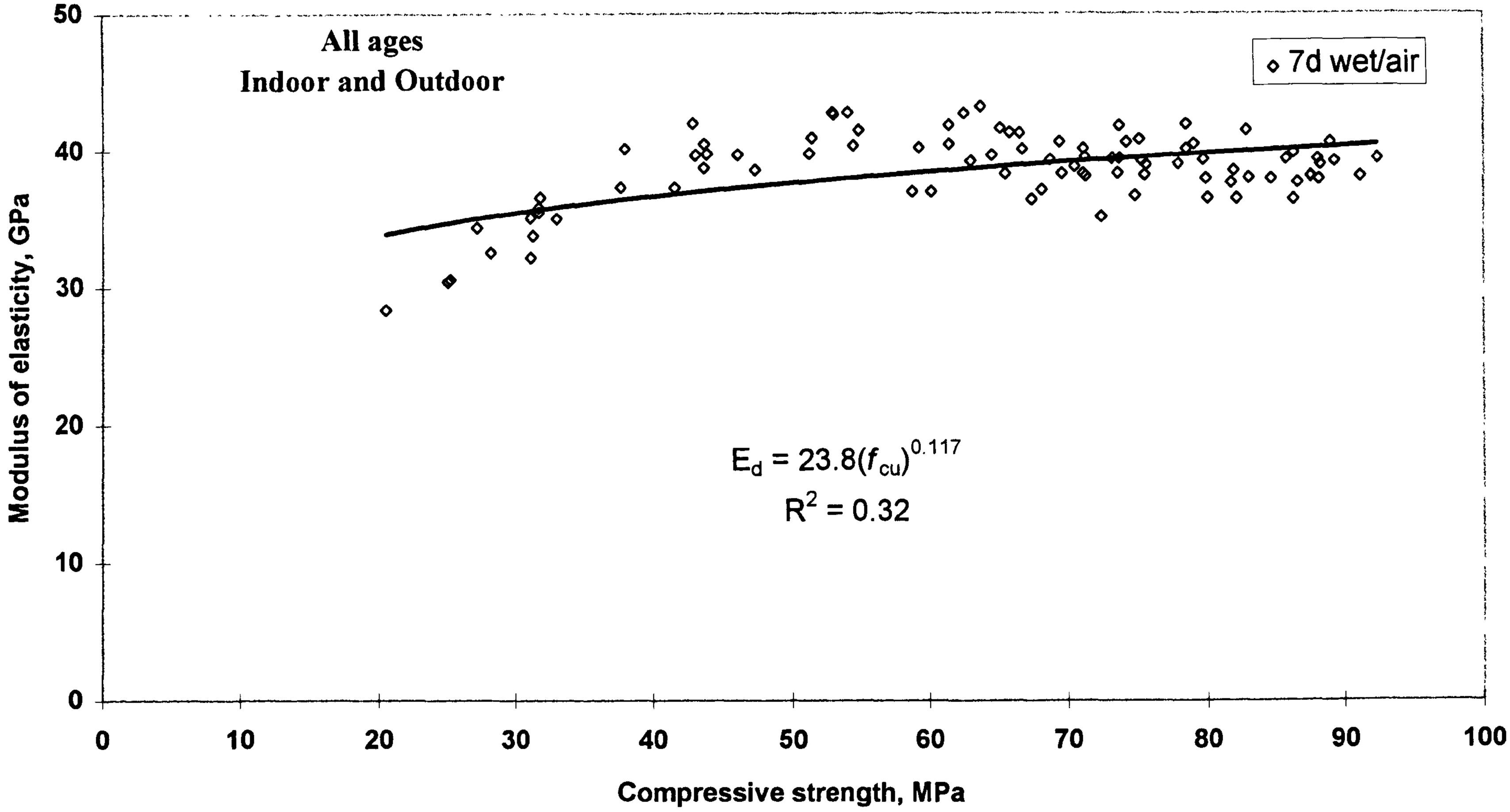

Fig. 5.41 : Relationship between dynamic modulus and compressive strength for all mixes under 7d wet/air curing.

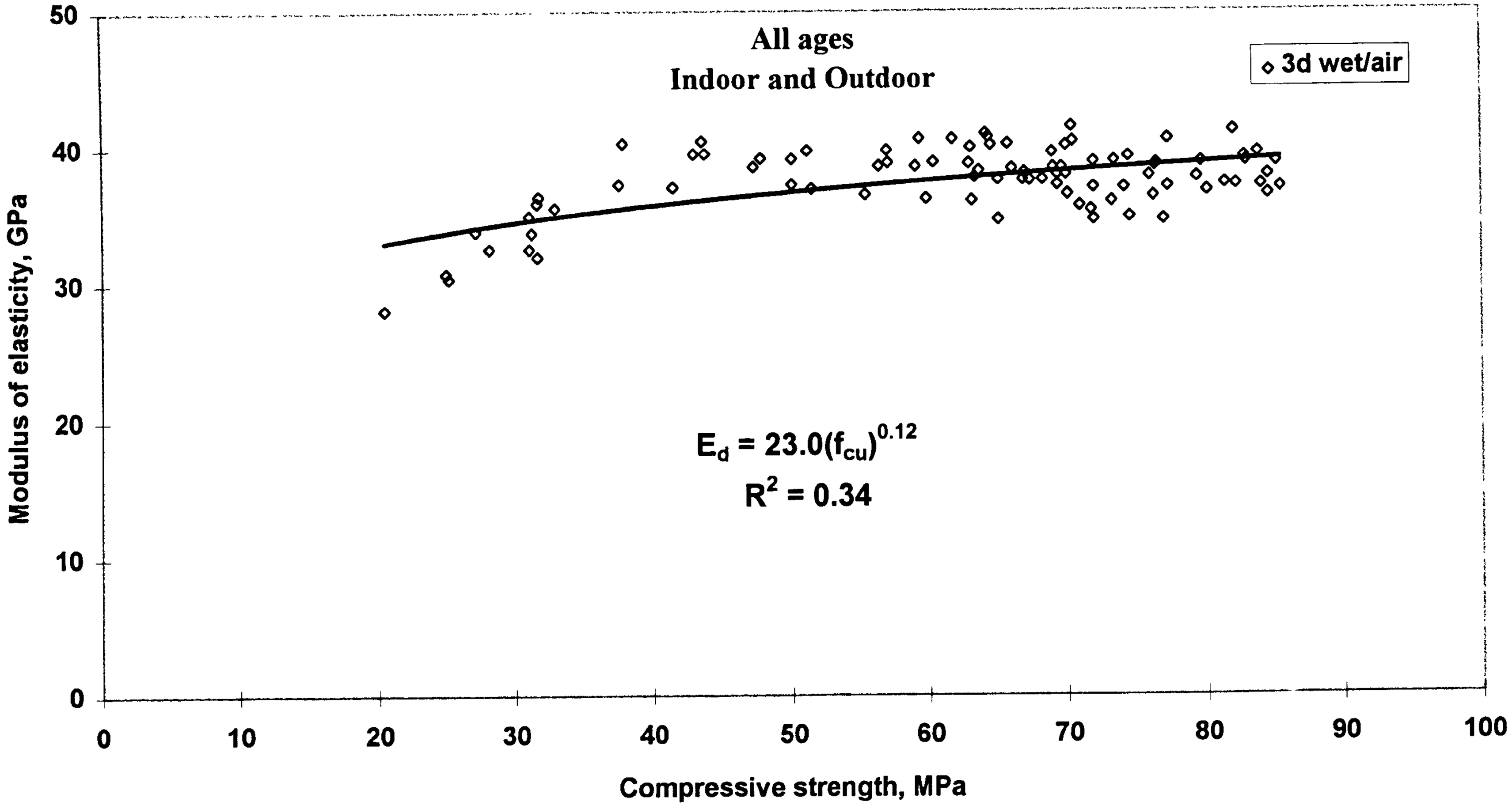

Fig. 5.42 : Relationship between dynamic modulus and compressive strength for all mixes under 3d wet/air curing.

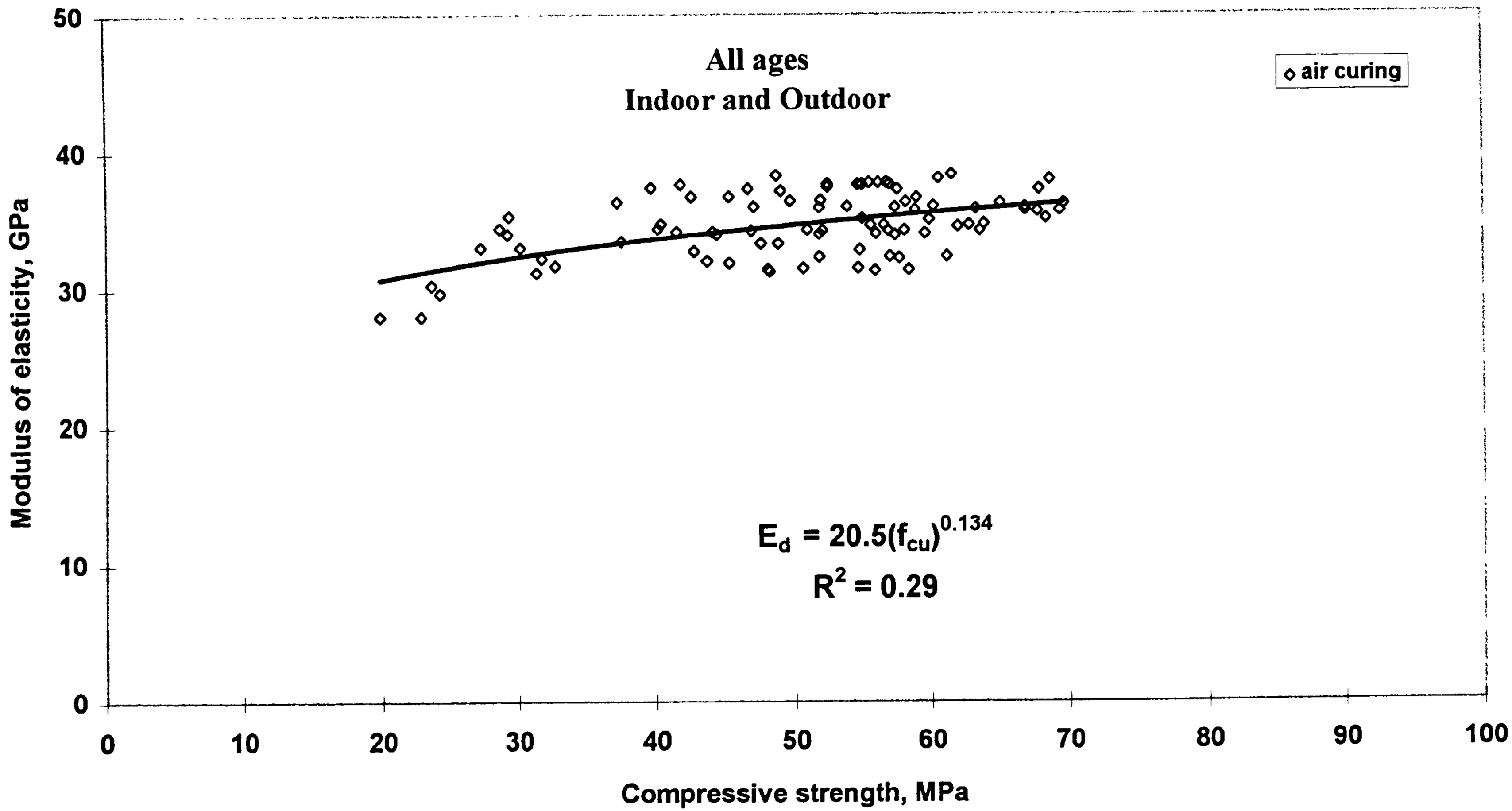

Fig. 5.43 : Relationship between dynamic modulus and compressive strength for all mixes under air curing.

cured in water show a good correlation factor of 0.88 between compressive strength and dynamic modulus.

5.5 Shrinkage and expansion

Shrinkage is generally affected by the volume and type of aggregate; aggregates with higher elastic modulus provide greater resistance to shrinkage of the cement paste. To achieve a low shrinkage, a stiff aggregate and a low water/binder ratio of 0.35, which was constant for all the mixes, was used in these tests. The shrinkage in this work was measured as a linear strain, and is thus dimensionless and is expressed as microstrains [52].

Figs. 5.44 to 5.56 show all the results of shrinkage and expansion measurements of the concretes used in this study. In these figures, every point on the graphs represents the average of eight measurements from two specimens. All the specimens were exposed to variable internal and external environmental conditions over several days as the shrinkage and expansion curves demonstrate.

5.5.1 Effect of curing, Indoor

Concrete shrinks and gains strength as it dries, and is the direct result of moisture loss as the material dries out and matures. The amount of shrinkage is greater than any subsequent expansion caused by wet curing whether the concrete is exposed to indoor or outdoor conditions. Generally, as far as the curing conditions are concerned, there is no significant difference between the two environments in all curing conditions for all the mixes, but the outdoor condition creates slightly lower values of expansion due to outdoor exposure when tested at 8 AM. As expected, for all mixes, longer wet curing contributed to shrinkage at a low level. In all curing conditions, the specimens show swelling up to the wetting time, and then shrinkage, but they never regained their original condition. However, the specimens cured in air show that the changes occurred at first day of curing as a result of the effect of the drying condition. In these tests the readings were not taken daily, they were rather taken only at the same time as the other engineering readings. The maximum shrinkage was achieved in air curing condition by mix E. The rest of the results of the shrinkage and expansion over the whole testing time for all the mixes are presented in Tables 5.8 and 5.9.

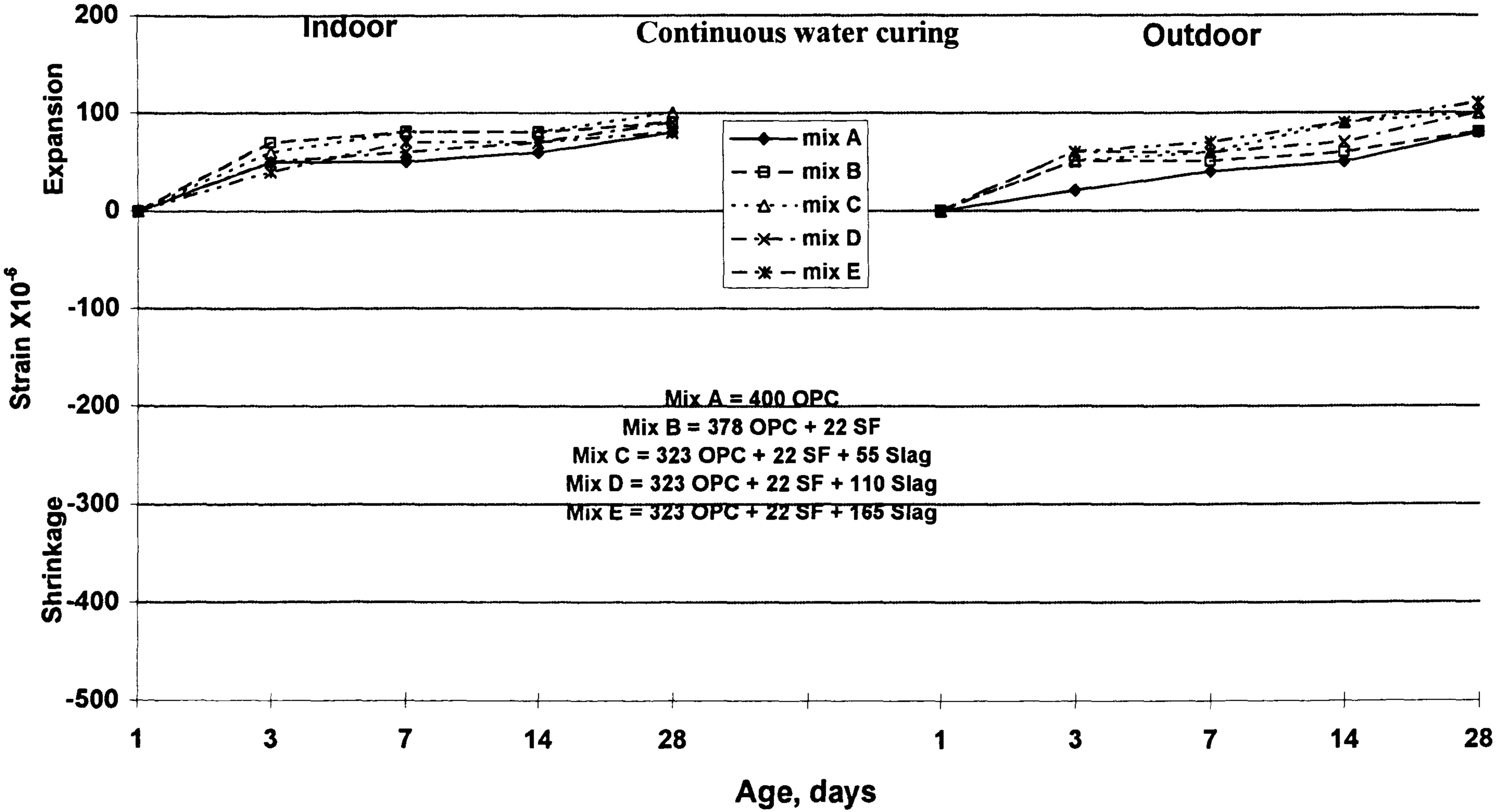

Fig. 5.44 : Influence of mix type on shrinkage and expansion under continuous water curing.

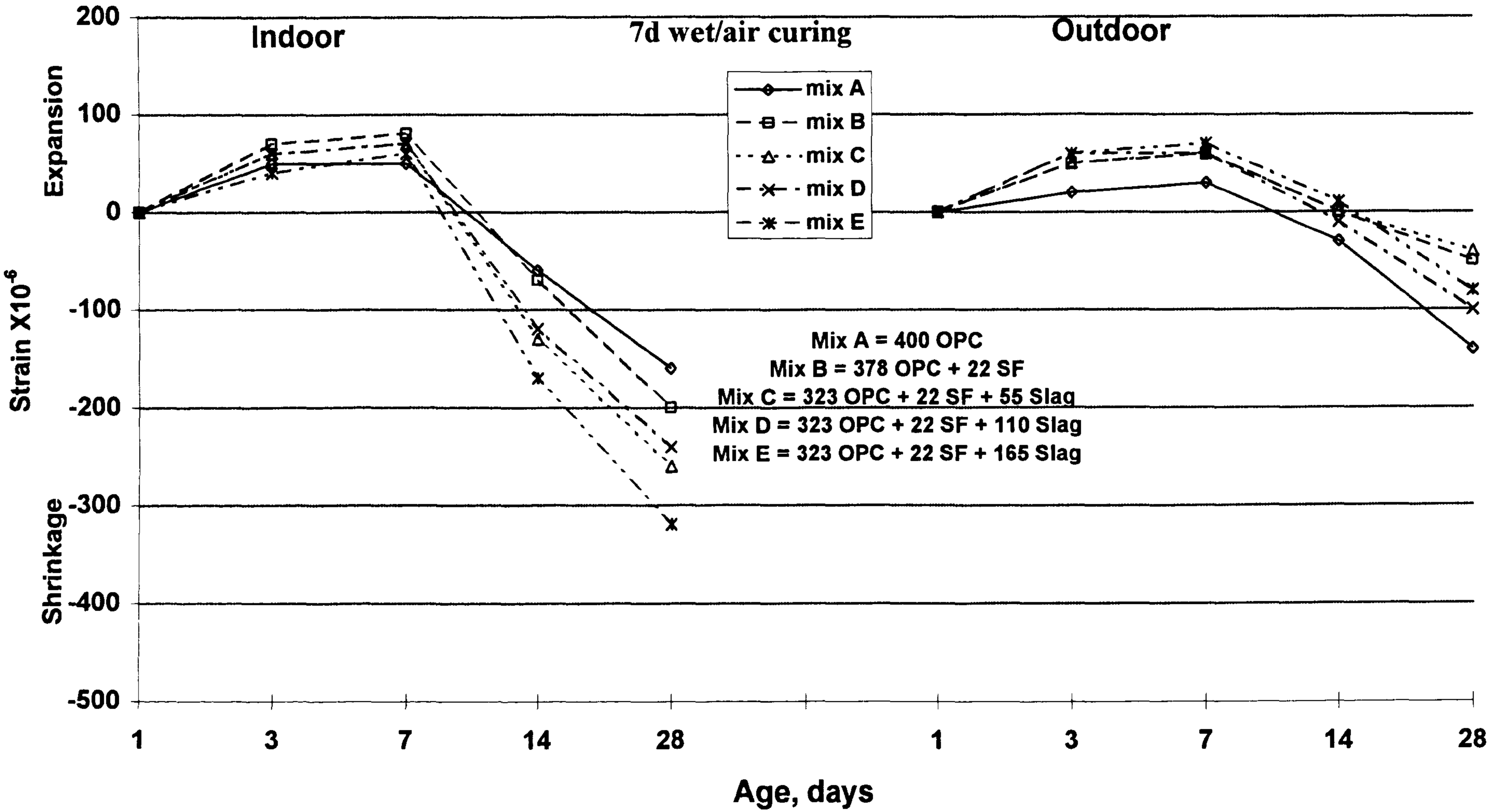

Fig. 5.45 : Influence of mix type on shrinkage and expansion under 7d wet/air curing.

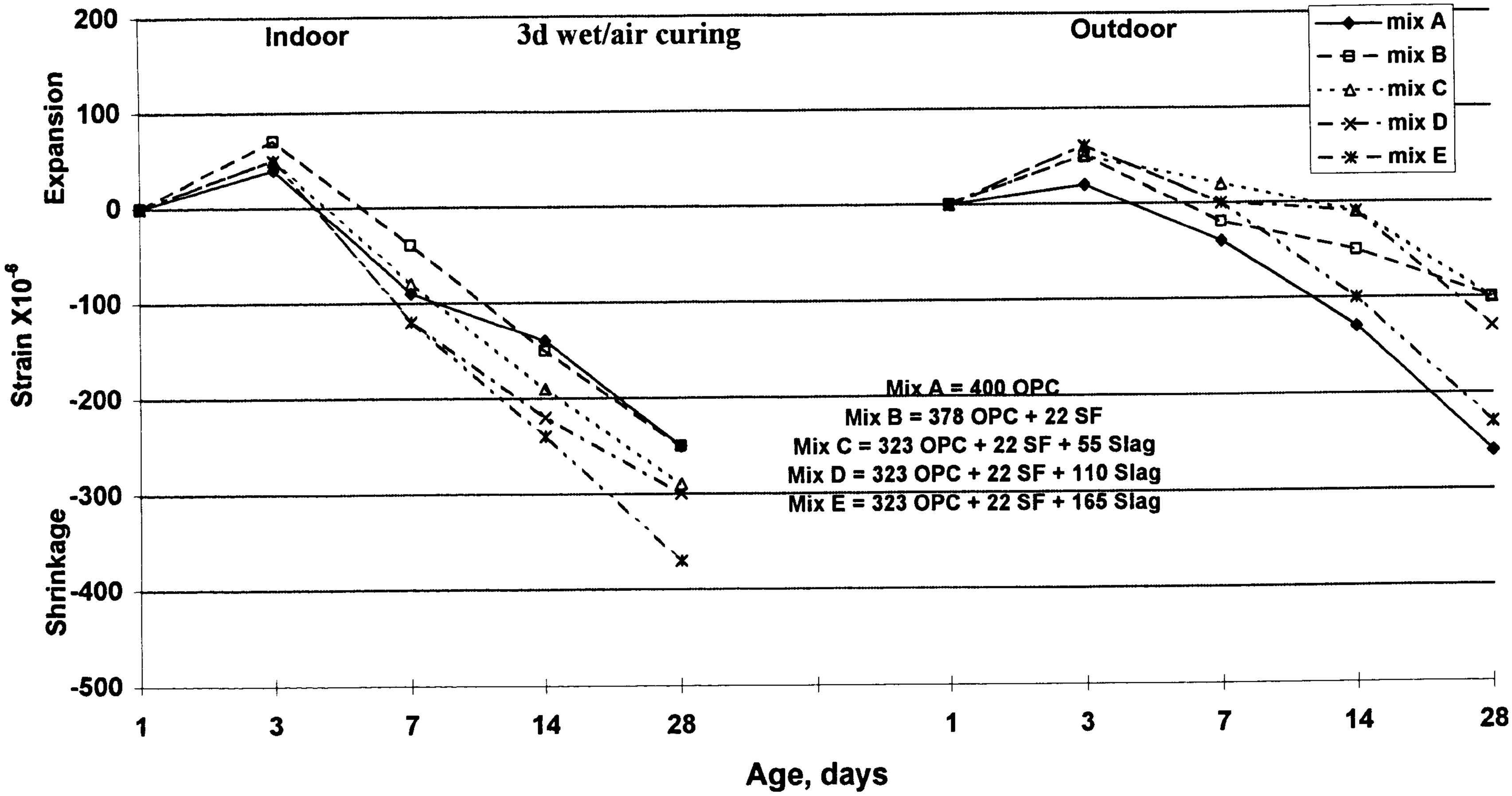

Fig. 5.46 : Influence of mix type on shrinkage and expansion under 3d wet/air curing.

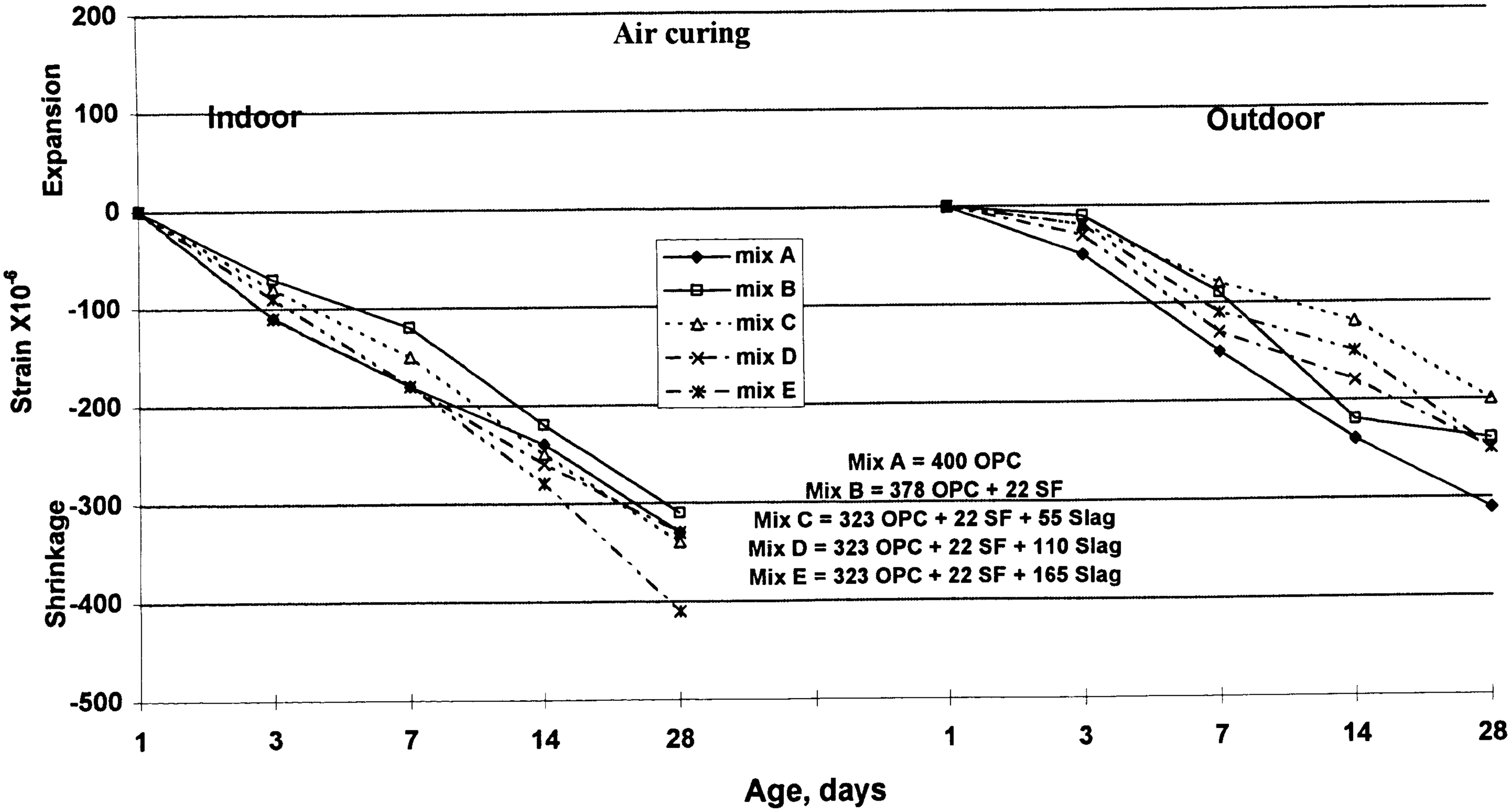

Fig. 5.47 : Influence of mix type on shrinkage and expansion under air curing regime.

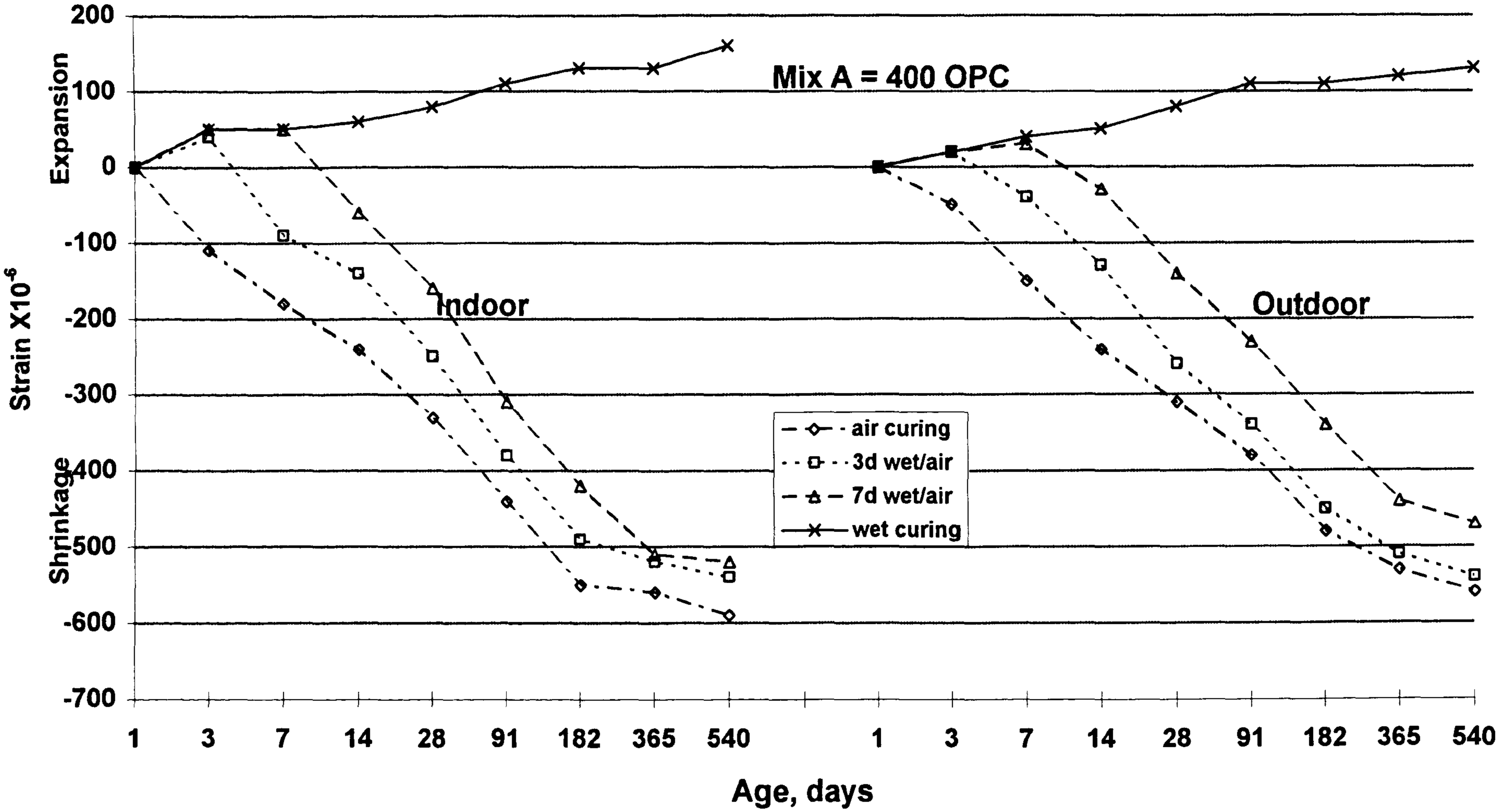

Fig. 5.48 : Influence of curing regime on shrinkage and expansion for mix A.

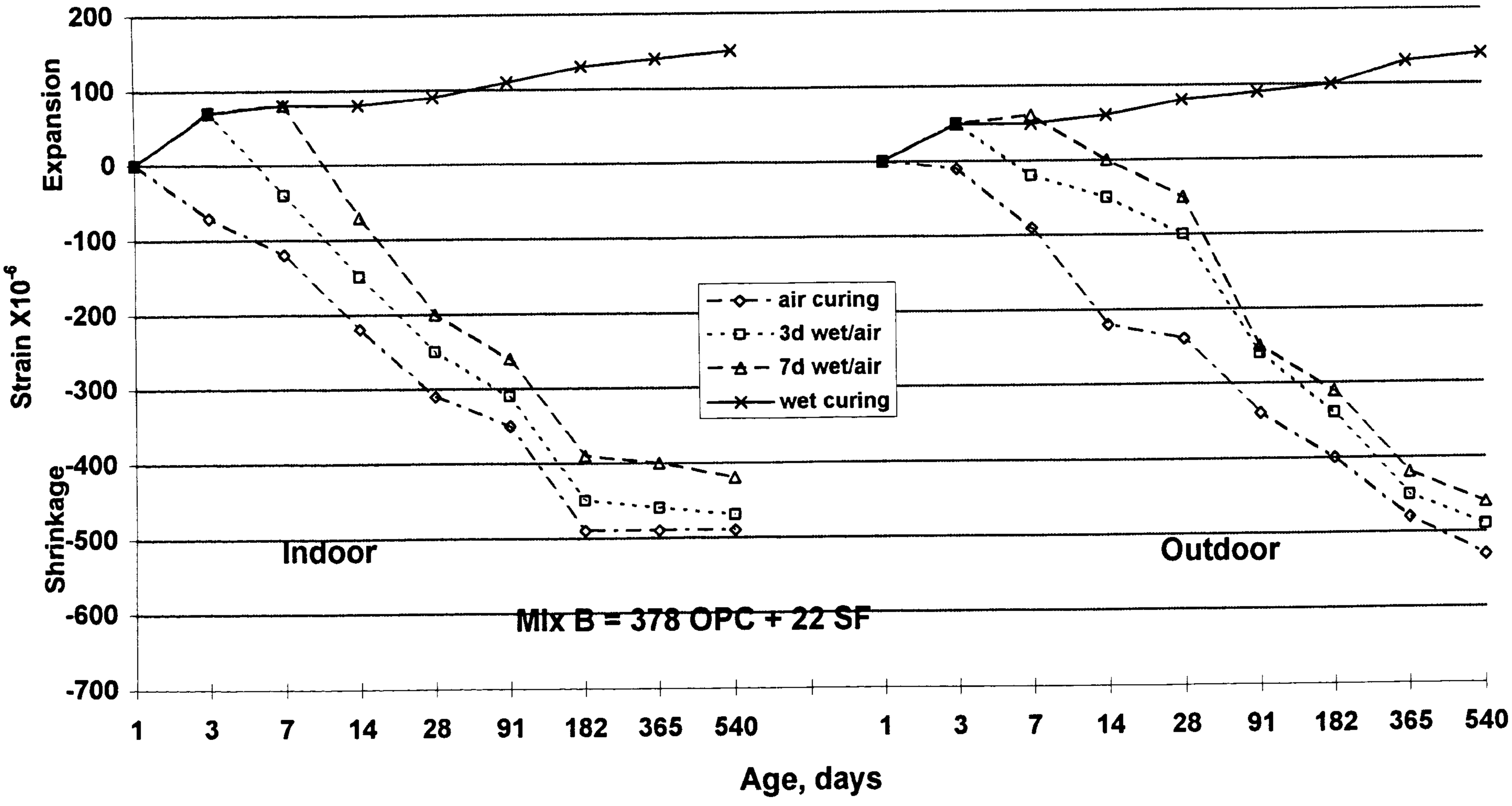

Fig. 5.49 : Influence of curing regime on shrinkage and expansion for mix B.

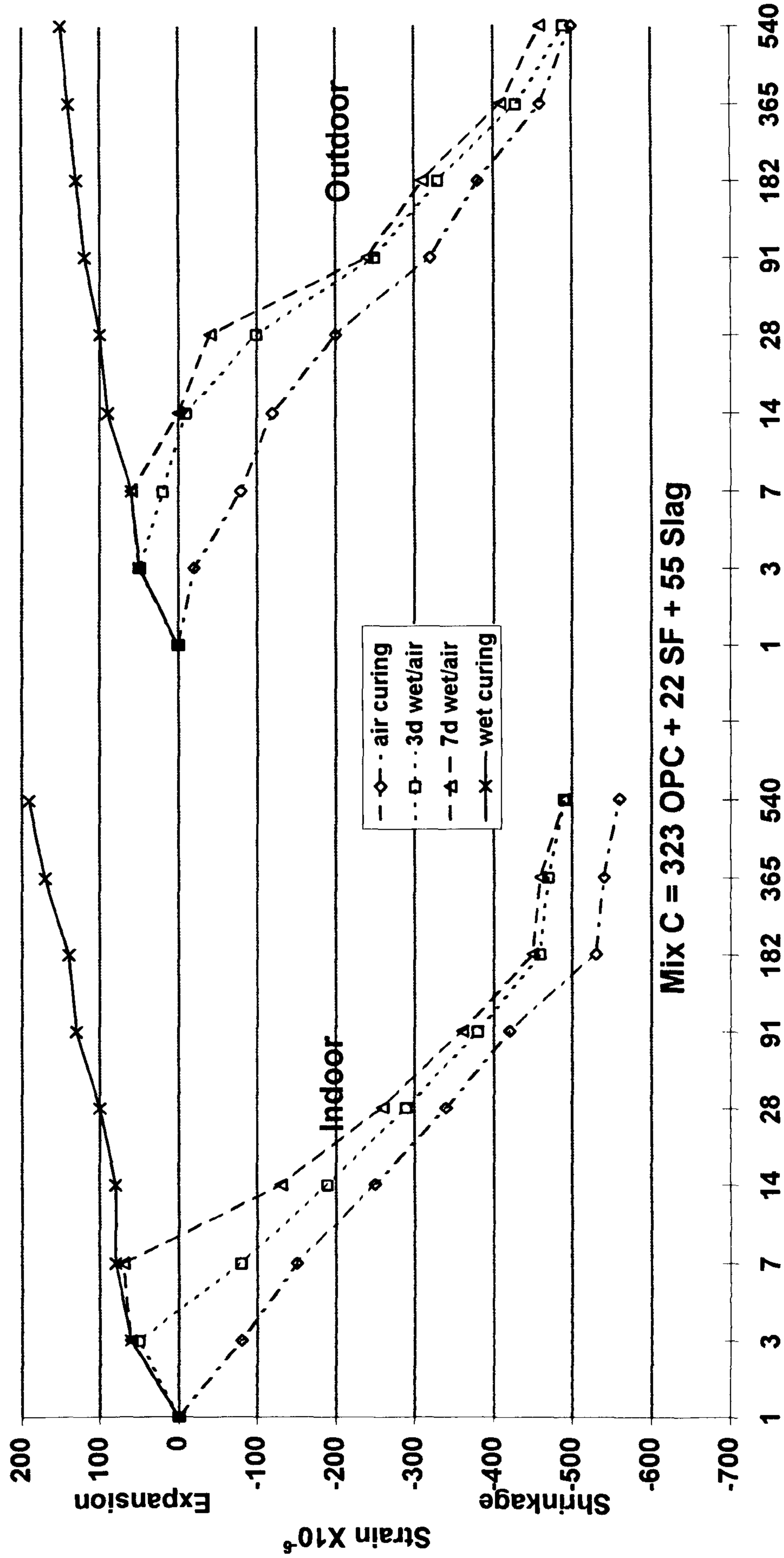

Fig. 5.50 : Influence of curing regime on shrinkage and expansion for mix C.

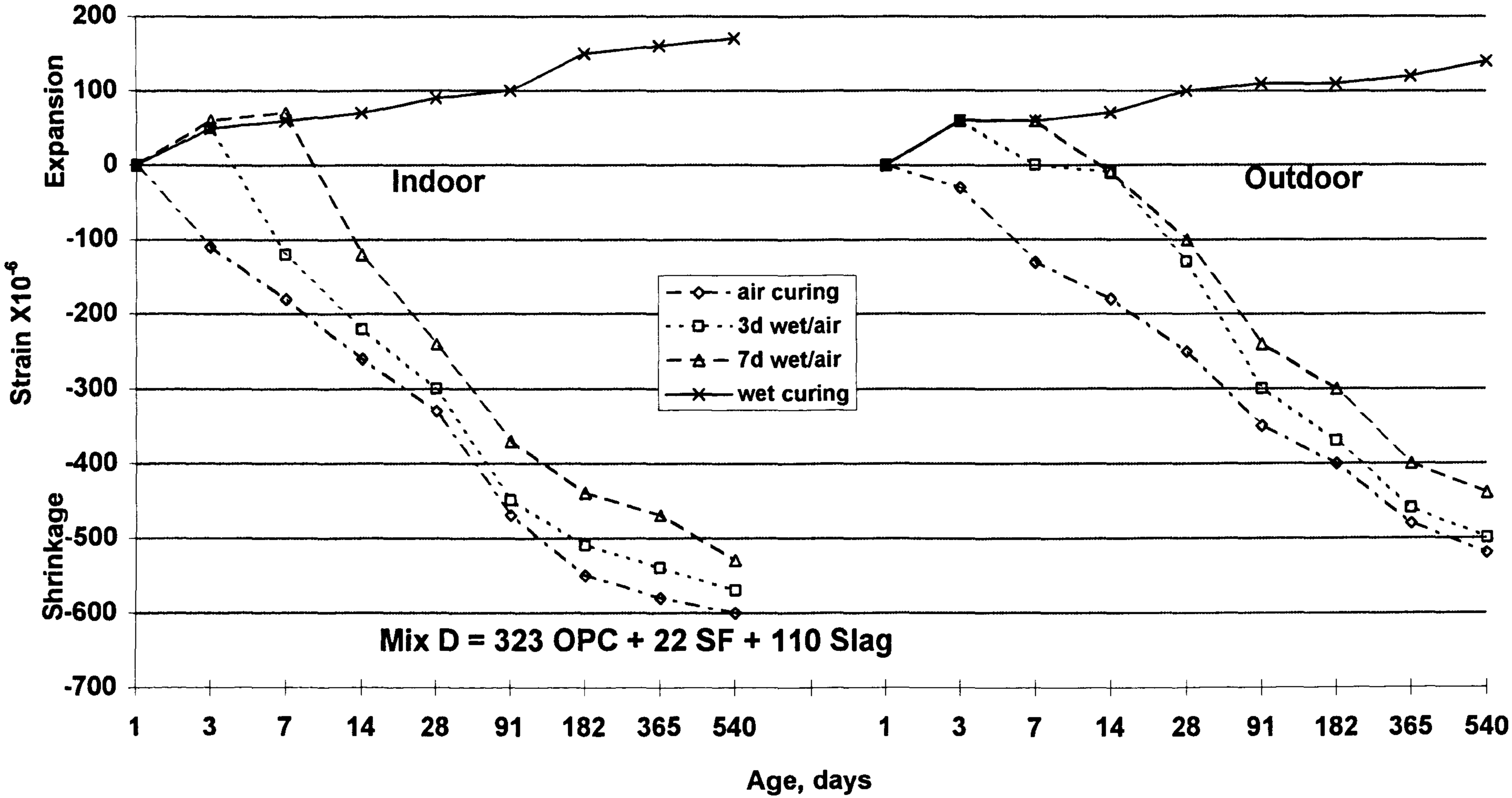

Fig. 5.51 : Influence of curing regime on shrinkage and expansion for mix D.

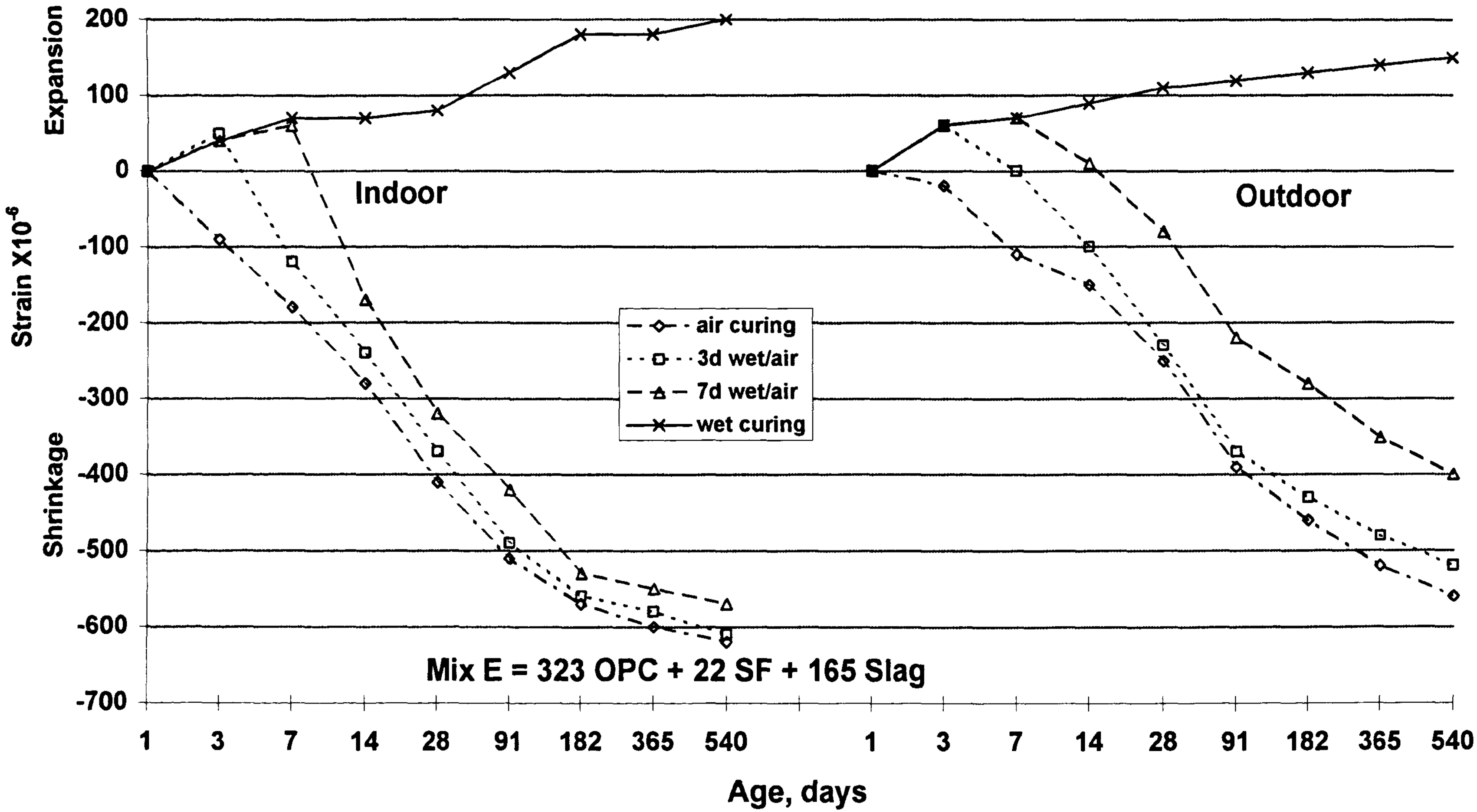

Fig. 5.52 : Influence of curing regime on shrinkage and expansion for mix E.

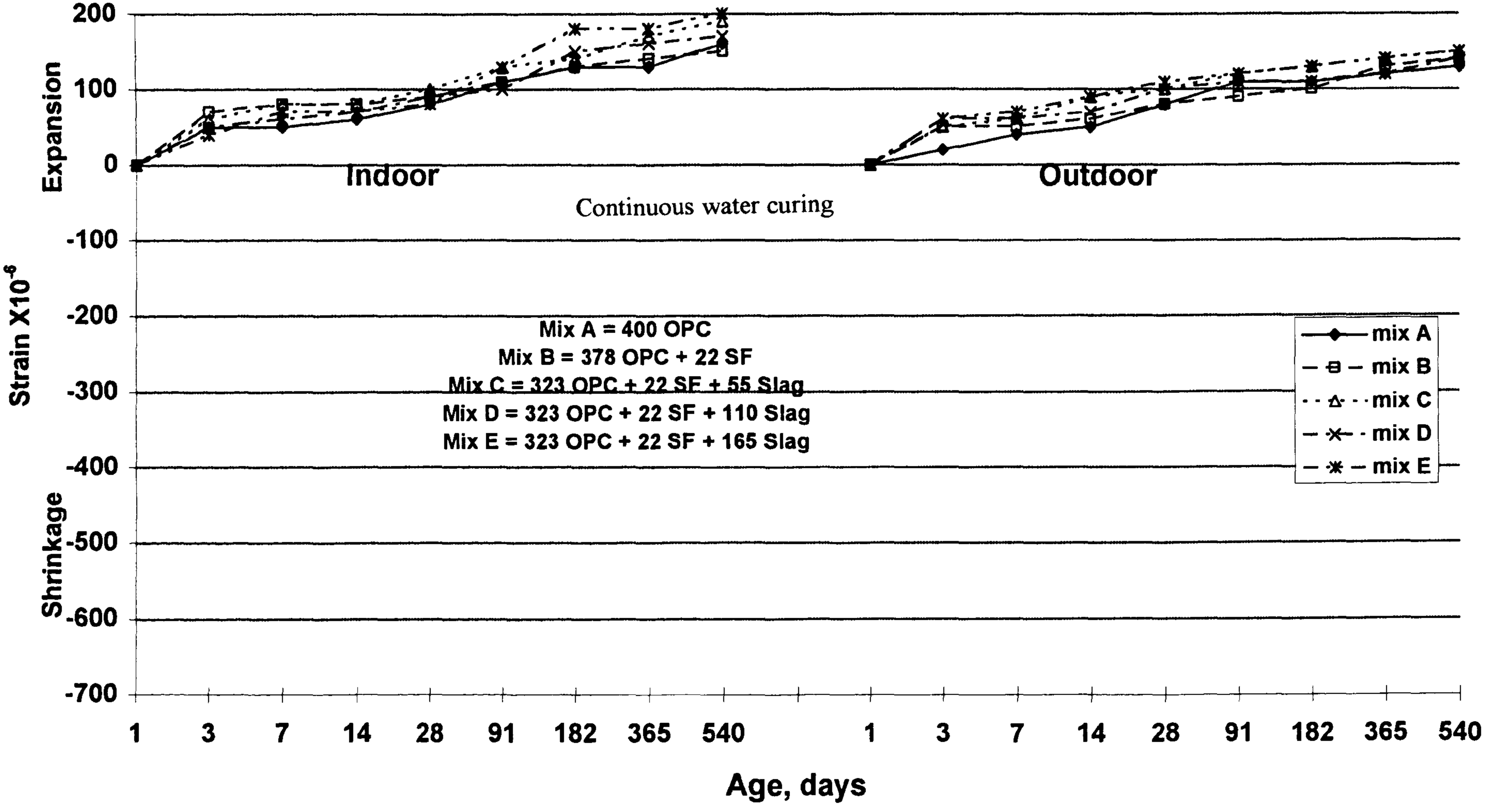

Fig. 5.53 : Influence of mix type on shrinkage and expansion under continuous water curing.

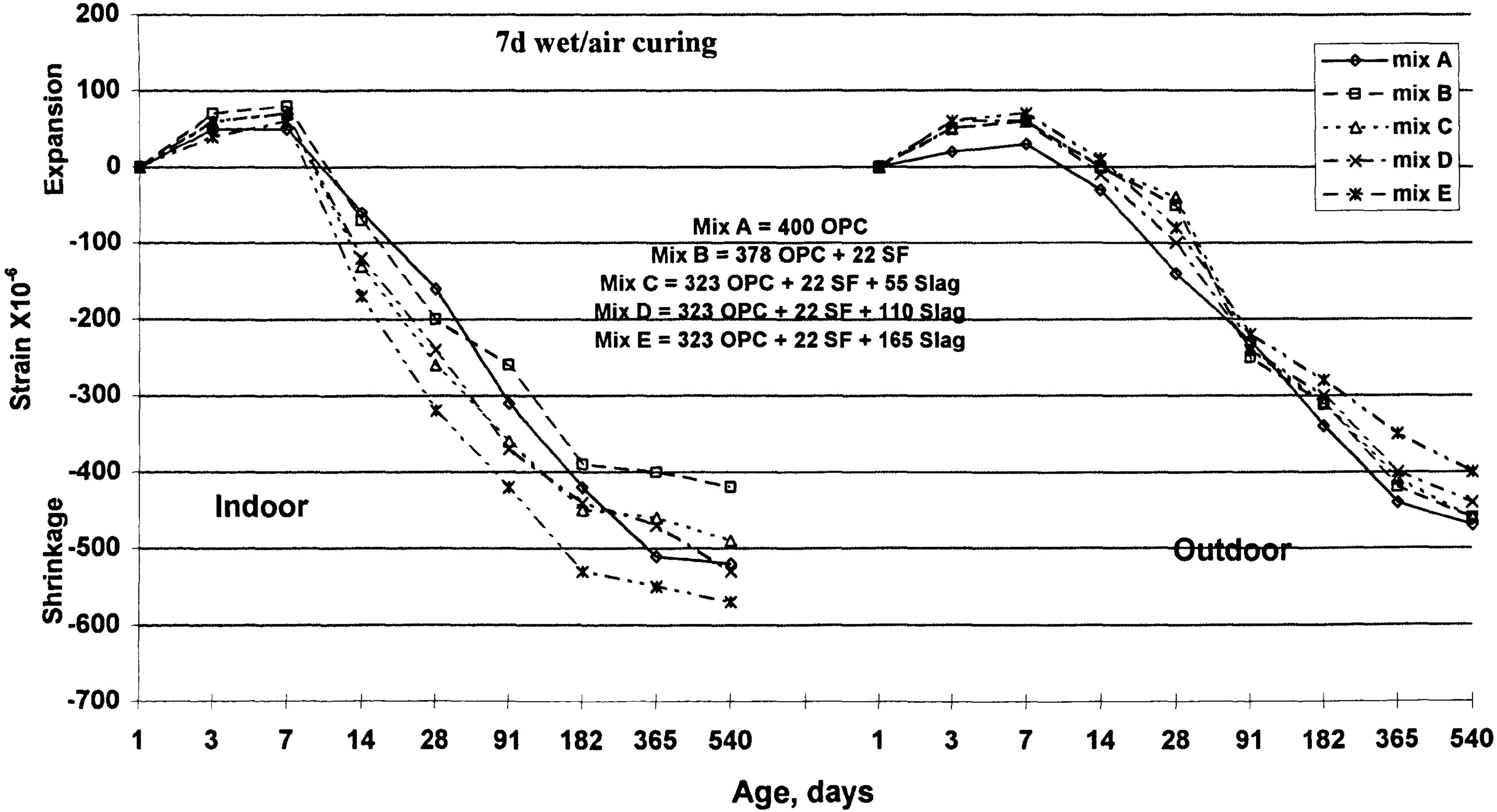

Fig. 5.54 : Influence of mix type on shrinkage and expansion under 7d wet/air curing.

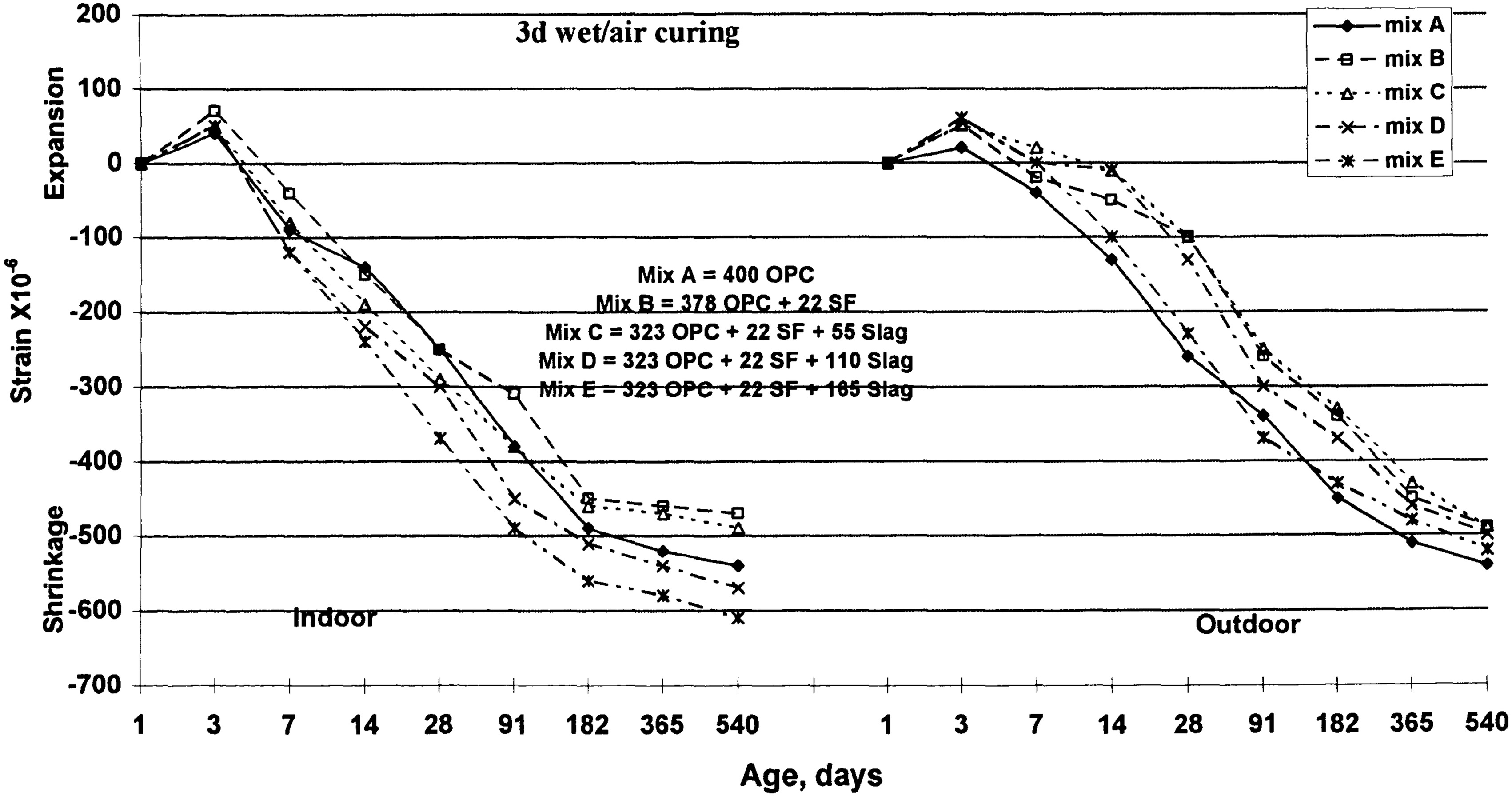

Fig. 5.55 : Influence of mix type on shrinkage and expansion under 3d wet/air curing.

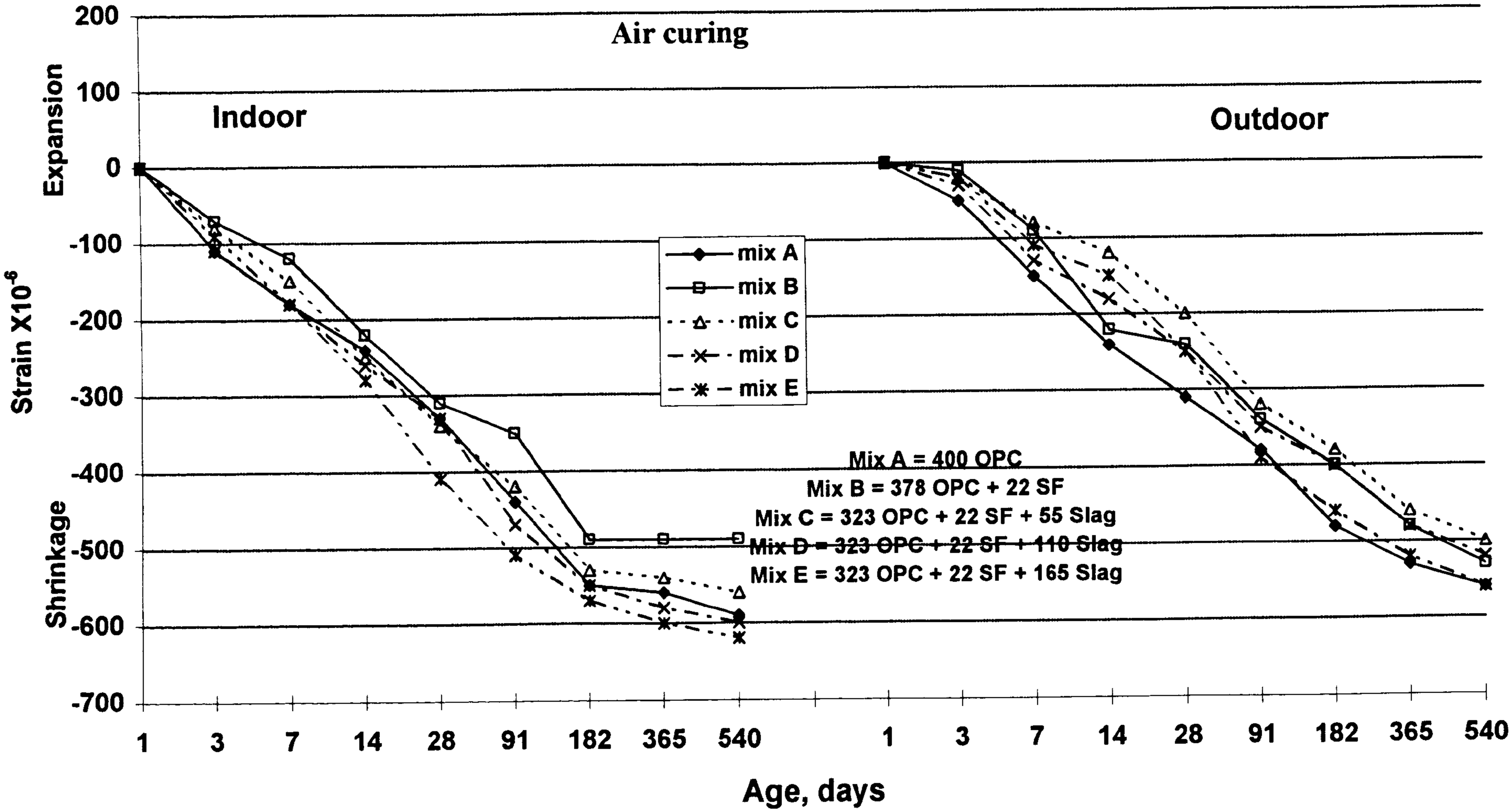

Fig. 5.56 : Influence of mix type on shrinkage and expansion under air curing regime.

The importance of moist curing, and the effect of the lack of any moist curing for OPC concrete, is illustrated in Fig. 5.48 and Table 5.8. These data emphasise dramatically the need for early curing and a minimum period of water curing as an integral part of mix proportioning for plain concrete. At 28 days, air cured specimens exhibited higher shrinkage values than the 7d wet/air or even the 3d wet/air cured specimens which registered differences of 24% and 52% respectively for 3d wet/air and 7d wet/air cured compared with air cured. However, with increasing age the gap between shrinkage of air cured and both 3d wet/air or 7d wet/air cured specimens was narrowed, the difference being 8% and 12% at the end of curing period of 18 months. This indicates that shrinkage of the specimens initially cured in water for period of 3 days or 7 days increased with time due to moisture loss through evaporation or hydration process. On the other hand, specimens continuously cured in water showed swelling with time and reached it is maximum values at 18 months.

Mixes B to E showed similar trend and followed approximately the same path as presented in Figs. 5.49 to 5.52 to mix A. Air cured specimens exhibited the highest shrinkage values followed by 3d wet/air and 7d wet/air curing respectively. However, when comparing the 7d wet/air with 3d wet/air curing, it appeared that differences are considered to be significant, and this is due to the fact of importance the early moist curing, and the same can be said when 3d wet/air cured specimens are compared to air cured specimens.

5.5.2 Effect of mix type, Indoor

The shrinkage of concrete depends on the shrinkage of the cement paste, but also on the volume fraction of the aggregate [136].

Also, Tables 5.8 and 5.9 and Figs. 5.53 to 5.56 show the effect of mineral admixtures on shrinkage and swelling properties. The figures show that the mix B at early age and long term under air curing exhibited shrinkage less than that of the control mix; this reduction is more pronounced at later ages. The shrinkage results of mix B subjected to 3d wet/air and 7d wet/air curing showed similar shrinkage to the control mix up to 28 days; beyond that age mix B exhibited lower shrinkage. This observation is in agreement with that of Carette and Malhotra [149] who carried out a study on concrete specimens initially cured in water for 28 days, then subsequently measured shrinkage 84 days after dried. The cement plus silica fume was kept constant at about 0

to 43% and w/b at 0.40% by using different amounts of superplasticizer. The pattern was less shrinkage for the concretes containing silica fume. Also the contribution of silica fume to drying shrinkage was studied by Khayat and Aitcin [69]. Three replacement levels of silica fume were used to replace part of OPC 0, 10 and 20% and w/b was between 0.37 and 2.11. All the specimens were initially cured in water for 7 day then dried in air at 60% RH. For concrete with w/b less than 0.6, the silica fume mixture was found to exhibit lower shrinkage values than plain concrete.

Under air curing, mix A exhibited higher shrinkage compared with that of mix B. The contribution of slag in mix C to drying shrinkage was higher where both mixes (mixes A and C) follow approximately the same path as presented in Fig. 5.56. The results show that mix C reduced the shrinkage compared to concrete with a higher amount of slag, mixes D and E. Mix E with the highest amount of slag exhibited the highest values of drying shrinkage for the period between 7 to 540 days. Wainwright cited study carried out by Heaton [45] who conducted tests on concrete replaced by 40% slag subjected to drying condition after 7 days water curing. From his study he concluded that after 400 days of drying the shrinkage of the concrete containing slag was 25% higher than that of the equivalent plain concrete. It has been reported elsewhere [146] that 50% slag as cement replacement increases shrinkage. This finding is similar to that of work of Bamforth reported by Wainwright [44], which concluded that concrete containing 70% slag had lower rate of drying shrinkage than the OPC concrete but in the long term the rate of shrinkage was accelerated by the use of slag. Hogan and Meusel [61] also concluded that drying shrinkage of concrete was somewhat increased through the addition of slag. This confirms the results obtained from mixes D and E. The higher the amount of slag, the higher is the shrinkage at constant water/binder ratio.

This behaviour is similar to that of mix A where the higher degree of hydration at early ages (1-7 days) due to using only OPC, which generates more heat, results in higher shrinkage as shown in Fig. 5.47.

Table 5.8: Shrinkage and expansion in microstrain in the indoor environment.

Age (days)		1	3	7	14	28	91	182	365	540
Mix type	Temp.	21°C	20°C	20°C	23°C	24°C	25°C	25°C	19°C	23°C
	R.H.	73%	72%	67%	67%	62%	84%	76%	85%	76%
A	air	0	-110	-180	-240	-330	-440	-550	-560	-590
	3d w/a	0	40	-90	-140	-250	-380	-490	-520	-540
	7d w/a	0	50	50	-60	-160	-310	-420	-510	-520
	wet	0	50	50	60	80	110	130	130	160
B	Temp.	18°C	19°C	22°C	21°C	20°C	25°C	25°C	20°C	25°C
	R.H.	62%	63%	66%	82%	81%	62%	58%	87%	77%
	air	0	-70	-120	-220	-310	-350	-490	-490	-490
	3d w/a	0	70	-40	-150	-250	-310	-450	-460	-470
	7d w/a	0	70	80	-70	-200	-260	-390	-400	-420
	wet	0	70	80	80	90	110	130	140	150
C	Temp.	24°C	23°C	23°C	23°C	20°C	25°C	25°C	21°C	24°C
	R.H.	52%	67%	67%	60%	81%	48%	57%	85%	76%
	air	0	-80	-150	-250	-340	-420	-530	-540	-560
	3d w/a	0	50	-80	-190	-290	-380	-460	-470	-490
	7d w/a	0	60	70	-130	-260	-360	-450	-460	-490
	wet	0	60	80	80	100	130	140	170	190
D	Temp.	23°C	20°C	23°C	22°C	25°C	25°C	25°C	20°C	25°C
	R.H.	61%	73%	60%	74%	62%	58%	65%	84%	76%
	air	0	-110	-180	-260	-330	-470	-550	-580	-600
	3d w/a	0	50	-120	-220	-300	-450	-510	-540	-570
	7d w/a	0	60	70	-120	-240	-370	-440	-470	-530
	wet	0	50	60	70	90	100	150	160	170
E	Temp.	23°C	24°C	22°C	20°C	23°C	25°C	25°C	22°C	24°C
	R.H.	75%	64%	74%	81%	60%	55%	56%	83%	78%
	air	0	-90	-180	-280	-410	-510	-570	-600	-620
	3d w/a	0	50	-120	-240	-370	-490	-560	-580	-610
	7d w/a	0	40	60	-170	-320	-420	-530	-550	-570
	wet	0	40	70	70	80	130	180	180	200

Table 5.9: Shrinkage and expansion in the outdoor environment at 8 AM.

Age (days)		1	3	7	14	28	91	182	365	540
Mix type	Temp.	33°C	34°C	34°C	34°C	33°C	30°C	17°C	33°C	19°C
	R.H.	50%9	54%	55%	55%	52%	57%	66%	52%	60%
A	air	0	-50	-150	-240	-310	-380	-480	-530	-560
	3d w/a	0	20	-40	-130	-260	-340	-450	-510	-540
	7d w/a	0	20	30	-30	-140	-230	-340	-440	-470
	wet	0	20	40	50	80	110	110	120	130
B	Temp.	33°C	34°C	34°C	32°C	34°C	31°C	16°C	33°C	18°C
	R.H.	52%	50%	54%	58%	50%	50%	55%	52%	57%
	air	0	-10	-90	-220	-240	-340	-400	-480	-530
	3d w/a	0	50	-20	-50	-100	-260	-340	-450	-490
	7d w/a	0	50	60	0	-50	-250	-310	-420	-460
	wet	0	50	50	60	80	90	100	130	140
C	Temp.	34°C	32°C	34°C	34°C	33°C	31°C	18°C	31°C	19°C
	R.H.	59%	60%	52%	61%	50%	58%	58%	52%	55%
	air	0	-20	-80	-120	-200	-320	-380	-460	-500
	3d w/a	0	50	20	-10	-100	-250	-330	-430	-490
	7d w/a	0	50	60	0	-40	-240	-310	-410	-460
	wet	0	50	60	90	100	120	130	140	150
D	Temp.	33°C	33°C	34°C	33°C	35°C	31°C	17°C	32°C	19°C
	R.H.	58%	62%	51%	59%	66%	62%	56%	57%	67%
	air	0	-30	-130	-180	-250	-350	-400	-480	-520
	3d w/a	0	60	0	-10	-130	-300	-370	-460	-500
	7d w/a	0	60	60	-10	-100	-240	-300	-400	-440
	wet	0	60	60	70	100	110	110	120	140
E	Temp.	33°C	35°C	35°C	33°C	33°C	28°C	16°C	33°C	19°C
	R.H.	56%	56%	60%	66%	50%	70%	55%	52%	61%
	air	0	-20	-110	-150	-250	-390	-460	-520	-560
	3d w/a	0	60	0	-100	-230	-370	-430	-480	-520
	7d w/a	0	60	70	10	-80	-220	-280	-350	-400
	wet	0	60	70	90	110	120	130	140	150

Fig. 5.53 shows the effect of continuous water curing on wetting expansion over a period of 18 months. The figure shows that for the control mix, 31% of the swelling was obtained in the first 3 days, and 50% at 28 days. Mix B exhibited 47% and 60% of swelling at the age of 3 and 28 days respectively; this rapid swelling at early age

indicates the ability of this mix to absorb large amount of water to enable its pozzolanic reaction to continue specially at an early age. Mix C also presented high swelling values similar to mix A, and any further increase in slag content decreased the swelling at early age, but increased it in the long term. The presence of GGBFS in mixes D and E slows down the hydration process at early ages, and activates it in the long term; at 3 days, these mixes exhibited values of 32 and 20% of their values at 18 months.

The final swelling strain of slag concrete was higher by about 13-33% than mix A and mix B. The swelling measured at 18 months were 190, 170, 200, 160 and 150 microstrain for mixes C, D, E, A and B respectively.

5.5.3 Effect of exposure environment

Concrete deterioration problems are diverse in nature. Each deterioration condition requires a clear understanding of what is causing deterioration. The specifier needs complete information on the properties of the environment, and how these control the properties of the concrete. For example, no precautions whatever are needed to prevent the deterioration of concrete by freeze-thaw cycling if the environment in which the concrete structure is used is one in which freezing and thawing cannot occur. In many cases, undesirable cracking in the concrete structures are the result of improper choice in matching the material specified and selected for use in a given environment with characteristics of that environment.

The data in Tables 5.8 and 5.9 and Figs. 5.48 to 5.56 show the effect of exposure environment at 8:00 AM on the strain measured on the different concrete mixes subjected to various curing regimes. It has been found that the addition of silica fume or SF/slag to concrete provides a significant decrease in the shrinkage of concrete. Concrete mix with limited amount of slag (mix C) subjected to 3d wet/air or air curing exhibited the lowest values of shrinkage followed by mix B. Any further increase in slag content (mixes D and E) increases the shrinkage. On the other hand, the control mix exhibited the highest values of shrinkage under this curing condition.

5.5.4 Effect of thermal expansion

Little information is available on the thermal expansion of high strength concrete. The shrinkage and expansion measurements of specimens exposed to the outdoor environment were taken at 8 AM in the morning and 1 PM in the afternoon to investigate the effects of the daily fluctuations of temperature and humidity on these

properties. These data emphasise that there are cyclic changes in shrinkage and expansion, and that these changes need to be taken into consideration in design. Before the effects of thermal expansion conditions on building elements can be determined, it is necessary to have information about the thermal and mechanical deformation properties of the materials involved, because concrete is a heterogeneous material, the physical characteristics of which are greatly affected by age and environment as well as by the properties of the constituent materials. In this situation, it has to be accepted that calculations of thermal expansion in concrete elements are necessary in the Arabian Gulf region.

Similar considerations should apply to estimates of boundary conditions; for example, in practice, there is no such thing as a freely supported slab: some degree of restraint is invariably present. Restrained drying shrinkage is probably the most common cause of the internal and surface volume changes due to thermal expansion causing concrete cracking in Arabian Gulf region.

In view of the complexity of the thermal expansion problem, a comparison of field experiments at early morning and afternoon is essential to substantiate the approximations on which calculations must be based. From the experimental work reported here, significant behaviour was found for all the mix specimens exposed to a continuous drying condition or initially cured in water and then dried in air. All the data are given in Figs. 5.57-5.65 and Tables 5.9 and 5.10. In general it can be seen that, with the exception of continuous wet curing, all the mixes showed considerably higher thermal expansion at 1 clock in the after noon than those tested at 8 clock morning. This can be attributed to the following parameters:

1- High variation in the ambient temperature during morning and after noon

2- Very high solar radiation in the after noon which raises the surface temperature of the specimens up to 60°C.

3- Low relative humidity in the after noon compared with the corresponding values in the morning.

4- The thermal properties of the materials and the inside thermal conditions which influence the transfer of heat at the inside face of the structure element.

5- The velocity of wind playing over the surface.

The above parameters show that the differences between the two values on the same day was as much as 200 microstrain within a time period of five hours. Also, these parameters will increase the surface temperature of the specimens faster than that in the bulk. Many specimens have been made where SF and SF/ slag were used in concrete as a portion of blended cement. Results of these studies generally indicate that when plain concrete was tested in comparison with OPC/SF and SF/slag, their resistances to thermal expansion were essentially the same.

The results show that drying condition has a significant effect on thermal expansion of concrete, as seen from Tables 5.9 and 5.10 and Fig. 5.57 to 5.65. As a result of thermal expansion the surface will be under tension and the bulk will be under compression. As a result of this microcracking will occur. It has been observed that concrete structures attaining high internal temperatures during setting and hardening tended to crack during subsequent cooling as reported by Lea and cited by Chatterji [150]. This aspect has also been studied by Hansen [150]. He concluded that cracking will occur whenever the temperature differences between the bulk of the structure and its surface exceed 20°C. Heat of hydration may accelerated in such environment similar to that in the Arabian Gulf region. It is important to note that, the inclusion of slag reduced the early rate of heat generation, and this reduction is directly proportional of GGBFS used [49].

In the Arabian Gulf, the exterior components will deteriorate more rapidly than the interior components due to the variation in the thermal expansion as mentioned above.

Consequently, the data collected suggest the following preliminary conclusions. Mix C achieved better properties than all the other mixes when all have the same total binder content. The former mixture is the best way to save more cement material, chemical admixture and reduce the shrinkage problem, whereas the early strength is controlled by using silica fume.

Clearly, more data are required to establish the effect of thermal expansion between maximum temperature in the afternoon, and minimum temperature at night of these mixes and concrete structures, particularly those having large surface areas such as walls, bridge slabs and pavement slabs which are very much susceptible to this type of deterioration mechanism for which the environment in the Arabian Gulf countries is ideal. The months of June, July and August are the hottest during the year.

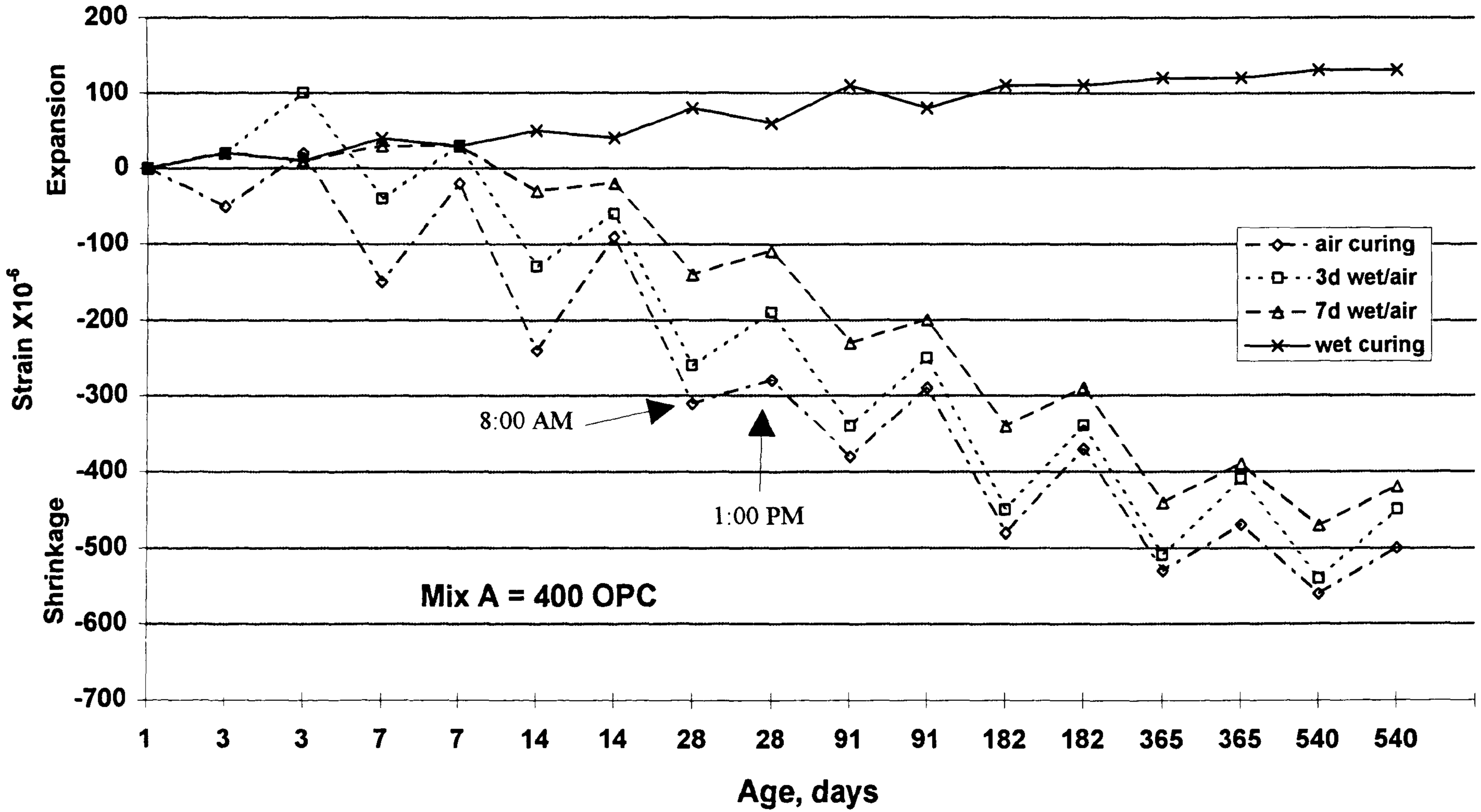

Fig. 5.57 : Influence of curing regime on thermal shrinkage and expansion for mix A.

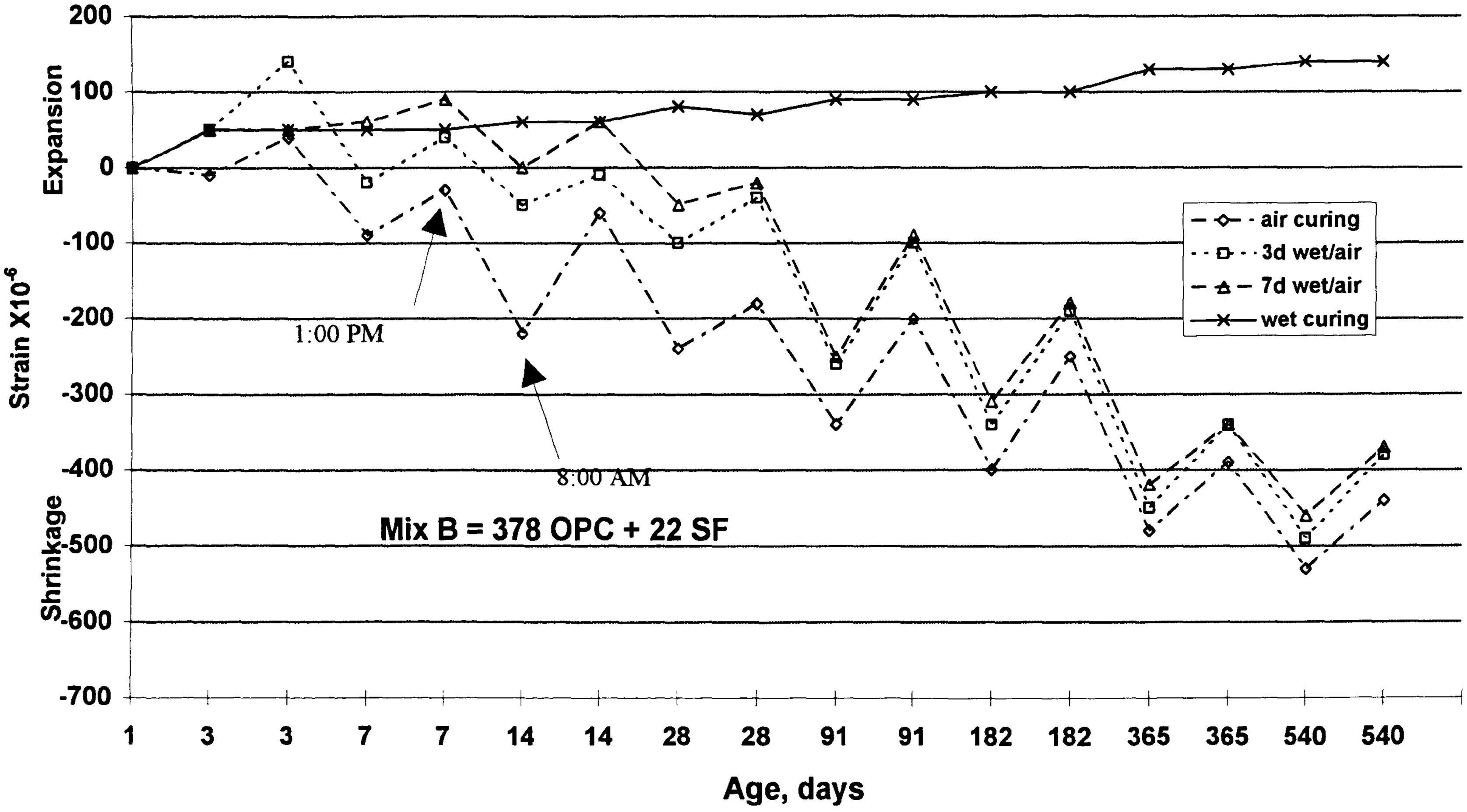

Fig. 5.58 : Influence of curing regime on thermal shrinkage and expansion for mix B.

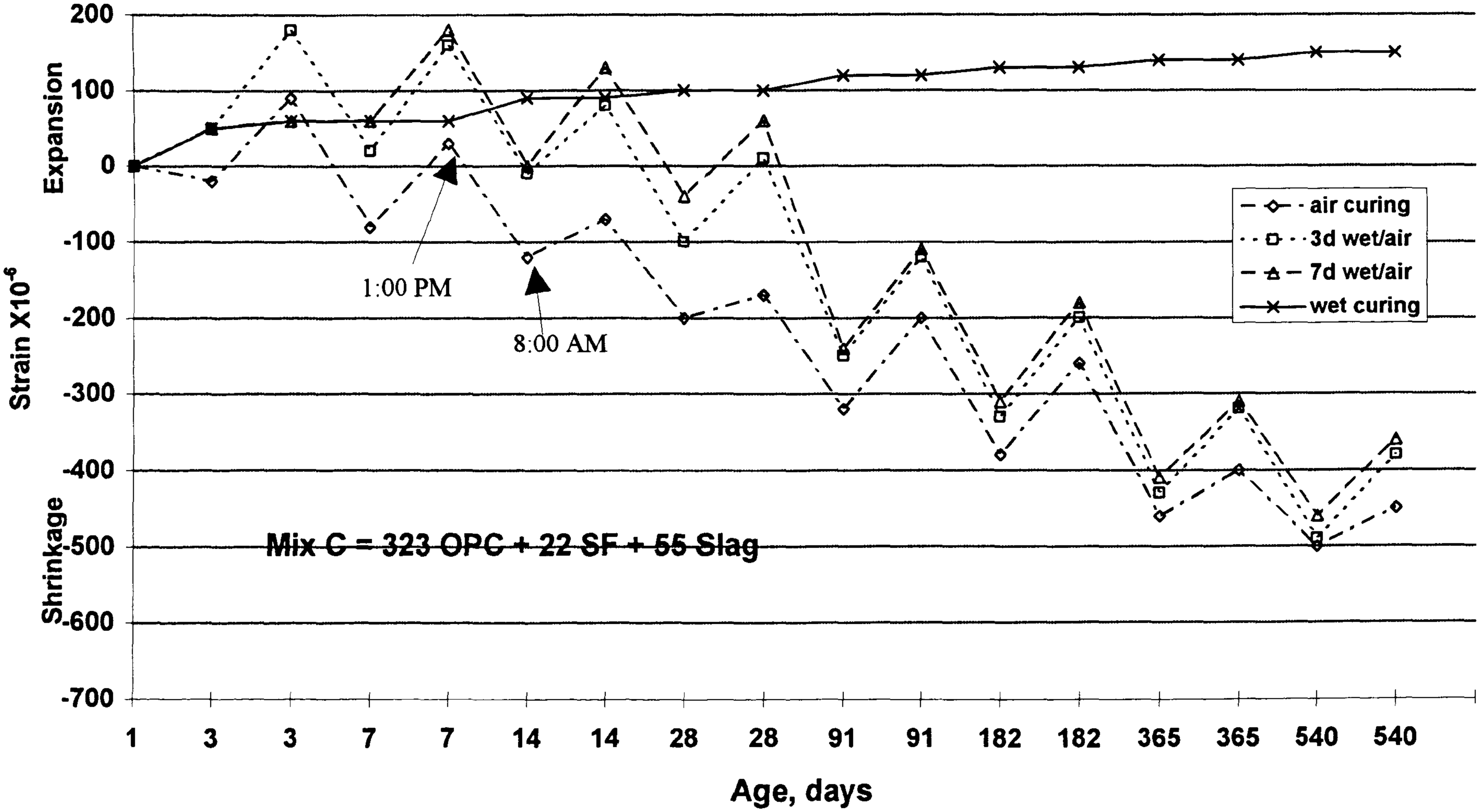

Fig. 5.59 : Influence of curing regime on thermal shrinkage and expansion for mix C.

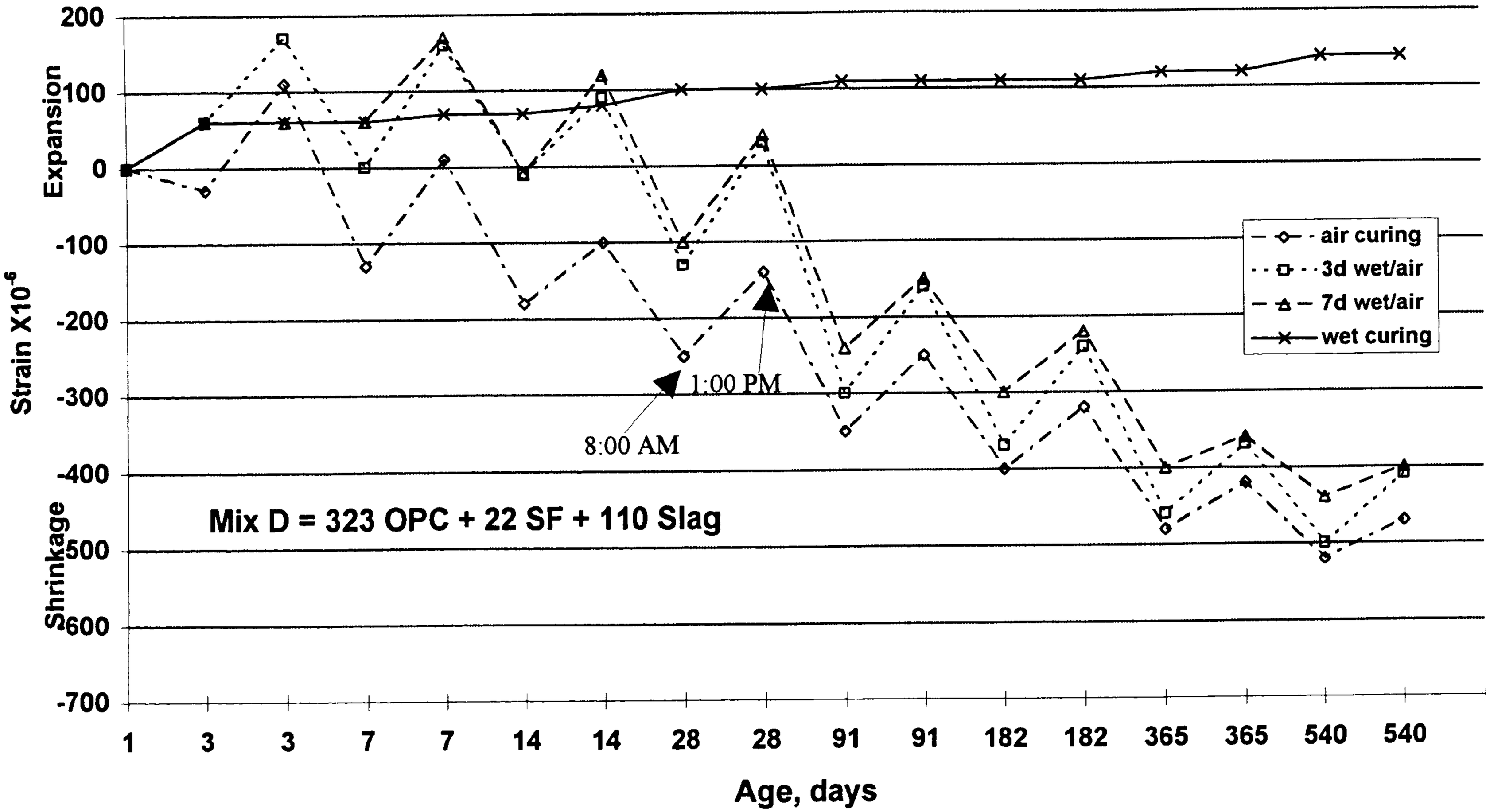

Fig. 5.60 : Influence of curing regime on thermal shrinkage and expansion for mix D.

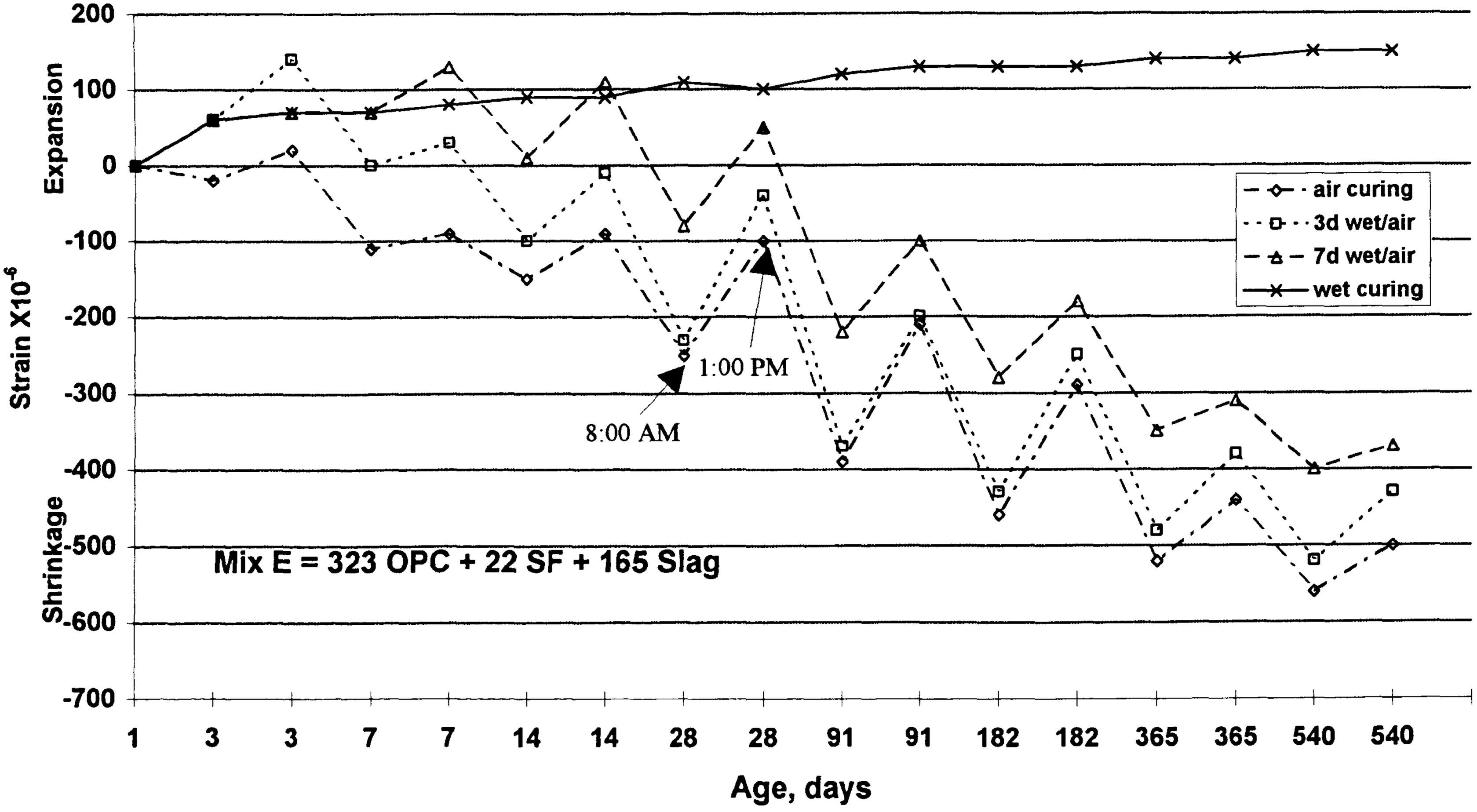

Fig. 5.61 : Influence of curing regime on thermal shrinkage and expansion for mix E.

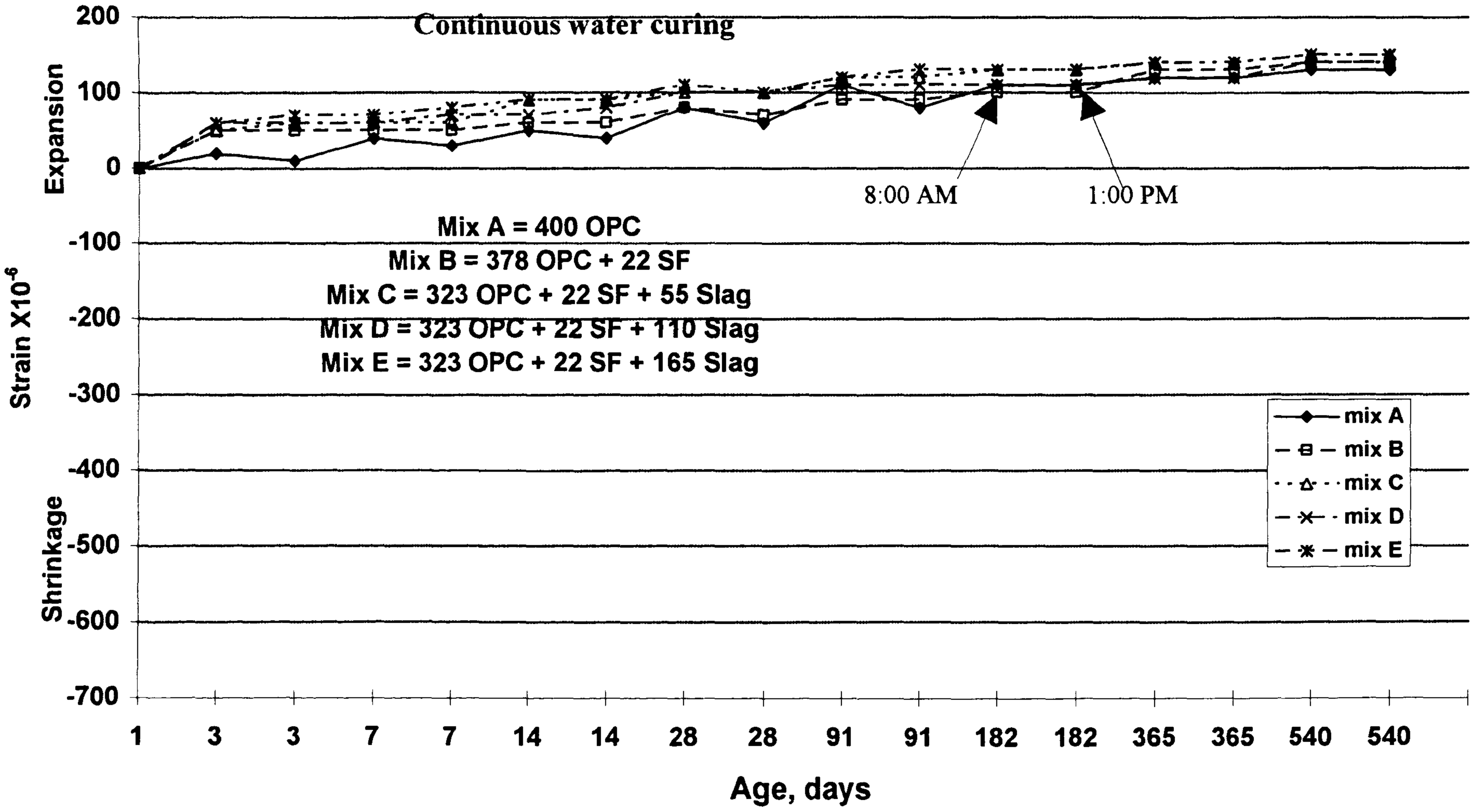

Fig. 5.62 : Influence of mix type on thermal shrinkage and expansion under continuous water curing.

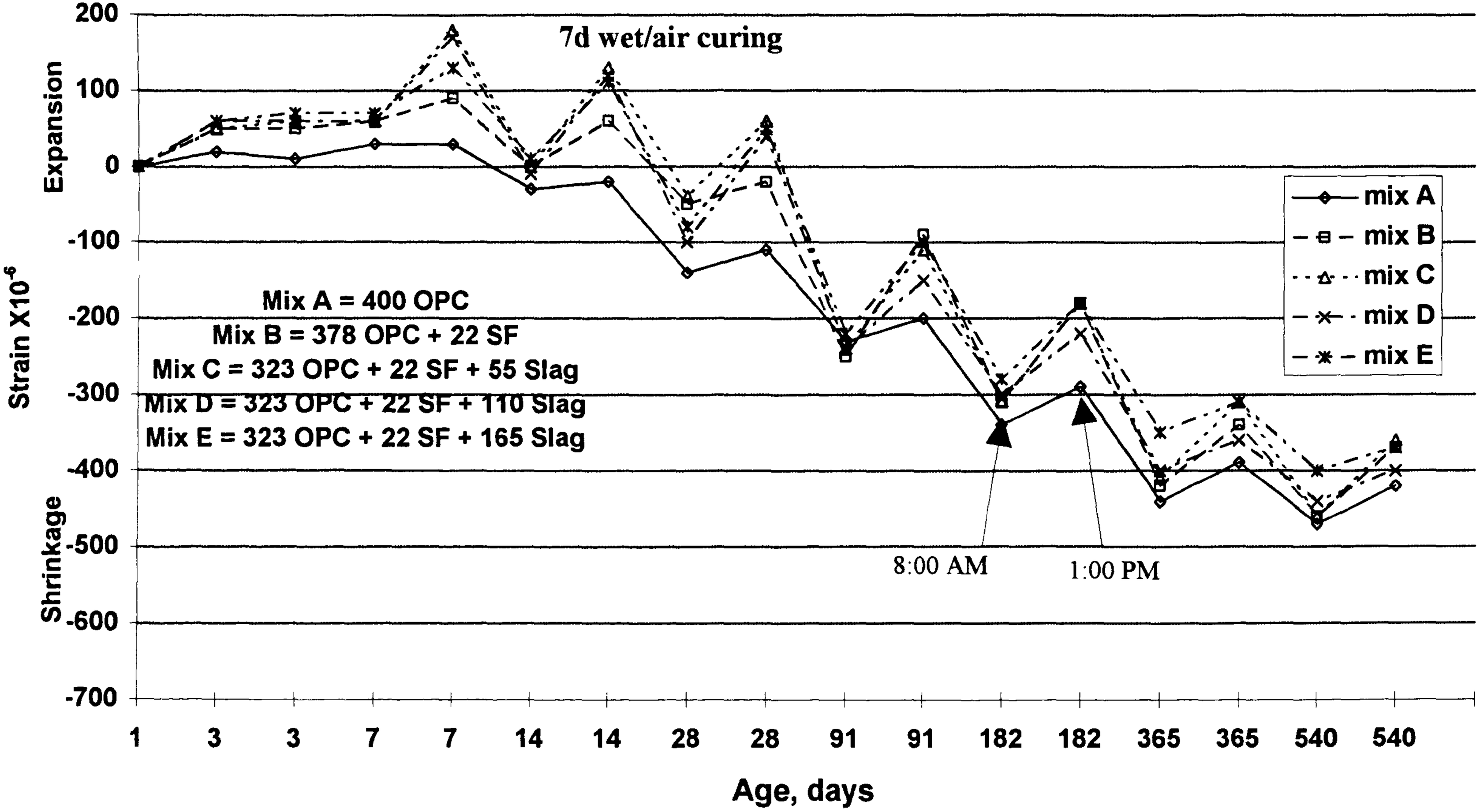

Fig. 5.63 : Influence of mix type on thermal shrinkage and expansion under 7d wet/air curing.

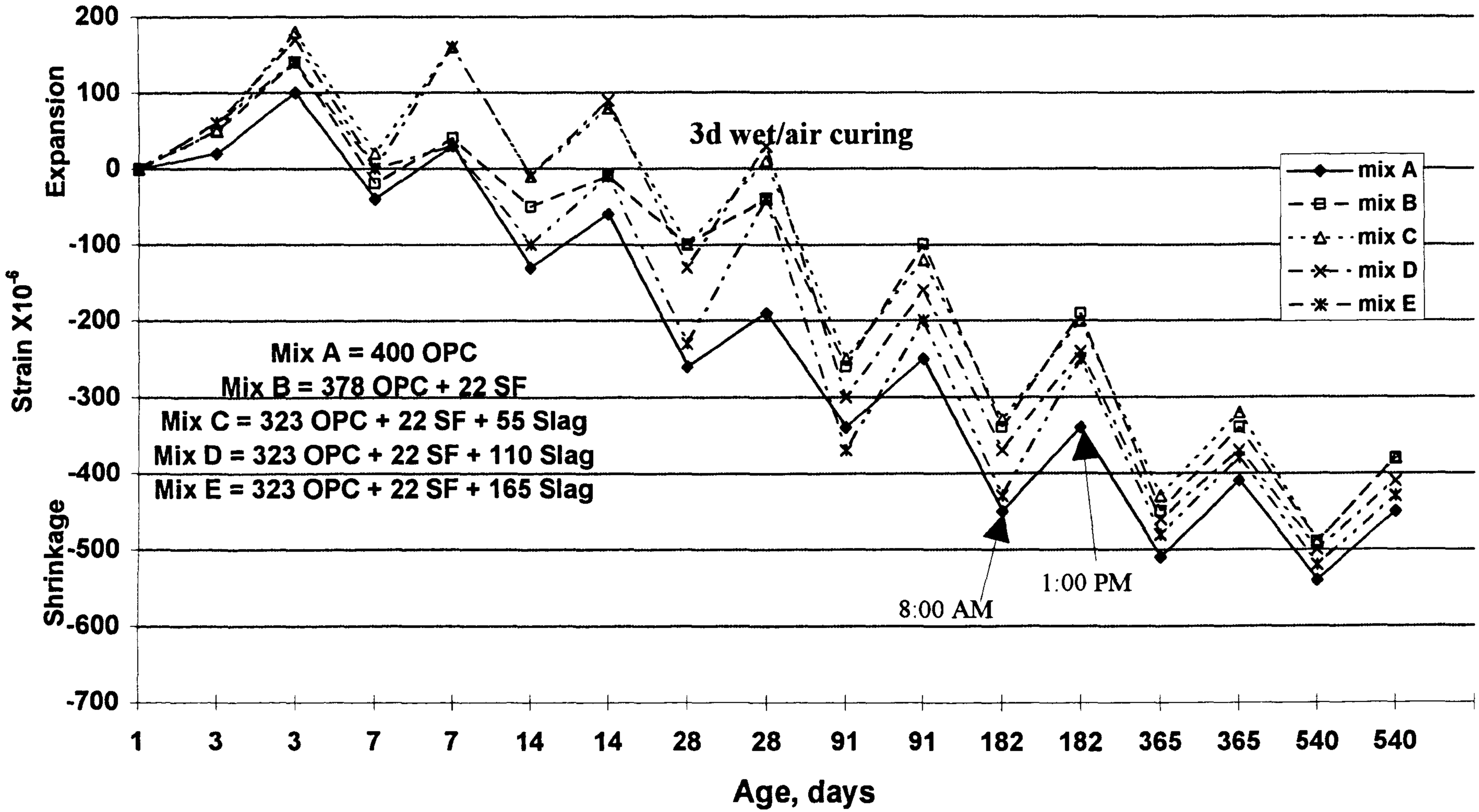

Fig. 5.64 : Influence of mix type on thermal shrinkage and expansion under 3d wet/air curing.

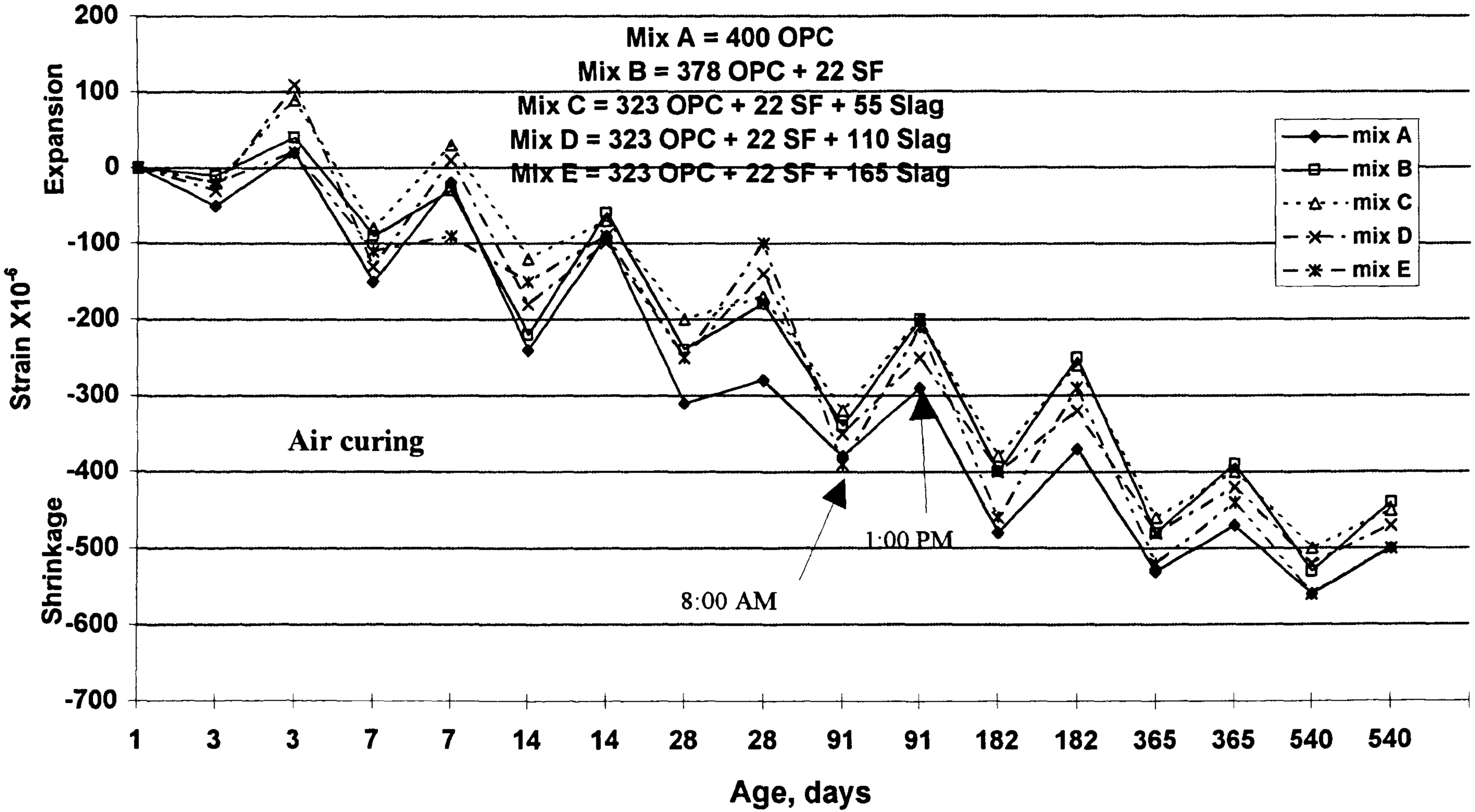

Fig. 5.65 : Influence of mix type on thermal shrinkage and expansion under air curing.

Table 5.10 Shrinkage and expansion in the outdoor environment at 1 PM.

Age (days)		1	3	7	14	28	91	182	365	540
Mix type	Temp.	39°C	40°C	40°C	45°C	41°C	43°C	22°C	40°C	23°C
	R.H.	44%	50%	56%	42%	49%	50%	50%	52%	50%
A	air	-	20	-20	-90	-280	-290	-370	-470	-500
	3d w/a	-	100	30	-60	-190	-250	-340	-410	-450
	7d w/a	-	10	30	-20	-110	-200	-290	-390	-420
	wet	-	10	30	40	60	80	110	120	130
B	Temp.	40°C	41°C	43°C	40°C	43°C	43°C	22°C	43°C	21°C
	R.H.	50%	52%	47%	60%	42%	52%	51%	52%	53%
	air	-	40	-30	-60	-180	-200	-250	-390	-440
	3d w/a	-	140	40	-10	-40	-100	-190	-340	-380
	7d w/a	-	50	90	60	-20	-90	-180	-340	-370
	wet	-	50	50	60	70	90	100	130	140
C	Temp.	41°C	43°C	40°C	39°C	44°C	43°C	23°C	41°C	22°C
	R.H.	58%	48%	60%	55%	38%	45%	54%	49%	57%
	air	-	90	30	-70	-170	-200	-260	-400	-450
	3d w/a	-	180	160	80	10	-120	-200	-320	-380
	7d w/a	-	60	180	130	60	-110	-180	-310	-360
	wet	-	60	60	90	100	120	130	140	150
D	Temp.	42°C	44°C	42°C	42°C	40°C	41°C	23°C	43°C	20°C
	R.H.	50%	50%	57%	48%	66%	59%	67%	52%	57%
	air	-	110	10	-100	-140	-250	-320	-420	-470
	3d w/a	-	170	160	90	30	-160	-240	-370	-410
	7d w/a	-	60	170	120	40	-150	-220	-360	-400
	wet	-	60	70	80	100	110	110	120	140
E	Temp.	39°C	40°C	44°C	45°C	44°C	46°C	22°C	41°C	20°C
	R.H.	60%	55%	45%	40%	43%	40%	56%	52%	57%
	air	-	20	-90	-90	-100	-210	-290	-440	-500
	3d w/a	-	140	30	-10	-40	-200	-250	-380	-430
	7d w/a	-	70	130	110	50	-100	-180	-310	-370
	wet	-	70	80	90	100	130	130	140	150

5.6 Conclusions

The results obtained from this part of the research so far lead to the following conclusions:

1. Mix B (378 OPC + 22 SF) under all curing conditions exhibited values of compressive strength higher than that of mix A (400 OPC); this increase in strength was observed from the first day of casting. It also produced the highest values of compressive strength among the five mixes at early ages, due to the high reactivity and fineness of the silica fume leading to accelerated reaction from the beginning of the first day.

2. Mix C which contained a limited amount of slag (323 OPC + 22 SF + 55 Slag) gave values of compressive strength lower than that of mix B at early ages, indicating that this small reduction in compressive strength of mix C was due to the small amount of slag added. The inclusion of silica fume compensated this, and produced values of compressive strength higher than that of mix A (400 OPC).

3. Because the early reactivity of GGBFS is lower than that of portland cement, the initial compressive strength (0-7 days) of slag concrete (mix E) was low compared to that of portland cement concrete (mix A), silica fume concrete(mix B) or even mixes containing limited amount of slag (mix C).

4. All mixes under the four curing regimes showed lower compressive strength at later ages in the outdoor environment compared with that in the laboratory environment.

5. Pulse velocity can vary quite widely with compressive strength when insufficiently cured concrete begins to dry with time. Prolonged drying can create moisture loss and possible adverse internal microcracking not readily indicated by compressive strength values. These results thus showed that, except for the case of moist curing, compressive strength should not be used as the only a criterion of concrete quality beyond 7-28 days.

6. With the exception of continuous wet curing, all the mixes in the outdoor environment exhibited loss in pulse velocity beyond 7-14 days after casting, while this trend was observed between 28-91 days in the indoor environment. This trend was more clear for specimens under continued air drying.

7. Mix E with the highest amount of slag exhibited the lowest values of pulse velocity in the outdoor environment for both early age and in the long term. On the other

hand, Mix C with limited amount of slag exhibited the highest values of pulse velocity at these corresponding ages.

8. Very rapid improvement in dynamic modulus of elasticity occurred on the first day, and up to 7 days under all curing conditions for all the mixes.

9. All the mixes cured in air exhibited the lowest values of dynamic modulus of elasticity, pulse velocity and compressive strength at early and later ages.

10. For all the five mixes, the initial rate of increase of the dynamic modulus was accelerated on the first day in the outdoor environment, while at 3 days and beyond, the outdoor environment gave values similar to or less than that in the indoor environment.

11. In the outdoor environment, mixes subjected to 7 days initial water curing and then dried in air showed sudden loss of dynamic modulus of elasticity after 7 days, whereas this loss was gradual in the indoor environment. This is considered to be due to rapid loss of water from specimens in the outdoor environment leading to a restricted hydration, and thus slowing down or stopping the development of the dynamic modulus of elasticity.

12. Mix C reduced the shrinkage compared to concrete with a higher amount of slag, such as mixes D and E. Mix B exhibited less shrinkage compared to mix C.

13. Thermal expansion showed large differences in its values in the same day by as much as 200 microstrains in a period of five hours. Thus the real effects on exterior components of structure will appear over a long period of exposure.

14. Mix C achieved better properties than all the other mixes when all the mixes had the same total binder content. This type of mixture appears to be the optimum to save cement, and chemical admixture and reduce the shrinkage problem, whereas the early strength can be controlled by incorporating an adequate amount of silica fume.

Chapter six

POROSITY AND PORE STRUCTURE OF BLENDED CEMENT CONCRETE

6.1 Introduction

The pore structure of the cement paste is one of the major characteristics controlling the durability properties of concrete such as permeability, water absorption and chloride intrusion. A measure of the pore size distribution of ordinary portland cement (OPC) and blended cement concrete is more definitive, and can lead to a basic understanding of the many phenomena occurring within the material. In this research the mercury intrusion porosimetry (MIP) technique was employed to determine the porosity and pore size distribution.

The main purpose of the work reported in this chapter was to investigate the effect of environment and age of the specimens on the porosity and pore size distribution of concrete, made from OPC and a combination of OPC/SF and OPC/SF/GGBFS subjected to four different curing regimes.

Variability of test results is influenced by many factors among which aggregate content plays an important part. Because of this, its is expected that concrete samples will result in greater variability than those of cement paste. To overcome this, small pieces of mortar (as shown in chapter 3, test procedure) were carefully taken from concrete sample, ensuring that no coarse aggregate particle was present, not even the smallest one, because such particles can be seen to have a great effect on pore size distribution when MIP results are being interpreted. Because of limitation of time, and the amount of work to be done, the results recorded here represent those obtained from one test on one specimen.

There are some factors and assumptions contributing to errors in the mercury porosimetry results. These assumptions include various corrections to pressure and volume data, such as pore shape factor, penetrometer expansion, liquid compression, sample compression, contact angle and surface tension values. In general, most of these corrections are made by the manufacturers in commercial porosimetry software. Some of these factors are discussed in the following sections:

Contact angle

The contact angle is dependent on several factors which have a large effect on the porosimetry data; these factors include mercury surface tension and the method of drying of the sample. The value of surface tension of mercury is usually taken by researchers to be in the range of 473 to 485 dyne/cm (0.473 to 0.485 N/m); the choice of surface tension within the range of commonly accepted values has a much smaller effect than does the choice of contact angle [151].

The choice of contact angle value has an important effect on the interpretation of pore structure results, which has the effect of shifting the intrusion curve horizontally. Increasing the contact angle leads to a shift of the intrusion curve to the coarser pore diameter.

In most of the published wok [115,151], the contact angle of mercury with the pore walls is assumed, and not determined. In this research a contact angle of 117°C was used to calculate the pore sizes. Winslow and Diamond [106] used hardened cement paste and made direct measurement of the pressure required to intrude 40 cylindrical pores. They found contact angle of 117°C for oven dried paste and 130°C for p-dried (equilibration over magnesium perchlorate hydrate) paste. Precise determination of contact angle is difficult for concrete materials. So far, there is no standard value of contact angle which is accepted by all researchers. To allow comparison with other researchers study, it is recommended that all researchers should state clearly the contact angle and the surface tension value used in the research.

Pore shape

The use of mercury intrusion in studies of the pore structure of the cement paste has been discussed by many researchers [106,110,151]. This method assumes that pores become narrower with depth while, in fact, some pores have a constricted entrance; this distorts the value of porosity measured by mercury intrusion porosimetry [152]. The Washburn equation was derived for pores of circular cross section. If a pore geometry other than a right cylinder is used, then the effect upon calculated pore size distribution curve is the same as that of the difference in the contact angle. This is attributed to mercury being trapped in the ink-bottle shaped pores of the specimens. This type of pore has an entry radius smaller than that of the pore itself, and is not filled until the pressure is high enough to force mercury to traverse through the narrow neck. The amount of mercury intruded through this type of pore is related to the radius of the neck which is smaller than the real radius of the pore.

Effect of drying method

The major difficulty with most techniques is that the water residing in the pores has to be removed in order to obtain the measurement [110]. Pre-treatment of hardened cement paste or concrete specimens can have a substantial effect on MIP results. During an examination of MIP, inter-pretation of results is restricted because the method is based on a number of underlying assumptions. Freeze-drying [115] and solvent exchange [110] are two drying methods which may reduce the amount of structural collapse which occurs. Direct and rapid oven-drying of specimens at 105°C could cause deformation under internal stresses induced by the removal of water. Feldman and Beaudoin [110] investigated the effect of the different pre-treatment procedures for water removal from hydrated cement pastes on pore structure. These methods are:

(1) Solvent replacement by two different solvents (methanol and isopropanol).

(2) Vacuum drying.

(3) Oven and vacuum drying and

(4) Pre-drying to 11% R.H.

They found that the solvent replacement by methanol increases the threshold pore diameter (the point where the initial rapid increase in dV/dD curve occurs) of the pore distribution curve, but no evidence of this occurring with isopropanol has been observed. Solvent replacement allows removal of water without major stress application. The method of drying which results in the least influence on the pore size distribution is isopropanol replacement followed by immediate evacuation and heating at 100°C for 20 hours.

The effects of three common drying procedures on cement paste were studied by Winslow and Diamond [106]. These were: equilibration over magnesium perchlorate hydrates (P drying), evacuation over a dry ice trap (D drying), and oven-drying at 105°C. The methods are given in order of increasing of water removal. They found that the data in the coarse pore region roughly coincide but that the extent of pore diameter smaller than about 0.1 μm, seems to be a direct function of the drying method. Therefore oven-drying was selected as the standard technique for characterizing the pore size distributions of the pastes, largely on the assumption that the more complete removal of water prior to the intrusion of mercury probably provides a truer assessment of the actual pore spaces present. Maukwa and Aitcin [115] also investigated the effect of drying methods on the pore system. They found that oven drying alter the pore structure by rearranging the hydration products.

Corrections to volume data

The compressibility of volume data is another source of error that requires a small correction. The uncorrected volume reading is not only a measure of the volume of intrusion into the sample, but it also contains significant volumes corresponding to the expansion of the machine, the compression of the mercury in the penetrometer, and the compression of the unintruded volume of the sample itself. The required correction due to the compression of mercury test is much less than the absolute loss in volume of the liquid since the penetrometer containing the mercury is also being compressed at the same time [106,151,153].

The significance of this correction increases with increasing sample size and decreasing porosity. The mercury being compressed as the pressure is increased which cause an increase in mercury temperature which cause additional correction may be given to temperature effects. While it is likely that the temperature increase causes expansion, these corrections for temperature effects, on the other hand, compensate some of the mercury compression [106,151].

Experimental results and discussion

6.2 Porosity

Table 6.1 and Fig. 6.1(a-d) summarize the total porosity of the five concrete mixes cured under the four curing conditions and exposed to both indoor and outdoor environment. Longer wet curing periods allow more time and sufficient moisture for continued hydration resulting in less porosity [10-12]. The results of the current work confirm this observation, as shown in Table 6.1. For example, the total porosity of concrete was reduced by about 30-50% when comparing water cured samples at the different ages and environments.

6.2.1 Effect of curing -6 months, indoor

Mix A (400 OPC) showed the highest porosity of 9.05% under air curing regime. the effect of continuous wet curing regime is very clear, the above value drops to 5.57%, a reduction of 38.5%. The corresponding values of 3d wet/air and 7d wet/air are 8.64 and 8.66% respectively, which indicates that with portland cement concrete, there was little difference in the total porosity when the 3 day water curing was extended to 7 days; this phenomenon is confirmed by the porosity data after 18 months exposure both indoor and outdoor.

Table 6.1 Influence of curing regime on total porosity.

Mix	Binder content kg/m^3 OPC/SF/Slag	Curing regime	Indoor Age = 6 months Porosity, % of volume	Indoor Age = 18 months Porosity, % of volume	Outdoor Age = 18 months Porosity, % of volume
A	400/0/0	air curing	9.05	10.09	11.06
		3d wet/air	8.64	8.98	9.56
		7d wet/air	8.66	8.13	9.61
		wet curing	5.57	4.82	5.40
B	378/22/0	air curing	10.45	9.47	11.56
		3d wet/air	9.39	9.49	9.38
		7d wet/air	7.99	6.11	8.62
		wet curing	6.82	6.27	5.83
C	323/22/55	air curing	9.73	9.47	11.48
		3d wet/air	6.92	7.19	7.29
		7d wet/air	6.19	5.76	6.46
		wet curing	5.24	4.49	4.67
D	323/22/110	air curing	10.50	10.12	13.40
		3d wet/air	7.75	7.98	7.92
		7d wet/air	6.62	6.46	7.40
		wet curing	4.64	4.31	6.21
E	323/22/165	air curing	11.66	11.22	14.18
		3d wet/air	7.75	8.42	9.45
		7d wet/air	7.90	5.32	8.60
		wet curing	6.05	4.92	6.88

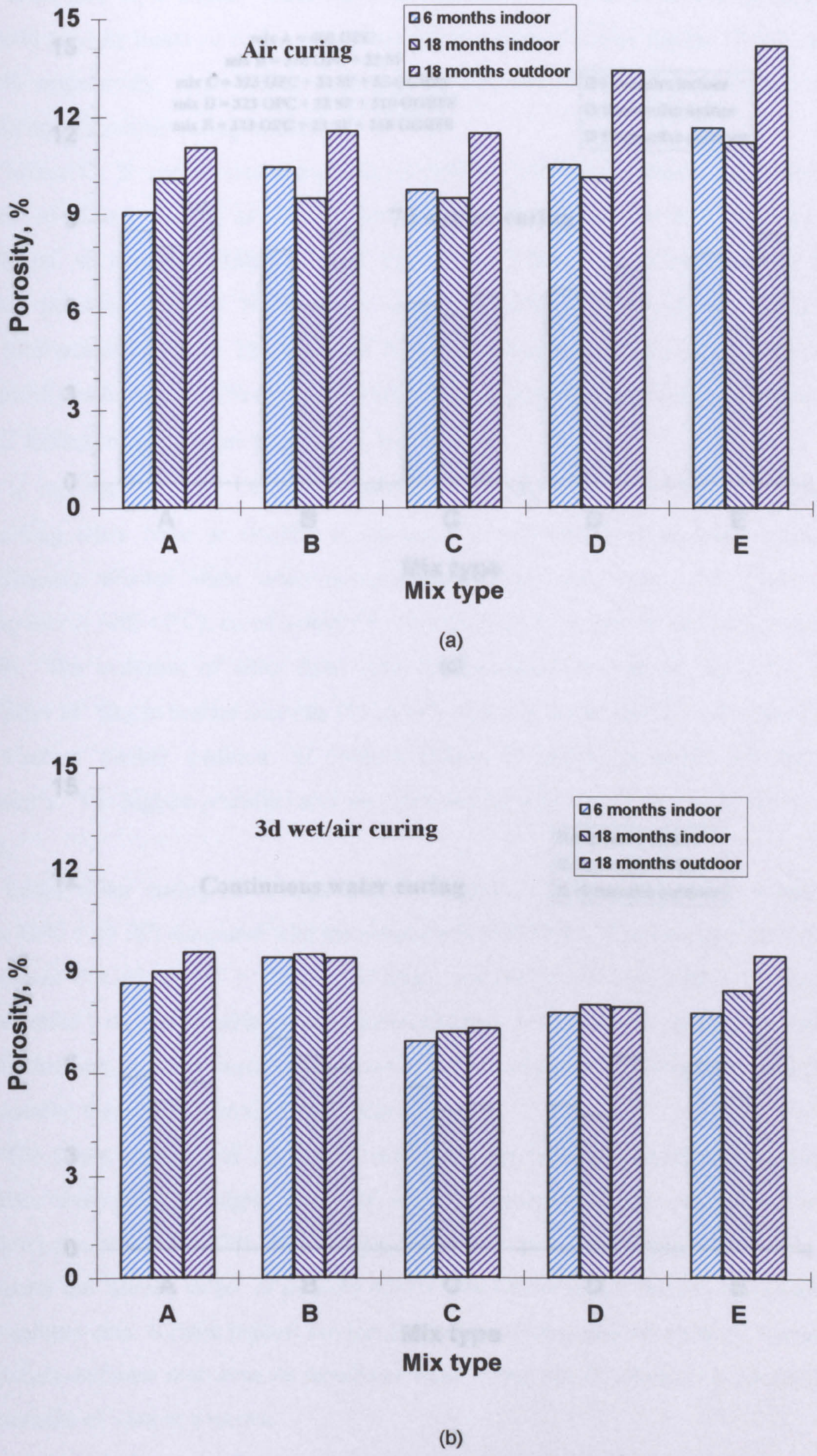

Fig. 6.1: Influence of age and exposure environment on porosity.

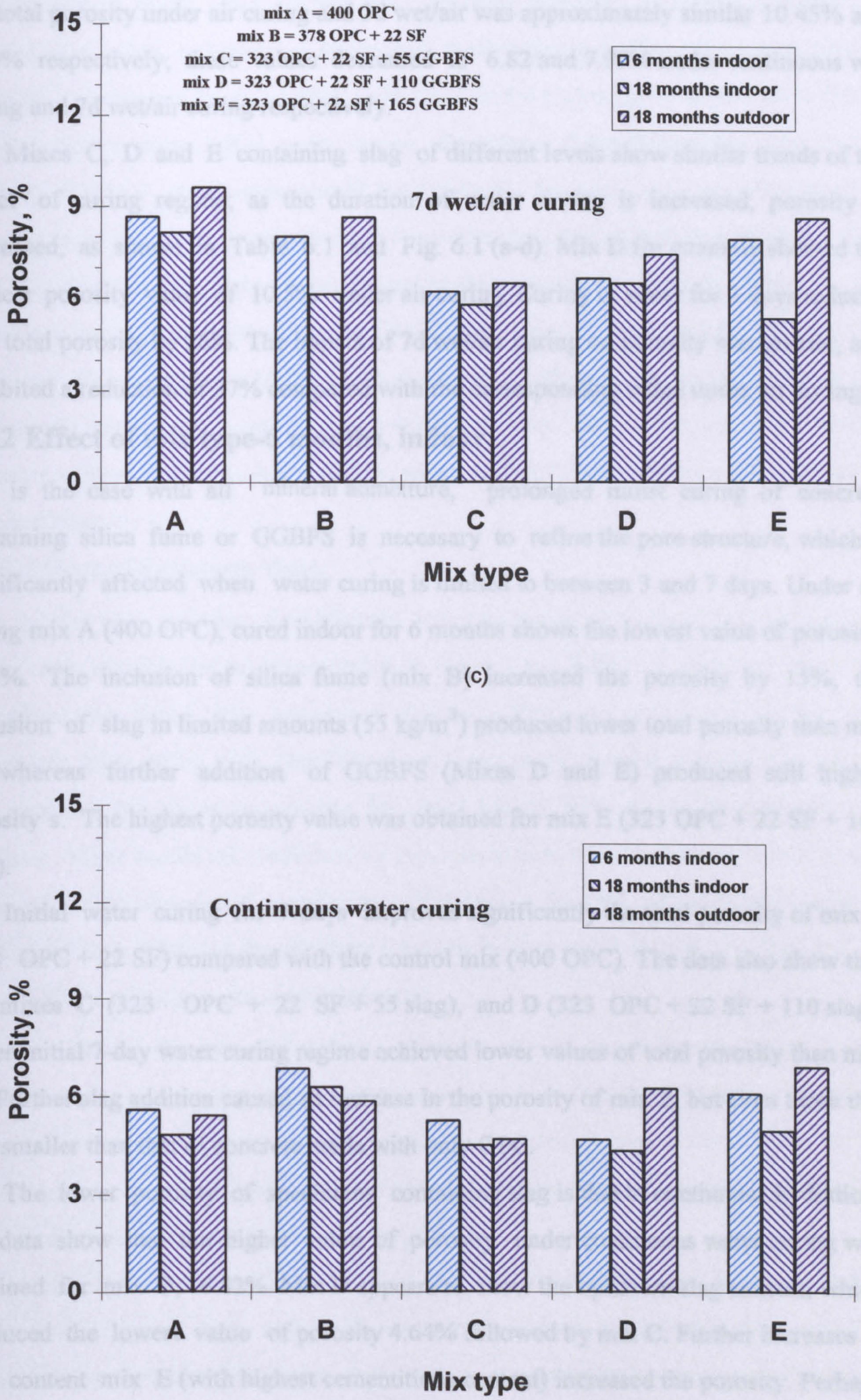

Fig. 6.1: Influence of age and exposure environment on porosity.

With mix B, a similar trend was observed due to the effect of the curing regime, the total porosity under air curing and 3d wet/air was approximately similar 10.45% and 9.39% respectively; these values decreased to 6.82 and 7.99% under continuous wet curing and 7d wet/air curing respectively.

Mixes C, D and E containing slag of different levels show similar trends of the effect of curing regime; as the duration of water curing is increased, porosity is decreased, as shown in Table 6.1 and Fig. 6.1 (a-d). Mix D for example showed the highest porosity value of 10.5% under air curing. Curing in water for 3 days reduced the total porosity by 26%. The impact of 7d wet/air curing on porosity was greater, and exhibited a reduction of 37% compared with the corresponding value under air curing.

6.2.2 Effect of mix type-6 months, indoor

As is the case with all mineral admixture, prolonged moist curing of concrete containing silica fume or GGBFS is necessary to refine the pore structure, which is significantly affected when water curing is limited to between 3 and 7 days. Under air curing mix A (400 OPC), cured indoor for 6 months shows the lowest value of porosity, 9.05%. The inclusion of silica fume (mix B) increased the porosity by 15%, the inclusion of slag in limited amounts (55 kg/m^3) produced lower total porosity than mix B, whereas further addition of GGBFS (Mixes D and E) produced still higher porosity's. The highest porosity value was obtained for mix E (323 OPC + 22 SF + 165 slag).

Initial water curing for 7-days improves significantly the total porosity of mix B (378 OPC + 22 SF) compared with the control mix (400 OPC). The data also show that the mixes C (323 OPC + 22 SF + 55 slag), and D (323 OPC + 22 SF + 110 slag), under initial 7-day water curing regime achieved lower values of total porosity than mix A. Further slag addition caused an increase in the porosity of mix E, but even those this was smaller than that of concrete made with only OPC.

The lower porosity of specimens containing slag is due to continuous hydration; the data show that the higher value of porosity under continuous water curing was obtained for mix B, 6.82%. Mix D appears to show the optimum slag content, which produced the lowest value of porosity 4.64% followed by mix C. Further increases in slag content mix E (with highest cementitious content) increased the porosity. Perhaps these data indicate that even six months of water curing are not adequate to obtain the full benefits of slag in concrete.

Many studies [10-13] have shown that the incorporation of slag produces a concrete with a much more refined pore structure than OPC concrete. Swamy [12] reported that, what influences pore structure most is curing, without any water curing, the 65% replacement level of OPC with slag had a higher porosity than plain OPC. However, once some initial water curing take place, these differences tend to be reduced. With a continuous humid environment, the pore sizes are dramatically reduced, It is this unique reduction in large pore sizes and refined pore structure that gives slag concrete its superior durability properties compared to OPC concrete.

Mixes containing silica fume or GGBFS/SF show the poorest performance in a prolonged air environment. Mix E which contained 32.4% slag and small amount of SF showed the highest value of total porosity at 6 months. This high porosity of blended cement concrete indicates the need for water curing to continue the reaction at early ages and later.

6.2.3 Effect of exposure time

Most of the pore structure development is completed when exposed to prolonged air curing after initial water curing as shown in Fig. 6.1 and Table 6.1. However, there are indications that when large amounts of slag are incorporated as in mix E, further pore refinement takes place with time. However, water cured samples showed reduction in total porosity for all mixes ranging by about 8% to 20% due to the availability of moisture. These results are confirmed by previous studies such as those of Winslow and Diamond [106] who found significant differences in the total pore volume between 1 day and 59 days, while the development between 59 days and 318 days was very low.

6.2.4 Effect of exposure environment

Table 6.1 shows that the real outdoor environment of Dubai has resulted in higher porosity when compared to similar concretes exposed to indoor environment. Samples were cast in the summer at a time when the temperature ranged from 38°C - 45°C. These results show that high curing temperatures result in greater porosity and other published results confirm this phenomena [1,2].

In addition to this, the adverse effect of environment on porosity in manifested in the samples exposed to air drying. The evaporation rate of mixing water from samples in outdoor environment is higher than that in the laboratory environment. Higher ambient temperature, lower relative humidity and high solar radiation accelerate this evaporation, resulting in a fast cessation of hydration due to lack of sufficient moisture.

The effect of outdoor environment on porosity is very clear, the difference in porosity in certain cases is up to 40% when compared to the laboratory environment. This is because of the large and continuous daily fluctuation in both temperature and relative humidity which initiates cycles of wetting and drying, causing subsequent adverse effects on hydration and initiates cracking. As seen from Table 6.1, mix A shows an increase in total porosity of about 10% when compared to the corresponding value at indoor exposure. The inclusion of silica fume in mix B (378 OPC + 22 SF) was more sensitive to water curing, and there was 22% increase in total porosity due to hot environment. On the other hand, mix C (323 OPC + 22 SF + 55 slag) with a similar SF content as mix B, shows that the inclusion of small amount of slag (55 kg/m^3) did not adversely effect the porosity under air curing. Further addition of slag to mixes D and E increased the porosity by 32 and 26% respectively, when compared with the corresponding values in indoor.

On the other hand, the outdoor environment affects the total porosity of concrete even when it is subjected to continuous water curing regime. Under these conditions, the control mix showed higher porosity in outdoor condition by 12% compared to the corresponding value at indoor. Mix B, however, showed a lower value of total porosity at outdoor than indoor, which is about 7% less. The presence of slag shows no change due to hot environment (mix C), but any further increase in slag content increased the porosity, as seen for both mixes D and E, the increase in porosity being about 40%. Similar trends were observed for specimens cured 3 days and 7 days in water then in air, all of which showed higher porosity when exposed to outdoor environment.

The results show that the total porosity in outdoor environment was increased as the level of GGBFS was increased from 24.2 to 32.4% (mix D and mix E) for all curing regimes, whereas, with the exception of air curing, the replacement level of GGBFS of 13.75% (mix C) reduced the total porosity. The lowest value of total porosity was obtained for mix C, the reduction being about 4.67%. The presence of silica fume produced similar values of total porosity when compared to the control mix at outdoor.

It is clear from these results that mixes containing slag in large amount were more affected by the nature of the environment. The adverse effect of the hot drying environment on total porosity is seen to be maximum for air-cured specimens. This high increase in the total porosity of slag specimens show that, slag samples are more sensitive to water curing in a hot environment.

Goto and Roy [1] found that, when porosity was calculated from the results of mercury intrusion porosimetry, significant increases were observed from 36% to 56% of total porosity as the curing temperature was increased from 27°C to 60°C.

6.3 Pore structure

The discussion of the characteristics of the pore structure is dealt with below in terms of the following parameters:

Total intrusion volume

This is the maximum volume of mercury intruded into the sample at the highest pressure during the test.

Coarse pore volume

The coarse pore volume which is greater than 0.1 μm.

Threshold diameter

The threshold diameter is taken as defined by other researchers [112-114] and as shown in Fig. 3.7 (chapter 3) via the turning point of the intrusion curve; above this point there is comparatively little intrusion into the specimens, and immediately below, the greatest portion of the intrusion.

Continuous pore diameter

The continuous pore diameter is as shown in Fig. 3.7 (chapter 3) is interpreted as the pore at which the maximum intrusion is filled. More details of these parameters are presented in chapter 3.

6.3.1 Effect of curing -6 months, indoor

A summary of the results of the pore structure is shown in Tables 6.2 to 6.4. A comparison of the cumulative intrusion volume against pore diameter under the four curing regimes, and the log differential intrusion volume against pore diameter of the same mixes is plotted is Figs. 6.2 to 6.11.

The results of the pore size distribution of OPC and blended concrete are presented in the following series of Figs. 6.12-6.15.

The duration of curing is, however, seen to have great effects on pore sizes than on total porosity. The volume of pores greater in diameter than 0.1 μm was reduced by about 55-75% when comparing continuous water cured samples to air cured samples, as shown in Fig. 6.13. Similar trends are also seen for continuous pore diameter and threshold diameter, (Figs. 6.14 and 6.15) Similar results have been reported elsewhere

Table 6.2 Influence of curing regime on pore size distribution.

Mix	Binder content kg/m^3 OPC/SF/Slag	Curing regime	Indoor Age = 6 months			Indoor Age = 18 months			Outdoor Age = 18 months		
			Intruded pore volume ml/g			Intruded pore volume ml/g			Intruded pore volume ml/g		
			Total pore volume	Coarse pore >0.1 μm	Fine pore <0.1 μm	Total pore volume	Coarse pore >0.1 μm	Fine pore <0.1 μm	Total pore volume	Coarse pore >0.1 μm	Fine pore <0.1 μm
A	400/0/0	air curing	0.0397	0.0120	0.0277	0.0411	0.0124	0.0287	0.0493	0.0280	0.0213
		3d wet/air	0.0385	0.0100	0.0285	0.0386	0.0100	0.0286	0.0412	0.0142	0.0270
		7d wet/air	0.0375	0.0070	0.0205	0.0364	0.0066	0.0298	0.0421	0.0103	0.0318
		wet curing	0.0245	0.0050	0.0195	0.0211	0.0048	0.0163	0.0240	0.0080	0.0160
B	378/22/0	air curing	0.0419	0.0100	0.0319	0.0420	0.0106	0.0314	0.0502	0.0282	0.0220
		3d wet/air	0.0408	0.0090	0.0318	0.0400	0.0090	0.0310	0.0422	0.0138	0.0284
		7d wet/air	0.0351	0.0060	0.0291	0.0265	0.0059	0.0206	0.0420	0.0096	0.0324
		wet curing	0.0283	0.0045	0.0238	0.0260	0.0038	0.0222	0.0260	0.0050	0.0210
C	323/22/55	air curing	0.0442	0.0130	0.0312	0.0440	0.0150	0.0290	0.0509	0.0280	0.0229
		3d wet/air	0.0322	0.0070	0.0252	0.0324	0.0076	0.0248	0.0333	0.0070	0.0263
		7d wet/air	0.0282	0.0057	0.0225	0.0262	0.0043	0.0219	0.0300	0.0065	0.0235
		wet curing	0.0226	0.0043	0.0183	0.0200	0.0039	0.0161	0.0210	0.0040	0.0170
D	323/22/110	air curing	0.0464	0.0220	0.0244	0.0481	0.0215	0.0266	0.0612	0.0351	0.0261
		3d wet/air	0.0360	0.0095	0.0265	0.0368	0.0102	0.0266	0.0382	0.0130	0.0252
		7d wet/air	0.0309	0.0060	0.0249	0.0300	0.0059	0.0241	0.0345	0.0121	0.0224
		wet curing	0.0217	0.0053	0.0164	0.0187	0.0042	0.0145	0.0291	0.0070	0.0221
E	323/22/165	air curing	0.0546	0.0250	0.0296	0.0546	0.0250	0.0296	0.0671	0.0423	0.0248
		3d wet/air	0.0371	0.0100	0.0271	0.0372	0.0117	0.0255	0.0465	0.0210	0.0255
		7d wet/air	0.0361	0.0085	0.0276	0.0251	0.0050	0.0201	0.0422	0.0134	0.0288
		wet curing	0.0281	0.0055	0.0226	0.0220	0.0042	0.0178	0.0332	0.0078	0.0254

Table 6.3 Percentage of coarse and fine pores.

Mix	Binder content kg/m^3 OPC/SF/Slag	Curing regime	Indoor Age = 6 months		Indoor Age = 18 months		Outdoor Age = 18 months	
			Coarse pore %	Fine pore %	Coarse pore %	Fine pore %	Coarse pore %	Fine pore %
A	400/0/0	air curing	30	70	30	70	57	43
		3d wet/air	26	74	26	74	34	66
		7d wet/air	19	81	18	82	24	76
		wet curing	20	80	23	77	33	67
B	378/22/0	air curing	24	76	25	75	56	44
		3d wet/air	22	78	23	77	33	67
		7d wet/air	17	83	22	78	23	77
		wet curing	16	84	15	85	19	81
C	323/22/55	air curing	29	71	34	66	55	45
		3d wet/air	22	78	23	77	21	79
		7d wet/air	20	80	16	84	22	78
		wet curing	19	81	20	80	19	81
D	323/22/110	air curing	47	53	45	55	57	43
		3d wet/air	26	74	28	72	34	66
		7d wet/air	19	81	20	80	35	65
		wet curing	24	76	22	78	24	76
E	323/22/165	air curing	46	54	46	54	63	37
		3d wet/air	27	73	31	69	45	55
		7d wet/air	24	76	20	80	32	68
		wet curing	20	80	19	81	23	77

Table 6.4 Influence of curing regime on threshold diameter and continuos pore diameter.

Mix	Binder content kg/m^3 OPC/SF/Slag	Curing regime	Laboratory environment Age = 6 months		Laboratory environment Age = 18 months		Outdoor environment Age = 18 months	
			Threshold diameter, μm	Continuous pore diameter, μm	Threshold diameter, μm	Continuous pore diameter, μm	Threshold diameter, μm	Continuous pore diameter, μm
A	400/0/0	air curing	0.140	0.070	0.160	0.095	0.280	0.200
		3d wet/air	0.090	0.065	0.100	0.065	0.180	0.130
		7d wet/air	0.065	0.033	0.065	0.060	0.130	0.090
		wet curing	0.030	0.020	0.020	0.017	0.025	0.018
B	378/22/0	air curing	0.130	0.065	0.130	0.070	0.310	0.210
		3d wet/air	0.080	0.030	0.080	0.060	0.190	0.150
		7d wet/air	0.050	0.019	0.055	0.030	0.130	0.100
		wet curing	0.025	0.011	0.020	0.020	0.030	0.017
C	323/22/55	air curing	0.130	0.065	0.150	0.070	0.300	0.200
		3d wet/air	0.035	0.023	0.070	0.035	0.075	0.060
		7d wet/air	0.025	0.020	0.030	0.015	0.070	0.060
		wet curing	0.020	0.018	0.020	0.013	0.025	0.017
D	323/22/110	air curing	0.300	0.085	0.350	0.130	0.400	0.235
		3d wet/air	0.032	0.018	0.040	0.022	0.120	0.065
		7d wet/air	0.030	0.019	0.025	0.017	0.110	0.070
		wet curing	0.022	0.014	0.020	0.015	0.025	0.017
E	323/22/165	air curing	0.400	0.065	0.500	0.080	0.500	0.260
		3d wet/air	0.080	0.025	0.060	0.019	0.190	0.100
		7d wet/air	0.070	0.018	0.038	0.017	0.120	0.055
		wet curing	0.030	0.016	0.020	0.011	0.040	0.014

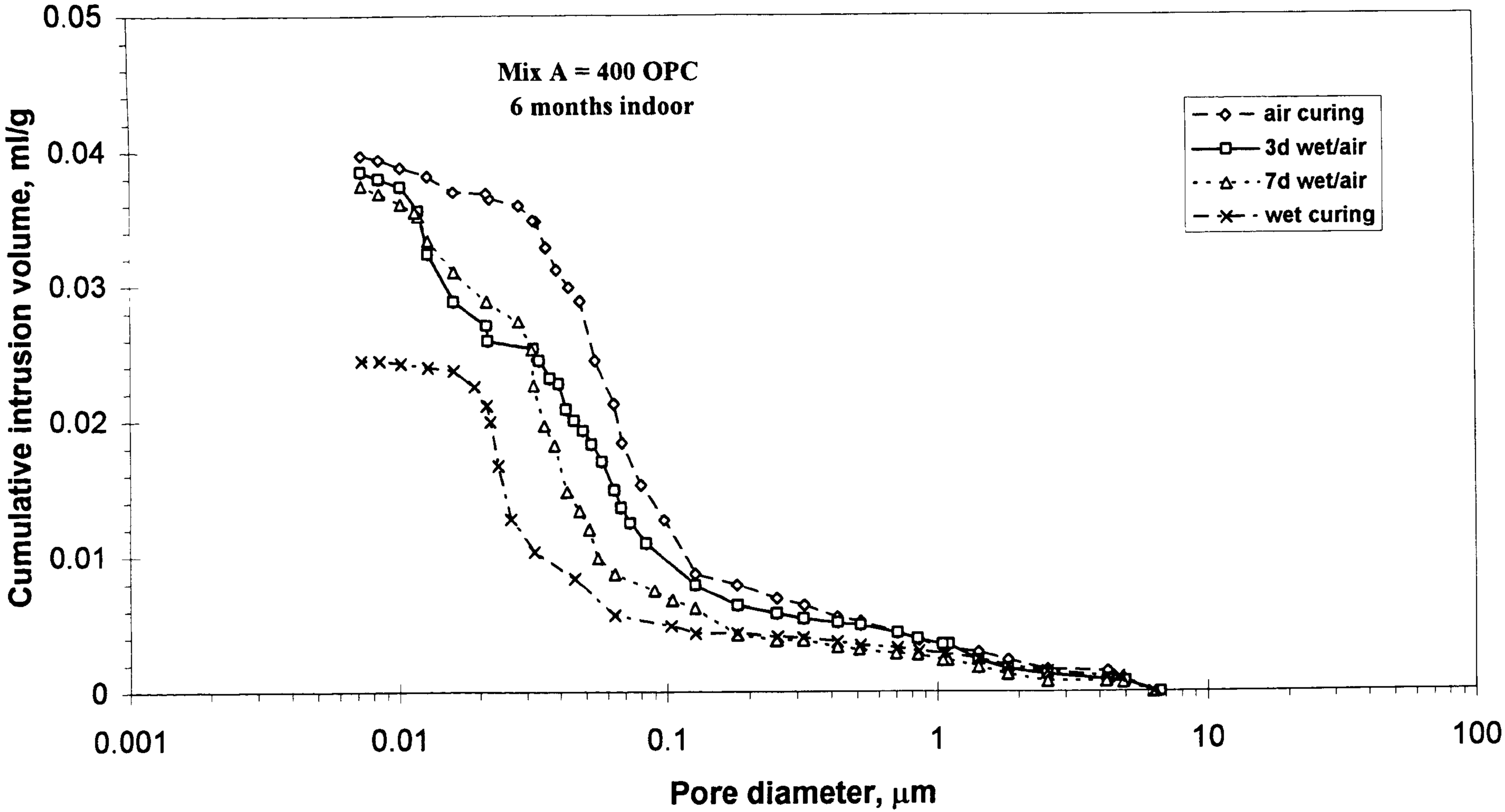

Fig. 6.2 : Influence of curing regime on pore size distribution for mix A.

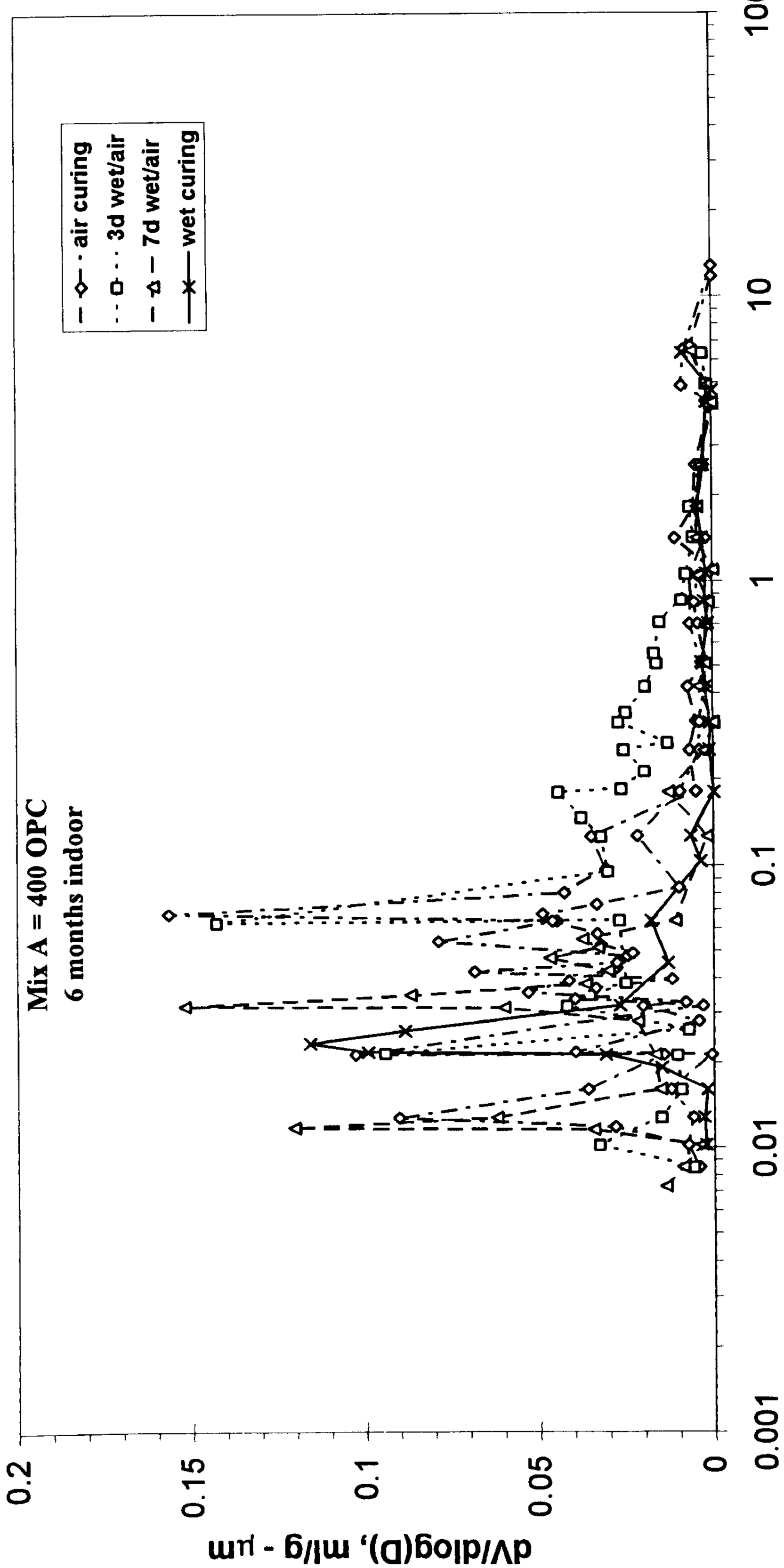

Fig. 6.3 : Differential pore size distribution for mix A.

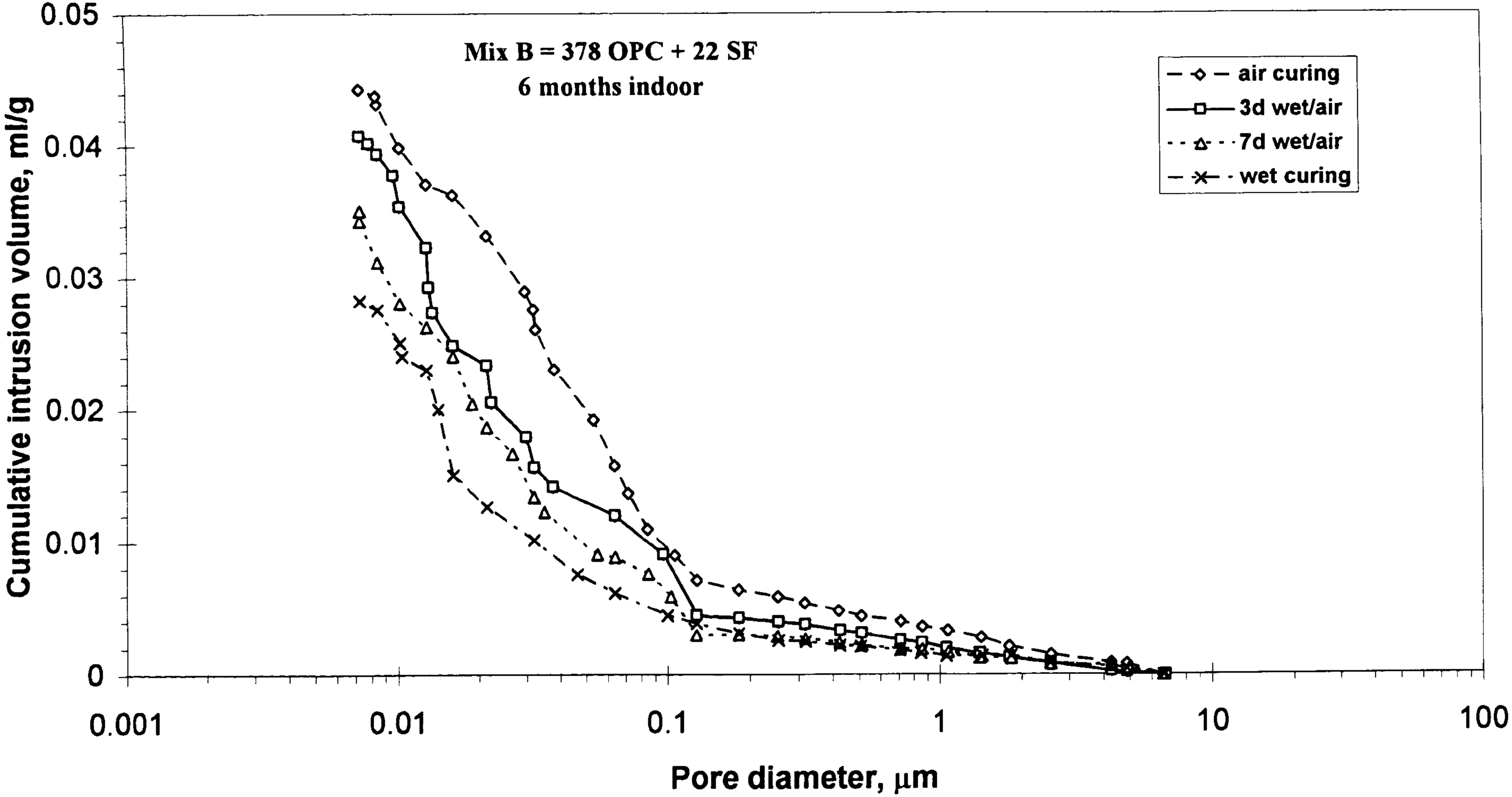

Fig. 6.4 : Influence of curing regime on pore size distribution for mix B.

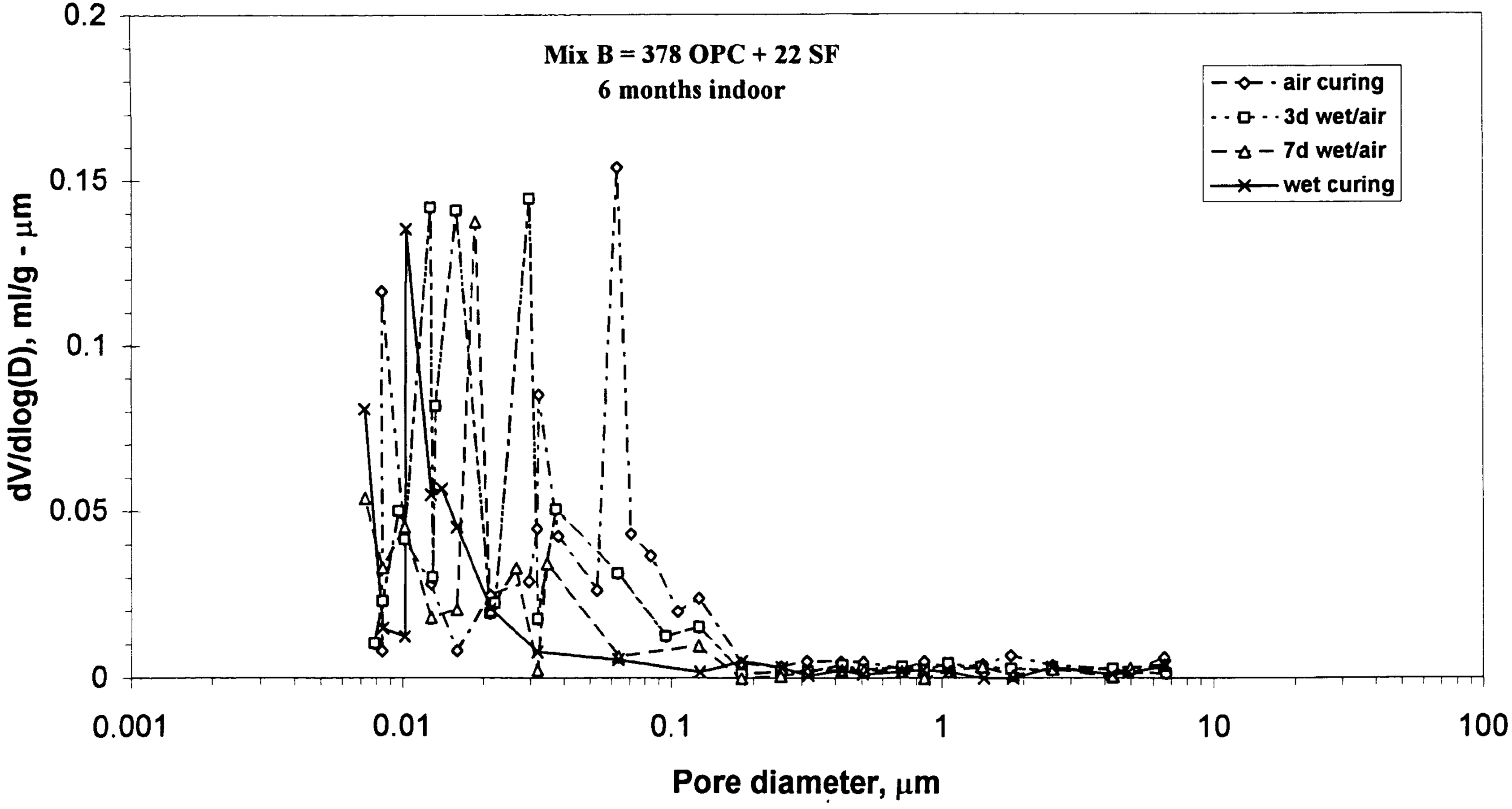

Fig. 6.5 : Differential pore size distribution for mix B.

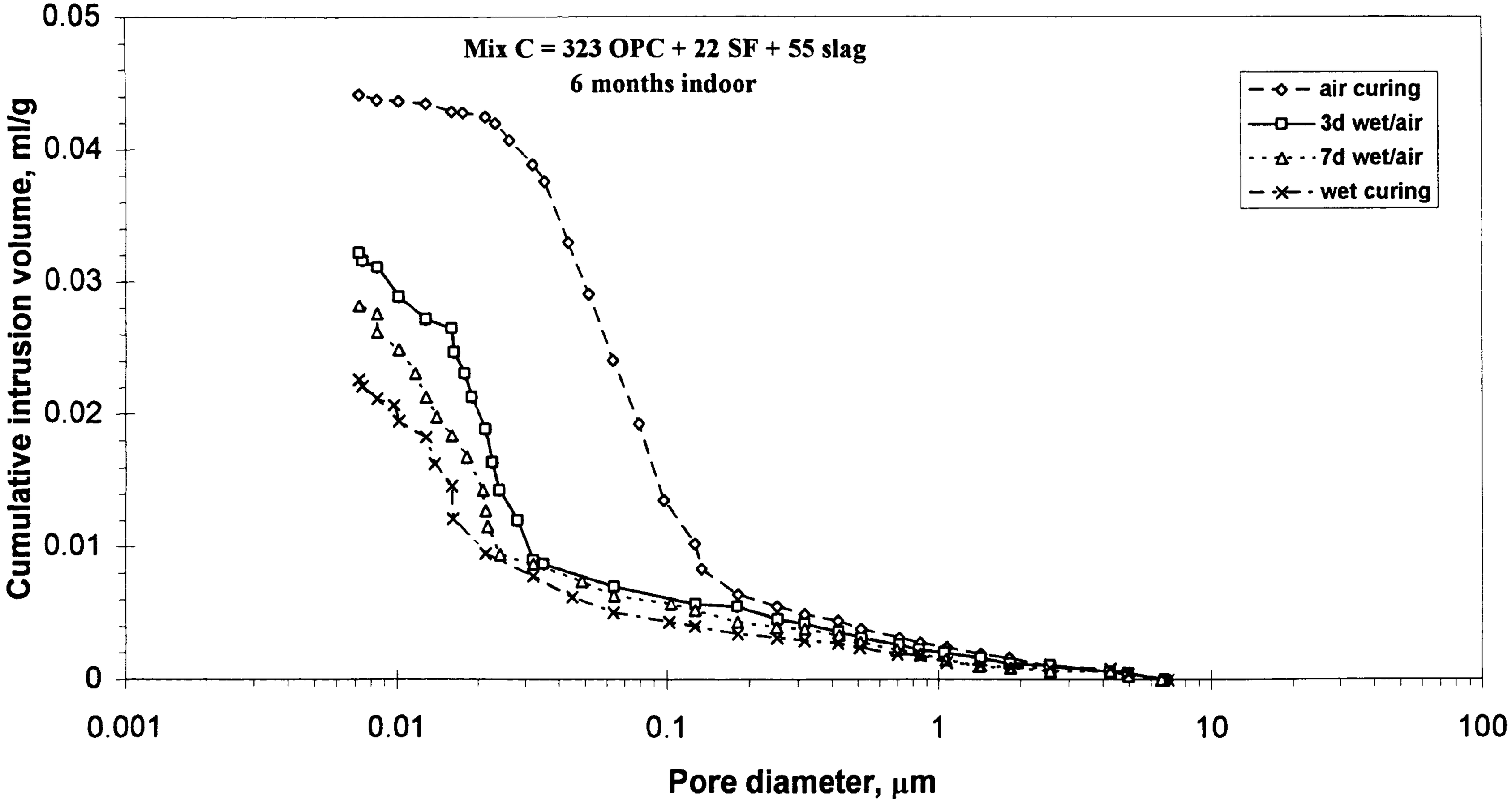

Fig. 6.6 : Influence of curing regime on pore size distribution for mix C.

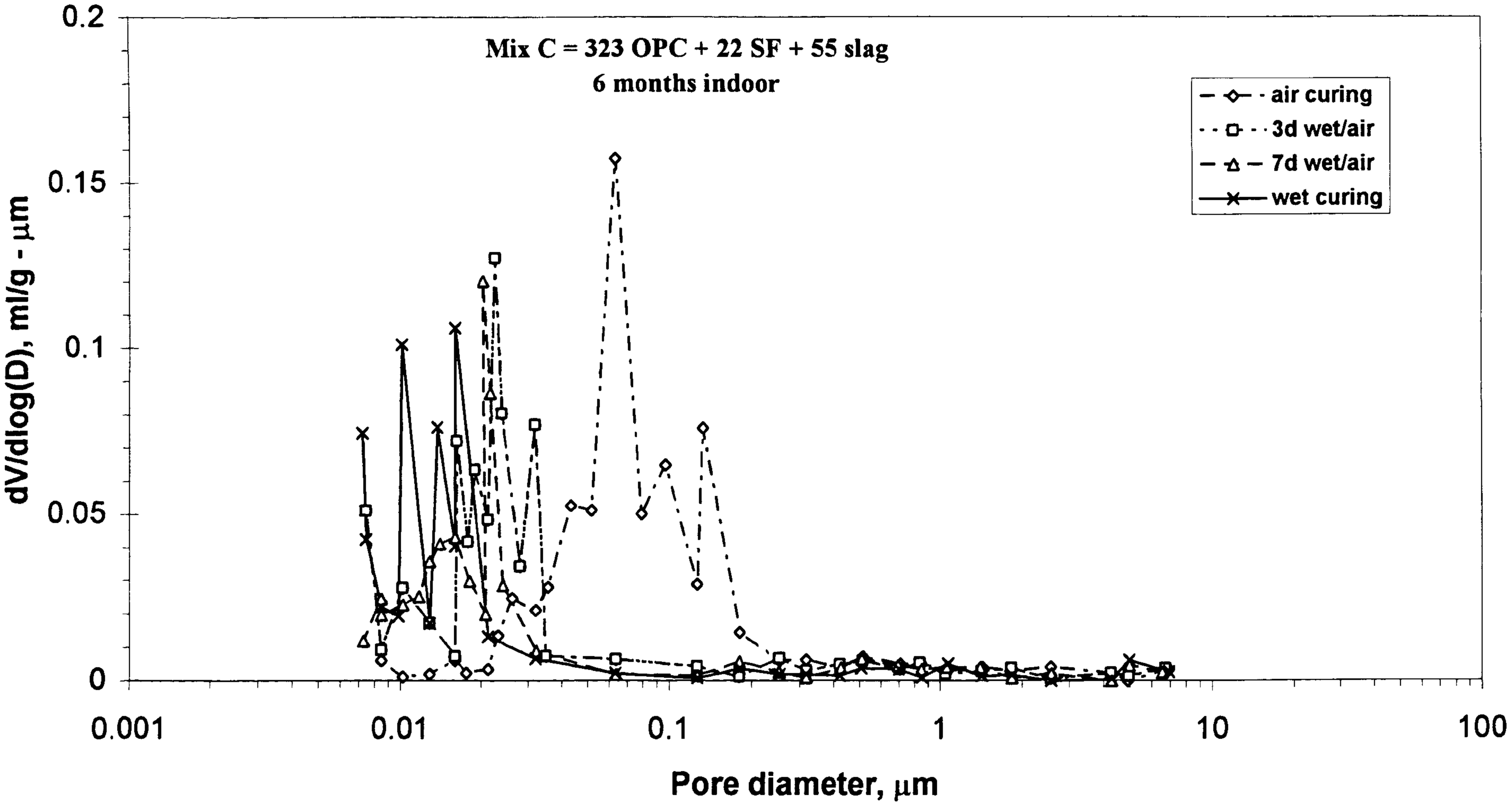

Fig. 6.7 : Differential pore size distribution for mix C.

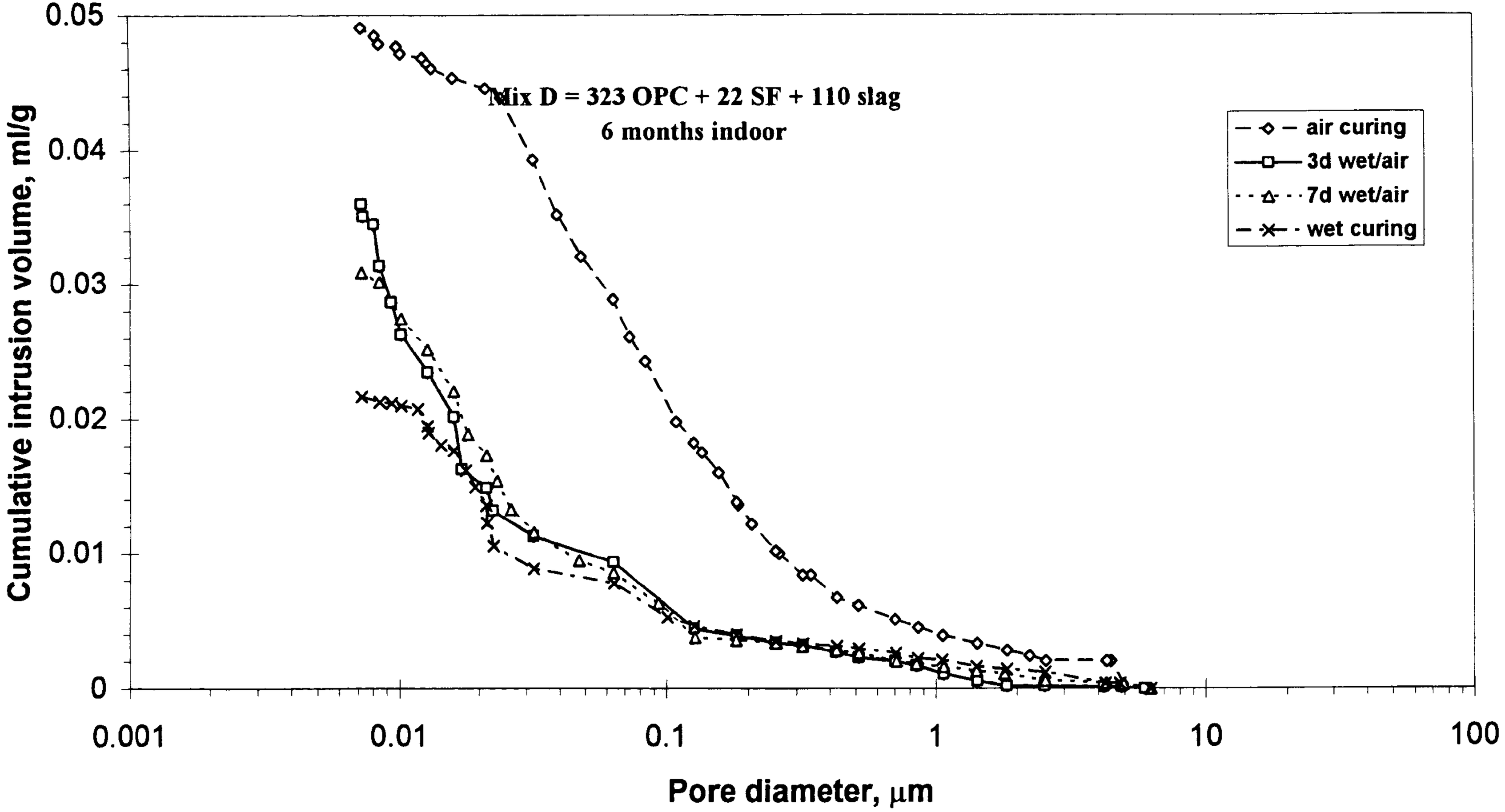

Fig. 6.8 : Influence of curing regime on pore size distribution for mix D.

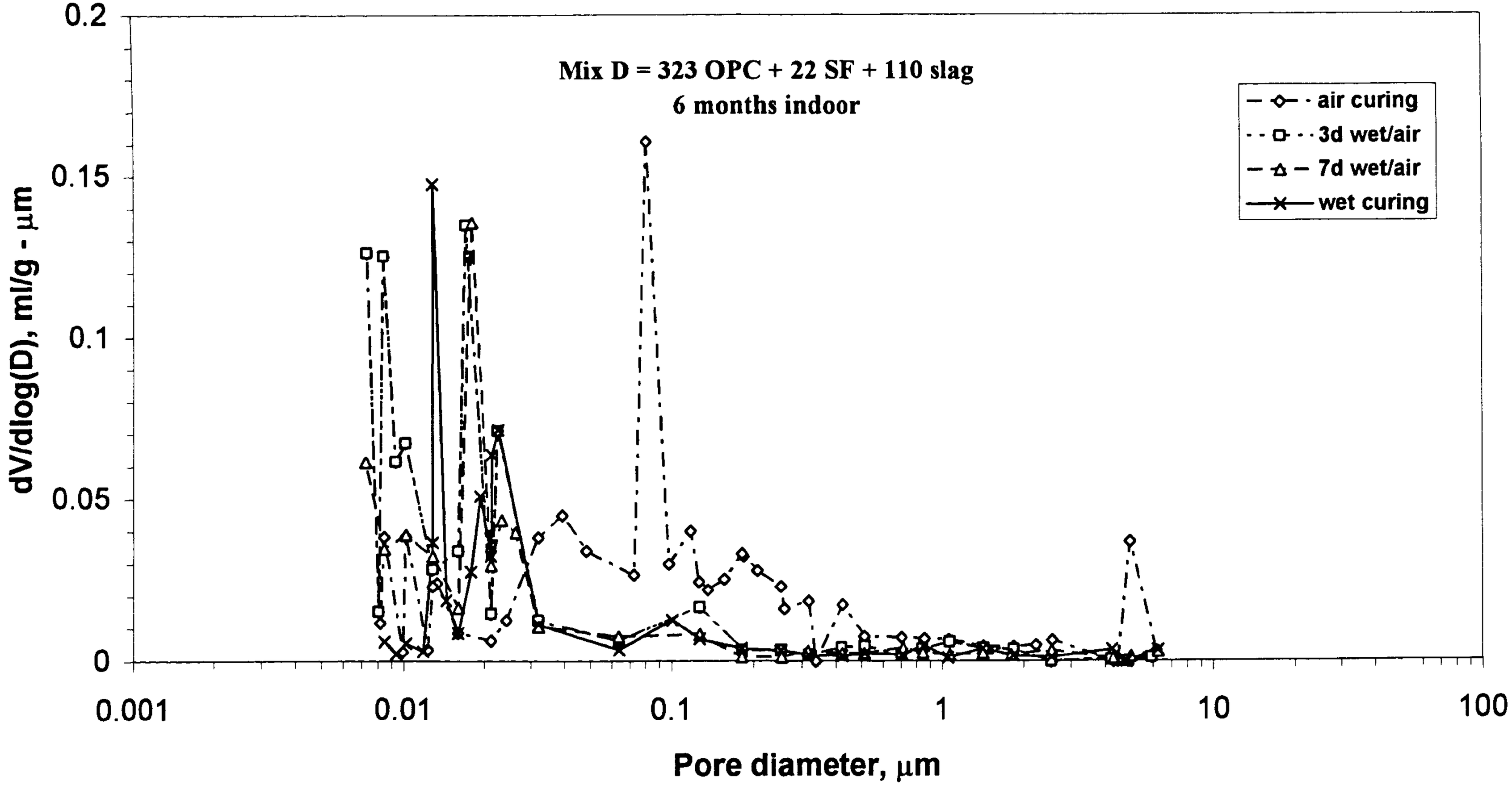

Fig. 6.9 : Differential pore size distribution for mix D.

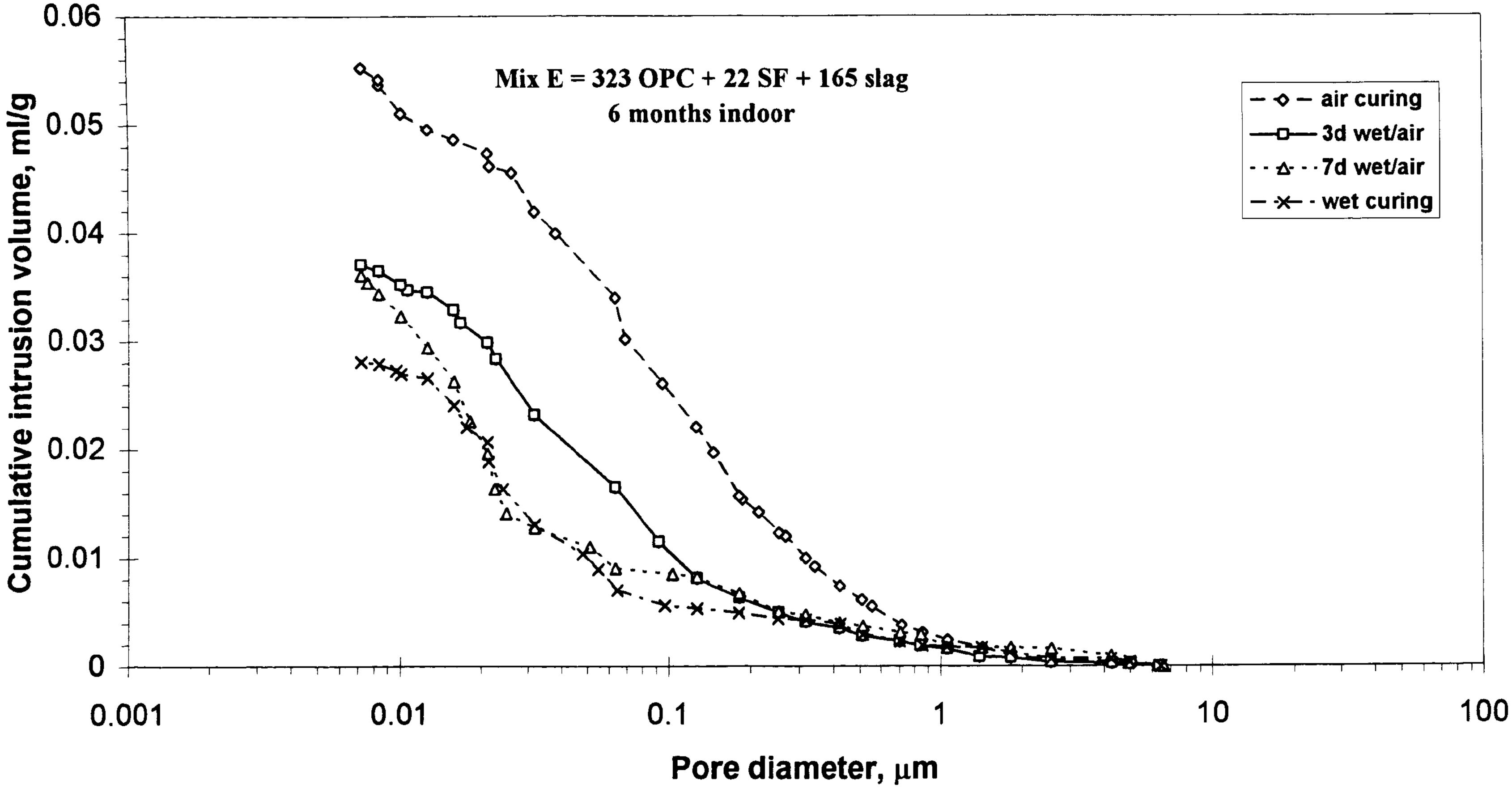

Fig. 6.10 : Influence of curing regime on pore size distribution for mix E.

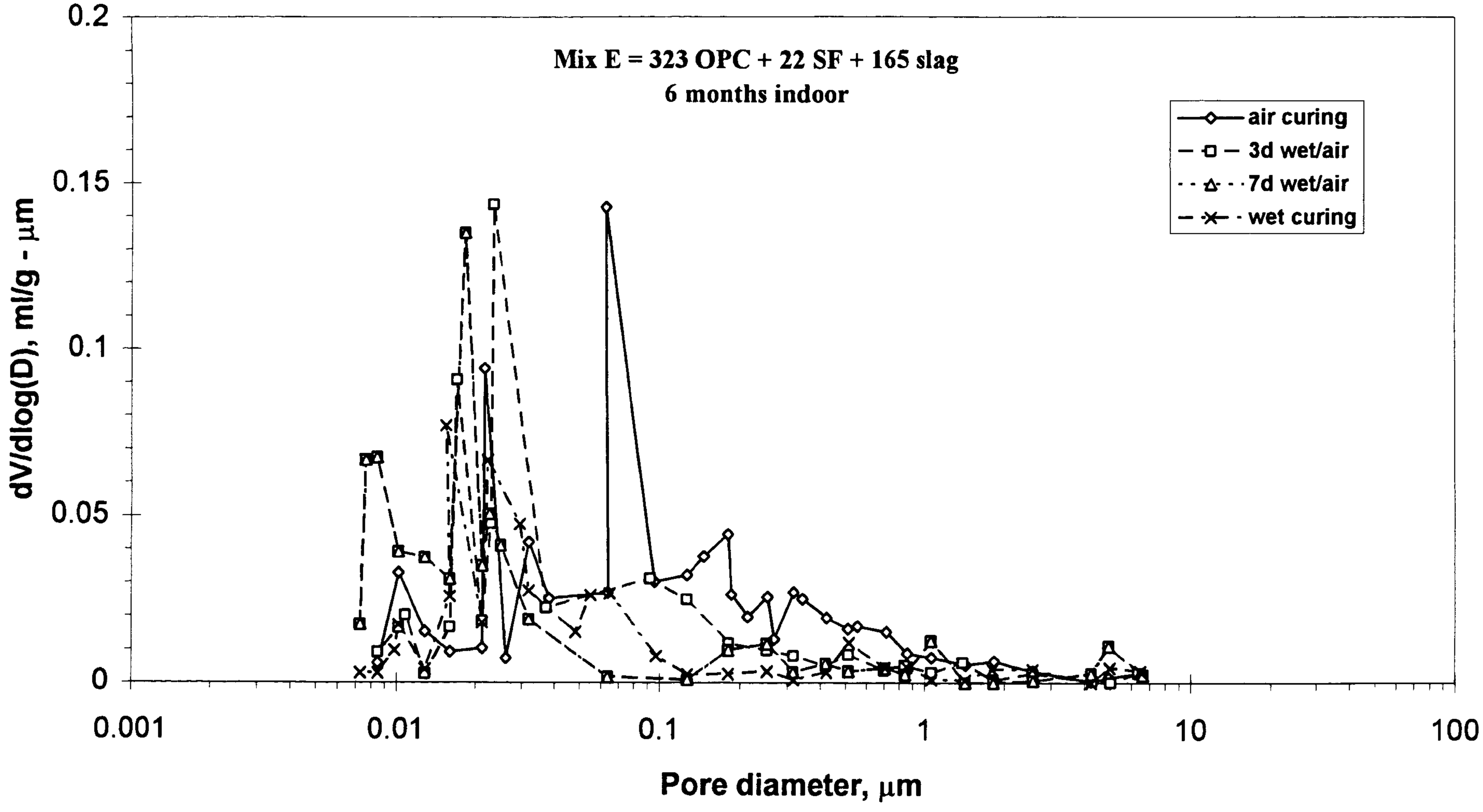

Fig. 6.11 : Differential pore size distribution for mix E.

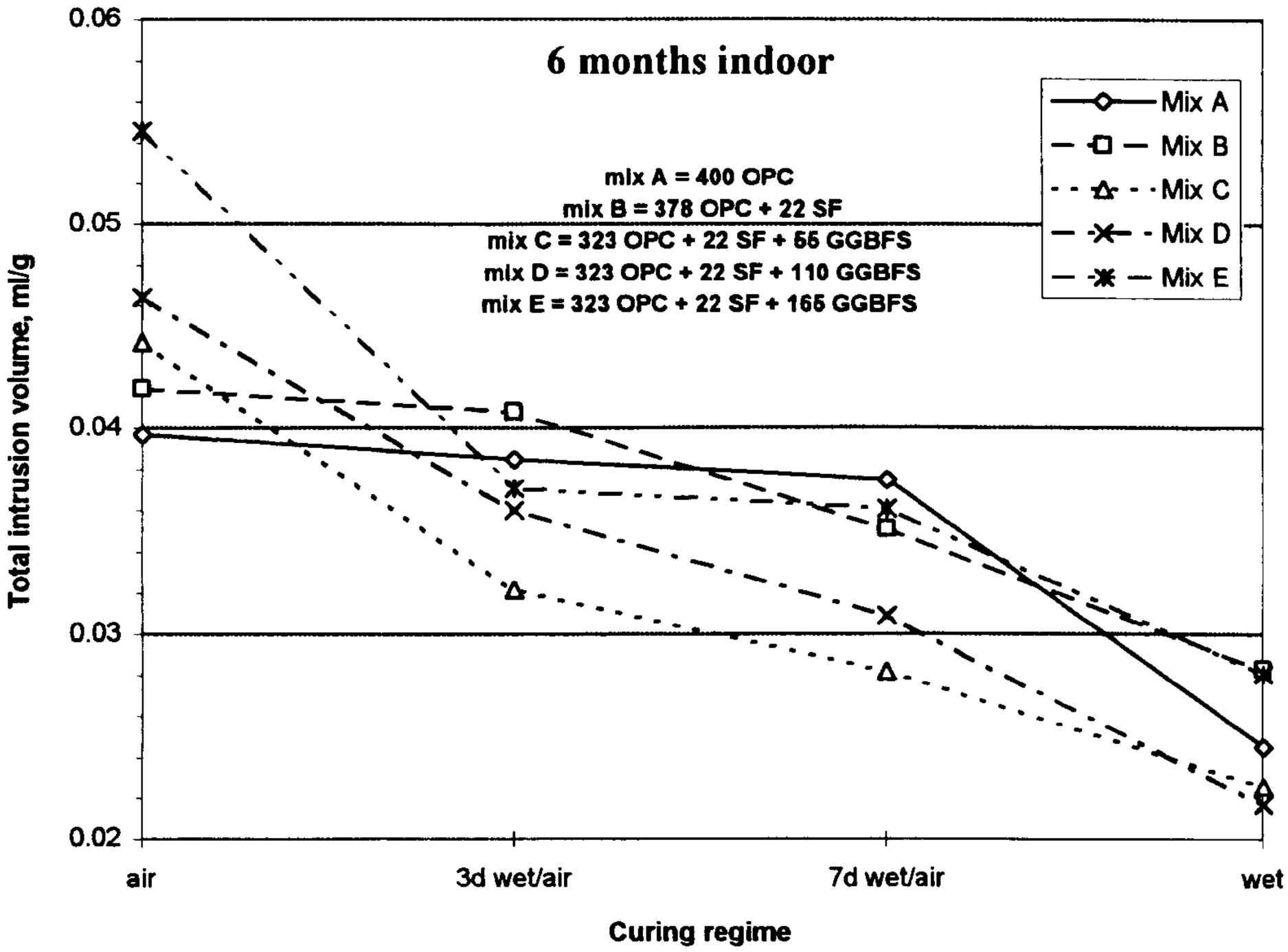

Fig. 6.12: Influence of curing regime and mix type on total intrusion volume.

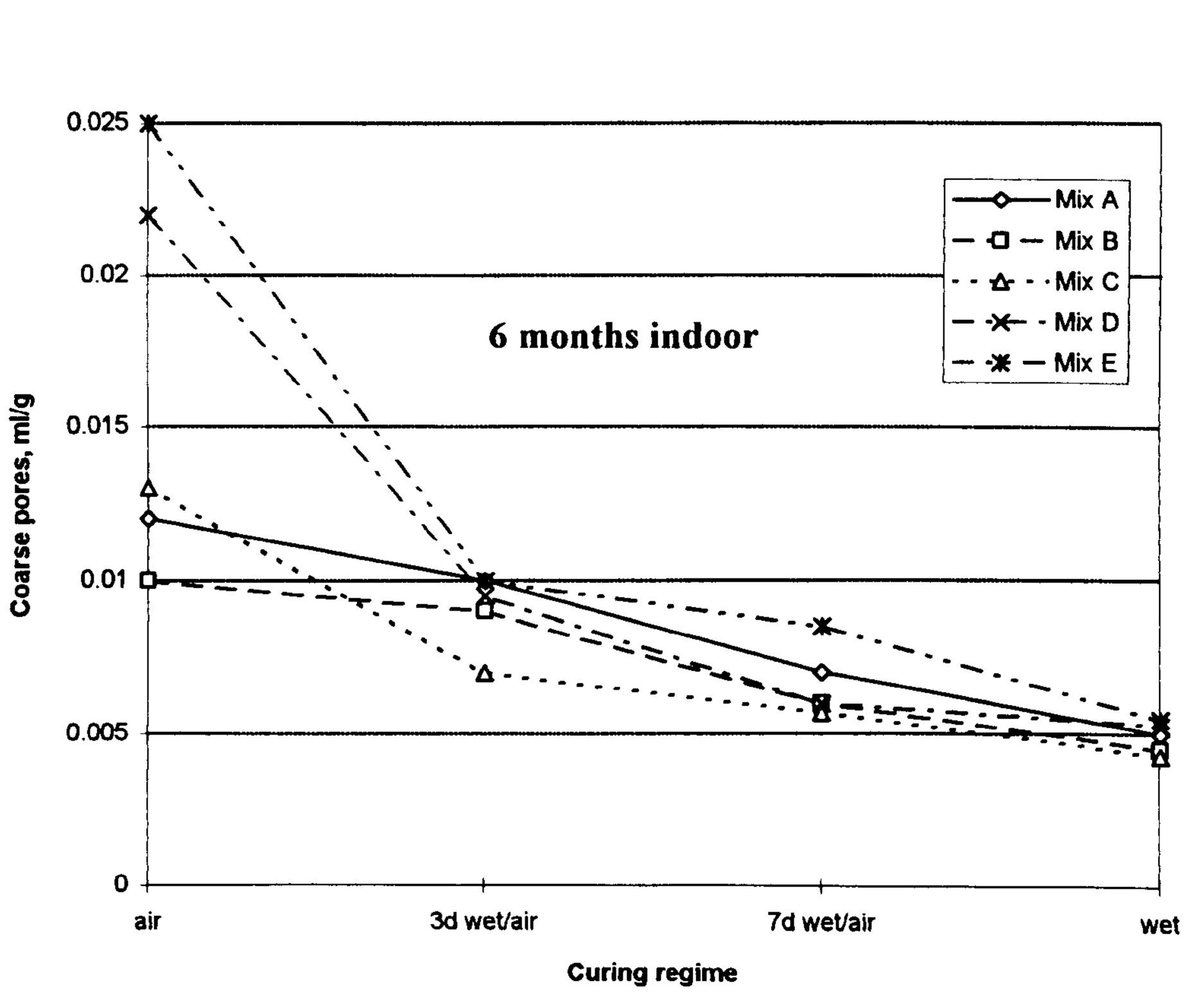

Fig. 6.13: Influence of curing regime and mix type on coarse pore volume.

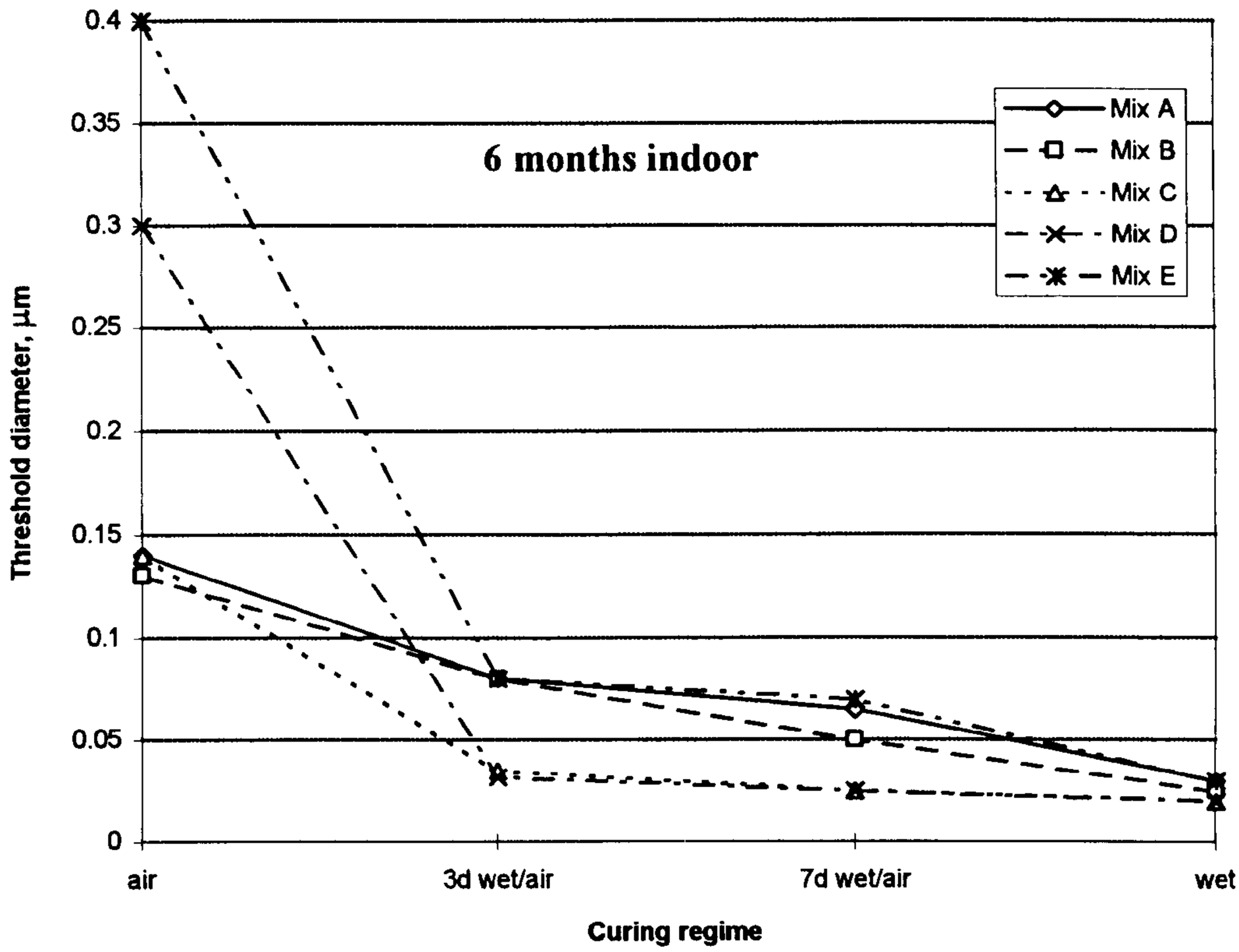

Fig. 6.14 Influence of curing regime and mix type on threshold diameter.

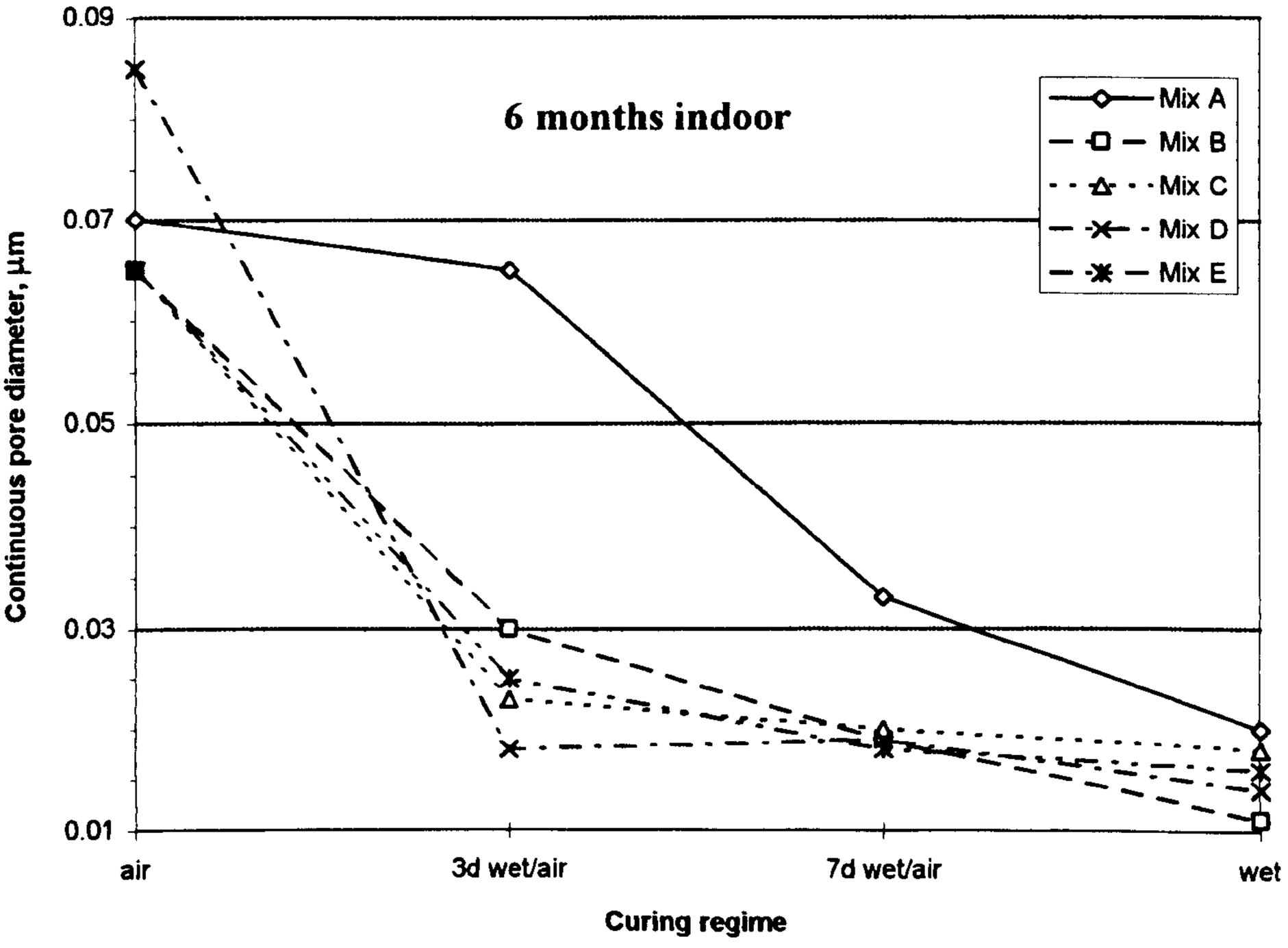

Fig. 6.15 Influence of curing regime and mix type on continuous pore diameter.

[142] showing that pore sizes are more effected by curing hydration than by total porosity.

The effect of curing regime on the pore size distribution of all the mixes at the age of 6 months in the laboratory environment was similar to those on total porosity; a longer curing period produced a finer pore structure. Mixes containing GGBFS show coarser pores than mixes A and B under air curing regime at the age of 6 months.

Fig. 6.2 shows a comparison of the cumulative intrusion volume against pore diameter for mix A under the four curing regimes at 6 months indoor. Also Fig. 6.12 and Table 6.2 show the influence of curing regime on the total intrusion volume. As seen in these data, the total intrusion volume of mix A (400 OPC) under air curing, 3d wet/air and 7d wet/air curing regime was approximately similar, being 0.0397, 0.0385, and 0.0375 ml/g, compared to the corresponding value is 0.0245 ml/g for continuous water curing, this shows a reduction in the total intrusion pore volume of 38.3%. More significant values were observed with the pore size distribution, the coarse pores decreasing as water curing increases. The air cured and 3d wet/air cured samples have a much higher pore volume than those exposed to both 7d wet/air curing and continuous water curing, which are 0.0120 and 0.0100 ml/g respectively, compared with 0.0070 ml/g for 7d wet/air and 0.0050 for continuous water curing. A similar effect on threshold diameter is also found. As seen from Table 6.4 specimens cured continuously in water also have a smaller threshold diameter. The threshold diameter under water curing is 0.030 μm, the corresponding values for air curing, 3d wet/air curing and 7d wet/air curing, being 0.140, 0.090 and 0.065 μm respectively.

The results of continuous pore diameter were obtained from dV/dlog(D) curves; these value are approximate, because the curves consist of one or more peaks, the first peak was taken as the value of the continuous pore diameter. As with the other results, air curing shows much larger continuous pore diameters than the other curing regimes. Air curing resulted in a continuous pore diameter of 0.070 μm, the corresponding value for 3d wet/air is very close to this, 0.065 μm. On the other hand, specimens cured continuous in water or for 7-day water curing, show significantly high reductions in continuous pore diameter, the corresponding values being 0.020 μm and 0.033 μm respectively.

Fig. 6.4 shows a comparison of the cumulative intrusion volume against pore diameter for mix B (378 OPC + 22 SF) under the four curing regimes at 6 months indoor exposure. Also, Fig. 6.12 and Table 6.2 show the influence of curing regime on

the total intrusion volume. It is clear from these data that the specimens under air curing and 3d wet/air curing regime have a much higher total pore volume than those at 7d wet/air curing and continuous water curing: these are 0.0419 and 0.0408 ml/g, respectively for air curing and 3d wet/air curing, compared with 0.0351 ml/g for 7d wet/air and 0.0283 ml/g for continuous water curing. As seen from Table 6.2, the specimens under air curing and 3d wet/air curing regime have a larger coarse pore volume, twice as much as the corresponding value under continuous water curing. Although there is a difference between the threshold diameters, as seen from Table 6.4 mix B under air curing regime has a large threshold diameter, more than five times as much as the corresponding value under continuous water curing regime: the values are 0.130 μm for the specimens under air curing regime and 0.025 μm for the specimens under continuous water curing regime. Also as water curing increased the threshold diameter decreased as seen for specimens under 3d wet/air curing and 7d wet/air curing, the values of threshold diameter being from 0.080 to 0.050 μm, with a value of 0.025μm for prolonged water curing.

Fig. 6.15 shows a comparison of the continuous pore diameter against curing regime; it is clear from this figure that water curing has a significant effect on the continuous pore diameter of mix B. Specimens under air curing exhibited a higher diameter of the continuous pore, while 3d wet/air curing decreased the continuous pore diameter from 0.065 to 0.030 μm, and further water curing shows a progressive reduction in continuous pore diameter, the corresponding values of 7d wet/air curing and continuous wet curing being 0.019 and 0.011 μm respectively.

Figs. 6.2to 6.12, and Table 6.2 show the influence of curing regime on pore size distribution for all mixes. The moist cured specimens of mix C (323 OPC + 22 SF + 55 slag) exhibited the lowest total pore volume which is 0.0226 ml/g. The corresponding values under air cured specimens displayed the highest value which is 0.0442 ml/g. Further water curing resulted in smaller pore volumes as seen for specimens under 3d wet/air and 7d wet/air curing regime, which had values of 0.0322 and 0.0282 ml/g respectively. Fig. 6.13 and Tables 6.2 and 6.3 show a comparison of the coarse pore volumes of all mixes under the four curing regimes. As seen,, the specimens of mix C under air curing and 3d wet/air curing regime have a larger coarse pore volume than 7d wet/air and continuous wet curing, these values being 0.0130 and 0.0070 ml/g respectively which represent a percentage of 29 and 22% of the total pore volume respectively. The corresponding values under continuous water curing and 7d wet/air

curing regime are 0.0043 and 0.0057 ml/g respectively, about 20% of the total volume. Although there is a difference between threshold diameters, as seen from Table 6.4 and Fig. 6.14, it varies as much as from 0.130 μm for specimens under air curing regime to 0.020 μm for specimens under continuous water curing regime.

Fig. 6.15 shows a comparison of continuous pore diameters with the curing regime. It is clearly seen that, for mix C continuous water curing regime obtained very low continuous pore diameter as compared to the value obtained under air curing, this value being 0.065 μm, and the corresponding value for continuous wet curing is 0.018 μm.

The effect of curing conditions on the cumulative intrusion volume development for mix D is shown in Fig. 6.8. A comparison of the four curing regimes on the pore size distribution development of mix D (323 OPC + 22 SF + 110 slag) is shown in Tables 6.2-6.4 and Fig. 6.12-6.15. It is generally observed that the pore size distribution changes from that of large size pores to that of small size ones with continued hydration due to water curing. Further, under continuous moist curing the pore distribution is smaller in size and the total pore volume is also less. On the other hand, as seen from Fig. 6.12 and Table 6.3 air curing regime shows a large size pore distribution which represents about 47% of the total pore volume. The corresponding value for 3d wet/air, 7d wet/air and continuous water curing are 26, 19 and 24% respectively. The corresponding values of threshold diameter are 0.300 μm for air cured specimens and 0.032, 0.030 and 0.022 μm for 3d wet/air, 7d wet/air and continuous wet curing respectively. These results confirm that longer duration of water curing for mixes containing slag must be taken into consideration.

Fig. 6.15 shows a comparison of the continuous pore diameter with curing regime, as seen, mix D specimens attained a very high continuous pore diameter of about 0.085 μm under air curing compared to other curing regimes, which produced values of about 0.018, 0.019 and 0.014 μm for 3d wet/air, 7d wet/air and continuous wet curing respectively.

Fig. 6.10 shows the cumulative intrusion volume against pore diameter for mix E. The effect of curing conditions on pore size distribution development is shown in Tables 6.2-6.4 and Figs. 6.12-6.15. The four curing regimes of mix E (323 OPC + 22 SF + 165 slag) yielded trends in values of pore structure, similar to the other four mixes more water curing producing a better pore structure. Specimens under air curing regime gave the highest values of total pore volume of 0.0546 ml/g, this value dropping to 0.0371 ml/g for the 3d wet/air curing. This high variation between the two values

indicates that, slag concrete is very sensitive to water curing. Specimens under continuous water curing show very low total pore volume as compared with specimens cured in air, the reduction was about 48.5%. Coarse pore volume (pores > 0.1μm) under air curing was 0.0250 ml/g, which is five times more than that of specimens cured continuously in water, the corresponding value under wet curing being 0.0055 ml/g. On the other hand, 7d wet/air and 3d wet/air curing gave values of 0.0085 and 0.0100 ml/g respectively. The threshold diameter found from the data obtained show that continuous water curing regime enabled the blended concrete to develop threshold diameter from 0.400 μm under air curing to only 0.030 μm under continuous wet curing. Also 3d wet/air and 7d wet/air developed pore refinement significantly, the corresponding values for these curing regimes being 0.080 and 0.070 μm respectively.

It is clear from Fig. 6.15 that the influence of water curing affects the continuous pore diameter of slag concrete significantly; the continuous pore diameter was 0.065 μm under air curing, it then drops to 0.025 μm for specimens cured 3d wet/air and to 0.018 μm for specimens cured 7d wet/air, the corresponding value under continuous wet curing being 0.016 μm.

Air curing regime, is obviously the worst, and leads to produce the largest threshold diameter and continuous pores; this is due to lack of water, sufficient to continue the hydration of cement and the cementitious action of the slag. The lack in curing water contributes to larger threshold diameters and continuous pore diameters, and therefore leading to permeable concrete.

Torii and Kawamura [154] reported the results of MIP measurement on OPC mortar and mortar containing 15% silica fume for periods of 1, 3, 7, 14, 28 and 91 days. It was observed that the general distribution curves shifted to the left (smaller pore diameter) with increasing curing time in water; that is the pore structure became increasingly finer with the curing time in water, and the total pore volume drastically decreased with increasing curing time in water.

6.3.2 Effect of mix type-6 months, indoor

A comparison of cumulative intrusion volume against pore diameter at the age of 6 months for plain OPC and blended cement concrete is presented in Figs. 6.16-6.19, while a comparison of the pore structure parameters against the curing regime for the five mixes is given in Figs. 6.12-6.15 and Table 6.2. The results show that, under air curing regime a high total pore volume was of 0.0546 ml/g observed in mix E, while

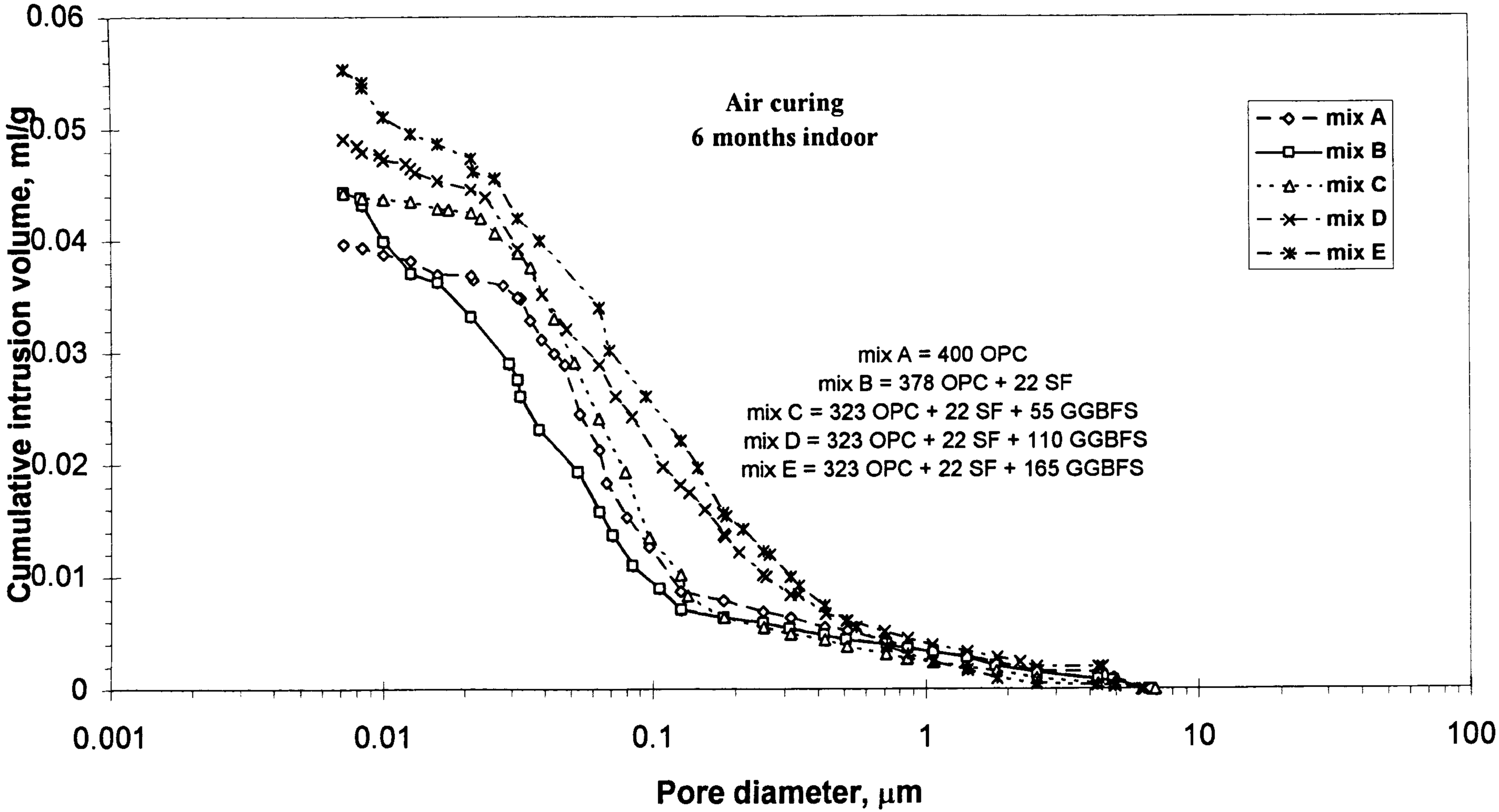

Fig. 6.16 : Influence of mix type on pore size distribution under air curing.

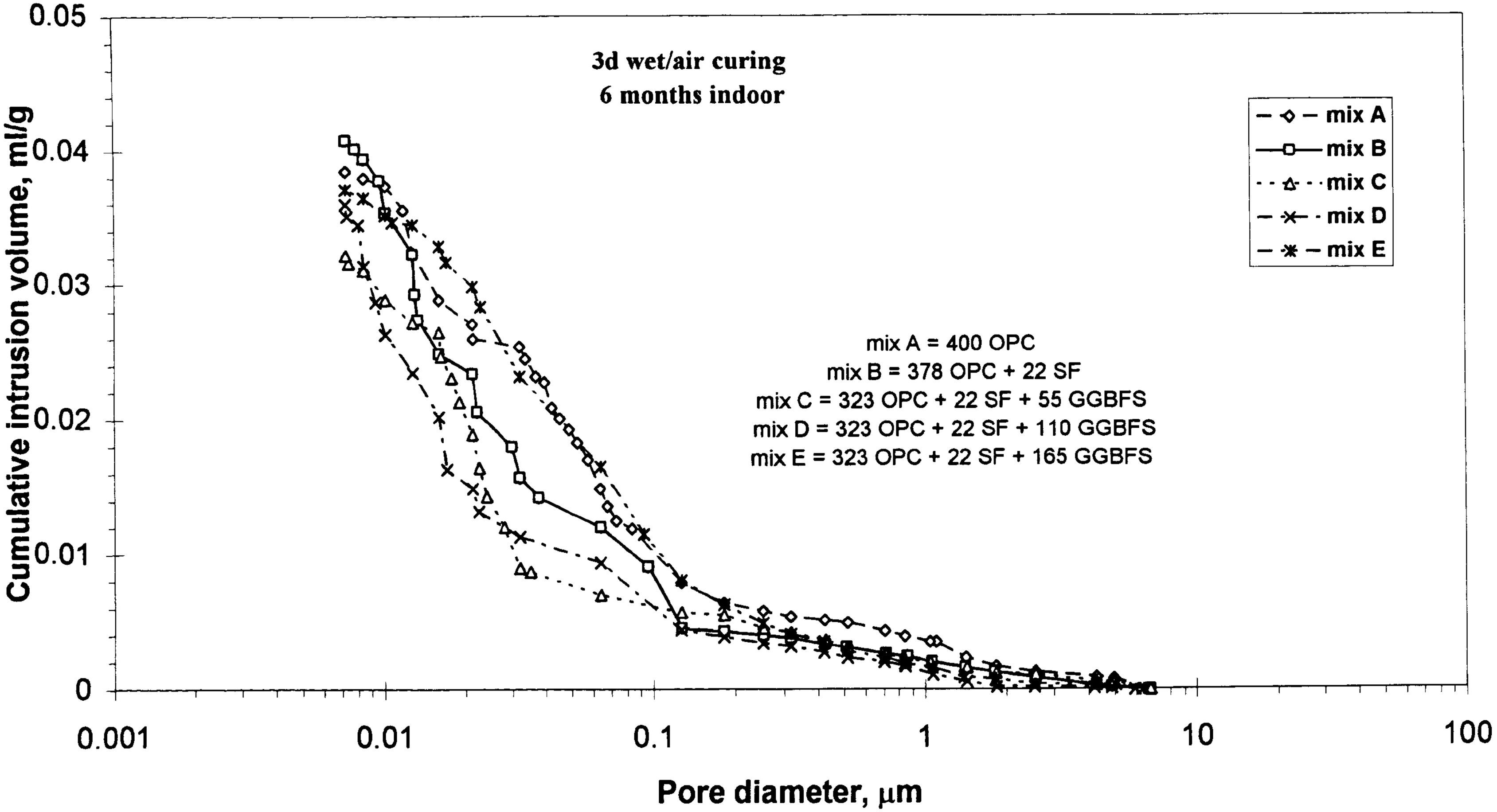

Fig. 6.17 : Influence of mix type on pore size distribution under 3d wet/air curing.

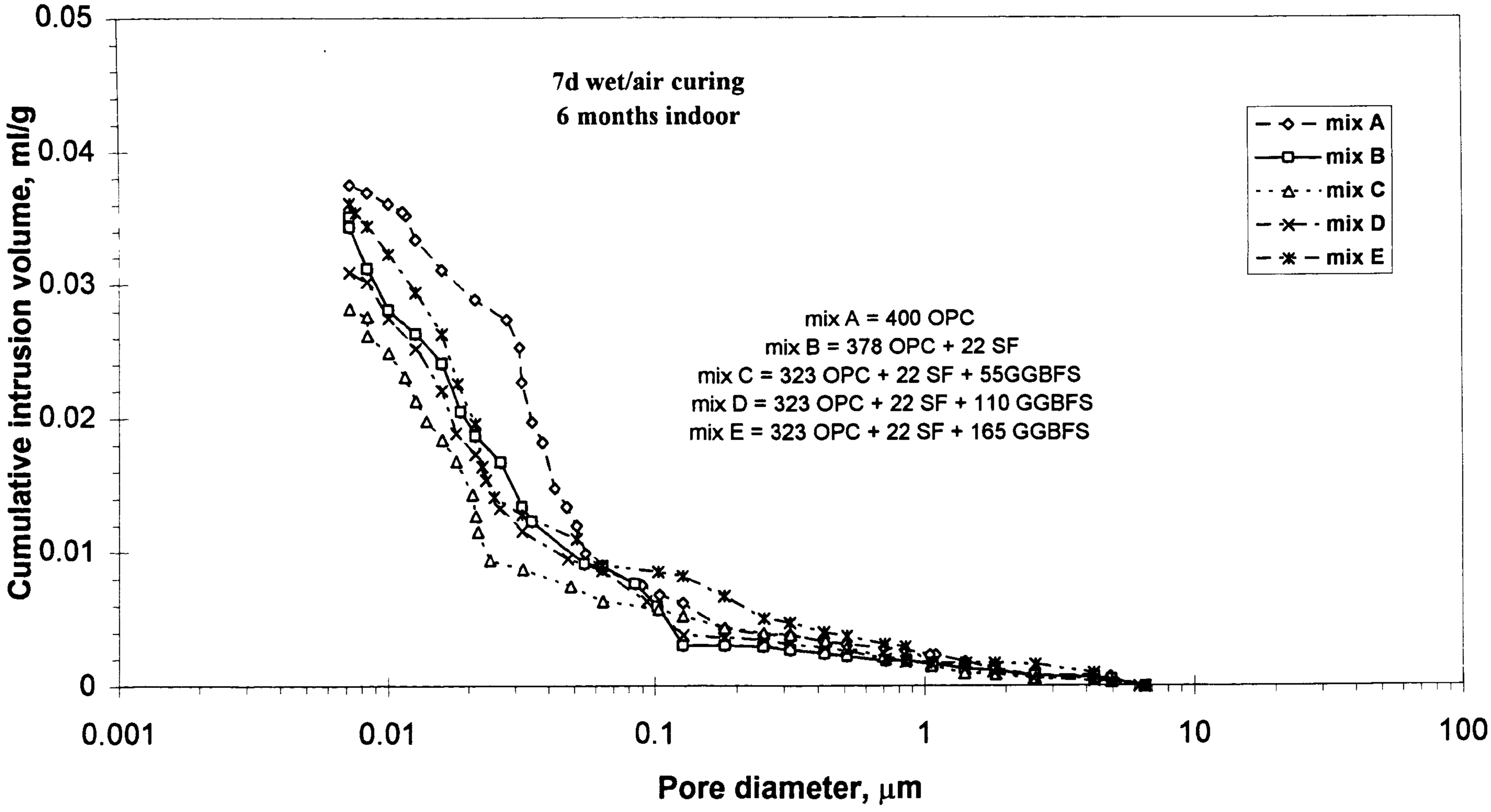

Fig. 6.18 : Influence of mix type on pore size distribution under 7d wet/air curing.

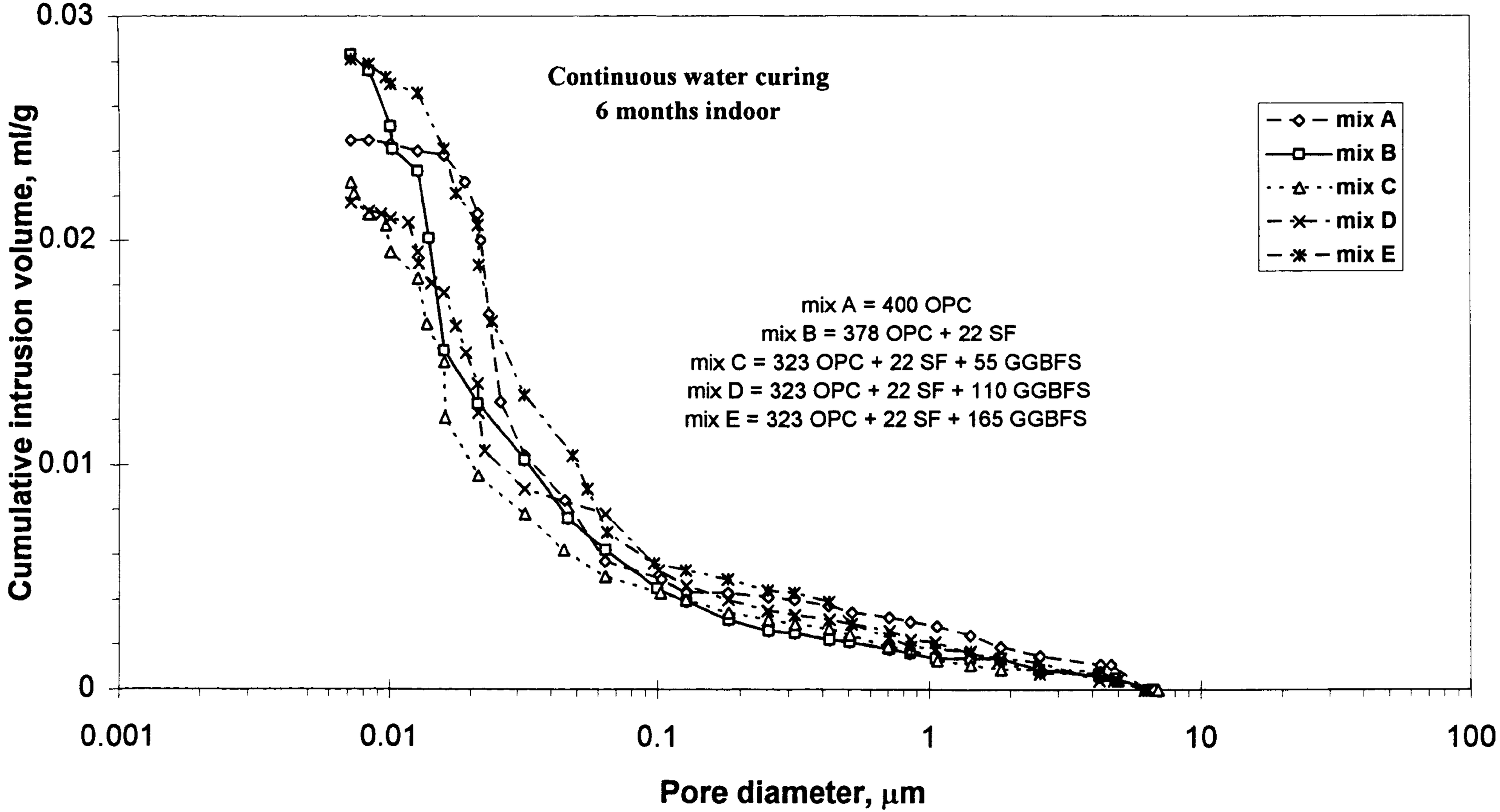

Fig. 6.19 : Influence of mix type on pore size distribution under continuous water curing.

mix A shows the lowest pore volume at a value of 0.0397 ml/g. The addition of silica fume does not affect the total intrusion volume as much as slag, the corresponding values for mixes B, C and D being 0.0419, 0.0442 and 0.0464 ml/g respectively.

It is very interesting to see that mix A specimens subjected 3 day wet/air curing and 7 day wet/air curing shows small reduction in intruded pore volume when compared to that in air curing regime; these values are 0.0385 and 0.0375 ml/g, respectively, while mixes C and D show values smaller than those for mix A i.e., 0.0322 and 0.0282 ml/g, for mix C, the reduction of total intrusion volume compared to the corresponding values of mix A being 16% and 25%, respectively. The values obtained for mix D are 0.0360 and 0.0309 ml/g with reduction of 6% and 18% respectively. With further increase in slag content, mix E, does not decrease the total intrusion volume, the corresponding values obtained for mix E being 0.0371 and 0.0361 ml/g respectively.

On the other hand the addition of silica fume produced little change to the values of total pore volume compared to mix A, with the exception of 7d wet/air curing. The total pore volume increased by about 6% and 16% for samples under both 3d wet/air and continuous water curing, The corresponding values are 0.0408 and 0.0283 ml/g respectively. The above finding is in agreement with published data [109].

Table 6.2 shows the coarse pore volume under the four curing regimes for all the mixes. Fig. 6.13 shows the coarse pore volume against curing regime for all the mixes. It is interesting to see that coarse pores for mix E and mix D are 0.0250 and 0.0220 ml/g for specimens cured in air, which are almost twice the value for mix A of 0.0120 ml/g. These values drop to 0.0100 and 0.0095 ml/g for specimens under 3d wet/air, where as the corresponding value of mix A is similar to these values, which is 0.0100 ml/g.

Under 7d wet/air curing regime, the addition of about 24% of slag (mix D) in concrete also improves significantly the performance of concrete as measured by the coarse pore volume when compared with mix A; any further increase in slag does not improve the coarse pores as seen in mix E.

Under continuous water curing condition, mix C shows the lowest coarse pore volume. followed by mix B, mix A, mix D and finally mix E, which yielded the highest value. The coarse pore volumes are 0.0043, 0.0045, 0.0050, 0.0053 and 0.0055 ml/g for mixes C, B, A, D and E respectively.

Table 6.4 shows the threshold diameter of the five mixes under the four curing regimes. Also, Fig. 6.14 shows threshold diameter against curing regime for all specimens at the age of 6 months. It is clear from these data that, under air curing, the threshold diameter of mixes containing slag were larger than those of the control mix. On the other hand, mixes B and C show similar values to mix A under air curing regime. Under 3d wet/air curing and 7d wet/air curing, mix C and mix D show the lowest values of the threshold diameter. Under continuous water curing, the concrete containing either SF or SF/Slag have almost the same values of threshold diameter as compared with the control mix. Table 6.4 also indicates that the threshold diameters for mix E and mix D drop from 0.400 and 0.300 μm under air curing to 0.030 and 0.022 under continuous water curing regime respectively. The corresponding values of the control mix dropped only from 0.140 to 0.030 μm under air curing and continuous wet curing respectively.

Table 6.4 shows the continuous pore diameter of the five mixes under the four curing regimes. Also, Fig. 6.15 shows the continuous pore diameter against curing regime at 6 months of age. Under air curing mix D specimens reached the highest value of continuous pore diameter, namely, 0.085 μm, the corresponding value of mix A was 0.070 μm. Under 3d wet/air and 7d wet/air curing mix A obtained the highest values of continuous pore diameter, namely, 0.065 μm and 0.033 μm respectively, while under 3d wet/air curing, mix D obtained the lowest value of continuous pore diameter, followed by mix C, E and B the values for which are 0.018, 0.023, 0.025 and 0.030 μm respectively. Under continuous wet curing, specimens for mix A show the highest value of continuous pore diameter, which is 0.020 μm; on the other hand specimens for mix B obtained the lowest continuous pore diameter which is 0.011 μm, with a reduction of 45% compared to mix A, the corresponding values for mixes D, E, and C being 0.014, 0.016 and 0.018 μm respectively.

From the above results it can be clearly seen that the inclusion of silica fume or SF/slag caused either pore refinement or transformation of coarse pores into fine pores. These observation were clear under 3d wet/air, 7d wet/air and continuous wet curing. on the other hand mixes containing slag and exposed to air curing regime, the pores become coarser which emphasizes the importance of good curing for mixes containing slag.

Many studies [2,12,155] show that in the long term, pore volume and pore size distribution of concretes containing slag decrease sharply with increasing slag content

provided that there is adequate initial water curing required for the slag concrete to enable it to develop superior microstructure and durability-related characteristics. Roy and Parker [2] reported that MIP measurements on the pore size distribution of 60:40 slag:OPC showed similar total porosity to OPC, but whereas that the slag cement had significantly lower critical pore radius from 0.0125 μm to 0.0035 μm as compared with the OPC mix.

Pigeon and Regourd [155] found similar results when they used two levels of slag replacement, namely, 28% and 60%. They found that the total porosity was similar, but there were significant differences in pore size distribution. Pores became much smaller as the percentage of slag increased, and at 66% slag content, they found that most of the pores were less than 0.020 μm in diameter.

Torii and Kawamura [154] reported the results of MIP measurement on OPC mortars, mortars containing 5, 10 and 15% silica fume for a period of 91 days under continuous moist curing regime. It was observed that the general distribution curves shifted to the left (to smaller pore diameter) with increasing silica fume content from 0 to 15%; that is, the fine pores increased with the replacement percentage by silica fume, although the total pore volume was almost equal to, or a little larger than the OPC mortar. Moreover; silica fume addition to the mortars resulted in an increase in pores of the range smaller than 0.040 μm and a decrease in pores of the range larger than 0.100 μm. The large increase in fine pore structure observed in the mortar containing silica fume is due really to the discontinuity of the fine pores formed in the process of pozzolanic reaction of silica fume with calcium hydroxide in the mortar [12].

Feldman [83] suggested an explanation as to the superiority of the pore structure of blended cements. He concluded from his study that the nature of the pore structure appears to be related to the calcium hydroxide content. He said that, calcium hydroxide produces an inhomogeneous body with pore bonding between the major components. Therefore, blended cements are superior in terms of durability due to reduction in the amount of continuous pores and calcium hydroxide content.

6.3.3 Effect of exposure time

A comparison of the cumulative intrusion volume against pore diameter for all the mixes in the indoor environment under the four curing regime at 6 months and 18 months and the corresponding log differential intrusion volume against pore diameter of the same samples are given in Figs. 6.2- 6.11 and Figs. 6.20-6.29. Further, a

comparison of the cumulative intrusion volume against pore diameter for all the mixes in the indoor environment at 6 months and 18 months is shown in Figs. 6.16-6.19 Figs. 6.30-6.33, while Fig. 6.34-(a-d) shows the total intrusion volume for the different mixes and for different curing regimes at 6 months and 18 months. In general, little effect of age on the total intrusion volume is seen for the air cured samples, 3d wet/air, and the 7d wet/air curing, although there is a definite visible improvement in pore structure with even limited water curing. The total intrusion pore volume for continuous water cured samples decreased when comparing exposure periods of 18 months and 6 months. The maximum effect is seen for mix E.

The total intrusion pore volume decreased by 22% (from 0.0281 for specimens at the age of 6 months to 0.0220 ml/g for specimens at the age 18 months). However, the other mixes also showed similar trends, but with less reduction, the corresponding reduction in total intrusion pore volume of mixes A, B, C and D being 14%, 8%, 11.5% and 14% respectively.

Mix E (323 OPC +22 SF + 165 slag) shows an increase in the coarse pore volume, at the age of 18 months, of about 17% for specimens subjected to 3d wet/air curing. This might be attributed to the fact that drying of slag concrete at an early age leads to restricted hydration in the specimens, and thus to higher coarse pores in the long-term.

Specimens cured continuously in water at the age of 18 months exhibited slight decrease in coarse pores compared to the water cured specimens at the age of 6 months. The greater the slag content, the greater was the decrease in coarse pore volume; these fractions are 9.3, 17 and 23.6% for mixes C, D and E respectively, while mix A shows no significant effect of age, only about 4% development. On the other hand, mix B which shows the effect of 5.5% silica fume, with 15% development in coarse pores. which also indicates that silica fume refines the pores and develops fine pores in the long term.

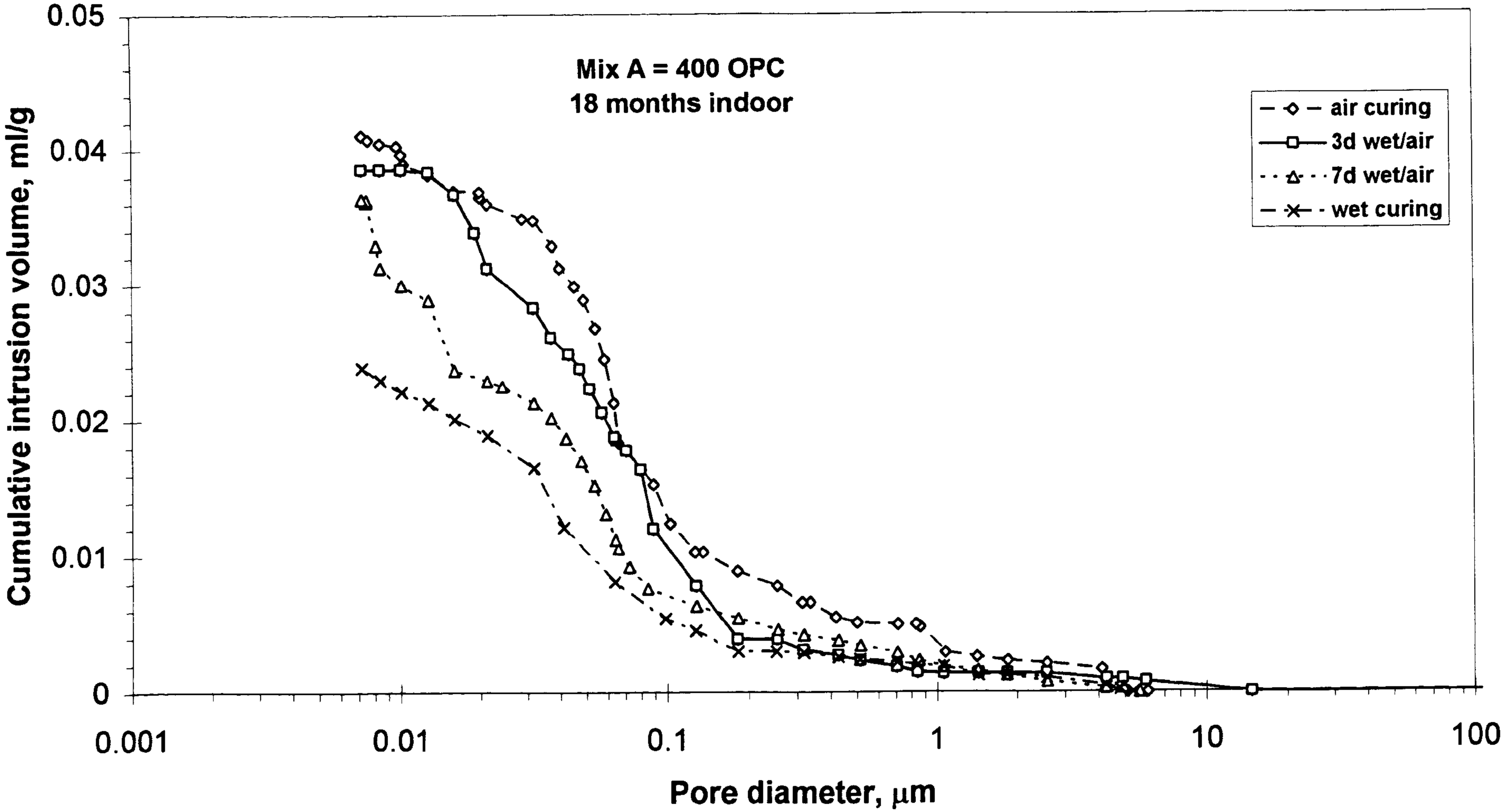

Fig. 6.20 : Influence of curing regime on pore size distribution for mix A.

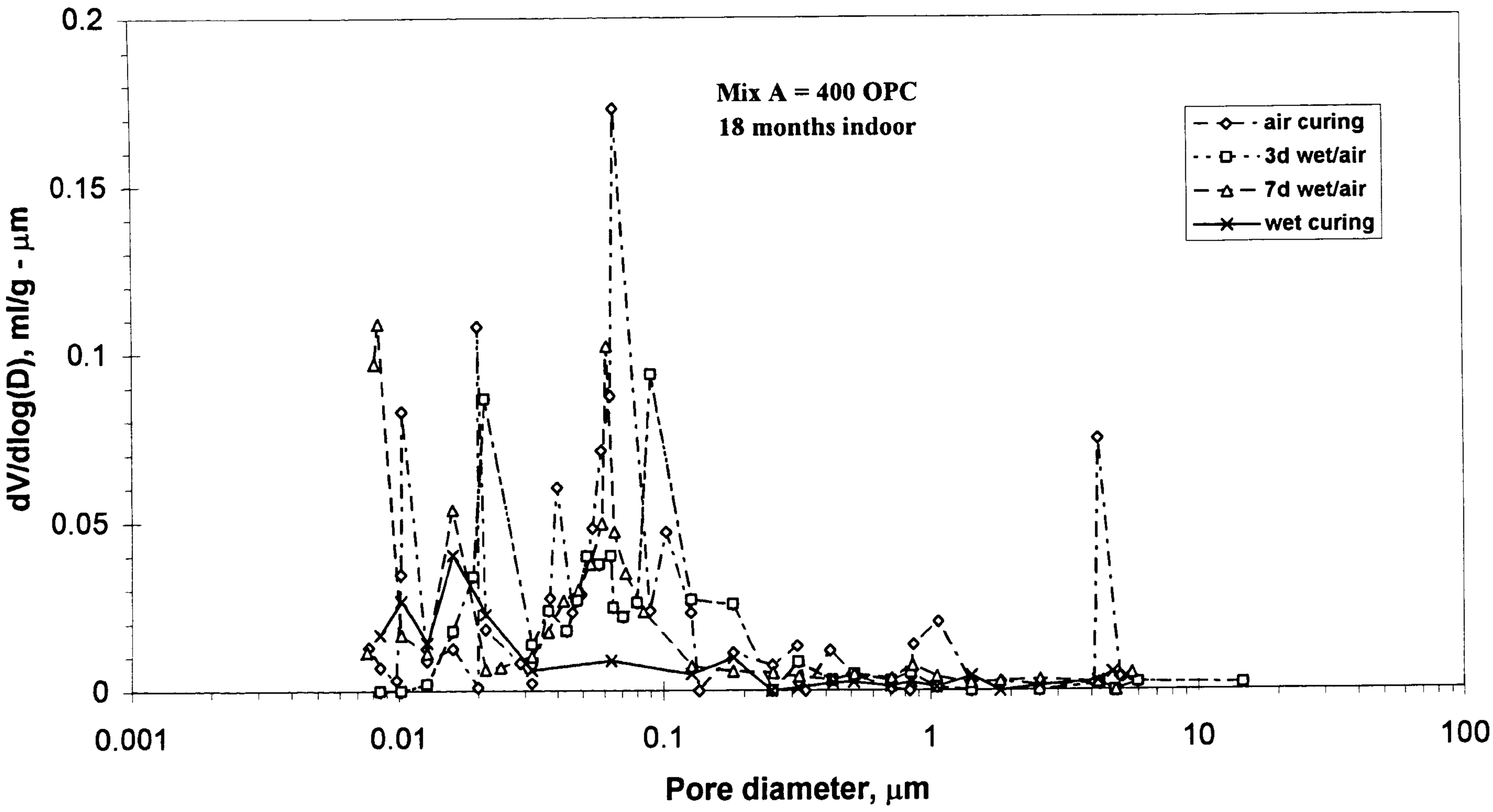

Fig. 6.21 : Differential pore size distribution for mix A.

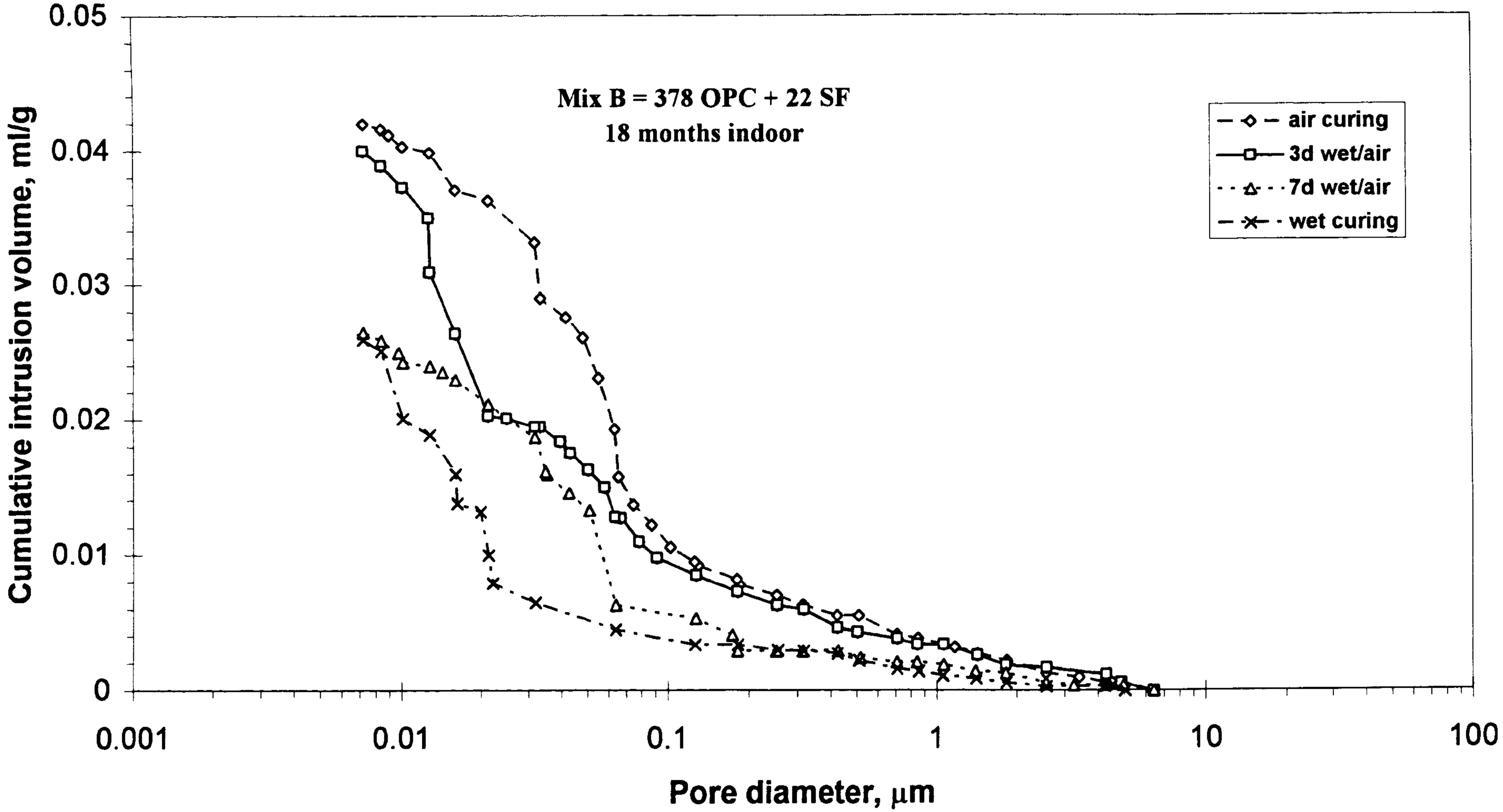

Fig. 6.22 : Influence of curing regime on pore size distribution for mix B.

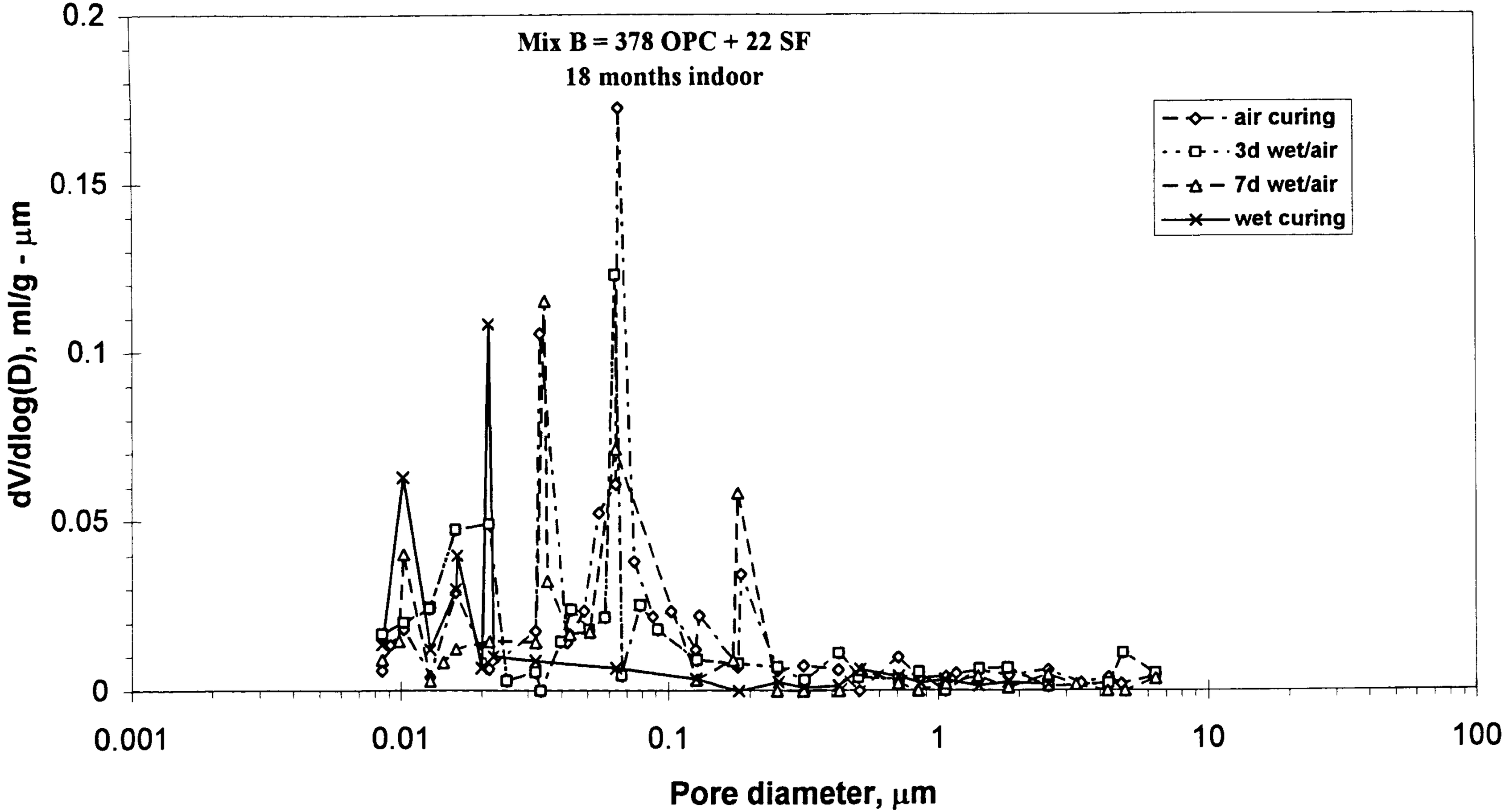

Fig. 6.23 : Differential pore size distribution for mix B.

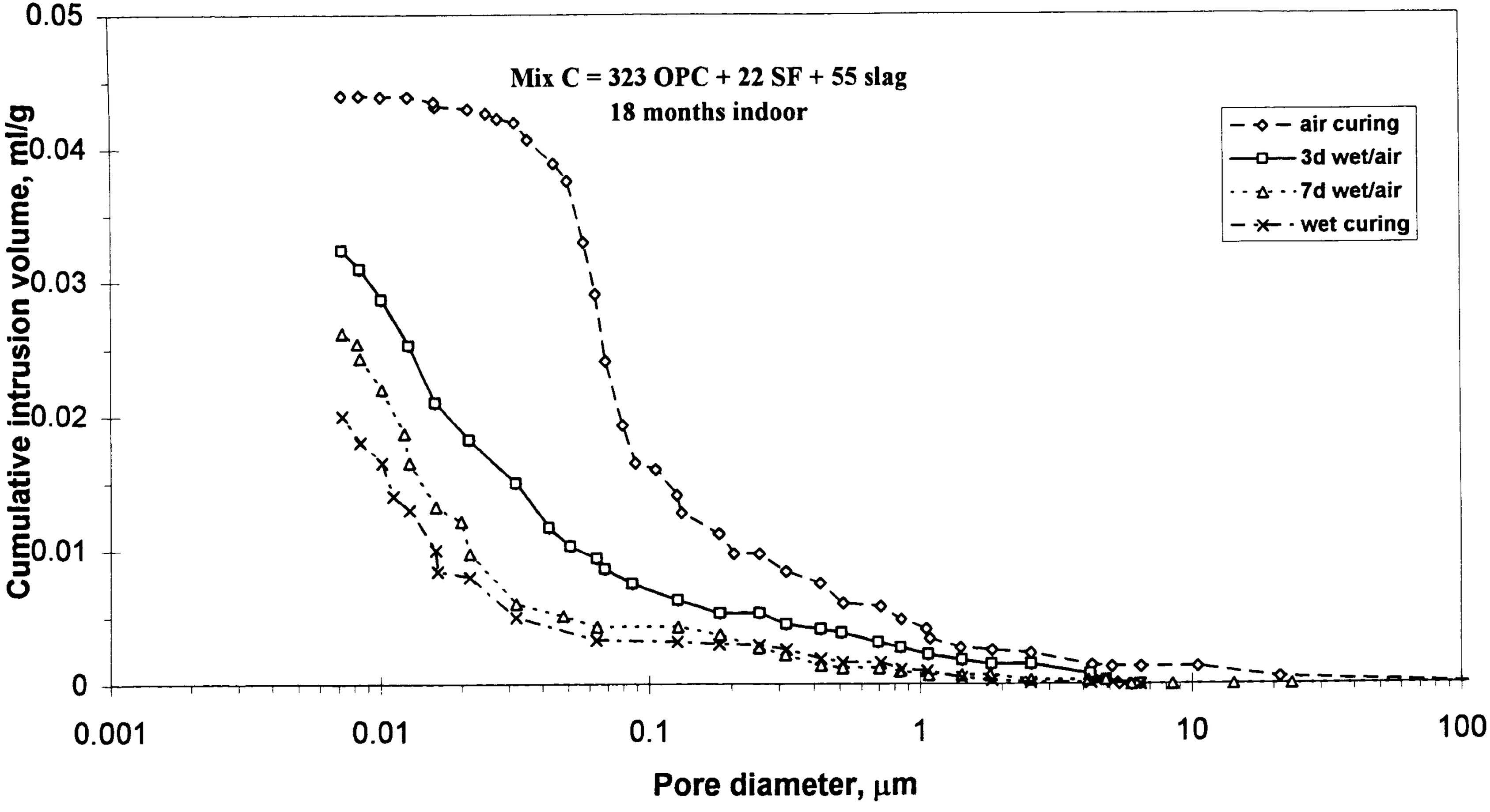

Fig. 6.24 : Influence of curing regime on pore size distribution for mix C.

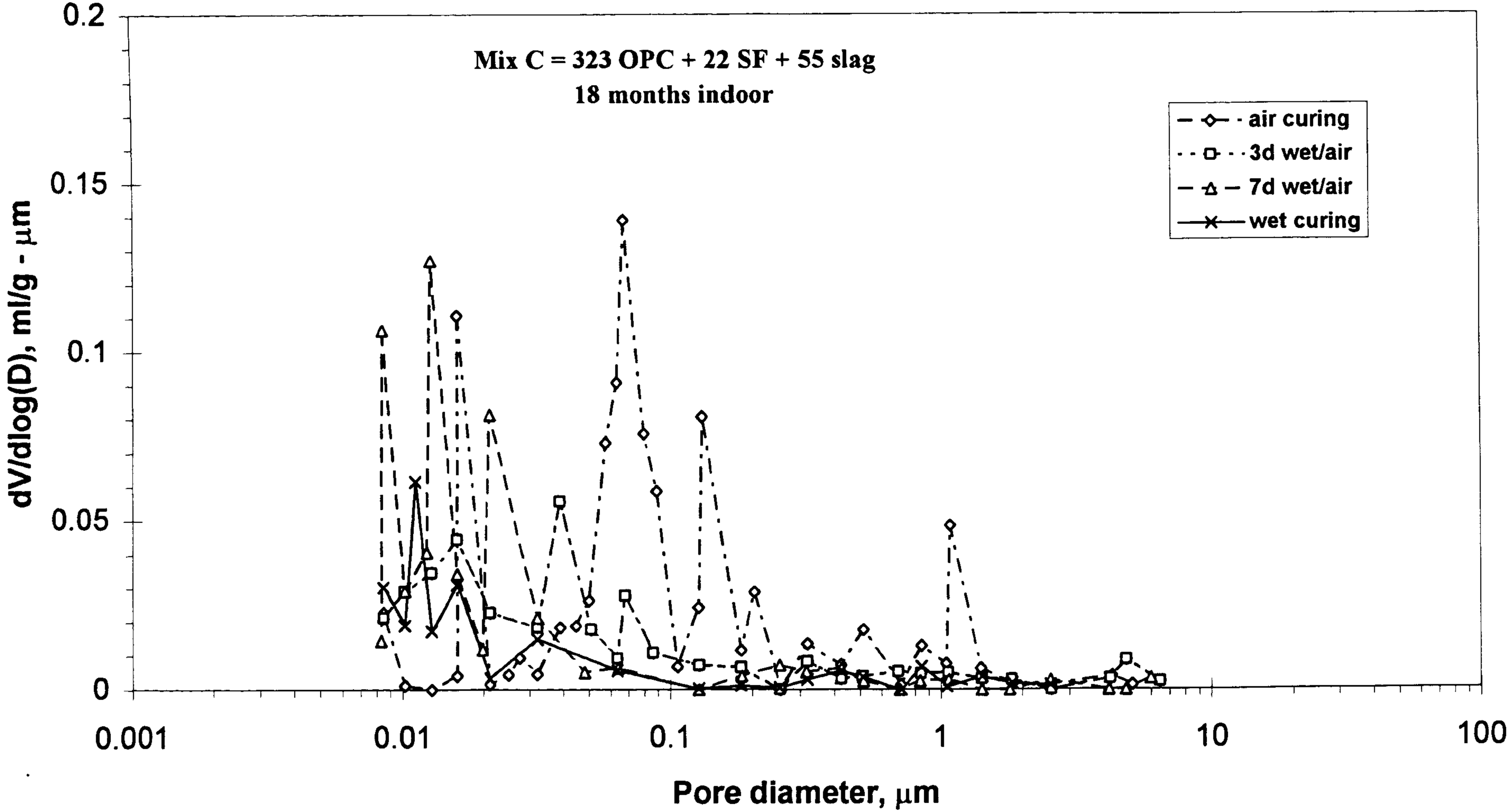

Fig. 6.25 : Differential pore size distribution for mix C.

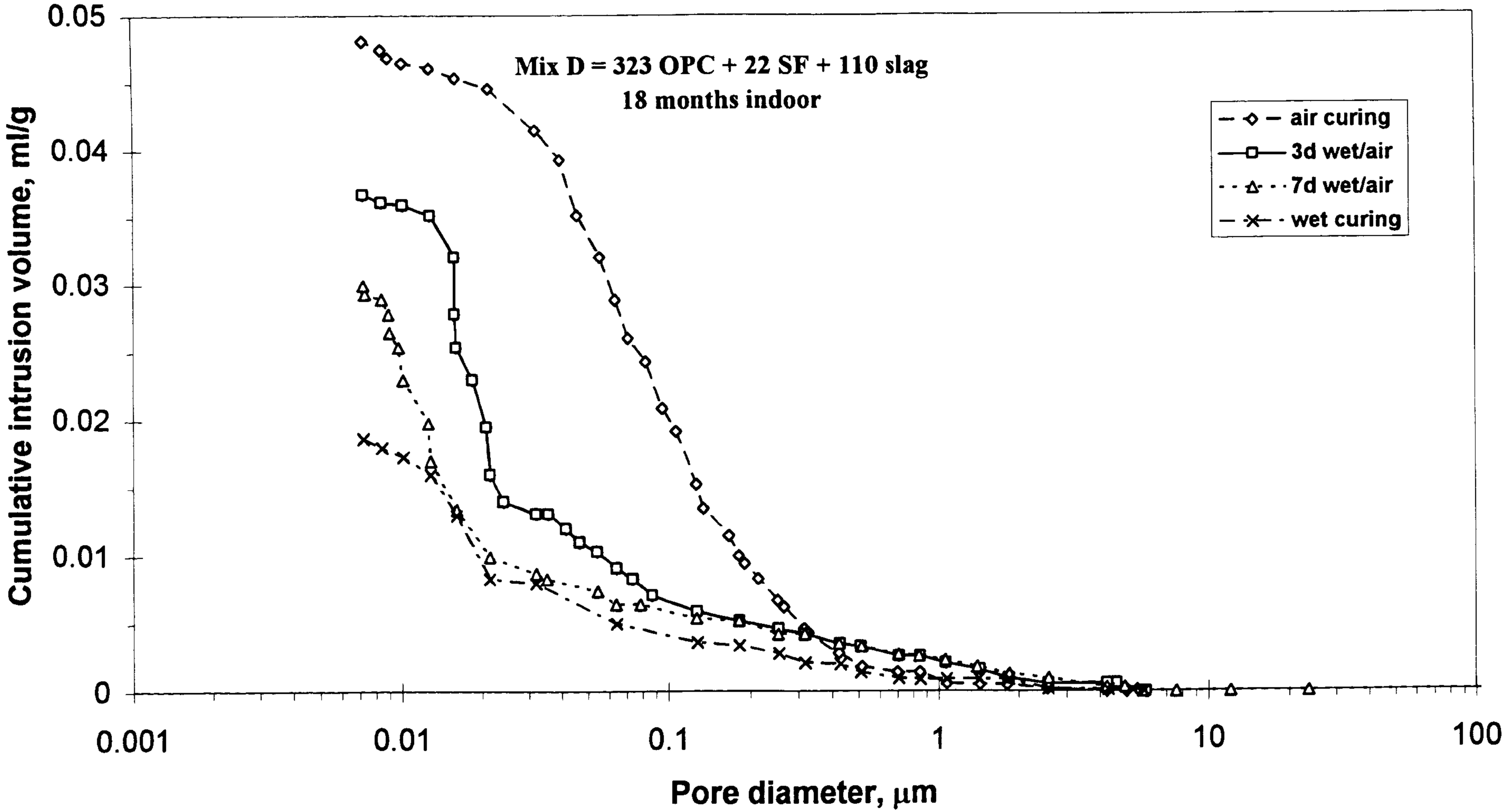

Fig. 6.26 : Influence of curing regime on pore size distribution for mix D.

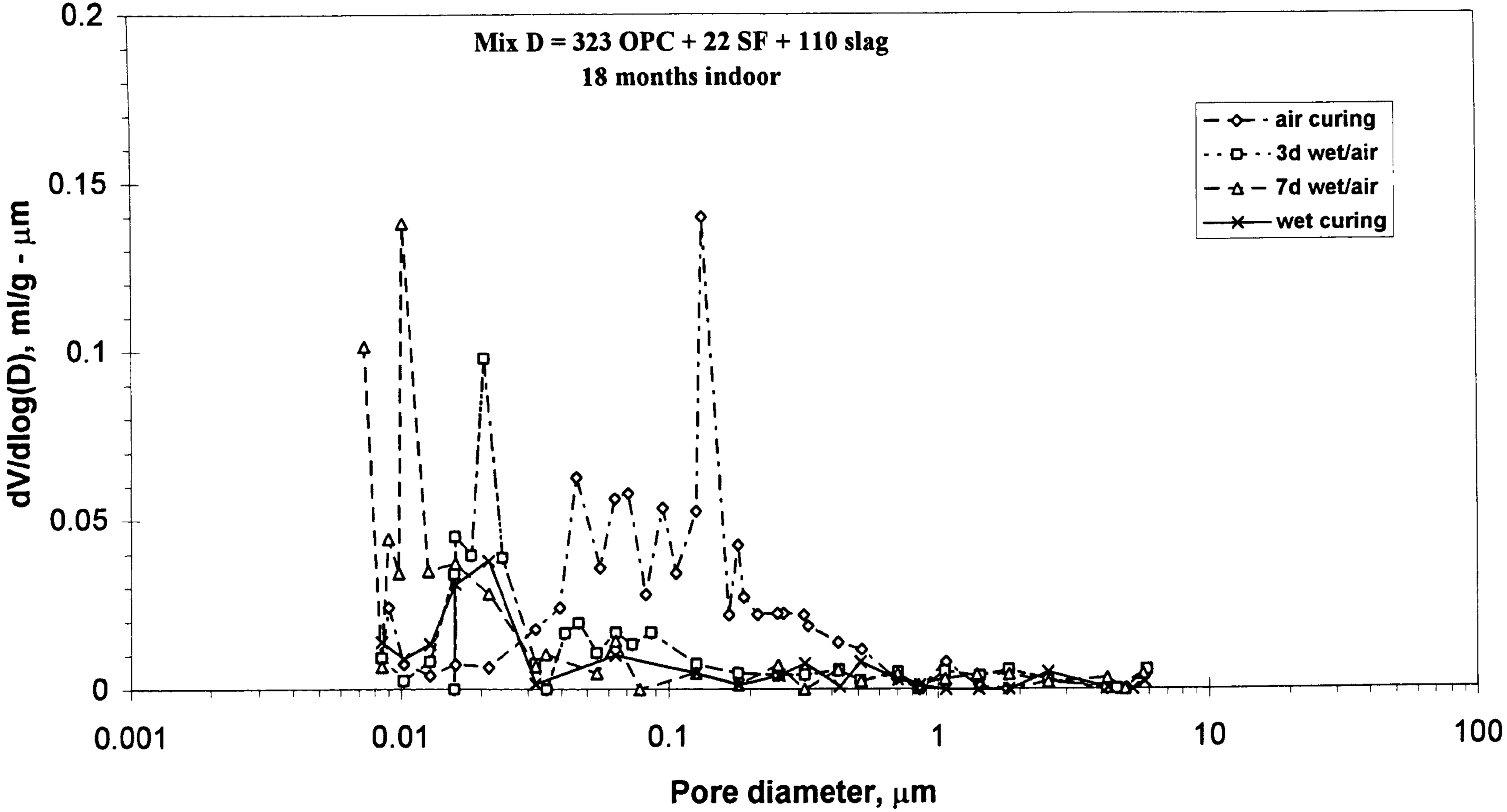

Fig. 6.27 : Differential pore size distribution for mix D.

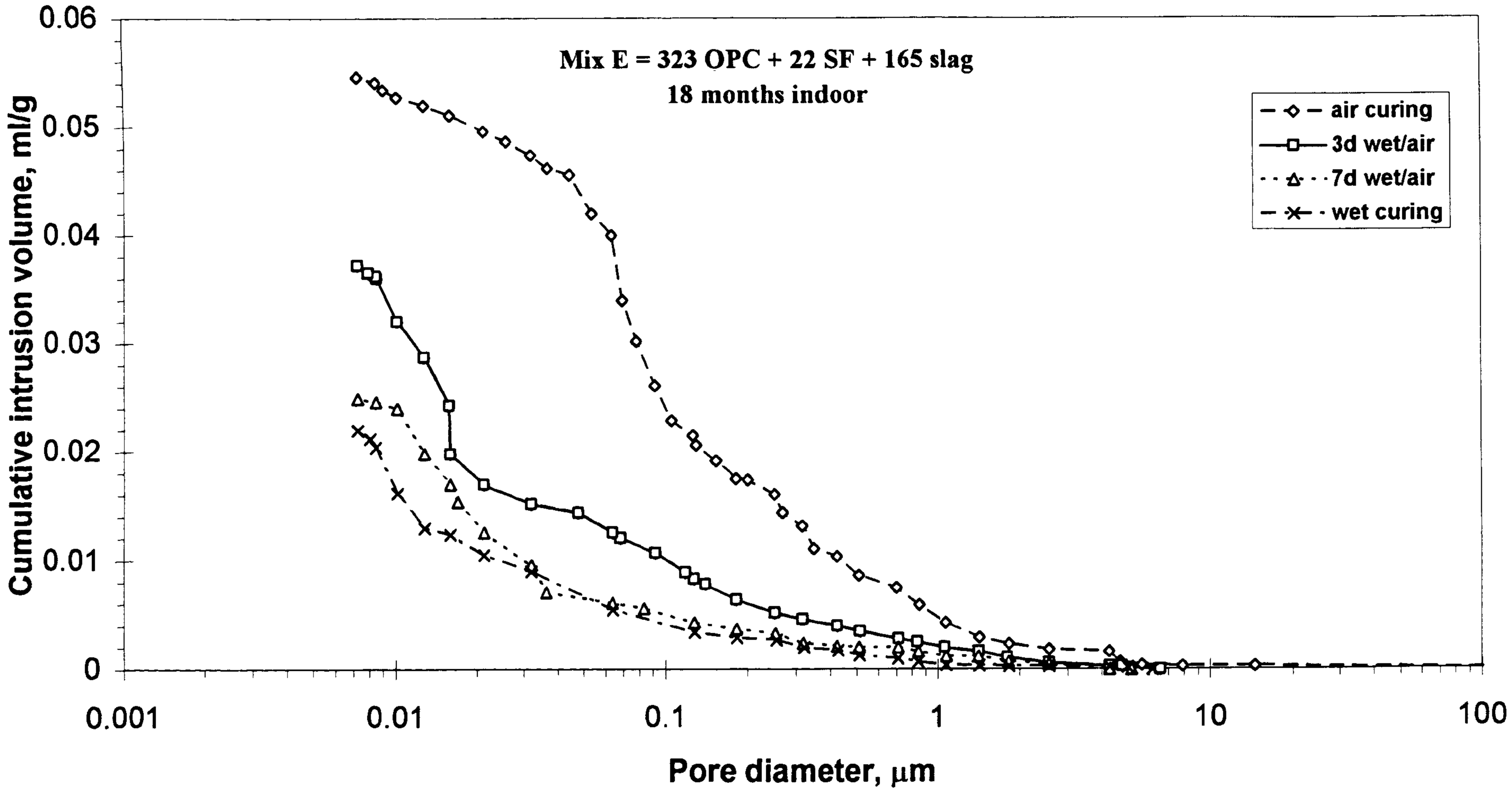

Fig. 6.28 : Influence of curing regime on pore size distribution for mix E.

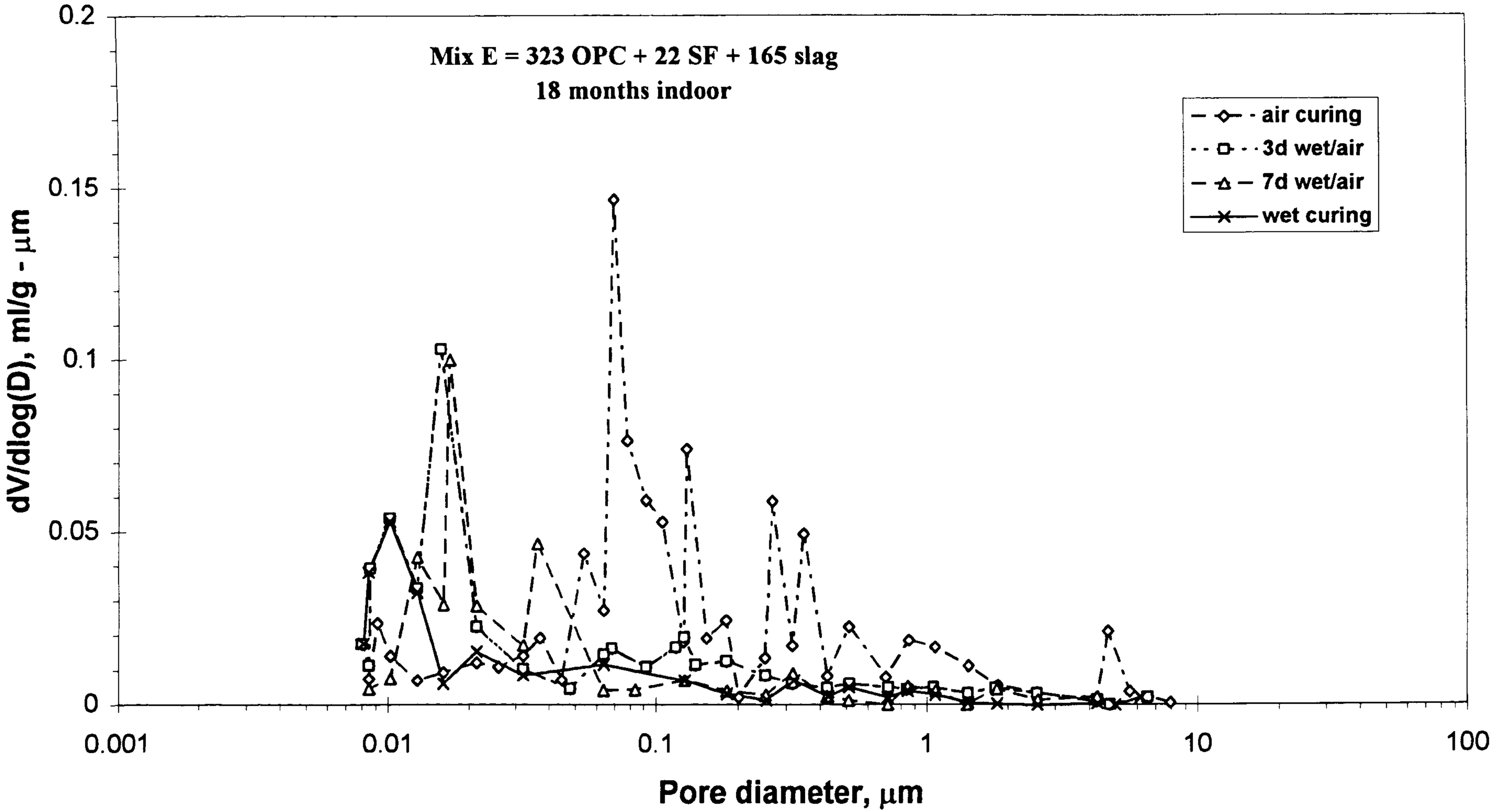

Fig. 6.29 : Differential pore size distribution for mix E.

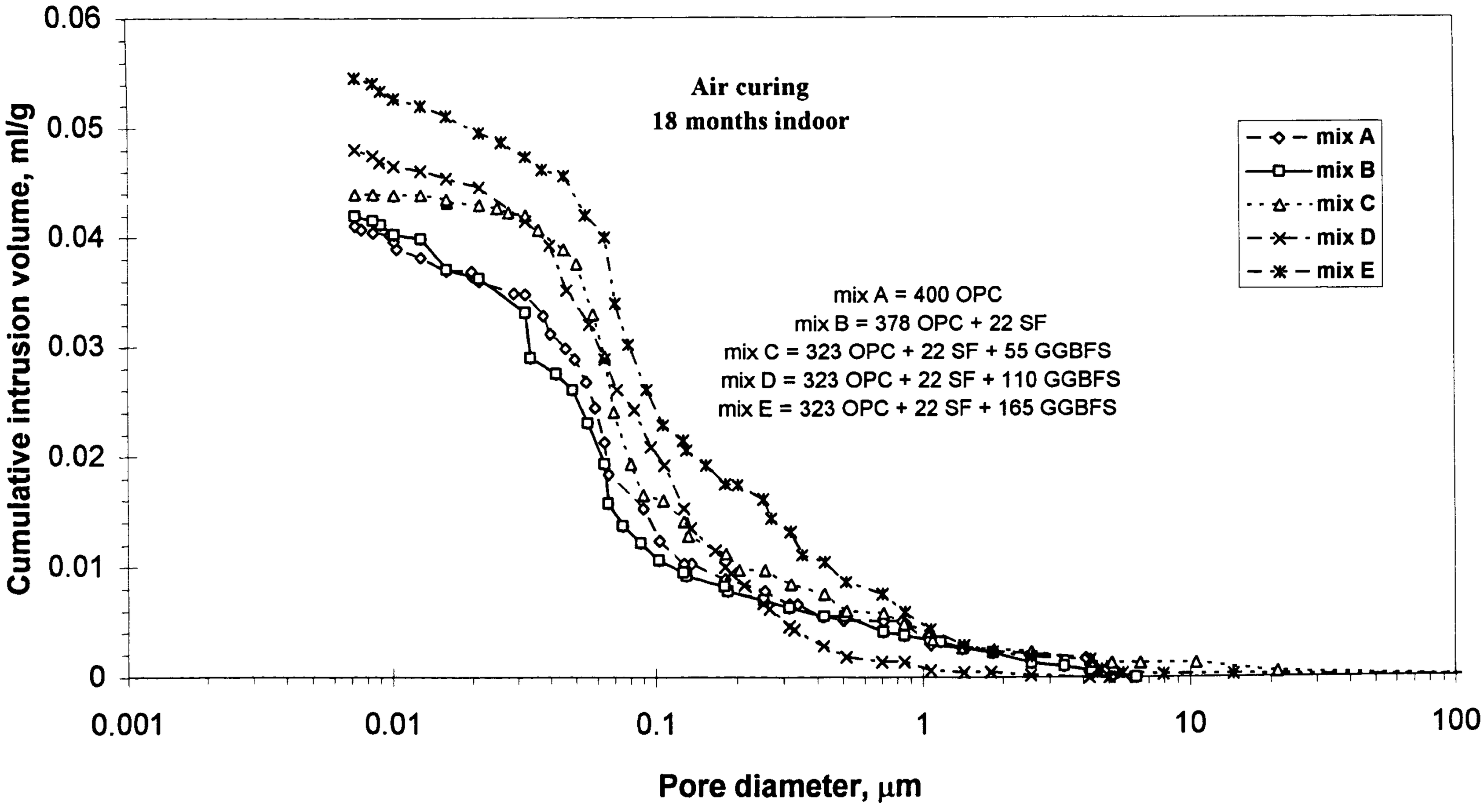

Fig. 6.30 : Influence of mix type on pore size distribution under air curing.

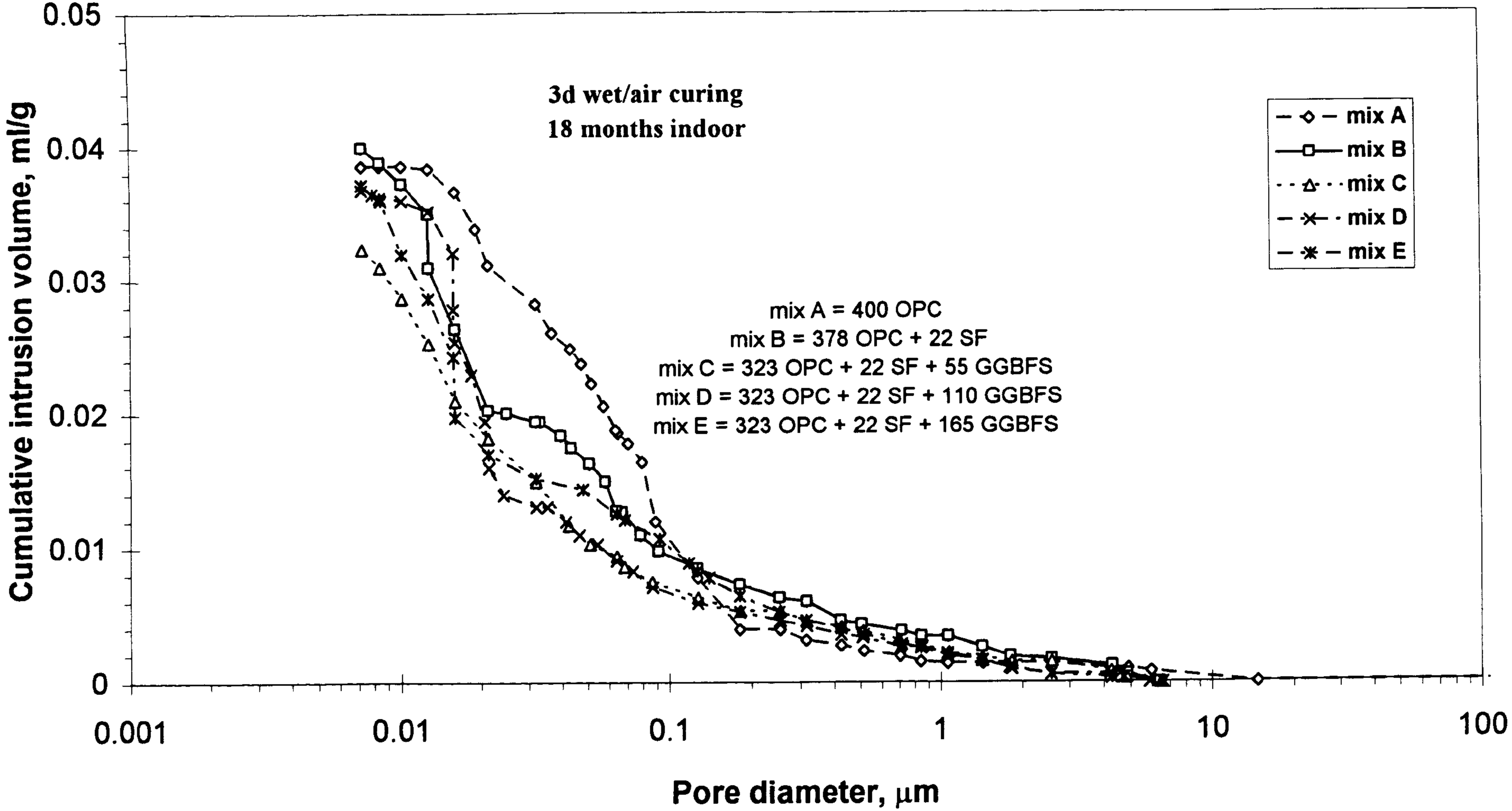

Fig. 6.31 : Influence of mix type on pore size distribution under 3d wet/air curing.

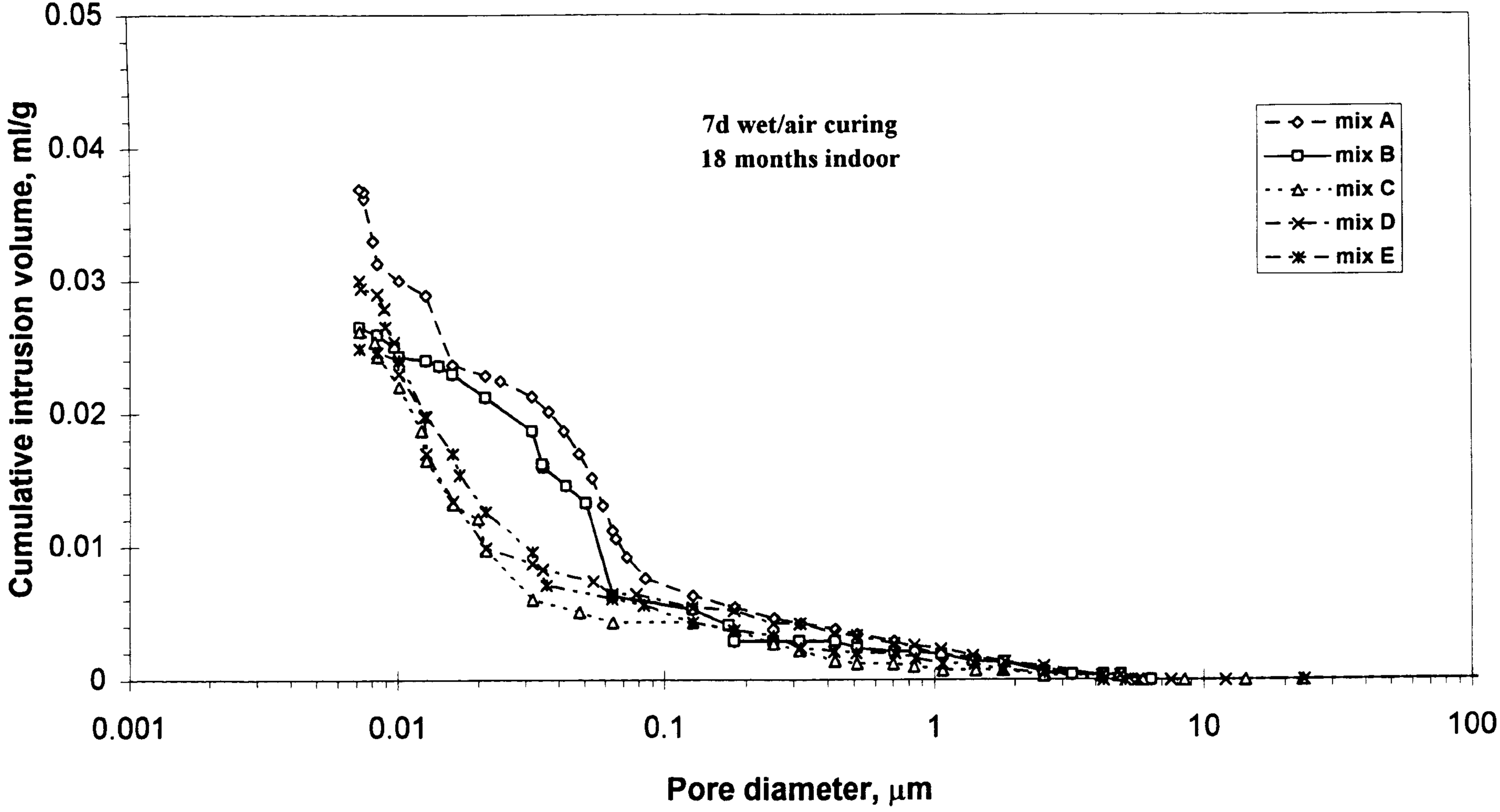

Fig. 6.32 : Influence of mix type on pore size distribution under 7d wet/air curing.

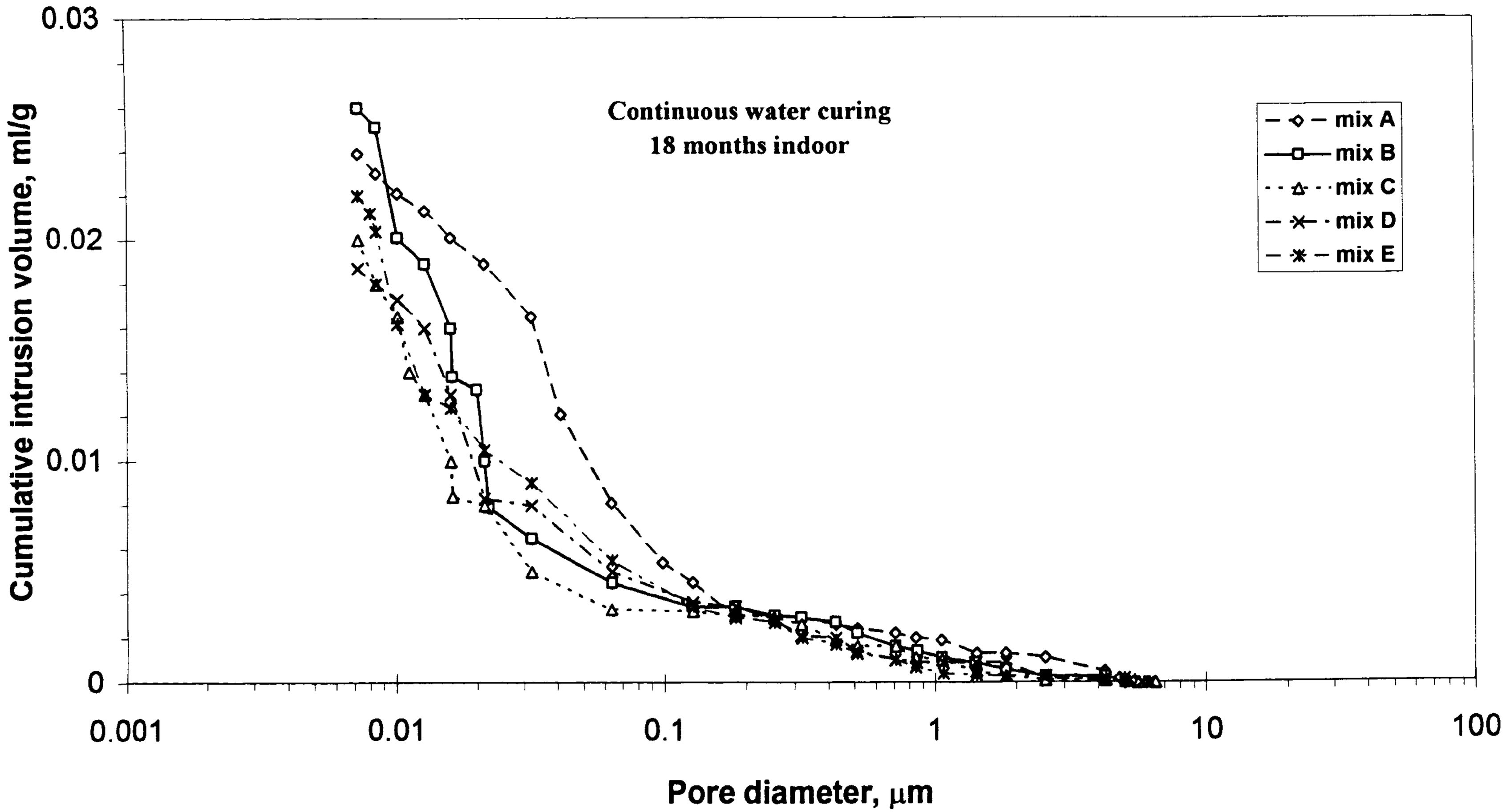

Fig. 6.33 : Influence of mix type on pore size distribution under continuous water curing.

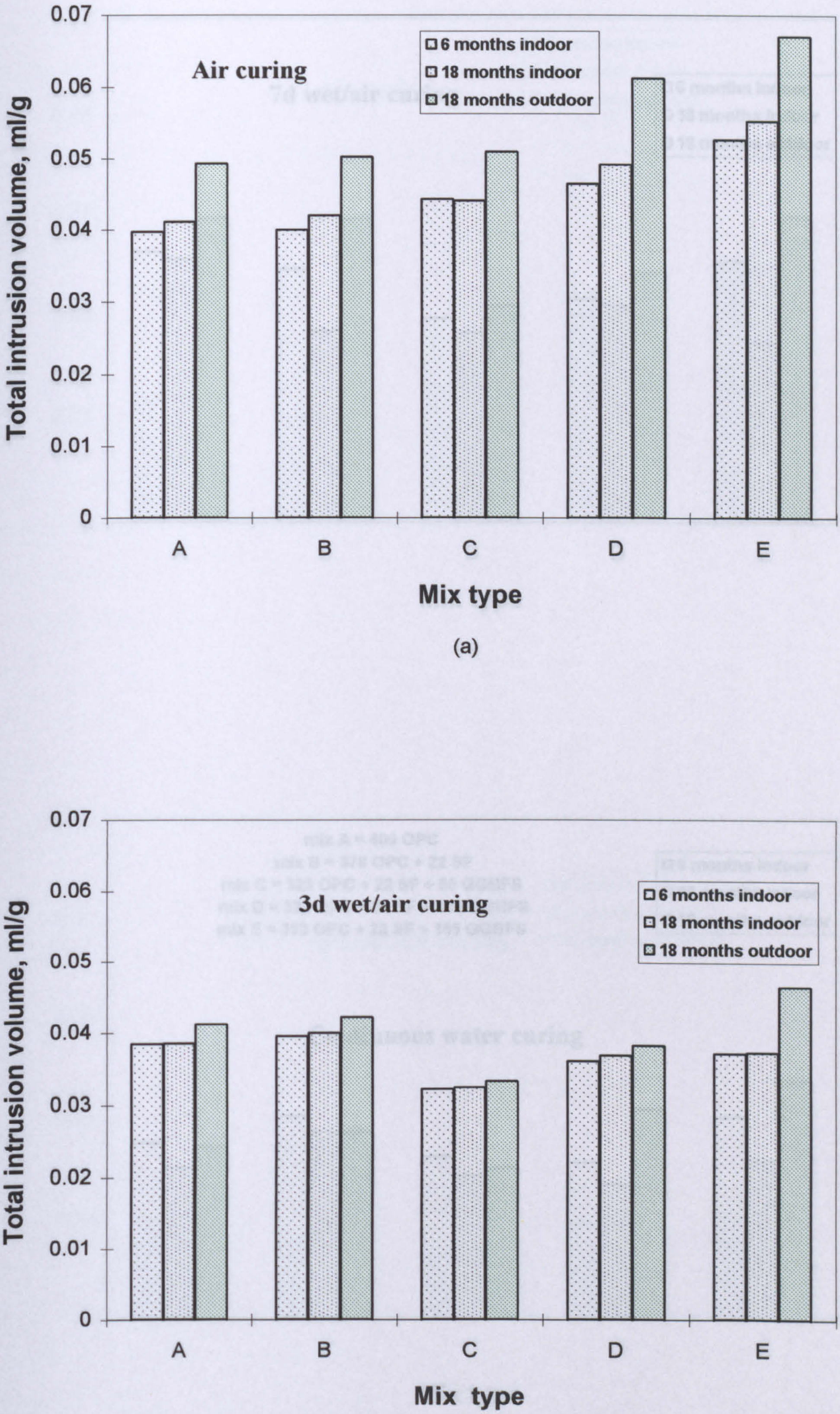

Fig. 6.34: Influence of specimens age and exposure environment on total intrusion volume.

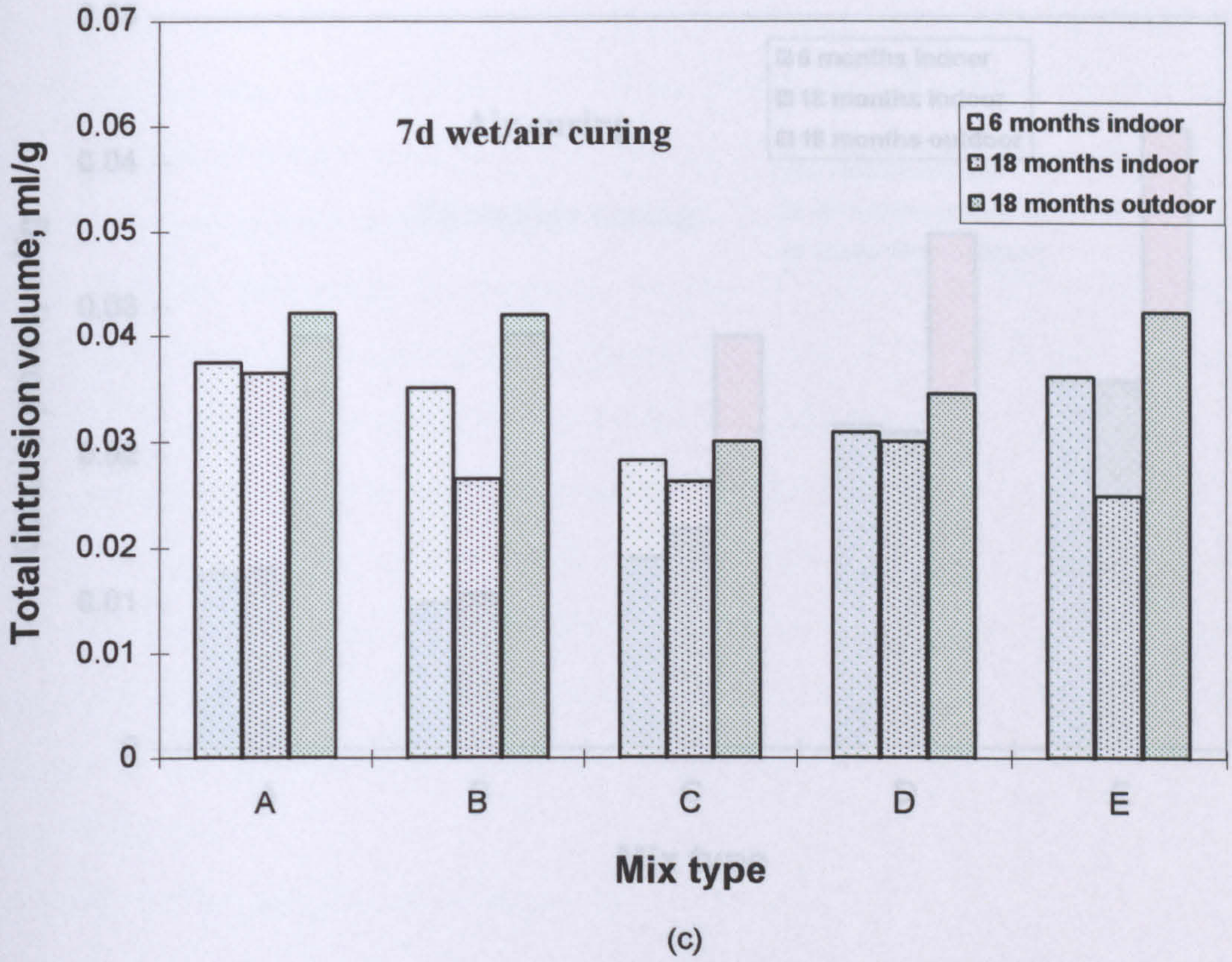

(c)

(d)

Fig. 6.34: Influence of specimens age and exposure environment on total intrusion volume.

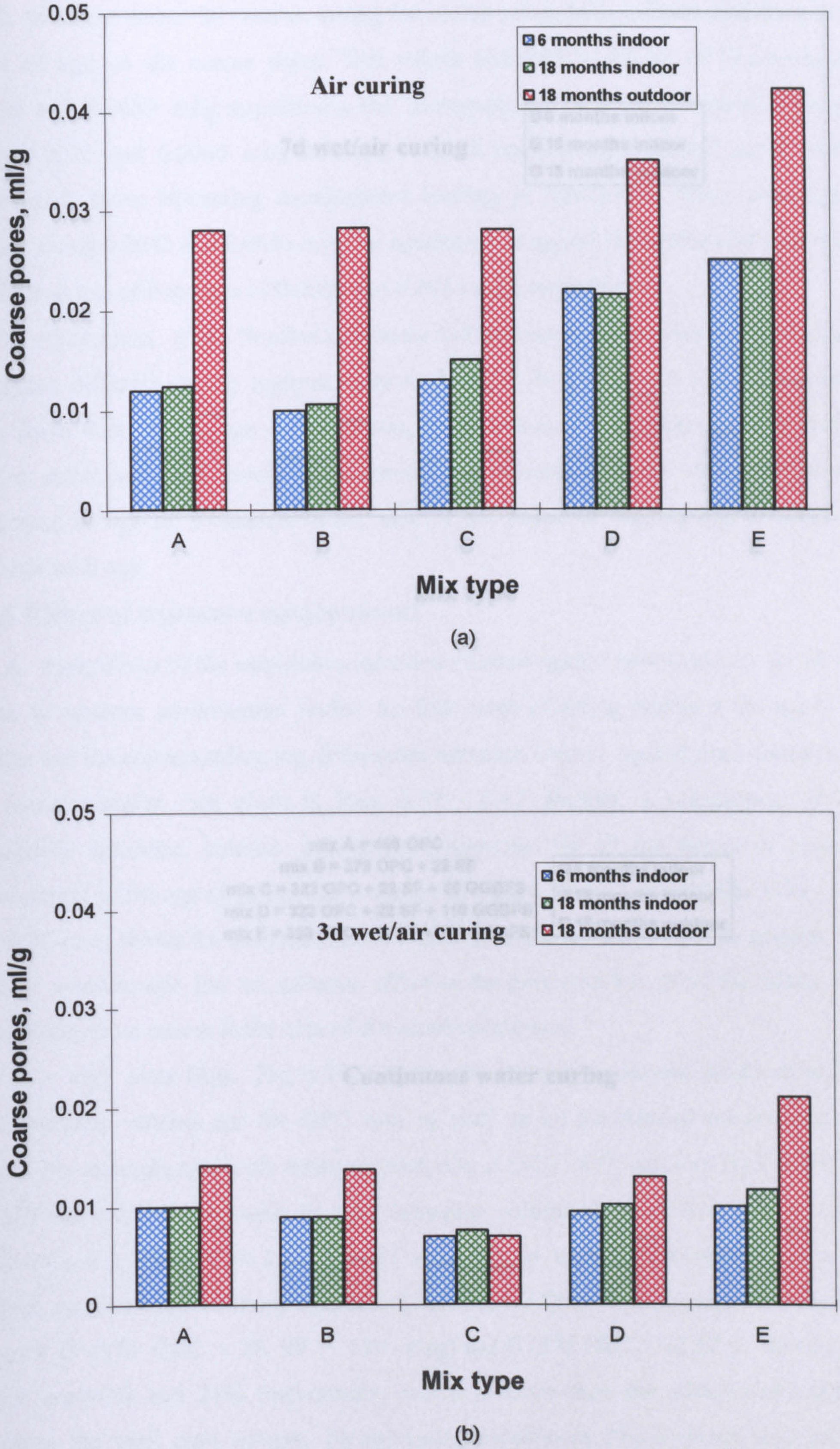

Fig. 6.35 : Influence of specimens age and exposure environment on coarse pores.

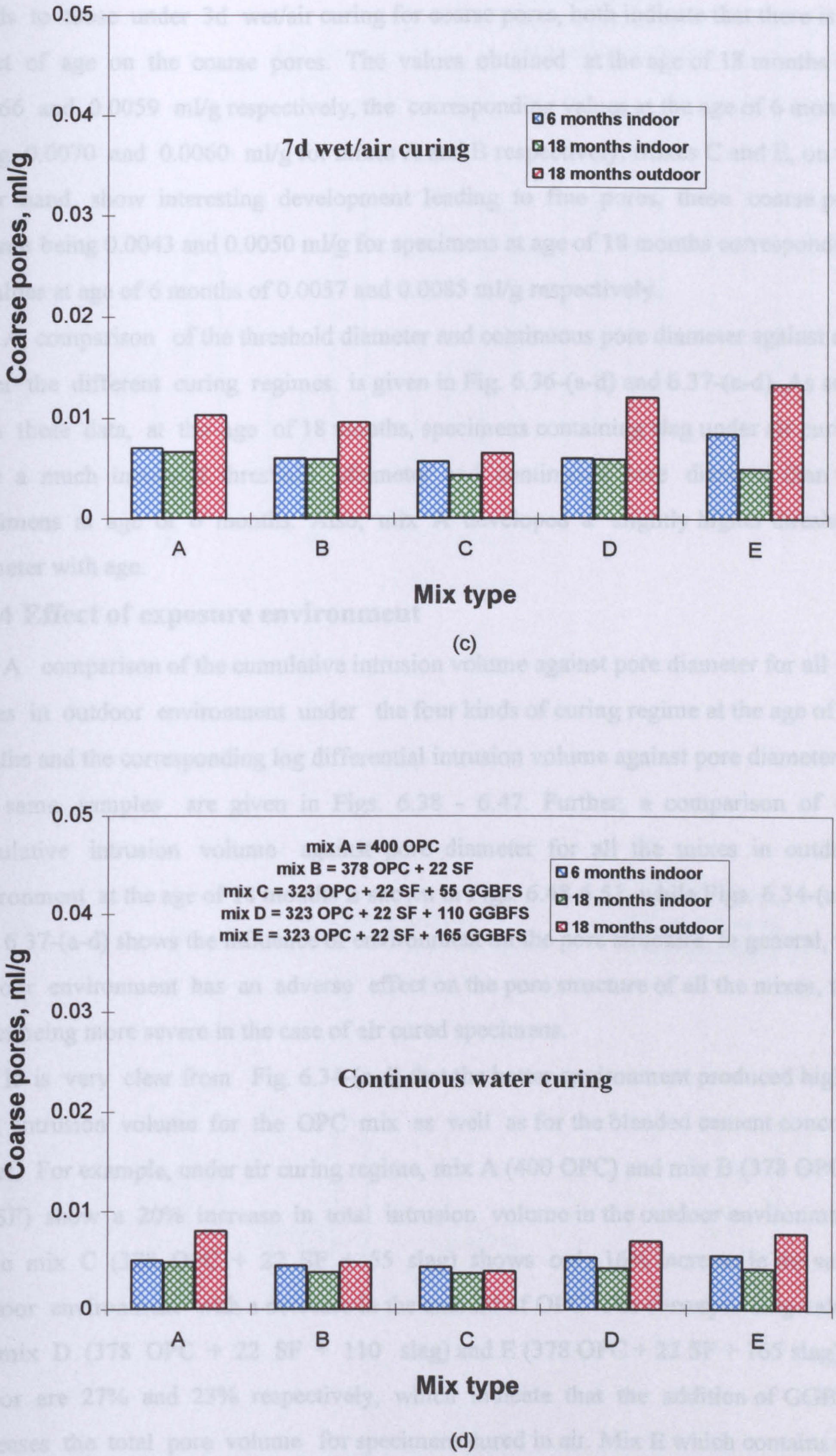

Fig. 6.35 : Influence of specimens age and exposure environment on coarse pores.

Under 7d wet/air curing regime, specimens of mix A and mix B show similar trends to those under 3d wet/air curing for coarse pores, both indicate that there is no effect of age on the coarse pores. The values obtained at the age of 18 months are 0.0066 and 0.0059 ml/g respectively, the corresponding values at the age of 6 months being 0.0070 and 0.0060 ml/g for mixes A and B respectively. Mixes C and E, on the other hand, show interesting development leading to fine pores, these coarse pore volume being 0.0043 and 0.0050 ml/g for specimens at age of 18 months corresponding to values at age of 6 months of 0.0057 and 0.0085 ml/g respectively.

A comparison of the threshold diameter and continuous pore diameter against age under the different curing regimes is given in Fig. 6.36-(a-d) and 6.37-(a-d). As seen from these data, at the age of 18 months, specimens containing slag under air curing have a much increased threshold diameter and continuous pore diameter than the specimens at age of 6 months. Also, mix A developed a slightly higher threshold diameter with age.

6.3.4 Effect of exposure environment

A comparison of the cumulative intrusion volume against pore diameter for all the mixes in outdoor environment under the four kinds of curing regime at the age of 18 months and the corresponding log differential intrusion volume against pore diameter of the same samples are given in Figs. 6.38 - 6.47. Further, a comparison of the cumulative intrusion volume against pore diameter for all the mixes in outdoor environment at the age of 18 months is shown in Figs. 6.48-6.51, while Figs. 6.34-(a-d) and 6.37-(a-d) shows the influence of environment on the pore structure. In general, the outdoor environment has an adverse effect on the pore structure of all the mixes, this effect being more severe in the case of air cured specimens.

It is very clear from Fig. 6.34-(a-d) that the hotter environment produced higher total intrusion volume for the OPC mix as well as for the blended cement concrete mixes. For example, under air curing regime, mix A (400 OPC) and mix B (378 OPC + 22 SF) show a 20% increase in total intrusion volume in the outdoor environment, while mix C (378 OPC + 22 SF + 55 slag) shows only 16% increase in the same outdoor environment with a decrease in the amount of OPC. The corresponding values for mix D (378 OPC + 22 SF + 110 slag) and E (378 OPC + 22 SF + 165 slag) at indoor are 27% and 23% respectively, which indicate that the addition of GGBFS increases the total pore volume for specimens cured in air. Mix E which contains the

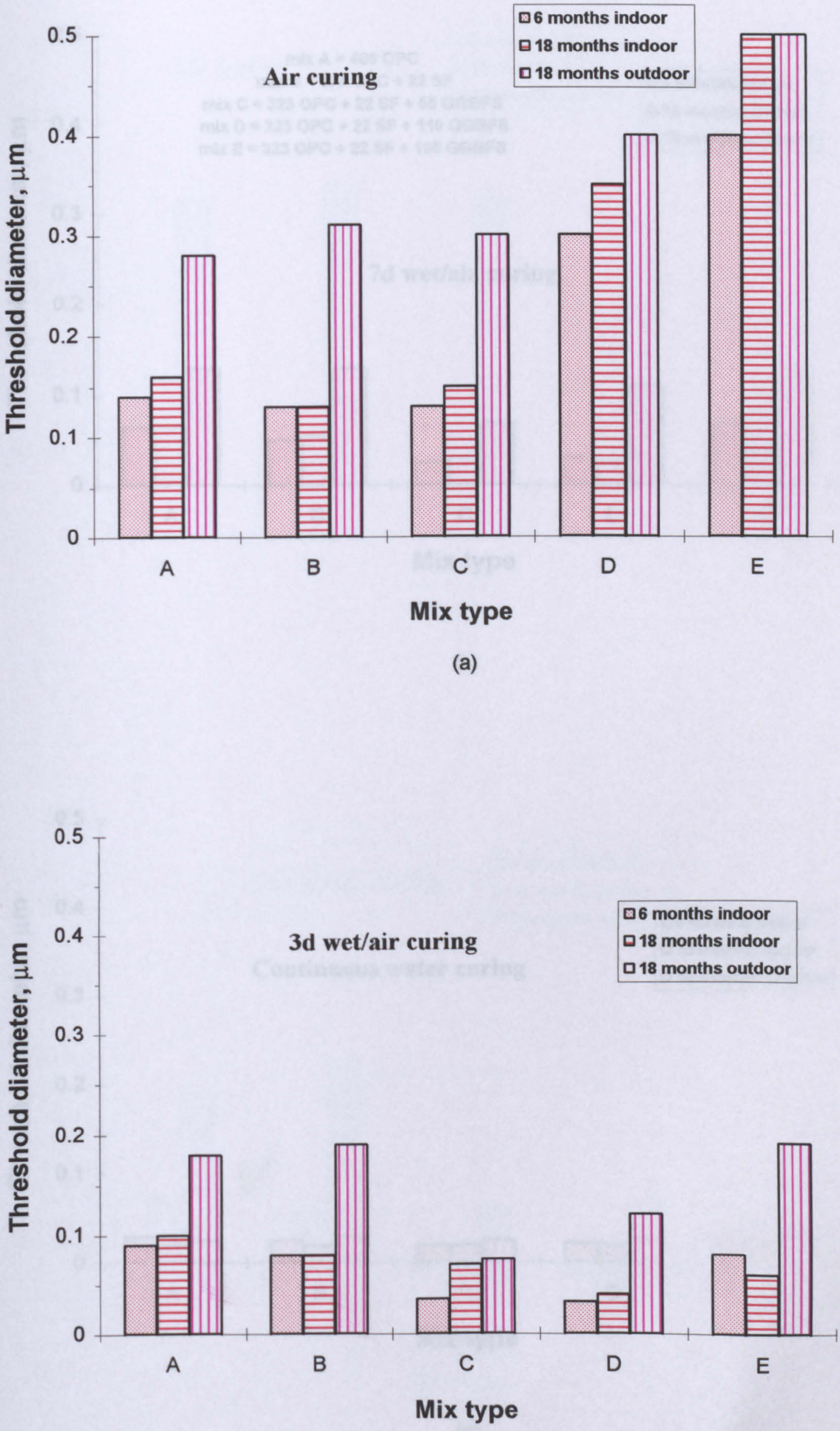

Fig. 6.36: Influence of specimens age and exposure environment on threshold diameter.

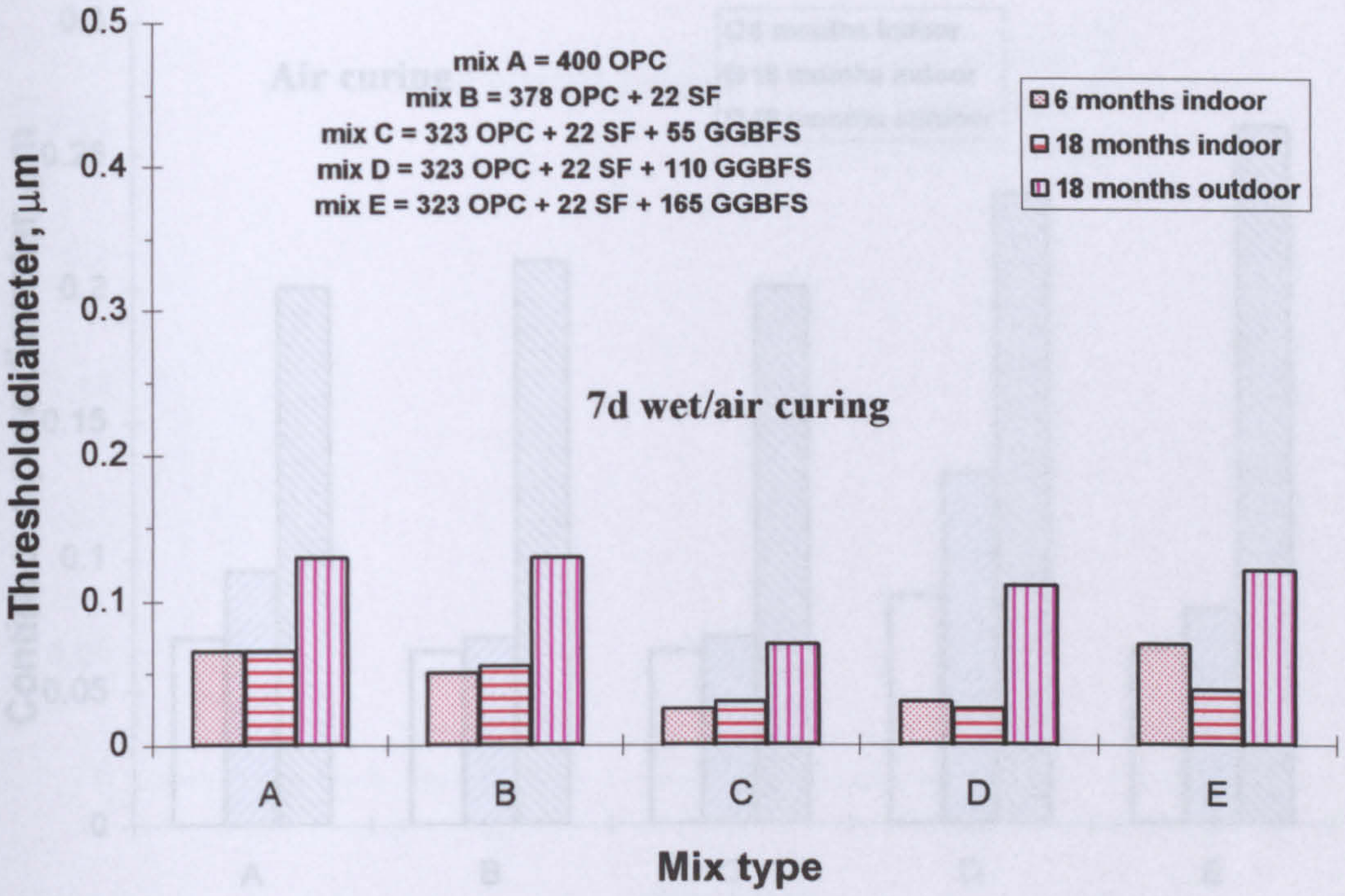

(c)

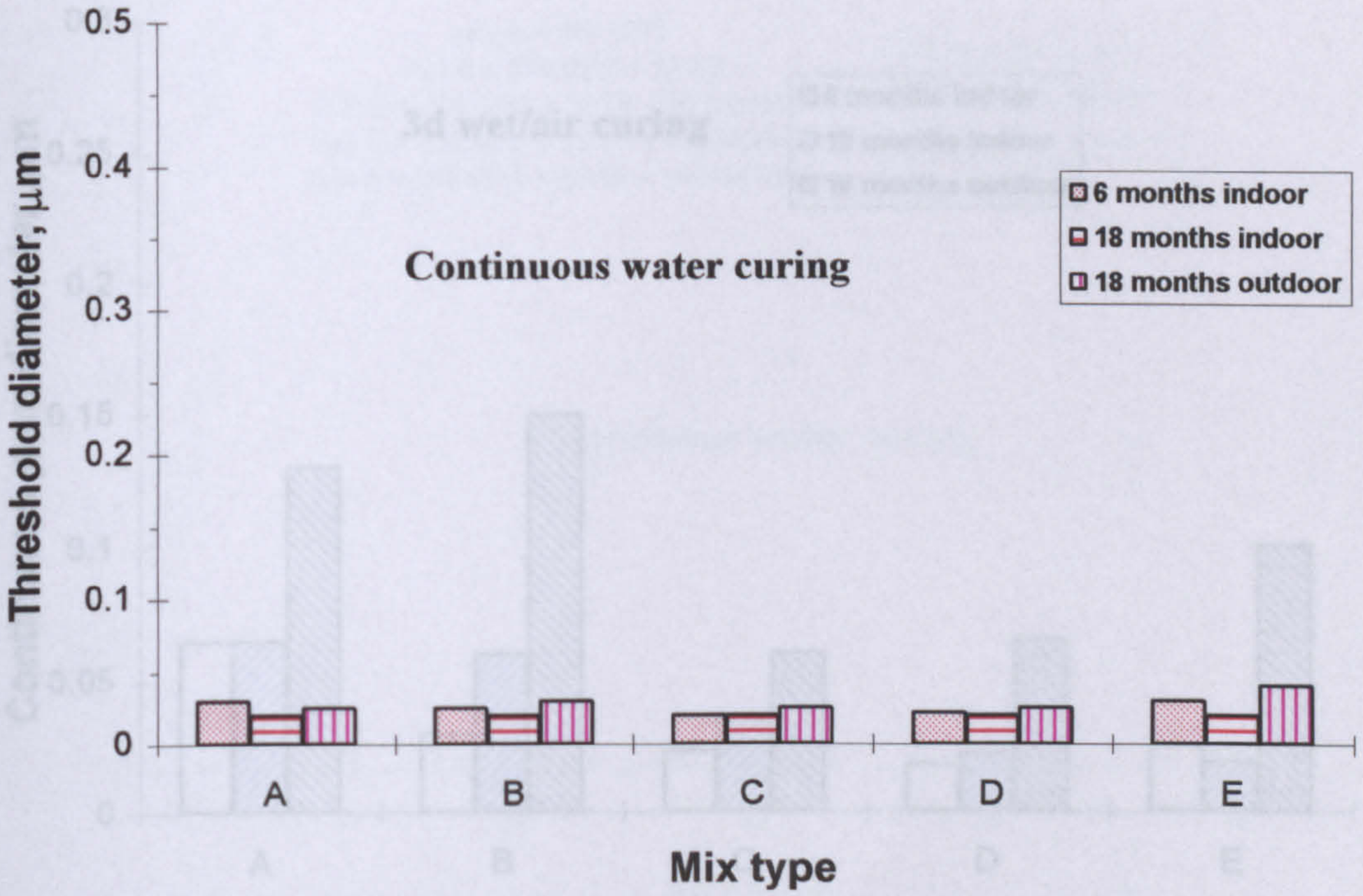

(d)

Fig. 6.36: Influence of specimens age and exposure environment on threshold diameter.

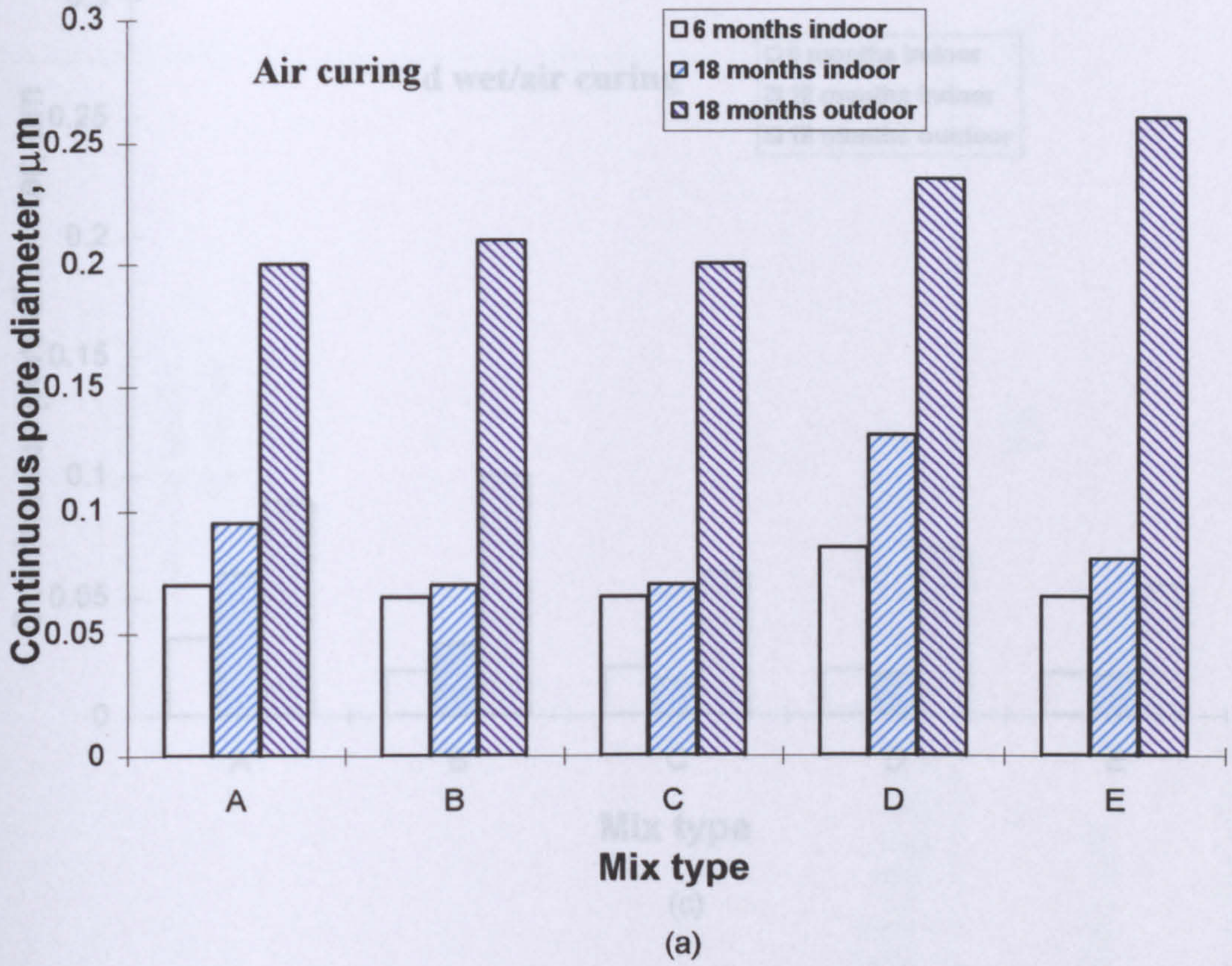

(a)

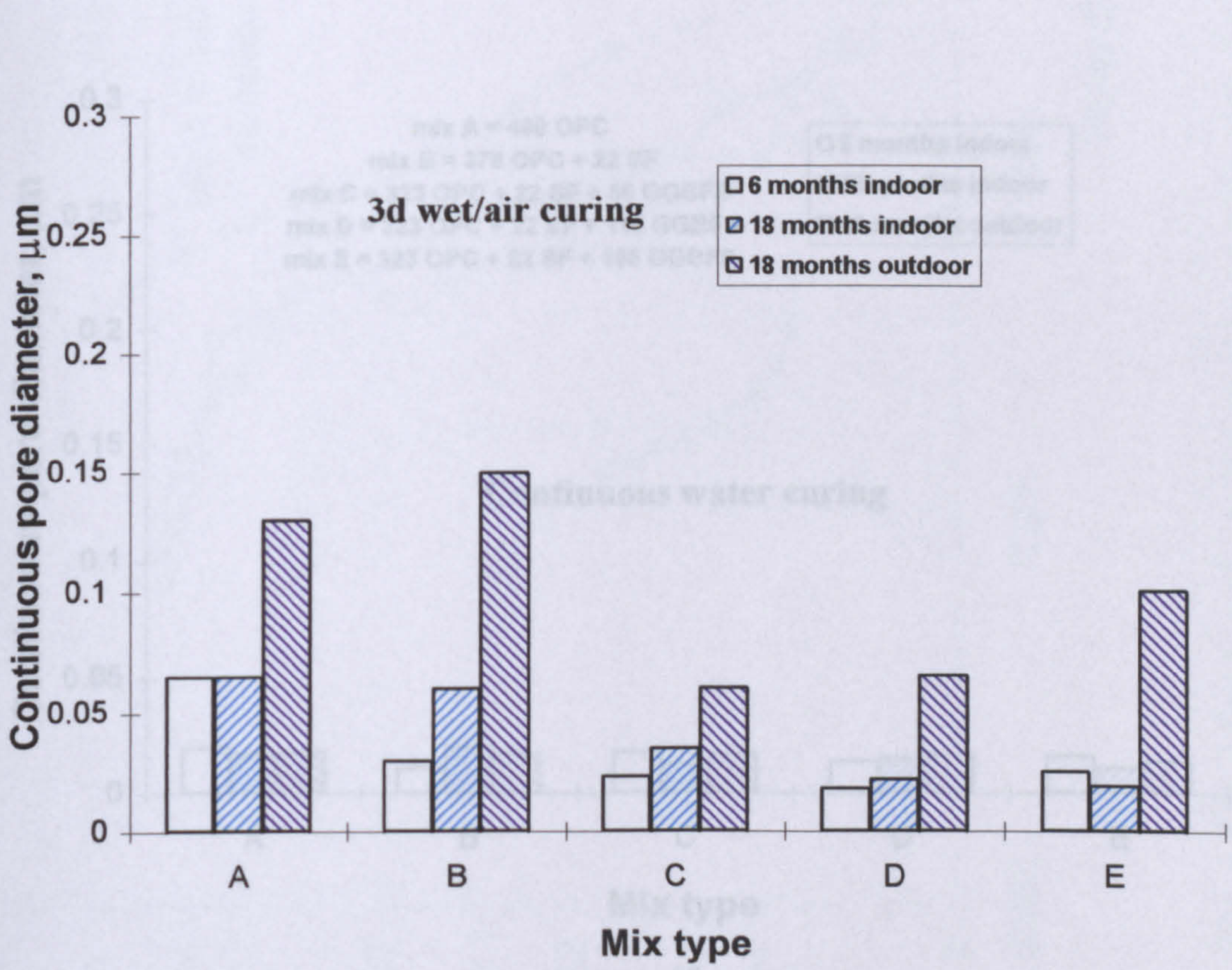

(b)

Fig. 6.37: Influence of specimens age and exposure environment on continuous pore diameter.

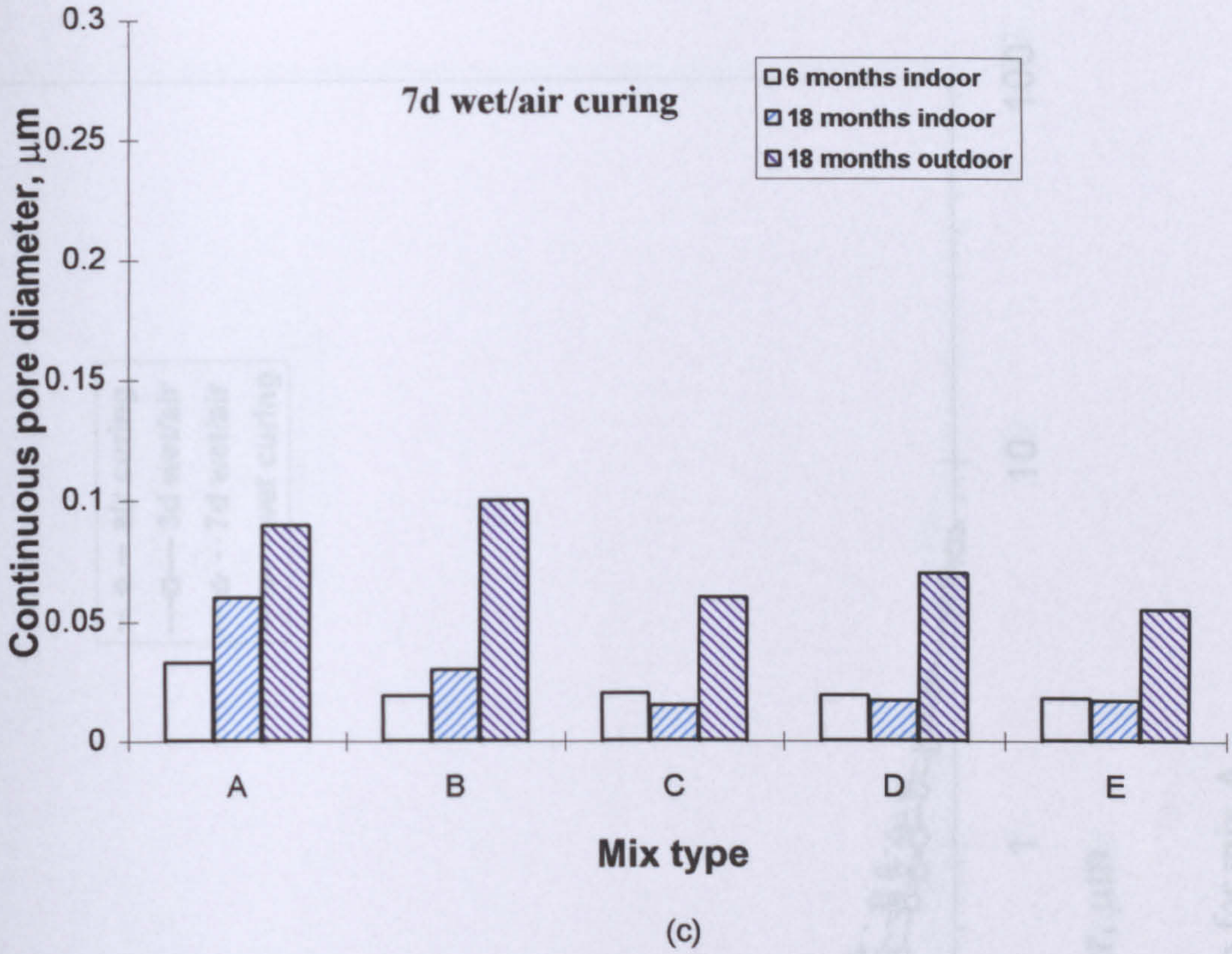

Fig. 6.37: Influence of specimens age and exposure environment on continuous pore diameter.

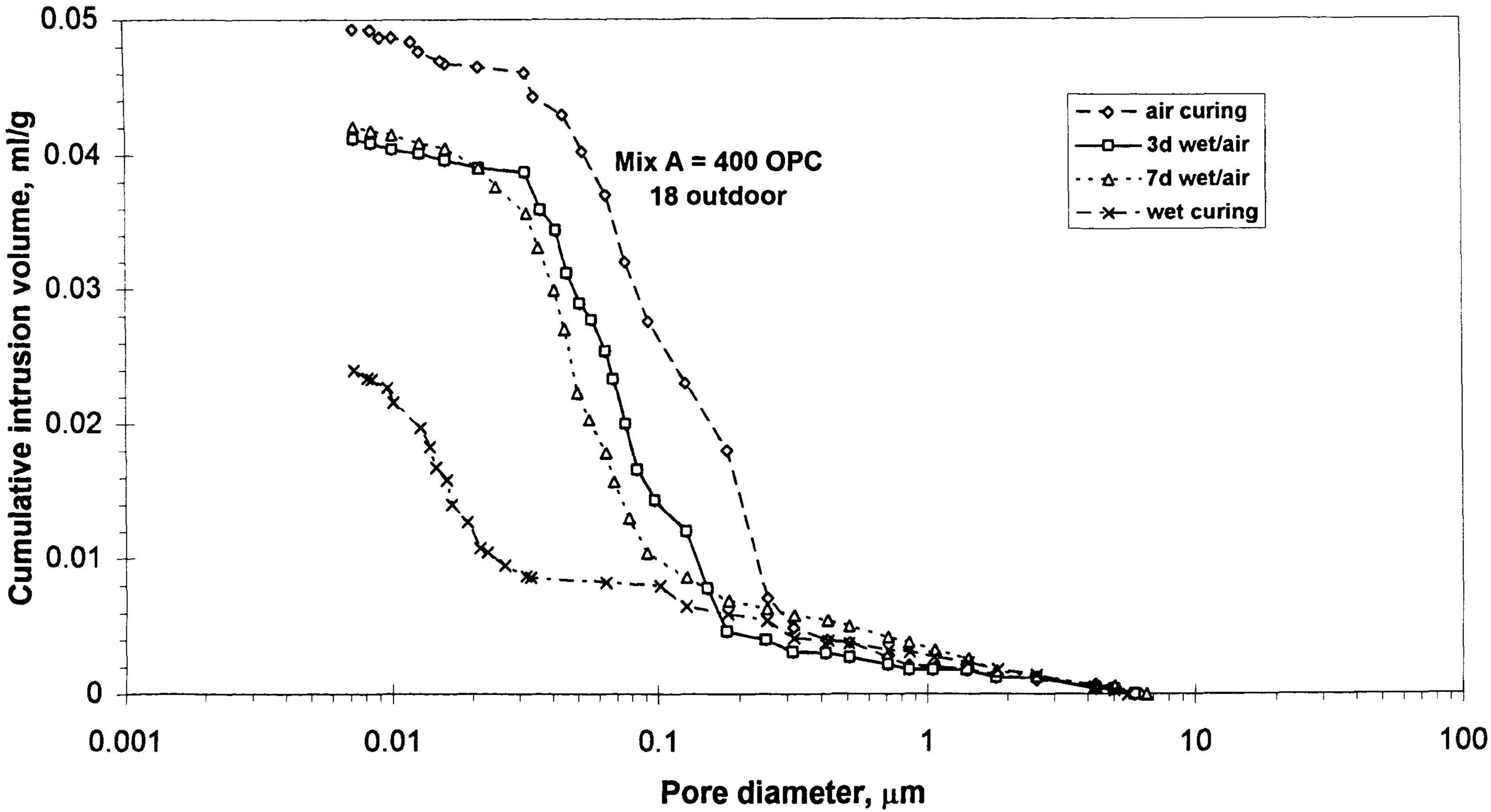

Fig. 6.38: Influence of curing regime on pore size distribution for mix A.

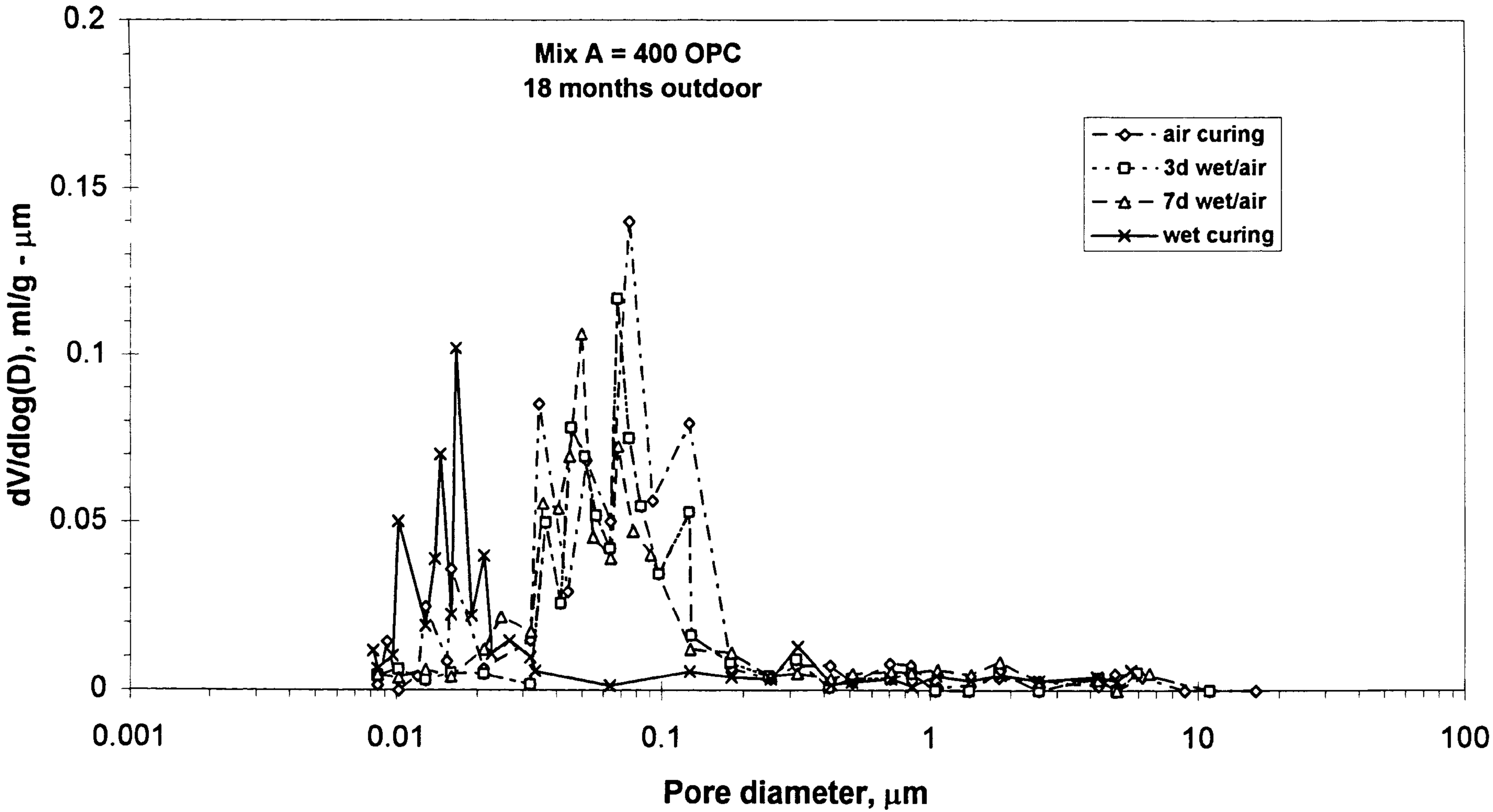

Fig. 6.39: Differential pore size distribution for mix A.

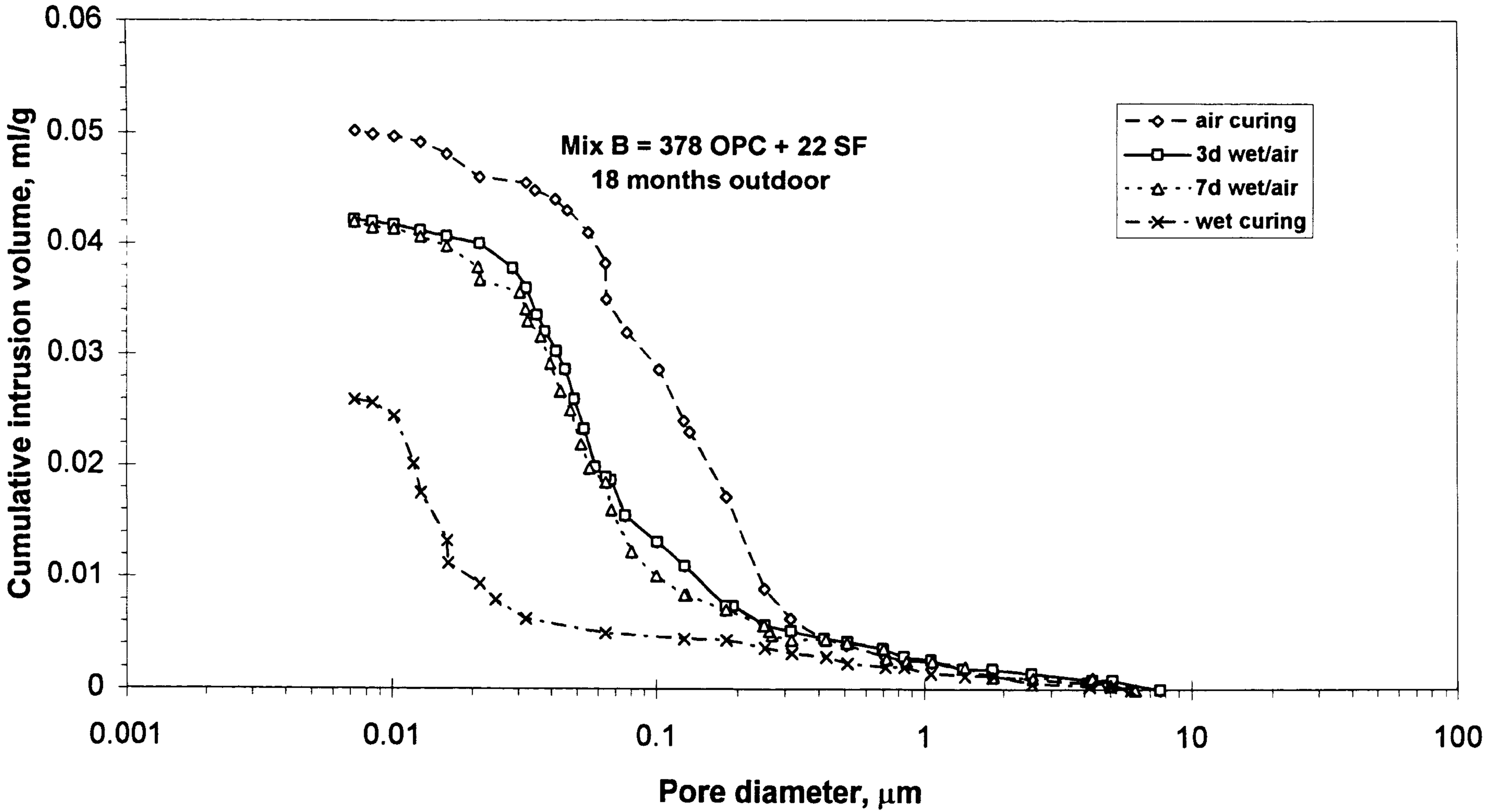

Fig. 6.40: Influence of curing regime on pore size distribution for mix B.

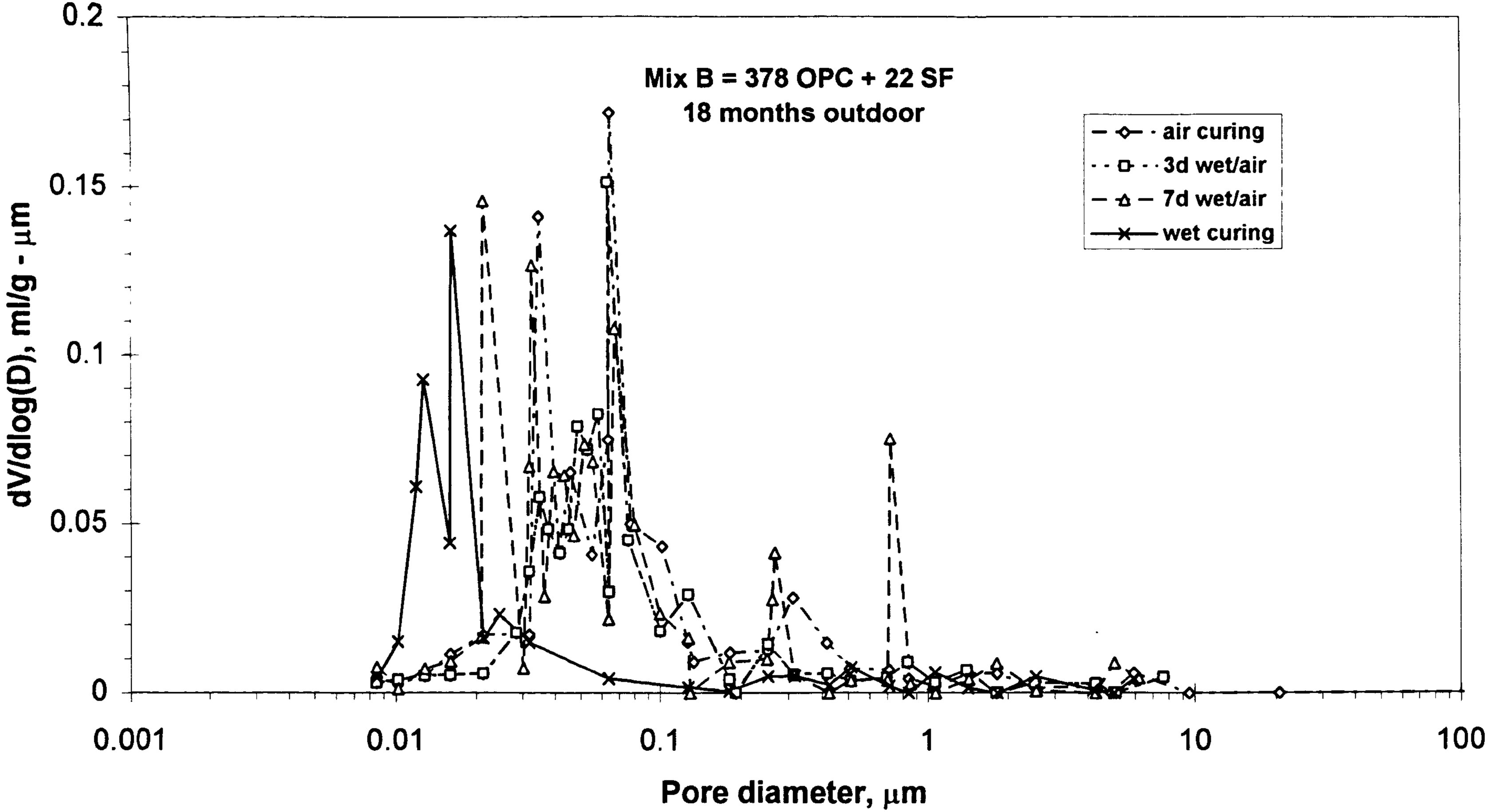

Fig. 6.41: Differential pore size distribution for mix B.

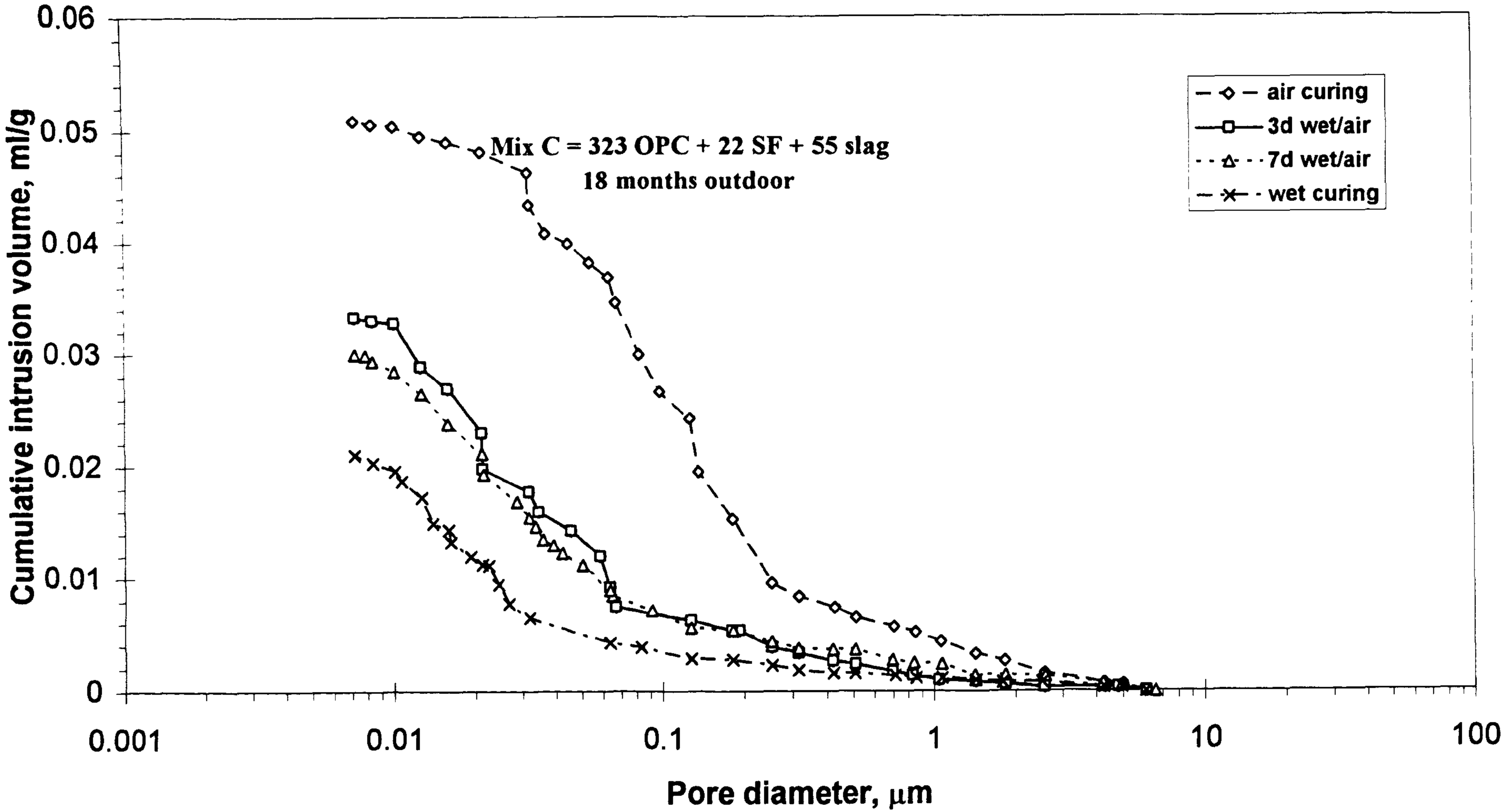

Fig. 6.42: Influence of curing regime on pore size distribution for mix C.

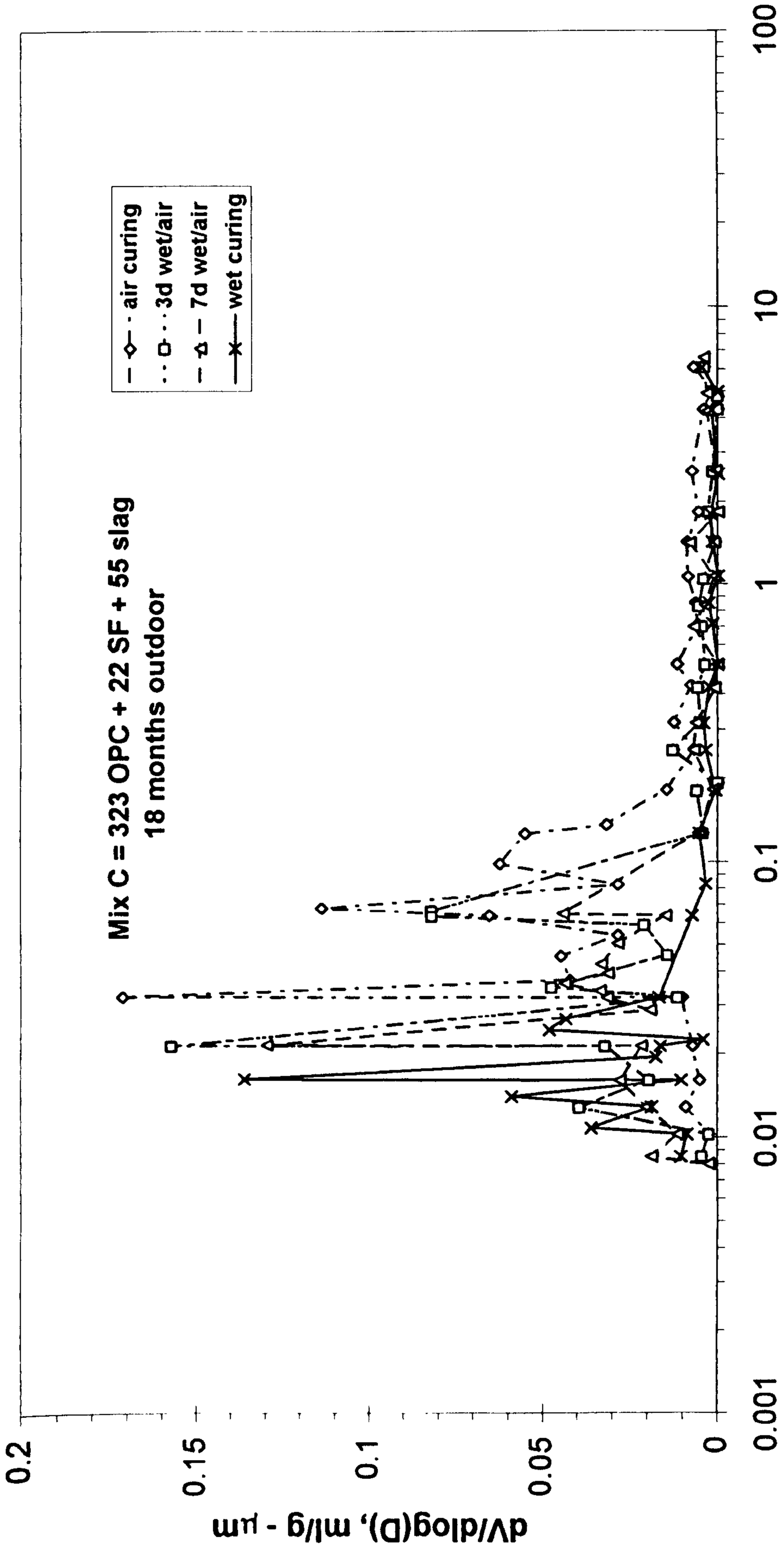

Fig. 6.43: Differential pore size distribution for mix C.

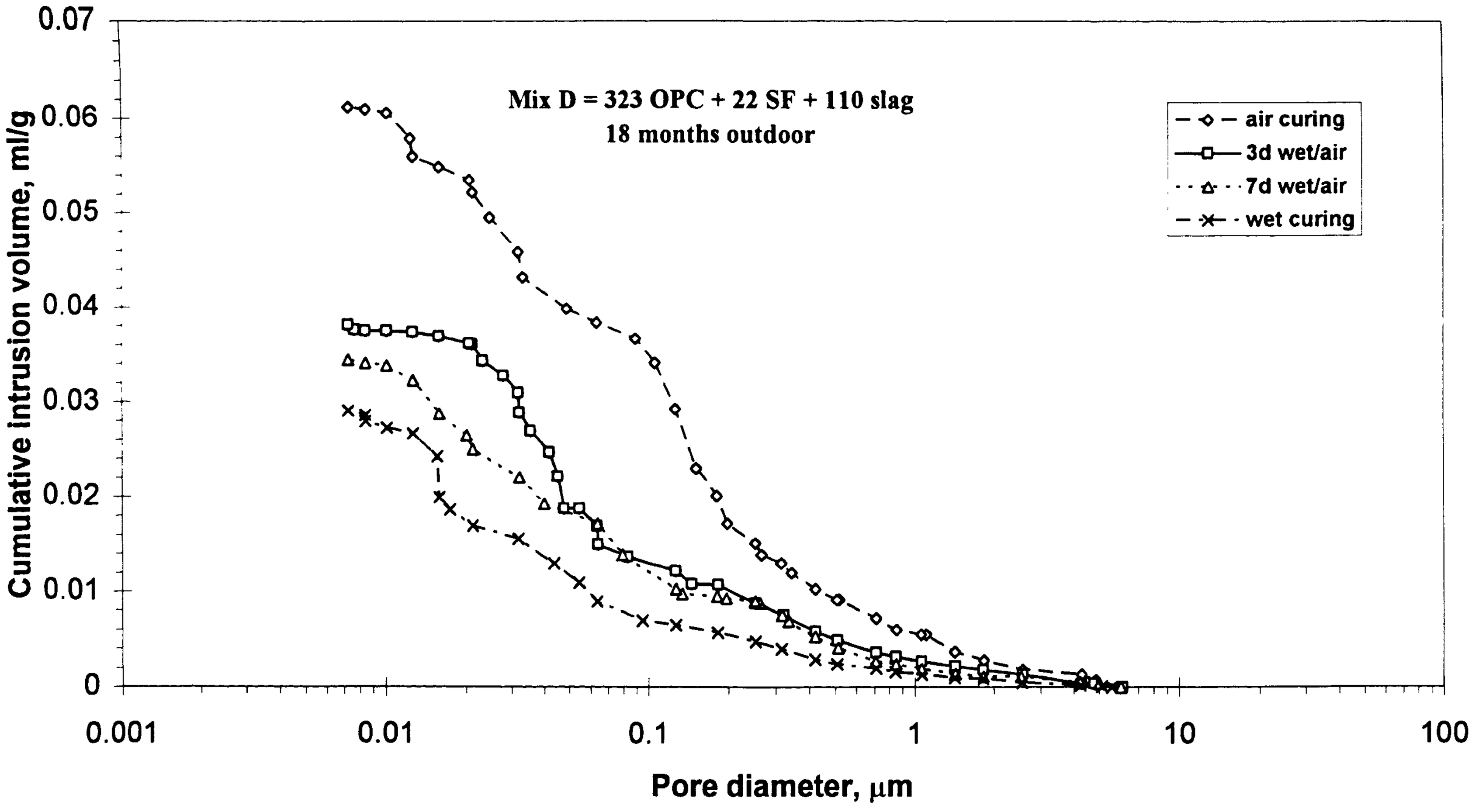

Fig. 6.44: Influence of curing regime on pore size distribution for mix D.

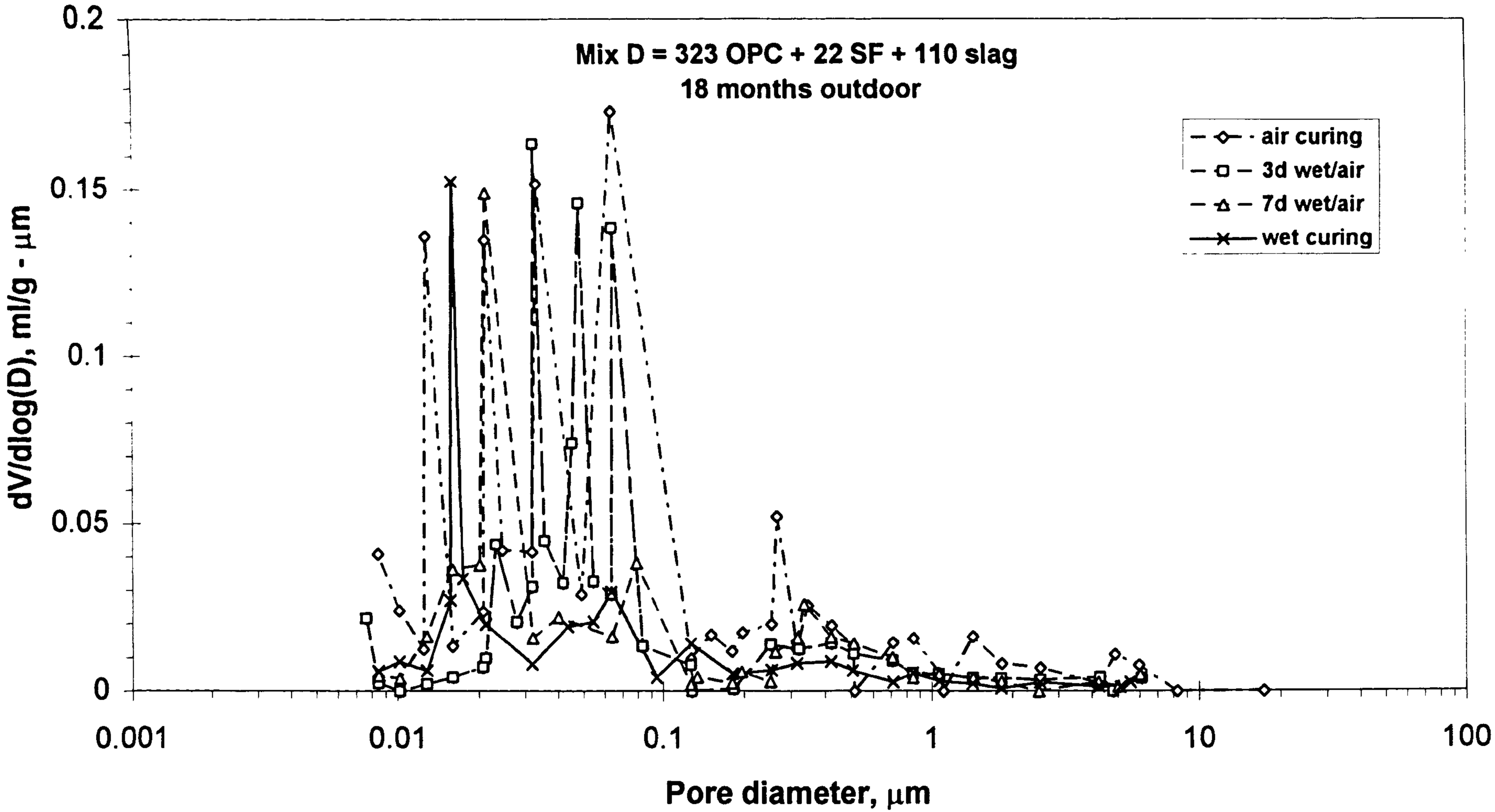

Fig. 6.45: Differential pore size distribution for mix D.

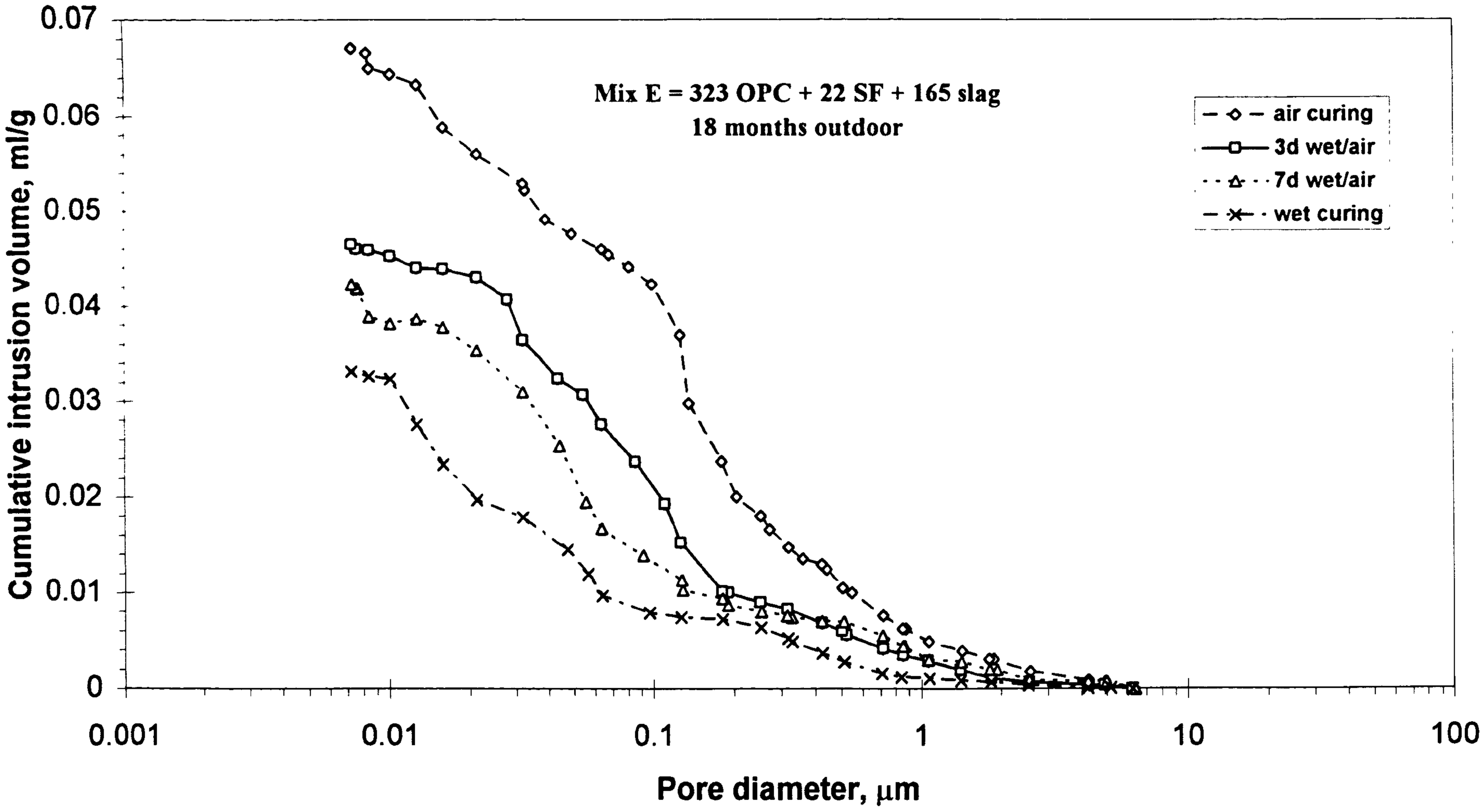

Fig. 6.46: Influence of curing regime on pore size distribution for mix E.

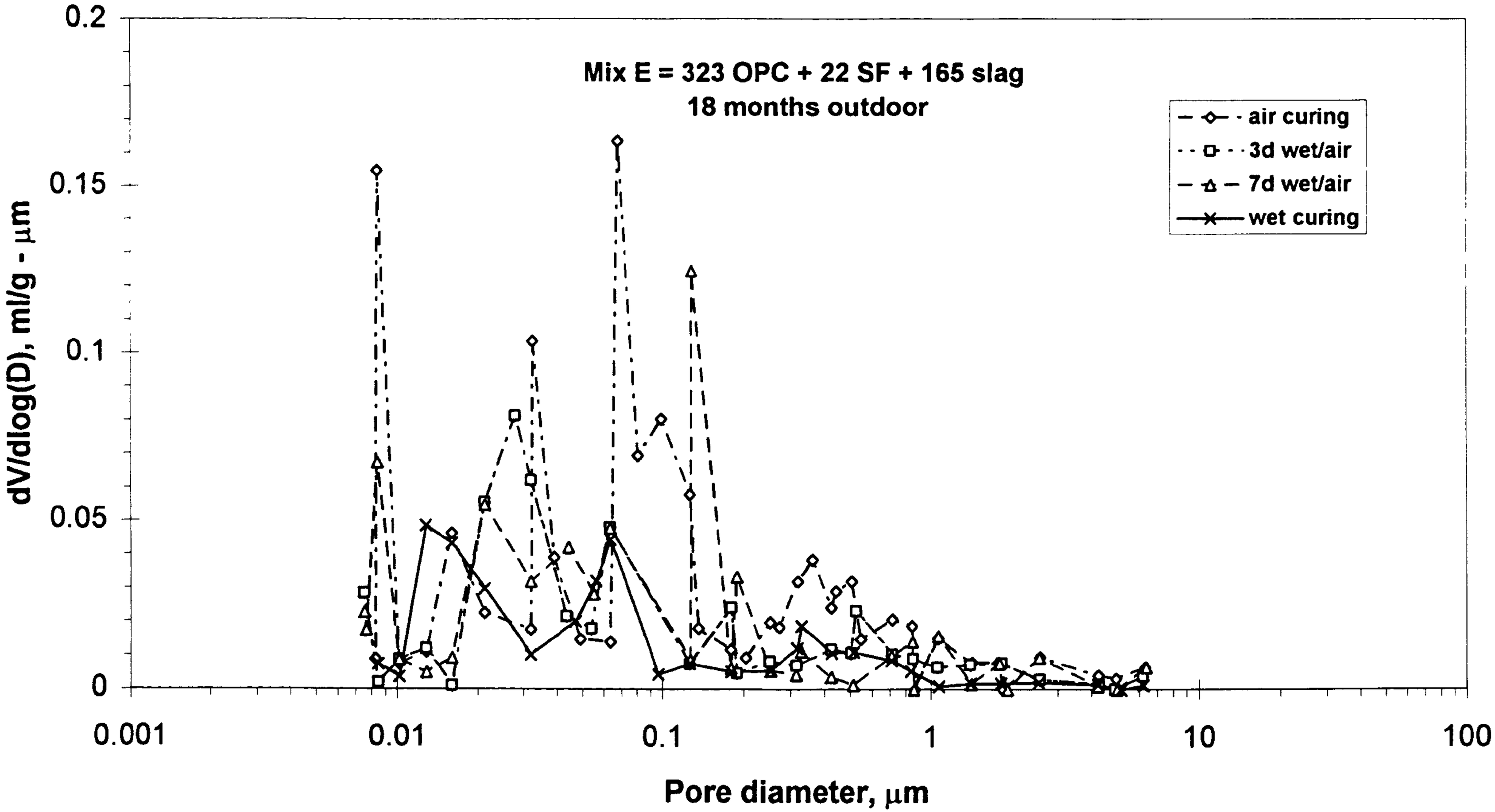

Fig. 6.47: Differential pore size distribution for mix E.

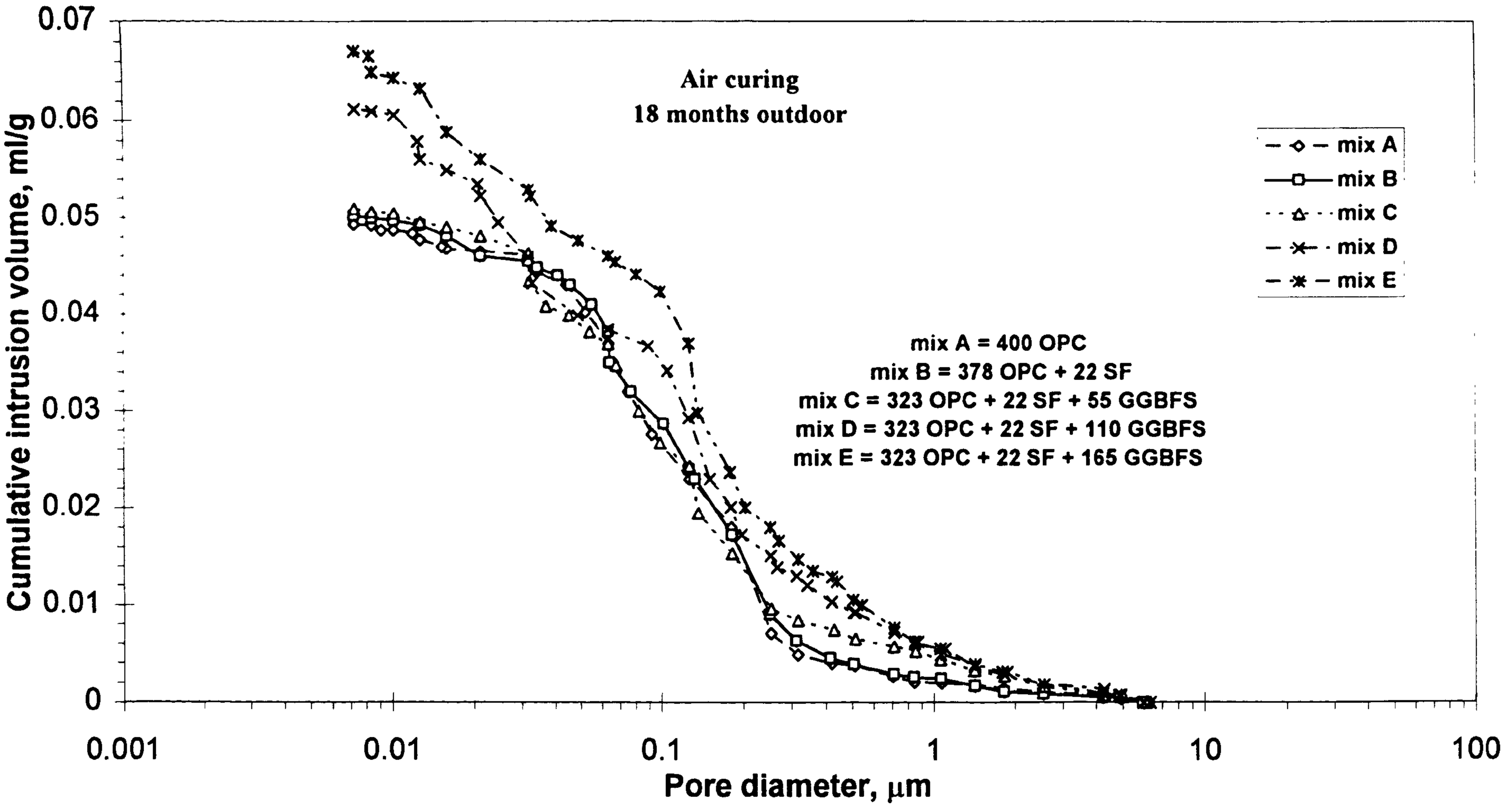

Fig. 6.48: Influence of mix type on pore size distribution under air curing.

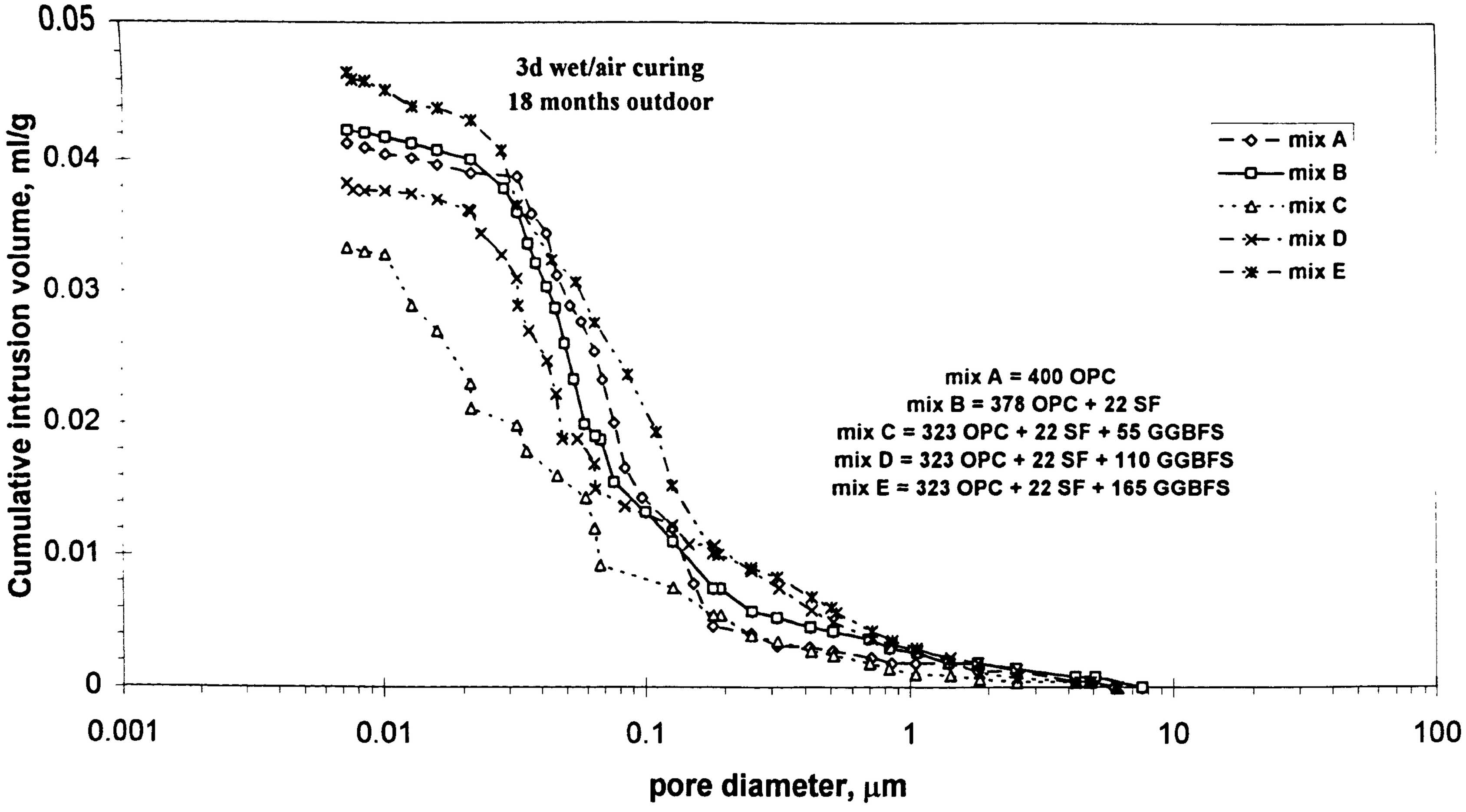

Fig. 6.49: Influence of mix type on pore size distribution under 3d wet/air curing.

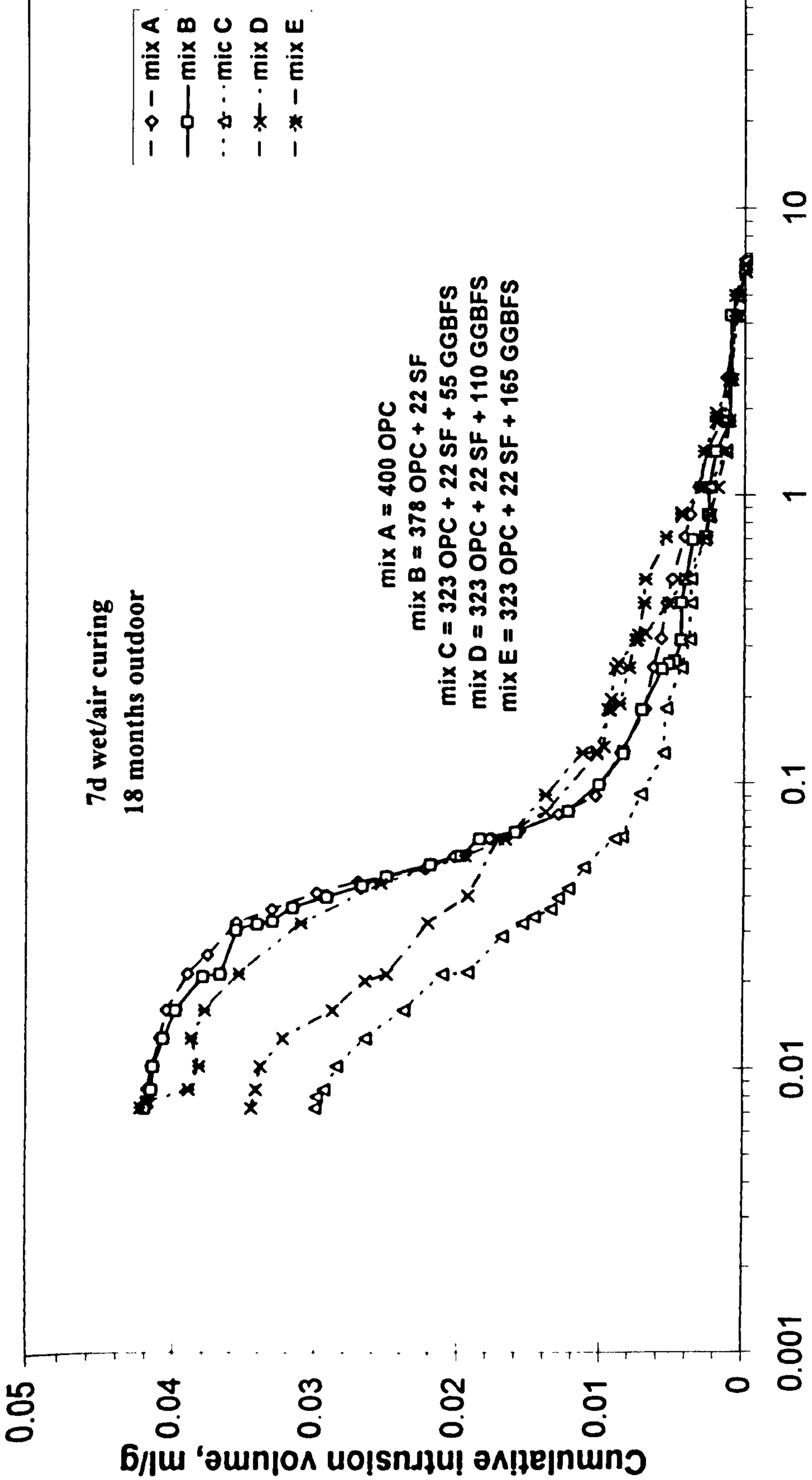

Fig. 6.50: Influence of mix type on pore size distribution under 7d wet/air curing.

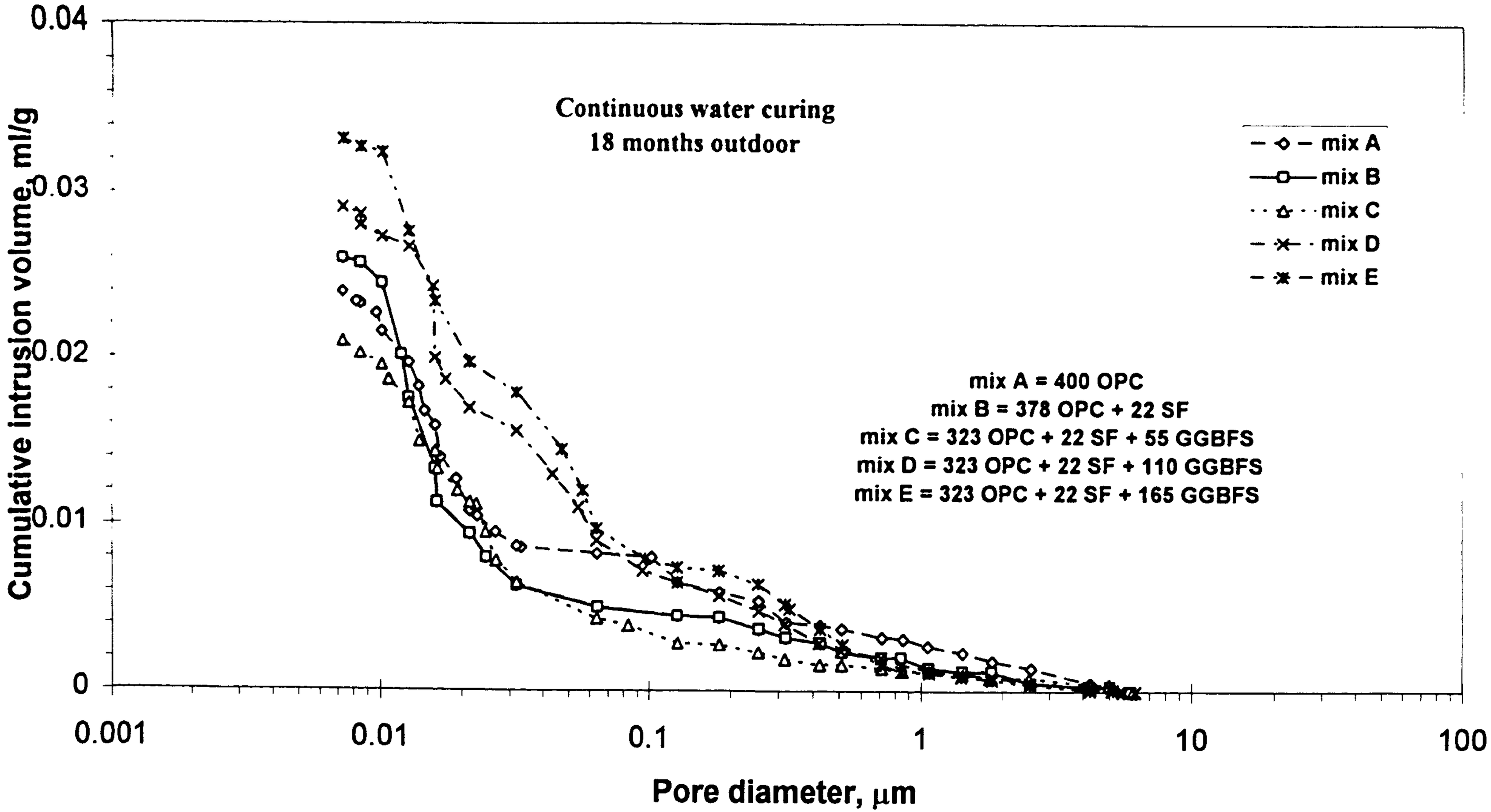

Fig. 6.51: Influence of mix type on pore size distribution under Continuous water curing.

highest volume of slag showed the greatest value of total intrusion volume; this value thus decreases as the slag content decreases, as given by 0.0671 , 0.0612, 0.0509 ml/g, for mixes E, D and C respectively, which is in agreement with a similar trend for concrete exposed in the indoor environment.

Fig. 6.35-(a-d) shows a comparison of coarse pores in both environments. It is very interesting to see that exposure to the outdoor environment leads to coarser pores. Under air curing, the hotter environment at outdoor produced coarser pores than that achieved in the laboratory environment. The control mix specimens (mix A), silica fume specimens and SF/slag specimens (mix C with the lowest volume of slag) have all similar values of coarse pore volume, and these values are approximately double those in the indoor environment. The values in the outdoor exposure are 0.0280, 0.0282 and 0.0280 ml/g, while the corresponding values in the laboratory environment were 0.0124, 0.0106 and 0.0150 ml/g respectively. Mix E samples with the highest amount of slag produced the largest coarse pore volume of all the five mixes, i.e., about 0.0423 ml/g, followed by mix D samples which produced 0.0351 ml/g. There is thus a significant difference between these values in outdoor exposure and indoors; a similar trend was also observed in the laboratory environment, but with a smaller difference between mixes E and D, namely 0.0250 and 0.0215 ml/g respectively.

The percentage of coarse pores to total pores volume under air curing, ranged from 55-63%, for all mixes in the outdoor environment, the corresponding values in the indoor environment ranged from 25-46%, as seen in Table 6.3. This large variation in the percentage of coarse pores is due primary to the major changes in the temperature and relative humidity in the day and night, which cause subsequent adverse effects of drying and wetting, may lead to the generation of cracks in concrete.

A possible explanation of this phenomena is suggested by Bakker [79] and Neville [35]. They said that high temperatures produce a physically poorer structure in the hydrated OPC pastes. According to Neville [35], Verbeck and Helmuth suggested that the temperature accelerated initial hydration rate retards the subsequent hydration, and produces a non-uniform distribution of the hydration products within the sample. The reason for this is, according to Neville, that the high initial rate of hydration does not provide sufficient time for the diffusion of the hydration products away from the cement grain as in the case of lower temperatures. Hence a high concentration of these products is precipitated in the vicinity of the hydrating grain, thus retarding the subsequent hydration.

Fig. 6.35-(b) shows the effect of hot environment on coarse pore volume under 3d wet/air curing. It is clear that increases in coarse pore volume were observed due to the hot environment; the volume of coarse pores of mix E samples in the outdoor was twice that of the indoor environment at the same age. The difference in the coarse pore volume values of mixes A, B, and D at outdoor is not as great as in mix E samples; mix C specimens show no increases with environment, and gave the minimum value of coarse pore volume of about 0.0070 ml/g.

Fig. 6.35-(c) presents results of coarse pore volumes under 7d wet/air curing. It is clear that specimens of mixes A and B show similar differences between the two environments. However, specimens in the outdoor environment were badly effected, and they had 56% and 63% higher coarse pore volume than similar specimens in the indoor environment. Mix C specimens were also influenced by the outdoor environment, but gave the smallest increase in coarse pore volume due to hot environment, about 51%. On the other hand, mixes E and D specimens show the largest increases in the values of coarse pore volumes, about 168% and 105% respectively more than the corresponding values in the indoor environment.

As expected the smallest volume of coarse pores occurred in specimens cured continuously in water as seen in Fig. 6.35-(d). However, it is interesting to see that, in mixes B and C specimens, there was no significant effect due to hot environment, which gave values of 0.0050 ml/g and 0.0040 ml/g in outdoor compared to the corresponding values in indoor of 0.0038 ml/g and 0.0039 ml/g respectively. In other mixes there are significant increases in the volume of coarse pores. A higher value was shown by mix A specimens followed by mixes E and D; these values in the outdoor being 0.0080, 0.0078 and 0.0070 ml/g respectively, compared to the corresponding values in the indoor environment of 0.0048, 0.0042 and 0.0042 ml/g respectively. The above results also show that mixes containing 24% or more slag are more sensitive to outdoor environment than mix C under continuous water curing.

The threshold diameter results for the two different environments for the concrete and blended concrete specimens are shown in Fig. 6.36-(a-d). The results show that the threshold diameter in the outdoor environment varied widely. Under air curing, the higher threshold diameters were obtained in mixes E and D, which had large amounts of slag. Specimens cured continuously in water show no effect of environment, and this was observed for all mixes. The 3d wet/air and 7d wet/air curing show an increase in

the threshold diameter in the outdoor environment. The trend here is generally the same as that shown by indoor environment specimens.

In general, air curing shows much higher continuous pore diameters than the other curing regimes in the outdoor environment, as shown in Fig. 6.37-(a). All values of continuous pore diameter almost doubled in the outdoor environment for specimens under air curing regime.

It is considered that these changes in continuous pore diameter are due to the ability of the presence of water in the specimens to have better hydration indoor than in the outdoor environment. These results also indicate the rapid loss of water in the outdoor environment than in indoor due to the high temperature, resulting in much more dry concrete specimens, and hence, the continuous pore diameter was higher.

Under continuous wet curing all the specimens showed a similar continuous pore diameter in the outdoor to that in the laboratory environment as seen in Fig. 6.37-(d). On the other hand, the effect of exposure environment on continuous pore diameter of specimens subjected to 3d wet/air and 7d wet/air curing shows that the outdoor environment produced a higher level of continuous pore diameter than the indoor environment under both curing regime, and that the difference in the two values was higher in the curing regime with the smaller exposure to water.

Fig. 6.52 shows a comparison of the volume of coarse pores (pores>0.1 μm) of specimens cured in 7d wet/air in outdoor with those of specimens cured 3d wet/air in indoor at 18 months. The 7d wet/air curing in the outdoor environment are higher than those of the 3d wet/air curing in the laboratory environment at the same age. This generation of higher coarse pores in specimens subjected to 7d wet/air curing in outdoor than specimens cured 3d wet/air in the laboratory environment, is thought to be due to the fact that mixes in outdoor are influenced by temperature and accelerated rates of initial hydration reactions more than mixes in the laboratory environment.

6.4 Conclusions:

1. Initially dry-cured specimens yield higher porosity, higher intruded pore volume, coarser pores, higher threshold and continuous pore diameter. The effect is more pronounced in OPC/SF/Slag mixes, with a high slag content.
2. Outdoor environment influences slag concrete more than the OPC concrete under air curing, while under 7d wet/air curing slag concrete showed development of porosity and pore structure better than the OPC concrete.

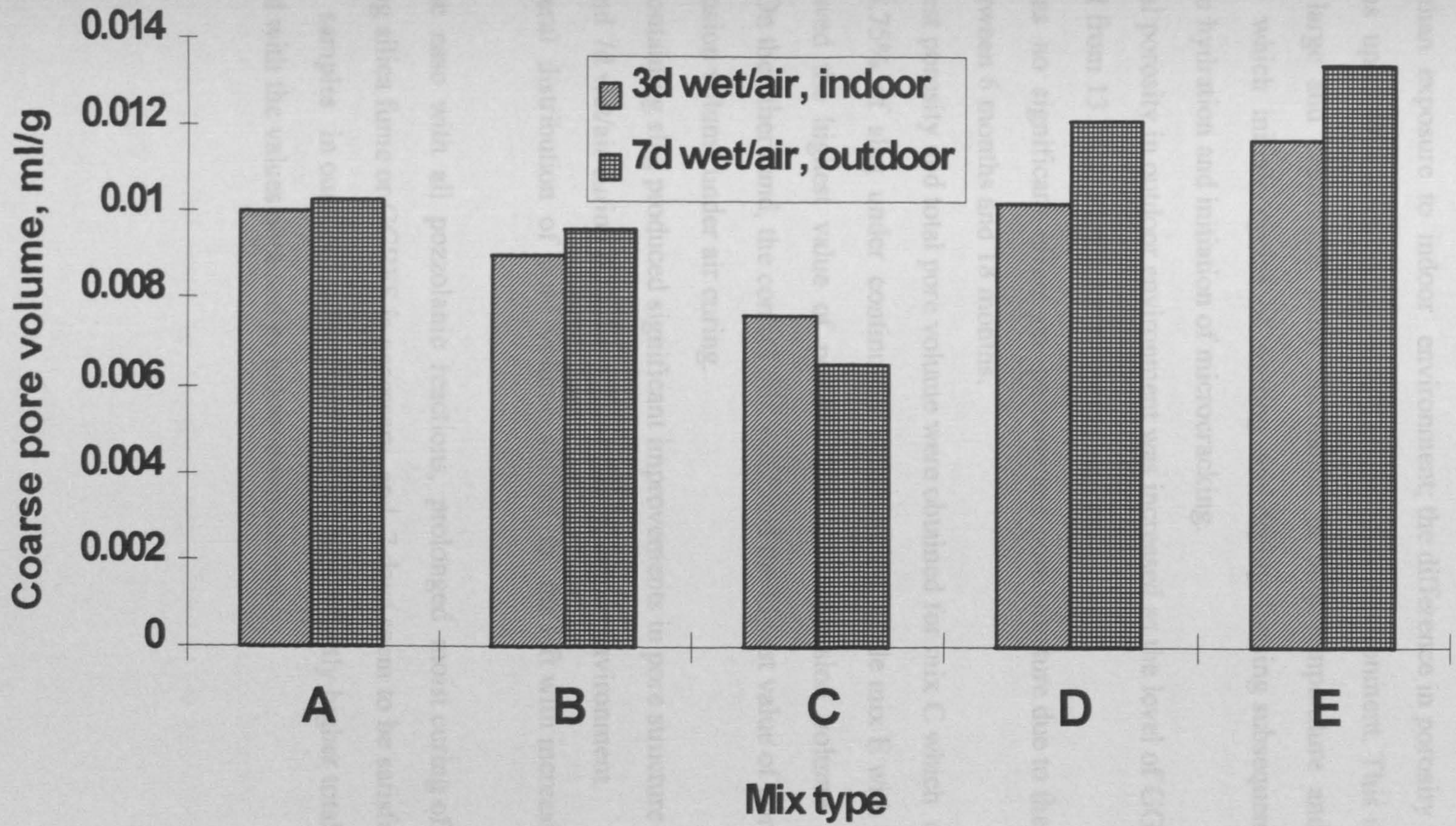

Fig. 6.52: Influence of exposure environment and curing condition on volume of coarse pore

3. Concrete specimens under air curing showed the poorest performance in terms of porosity, total intrusion volume, coarse pores, threshold diameter and continuous pore diameter.
4. Exposure to outdoor environment produced higher porosity and total intrusion volume than exposure to indoor environment; the difference in porosity in certain cases was up to 40% when compared to the laboratory environment. This is because of the large and continuous daily fluctuation in both temperature and relative humidity which initiate cycles of wetting and drying, causing subsequent adverse effects on hydration and initiation of microcracking.
5. The total porosity in outdoor environment was increased as the level of GGBFS was increased from 13.75 to 32.4% for all curing regimes.
6. There was no significant effect on porosity and pore structure due to the effect of aging between 6 months and 18 months.
7. The lowest porosity and total pore volume were obtained for mix C which contained about 13.75% of slag under continuous water curing, while mix E with 32.4% of slag showed the highest value of porosity and total intrusion volume under air curing. On the other hand, the control mix exhibited the lowest value of porosity and total intrusion volume under air curing.
8. Mixes containing slag produced significant improvements in pore structure under 3d wet/air and 7d wet/air curing than the control mix in indoor environment.
9. The general distribution of pore volume shifted to the left with increasing water curing.
10. As is the case with all pozzolanic reactions, prolonged moist curing of concrete containing silica fume or GGBFS is necessary, and 7 days seem to be satisfactory.
11. All mix samples in outdoor environment showed significantly higher total porosity compared with the values obtained in indoor environment.

Chapter seven

DURABILITY-RELATED PROPERTIES OF BLENDED CEMENT CONCRETE

7.1 Introduction

Durable concrete should have the ability to maintain its structural integrity and protective capacity over long period of time when exposed to natural elements. The durability of concrete may be evaluated by determining its ability to withstand freeze-thaw cycles, chloride ingress, sulfate attack and to maintain long-term strengths [156].

As far as the diffusion of gases is concerned, carbon dioxide and oxygen are of primary interest. Oxygen diffusion through concrete is strongly affected by moist curing, prolonged curing reducing the diffusion coefficient. The moisture condition of the concrete under test also has a large influence because the water in the pores significantly reduces the diffusion. One of the factors influencing the diffusion of external agents into concrete is the presence or absence of mineral admixtures in the concrete.

Permeability of concrete is one of the most critical parameters in the determination of concrete durability. As the permeability of concrete is lowered, its resistance to chemical attack increases. The aspect of the structure of hardened cement paste most relevant to permeability is the nature of the pore system as well as the characteristics of the interface zone between the cement paste and the aggregate. The interface zone occupies as much as one-third to one-half of the total volume of hardened cement paste in concrete and is know to have a different microstructure from the bulk of the hardened cement paste. The interface is also the locus of early microcracking. For these reasons, the interface zone can be expected significantly to contribute to the permeability of concrete [35].

7.2 Aims and objectives

The main objectives of this part of the project are as follows:

- To study the effect of exposure environments on the durability-related properties using combination of mineral admixture. Water absorption and carbonation depth of the surface layer of concrete are of considerable importance, especially in relation to

the thickness of the concrete cover. Also, gas permeation into concrete is not a simple function of total porosity of concrete, but depends on the pore size distribution and continuous pore diameter. While permeability of concrete is one of the most critical parameters in determining concrete durability, the effect of aggressive environmental conditions on the oxygen permeability of concrete with different mineral admixtures subjected to four curing regimes also have been evaluated.

The durability-related properties investigated include water absorption, carbonation depth and oxygen permeability over a period of time of 18 months. The full details of the experimental programme are presented in chapter three and the test results are presented below:

7.3 Oxygen permeability

7.3.1 Effect of curing-indoor

Figs. 7.1 to 7.5 show the variation of oxygen permeability against with age under the four curing regimes for all mixes tested in this study. The corresponding quantitative results are presented in Table 7.1. It is clear from the figures that, as the period of water curing increased, permeability decreased; specimens dried continuously in air exhibited the highest values of oxygen permeability, followed by those exposed to 3d wet/air, 7d wet/air and continuous wet curing specimens at all ages. For example, as seen from Fig. 7.1 the control mix (400 OPC) at the age of 28 days in the laboratory environment, under continuous air curing showed a permeability value of 0.992×10^{-16} m^2; on the other hand, the corresponding value under continuous water curing regime exhibited the lowest value of 0.396×10^{-16} m^2, which is a reduction of some 60% due to moist curing. Specimens exposed to 3d wet/air and 7d wet/air curing also exhibited values lower than air curing specimens, namely, 0.405 and 0.478 $\times 10^{-16}$ m^2, respectively. These values are close to that of specimens under continuous wet curing, which indicates the importance of early water curing. At the age of 6 and 18 months the specimens under air curing, 3d wet/air and 7d wet/air curing show an increase in permeability; as the age of specimens increased these values also increased. For example, at the age of 18 months, the permeability of specimens under 3d wet/air and 7d wet/air curing were about doubled compared comparatively there permeability at 28 days, whereas the wet cured specimens showed a progressive reduction in permeability,

as would be expected, giving values of permeability at these ages (under wet curing) of 0.0396 x10^{-16}, 0.275 x10^{-16} and 0.274 x10^{-16} m^2 respectively.

Fig. 7.2 shows the oxygen permeability coefficient of mix B (378 OPC + 22 SF) concrete specimens under the four curing regimes. As expected air drying leads to a high oxygen permeability coefficients. However, with initial wet curing i.e., with 3d wet/air and 7d wet/air curing, the oxygen permeability coefficients were very close to that due to wet curing regime at the age of 28 days, very much lower than that of the air cured specimens. At 18 months, however, large differences in oxygen permeability were obtained between continuous water curing and the other curing regimes. For example, specimens under wet curing, at the age of 18 months in the indoor environment showed a permeability value of 0.202 x10^{-16} m^2; drying continuously in air increased this coefficient by more than 4.7 times to register a value of 0.954 x10^{-16} m^2.

Table 7.1: Influence of mix type on oxygen permeability x10^{-16} m^2.

Mix	Binder content kg/m^3 OPC/SF/Slag	Curing regime	Indoor environment			Outdoor environment		
			Age			Age		
			28 days	6 months	18 months	28 days	6 months	18 months
A	400/0/0	air curing	0.992	1.030	1.136	3.235	7.324	9.913
B	378/22/0	air curing	0.806	0.993	0.954	3.884	6.187	9.020
C	323/22/55	air curing	1.052	1.148	1.163	3.710	4.832	7.077
D	323/22/110	air curing	1.027	1.264	1.271	1.658	2.941	6.108
E	323/22/165	air curing	1.082	1.330	1.313	2.421	6.260	9.684
A	400/0/0	3d wet/air	0.405	0.611	0.945	1.563	2.020	2.201
B	378/22/0	3d wet/air	0.354	0.530	0.787	1.067	1.293	1.519
C	323/22/55	3d wet/air	0.227	0.245	0.278	0.770	1.215	1.503
D	323/22/110	3d wet/air	0.185	0.199	0.236	0.825	1.122	0.981
E	323/22/165	3d wet/air	0.212	0.443	0.605	0.97	1.495	2.995
A	400/0/0	7d wet/air	0.478	0.584	0.892	1.394	1.848	2.399
B	378/22/0	7d wet/air	0.354	0.414	0.708	1.065	1.031	1.295
C	323/22/55	7d wet/air	0.134	0.190	0.191	0.84	0.981	1.144
D	323/22/110	7d wet/air	0.128	0.158	0.186	0.739	1.121	1.224
E	323/22/165	7d wet/air	0.216	0.310	0.437	0.880	1.451	2.666
A	400/0/0	wet curing	0.396	0.275	0.274	0.988	0.985	0.913
B	378/22/0	wet curing	0.277	0.234	0.202	0.888	0.494	0.477
C	323/22/55	wet curing	0.101	0.174	0.139	0.685	0.412	0.327
D	323/22/110	wet curing	0.130	0.130	0.126	0.798	0.718	0.617
E	323/22/165	wet curing	0.160	0.134	0.164	0.992	0.934	0.936

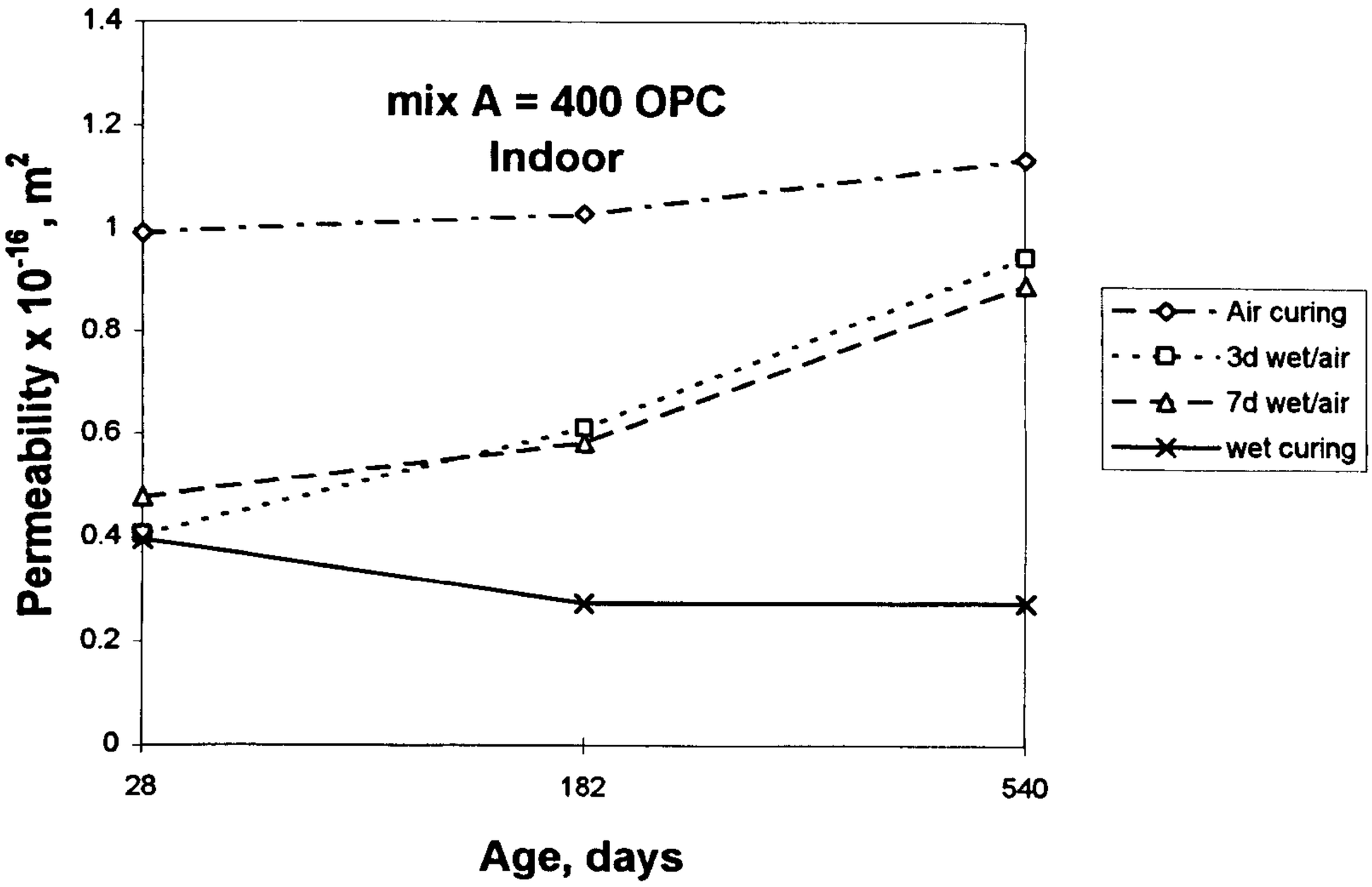

Fig. 7.1: Influence of curing regime on oxygen permeability of mix A.

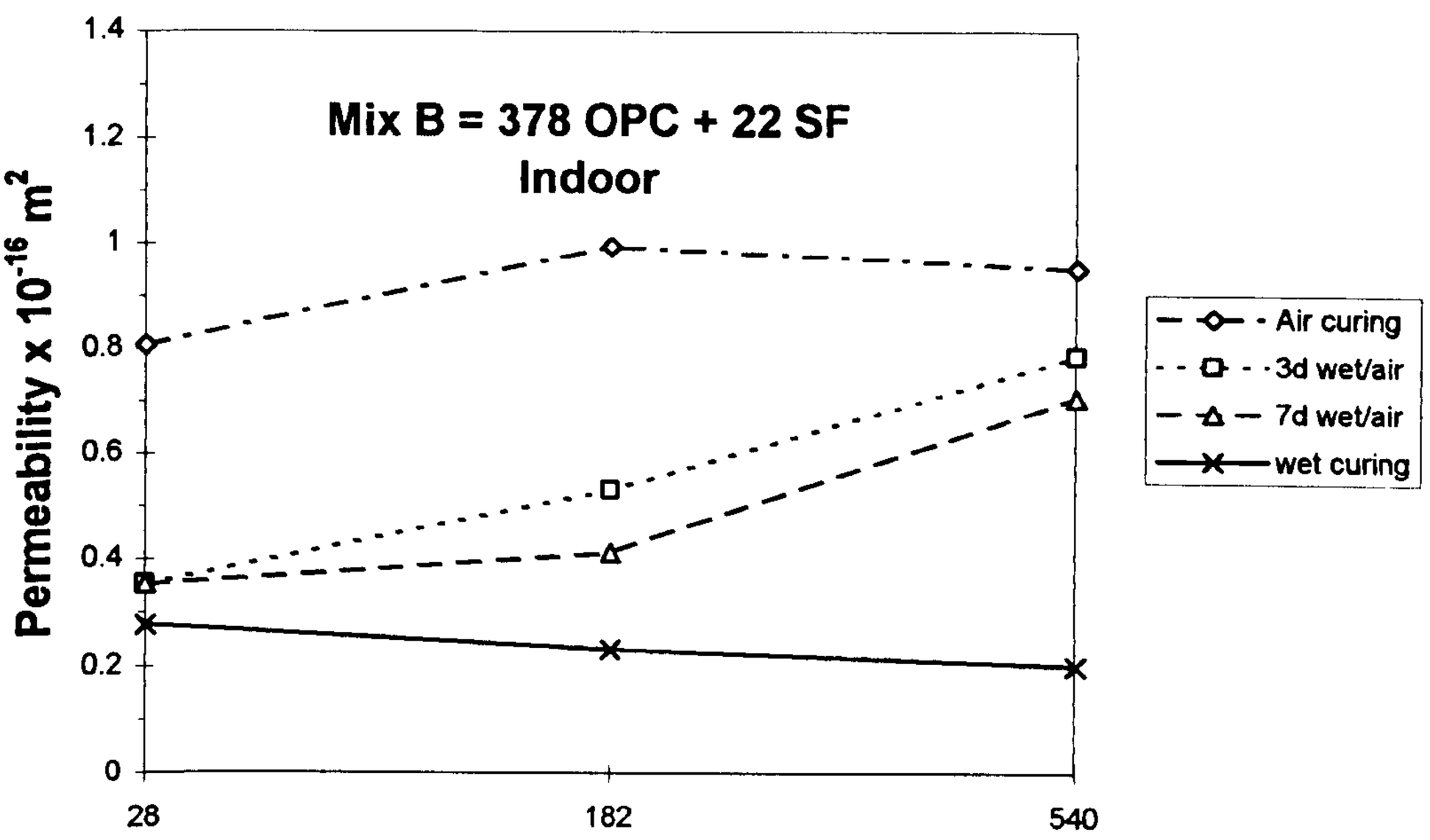

Fig. 7.2: Influence of curing regime on oxygen permeability of mix B.

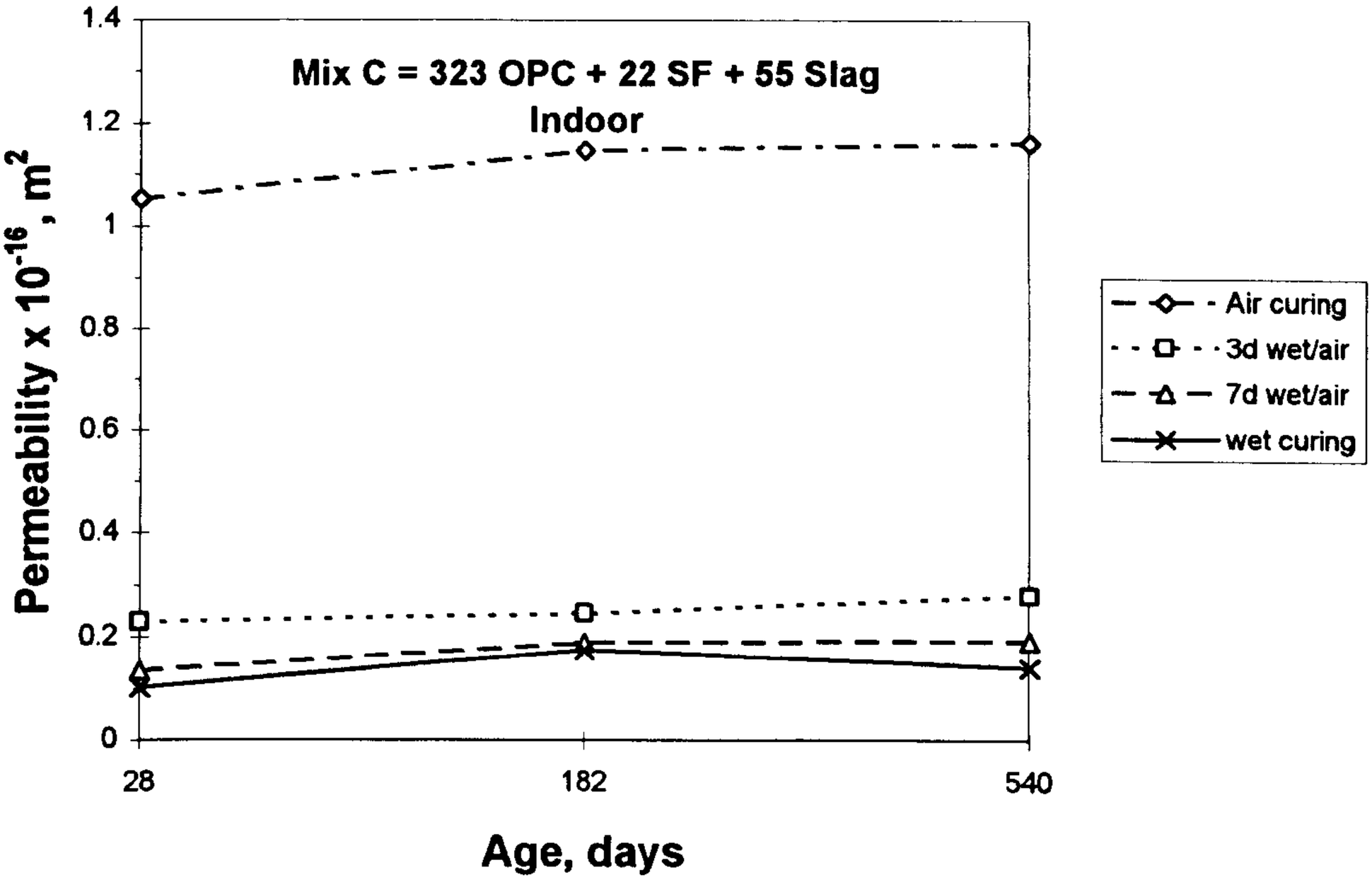

Fig. 7.3: Influence of curing regime on oxygen permeability of mix C.

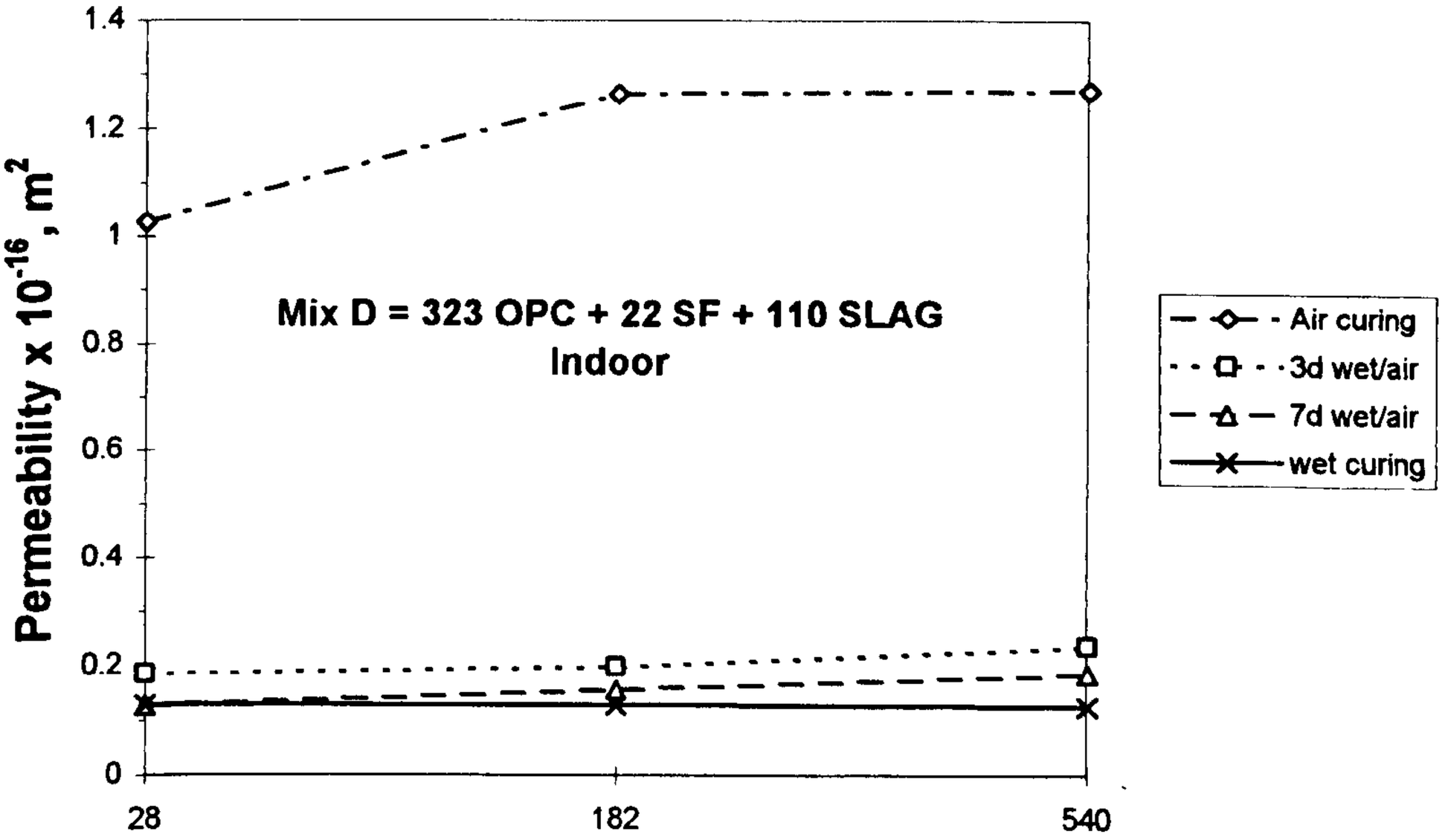

Fig. 7.4: Influence of curing regime on oxygen permeability of mix D.

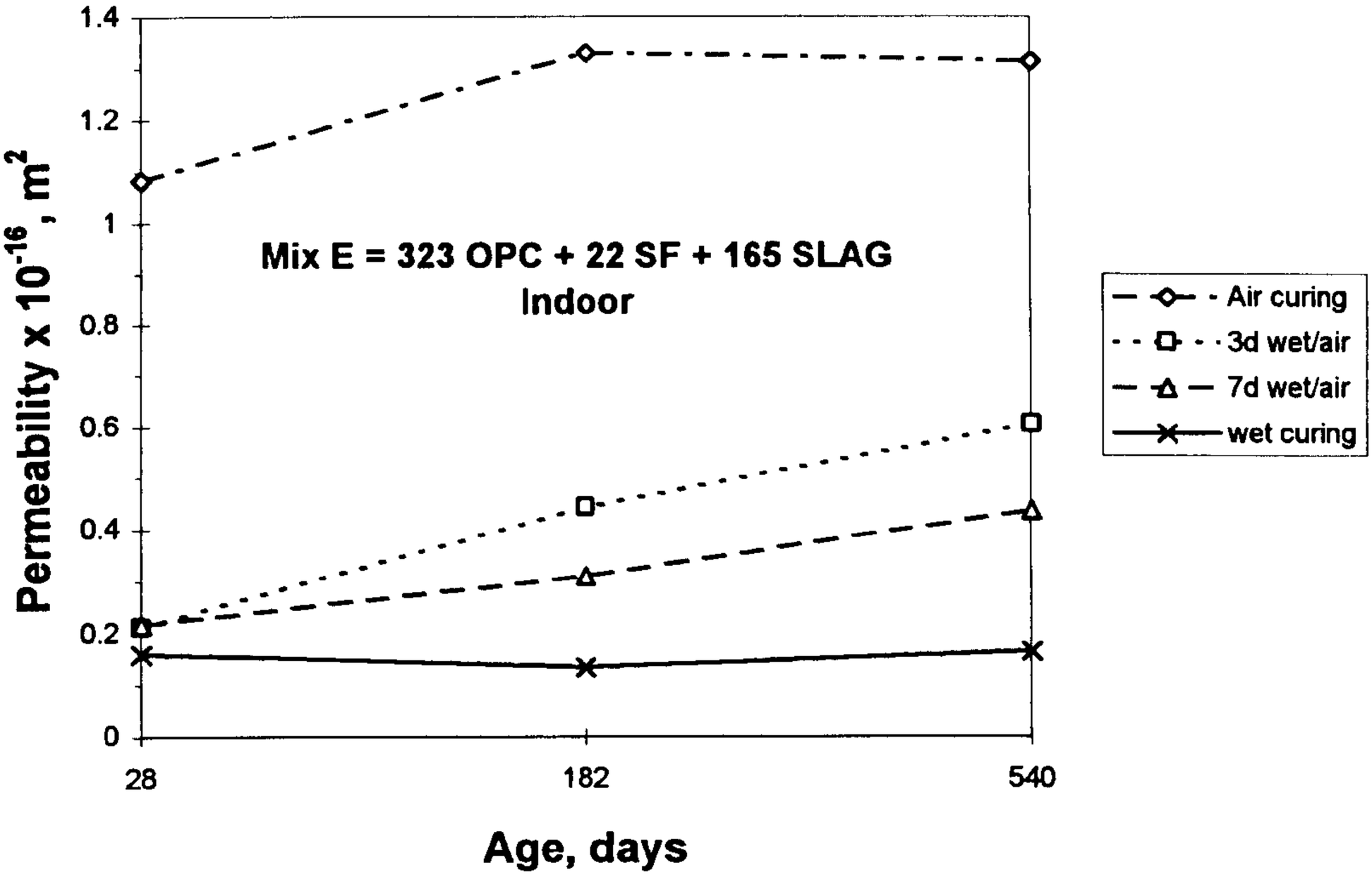

Fig. 7.5: Influence of curing regime on oxygen permeability of mix E.

Figs. 7.3 and 7.4 shows the oxygen permeability coefficient of mix C specimens (323 OPC + 22 SF + 55 slag), under the four curing regimes, and of mix D specimens (323 OPC + 22 SF + 110 slag) respectively. Both mixes recorded similar trends, specimens under air curing show high coefficients of permeability than those cured 3 days in water and beyond. For example, at age of 18 months, the oxygen permeability of mix C under continuous moist curing was 0.139 $x10^{-16}$ m^2, the corresponding values for air cured specimens were higher by 8.4 times, while the 3d wet/air and 7d wet/air specimens showed increased of 2 and 1.4 times respectively.

The effect of curing regime on oxygen permeability of mix E specimens (323 OPC + 22 SF + 165 slag) is presented in Fig. 7.5. It is clearly indicated that, at the age of 18 months, specimens which were cured continuously in air have a much higher coefficient of permeability than those initially cured in water. Air curing displayed the highest value of oxygen permeability, about eight times that at continuous wet curing. The 3d wet/air, 7d wet/air and wet curing gave values of 1.313 $x10^{-16}$, 0.605 $x10^{-16}$, 0.437 $x10^{-16}$ and 0.164 $x10^{-16}$ m^2 respectively.

The above finding is in general agreement with other published data [5,78,157]. Kasai et al [78] found that the coefficient of air permeability varies with curing time and initial curing. The specimens which were not cured in water at early ages gave a

higher coefficient of air permeability than those subjected to 3d wet/air or 7d wet/air curing. The specimens cured 7d wet/air showed small values of coefficient of air permeability; the reason is that the specimens subjected to 7d wet/air curing have more moisture, and a denser structure because of more hydration than specimens cured in air or 3d wet/air.

7.3.2 Effect of mix type- indoor

Figs. 7.6-7.9 and Table 7.1 show the influence of mineral admixture on the oxygen permeability of concrete. As seen from Figure 7.6, at the age of 18 months in the indoor environment, mix E (323 OPC + 22 SF + 165 slag) presented the highest value of oxygen permeability for specimens dried continuously in air, namely 1.313 $x10^{-16}$ m^2. This was followed by mix D (323 OPC + 22 SF + 110 slag) which gave value of 1.271 $x10^{-16}$ m^2; the lowest values were obtained for mix B (378 OPC + 22 SF) which produced a value of 0.954 $x10^{-16}$ m^2. Mix C (232 OPC + 22 SF + 55 slag) showed a value better than those of the other mixes containing slag, namely 1.163 $x10^{-16}$ m^2, which is close to the corresponding value of mix A 1.136 $x10^{-16}$ m^2. As seen above, all mixes containing slag exhibited an increase in oxygen permeability compared with the control mix (400 OPC) when they were exposed to a drying environment from the beginning. These increases in permeability indicate that mixes containing slag are more sensitive to water curing than the portland cement mix or mix containing silica fume in small amounts. The above findings are in agreement, with the data reported by Austin et al [3] found that, the 50% GGBFS concrete was less permeable than the OPC concrete when it received moist curing. However, when air curing was provided the 50% GGBFS concrete suffered more than the OPC concrete and was highly permeable.

It is clear from the Fig. 7.7 that, at the age of 18 months in the indoor environment, mix A specimens subjected to 3d wet/air curing the highest value of oxygen permeability followed by mixes B and E, the values obtained being 0.945 $x10^{-16}$, 0.787 $x10^{-16}$ and 0.605 $x10^{-16}$ m^2 respectively. On the other hand, mixes C and D showed similar values, 30% and 25% less respectively than the corresponding value of the control mix. This might be attributed to increases in the density due to curing of such concrete containing slag, resulting in the transformation of large pores into fine pores and therefore causing pore refinement [1,158]. On the other hand, for specimens under continuous water curing, shown in Fig. 7.9, at the age of 18 months the oxygen permeability of mix C and mix D are much lower than that of the control mix; both

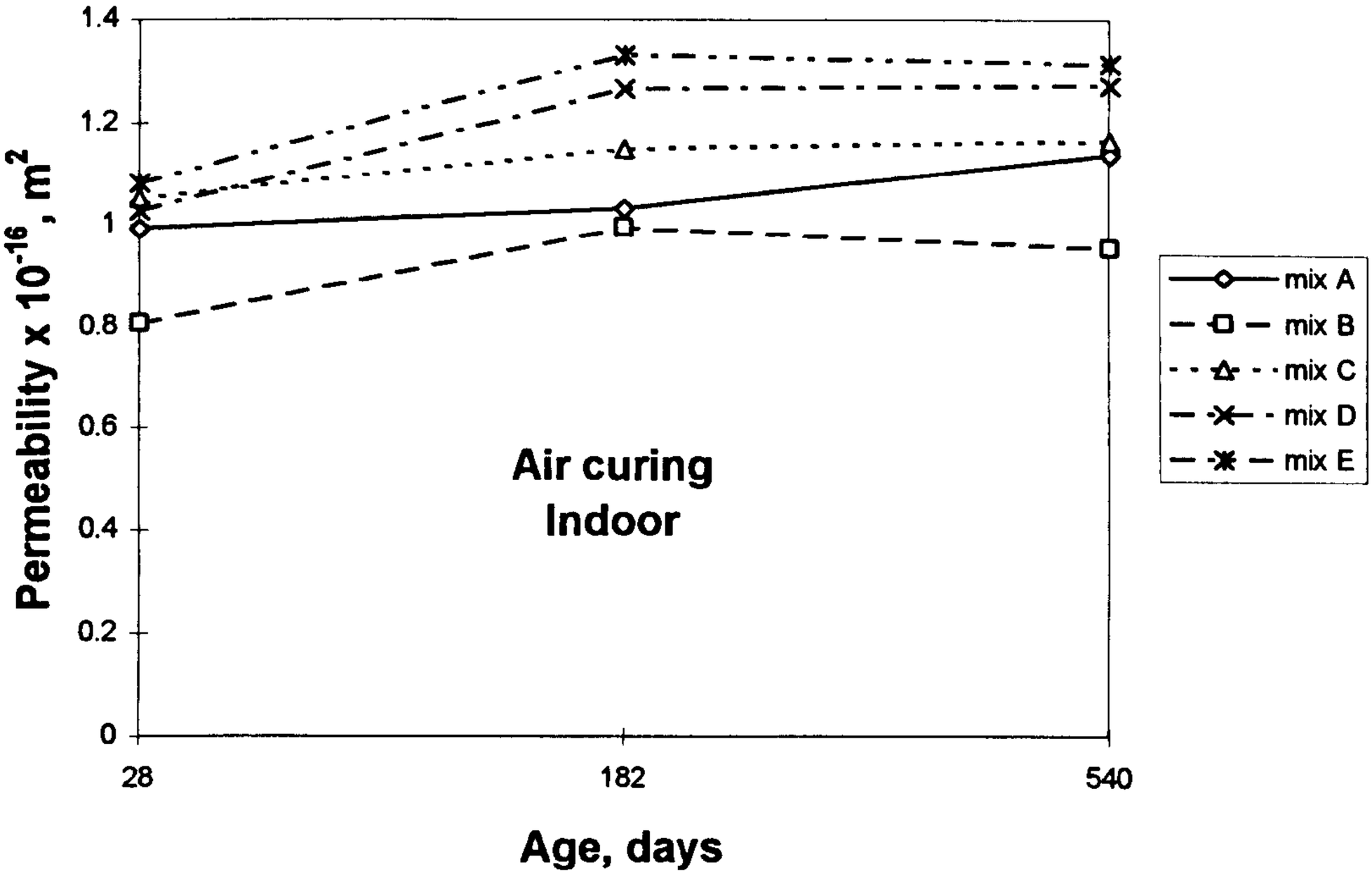

Fig. 7.6: Influence of mix type on oxygen permeability under air curing.

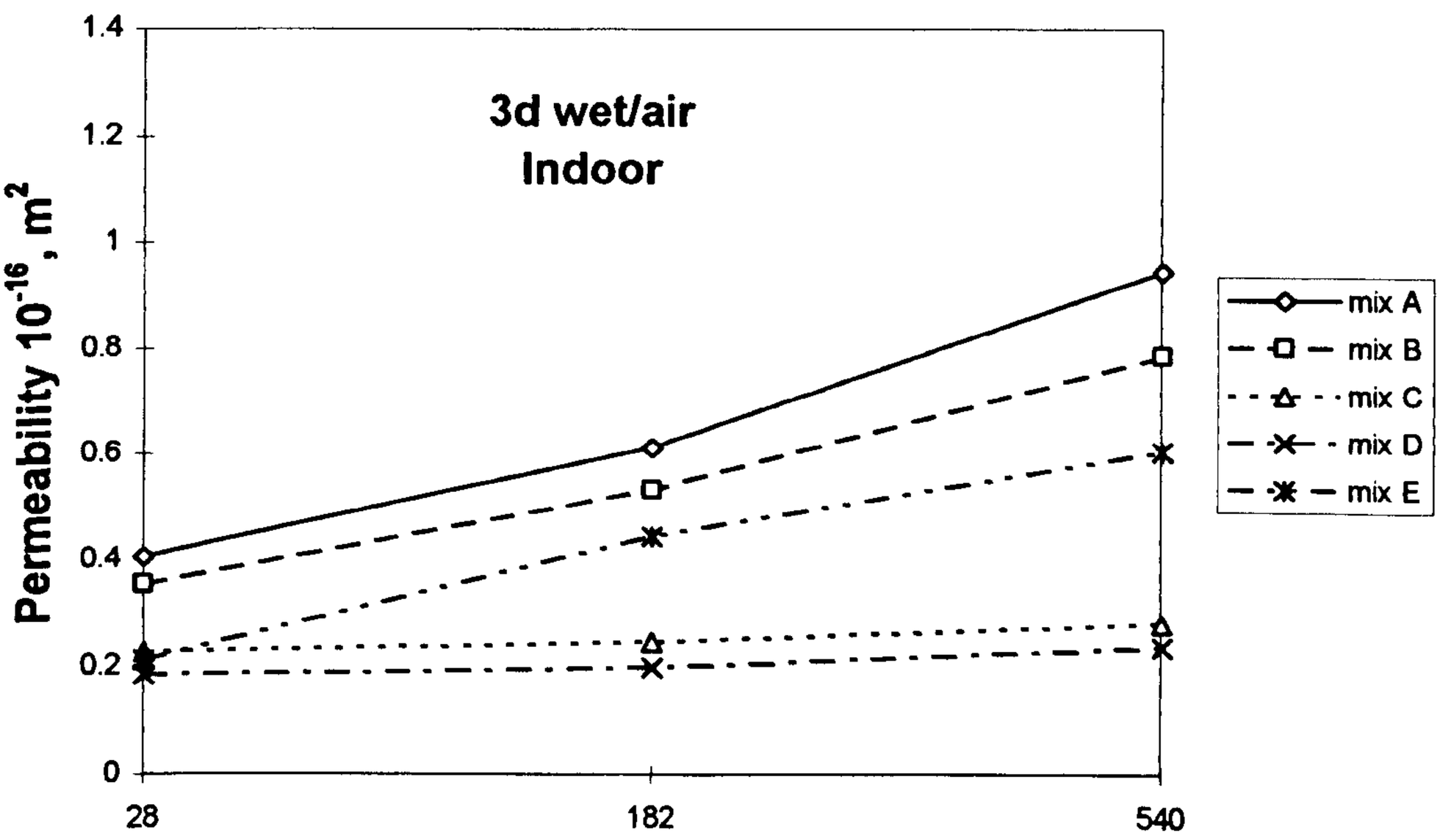

Fig. 7.7: Influence of mix type on oxygen permeability under 3d wet/air curing.

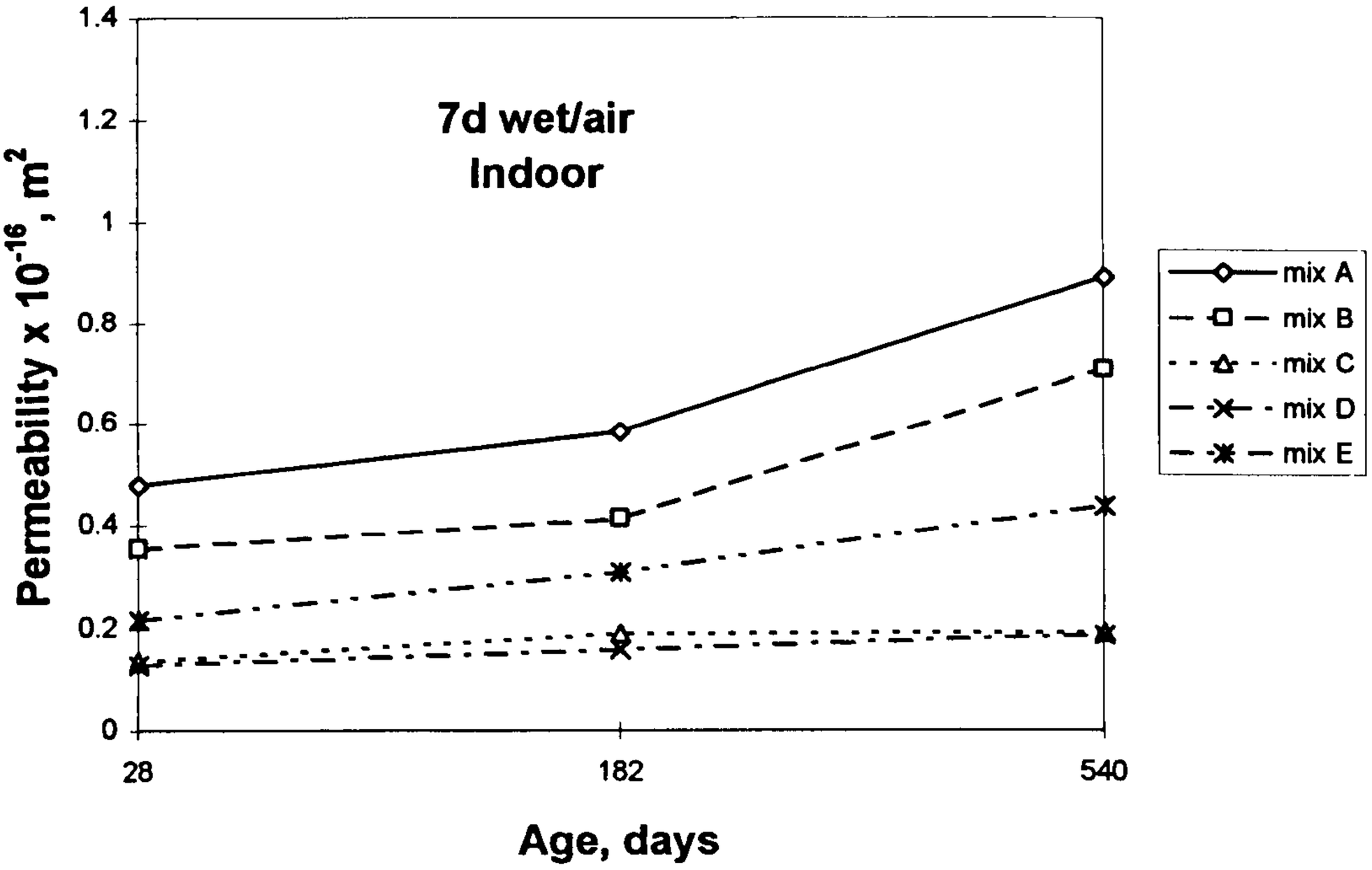

Fig. 7.8: Influence of mix type on oxygen permeability under 7d wet/air curing.

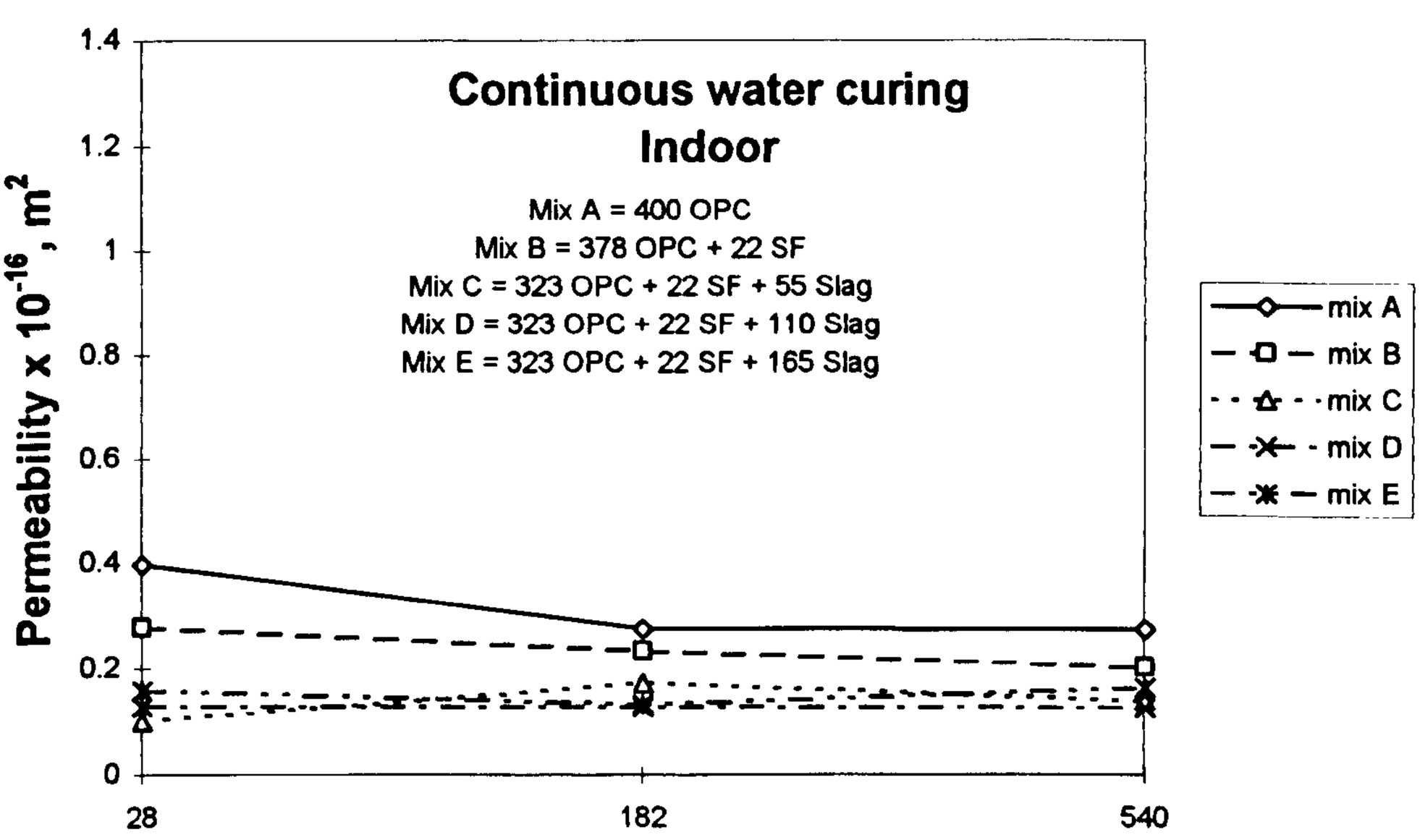

Fig. 7.9: Influence of mix type on oxygen permeability continuous water curing.

reached permeability values, about half of that of the control mix. Mix E with the highest amount of slag improved permeability significantly; as seen from the figure, it gained about 40% improvement compared with the control mix, which illustrates the importance of using slag to reduce the permeability of concrete. Also, it can be seen that mix E under continuous water curing shows a value of oxygen permeability greater than those of mixes containing limited amount of slag (mixes C and D). This probably indicates that the optimum slag content was obtained by mix D. This increase in the permeability of mix E may be due to its higher water content. As seen in the chapter 3, Table 3.5, all the mixes had fixed w/b ratio of 0.35; for the first three mixes the total cementitious material content was 400 kg/m^3, the corresponding value of the free water content is 140 l/m^3. On the other hand, the corresponding value of mixes D and E, which had total cementitious material contents of 455 and 510 kg/m^3 are 159 and 178.5 l/m^3 respectively; this increase in water content may have lead to high permeability.

All specimens made using slag or silica fume exhibited lower coefficient of oxygen permeability, especially for the 3 and 7 day water cured concrete, when compared to similar specimens made with OPC. However, there is significant improvement if the curing duration is raised to continuous water curing, as seen in mixes C, D and E.

Fig. 7.8 present results of oxygen permeability for specimens cured 7d in water then in air, it can be seen that the trend in oxygen permeability for 7d wet/air curing is similar to the trend obtained for 3d wet/air curing. At all ages the 7d wet/air curing yielded a permeability slightly better than mixes subjected to 3d wet/air curing, which illustrates the importance of early water curing on permeability.

Kasai et al [78] found that the higher the amount of GGBFS, the greater was the coefficient of air permeability than the OPC. On the other hand, others [79,157] showed that, for seven day cured samples which were tested at the end of curing period, specimens containing slag exhibited less permeability than the OPC [79].

The presence of silica fume (mix B) helps to enhance long term permeability; 26% improvement was seen for the oxygen permeability compared with the control mix. In the investigation by Grove and Markestad reported by Malhotra [128], water permeability tests were conducted on concretes with cement contents ranging from 100 to 500 kg/m^3. When 10% silica fume was incorporated in the concrete with 100 kg/m^3 cement, the permeability decreased from 1.6 x10^{-7} to 4.0 x10^{-10} m/s. The permeability of concrete containing 100 kg/m^3 cement and 20% silica fume was found to be

equivalent to that of a concrete containing 250 kg/m^3 portland cement without any silica fume.

It is generally agreed from the above observations that concrete mixes containing mineral admixtures have probably the greatest influence on concrete permeability, provided that adequate water curing at early ages is carried out. This is resulted from pore refinement leading to dense concrete. This pore refinement improves the impermeability of specimens containing cement replacement materials, Many researchers [10-13,128] attributed this decreases in the permeability due to pore refinement, occurring due to the conversion of $Ca(OH)_2$ by pozzolanic activity into a secondary calcium silicate hydrate (C-S-H) gel, which effectively fills up large voids in hydrated specimens; therefore pore interconnections will not be established, and the permeability will be reduced.

Besides the beneficial effect of mineral admixture on the permeability of hardened concrete, as discussed above, there is yet another component of the concrete microstructure (namely the transition zone between cement paste and aggregate particles) which is greatly strengthened by the use of mineral admixture. When using plain concrete without a mineral admixture, the bleeding will be much more, the internal sedimentation and bleeding effect in the vicinity the of aggregate particles will cause the transition zone to be porous and weak. A weak transition zone is vulnerable to microcracking easily when the concrete is subjected to the environment stresses (i.e. thermal and humidity cycles) [35].

7.3.3 Effect of exposure environment

The results of oxygen permeability tests of control, OPC/SF and OPC/SF/slag concrete mixes, in both environments, indoor as well as outdoor, subjected to four curing regime, are summarized in the series of Figs. 7.10-7.18 and Table 7.1. The permeability results shown indicate that there are significant differences arising from the type of exposure for all concrete mixes. However, the five mixes show similar trends but with different magnitudes of oxygen permeability. An increase in the curing temperature promotes an increase of permeability coefficient. This effect is more pronounced for air-cured specimens than for specimens cured in water, because of the higher amount of water evaporated do to air curing. To obtain good concrete, the placing of an appropriate mix must be followed by water curing in a suitable environment during the early stages of hardening. The necessity of curing arises from the fact that hydration of

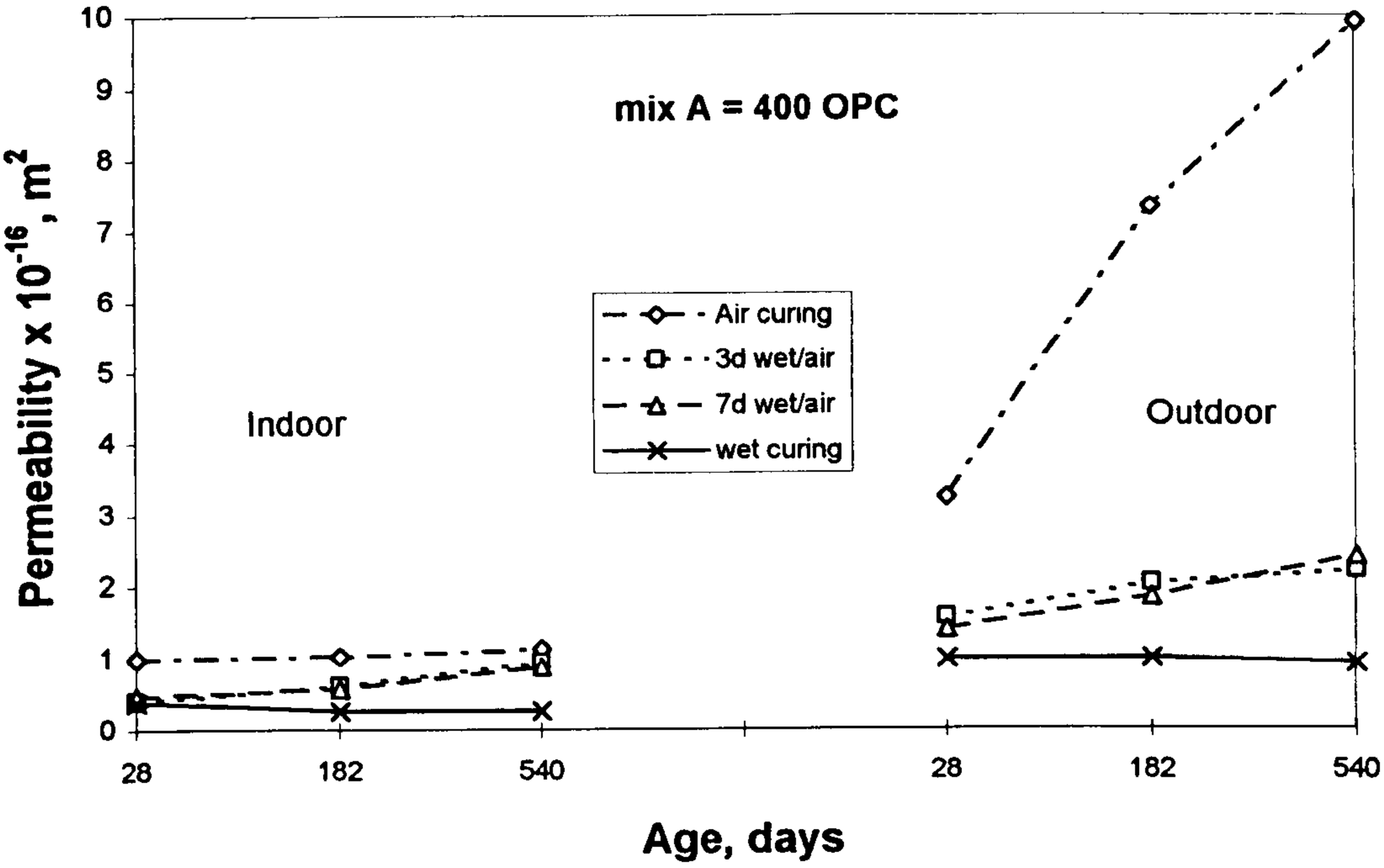

Fig. 7.10 Influence of curing regime on oxygen permeability for mix A.

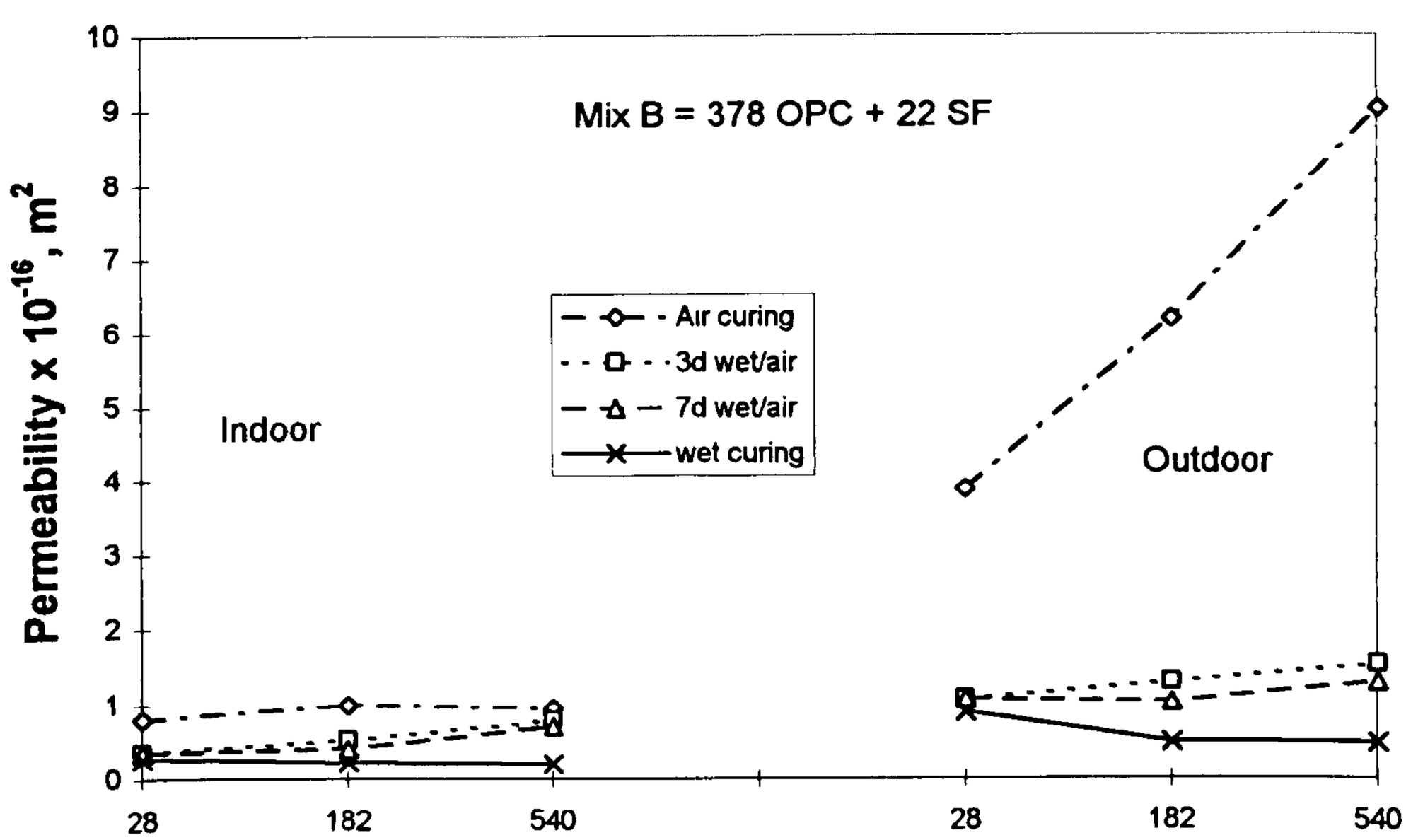

Fig. 7.11 Influence of curing regime on oxygen permeability for mix B.

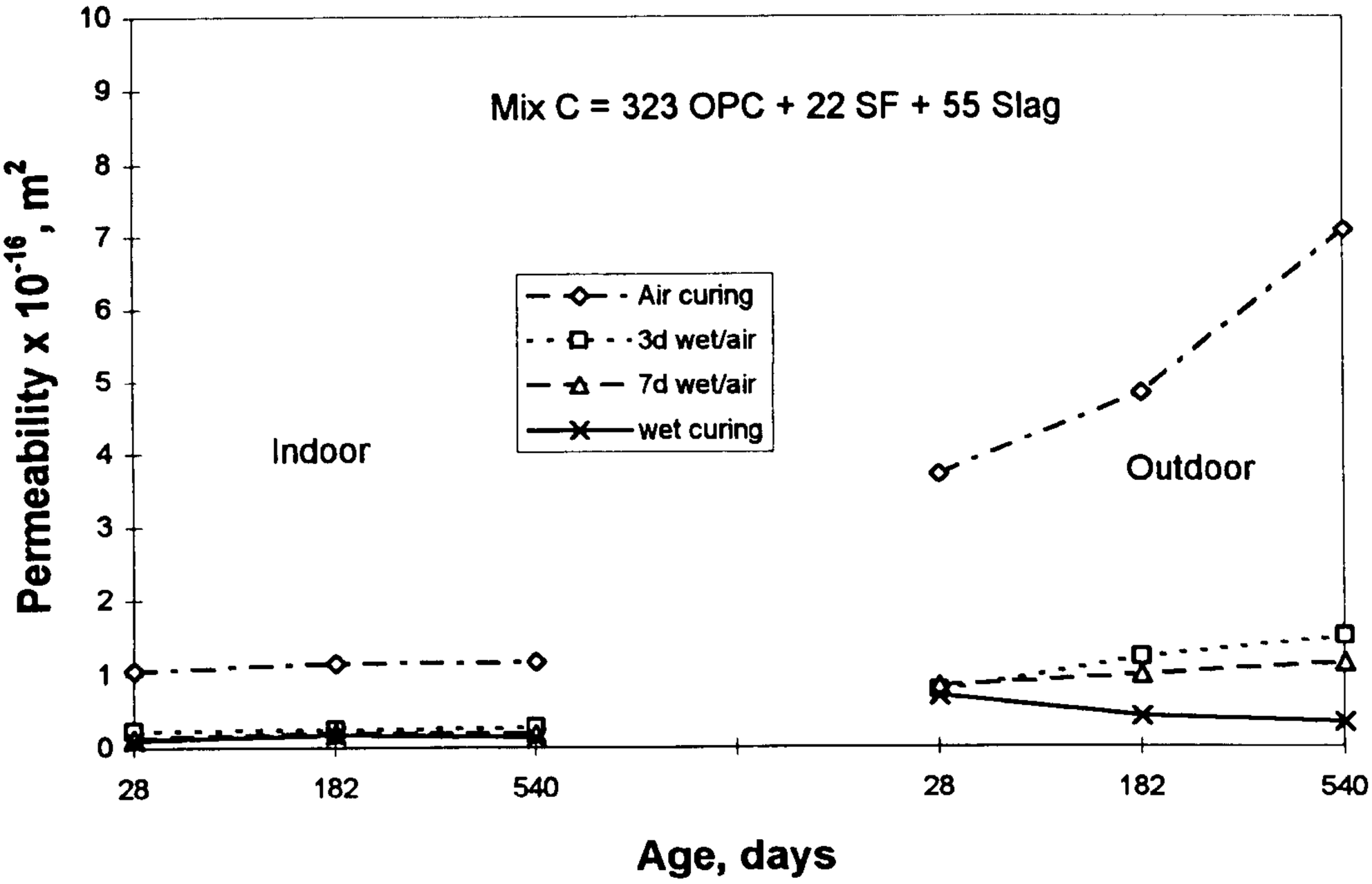

Fig. 7.12 Influence of curing regime on oxygen permeability for mix C.

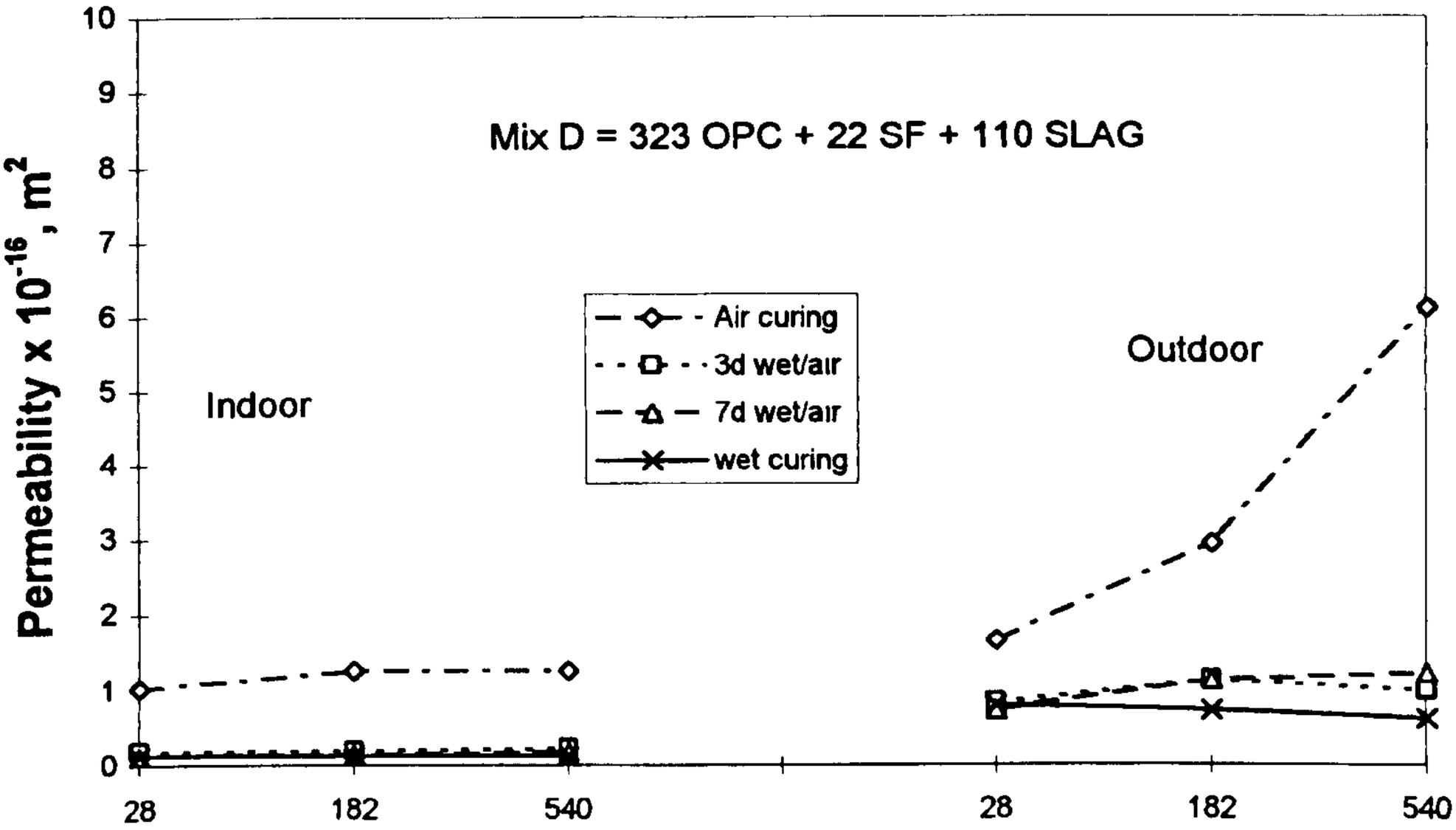

Fig. 7.13 Influence of curing regime on oxygen permeability for mix D.

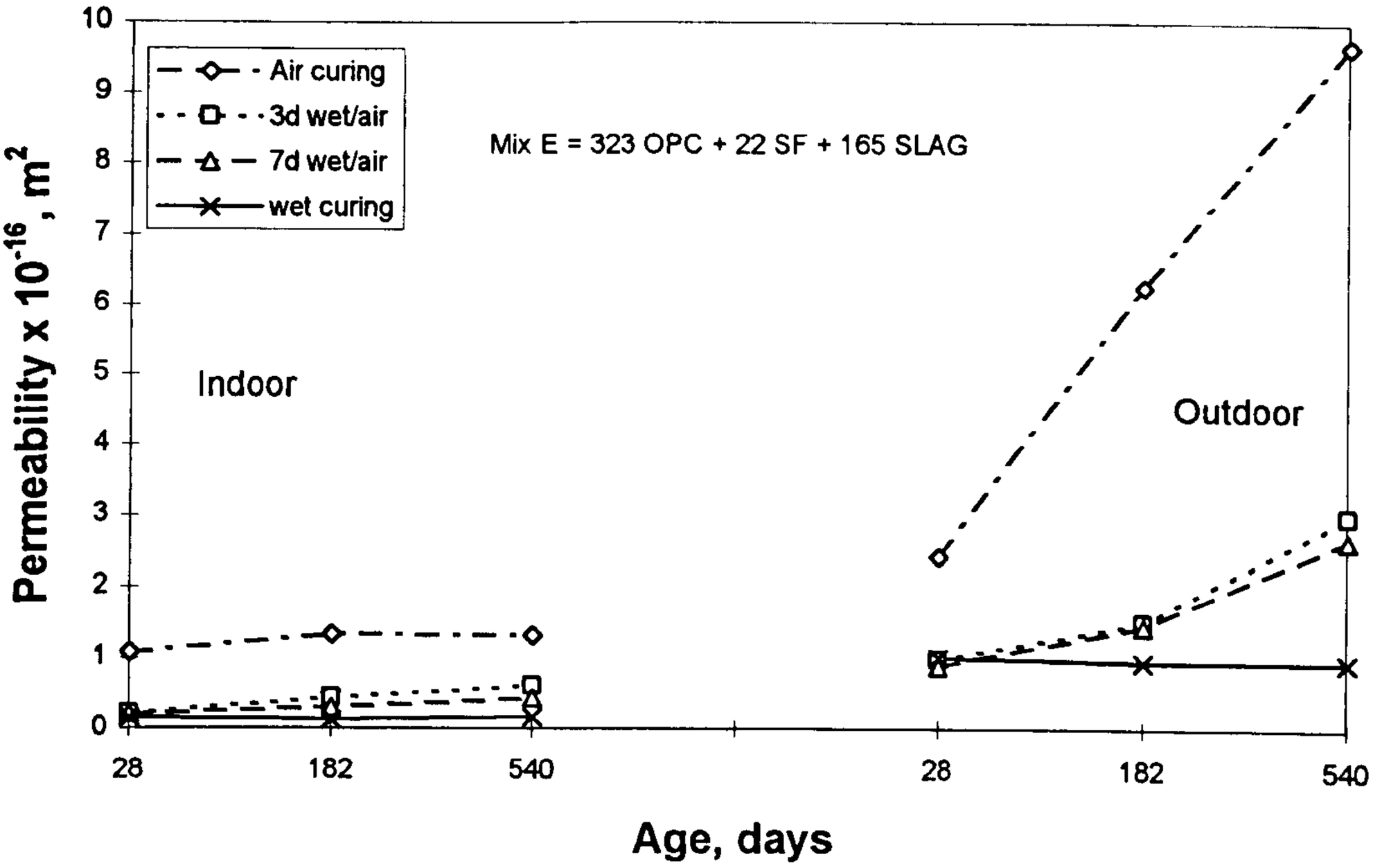

Fig. 7.14 Influence of curing regime on oxygen permeability for mix E.

cement can take place satisfactorily only if concrete is kept moist. For this reason, the loss of water by evaporation from the concrete must be prevented, specially in the Arabian Gulf environment.

Fig. 7.15 shows the influence of exposure environment on oxygen permeability under air curing. It can be seen that dramatic increases in permeability occur in the outdoor specimens compared with indoor environment specimens. For example, at the age of 18 months in the outdoor environment, mix A exhibited a permeability value of concrete higher than the corresponding value in the indoor by a factor of 9. The corresponding values for oxygen permeability of mixes B, C, D and E in the outdoor environment were higher than that in the indoor by factors of 9, 6, 5 and 7 respectively. This dramatic increase in the permeability for the outdoor specimens is attributed to the severs drying immediately after casting, as well as to the daily cycles of thermal expansion, (as clearly discussed in the chapter 5); these factors may induce microcracking, and modify the large pores (as seen in chapter 6 Figs. 6.34-6.37). These changes in microstructure obviously lead to higher permeability values.

Generally, it is accepted by many researchers [1,5,6] that permeability would increase with increasing temperature of curing; as a result of this, water will evaporate from the specimens, and hydration will stop, which will lead to increased continuity of the large pores as they do not become filled with hydration products.

Figs. 7.16-7.17 show the influence of exposure environment on the oxygen permeability of specimens subjected to 3d wet/air and 7d wet/air curing. Both figures present similar trends of exposure environment on the mix type. In general, the control mix specimens exhibited the highest values of oxygen permeability at all ages and in both environments. The effect of hot environment is more clear, and outdoor environment is more severe on the plain concrete. For example, mix A (400 OPC) specimens in the indoor presented for 3d and 7d wet/air curing values, very close to the other mixes (mixes B, C and D), while in the outdoor environment, the difference was much more than that for the other mixes (mixes B, C and D) for both curing regimes. However, mixes D, C and B in the outdoor environment present much lower values than those of mix A and mix E. For example, specimens at the age of 18 months, cured 7d wet/air in the outdoor, showed values of 1.224×10^{-16}, 1.144×10^{-16} and 1.295×10^{-16} m^2 for mixes D, C and B respectively; the corresponding values for mixes A and E were 2.399 and 2.666×10^{-16} m^2 respectively, which are about twice of former. This also indicates that increases in slag content up to 33% (mix E) increases the permeability in the long term (as seen in Figs. 7.16-7.17). This increase in permeability may be attributed to the fact that mixes containing slag in large amounts (165 kg/m^3) need more water to continue the pozolanic reaction. When the specimens are taken out from the water tank at 3 days or even at 7 days, and then are subjected to drying in hot environments, the specimens lose their moisture within few hours. This causes a lack of water to continue the hydration process. In the other mixes containing limited amounts of slag (55 or 110), this increases did not appear.

It is interesting to see that mix B specimens (378 OPC + 22 SF), subjected to 7d wet/air curing in the outdoor, showed values about one half of the corresponding value of the control mix at the age of 18 months, which means that the performance of mix B is better than that of mix A in the outdoor environment. For example, at the age of 18 months in the indoor environment, mix B exhibited values of 0.787×10^{-16} and 0.708×10^{-16} m^2 for 3d wet/air and 7d wet/air curing respectively; the corresponding values of permeability in the outdoor were generally higher than that in the indoor by a factor of two 1.519×10^{-16} and 1.295×10^{-16} m^2. On the other hand, the corresponding values of mix A in the same environment were increased by 30 and 46% than the corresponding values of mix B for the same curing regimes respectively, which indicates that the presence of silica fume helps to enhance early and long term permeability.

Fig. 7.18 shows a comparison of oxygen permeability for specimens cured continuously in water and subjected to the both environments, indoor as well as outdoor. These results show that even when the specimens are cured continuously in water in the outdoor environment, they develops higher permeability values than the corresponding specimens cured in the indoor environment. For example, the specimens of the control mix (400 OPC) at the age of 18 months in the outdoor environment presented a value of 0.913×10^{-16} m^2; this is generally higher than the permeability of the corresponding concrete in the indoor environment by about three times, namely, 0.274×10^{-16} m^2. On the other hand, mixes D and E specimens also shows higher permeability values in the outdoor than indoor, which is about five and six times more than the corresponding values in the indoor environment respectively. However, mix D even through it had a high increase in permeability in the outdoor environment, it is still lower than the corresponding value of the control mix. The corresponding values of mixes D and A were 0.617×10^{-16} and 0.913×10^{-16} m^2 respectively. Mixes B and C show much lower values in the hot environment in the long term compared with the other mixes, but it is greater than the corresponding values in the indoor environment; these values increased by a factor of two-namely, values of 0.477×10^{-16} and 0.327×10^{-16} m^2 in the outdoor compared to values in the indoor of 0.202×10^{-16} and 0.139×10^{-16} m^2 respectively. Mix C specimens presented the lowest value of permeability compared with the other four mixes in the outdoor environment at all ages.

This increase in oxygen permeability in the outdoor environment for mixes cured continuously in water can be attributed to the fact that the specimens after casting were put immediately in the outdoor environment exposed to solar radiation and high ambient temperature. This temperature rises to 60°C on specimens surfaces, accompanied by relative humidity values of 55% at mid day, and then dropping to 30°C + 90% RH at night. This high temperature and also high variation in the temperature and humidity when the concrete is in the plastic stage led to accelerated setting, and accelerated the hydration, causing high evaporation of the water from the specimens at first day, causing adverse effects on the specimen durability in the long term.

Goto et al [1] have studied the effect of temperature on permeability; they found that the permeability of samples cured at 60°C was higher than of those cured at 27°C for the same mix concrete. This observation was due to the larger diameter pores resulting from the high temperatures.

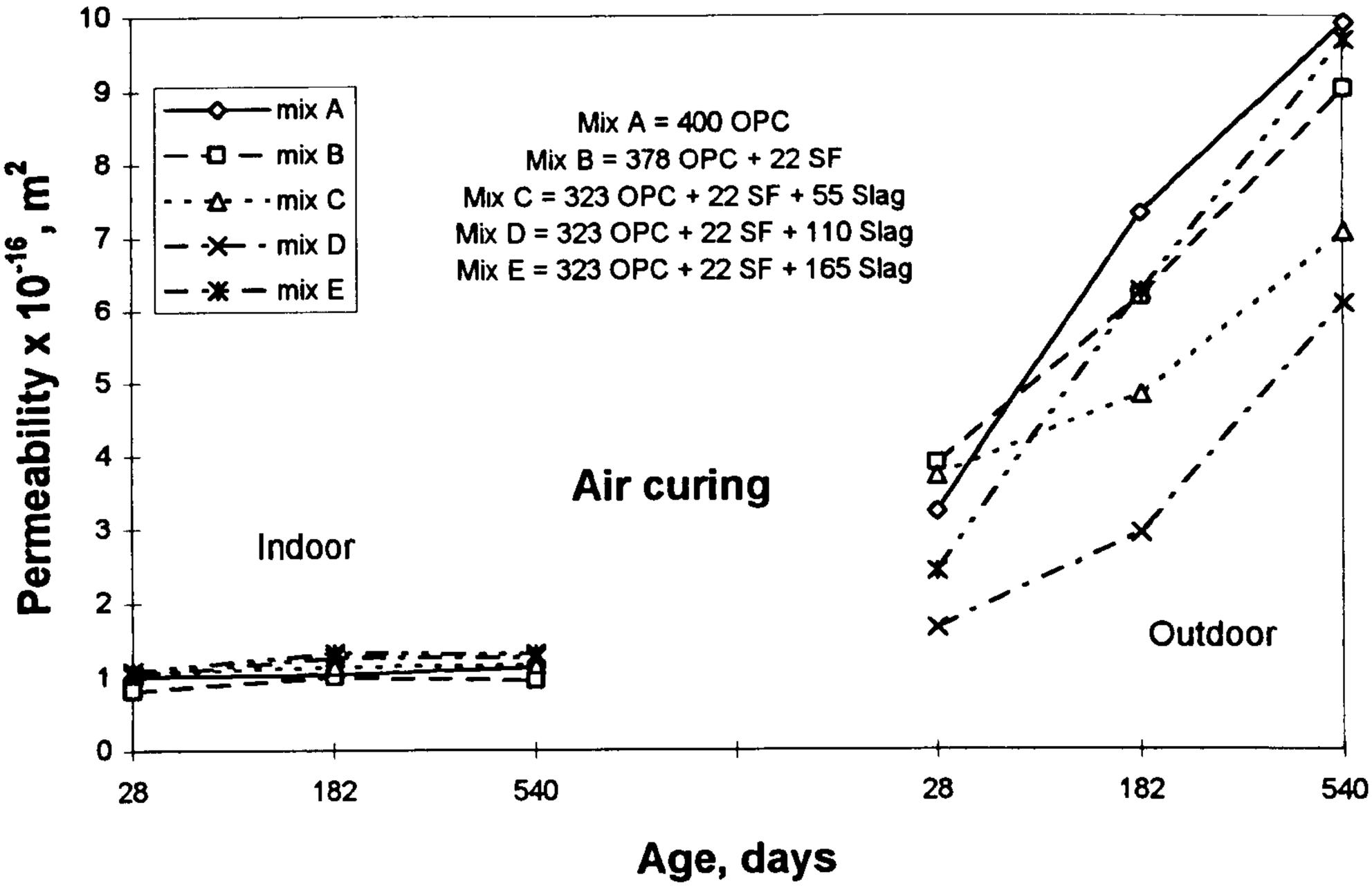

Fig. 7.15 Influence of mix type on oxygen permeability under air curing.

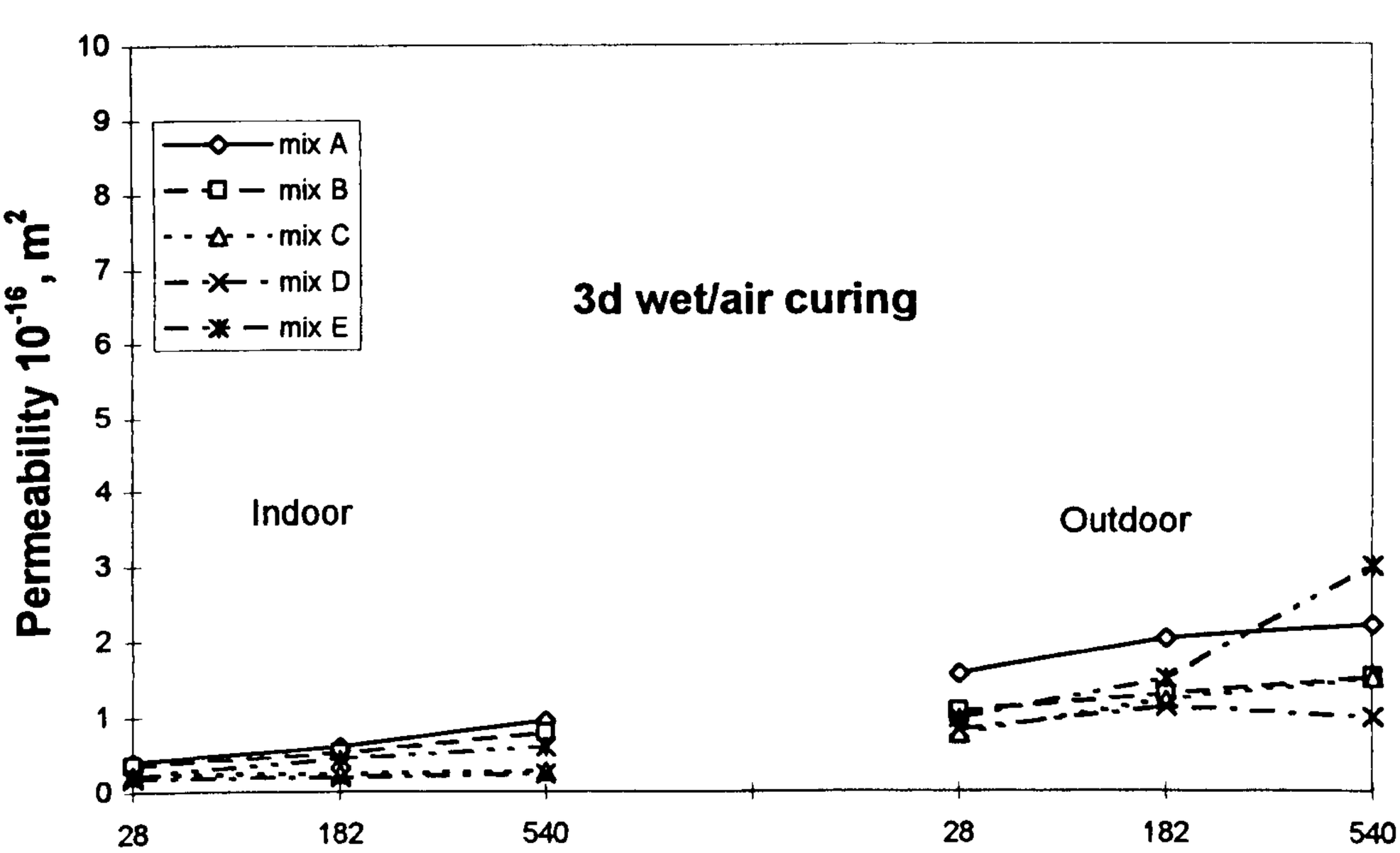

Fig. 7.16 Influence of mix type on oxygen permeability under 3d wet/air curing.

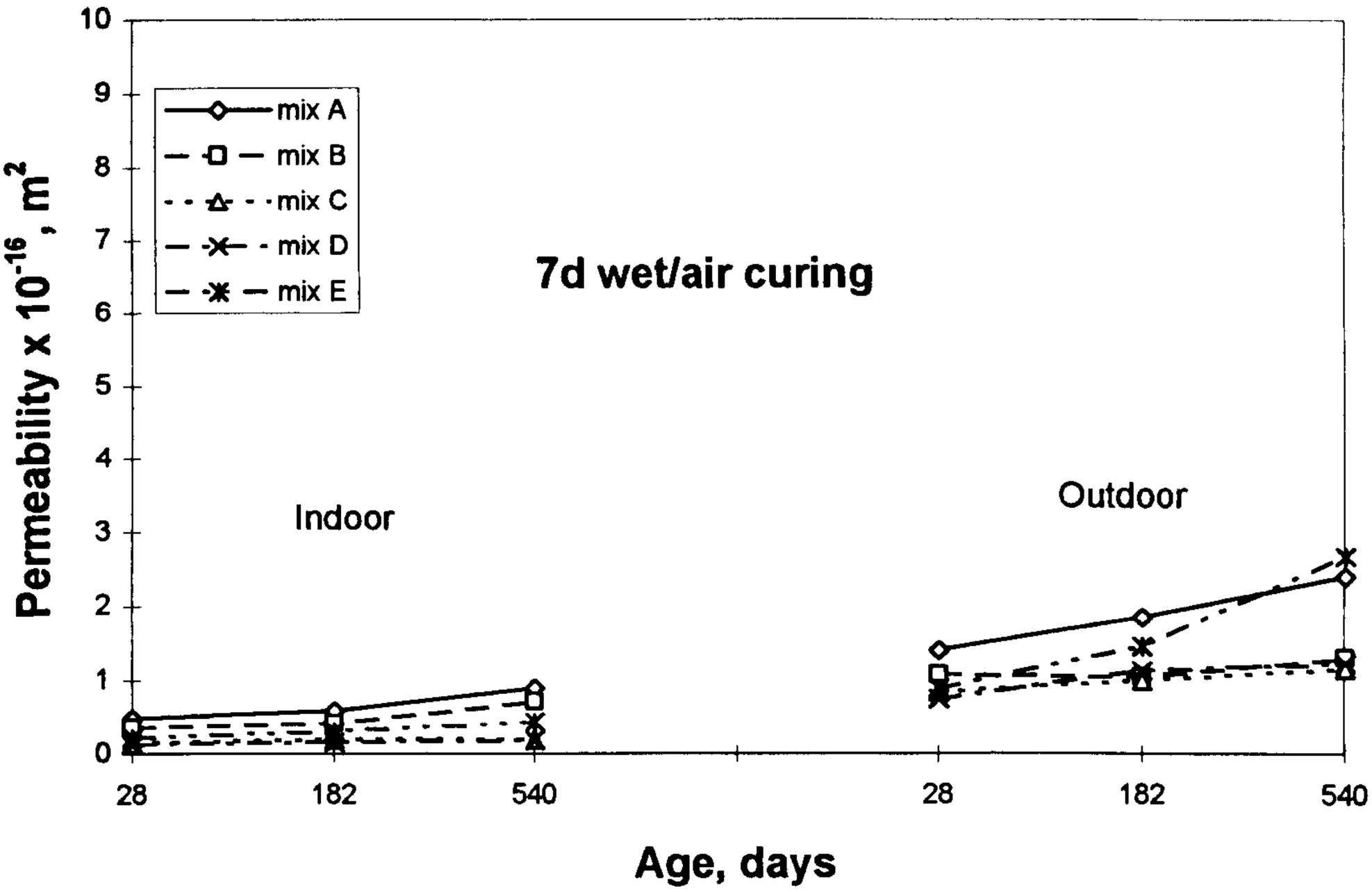

Fig. 7.17 Influence of mix type on oxygen permeability under 7d wet/air curing.

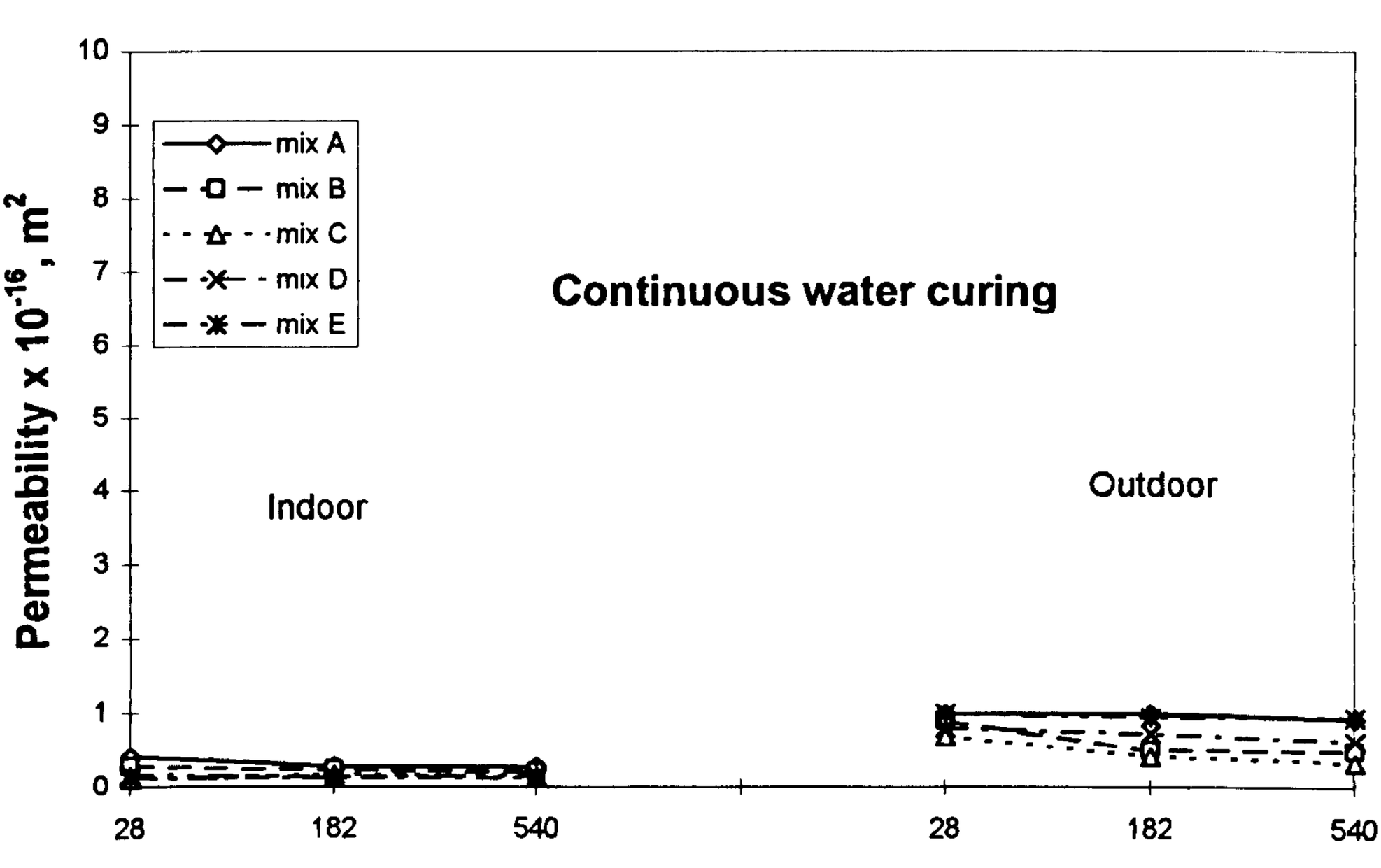

Fig. 7.18 Influence of mix type on oxygen permeability under wet curing.

Malhotra reported an investigation done by Skurdal [128] who observed in an investigation of the effect curing of concretes, with and without silica fume, that elevated temperatures resulted in increased permeability. The reference concrete and the concrete containing 10% silica fume were cured at 20°C. The permeability coefficients for these concretes were found to be 7.2 $x10^{-13}$ for the reference concrete and $0.5x10^{-13}$ m/s for silica fume concrete. When cured at a temperature of 30°C, the permeability coefficients were 27 $x10^{-13}$ and 0.8 $x10^{-13}$ m/s for reference and silica fume concretes respectively. At 50°C curing, the permeability coefficients were 90 $x10^{-13}$ and 74 $x10^{-13}$ for reference and silica fume concrete respectively. In all the different curing regime, the silica fume concrete had consistently lower permeability values than the reference concrete.

There are factors other than the characteristics of concrete materials and mix proportions which govern the permeability of concrete. Most of these factors occur in Arabian Gulf region which are known as environmental factors these factors involve solar radiation, high ambient temperature, high materials temperature, salt saturated humidity, thermal cycles etc. The areas of microstructural inhomogeneity turn out to be the potential sites for crack initiation. The incorporation of mineral admixture into superplasticized concrete mixture provide an excellent solution to the bleeding problem, it is almost imperative to use a mineral admixture in combination with high range water reducer whenever the durability of concrete is of primary concern. As seen above, mix C under 7d wet/air curing, which is the curing method usually used in the Arabian Gulf region, improves the permeability of concrete in the long term by about two orders of magnitude. It should be noted that, when their quality and quantity in a concrete mixture are adequate, the mineral admixtures not only have the ability to enhance the workability and the impermeability but also the resistance of concrete to cracking by thermal stresses due to heat of hydration in deep members, thermal cycles, chloride ingress and sulfate attack.

7.3.4 Effect of exposure time

The effect of age on oxygen permeability of control and blended cement concrete specimens, in both environments, indoor as well as outdoor environment, subjected to the four curing regime are presented in the following series of Figs. 7.10-7.18. The permeability of specimens cured in air, 3d wet/air and 7d wet/air show significant increases in permeability with age in the outdoor environment. As seen from Fig. 7.15,

this effect is more critical when specimens are cured in air. These values increased from 3.235 $x10^{-16}$ m^2 at age of 28 days by about two to three orders in magnitude at the ages of 6 and 18 months. On the other hand, the same figure presents the results for the indoor environment; it is clear that; the effect of the age in the indoor exposure is much lower than that in the outdoor for the same curing regime. For example, the values of mix A specimens at the age of 28 days increased from $0.992 x10^{-16}$ to $1.030 x10^{-16}$ and $1.136x10^{-16}$ m^2 at the ages of 6 and 18 months respectively. Similar results have been found for pore structure, ultrasonic pulse velocity and dynamic modulus of elasticity. This may be attributed to the fact that shrinkage cracks were generated in the long term, for specimens cured in air, or dried in air after a certain period of curing in water.

Fig. 7.16 shows the effect of replacement material on oxygen permeability of specimens subjected to 3d wet/air curing; it is clear from this figure that at the age of 28 days in the indoor environment all specimens present small values compared with the values at 18 months. The values of permeability obtained at 18 moths for mixes A, B and E are much higher than those at 28 days, these increases being about twice. On the other hand, mixes C and D showed very little change in oxygen permeability compared with specimens at 28 days of age; this might be attributed to increase in the denseness of such concrete arising from addition of a limited amount of slag, resulting in the transformation of large pores into fine pores and causing pore refinement, while the specimens of mix E need more time to develop its microstructure.

Also, Table 7.1 shows significant increase in permeability due to effect of age; as seen, mix A specimens dried continuously in air at the age of 18 months in the outdoor presented values about three times of the corresponding value at 28 days. The corresponding values for mix B and mix C were increased by about two orders of magnitude. On the other hand, mix D and mix E exhibited much higher values of permeability at 18 months in the outdoor, about four times the corresponding values at 28 days.

It is clear from Fig. 7.18 and Table 7.1 that most of specimens cured continuously in water, exhibited very little decrease in permeability with increasing age from 28 days to 6 months, but that there was no significant change between the ages of 6 months and 18 months. Similar trends have been observed by others [78,159] Kasai et al [78] investigated specimens of OPC and slag under three curing regime, namely, air curing, 3d wet/air and 7d wet/air curing. Significant increases were observed for air

permeability for specimens at the age of 3 months compared with specimens at age of 1 month. Also Sanjuan et al [159] investigated the variation of concrete permeability with time. Air permeability results recorded for 20 years in 0.2 m^3 concrete slabs are presented in these studies. It was found that the air permeability coefficient increases with time, reaching an almost stable value after 20 years. To clearly distinguish the reason for such observation, three different regions with time were divided, 0-4, 4-12 and 12-20 years. During the first region, several chemical and physical processes occur simultaneously: cement paste hydration, carbonation, drying out and shrinkage of the concrete which induces its microcracking. The drying shrinkage and microcracking processes led to great increase in permeability during the first 4 years of testing.

Other studies [78,160] show that permeability decreases with age. For example, Cabrera et al [71] investigated the effect of mix variables and age on oxygen permeability. The results obtained show clearly the sensitivity of the change taking place due to mix composition and age; high decreases in permeability was observed during the first week, while, on the other hand, very little decreases was found between the period of 1-3 months.

Dhir et al [160] reported the results of the effect of air curing on permeability compared with continuous water curing. These show that air curing significantly increases the permeability of concrete, and that this increases with age when tested at 28 days and 180 days. Continuous water curing showed that, contrary to the air curing, samples at the age of 18 months exhibited little decrease in permeability compared with those at age of 28 days.

7.3.5 Relationship between permeability and pore structure

Many researchers have attempted to correlate permeability to different parameters representing the pore structure of concrete [10,107,111,112,161,162]. For example Mehta [111] reported that a correlation is found between the permeability of cement paste and the volume of pores greater than 0.132 μm diameter. Also, in other studies [107,112,162], the threshold diameter is used to correlate the pore structure of concrete to its permeability.

In this study, an attempt has been made to examine if a relationship exists between oxygen permeability and the pore structure parameters; the parameters considered include coarse pore volume (pores >0.100 μm), threshold diameter and maximum continuous pore diameter.

Reasonable correlation coefficients (R^2) between oxygen permeability and the pore structure parameters were found. These correlation coefficients are shown in Figs. 7. 19 -7.21. The following power equation was used to establish quantitative relations:

$$k = aP^b \tag{7.1}$$

where

k = Oxygen permeability, m^2

P = pore structure parameter

a and b are constants related to the properties of the concrete and the materials in the each mix.

Table 7.2 shows the correlation coefficients obtained between oxygen permeability and the different variables defined from the mercury porosimetry data. The results imply that the maximum continuous pore diameter has the more important effect on permeability. Examination of the correlation coefficients in Table 7.2 indicates that the highest and significant correlation occurred with the maximum continuous pore diameter. However, significant correlations also existed with the threshold diameter and the volume of pores larger than 0.100 μm. Figs. 7.19-7.21 show the scattergraphs of the relationships between oxygen permeability and the pore structure variables. Their regression analysis equations also are shown in the corresponding figures and Table 7.2.

Table 7.2: Relationship between oxygen permeability and pore structure.

Pore structure variable	Equation	R^2
Coarse pore volume (pore>0.100 μm), ml/g	$k = 1112(P_{cr})^{1.58}$	0.73
Threshold diameter, μm	$k = 9.76(d_{th})^{1.01}$	0.74
Maximum continuous pore diameter, μm	$k = 27.05(d_{con})^{1.14}$	0.81

These variables have correlation factors ranging from 0.73 to 0.81, emphasizing the reasonable relationship between permeability and pore structure. These results mean that the coarse pore volume, threshold diameter and maximum continuous pore diameter are all importants factor affecting permeability, but they are not the only factors. For cementitious materials, the pore space can be generally divided into capillary pores and gel pores. These pores are in a continuous dynamic change in geometry and connectivity as the hydration of the matrix is continuous with time. For gas flow through cementitious materials, only the connected capillary pores dominate the flow [79].

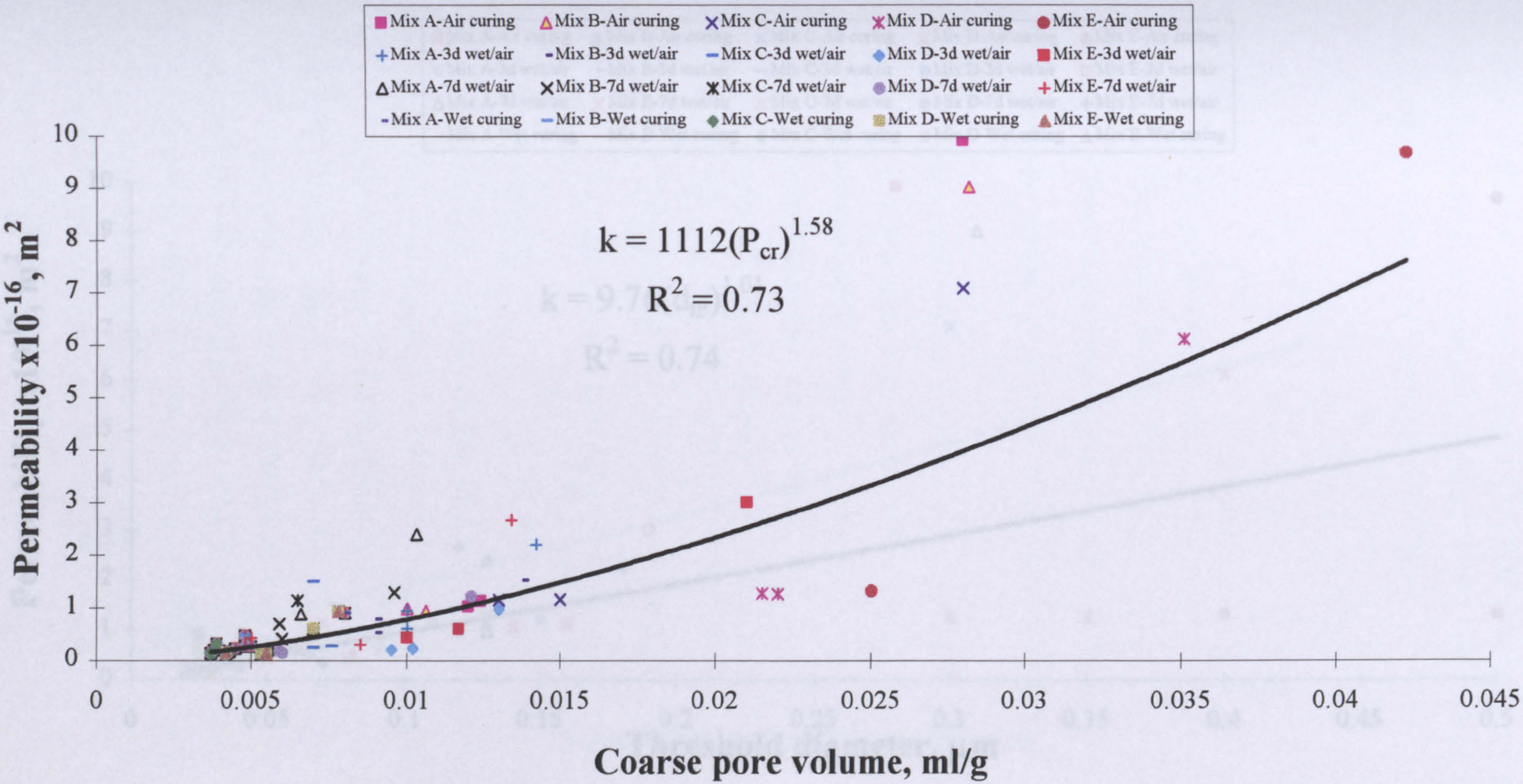

Fig. 7.19 : Relationship between oxygen permeability and coarse pore volume.

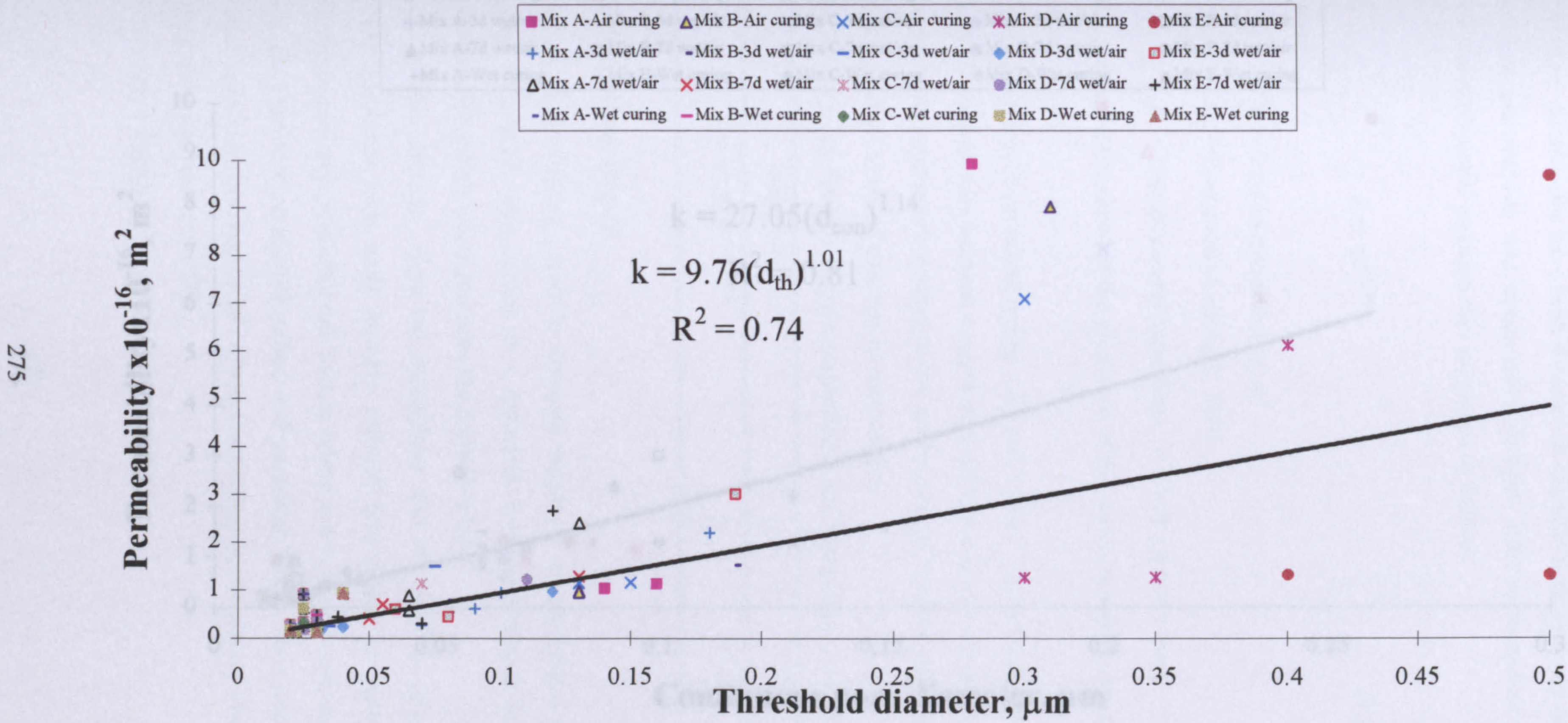

Fig. 7.20 : Relationship between oxygen permeability and threshold diameter.

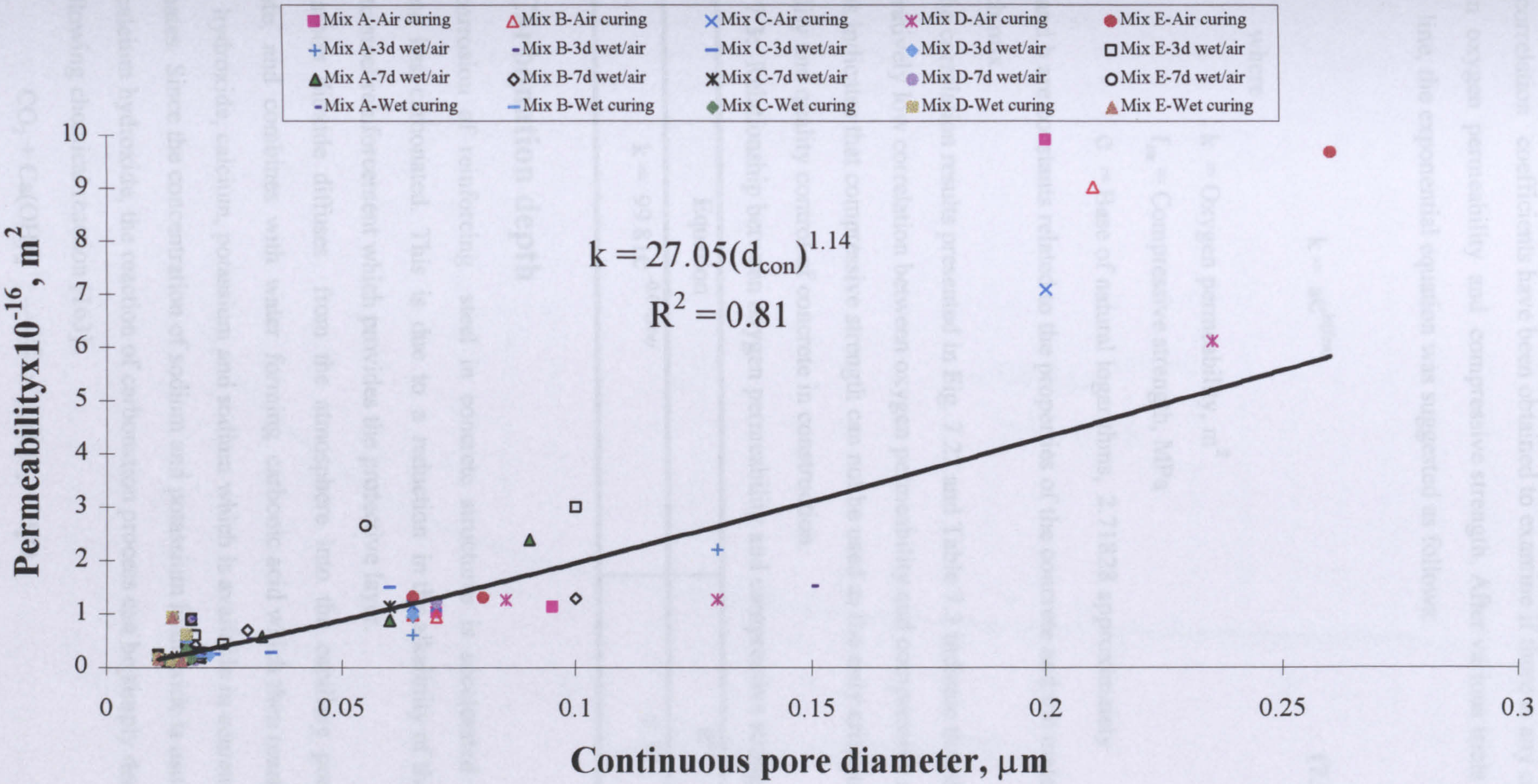

Fig. 7.21: Relationship between oxygen permeability and continuous pore diameter.

7.3.6 Relationship between permeability and compressive strength

Also, correlation coefficients have been obtained to examine if there is any correlation between oxygen permeability and compressive strength. After various trials to get the best fit line, the exponential equation was suggested as follows:

$$k = ae^{b(f_{cu})} \tag{7.2}$$

where

k = Oxygen permeability, m^2

f_{cu} = Compressive strength, MPa

e = Base of natural logarithms, 2.71828 approximately

a and b are constants related to the properties of the concrete and the materials in the each mix.

The correlation results presented in Fig. 7.22 and Table 7.3 indicate that there is comparatively low correlation between oxygen permeability and compressive strength, and this indicates that compressive strength can not be used as the only criterion for the durability and quality control of concrete in construction.

Table 7.3: Relationship between oxygen permeability and compressive strength

Equation	R^2
$k = 99.81e^{-0.07(f_{cu})}$	0.58

7.4 Carbonation depth

The corrosion of reinforcing steel in concrete structures is accelerated when the concrete has carbonated. This is due to a reduction in the alkalinity of the concrete cover to steel reinforcement which provides the protective layer.

Carbon dioxide diffuses from the atmosphere into the capillary pores of the concrete, and combines with water forming carbonic acid which then reacts with the alkali hydroxide, calcium, potassium and sodium which is available in cement, forming carbonates. Since the concentration of sodium and potassium hydroxide is usually lower than calcium hydroxide, the reaction of carbonation process can be simply described by the following chemical reaction [163]:

$$CO_2 + Ca(OH)_2 \xrightarrow{H_2O} CaCO_3 + H_2O \tag{7.3}$$

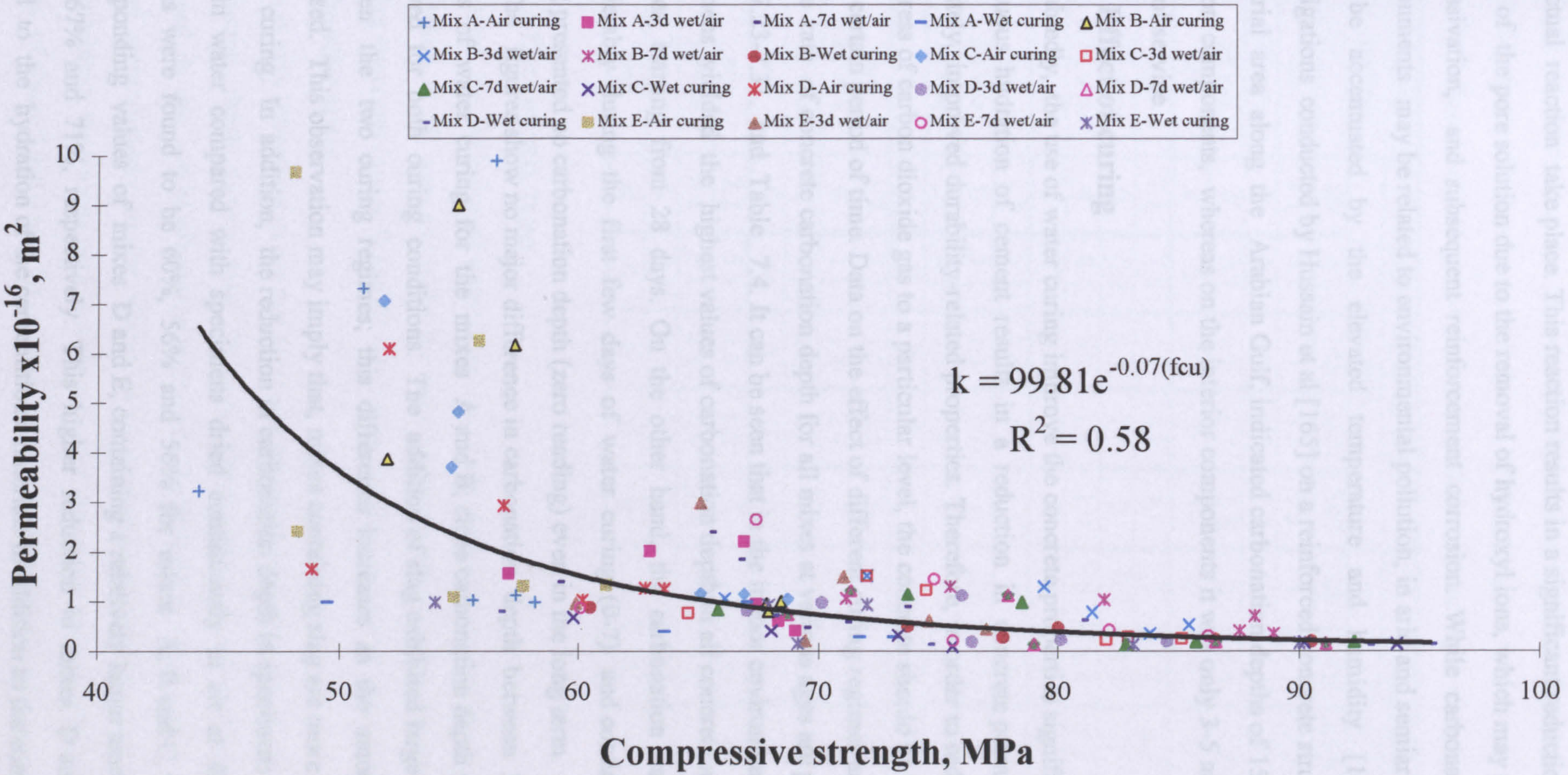

Fig. 7.22 : Relationship between oxygen permeability and compressive strength .

The above equation represents only the final result of several steps through which the actual reaction take place. This reaction results in a significant reduction in the pH value of the pore solution due to the removal of hydroxyl ions, which may lead to steel despassivation, and subsequent reinforcement corrosion. While carbonation in hot environments may be related to environmental pollution, in arid and semiarid regions it may be accentuated by the elevated temperature and humidity [164]. In-situ investigations conducted by Hussain et al [165] on a reinforced concrete structure, in an industrial area along the Arabian Gulf, indicated carbonation depths of 15 mm on the exterior components, whereas on the interior components it was only 3-5 mm, after six years of service.

7.4.1 Effect of curing

Undoubtedly, the use of water curing improve the concrete properties significantly. The continuous hydration of cement results in a reduction in concrete permeability and ultimately, improved durability-related properties. Therefore, in order to reduce the rate of ingress of carbon dioxide gas to a particular level, the concrete should be water cured for a certain period of time. Data on the effect of different curing regimes and mix type on the rate of concrete carbonation depth for all mixes at various ages are presented in Figs 7.23-7.31. and Table 7.4. It can be seen that in the indoor environment air-cured specimens yielded the highest values of carbonation depth in all concrete mixes and at all ages, starting from 28 days. On the other hand, the carbonation rates reduced considerably during the first few days of water curing (0-7) and continuous water curing presented no carbonation depth (zero reading) even in the long term.

The figures show no major difference in carbonation depth between 3 days and 7 days of water curing for the mixes A and B; close carbonation depth values were observed for both curing conditions. The addition of slag exhibited large differences between the two curing regimes; this difference increases as the amount of slag increased. This observation may imply that, mixes containing slag are more sensitive to water curing. In addition, the reduction in carbonation depth in specimens cured for 7 days in water compared with specimens dried continuously in air at the age of 18 months were found to be 60%, 56% and 56% for mixes A, B and C, whereas the corresponding values of mixes D and E, containing a relatively larger amount of slag, were 67% and 71%, respectively. This higher reduction in mixes D and E may be related to the hydration of the cementitious materials in addition to the continued slag

hydration at later ages. Air dried specimens of mix E at the age of 28 days showed that, the depth of carbonation was considerably higher than the value recorded at 18 months for specimens cured 7 days in water followed by air-curing.

Table 7.4 Influence of curing and exposure condition on the depth of carbonation, mm.

Mix	Curing regime	Indoor environment					Outdoor environment				
		Age, days					Age, days				
		28	91	182	365	540	28	91	182	365	540
	air	1.1	1.2	2.1	3.5	3.8	1	1.3	2.5	3.5	4.2
A	3d w/a	0	0.2	0.3	1.5	1.8	0.4	0.5	2	2	2.5
	7d w/a	0	0.1	0.2	1.2	1.5	0	0.4	1.5	1.6	2
	wet	0	0	0	0	0	0	0	0	0	0
	air	1.1	1.5	2.1	3.3	4.3	1	1.7	2.5	3.5	4.1
B	3d w/a	0	0.2	0.3	1.5	2	0.3	0.7	2	2	2.8
	7d w/a	0	0.1	0.2	1.4	1.9	0	0.4	1.5	1.5	2
	wet	0	0	0	0	0	0	0	0	0	0
	air	1.1	1.7	2.4	3.5	4.5	1	2	3	3.5	4.2
C	3d w/a	0	1.1	1.3	2.7	3	0.4	1.3	2	2	2.5
	7d w/a	0	0.1	0.3	1.9	2	0	0.6	1.5	1.5	2
	wet	0	0	0	0	0	0	0	0	0	0
	air	1.7	2.7	3.7	4.5	6	1	2	3	3.5	4.8
D	3d w/a	0	1.1	1.8	2.4	3	0.4	1.3	2	2	2.3
	7d w/a	0	0.1	0.5	1.7	2	0	0.6	1.5	1.5	2
	wet	0	0	0	0	0	0	0	0	0	0
	air	2.2	3.1	4.6	5.8	7	1	2	3	4.7	6
E	3d w/a	0.4	1.1	2.1	2.8	3.5	0.4	1.4	2	2.7	3.5
	7d w/a	0	0.1	0.7	1.7	2	0	0.9	1.5	2	2.5
	wet	0	0	0	0	0	0	0	0	0	0

7.4.2 Effect of mix type

In general the inclusion of a small amount of silica fume had no effect on the depth of carbonation at all ages and under the different curing regime when compared with mix A. Slag concretes (mixes D and E) achieved a significantly higher depth of carbonation than the other mixes.

It is very interesting to see that all mixes subjected to continuous air drying showed carbonation depth starting from 28 days. These values of carbonation depth then increased as the age of specimens increased. The first three mixes (mixes A, B and C) showed approximately similar values at all ages while mixes with a higher amount of slag exhibited the poorest performance to record maximum values of carbonation at 18 months of about 7 and 6 mm for mixes E and D respectively. The corresponding values of mixes A, B and C were 3.8, 4.3 and 4.5 mm, respectively.

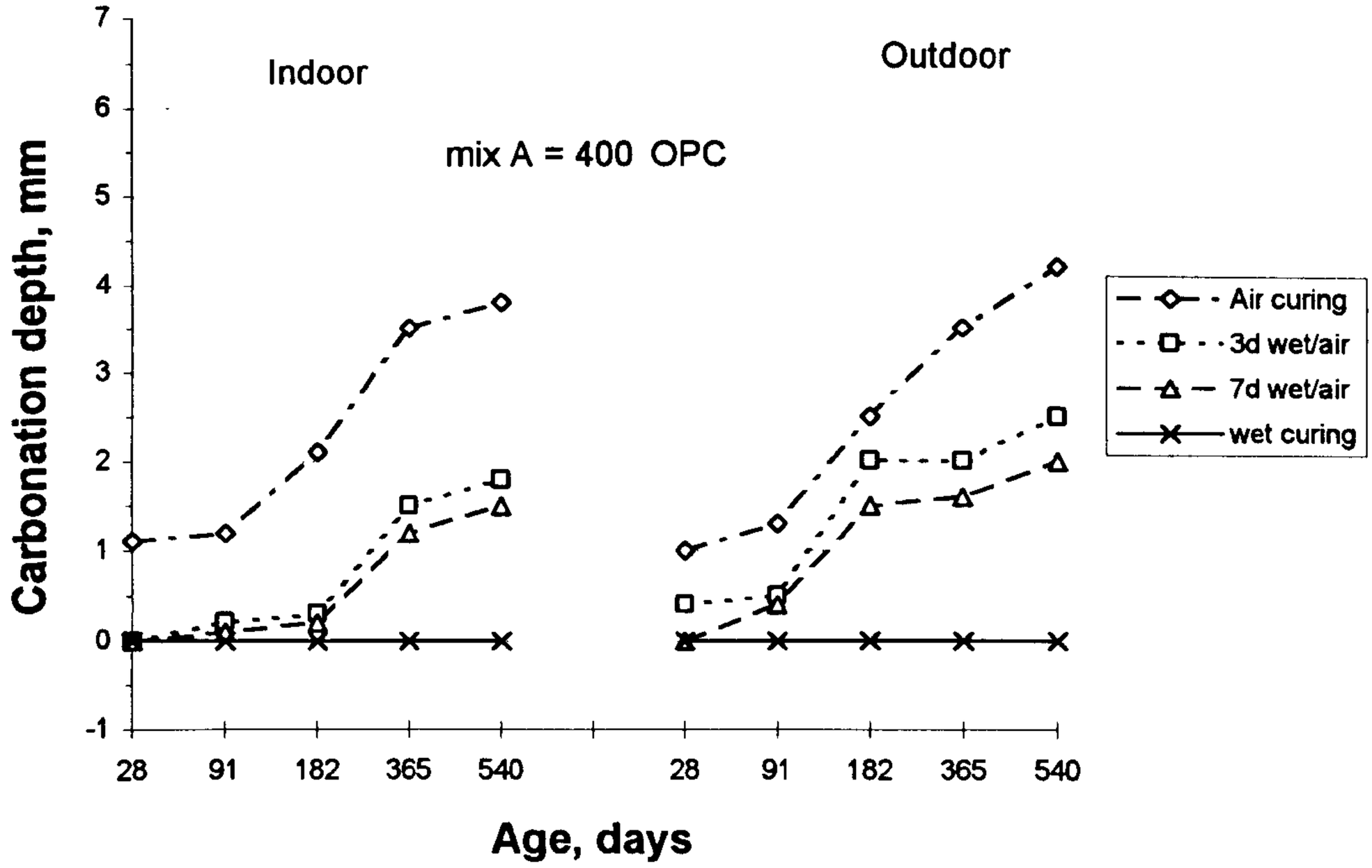

Fig. 7.23: Effect of curing regime on carbonation depth for mix A.

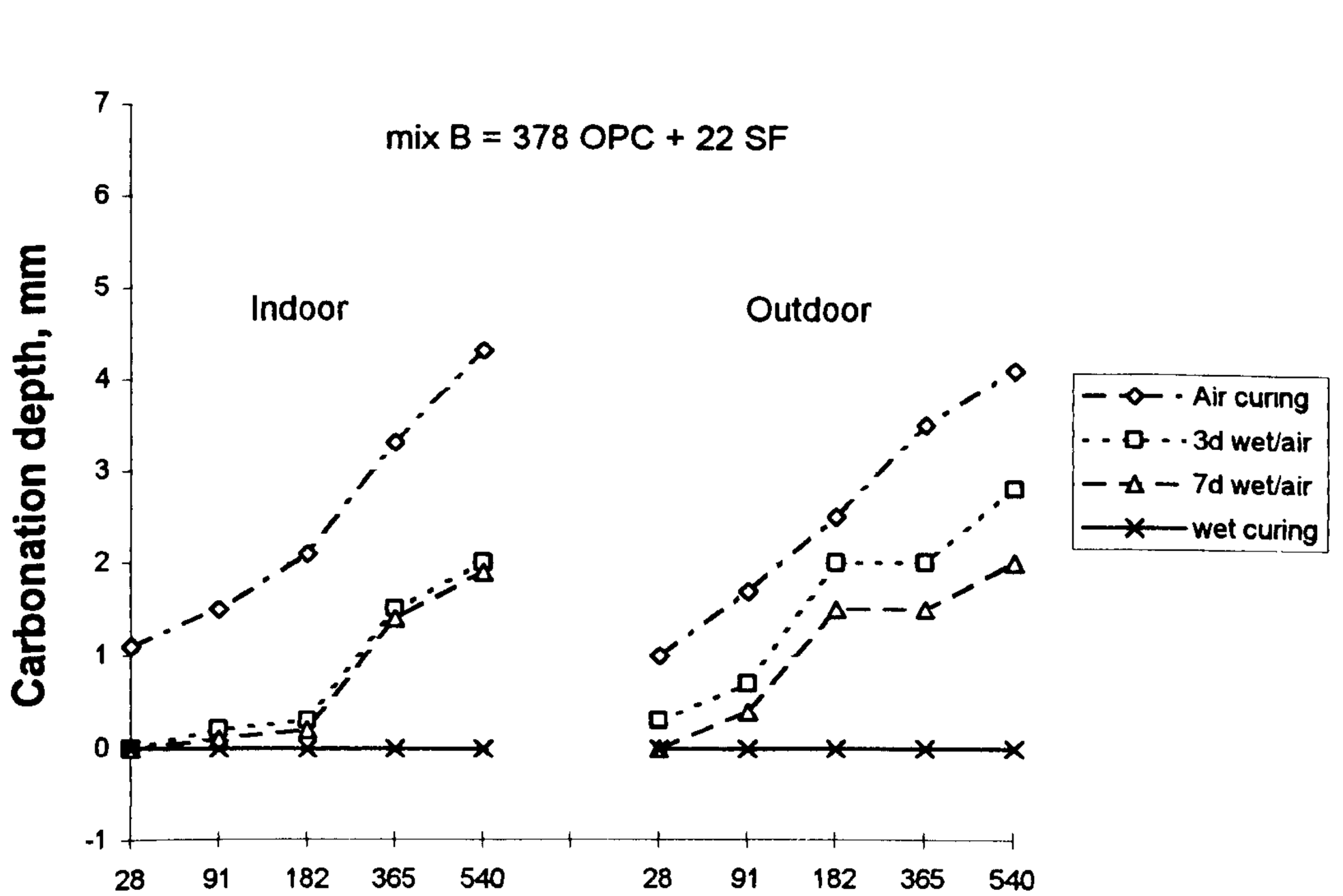

Fig. 7.24: Effect of curing regime on carbonation depth for mix B.

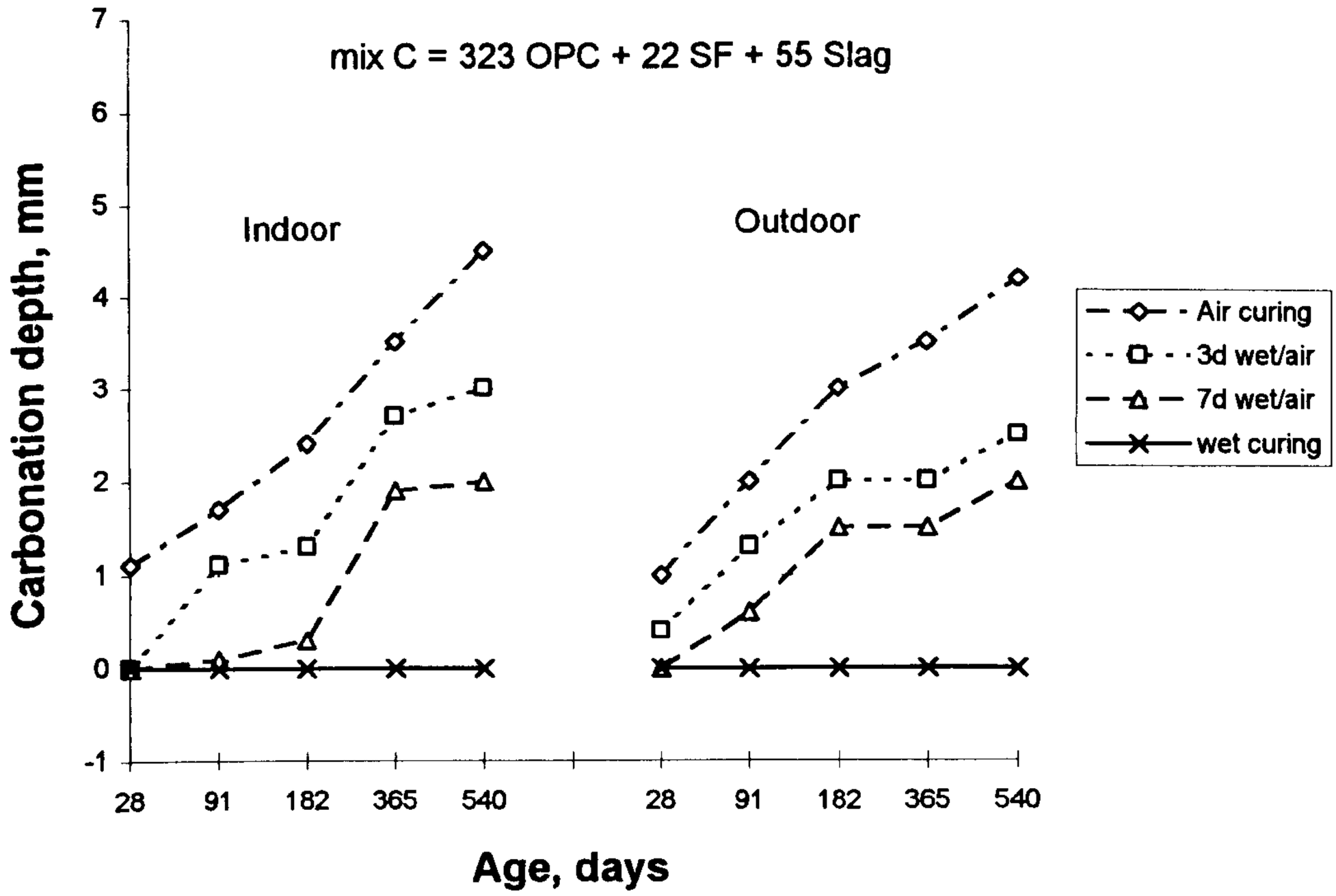

Fig. 7.25: Effect of curing regime on carbonation depth for mix C.

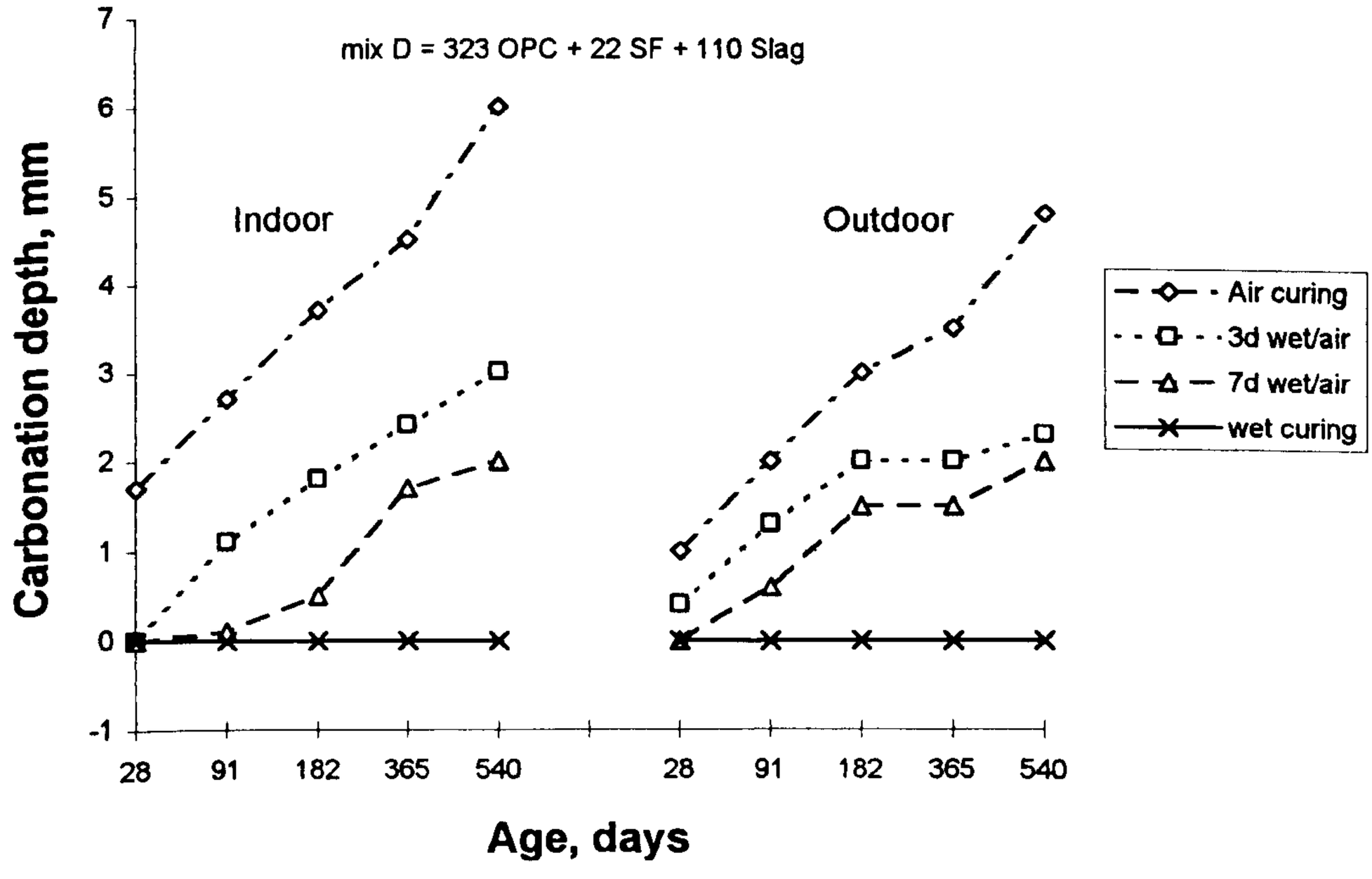

Fig. 7.26: Effect of curing regime on carbonation depth for mix D.

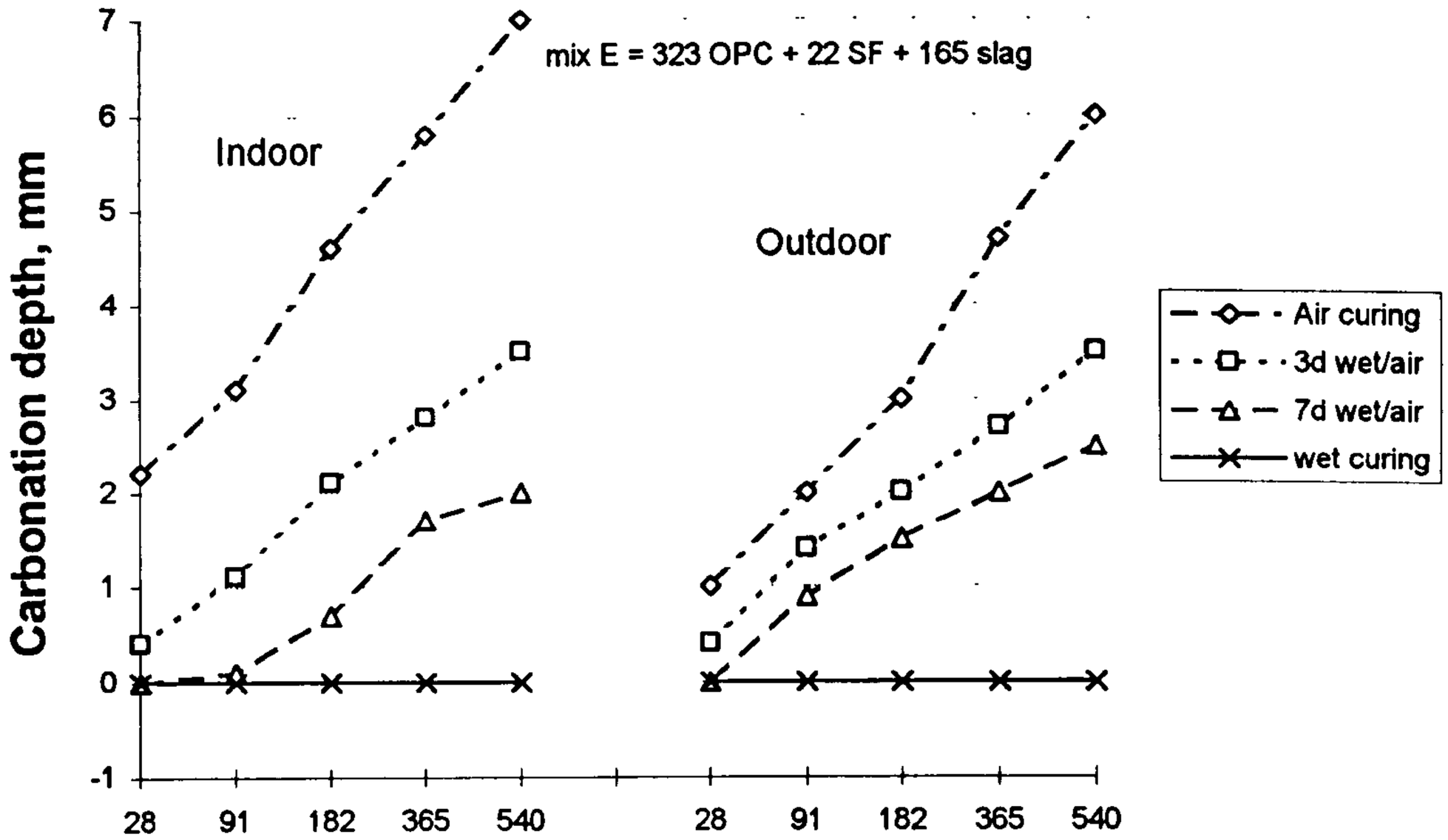

Fig. 7.27: Effect of curing regime on carbonation depth for mix E.

Specimens cured 3 days in water then dried in air, showed similar effects for mixes A and B; it indicates that the development of pozzolanicity of the silica fume is such that the quality of the silica fume concrete is identical to the corresponding plain concrete in resisting the neutralization due to carbonation. Under this condition, carbonation depth would become 0.3 mm at 6 months, whereas in mixes containing slag these values were increased to 1.3, 1.8 and 2.1 mm for mixes C, D and E, respectively. On the other hand, these values decreased significantly for mixes containing slag subjected to 7 days water curing; this is due to the development of pore refinement of slag, the corresponding values for mixes C, D and E being 0.3, 0.5 and 0.7 mm, respectively, compared with the values of 0.2 mm for mixes A and B, respectively.

7.4.3 Effect of exposure environment

When concrete is exposed to the outside environment, specimens dried continuously in air showed lower values of depth of carbonation for mixes D and E when compared with the corresponding values in indoor environment at the age of 18 months, whereas the other mixes presented similar values for both environments. On the other hand, 7 days wet/air curing improves the quality of plain concrete and concrete with mineral admixture in the indoor as well as outdoor environments, but the specimens in the outdoor showed depths of carbonation start from 91 days, while in the laboratory environment, the depth of carbonation started at age of 6 months; similar observations were found for 3 days wet/air curing.

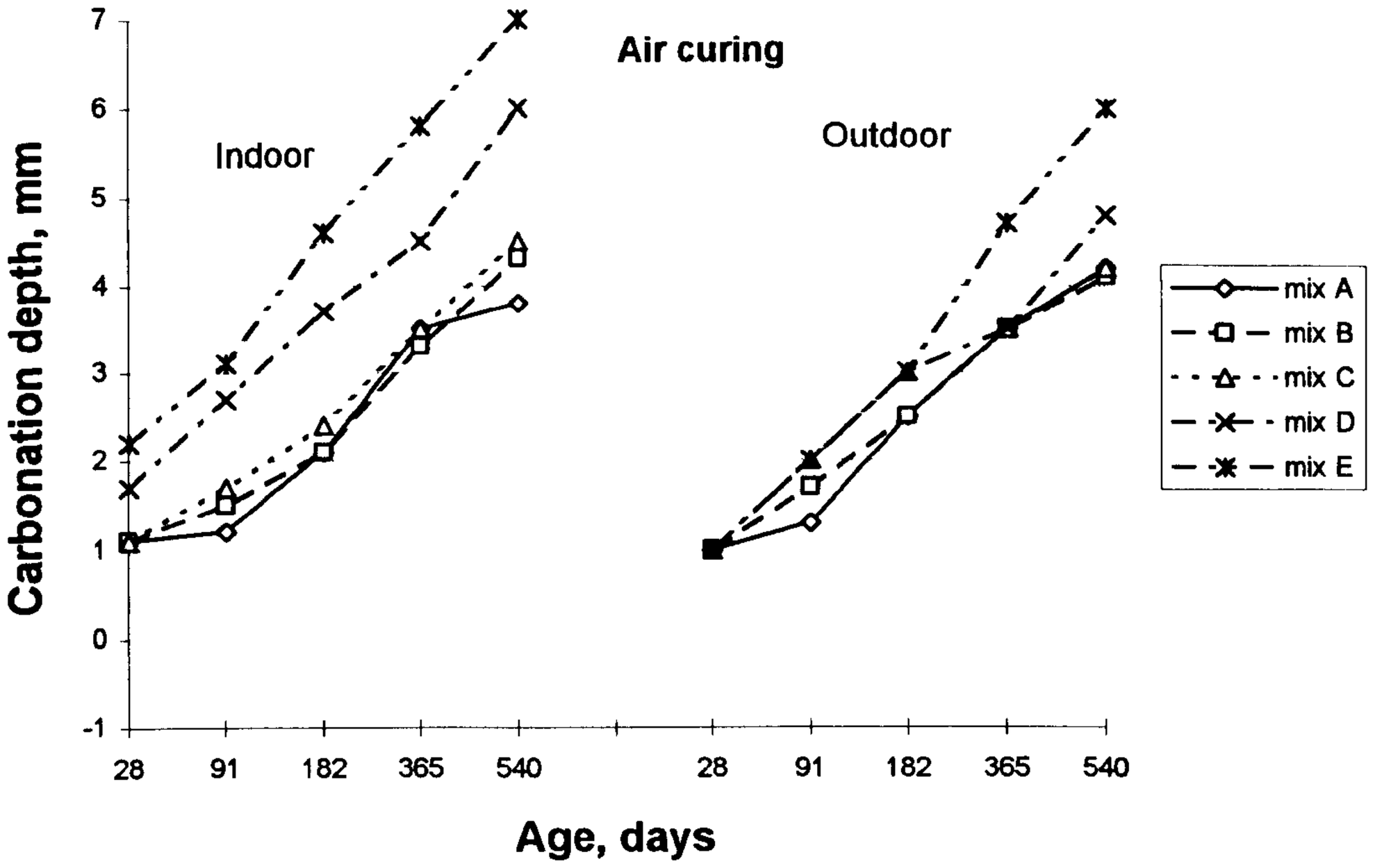

Fig. 7.28: Effect of mix type on carbonation depth under air curing.

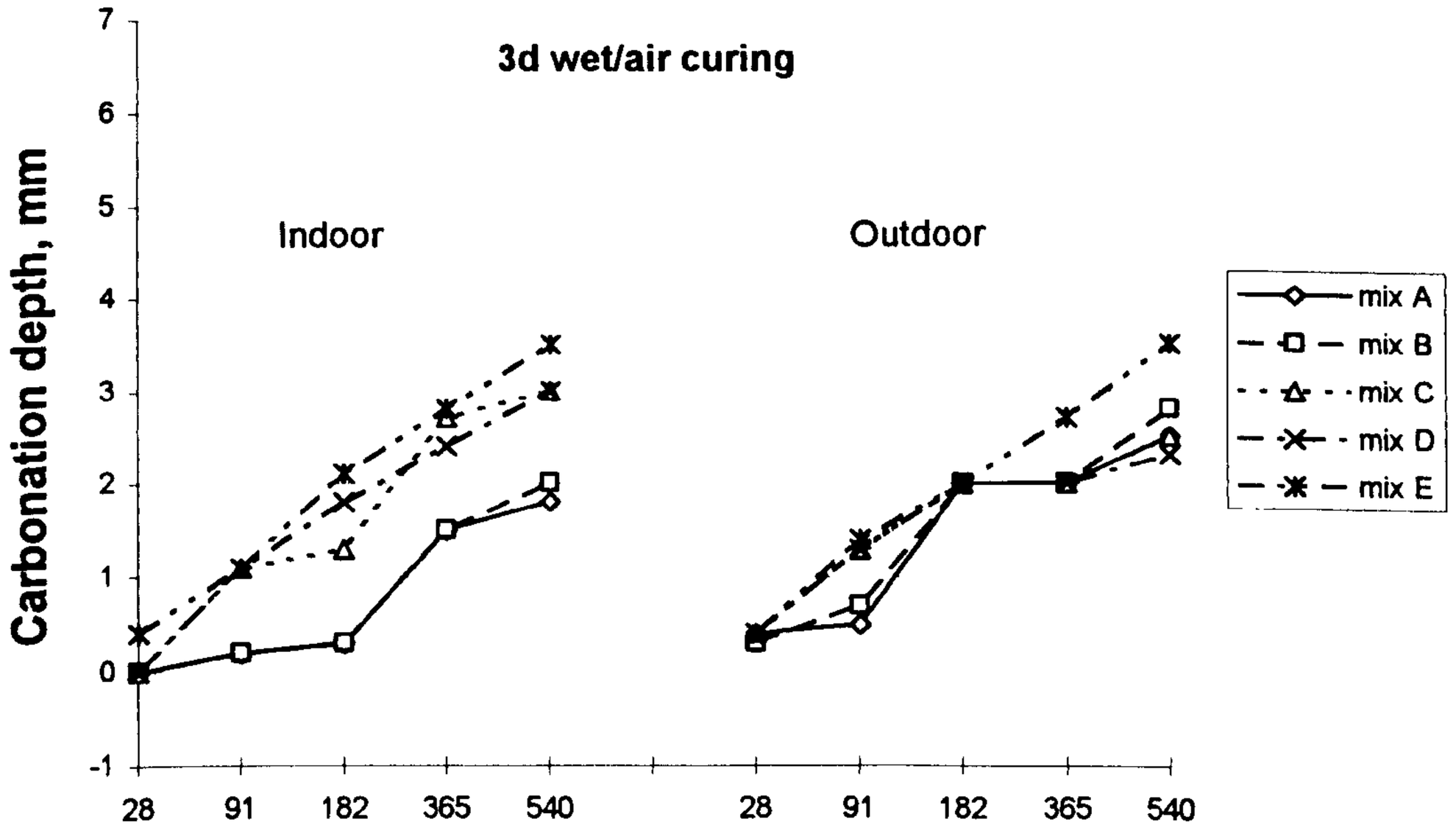

Fig. 7.29: Effect of mix type on carbonation depth under 3d wet/air curing.

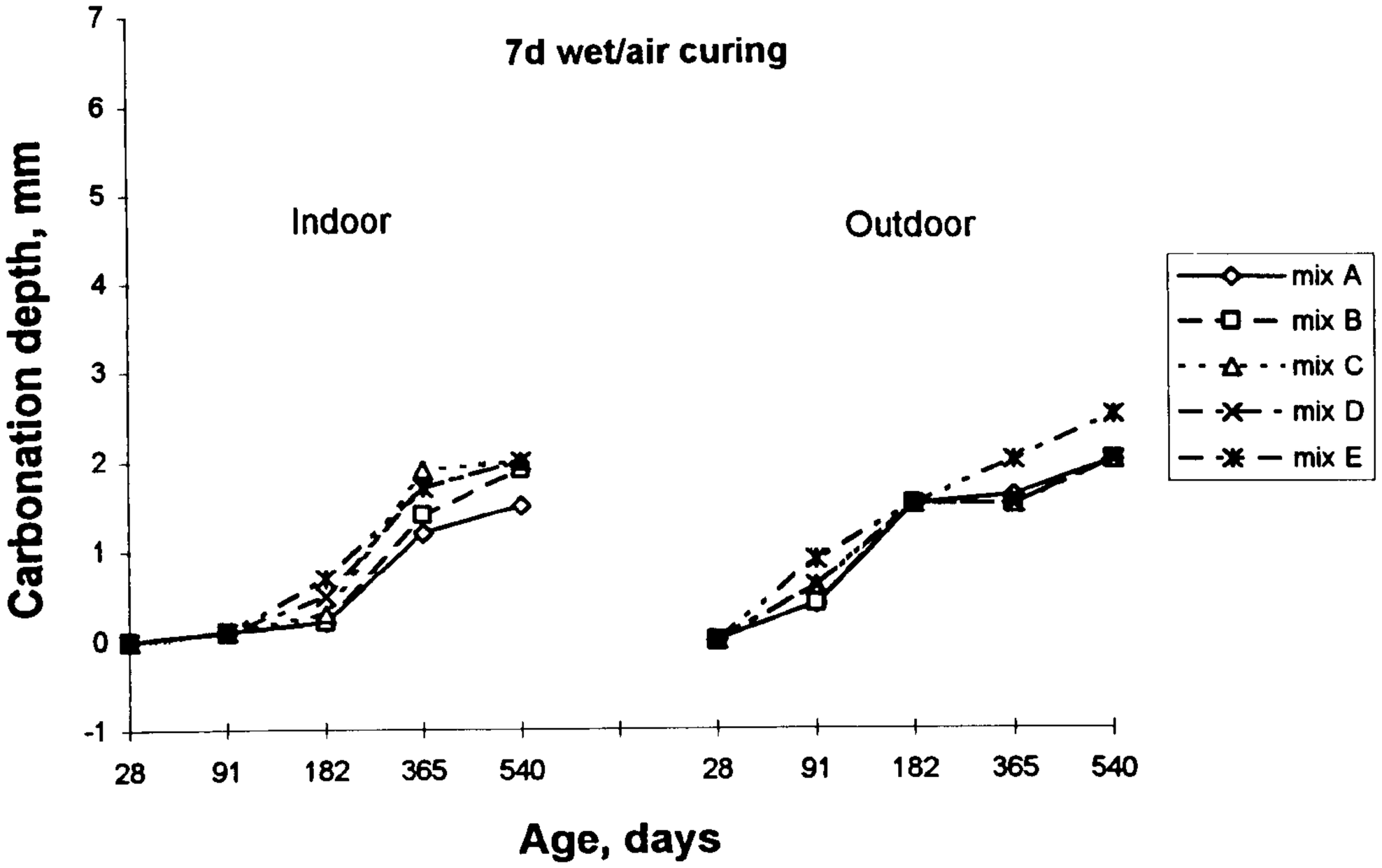

Fig. 7.30: Effect of mix type on carbonation depth under 7d wet/air curing.

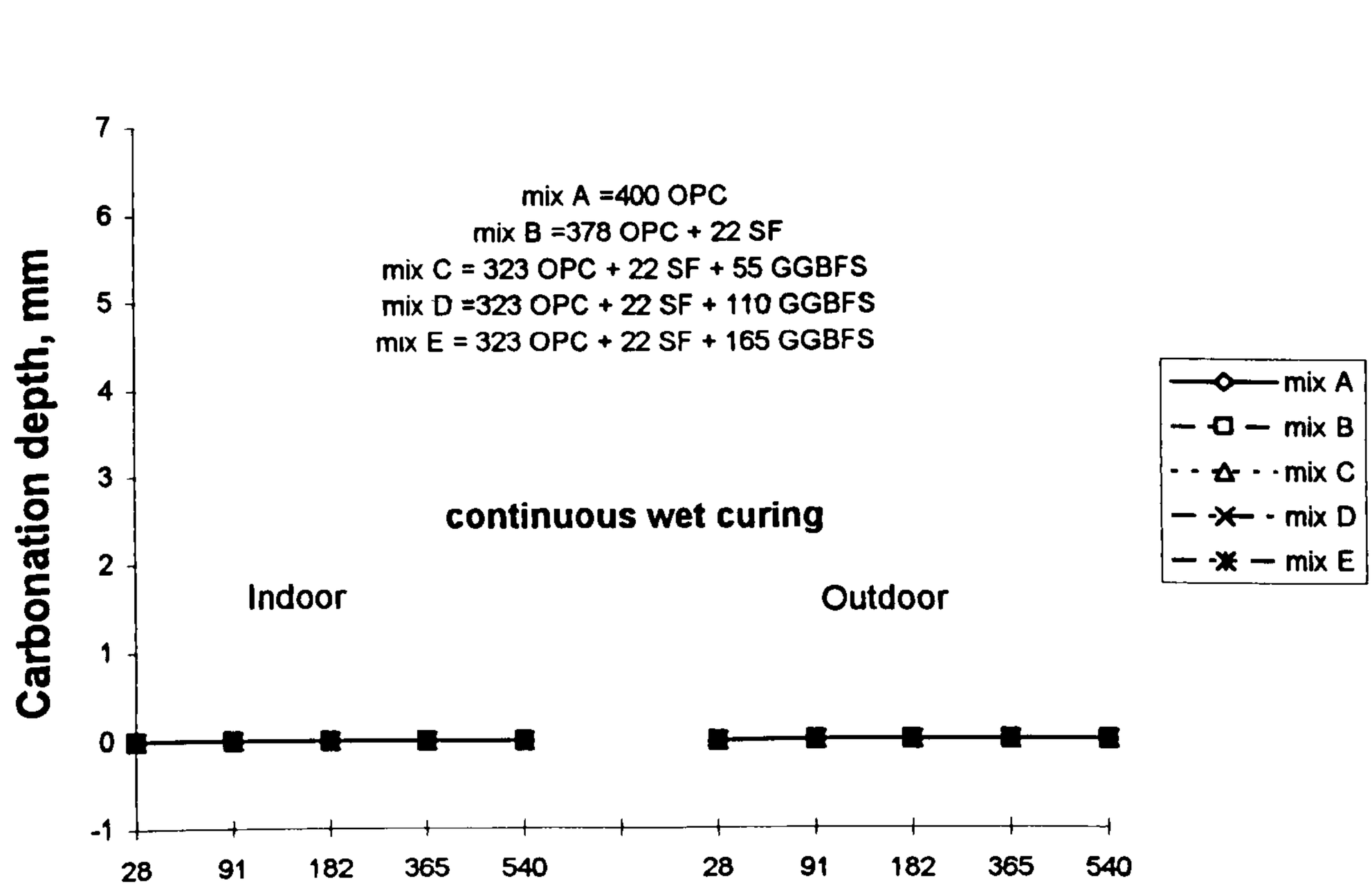

Fig. 7.31: Effect of mix type on carbonation depth under continuous water curing.

7.5 Water absorption

Water absorption of the surface layer of concrete is of considerable importance, especially in relation to the thickness of the concrete cover. However, water movement into concrete is not a simple function of porosity, but it also depends on the pore size distribution and continuous pore diameter. It has become increasingly clear that there can be significant differences between cover concrete and the underlying material; the variations of water absorption of exposed surfaces are then attributable to differences of permeable pores that arise from drying, limitation of cement hydration and carbonation. A short curing period causes a higher surface permeability due to a limitation of cement hydration which is relevant to coarse pores. The results presented in this part are concerned with the effects of curing regime, binder type and exposure to laboratory and field conditions. Many researchers have reported the results of the measurements of water absorption by concrete. Unfortunately, there are considerable differences in the way the results are presented and in the units used. Parrott [166] discusses results in terms water absorption in kg/m^2 after given wetting time of the 100 mm cubes samples sealed against moisture exchange on five faces. Sealing was accomplished firstly by applying a bituminous waterproofing coat to the concrete; this acted as an adhesive for the aluminum foil water-vapor barrier. The final stage of sealing involved wrapping with self-adhesive, weatherproof plastic tape. McCarter et al [167] discusses results in terms of weight increase of the samples which were sealed with a bituminous paint with ends of the cylinder unsealed. Saricimen et al [168] measured the increase in weight of concrete specimens immersed 48 hours in water. However, in this work the method used was that specified in BS 1881:122:1983 [103], using 100 mm concrete cubes instead of concrete cores (as recommended by BS) to monitor the surface capillary porosity. The BS1881 data at 28, 182 and 540 days for water absorption (30 minutes immersion) of 100 mm concrete cubes dried at 105°C are presented as an increase in weight.

7.5.1 Effect of curing

Table 7.5 shows a summary of the water absorption data for all mixes under the four curing regimes and both environments. Figs. 7.32-7.36 show the effect of curing regime on water absorption. In general, as the curing period increases, the water absorption decreases for all mixes. However; specimens dried continuously in air presented the highest values at all ages in the indoor as well as in the outdoor environment. This is

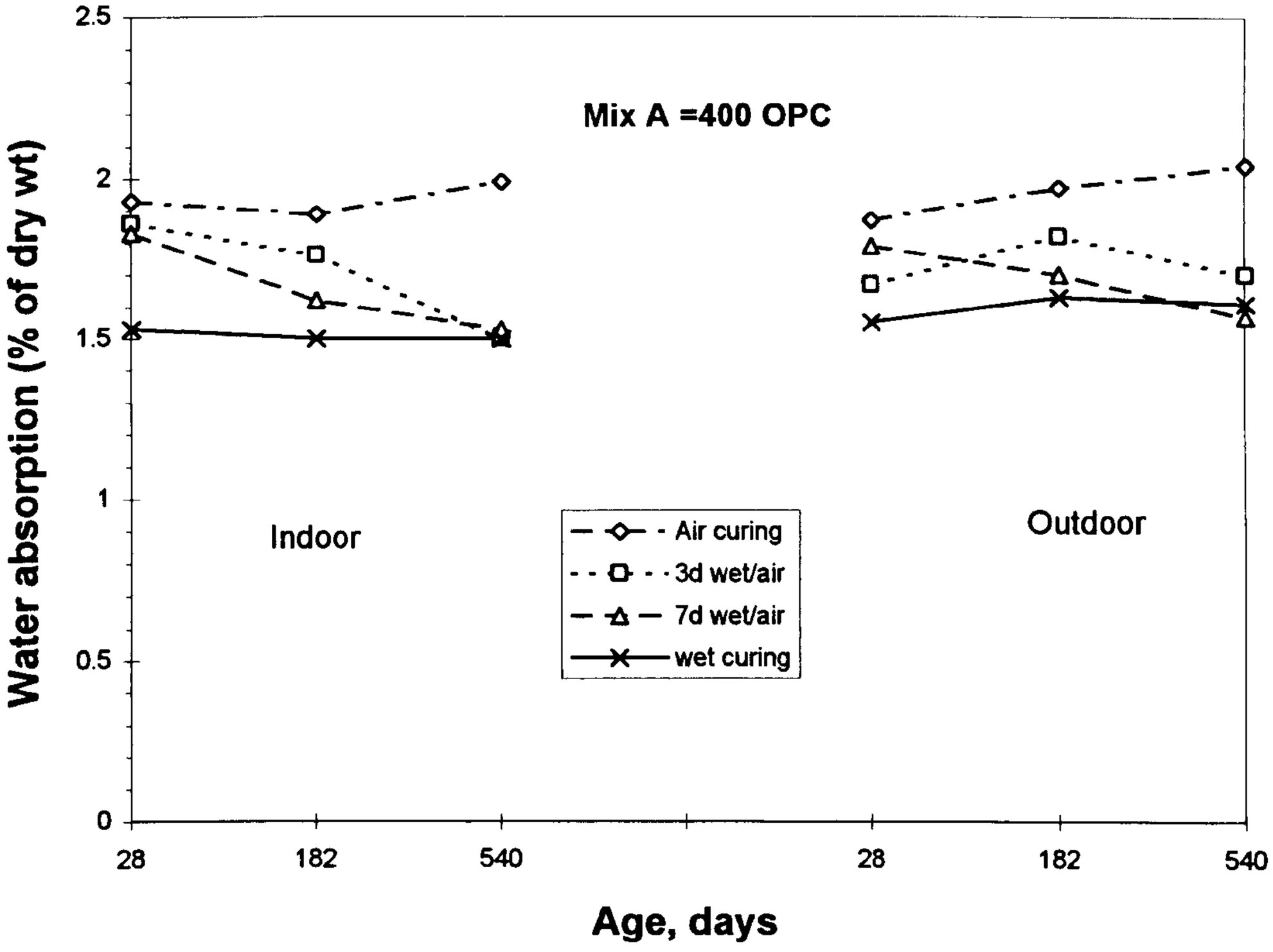

Fig. 7.32: Influence of curing regime on water absorption for mix A.

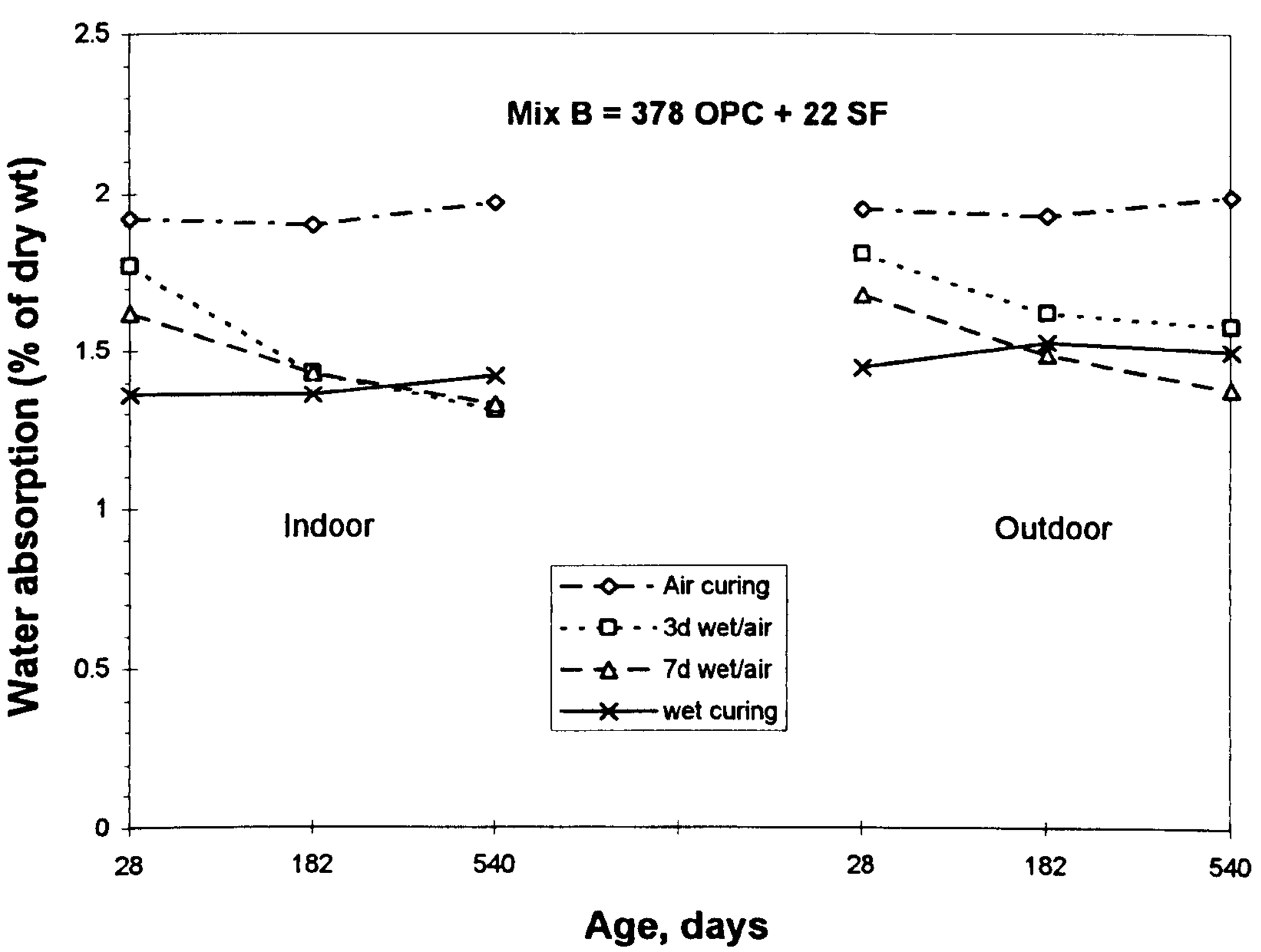

Fig. 7.33: Influence of curing regime on water absorption for mix B.

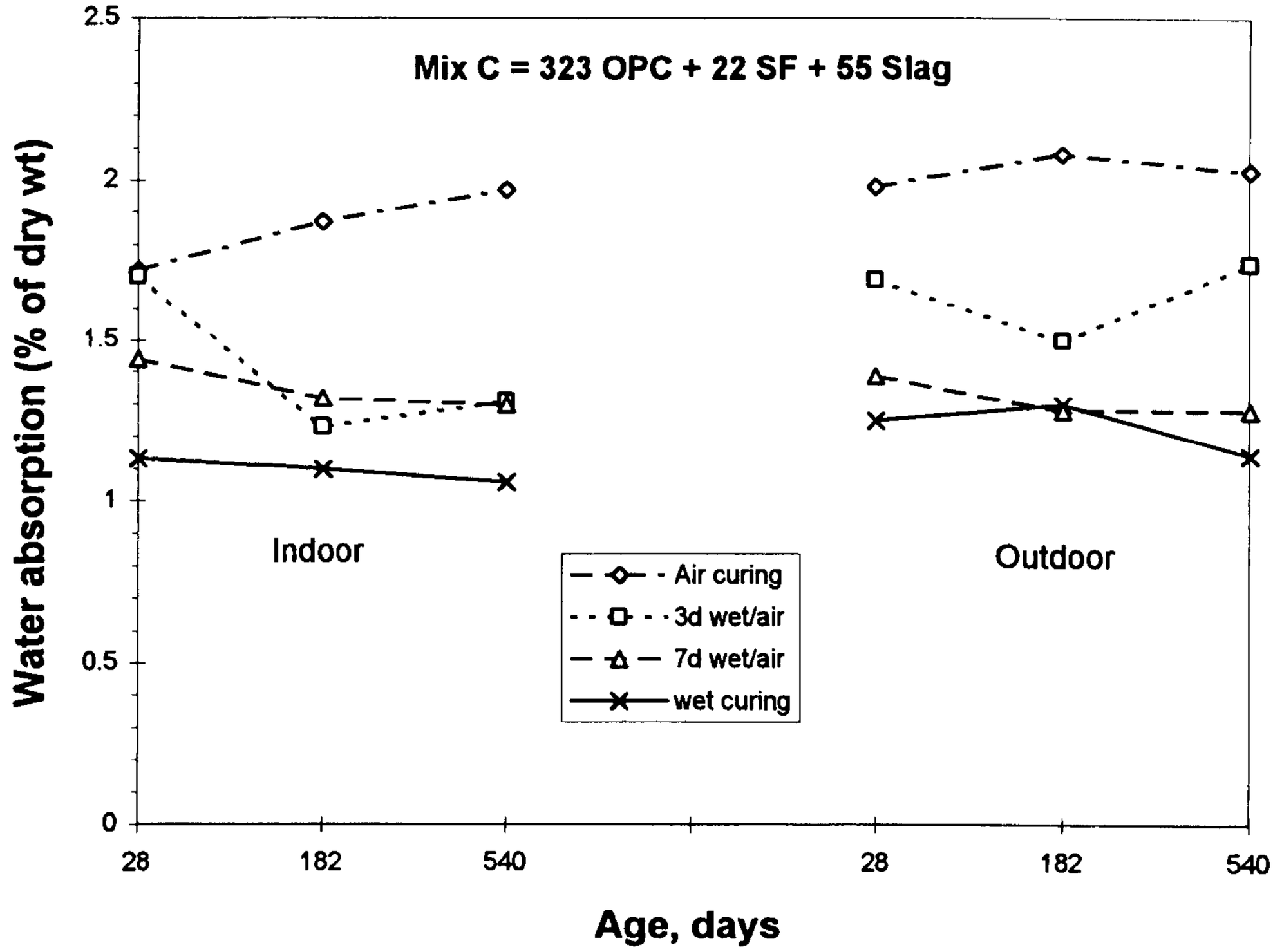

Fig. 7.34: Influence of curing regime on water absorption for mix C.

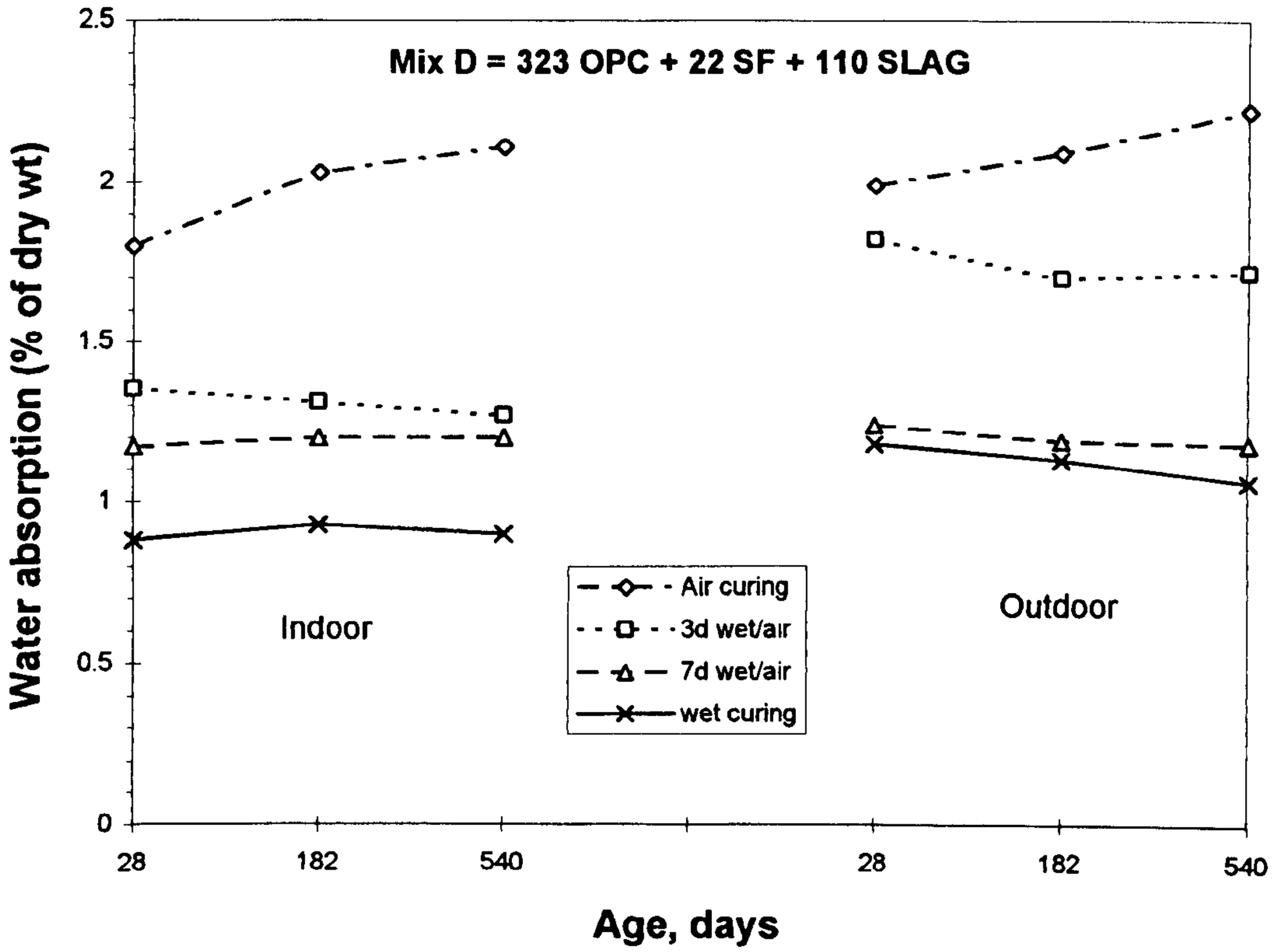

Fig. 7.35: Influence of curing regime on water absorption for mix D.

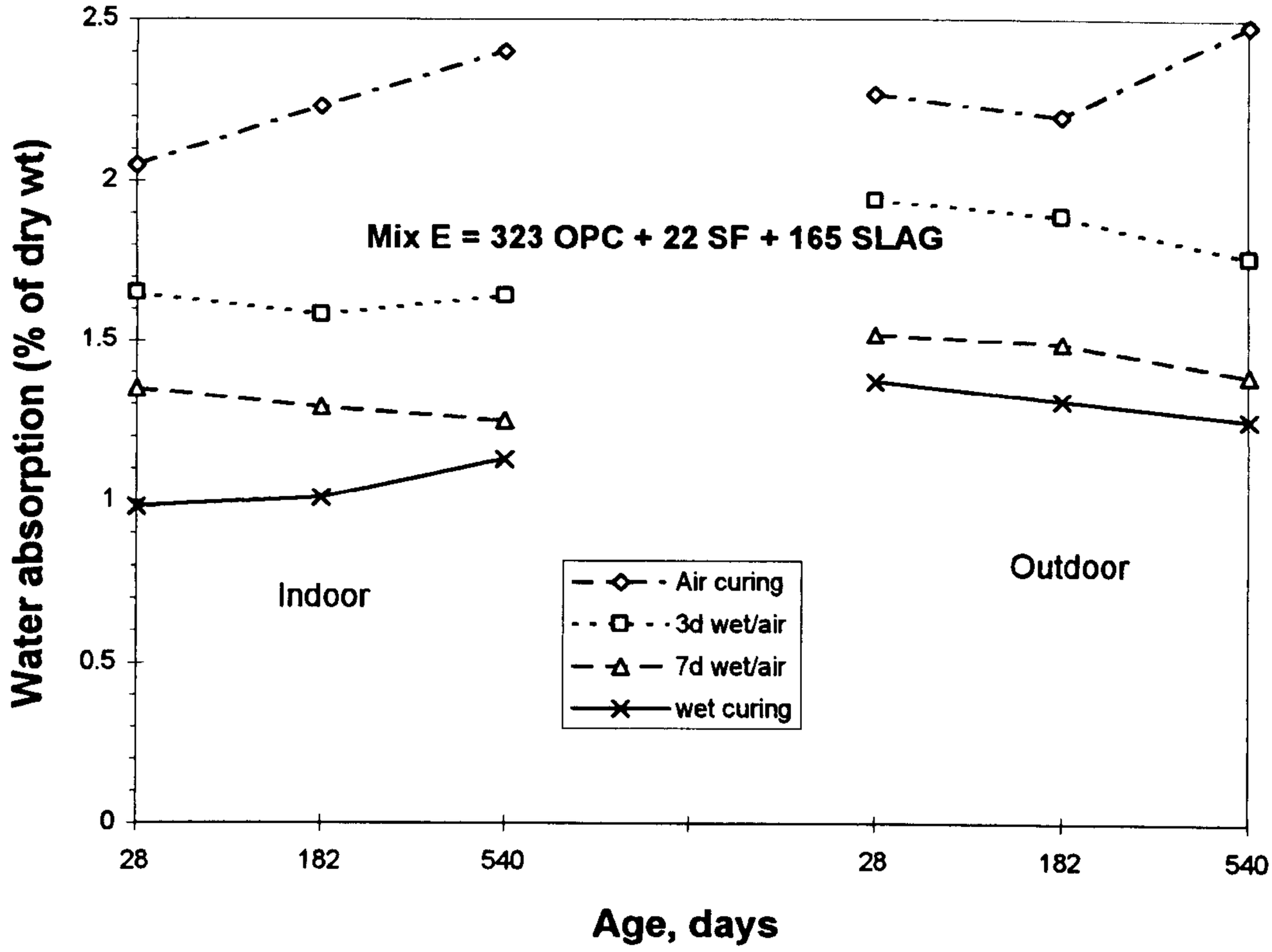

Fig. 7.36: Influence of curing regime on water absorption for mix E.

due to insufficient hydration at early ages which will step down the hydration products to fill the pores. Curing the specimens for 7 days in water lowers the water absorption at later ages (18 months) in the range of 23%-48% for all mixes compared with air curing in the laboratory environment.

7.5.2 Effect of mix type

Figs. 7.37-7.40 show the effect of cement replacement materials on water absorption. In the indoor environment under continuous wet curing conditions, all mixes containing slag have much lower values of water absorption than the control mix (mix A) or even the mix containing small amount of silica fume (mix B). The values obtained at 18 months were reduced by about 29%, 40% and 24% for mixes C, D and E, respectively compared with mix A. The corresponding value for mix B was reduced only by 5%. These results mean that all mixes containing slag have a finer pore diameter near the surface compared with that of the control mix. In other words, all mixes containing slag have a refinement of pores compared with the control mix.

Table 7.5: Water absorption results for indoor and outdoor specimens.

Mix	Binder content kg/m³ OPC/SF/Slag	Curing regime	Indoor environment			Outdoor environment		
			Age			Age		
			28 days	6 months	18 months	28 days	6 months	18 months
A	400/0/0	air curing	1.93	1.89	1.99	1.87	1.97	2.04
B	378/22/0	air curing	1.92	1.90	1.97	1.95	1.93	1.99
C	323/22/55	air curing	1.72	1.87	1.97	1.98	2.08	2.03
D	323/22/110	air curing	1.80	2.03	2.11	1.99	2.09	2.22
E	323/22/165	air curing	2.05	2.23	2.40	2.27	2.20	2.48
A	400/0/0	3d wet/air	1.86	1.76	1.50	1.67	1.82	1.70
B	378/22/0	3d wet/air	1.77	1.43	1.31	1.81	1.62	1.58
C	323/22/55	3d wet/air	1.70	1.23	1.31	1.69	1.50	1.74
D	323/22/110	3d wet/air	1.35	1.31	1.27	1.82	1.70	1.72
E	323/22/165	3d wet/air	1.65	1.58	1.64	1.94	1.89	1.76
A	400/0/0	7d wet/air	1.83	1.62	1.53	1.79	1.70	1.57
B	378/22/0	7d wet/air	1.62	1.43	1.33	1.68	1.37	1.38
C	323/22/55	7d wet/air	1.44	1.32	1.30	1.39	1.28	1.28
D	323/22/110	7d wet/air	1.17	1.2	1.20	1.24	1.19	1.18
E	323/22/165	7d wet/air	1.35	1.29	1.25	1.52	1.39	1.35
A	400/0/0	wet curing	1.53	1.50	1.50	1.55	1.63	1.61
B	378/22/0	wet curing	1.36	1.36	1.42	1.45	1.53	1.50
C	323/22/55	wet curing	1.13	1.10	1.06	1.25	1.30	1.14
D	323/22/110	wet curing	0.88	0.93	0.90	1.18	1.13	1.06
E	323/22/165	wet curing	0.98	1.01	1.13	1.37	1.31	1.25

The same trends occurred for the two curing regimes of 3 days and 7 days wet/air curing; all mixes containing mineral admixtures gave smaller values of water absorption than those of the control mix. These results confirm that all mixes containing cement replacement materials have a refinement of pores, which is similar to the trends observed in the results obtained from pore size distribution, as seen in chapter 6.

Under continuous drying in air, mix E specimens which contain the highest amount of slag presented the highest values of water absorption at all ages followed by mix D. The inclusion of silica fume or small amount of slag presented similar values to the control mix at 6 months and 18 months. It could be concluded from these results that the incorporation of a relatively large amount of slag is sensitive to drying due to the lack of water required by the slag for hydration process. All mix specimens in the indoors exhibited lowest absorption at the first 28 days, which subsequents that became higher; the same trend was observed in the outdoor environment. This observation may

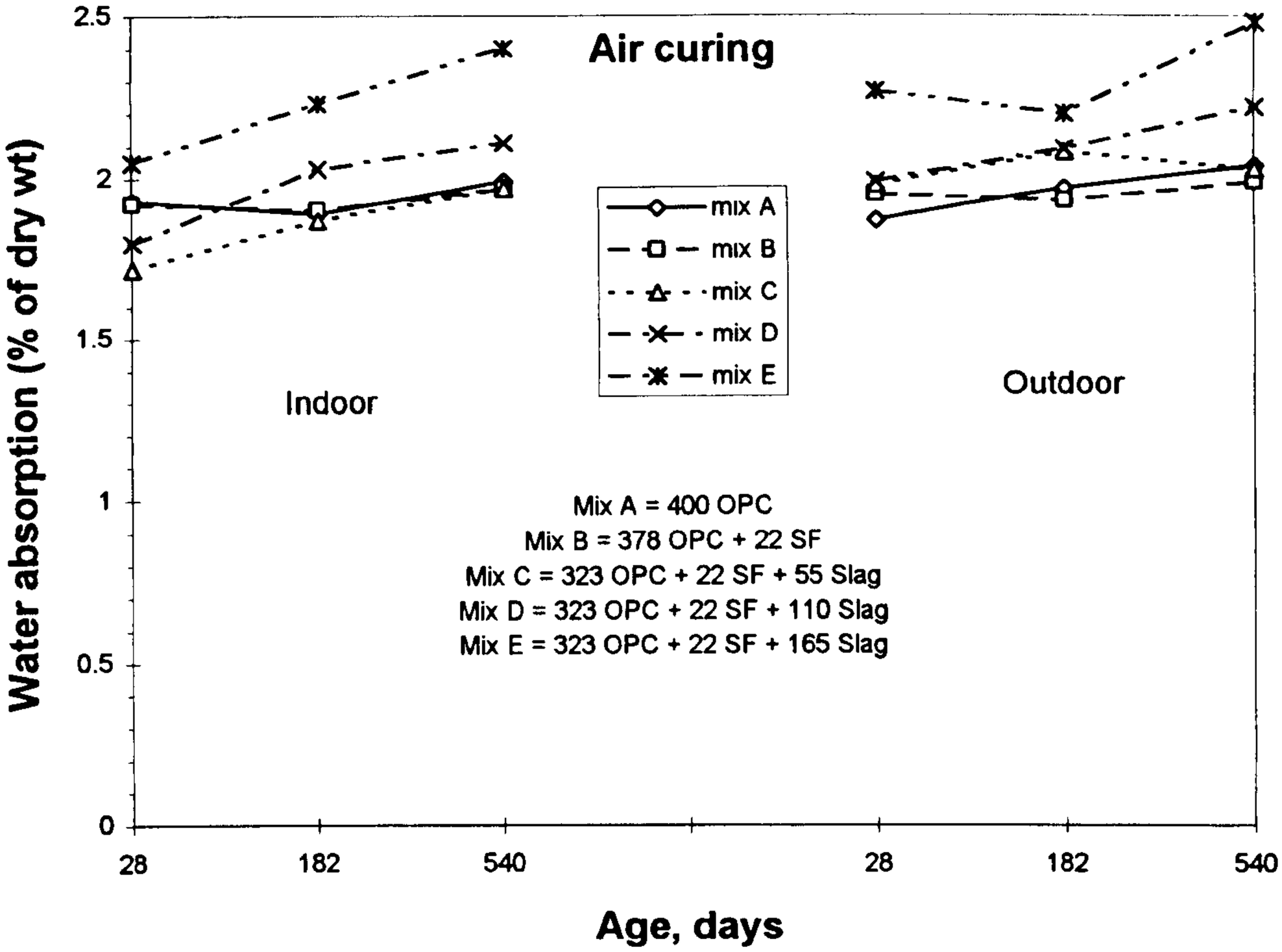

Fig. 7.37: Influence of mix type on water absorption under air curing.

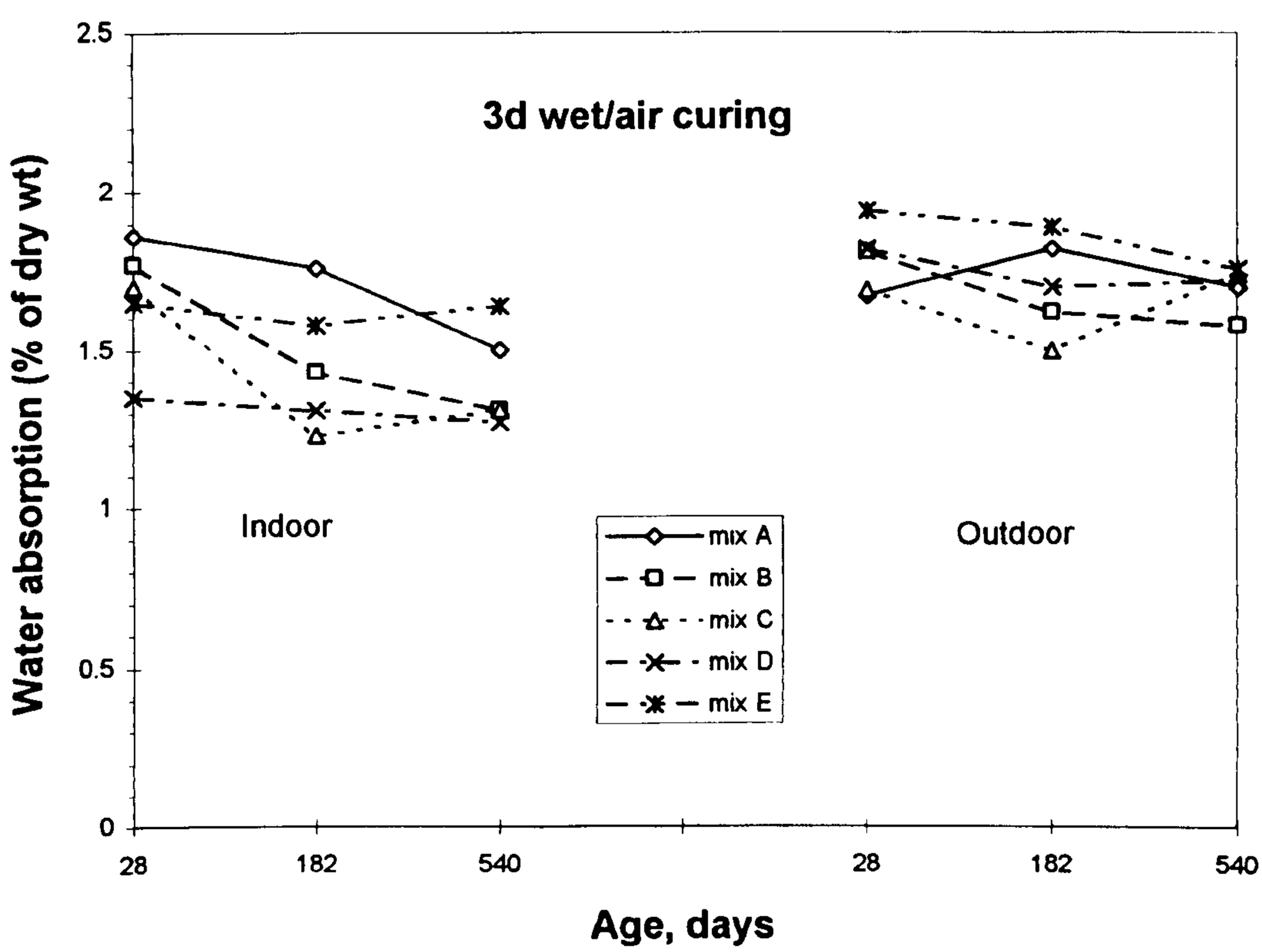

Fig. 7.38: Influence of mix type on water absorption under 3d wet/air curing.

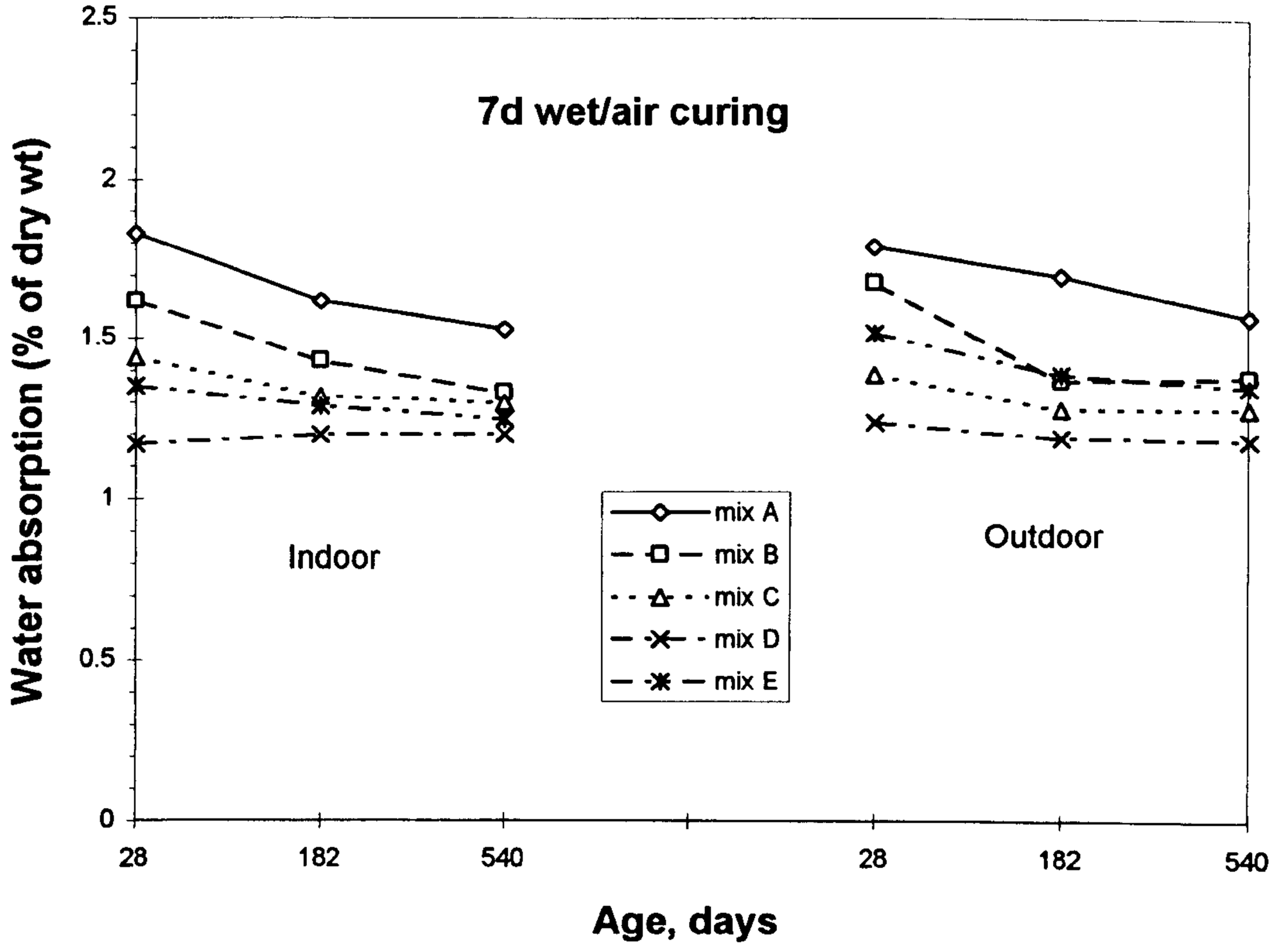

Fig. 7.39: Influence of mix type on water absorption under 7d wet/air curing.

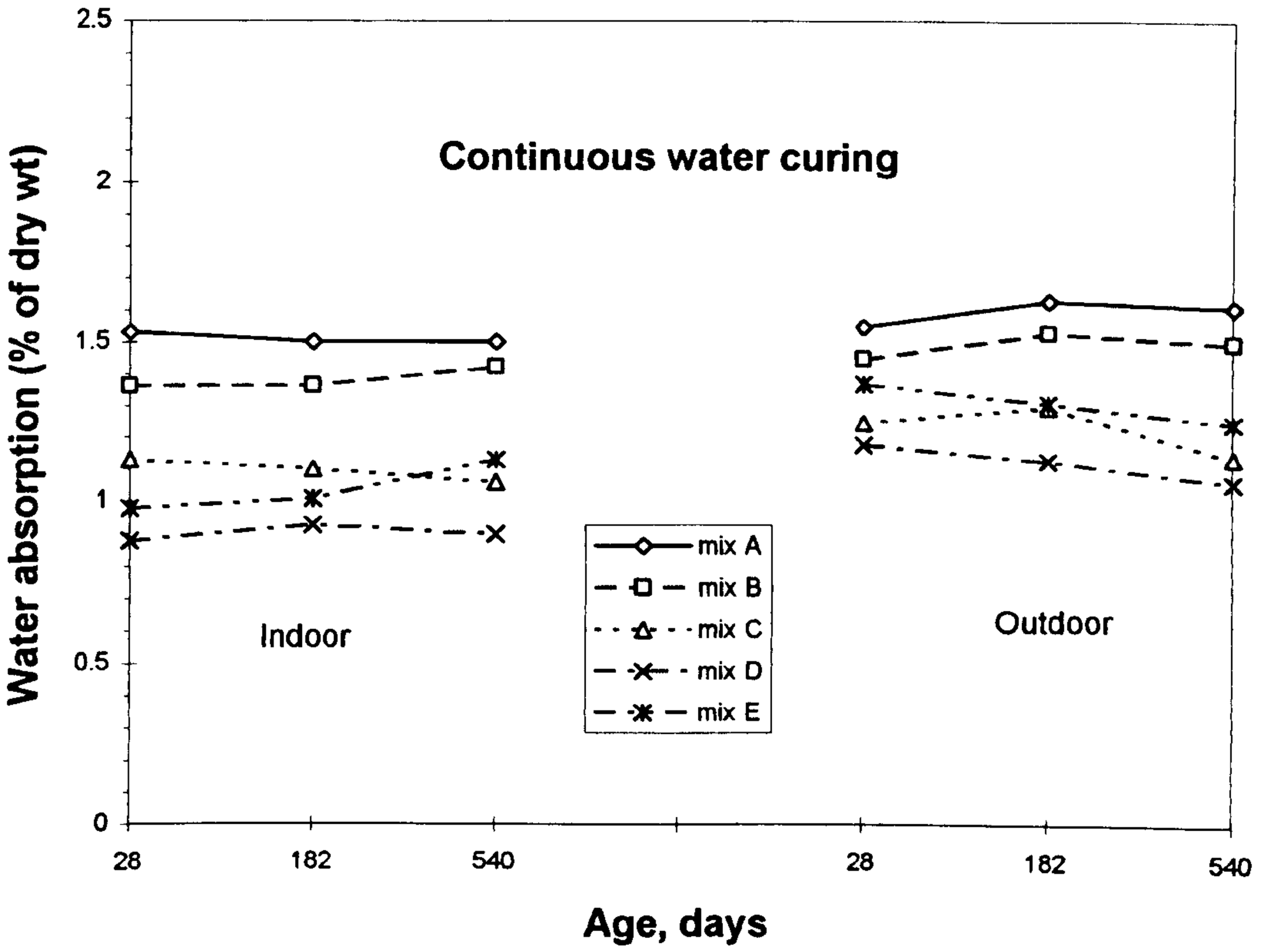

Fig. 7.40: Influence of mix type on water absorption under wet curing.

be attributed to the fact that continuous drying leads to initiation of microcracking which increases with time due to loss of moisture.

7.5.3 Effect of exposure environment

The same figures present the effect of environment on water absorption. In general, a similar trend in the outdoor was observed for all mixes and under the four curing regimes, but with slight increase in the values of water absorption. Under continuous wet curing, all the mixes exhibited an increase in the range of 6%-18% for all mixes at the age of 18 months. Mix D presented the lowest values of water absorption in the indoor as well in the outdoor environment, while the control mix presented the highest values for the corresponding conditions. Mix E under air curing regime at the age of 18 months in the outdoor environment presented the highest value followed by mix D, with approximately no change between the two environments.

Specimens cured 3 days in the water followed by air curing exhibited an increase in water absorption in the range of 13-35% for all mixes at 18 months compared to the corresponding values in the indoor environment. An increase in the water curing to 7 days reduced these values in the range of 2-8%, which indicates the importance of water curing in hot environments.

7.5.4 Relationship between water absorption and oxygen permeability

Imperical model relating water absorption to permeability involving a power equation is suggested as follows:

$$WA = ak^b \tag{7.4}$$

where

WA = Water absorption, %

k = Oxygen permeability, m^2

a and b are constants related to the properties of the concrete and the materials in each mix.

Fig. 7.41 and Table 7.6 show the equation suggested. The regression analysis of the relationship between water absorption and oxygen permeability does not show significant correlation, with a low correlation coefficient of 0.51. This mean for this lack of correlation is that the phenomenon controlling water absorption is different from that of permeability, and it may well be due to the fact that water absorption depends on the surface tension of water surrounding the pores of the surface layer of specimens,

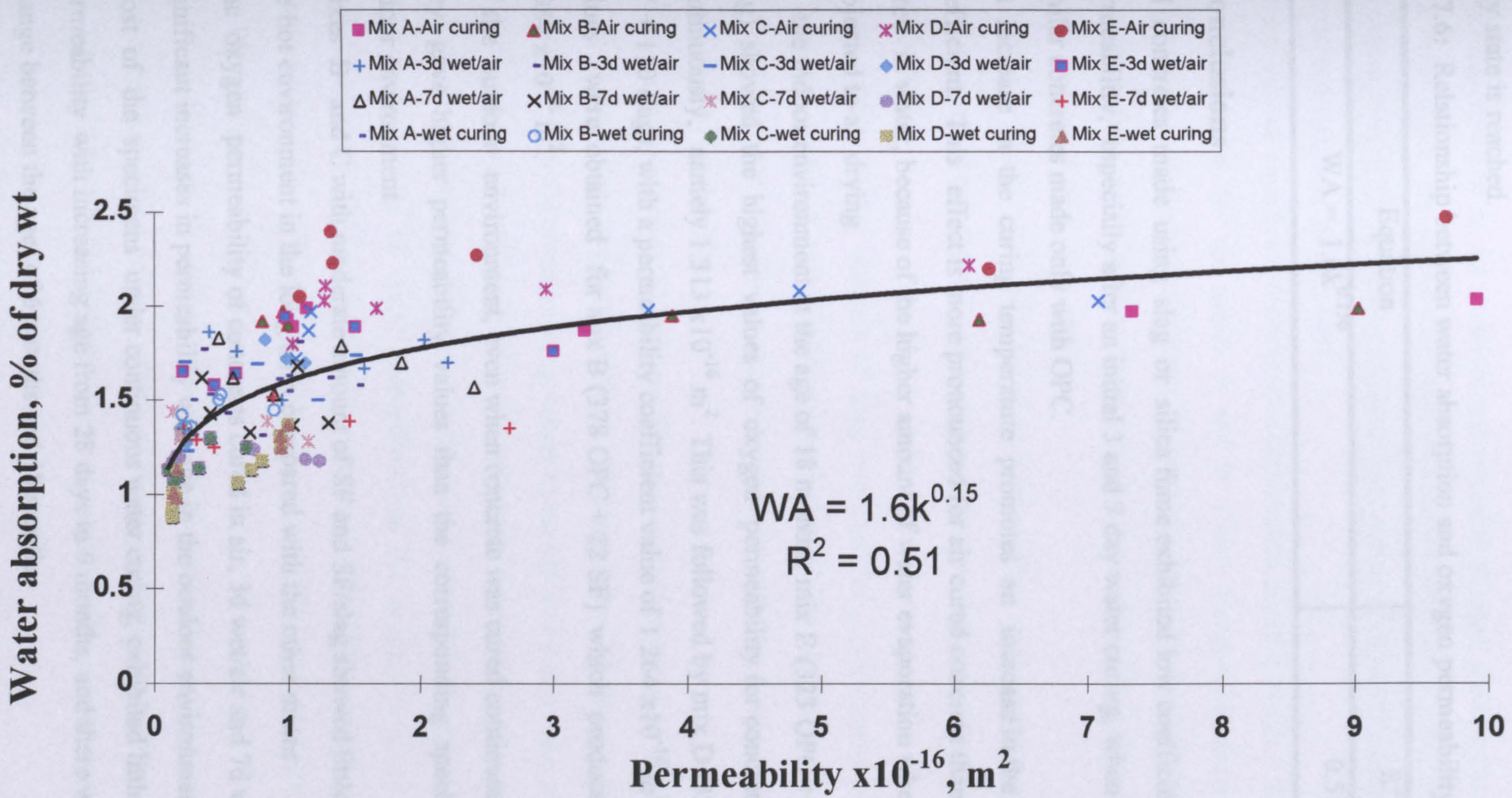

Fig. 7.41 Relationship between water absorption and oxygen permeability.

whereas in the oxygen permeability, the gas will pass through the whole specimen until a steady state is reached.

Table 7.6: Relationship between water absorption and oxygen permeability

Equation	R^2
$WA = 1.6k^{0.150}$	0.51

7.5 Conclusions

1. All concretes made using slag or silica fume exhibited low coefficient of oxygen permeability, especially after an initial 3 and 7 day water curing, when compared to similar concretes made only with OPC.
2. An increase in the curing temperature promotes an increase in the permeability coefficient. This effect is more pronounced for air cured concrete than for concrete cured in water, because of the higher amount of water evaporation when concrete is subjected to air drying.
3. In the indoor environment at the age of 18 months, mix E (323 OPC + 22 SF + 165 slag) showed the highest values of oxygen permeability for concrete dried in air continuously, namely 1.313×10^{-16} m^2. This was followed by mix D (323 OPC + 22 SF + 110 slag), with a permeability coefficient value of 1.264×10^{-16} m^2. The lowest values were obtained for mix B (378 OPC + 22 SF) which produced a value of 0.954×10^{-16} m^2.
4. In the outdoor environment, even when concrete was cured continuously in water, they gave higher permeability values than the corresponding specimens in the indoor environment.
5. Mixes B and C with moderate amount of SF and SF/slag showed little influence of the hot environment in the long term compared with the other mixes
6. The oxygen permeability of concretes cured in air, 3d wet/air and 7d wet/air shows significant increases in permeability with age in the outdoor environment.
7. Most of the specimens under continuous water curing, exhibited little decrease of permeability with increasing age from 28 days to 6 months, and there was no major change between the ages of 6 months and 18 months.
8. There is reasonable correlations between oxygen permeability and coarse pore volume, threshold diameter and maximum continuous pore diameter. These correlation factors ranged from 0.73-0.81.

9. In the indoor environment, the air-cured concretes yielded the highest values of carbonation depth in all concrete mixes and at all ages, starting from 28 days. On the other hand, the carbonation rates reduced considerably during the first few days of water curing (0-7) and continuous water curing presented no carbonation depth (zero reading), even at long term.
10. There was no significant difference in carbonation depth between 3 days and 7 days of water curing for the mixes A and B. Close carbonation depth values were observed for both curing conditions. The addition of slag exhibited a high difference in carbonation depth between the two curing regimes, and this difference increased as the amount of slag increased.
11. In general, the inclusion of silica fume had no effect on the depth of carbonation at all ages and under the different curing regimes when compared with the control mix (mix A).
12. Mixes with a higher amount of slag exhibited the poorest performance to record maximum values of carbonation at 18 months, of about 7 mm and 6 mm for mixes E and D respectively. The corresponding values of mixes A, B and C were 3.8, 4.3 and 4.5 mm respectively.
13. When concrete is exposed to the outside environment, specimens dried continuously in air showed lower values of depth of carbonation for mixes D and E when compared with the corresponding values in the indoor environment at the age of 18 months, whereas the other mixes presented similar values for both environments.
14. In indoor environment under wet curing conditions all mixes containing slag have much lower values of water absorption than the control mix or even the mix containing a small amount of silica fume (mix B). The values obtained at 18 months were reduced by 29%, 40% and 24% for mixes C, D and E respectively compared with that of mix A.
15. Under continuous air curing, mix E, which contained the highest amount of slag, presented the highest values of water absorption at all ages, and this was followed by mix D. The inclusion of silica fume or a small amount of slag presented similar values to the control mix at 6 months and 18 months.
16. Mix D presented the lowest values of water absorption in indoor as well in outdoor environment for specimens cured continuously in water, while the control mix presented the highest values for the corresponding regimes.

Chapter Eight

CONCLUSIONS AND RECOMMENDATIONS FOR FUTURE RESEARCH

8.1 Overall conclusions

The conclusions drawn from this project are shown at the end of each chapter, the overall major conclusions which can be extracted from the test results presented in this thesis, may be summarized as follows. These conclusions are offered within the limitation of the test conditions and test procedures used:

1. The inclusion of GGBFS showed an increase in both setting times in both environments.
2. The inclusion of GGBFS and chemical admixture showed faster loss of slump than plain OPC concrete when tested in the laboratory environment, while plain OPC concrete in real outdoor environment showed faster loss of slump than GGBFS concrete.
3. The effect of superplasticizer was found to be in hot environment was limited. Using GGBFS to extend of working time better than using superplasticizer.
4. With the exception of continuous wet curing, all the mixes in the outdoor environment exhibited loss in pulse velocity beyond 7-14 days after casting, while this trend was observed between 28-91 days in the indoor environment. This trend was more well defined for specimens under continued air drying.
5. Pulse velocity can vary quite widely with compressive strength when insufficiently cured concrete begins to dry with time. Prolonged drying can create moisture loss and possible adverse internal microcracking not readily indicated by compressive strength values These results thus showed that, except for the case of moist curing, compressive strength should not be used as the only a criterion of concrete quality beyond 7-28 days.
6. Very rapid improvement in dynamic modulus of elasticity occurred on the first day, and up to 7 days under all curing conditions and for all the mixes.
7. In the outdoor environment, mixes subjected to 7 days water curing and then dried in air showed sudden loss of dynamic modulus of elasticity after 7 days, whereas this

loss was gradual in the indoor environment. This is considered to be due to rapid loss of water from specimens in the outdoor environment leading to a restricted hydration, and thus slowing down or stopping the development of the dynamic modulus of elasticity.

8. Thermal expansion showed large differences in its values in the same day by as much as 200 microstrains in a period of five hours. Thus the real effects on exterior components of structure will appear over a long period of exposure.
9. Mix C (323 OPC + 22 SF + 55 slag) achieved better properties than all the other mixes when all the mixes had the same total binder content. This type of mixture appears to be the optimum to save cement, and chemical admixture and reduce the shrinkage problem, whereas the early strength can be controlled by incorporating an adequate amount of silica fume.
10. Outdoor environment caused higher porosity and total intrusion volume than indoor environment; the difference in porosity in certain cases was up to 40% when compared to the laboratory environment. This is because of the large and continuous daily fluctuation in both temperature and relative humidity which initiates cycles of wetting and drying, causing subsequent adverse effects on hydration and crack initiation.
11. All specimens made using slag or silica fume exhibited lower coefficient of oxygen permeability, especially for 7 day water cured concrete, when compared to similar specimens made with OPC.
12. An increase in the curing temperature promotes an increase of permeability coefficient. This effect was more prominent in air cured specimens than specimens cured in water, because of the higher amount of water evaporation in air.
13. In the outdoor environment even if the specimens were cured continuously in water, they showed higher permeability than the corresponding specimens in the indoor environment.
14. There was good correlation between oxygen permeability and coarse pore volume, threshold diameter and maximum continuous pore diameter; these correlation factors ranged from 0.73-0.81, while there was poor correlation between oxygen permeability and compressive strength which had a correlation factor of 0.36.

15. In the indoor environment the air-cured specimens yielded the highest values of carbonation depth in all concrete mixes and at all ages, starting from 28 days. On the other hand, the carbonation rates reduced considerably during the first few days of water curing (3 and 7 days) and continuous water curing presented no carbonation depth (zero reading) even in the long term.
16. When concrete was exposed to the outside environment, specimens dried continuously in air showed lower values of depth of carbonation for mixes D and E when compared with the corresponding values in the indoor environment at the age of 18 months, whereas the other mixes presented similar values for both environments.
17. In indoor environment under wet curing conditions all the mixes containing slag had much lower values of water absorption than the control mix or even the mix containing small amount of silica fume (mix B), the values obtained at 18 months were reduced 29%, 40% and 24% for mixes C, D and E, respectively as compared with mix A.

8.2 Limitations of the present works

The main limitations within which this work was carried out were as follows:

1. Only one water binder ratio and silica fume replacement level were used throughout this work.
2. Pore size distribution test was carried out only using one sample conditioning method.
3. Pore size distribution was studied at 18 months in the outdoor and at 6 months and 18 months in the indoor environment.
4. For 400 kg/m^3 binder content series, one mix (mix C) with slag was only used throughout this work.

8.3 Recommendations for future work

During this investigation many interesting points have been noted, which could not be investigated because of the limited time available. To improve the durability of concrete structure in the Arabian Gulf region, the following research is recommended to be undertaken in the future:

1. Sulphate attack and chloride diffusion of all mixes to establish the role and effectiveness of mineral admixture on sulphate attack and chloride diffusion into concrete with different cement replacement levels.

2. Corrosion resistance of different types of steel bars, such as uncoated bars, epoxy coated bars, stainless steel bars and galvanized bars in the various concrete mixes subjected to field condition such as real outdoor environment and splash zone in coastal area in the Arabian Gulf region.

References

1. Goto S. and Roy D. M., "*The effect of w/c ratio and curing temperature on the permeability of hardened cement paste*," Cement and Concrete Research Vol. 11, No. 4, 1981, pp. 575-579.

2. Roy, D. M. and Parker K.M., *"Microstructure and properties of granulated slag-portland cement blends at normal and elevated temperatures,"* Proceeding of the 1st International conference on the use of fly ash, silica fume, slag and other mineral by products in concrete, ACI SP 79, Vol. 1, Canada, 1983, pp. 397-414.

3. Verbeck, G. J. and Helmuth, R. H., *"Structure and physical properties of cement paste,"* Proceeding 5th International Congress on the Chemistry of Cement, Tokyo, 1968, Vol. 2 pp. 137-146.

4. Detwiler, R. J., Kjellsen, K. O. and Gjorv, O. E., *"Resistance to chloride intrusion of concrete cured at different temperatures,"* ACI Materials Journal, Vol. 88, No. 1, 1991, pp. 19-24.

5. Austin, S. A, Robins, P. J. and Issaad, A, *"Influence of curing method on the strength and permeability of GGBFS concrete in a simulated arid climate,"* Cement and Concrete Composites Vol. 14, 1992, pp. 157-167.

6. Roy, D. M., *"Relationships between permeability, porosity, diffusion and microstructure of cement pastes, mortar and concrete at different temperatures,"* Material research Society Proceeding, Vol. 137. 1989.

7. Cebeci O.Z., *"Strength of concrete in warm and dry environment,"* Materials and Structures, Vol. 20, No. ,1987, pp. 270-272.

8. Rose, J.H., *"The influence of curing temperature on the strength of concrete containing granulated blast-furnace slag,"* Proceeding of the 2nd International Conference on the Use of Fly Ash, Silica Fume, Slag and Natural Pozzolans in Concrete, ACI Special Publication SP-91, Vol. 1, Madrid, Spain, 1986, pp. 445-463.

9. Klieger, P., *"Effect of mixing and curing temperature on concrete strength,"* Journal of American Concrete Institute, June 1958, pp. 1063-1081.

10. Manmohan, D. and Mehta, P.K., *"Influence of pozzolanic slag and chemical admixtures on pore size distribution and permeability of hardened cement pastes,"* Cement Concrete and Aggregates, Vol. 3, No. 1, Summer 1981, pp. 63-67.

11. Hooton, R.D., *"Permeability and pore structure of cement pastes containing fly ash, slag and silica fume,"* Blended cements, Edited by G. Frohnsdrorff, American Society for Testing and Materials, ASTM STP-897, Philadelphia, 1986, pp. 128-143.

12. Swamy, R.N., *"Concrete with slag: High performance and durability without tears,"* Proceeding of the 4th international Conference on Structural Failure, Durability and Retrofitting, Singapore, 14-15 July 1993, pp. 206-235.

13. Swamy, R.N. and Bouikni, A., *"Some engineering properties of slag concrete as influenced by mix proportioning and curing,"* ACI Materials Journal, Vol. 87, No. 3, May-June 1990, pp. 210-220.

14. Feldman, R. F., *"Durability of blended cement to high concentration chloride solutions,"* Proceeding 5th International Symposium on Concrete Technology, Monterrey, Mexico, 1981, pp. 262-288.

15. Al-Rabiah, A., *"Performance of the largest slag cement concrete structure in the Arabian Gulf marine environment,"* Proceeding of the 4th International Conference on Deterioration and Repair of Reinforced Concrete in the Arabian Gulf, Bahrain, Vol. 2, 10-13 October 1993, pp. 215-232.

16. ACI Committee 305, *Recommended practice for hot weather concreting,* American Concrete Institute, Detroit, 1991.

17. Rasheeduzzafar, Dakhil, F. H. and Mukarram, K., *"Influence of cement composition and content on the corrosion behaviour of reinforcing steel in concrete,"* American Concrete Institute, Special Publication SP-100, Detroit, pp. 1477-1503.

18. Berke, N. S., Gianetti, F., Tourney, P. G. and Matta, Z. G., *"The use of calcium nitrite corrosion inhibitor to improve the durability of reinforced concrete in the Arabian Gulf,"* Proceeding of the 4th International Conference on Deterioration and

Repair of Reinforced Concrete in the Arabian Gulf, Bahrain, Vol. 2, 10-13 October 1993, pp. 873- 893.

19. Rasheeduzzafar, Hussain, S. E. and Al-Saadoun, S. S., *"Effect of tricalcium aluminate content of cement on chloride binding and corrosion of reinforcing steel in concrete,"* ACI Materials Journal, Vol. 89, No. 1, 1992, pp. 3-12.

20. Rasheeduzzafar, Dakhil, F. H., and Al-Gahtani, A. S., *"Deterioration of concrete structures in the environment of the Middle East,"* ACI Materials Journal, Vol. 81, No. 1, January-February 1984, pp. 13-20.

21. Al-Tayyib, A. J., Rasheeduzzafar and Al-Mana, A. I., *"Deterioration of concrete structure in the Arabian Gulf State,"* Proceeding of the 1st International Conference on Deterioration and Repair of Reinforced Concrete in the Arabian Gulf, Bahrain, Vol. 1, 26-29 October 1985, pp. 10-27.

22. Rasheeduzzafar, Dakhil, F. H., and Al-Gahtani, A. S., *"Corrosion of reinforcement in concrete structures in the Middle East,"* Concrete International, September 1985, Vol. 7, No. 9, pp. 48-55.

23. Rasheeduzzafar, Dakhil, F. H., and Al-Gahtani, A. S., *"The deterioration of concrete structures in the environment of Saudi Arabia,"* The Arabian Journal of Science and Engineering, Vol. 7, No. 3, 1982, pp. 191-232.

24. Saricimen, H. *"Concrete durability problems in the Arabian Gulf region - a review,"* Proceeding of the 4th International Conference on Deterioration and Repair of Reinforced Concrete in the Arabian Gulf, Vol. 2, 10-13 October 1993, Bahrain, pp. 943- 959.

25. Al-Amoudi O. S., Rasheeduzzafar, Maslehuddin, M. and Almusallam A. A., *"Improving concrete durability in the Arabian Gulf,"* Proceeding of the 4th International Conference on Deterioration and Repair Reinforced Concrete in the Arabian Gulf, Vol. 2, 10-13 October 1993, Bahrain, pp. 927- 941.

26. Rasheeduzzafar and Al-Kurdi, S. M. A., *"Effect of hot weather conditions on the microcracking and corrosion cracking potential of reinforced concrete,"* Durable Concrete in Hot Climates, ACI Special Publication SP 139-1, Detroit, 1993, pp. 1-20.

27. Metso, J., Makinen, S. and Kajaus, E., *"Use of blast furnace slag as mining fill,"* Proceeding of the 1st International Conference on the use of Fly Ash, Silica Fume, Slag and Other Mineral Admixture By- Products in Concrete, American Concrete Institute Special Publication SP 79, Vol. 2, Canada, 1983, pp. 1111-1113.

28. Al-Rabiah, A. R., *"Behaviour of slag concrete exposed to the Arabian Gulf marine environment- case study,"* Proceeding of the 7th Arab Structural Engineering Conference, 24 - 26 November 1997, Kuwait, Vol. 1, pp. 149 - 163.

29. BS 8110: Part I, *"Structural use of concrete-code of practice for design and construction,"* British Standards Institution, London, 1985.

30. Dhir, R. K., *"The use of GGBS and PFA in concrete,"* Concrete Society Technical Report No. 40, UK 1991, pp. 96.

31. Mehta, R. K., *"Pozzolanic and cementitious by-products as mineral admixtures for concrete- a critical review,"* Proceeding 1st International conference on the use of fly ash, silica fume, slag and other mineral by products in concrete, ACI SP 79, Vol. 1, Canada, 1983, pp. 1-46.

32. Daube, J. and Bakker, R., *"Portland blast-furnace slag cement: a review,"* Blended Cements, ASTM STP 897, Edited by G. Frohnsdorff, American Society for Testing and Materials, Philadelphia, 1986, pp. 5-14.

33. Douglas, E., *"Blast-furnace slag cement mortar and concrete; durability aspects, in supplementary Cementing Materials for Concrete,"* ACI SP 86-8E, Edited by V. M. Malhotra, 1987, pp. 335-369.

34. Malhotra, V. M., *"Properties of fresh and hardened concrete incorporating ground gramulated blast furnace slag, in supplementary Cementing Materials for Concrete,"* SP 86-8E, Edited by V. M. Malhotra, 1987, pp. 289-333.

35. Neville, A. M., *"Properties of concrete,"* 4th Edition, London 1995.

36. Malhotra, V.M., Ramachandran, V.S., Feldman, R.F. and Aitcin, P.C., *"Condensed silica fume in concrete,"* CRC Press, 1987, 221 pp.

37. Mehta, P. K., *"Condensed silica fume," Cement Replacement Materials,"* Edited by R. N. Swamy, Vol. 3, 1986, pp. 134-170.

38. Birt, J. C., *"Curing concrete an appraisal of attitudes, practices and knowledge,"* Construction Industry Research and Information Association, CIRIA Report 43, 1981, pp. 33.

39. ACI committee 308, *"Standard practice for curing concrete,"* American concrete institute, Detroit, August 1981.

40. The Concrete Society, *"Permeability of concrete and its control,"* 1 day conference London, December 1985.

41. Powers, T. C., Copeland L. E., Hyes, J. C. and Mann, H. M., *"Permeability of portland cement paste,"* ACI Journal, November 1954, pp. 285-298.

42. Khan, M. S. and Ayers M. E., *"Minimum length of curing silica fume concrete,"* Journal of Materials in Civil Engineering, May 1995, Vol. 7, No. 2, pp. 135-139.

43. Hussain, S., Paul I., and Bashenini M., *"Design considerations for durable structures in the Arabian Gulf environment,"* Proceeding of 4th International Conference on Structural Failure, Durability and Retrofitting, 14-15 July 1993, Singapore. pp. 237-244.

44. Wainwright, P.J., *"Properties of fresh and hardened concrete incorporating slag cement,"* Cement Replacement Materials, Edited by R. N. Swamy, Vol. 3, 1986, pp. 100-128.

45. Popovics S. M. and Malhotra, V. M., *"Effect of high temperatures on the properties of concrete,"* Eliskan wa ettamir, 4th year, Vol. 5 and 6, April, 1988 (Arabic Magazine).

46. Alshamsi, A. M., *"Efficiency of the use of set-retarding superplasticizers in hot climates,"* Arabian Gulf Journal of Scientific Research, Vol. 12, No. 1, 1994.

47. Shattaf N. R., and Alshamsi A. M., *"The Effect of Condensed Silica Fume on Some Properties of Concrete in Hot Climate,"* First International Conference on Reinforced Concrete Materials in Hot Climates, April 24th -27th, Alain, U.A.E, 1994, Vol. I, pp. 147-158.

48. Malhotra V. M. and Carette G. G., *"Silica Fume a Pozzolan of New Interest for Use in Some Concretes,"* Concrete Construction, May 1982, pp. 443-447.

49. ACI Committee 226, *"Ground Granulated Blast- Furnace Slag as a Cemetitious Constituent in Concrete,"* ACI Materials Journal, Vol. 84 , No. 4, July-August, 1987, pp. 327-342..

50. Dubbovoy, V. S., Gelber, S. H., Klieger, P. and Whiting, D. A, *" Effects of ground granulated blast furnace slags on some properties of pastes, mortars and concretes,"* Blended cements, Edited by G. Frohnsdrorff, American Society for Testing and Materials, ASTM STP-897, Philadelphia, 1986.

51. Mehta, R. K., *"Pozzolanic and cementitious by-products in concrete- Another look,"* ACI Special Publication SP 114, Trondheim Conference, 1989, pp. 1-43.

52. Neville, A. M. and Brooks, J. J. *"Concrete Technology,"* 1st Edition New York, 1987.

53. Portland Cement Association (PCA), *"Design and control of concrete mixtures,"* 12th Edition, USA

54. Working Group FIP, *"Concrete in Hot Countries,"* 1st Edition, Published by Stuvo, Netherlands.

55. Shalon R. and Ravina D., *"Silica fume in PCC: the effect of form on engineering performance,"* International Design and Construction Magazine, Vol. 41 No. 149, December, 1989.

56. Shalon, *"Report on behaviour of concrete in hot climate,"* Materials and Structures, Vol. 11, No. 62, March-April 1978, pp. 127-131.

57. Working Group FIP on Condensed Silica Fume in Concrete, *"Condensed silica fume in concrete,"* 1st Published, London, 1988.

58. Meusel, J. W. and Rose, J. H., *"Production of granulated blast furnace slag at sparrows point, and the workability and strength potential of concrete incorporating the slag,"* Fly Ash, Silica Fume, Slag and Other Mineral Admixture By- Products in Concrete, ACI SP-79, Vol. 2, 1983, PP. 867-890.

59. Malhotra, V. M. and Carette, G. G., *"Mechanical properties of concrete incorporating both fly ash and condensed silica fume,"* proc. ACI/RILEM Symp. Technology of concrete when pozzolans, slags and chemical admixtures are used, Monterey, March 1985, pp. 395-414.

60. Hwang C. L and Lin C. Y., *"Strength development of blended blast furnace slag cement mortars,"* Proceeding of the 2nd International Conference on the Use of Fly Ash, Silica Fume, Slag and Natural Pozzolans in Concrete, ACI SP 91, Vol. 1, Madrid, Spain, 1986, pp. 1323-1337.

61. Hogan, F. J., and Meunsel, J. W., *"The evaluation of durability and strength development of a ground granulated blast-furnace slag,"* Cement Concrete and Aggregates, Vol. 3, No. 1, Summer 1981, pp. 41-52.

62. Price , W. H. *"Factors influencing concrete strength,"* Journal of American Institute, Vol. 47, Feb. 1951, pp. 417-32.

63. Qamaruddin M., Al-Oraimi S. and Al-Harthy A., *"Effect of hot weather on concrete curing and strength,"* Proceeding of the 7th Arab Structural Engineering Conference, Kuwait, 24 - 26 November 1997, Vol. 1, pp. 165 - 172.

64. Al-Mashary F. A. *"Effect of curing temperature on concrete strength,"* Proceeding of the 7th Arab Structural Engineering Conference, 24 - 26 November 1997, Vol. 1, pp. 173 - 180.

65. Abbasi A. F. and Al-Tayyib A. J., *"Effect of hot weather on pulse velocity and modulus of elasticity of concrete,"* Materials and Structures, Vol. 23, 1990, pp. 334-340.

66. Robins P. J., Austin S. A. and Issaad A., *"Suitability of GGBFS as a cement replacement for concrete in hot arid climates,"* Materials and Structure, Vol. 25, 1992, pp. 598-612.

67. Wainwright, P. J. and Tolloczko, J. J. A., *"The early and later age properties of temperature cycled slag-OPC concretes,"* Proceeding of the 2nd International Conference on the use of fly ash, silica fume, slag and natural pozzolans in concrete, April 1986, Madrid, Vol. 2, pp. 1293-1321.

68. Sellevold, E. J., *"Review: Microsilica in concrete,"* Norwegian Building Research Institute, Project No. 8037, Oslo, January 1984, pp. 44.

69. Kayat, K. H and Aitcin, P. C., *"Silica fume in concrete - An overview,"* ACI Special Publication SP-132, Istanbul Conference, 1992, pp. 835-872.

70. Kristensen, L. and Hansen, T. C., *"Cracks in concrete core due to fire or thermal heating shock,"* ACI Materials Journal, Vol. 91, No. 5, 1994, pp. 453-459.

71. Cabrera J. G. and Lynsdale C. J., *"A new gas permeameter for measuring the permeability of mortar and concrete,"* Magazine of Concrete Research, Vol. 40, No. 144, September 1988, pp. 177-182.

72. Cather R., Figg J. W., Marsden, A. F. and O`Brain, T. P., *"Improvement to the Figg method for determining the air permeability of concrete,"* Magazine of Concrete Research, Vol. 36, No. 129, December 1984, pp. 241-245.

73. BS 1881: Part 5, *"Method for testing concrete for other than strength,"* British Standards Institution, London, 1970.

74. Graf, H. and Grube, H., *"The influence of curing on the gas permeability of concrete with different compositions,"* Proceeding of RILEM seminar on Durability of Concrete Struvture Under Normal Outdoor Exposure, Hanover University, Germany, March 1984, pp. 102-115.

75. Reeve, C. M., *"The use of GGBFS to produce durable concrete, improvement of concrete durability,"* Thomas Telford, London, 1985, pp. 59-76.

76. Ozylidrim, C., *"Laboratory investigation of low-permeability concretes containing slag and silica fume,"* ACI Materials Journal, Vol. 91, No. 2, Nov.-Dec. 1994, pp. 197-202.

77. Swamy, R. N., *"Design for durability and strength through the use of fly ash and slag in concrete,"* Advances in Concrete Technology, SP-171, 1997, pp. 1-72.

78. Kasai Y. Matsui I. Fukushima and Kamohara, *"Air permeability and carbonation of blended cements mortars,"* 1st International conference on the use of fly ash, silica fume, slag and other mineral by products in concrete, ACI SP-79, Vol. 2, Canada, 1983, pp. 435-451.

79. Bakker R. F. M., *"Permeability of blended cements concretes,"* 1st International conference on the use of fly ash, silica fume, slag and other mineral by products in concrete, ACI SP-79, Vol. 2, Canada,, 1983, pp. 589-609.

80. Mehta, P. K., *"Sulfate resistance of blended portland cements containing pozzolans and gramulated blastfurnace slag,"* 5th International Symposium on Concrete Technology, Durability, Monterey, Mexico. March 1981.

81. Roy D. M. and Idorn G. M., *"Hydration, Structure, and Properties of Blast Furnace Slag Cements, Mortars, and Concrete,"* ACI Materials Journal, November-December, 1982, pp. 444-457.

82. Mehta, P. K., *"Durability of concrete in marine environment - A review,"* ACI Special publication SP -65, 1983, pp. 1-20.

83. Feldman R.F. *"Significance of porosity measurement on blended cement performance,"* 1st International conference on the use of fly ash, silica fume, slag and other mineral by products in concrete, ACI SP 79, Vol. 2, Canada,, 1983, pp. 415-433

84. Sellevold, E. J., Bager, D. H., Klitgaard Jensen, E. and Knudsen, T., *"Silica fume-cement paste: hydration and pore structure,"* Norwegian Institute of Technology, Report No. 82.610, Tronheim, 1982, pp. 19-50.

85. Osberne, G. J., *"Carbonation of blastfurnace slag cement concretes,"* Durability of building materials, Elsevier Science, Amsterdam, Vol. 4, 1986, pp. 81-96.

86. Horighuchi, K., *"The rate of carbonation in concrete made with blended cement,"* Third International Conference on the Durability of Concrete, ACI SP-145, Detroit, Vol. 2, 1994, pp. 917-931.

87. Jones M. R., *"Performance in carbonating and chloride-bearing exposures,"* Euro-Cements: Impact of ENV 197 on Concrete Construction, Edited by R. K. Dhir and M. R. Jones, 1994, by E & FN Spon, London, UK, pp.149-167.

88. Suryavanshi A. K., Scantlebury L. D. and Lyon S. B., *"Pore size distribution of OPC and SRPC mortars in presence of chlorides,"* Cement and Concrete Research Vol. 25, No. 5, 1995, pp. 980-988.

89. Al-Amoudi O. S. B., Rasheeduzzafar, Maslehuddin M and Abduljawad S. N., *"Influence of chloride ions on sulphate deterioration in plain and blended cements,"* Magazine of Concrete Research, Vol. 46, No. 167, June 1994, pp. 113-123.

90. BS 12, Determination of setting time and soundness, British Standard Institution, London, 1991.

91. BS 882, *"Specification for aggregate from natural sources for concrete,"* British Standard Institution, London, 1992.

92. BS 3148, *"Methods of test for water for making concrete (including notes on the suitability of the water),"* British Standard Institution, London, 1980.

93. BS 5075: Part 3, *"Specification for superplasticizing admixture,"* British Standard Institution, London, 1985.

94. Al Gurg Fosroc *"Admixtures manual,"* Dubai, 1993.

95. Dubai Airport private communications.

96. BS 4550: Part 3, *"Methods of testing cement,"* British Standard Institution, London, 1978.

97. BS 4027, *"Specification for sulphate-resisting cement,"* British Standard Institution, London, 1980.

98. BS 1881: Part 102, *"Method for determination of slump,"* British Standard Institution, London, 1983.

99. BS 1881: Part 116, *Method for determination of compressive strength of concrete cubes,"* British Standard Institution, London, 1983.

100. BS 1881: Part 203, *Recommendations for measurement of velocity of ultrasonic pulses in concrete,"* British Standard Institution, London, 1986.

101. BS 1881: Part 209, *"Recommendations for the determination of dynamic modulus of elasticity of plain concrete in the laboratory using resonance of vibration in the longitudinal mode,"* British Standard Institution, London, 1990.

102. BS 1881: Part 206, "*Recommendations on method and devices which can be used to determine strain in concrete,"* British Standard Institution, London, 1986.

103. BS 1881: Part 122, *"Method for determination of water absorption,"* British Standard Institution, London, 1983.

104. Grube, H. and Lawrence, C. D. *"Permeability of concrete to oxygen,"* Proceeding of RILEM Seminar, Durability of concrete structures under normal outdoor

exposure. University of Hanover, Institute fur Baustoffkunde und Materialprufung, 1984. pp. 68-79.

105. RILEM Draft recommendation CPC - 18, *"Measurement of hardened concrete carbonation,"* by concrete permanent committee, Materials and Structures, Vol. 17, No 102,1984, pp 437-440.

106. Winslow D. N. and Diamond S., *"A mercury Porosimetry Study of the evaluation of porosity in portland cement,"* Journal of Materials, Vol. 5, No. 3, September 1970, pp. 564-585.

107. Nyame, B.K. and Illston, J.M., *"Capillary pore structure and permeability of hardened cement paste,"* Proceeding of the 7th International Congress on the Chemistry of Cement, Paris, Vol. 3, 1980, pp. 181-185.

108. Mehta, P.K., *"Studies of Blended Cements Containing Santorin Earth," Cement and Concrete Research,"* Vol. 11, No. 4, July 1981, pp. 507-518

109. Hooton, R. D. *"Influence of silica fume replacement of cement on physical properties and resistance to sulfate attack, freezing and thawing, and alkali-silica reactivity,"* ACI Materials Journal, Vol. 90, No. 2, 1993, pp. 143-151.

110. Feldman R. F. and Beaudoin J. J., *"Pretretment of hardened hydrated cement pastes for mercury intrusion measurements,"* Cement and Concrete Research Vol. 21, No. 2/3, 1991, pp. 297-308.

111. Mehta, P. K. and Manmohan. D., *"Pore size distribution and permeability of hardened cement pastes,"* 7th International Congress on the Chemistry of Cement, Paris, 1980, Vol. 3, pp. VII-1-5.

112. Young, J. F. *"A Review of the pore structure of cement paste and concrete and its influence on permeability,"* Permeability of Concrete, American Concrete Institute, SP-108, 1988 pp. 1-18.

113. Pereira, C. J., Rice, R. W. and Skalny, J. P., *"Pore structure and its relationship to properties of materials,"* Materials Research Society Symposium Proceeding Vol. 137, 1989, pp. 3-21.

114. Whiting D and Walitt A., *"Permeability of concrete,"* American Concrete Institute, SP 108-1, 1988.

115. Moukwa M. and Aitcin P. C. *"The effect of drying on cement pastes pore structure as determined by mercury porosimetry,"* Cement and Concrete Research Vol. 18, No. 5, 1988, pp. 745-752.

116. Alshamsi A. M., Sabouni A. R. and Bushlaibi A. H., *"Influence of set-retarding superplasticizers and microsilica on stting times of pastes at various temperatures,"* Cement and Concrete Research Vol. 23, 1993, pp. 592-598.

117. Reeves, C. M., *"The production, properties and applications of blast-furnace slag with particular reference to portland-blast-furnace cement, mortars and grouts made with Cemsave,"* ACI Dissertation, 1980, Cement and Concrete Assoc., Slough, England.

118. Pistilli, M. F., Wintersteen, R. and Cechner, R. *"The uniformity and influence of silica fume source on the properties of portland cement concrete,"* Cement, Concrete and Aggregates, Vol. 6, No. 2, 1984, pp. 120-124.

119. Hwang C-L and Shen D-H., *"The effect of blast-furnace slag and fly ash on the hydration of portland cement,"* Cement and Concrete Research Vol. 21, No. 4, 1991, pp. 410-425.

120. Swamy, R. N., Sakai, M., and Nakamura, N., *"Role of superplasticizer and slag for high performance concrete, Superplasticizer and other chemical admixtures in concrete,"* ACI SP-148, Edited by V. M. Malhotra, 1994, pp. 1-26.

121. Douglas, E., Wilson, H. and Malhotra, V. M., *"Production and evaluation of a new source of granulated blastfurnace slag,"* Proceeding International Workshop on Ground Blastfurnace Slag, CANMET, Ottawa, 1987, pp. 79-112.

122. Malhotra, V.M., Carette, G.G., and Bremner, T.W., *"Durability of granulated blastfurnace slag concrete in marine environment,"* Proceeding International Workshop on Ground Blastfurnace Slag, CANMET, Ottawa, 1987, pp. 171-201.

123. Wainwright, P.J., *'The influence of slag cement on some of the properties of concrete related to thermal cracking,"* Proceeding International Workshop on Ground Blastfurnace Slag, CANMET, Ottawa, 1987, pp. 203-227.

124. Cesareni, D. and Frigione, G. *"A contribution to the study of the physical properties of hardened paste of portland cement containing Ground Blast-furnace*

Slag," Proceeding, 5th International Symposium on the Chemistry of Cement, Cement Association of Japan, Tokyo, Vol. 4, 1968, pp. 237-247.

125. Lea, F. M., *"The chemistry of cement and concrete,"* 3rd Edition, Chemical Publishing Co., New York, 1971, pp. 454-489.

126. Mangialardi T and Paolini A. E., *"Workability of superplasticized microsilica-portland cement concretes,"* Cement and Concrete Research. Vol. 18, 1988, pp. 351-362.

127. Punkki, J., Golaszewski, J and Gjorv O., *"Workability loss of high-strength concrete,"* ACI Materials Journal, Vol. 93, No. 5, September- October 1996, pp. 427-431.

128. Malhotra, V. M., Carette G. G. and Sivasundaram V., *"Role of silica fume in concrete: A review,"* Advance in Concrete Technology Edited by Malhotra, V.M., 1994, pp. 925-991.

129. Whiting D., *"Evaluation of super-water reducers for highway application,"* FHWWA/RD-80/132, Federal Highway Administration, Washington, DC, March 1981.

130. Whiting D. and Dziedzic W., *"Behaviour of cement reduced and 'flowing' fresh concretes containing convential water-reducing and 'second-generation' high-range water- reducing admixtures,"* Cement, Concrete, and Aggregates, Vol. 11, No. 1, Summer 1989, pp. 30-39.

131. Fookes, P.G., Pollock, D.G. and Kay, E.A., *"Rates of deterioration,"* Concrete, September 1981, pp. 12-19.

132. Swamy R. N., *"Properties of high-strength concrete,"* Cement, Concrete, and Aggregates, Vol. 8, No 1, Summer 1986, pp.-41.

133. Al-Khaja W. A. *"Strength and time-dependent deformations of silica fume concrete for use in Bahrain,"* Construction and Building Materials, Vol. 8, No. 3, 1994, pp. 169-172.

134. ACI Committee 226 "*Silica fume in concrete*," ACI Materials Journal, 1987, March-April, pp. 158-166.

135. Carette, G.G. Malhotra, V.M. *"Early-age strength development of concrete incorporating fly ash and condensed silica fume,"* Proceeding of the 1st International Conference on the use of Fly Ash, Silica Fume, Slag and Other Mineral By-Products in Concrete, ACI SP-79, Canada, Vol. 2, 1983, pp. 665-684.

136. State of art report, "*Condensed silica fume in concrete,"* Published by Thomas Telford Ltd, London, 1st Edition 1988, pp. 1-37.

137. Ozyildirim C., *"Laboratory investigation of low permeability concrete 's containing slag and silica fume,"* ACI materials Journal, Vol. 91, No. 2, March-April 1994, pp. 197-202.

138. Djellouli J., Aitcin P. C. and Chaallal O., *"Use of ground granulated slag in high-performance concrete,"* ACI SP-121, 1991, pp. 351-368.

139. Khan M. S. and Ayers M. E., *"Curing requirements of silica fume and fly ash mortars,"* Cement and Concrete Research Vol. 23, No. 6, 1993, pp. 1480-1490.

140. Ramezanianpour, A. A. and Malhotra, V. M., *"Effect of curing on the compressive strength, resistance to chloride-ion penetration and porosity of concretes incorporating slag, fly ash or silica fume,"* Cement and Concrete Composites, Vol. 17, 1995, pp. 125-133.

141. Videla C.C., Convarrubias J. P. T. and Pascual J. M. D., *"Behaviour in extreme climates of concrete made with different types of cement,"* Appropriate Concrete Technology, Edited by Dhir R.K. and McCarthy M.J., London, UK, 1996, pp. 213-224.

142. Alamri, A. M., *"Influence of curing on the properties of concretes and mortars in hot climates,"* Ph. D. thesis, October 1988, Leeds University, Leeds, UK.

143. Popovics, S., *"Effect of curing method and final moisture condition on compressive strength of concrete,"* ACI Materials Journal, July-August 1986, Vol. 83, No. 3, pp. 650-65.

144. Roy, D. M., *"Fly ash and silica fume chemistry and hydration,"* Fly ash, Silica Fume Slag and natural pozzolans in concrete, ACI SP-114, ACI, Detroit, 1989.

145. De Larrard F. and Bostvironnois J. -L., *"On the long-term strength losses of silica fume high strength concretes,"* Magazine of Concrete Research, Vol. 43, No. 155, June 1991, pp. 109-119.

146. Tomosawa, F. and Noguchi, T., *"Relationship between compressive strength and modulus of elasticity of high-strength concrete,"* Utilisation of High Strength Concrete, Symposium in Lillehammer, Norway, June 20-23, 1993, Edited by Ivar Holand & Erik Sellevold, Vol. 2, pp. 1247-1254.

147. Swamy, R.N. and Rigby, G., *"Dynamic properties of hardened paste, mortar and concrete,"* Materials and Structure, 1971, No. 4, pp. 13-40.

148. Lydon F. D. and Lacovou M., *"Some factors affecting the dynamic modulus of elasticity of high strength concrete,"* Cement and Concrete Research Vol. 25, No. 6, 1995, pp. 1246-1256.

149. Carette G. G. and Malhotra V. M., *"Mechanical properties, durability and drying shrinkage of portland cement concrete incorporating silica fume,"* Cement, Concrete and Aggregates, 1983, Vol. 5, No. 1, Summer, pp. 3-13.

150. Chatterji, S. *"Probable mechanisms of crack formation at early ages of concretes: A literature survey,"* Cement and Concrete Research, Vol. 12, 1982, pp. 371-376.

151. Cook, R. A. and Hover, K. C., *"Mercury porosimetry of cement-based materials and associated correction factors,"* ACI Materials Journal, Vol. 90, No. 2, March-April 1993, pp. 152-161.

152. Hearn, N., Hooton, R. D. and Mills, R. H., *"Pore structure and permeability in concrete and concrete-making materials,"* ASTM SP Technical Publication No. 169C, 1994, pp. 241-262.

153. Micromeritics instruction manual for mercury porosimetry model 9320, part No. 932-42801-01, September 1989.

154. Torii, K. and Kawamura, M., *"Pore structure and chloride ion permeability of mortars containing silica fume,"* Cement and Concrete Composites, 16, 1994, pp. 279-286.

155. Pigeon M. and Regourd M., *"Freezing and thawing durability of three cements with various granulated blastfurnace slag contents,"* Proceeding of the 1st International conference on the use of fly ash, silica fume, slag and other mineral by products in concrete, ACI SP-79, Vol. 2, Canada, 1983, pp. 979-998.

156. Ramachandran V.C., Feldman R.F. and Beaudoin J. J., *"Concrete science,"* Heyden and Son Ltd, London, UK, 1981.

157. Dinku A and Reinhardt, *"The influence of storage conditions on the gas permeability and carbonation of concrete,"* Proceeding of the International Conference on "Concrete Repair, Rehabilitation and Protection," Edited by R. K. Dhir and M. R. Jones, University of Dundee, Scotland, UK, 1996, pp. 195-204.

158. Feldman, R. F., *"Pore structure Formation during Hydration of Fly Ash and Slag Cement Blends,"* Proceeding Symposium on Fly Ash Utilisation in cement and Concrete, Materials Research Society, 1981, pp. 124-133.

159. Sanjuan, M. A. and Munoz-Martialay, R., *"Influence of the age on air permeability of concrete,"* Journal of Materials Science Vol. 30, 1995, pp. 5657-5662.

160. Dhir R. K. and Byars E. A., *"Pulverized fuel-ash concrete: Intrinsic permeability,"* ACI Materials Journal, Vol. 90, No 6, November-December 1993, pp. 571-580.

161. Hughes, D. C., *"Pore structure and permeability of hardened cement paste,"* Magazine of Concrete Research, Vol. 17, No. 133, 1985, pp. 227-233.

162. Nyame B. K. and Illston J. M., *"Relationships between permeability and pore structure of hardened cement paste,"* Magazine of Concrete Research, Vol. 33, No. 116, September 1981, pp. 139-146.

163. Saetta, A. V., Schrefler A. and Vitaliani, R. V., *"The carbonation of concrete and the mechanism of moisture, heat and carbon dioxide flow through porous materials,"* Cement and Concrete Research, Vol. 23, 1993, pp. 761-772.

164. Maslehuddin, M., Page, C. L. and Rasheeduzzafar, *"Effect of temperature and salt contamination on carbonation of cements,"* Journal of Materials in Civil Engineering, Vol. 63 May 1996.

165. Hussain, S. E, Paul, I. S. and Ruthaiyea, H. M., *"Evaluation and repair strategies for shallow foundations,"* Proceeding of the 6th Middle East corrosion conference, Bahrain Society of Engineers, Manama, 1994, pp. 613-628.

166.Parrott, L. J., *"Water absorption in cover concrete,"* Materials and Structures, Vol. 25, 1992, pp. 284-292.

167.McCrter, W. J., Ezirim, H. and Emerson, M., *"Absorption of water and chloride into concrete,"* Magazine of Concrete Research, Vol. 44, No. 158, 1992, pp. 31-37.

168.Saricimen H, Maslehuddin M, Al-Tayyib A and Al-Mana A., *"Permeability and durability of plain and blended cement concretes cured in field and laboratory conditions,"* ACI Materials Journal, Vol. 92, No 3, May-June 1995, pp. 111-116.